ZooKeys 1224: 1–28 (2025)
DOI: 10.3897/zookeys.1224.130537

Research Article

Phylogeny of *Macrobrachium* spp. (Decapoda, Pleocyemata) from Peru based on mitochondrial and nuclear data reveals a species complex comprising *M. digueti* (Bouvier, 1895) and *M. transandicum* Holthuis, 1950

Eliana Zelada-Mázmela[1], Lorenzo E. Reyes-Flores[1], Luis De Stefano-Beltrán[2]

1 *Laboratory of Genetics, Physiology and Reproduction, National University of Santa, Av. Pacífico 508, Nuevo Chimbote, Ancash, Peru*
2 *Peruvian University Cayetano Heredia, Av. Honorio Delgado 430, San Martín de Porres, Lima, Peru*
Corresponding author: Eliana Zelada-Mázmela (ezelada@uns.edu.pe)

Abstract

Prawns of the genus *Macrobrachium* represent a highly diverse group of high commercial value worldwide. Eight *Macrobrachium* species have been reported from the Peruvian Pacific slope, but their phylogenetic relationships are still unknown. To investigate the systematics of *Macrobrachium* species from Peru, morphological identification and molecular data from nucleotide sequences of three genes were used: cytochrome *c* oxidase subunit I, 16S rRNA, and 28S rRNA. Based on morphological taxonomy, six species were successfully identified: *M. americanum*, *M. digueti*, *M. gallus*, *M. inca*, *M. panamense*, and *M. transandicum*. However, the phylogenetic inference results supported the species validity of only the first five species; all prawn individuals that were morphologically identified as *M. transandicum* were recovered within the *M. digueti* group, showing interspecific genetic distances near zero, suggesting that both species belong to the same species-level lineage, which may represent in the "*olfersii* species complex". Our analyses also corroborated the genetic proximity of sibling species *M. inca*–*M. americanum* and *M. gallus*–*M. panamense*, and the monophyletic origin of *Macrobrachium* species from Peruvian populations. This study represents the first comprehensive phylogenetic analyses of *Macrobrachium* species from Peru, and contributes the first publicly available DNA sequences for *M. inca* and *M. gallus*, as well as the first sequences of *M. americanum*, *M. panamense*, *M. digueti*, and *M. transandicum* collected from Peruvian rivers.

Key words: Genetic variability, *Macrobrachium*, molecular phylogenetics, *olfersii* species complex, Peruvian river prawns, systematics

Academic editor: Luis Ernesto Bezerra
Received: 30 June 2024
Accepted: 11 November 2024
Published: 20 January 2025

ZooBank: https://zoobank.org/51672CCD-390B-4D2D-821D-F9349F5B46CC

Citation: Zelada-Mázmela E, Reyes-Flores LE, De Stefano-Beltrán L (2025) Phylogeny of *Macrobrachium* spp. (Decapoda, Pleocyemata) from Peru based on mitochondrial and nuclear data reveals a species complex comprising *M. digueti* (Bouvier, 1895) and *M. transandicum* Holthuis, 1950. ZooKeys 1224: 1–28. https://doi.org/10.3897/zookeys.1224.130537

Introduction

Prawns of the genus *Macrobrachium* Spence Bate, 1868 are cosmopolitan species inhabiting freshwater and estuarine ecosystems (Bowles et al. 2000). This speciose crustacean genus currently encompasses 319 accepted species in the World Register of Marine Species (WoRMS Database 2024) database, many of them being of high commercial value worldwide (Makombu

et al. 2019); however, several studies have suggested the existence of cryptic species causing taxonomic issues that are yet to be resolved (Liu et al. 2007). This crustacean group is also known for the presence of strong interspecific conservatism and intraspecific variation, which makes it taxonomically recalcitrant (Pileggi and Mantelatto 2010; Rossi and Mantelatto 2013), especially when systematics studies have been based mainly on comparison of external morphological traits (de Bruyn 2005; Nogueira et al. 2023). Arguably, the palaemonid prawn classification scheme given by Holthuis (1950, 1952) is the most widely used for the taxonomic classification of freshwater prawns from the Americas (Murphy and Austin 2002, 2003). However, the diagnostic characters determined by Holthuis have been critically debated due to their complex morphological variation (Murphy and Austin 2002, 2003).

More recently, this group has received special attention with studies mainly related to taxonomy and molecular systematics (Nogueira et al. 2023). Molecular phylogenetics has become a powerful tool and more studies are combining molecular and morphological data aiming to obtain a more robust insight into the classification of *Macrobrachium* species. Nuclear and mitochondrial DNA markers have been successfully used to solve taxonomic issues in highly diversified decapod groups (Murphy and Austin 2004; Siriwut et al. 2020 and references therein) including the description of cryptic species from *Macrobrachium* (Pileggi et al. 2014; Fuke and Imai 2018; Siriwut et al. 2020; Rossi et al. 2023). Despite the large diversity of *Macrobrachium* species and species complexes existing in populations from Latin America (García-Guerrero et al. 2013; Pileggi et al. 2014), to date most taxonomic studies on *Macrobrachium* have mainly focused on species from the Indo-Pacific region (where a higher number of *Macrobrachium* species occur), and only a few studies have used molecular and morphological data to analyze *Macrobrachium* populations from Brazil and Mexico (Pileggi and Mantelatto 2010; Rossi and Mantelatto 2013; Pileggi et al. 2014; García-Velazco et al. 2017; Rossi et al. 2023). A comprehensive systematic review of *Macrobrachium* by Anger (2013), concluded that *Macrobrachium* species from the Americas represent a separate group, including up to 57 species, of which three (*M. gallus* Holthuis, 1952, *M. inca* Holthuis, 1950, and *M. transandicum* Holthuis, 1950) are endemic to the western slopes of the Andes (Holthuis 1950; Anger 2013).

In Peru, eight *Macrobrachium* species (*M. gallus*, *M. inca*, *M. transandicum*, *M. americanum* Bate, 1868, *M. tenellum* (Smith, 1871), *M. digueti* (Bouvier, 1895), *M. hancocki* Holthuis, 1950, and *M. panamense* Rathbun, 1912) have been reported to occur on the Pacific slope (Amaya and Guerra 1976; Méndez 1981; Valencia and Campos 2007; Luque 2008; Hendrickx and Wicksten 2011, Campos 2014), but only the first three species are endemic to the Ecuadorian and Peruvian Pacific slope, while the latter five species also occur in Central America and Mexico (Valencia and Campos 2007; Hernández 2008; Mc Larney et al. 2010).

Currently, there is no established *Macrobrachium* prawn fishery in Peru, and as with other *Macrobrachium* species, as it is generally a complementary and artisanal activity associated with the rainy season. The organisms caught are consumed locally or marketed in places close to the fishing grounds. However,

their widespread use means that fishing pressure is increasing and the availability of areas for natural production is decreasing, aggravated by pollution, which limits the potential of natural populations. (López-Uriostegui et al. 2013). Despite the economic and culinary importance of prawns, studies on Peruvian freshwater prawns are scarce and those that exist are mostly related to *Cryphiops* (*Cryphiops*) *caementarius* (Molina, 1782) from central and southern Peruvian rivers (Zacarías and Yépez 2008). Furthermore, official inland capture fishery statistics of different *Macrobrachium* prawns are registered using the generic term "river prawn" (PRODUCE 2023) with no species-specific records. This common practice can lead to serious conservation problems, highlighting the urgent need for more taxonomic and population studies of *Macrobrachium* species from Peru.

Prawns are key elements of the food chain from freshwater environments, playing a major role not only as omnivorous scavengers and detritus feeders, but also as prey for fish, birds, and reptiles. Furthermore, they are considered important ecosystem engineers (García-Guerrero et al. 2013). To the best of our knowledge, despite the ecological (*Macrobrachium* prawns are key to the functionality and health of aquatic ecosystem) and commercial value of freshwater prawns, to date no study has applied nuclear and mitochondrial DNA markers to study the phylogeny of *Macrobrachium* species from Peruvian populations. The present study aimed to analyze the phylogenetic relationships among six *Macrobrachium* species collected from Peruvian rivers of the Pacific slope using morphological and molecular data. Phylogenetic relationships were inferred based on partial sequences of two mitochondrial makers, namely cytochrome *c* oxidase subunit I and 16S ribosomal RNA (hereafter referred to as COI and 16S rRNA, respectively), and one nuclear gene fragment, namely 28S ribosomal RNA (hereafter referred to as 28S rRNA).

Materials and methods

Field sampling and morphological identification

A total of 136 specimens belonging to the genus *Macrobrachium* were collected between December 2012 and February 2016 in rivers and estuaries from six Peruvian coastal regions including Tumbes, Piura, Lambayeque, La Libertad, Ancash, and Lima (Fig. 1; Suppl. material 2: table S1). The organisms were either bought from local fishermen or extracted using cast nets with a mesh size of 1 mm, landing nets, or by sieving seagrass beds and rocky bottoms of estuaries. Additionally, we also collected samples of the tropical river prawn *Palaemon hancocki* (Holthuis, 1950) to be used as an outgroup in phylogenetic analyses. Specimens were preserved in 96% ethanol, labeled by river name and collection date, and deposited in the voucher collection of the Laboratory of Genetics, Physiology, and Reproduction of the Universidad Nacional del Santa (**LGFyR-UNS**, Ancash, Peru). Morphological species identification was performed according to Méndez (1981) and Valencia and Campos (2007). The current accepted prawn scientific names and authorities were checked in WoRMS, which also includes the current revised taxonomy of freshwater species.

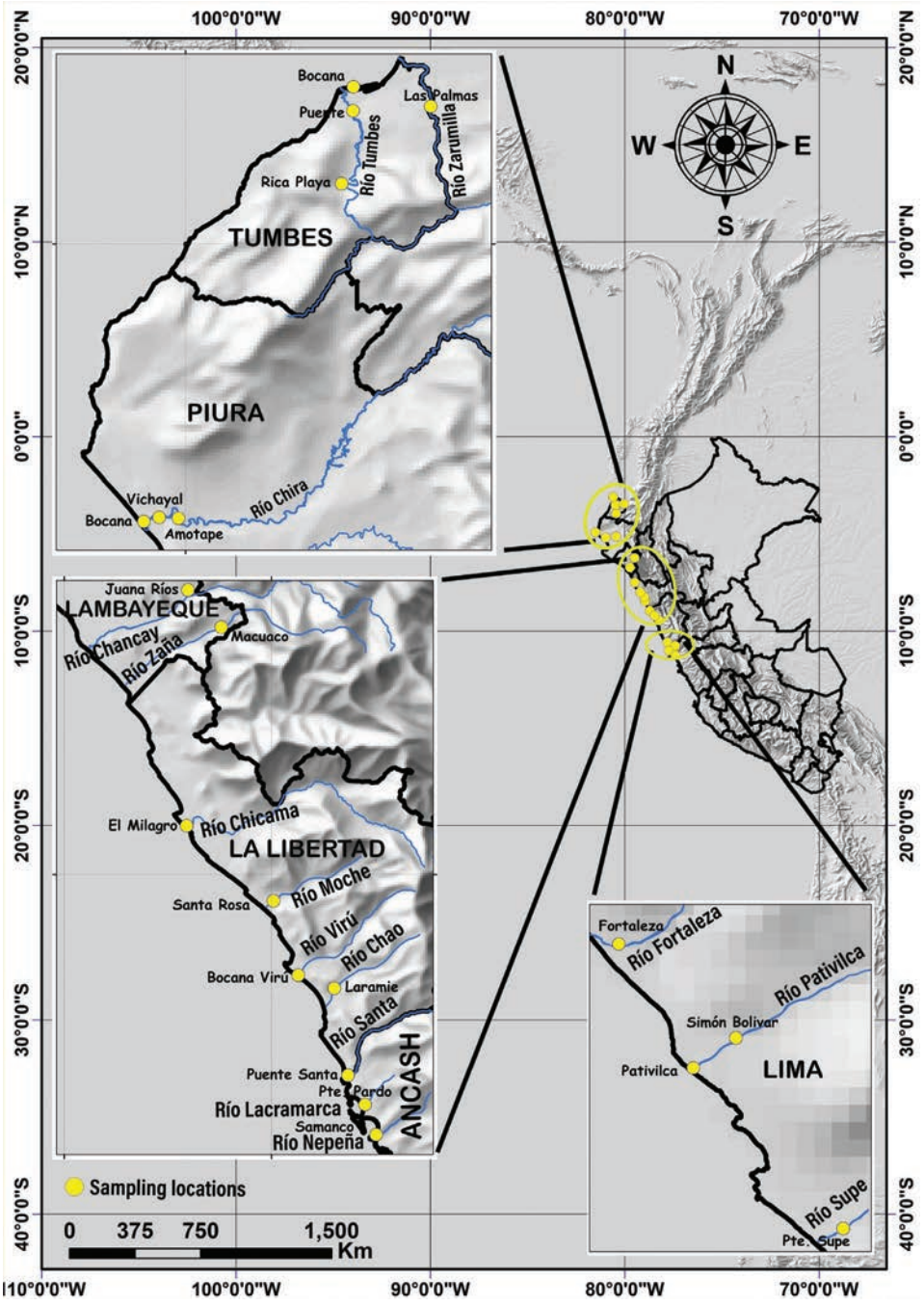

Figure 1. Geographic map of Peru showing sampling locations of *Macrobrachium* species (adapted from https://www.naturalearthdata.com/downloads/10m-raster-data/10m-shaded-relief/).

DNA extraction, PCR amplification, and sequencing

Total genomic DNA was extracted from the muscle tissue of the pleopods, using the commercial GeneJET Genomic DNA Purification Kit (Thermo Fisher Scientific, Carlsbad, CA, USA). DNA quantification was calculated using an Epoch spectrophotometer (BioTek Instruments, Winooski, VT, USA). Extracted DNA quality was assessed by the 260/280 ratio and its integrity was observed by 1% agarose gel electrophoresis using GelRed Nucleic Acid Gel Stain as a DNA intercalator. Oligonucleotide sequences used for the polymerase chain reaction (PCR) amplification of partial fragments of COI, 16S rRNA, and 28S rRNA genes

are shown in Table 1. All PCR amplifications were performed in a Veriti 96-Well Thermal Cycler (Applied Biosystems, Foster City, CA, USA) using Maximo *Taq* DNA Polymerase (GeneOn GmbH, Nurnberg, Germany) with the following master mix composition for COI y 16S rRNA: 1.14 µL of 25 mM $MgCl_2$, 1.5 µL of 10X buffer, 0.75 µL of 2.5 mM dNTPs, 0.15 µL of each primer (50 µM), 0.15 µL of 5U μL^{-1} of *Taq* polymerase, 1 µL template DNA, and 10.16 µL of PCR Water (Invitrogen) to reach a total reaction volume of 15 µL. For 28S rRNA, the master mix composition was 1.3 µL of 25 mM $MgCl_2$, 1.5 µL of 10X buffer, 0.75 µL of 2.5 mM dNTPs, 0.15 µL of each primer (50 µM), 0.15 µL of 5U μL^{-1} of *Taq* polymerase, 1 µL template DNA, and 10 µL of PCR Water (Invitrogen) to reach a total reaction volume of 15 µL. COI gene fragments were amplified with the following thermal cycler protocol: initial denaturation at 94 °C for 3 min, followed by 35 cycles of 94 °C for 45 s, 42 °C for 60 s, and 72 °C for 60 s, and a final extension step at 72 °C for 6 min. 16S rRNA gene fragments were amplified with the following thermal cycler protocol: initial denaturation at 94 °C for 3 min, followed by 30 cycles of 95 °C for 60 s, 40 °C for 60 s, and 72 °C for 60 s, and a final extension step at 72 °C for 10 min. 28S rRNA gene fragments were amplified with the following thermal cycler protocol: initial denaturation at 94 °C for 5 min, followed by 38 cycles of 94 °C for 30 s, 56 °C for 30 s, and 72 °C for 38 s, and a final extension step at 72 °C for 7 min. Successful PCR amplifications were verified in a 1% agarose electrophoresis using GelRed Nucleic Acid Gel Stain as a DNA intercalator. For DNA sequencing, all PCR products were purified using Exonuclease I and Shrimp Alkaline Phosphatase enzymes following Werle et al. (1994). Purified amplicons were Sanger sequenced bidirectionally by Macrogen Inc. (Rockville, MD, USA) in an ABI 3730Cl genetic analyzer (Applied Biosystems, Foster City, CA). For DNA electropherogram quality control, all sequences were manually checked and edited by removing ambiguous base callings, and COI sequences were checked for premature stop codons and frameshift indels that might indicate the presence of nuclear mitochondrial pseudogenes (NUMTs).

DNA sequence and genetic distance analyses

A matrix containing multi-aligned sequences was constructed for each gene analyzed gene (COI, 16S rRNA, and 28S rRNA) using all the obtained sequences from *M. americanum*, *M. digueti*, *M. panamense*, and *M. transandicum*. In each matrix, we included sequences from three specimens of *M. gallus* and *M. inca* collected from each river of our field surveys, avoiding common or shared haplotypes. *Palaemon hancocki* was used as an outgroup. All DNA sequences obtained in this study have been deposited in GenBank/EMBL/DDBJ databases with accession numbers from OR941326–OR941602 (Suppl. material 2: table S2). All sequences were multi-aligned using the ClustalW algorithm as implemented in MEGA v. 7.0.21 (Kumar et al. 2016). Intraspecific and interspecific pairwise genetic distances were calculated using the Kimura 2-parameter model using MEGA v. 7.0.21. Basic sequence analysis statistics such as nucleotide composition, conserved sites, variable sites, parsimony informative sites, transitions and transversions rates, and amino acid composition were determined using MEGA v. 7.0.21, considering the start codon nucleotide position for the COI gene. The complete amino acid COI sequence from *M. rosenbergii* (De Man, 1879) (GenBank accession AY659990) was used to determine the correct start codon position in our partial COI fragment sequences.

Table 1. Primer sequences used to amplify mitochondrial (COI and 16S rRNA) and nuclear (28S rRNA) genes.

Primer name	Direction	Sequence (5' -- 3')	Gene	Reference
Col6bF	Forward	ACAAATCATAAAGATATYGG	COI	Schubart and Heber (2006)
COH6R	Reverse	TADACTTCDGGRTGDCCAAARAAYCA		
1471	Forward	CCTGTTTANCAAAAACAT	16S rRNA	Munashinge (2010); Liu et al. (2007)
1472	Reverse	AGATAGAAACCAACCTGG		
28RDDF D2CFD45F	Forward	TACCGTGAGGGAAAGTTGAAA	28S rRNA	Suresh et al. (2012); Ndong et al. (2012)
28D2CRD45R	Reverse	AGACTCCTTGGTCCGTGTTT		

Phylogenetic analyses

Three different phylogenetic methods were performed for each of the three selected genes including maximum parsimony (MP), maximum likelihood (ML) and Bayesian inference (BI), implemented in PAUP v. 4.0 (Swofford 2002), RAxML v. 8.2.13 (Stamatakis 2014), and MrBayes v. 3.2.2 (Ronquist et al. 2011) respectively. For the construction of the MP phylogenetic tree, which treats gaps as a fifth state character, node reliability was evaluated using 1000 bootstrap replicates. The ML approach was performed with default parameters and employing the GTRGAMMA model of evolution, using 1000 bootstrap replicates to verify tree topology and clade support. The BI approach, which is a probabilistic model of multiple sequence alignments that accounts for insertion and deletion events in addition to substitution (Palero and Crandall 2009), was performed using two independent runs, each with four Markov chains under the Metropolis-Hasting algorithm (MCMC). To find the best-fit model of evolution we used jModelTest 2 (Darriba et al. 2012) under the Bayesian Information Criterion (BIC). The analyses were run for 1,000,000 generations with sampling every 100 generations, until reaching a standard deviation of less than 0.01. The first 25% of the sampled trees were discarded as burn-in. All phylogenetic trees were drawn using the Figtree v. 1.4.2 program (Rambaut 2014). Additionally, aiming to obtain further evolutionary insights that might not be resolved with single gene phylogenetic analysis, three different concatenated gene datasets (COI-16S rRNA, COI-28S rRNA, 16S rRNA-28S rRNA) were constructed using SeaView v. 4.5.4 (Gouy et al. 2010). jModelTest 2 (Darriba et al. 2012) under BIC was used to find the best-fit model of evolution of the concatenated gene datasets. MP, ML and BI analyses were performed using the same parameters described above for phylogenetic analysis of a single gene locus. Substitution saturations in single codon positions from each COI and the level of nucleotide substitution and genetic variability in the 16S rRNA and 28S rRNA genes were evaluated using an entropy-based index as implemented in DAMBE 6 (Xia 2017).

Results

Morphological and molecular species identification

Among the 136 collected specimens, a total of six *Macrobrachium* species (Suppl. material 2: table S2) were identified based on morphological analyses following the taxonomic key reported by Méndez (1981) and Valencia and Campos (2007) (Suppl. material 1: figs S1–S9; Suppl. material 2: table S3).

Phylogenetic relationships of COI dataset

Overall, the results of phylogeny estimation approaches (MP, ML and BI) inferred with single and concatenated gene datasets showed similar topologies, branch lengths, and high bootstrap support and posterior probabilities. All approaches (MP, ML, and BI) (Figs 2–4, respectively) for the COI dataset (n = 83 sequences) showed that the six *Macrobrachium* species included in our analyses were recovered in five discrete clades: *M. inca* (Mi, n = 45), *M. gallus* (Mg, n = 7), *M. americanum* (Ma, n = 7), *M. panamense* (Mp, n = 4), and a single clade that grouped both *M. digueti* (Md, n = 6) and *M. transandicum* (Mt, n = 10). *Palaemon hancocki* (Ph, n = 4) was used as the outgroup. All substitution models used in our phylogenetic analyses are shown in Suppl. material 2: table S4. The MP, ML, and BI phylogenetic trees for COI sequences recovered *M. inca* and *M. americanum* in

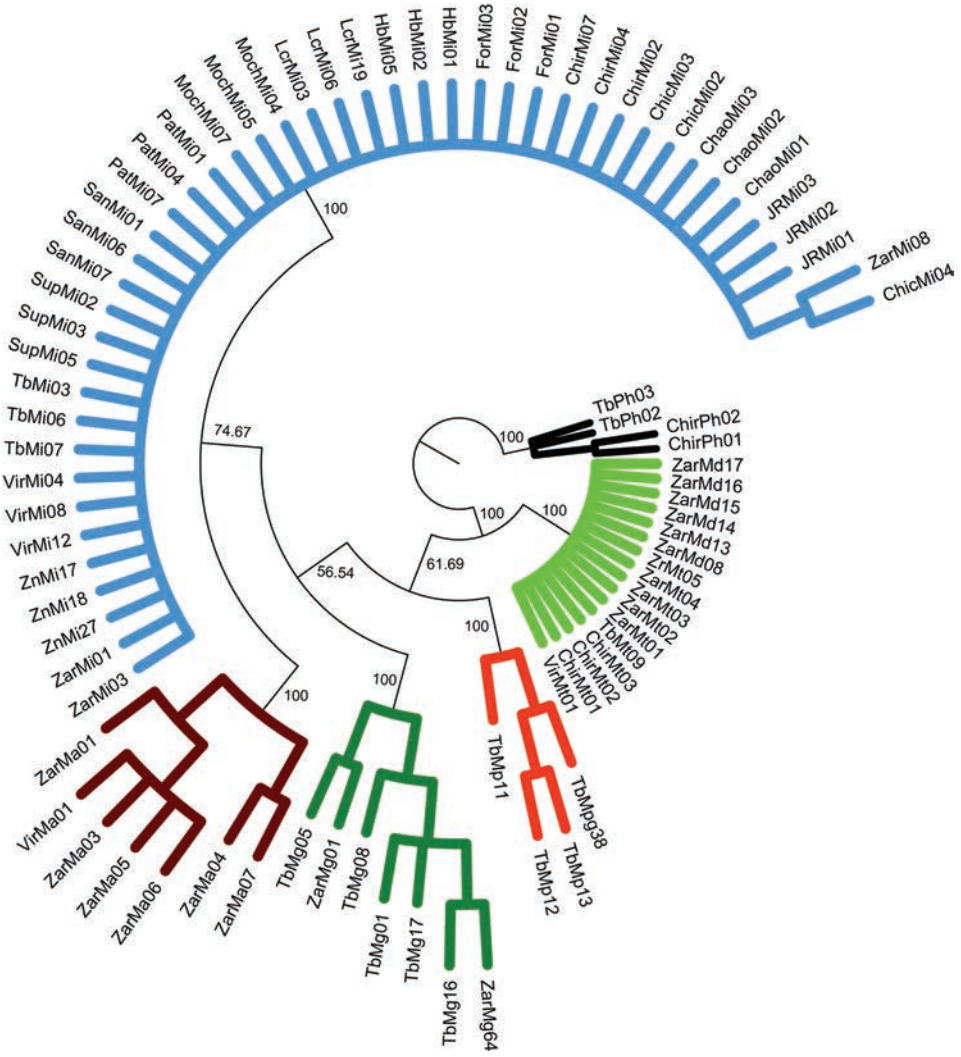

Figure 2. Phylogenetic tree based on maximum parsimony generated using 83 partial sequences of the mitochondrial COI gene from six *Macrobrachium* species collected in Peruvian rivers of the Pacific slope. Bootstrap values ≥ 50% are shown. *P. hancocki* was used as outgroup. GenBank accession numbers OR941326–OR941408. Abbreviations: Mt: *M. transandicum*; Mp: *M. panamense*; Mi: *M. inca*; Mg: *M. gallus*; Ma: *M. americanum*; Md: *M. digueti*, Ph: *P. hancocki*; Chir: Chira River; Tb: Tumbes River; Zr, Zar: Zarumilla River; Vir: Virú River; Pat: Pativilca River; JR: Juana Ríos River; Chao: Chao River; Lcr: Lacramarca River; Hb: Nepeña River; For: Fortaleza River; San: Santa River; Moch: Moche River; Chic: Chicama River; Sup: Supe River; Zn: Zaña River.

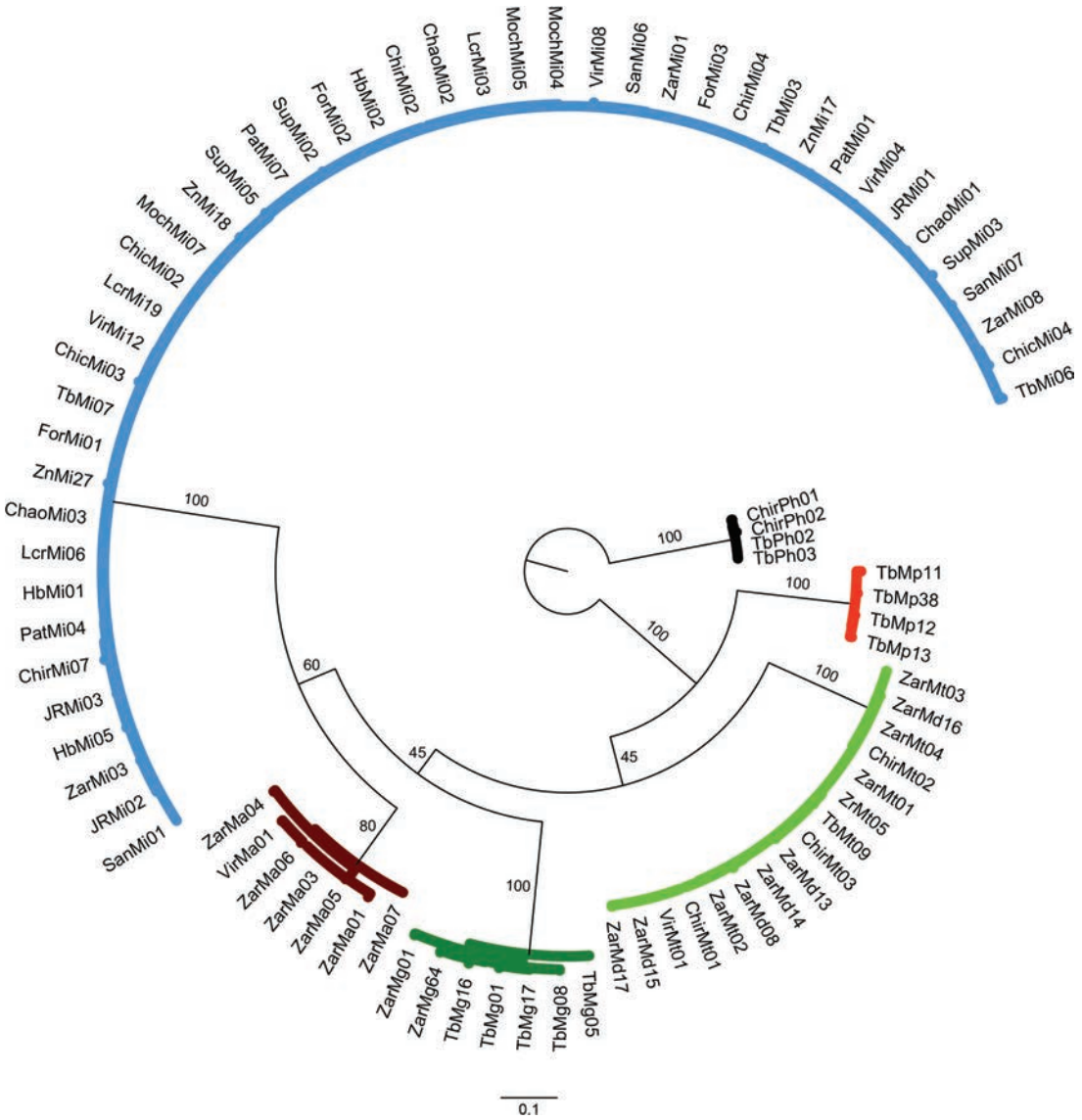

Figure 3. Phylogenetic tree based on maximum likelihood inference generated under the GTRGAMMA substitution model using 83 partial sequences of the mitochondrial COI gene from six *Macrobrachium* species collected in Peruvian rivers of the Pacific slope. Bootstrap values ≥ 50% are shown. *P. hancocki* was used as outgroup. GenBank accession numbers OR941326–OR941408. Abbreviations: Mt: *M. transandicum*; Mp: *M. panamense*; Mi: *M. inca*; Mg: *M. gallus*; Ma: *M. americanum*; Md: *M. digueti*; Ph: *P. hancocki*; Chir: Chira River; Tb: Tumbes River; Zr, Zar: Zarumilla River; Vir: Virú River; Pat: Pativilca River; JR: Juana Ríos River; Chao: Chao River; Lcr: Lacramarca River; Hb: Nepeña River; For: Fortaleza River; San: Santa River; Moch: Moche River; Chic: Chicama River; Sup: Supe River; Zn: Zaña River.

two sister clades with high bootstrap support (74.7, 60%) and posterior probabilities (87%), which is consistent with shared morphological characteristics between both species (short rostrum and similar shape of the second pair of pereiopods). Intraspecific genetic distance values of COI for the six *Macrobrachium* species analyzed in this study are shown in Table 2, ranging from 0.43% in *M. transandicum* to 1.78% in *M. americanum*. Interspecific genetic distances for COI (Table 3) ranged from 0.53% (between *M. transandicum* and *M. digueti*) to 23.9% (between *M. digueti* and *M. inca*). The short interspecific genetic distance found between *M. digueti* and *M. transandicum* (0.53%) caused the recovery of both species into a single clade in all phylogenetic trees (MP, ML and BI) with high statistical support (100% bootstrap value and posterior probabilities).

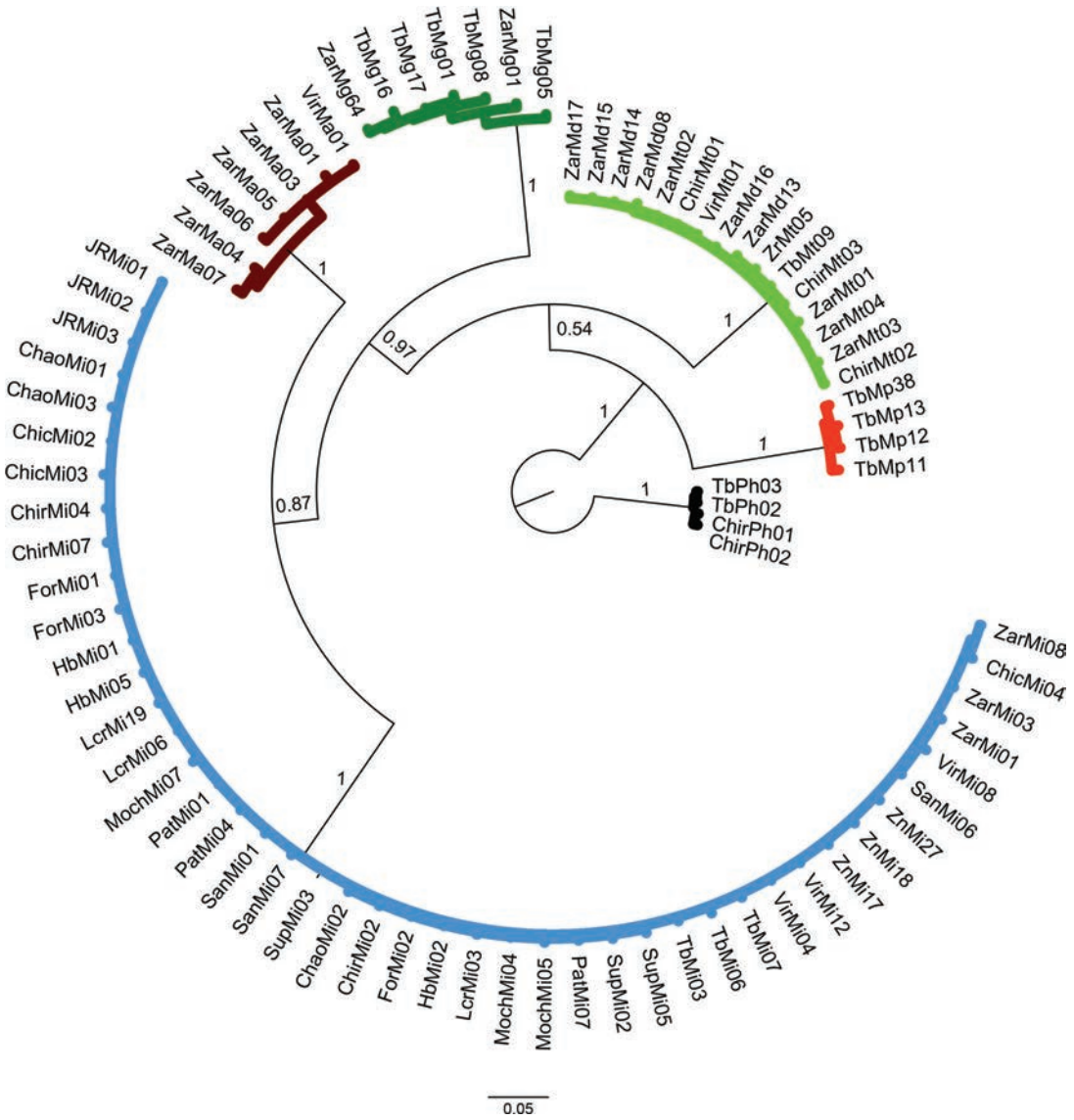

Figure 4. Phylogenetic tree based on Bayesian Inference approach generated under the GTR+I+G substitution model using 83 partial sequences of the mitochondrial COI gene from six *Macrobrachium* species collected in Peruvian rivers of the Pacific slope. Bootstrap values ≥ 50% are shown. *P. hancocki* was used as outgroup. GenBank accession numbers OR941326–OR941408. Abbreviations: Mt: *M. transandicum*; Mp: *M. panamense*; Mi: *M. inca*; Mg: *M. gallus*; Ma: *M. americanum*; Md: *M. digueti*; Ph: *P. hancocki*; Chir: Chira River; Tb: Tumbes River; Zr, Zar: Zarumilla River; Vir: Virú River; Pat: Pativilca River; JR: Juana Ríos River; Chao: Chao River; Lcr: Lacramarca River; Hb: Nepeña River; For: Fortaleza River; San: Santa River; Moch: Moche River; Chic: Chicama River; Sup: Supe River; Zn: Zaña River.

Table 2. Intraspecific genetic distances based on a partial fragment of the COI gene. Analyses were conducted using the Kimura 2-parameter model (K2P) with 1000 bootstrap replicates.

Species	Genetic distance (d)	Standard error (SE)
M. inca	0.007875916	0.001348432
M. gallus	0.016703893	0.002978309
M. panamense	0.009035682	0.002716602
M. transandicum	0.004338227	0.0015591
M. digueti	0.006141983	0.001761096
M. americanum	0.017789742	0.003291708
P. hancocki	0.003437498	0.001656147

Table 3. Interspecific genetic distances (below diagonal) based on a partial fragment of the COI gene. Analyses were conducted using the Kimura 2-parameter model (K2P) with 1000 bootstrap replicates. Standard error estimates are shown above the diagonal.

Species	*M. inca*	*M. americanum*	*M. digueti*	*M. panamense*	*M. transandicum*	*M. gallus*	*P. hancocki*
M. inca	–	0.017348	0.020433	0.021025	0.020447	0.019419	0.022040
M. americanum	0.179606	–	0.018468	0.017899	0.018470	0.018310	0.021414
M. digueti	0.238992	0.188721	–	0.019072	0.001463	0.017165	0.019316
M. panamense	0.228502	0.186465	0.203847	–	0.019046	0.021432	0.021106
M. transandicum	0.237390	0.188609	0.005268	0.202176	–	0.017119	0.019351
M. gallus	0.213766	0.198608	0.189913	0.236212	0.187403	–	0.021735
P. hancocki	0.262074	0.238108	0.211475	0.241439	0.210927	0.253760	–

Phylogenetic relationships of 16S rRNA dataset

16S rRNA gene phylogenetic trees based in MP (Fig. 5), ML (Fig. 6), and BI (Fig. 7) showed similar topologies. In all trees, the monophyletic clades that recovered all *M. gallus* and *M. inca* sequences were placed in the basal and apical position of the tree, respectively. However, the phylogenetic trees recovered the two sequences representing *M. panamense* (TbMp16 GenBank accession OR941679 and TbMp17 GenBank accession OR941680) within the *M. inca* clade. Similar to the results obtained with the COI dataset, all sequences from *M. digueti* (Md, *n* = 6) and *M. transandicum* (Mt, *n* = 12) were recovered in a single clade with high bootstrap support (60% and 99%) and posterior probabilities (100%). The results of the intraspecific genetic distance values of the 16S rRNA gene dataset for the six *Macrobrachium* species analyzed in this study were found to be lower than those of the COI gene (Table 4) ranging from 0.11% in *M. americanum* to 0.72% in *M. gallus*. Interspecific genetic distances for 16S rRNA (Table 5) ranged from 0.19% (between *M. transandicum* and *M. digueti*) to 11.76% (between *M. gallus* and *M. digueti*). We should mention that COI and 16S rRNA gene sequences from *M. panamense* were obtained from different specimens and, in contrast to the COI genetic distance observed between *M. panamense* and *M. inca* (22.9%), the 16S rRNA distance observed for the same species pair was 0.53%, which was reflected in the recovery of both species within a single clade (Figs 2–4).

Table 4. Intraspecific genetic distances based on a partial fragment of the 16S rRNA gene. Analyses were conducted using the Kimura 2-parameter model (K2P) with 1000 bootstrap replicates.

Species	Genetic distance (d)	Standard error (SE)
M. inca	0.005080317	0.001149334
M. americanum	0.001143241	0.00077876
M. digueti	0.002001609	0.001112749
M. panamense	0.004003013	0.002731773
M. transandicum	0.001942077	0.000888224
M. gallus	0.007245067	0.002351216
P. hancocki	0.002803217	0.001658205

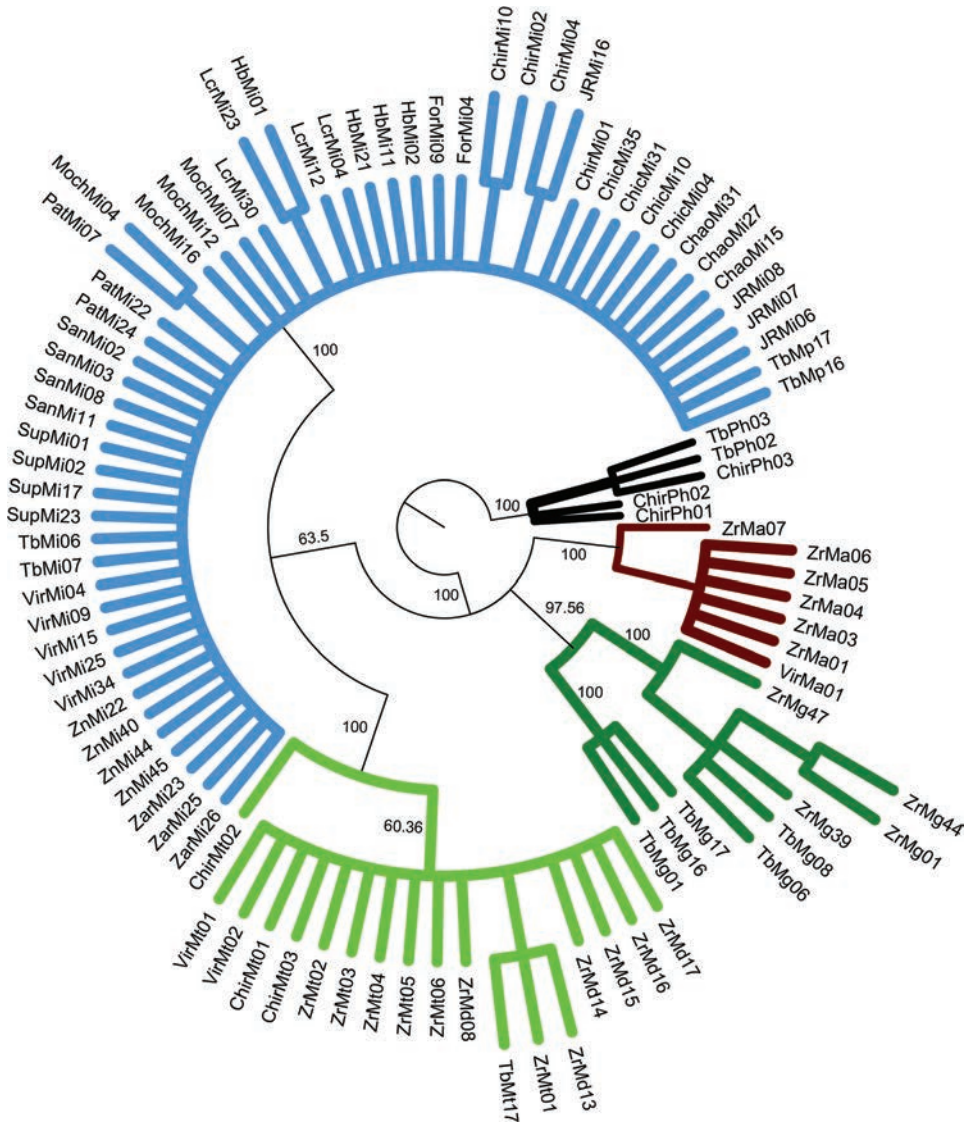

Figure 5. Phylogenetic tree based on Maximum Parsimony approach generated using 93 partial sequences of the mitochondrial 16S rRNA gene from six *Macrobrachium* species collected in Peruvian rivers of the Pacific slope. Bootstrap values ≥ 50% are shown. *P. hancocki* was used as outgroup. GenBank accession numbers OR941603–OR941697. Abbreviations: Mt: *M. transandicum*; Mp: *M. panamense*; Mi: *M. inca*; Mg: *M. gallus*; Ma: *M. americanum*; Md: *M. digueti*; Ph: *P. hancocki*; Chir: Chira River; Tb: Tumbes River; Zr, Zar: Zarumilla River; Vir: Virú River; Pat: Pativilca River; JR: Juana Ríos River; Chao: Chao River; Lcr: Lacramarca River; Hb: Nepeña River; For: Fortaleza River; San: Santa River; Moch: Moche River; Chic: Chicama River; Sup: Supe River; Zn: Zaña River.

Table 5. Interspecific genetic distances (below diagonal) based on a partial fragment of the 16S rRNA gene. Analyses were conducted using the Kimura 2-parameter model (K2P) with 1000 bootstrap replicates. Standard error estimates are shown above the diagonal.

Species	*M. inca*	*M. americanum*	*M. digueti*	*M. panamense*	*M. transandicum*	*M. gallus*	*P. hancocki*
M. inca	–	0.014232	0.012861	0.001992	0.012809	0.014017	0.023743
M. americanum	0.098973	–	0.014303	0.014626	0.014328	0.013072	0.023497
M. digueti	0.077575	0.095831	–	0.013265	0.000785	0.015049	0.023423
M. panamense	0.005348	0.101574	0.079840	–	0.013213	0.014356	0.024126
M. transandicum	0.077179	0.096172	0.001891	0.079458	–	0.015013	0.023423
M. gallus	0.102915	0.092403	0.117623	0.104548	0.117217	–	0.024178
P. hancocki	0.209718	0.207972	0.216827	0.213408	0.216353	0.229778	–

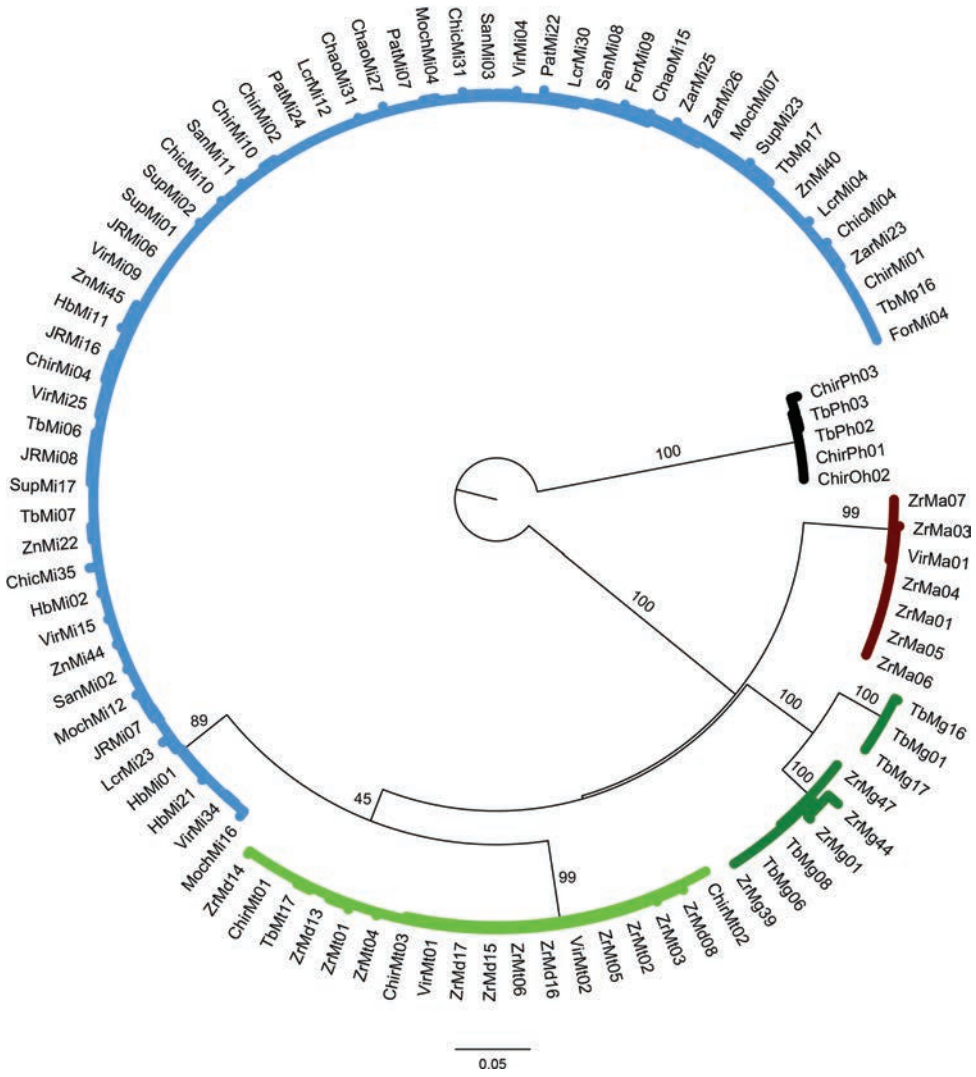

Figure 6. Phylogenetic tree based on maximum likelihood inference generated under the GTRGAMMA substitution model using 93 partial sequences of the mitochondrial 16S rRNA gene from six *Macrobrachium* species collected in Peruvian rivers of the Pacific slope. Bootstrap values ≥ 50% are shown. *P. hancocki* was used as outgroup. GenBank accession numbers OR941603–OR941697. Abbreviations: Mt: *M. transandicum*; Mp: *M. panamense*; Mi: *M. inca*; Mg: *M. gallus*; Ma: *M. americanum*; Md: *M. digueti*; Ph: *P. hancocki*; Chir: Chira River; Tb: Tumbes River; Zr, Zar: Zarumilla River; Vir: Virú River; Pat: Pativilca River; JR: Juana Ríos River; Chao: Chao River; Lcr: Lacramarca River; Hb: Nepeña River; For: Fortaleza River; San: Santa River; Moch: Moche River; Chic: Chicama River; Sup: Supe River; Zn: Zaña River.

Phylogenetic relationships of 28S rRNA dataset

The results from phylogenetic approaches (MP, Fig. 8; ML, Fig. 9 and BI, Fig. 10) for the 28S rRNA were highly similar, except for *M. digueti* (*n* = 5) and *M. transandicum* (*n* = 4) which were grouped in a single discrete clade with high statistical support (100% bootstrap value and posterior probability). All the other species (*M. americanum*, *M. gallus*, *M. inca*, and *M. panamense*) were recovered in unique clades with high bootstrap values (98–100%) and posterior probabilities (100%). The MP, ML, and BI phylogenetic tree results using the 28S rRNA dataset successfully recovered all *M. panamense* sequences in a single clade, including individuals TbMp16 (GenBank accession OR941594) and TbMp17 (GenBank accession OR941595) (see Figs 8–10), which under the 16S rRNA gene dataset were recovered within the *M. inca* group (see Figs 5–7).

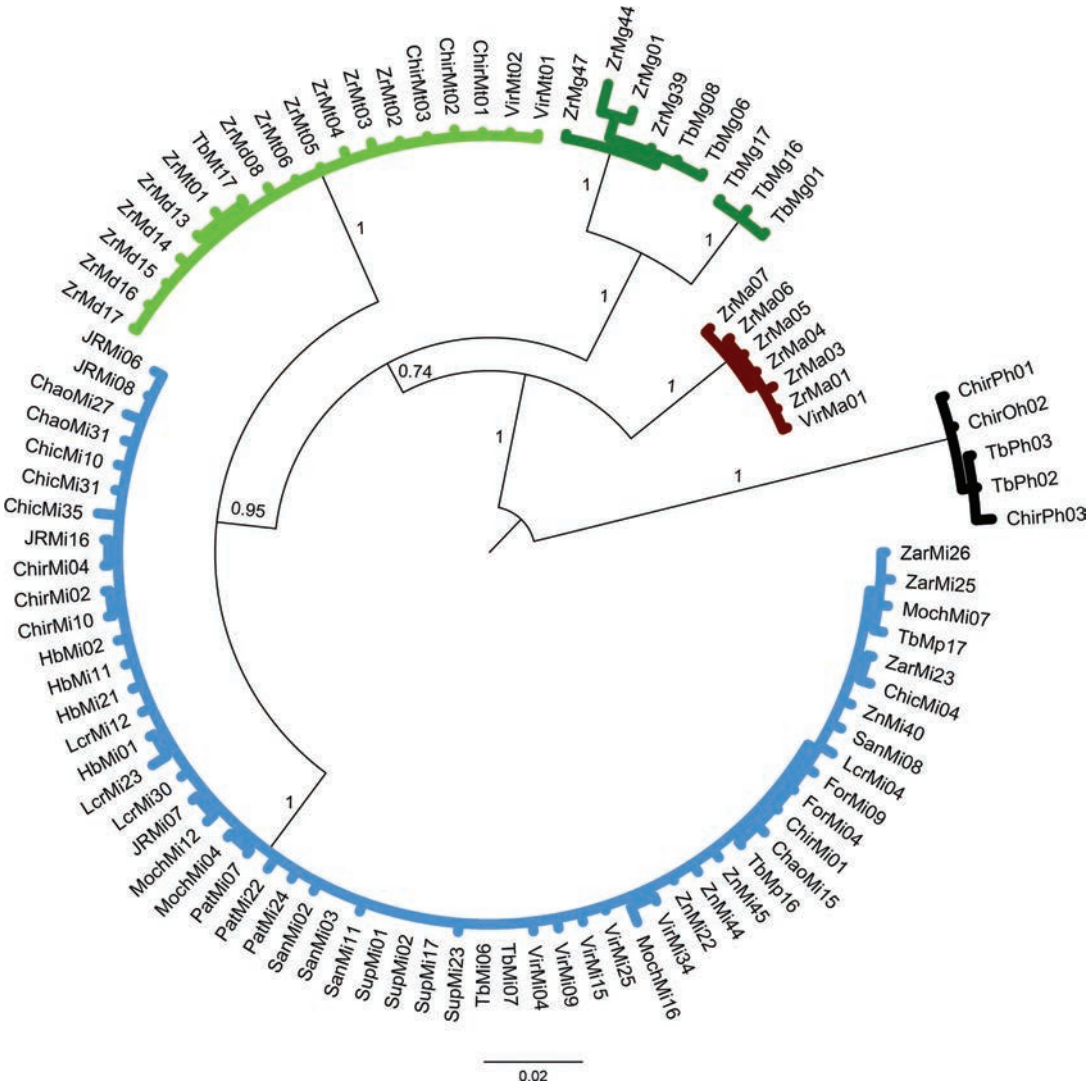

Figure 7. Phylogenetic tree based on Bayesian Inference approach generated under the K80+I+G substitution model using 93 partial sequences of the mitochondrial 16S rRNA gene from six *Macrobrachium* species collected in Peruvian rivers of the Pacific slope. Bootstrap values and posterior probabilities ≥ 50% are shown. *P. hancocki* was used as outgroup. GenBank accession numbers OR941603–OR941697. Abbreviations: Mt: *M. transandicum*; Mp: *M. panamense*; Mi: *M. inca*; Mg: *M. gallus*; Ma: *M. americanum*; Md: *M. digueti*; Ph: *P. hancocki*; Chir: Chira River; Tb: Tumbes River; Zr, Zar: Zarumilla River; Vir: Virú River; Pat: Pativilca River; JR: Juana Ríos River; Chao: Chao River; Lcr: Lacramarca River; Hb: Nepeña River; For: Fortaleza River; San: Santa River; Moch: Moche River; Chic: Chicama River; Sup: Supe River; Zn: Zaña River.

The topology in the phylogenetic trees was also similar: *M. americanum* and *M. panamense* were recovered in two discrete clades with high bootstrap support (100 and 98%) and posterior probabilities (100%). The results also showed that the BI phylogenetic tree grouped *M. gallus* with *M. panamense* and *M. americanum* with *M. inca* in sister clades with high nodal support (100% and 86%, respectively). The two former species have a long rostrum while the two latter species share a similar long and robust shape of the second pair of pereiopods. As shown in Table 6, all the prawn species had no intraspecific genetic distance (0%) for the analyzed 28S rRNA fragment, except for *M. americanum* and *M. panamense* which displayed genetic distance values above zero (7.22% and 2.11% respectively). The calculated interspecific genetic distances for 28S rRNA among the *Macrobrachium* species analyzed herein resolved the

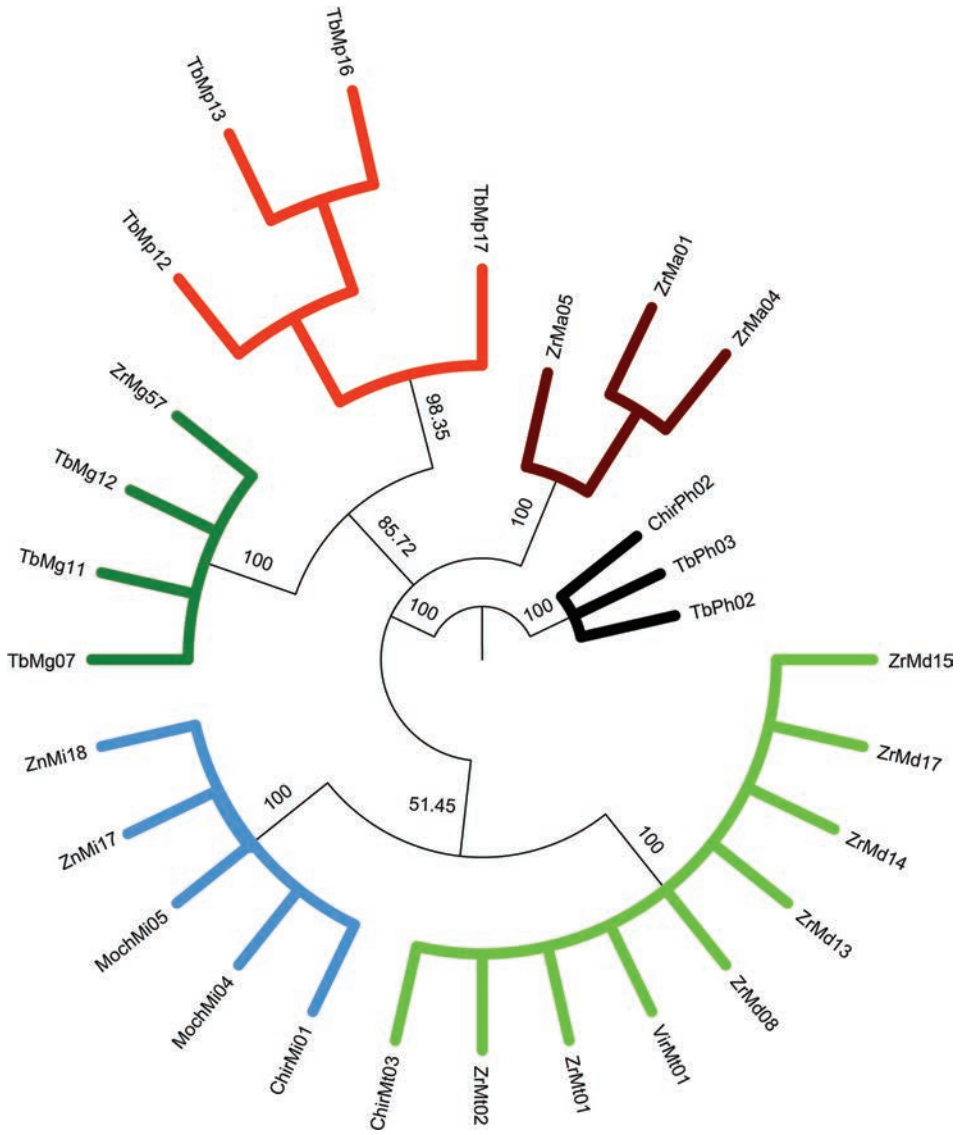

Figure 8. Phylogenetic tree based on Maximum Parsimony approach generated using 28 partial sequences of the nuclear 28S rRNA gene from six *Macrobrachium* species collected in Peruvian rivers of the Pacific slope. Bootstrap values ≥ 50% are shown. *P. hancocki* was used as outgroup. GenBank accession numbers OR941575–OR9411602. Abbreviations: Mt: *M. transandicum*; Mp: *M. panamense*; Mi: *M. inca*; Mg: *M. gallus*; Ma: *M. americanum*; Md: *M. digueti*; Ph: *P. hancocki*; Chir: Chira River; Tb: Tumbes River; Zr, Zar: Zarumilla River; Vir: Virú River; Pat: Pativilca River; JR: Juana Ríos River; Chao: Chao River; Lcr: Lacramarca River; Hb: Nepeña River; For: Fortaleza River; San: Santa River; Moch: Moche River; Chic: Chicama River; Sup: Supe River; Zn: Zaña River.

taxonomic relationship between *M. panamense* and *M. inca*, showing a genetic distance of 12.3% (Table 7) with both species recovered in separate clades with high nodal support (MP: 98.3% and 100% respectively; ML: 96% and 100%, respectively; BI 100% for both species), supporting their status as different species and resolving the confusion as to their placement and classification obtained in the phylogenetic results from 16S rRNA. Our 28S rRNA data analysis results also revealed that there was no interspecific genetic distance gene between *M. digueti* and *M. transandicum* (0%, Table 7) confirming the phylogenetic grouping of these two species into a single discrete clade (MP, Fig. 8; ML, Fig. 9; BI, Fig. 10), which was also observed in the phylogenetic trees (MP, ML, and BI) from COI and the 16S rRNA gene datasets.

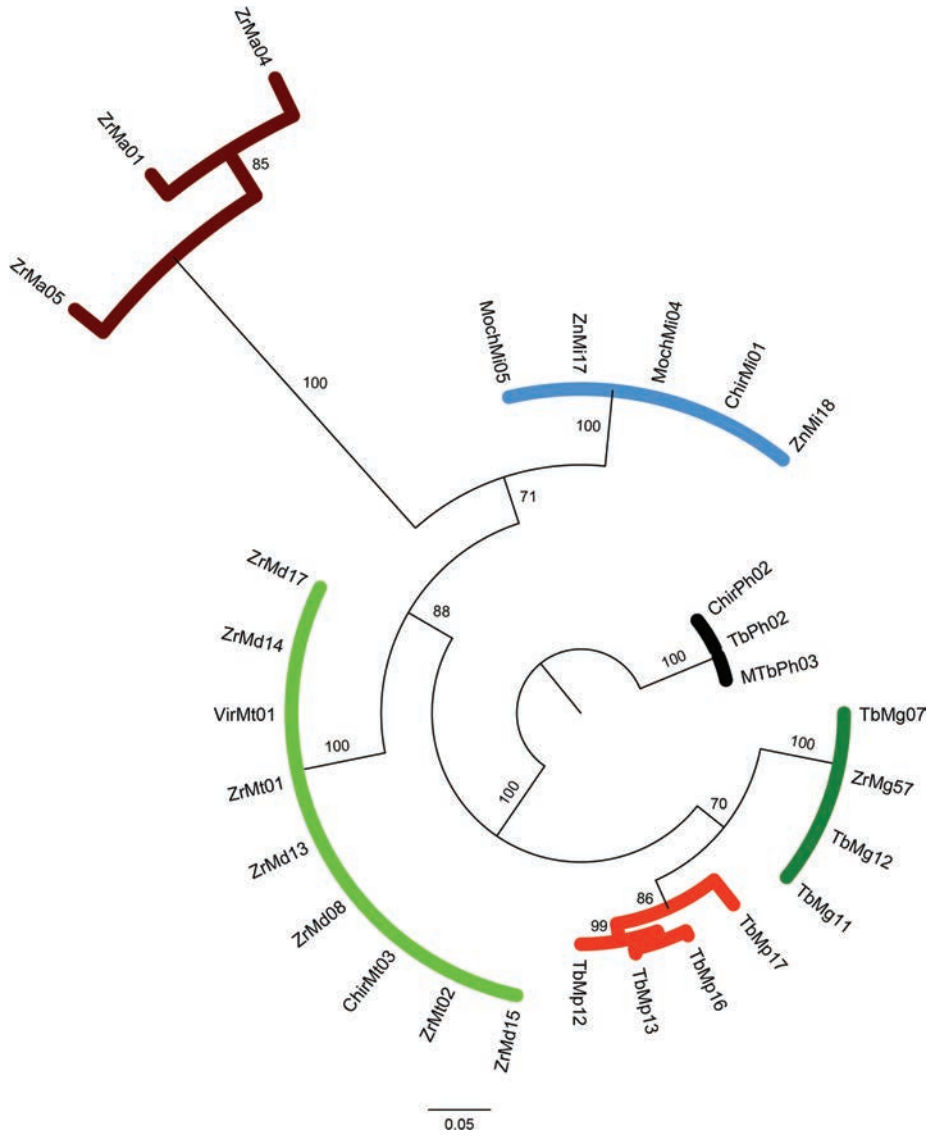

Figure 9. Phylogenetic tree based on maximum likelihood inference generated under the GTRGAMMA substitution model using 28 partial sequences of the nuclear 28S rRNA gene from six *Macrobrachium* species collected in Peruvian rivers of the Pacific slope. Bootstrap values ≥ 50% are shown. *P. hancocki* was used as outgroup. GenBank accession numbers OR941575–OR9411602. Abbreviations: Mt: *M. transandicum*; Mp: *M. panamense*; Mi: *M. inca*; Mg: *M. gallus*; Ma: *M. americanum*; Md: *M. digueti*; Ph: *P. hancocki*; Chir: Chira River; Tb: Tumbes River; Zr, Zar: Zarumilla River; Vir: Virú River; Pat: Pativilca River; JR: Juana Ríos River; Chao: Chao River; Lcr: Lacramarca River; Hb: Nepeña River; For: Fortaleza River; San: Santa River; Moch: Moche River; Chic: Chicama River; Sup: Supe River; Zn: Zaña River.

Table 6. Intraspecific genetic distances based on a partial fragment of the 28S rRNA. Analyses were conducted using the Kimura 2-parameter model (K2P) with 1000 bootstrap replicates.

Species	Genetic distance (d)	Standard error (SE)
M. americanum	0.072173333	0.008788746
M. digueti	0	0
M. transandicum	0	0
M. gallus	0	0
M. inca	0	0
M. panamense	0.021090406	0.004236636
P. hancocki	0	0

Table 7. Interspecific genetic distances (below diagonal) based on a partial fragment of the 28S rRNA. Analyses were conducted using the Kimura 2-parameter model (K2P) with 1000 bootstrap replicates. Standard error estimates are shown above the diagonal.

Species	*M. americanum*	*M. digueti*	*M. transandicum*	*M. gallus*	*M. inca*	*M. panamense*	*P. hancocki*
M. americanum	–	0.018854	0.018854	0.019530	0.019097	0.019233	0.020815
M. digueti	0.198629	–	0.000000	0.014078	0.013348	0.013639	0.016511
M. transandicum	0.198629	0.000000	–	0.014078	0.013348	0.013639	0.016511
M. gallus	0.213409	0.114759	0.114759	–	0.013662	0.010068	0.015985
M. inca	0.199487	0.112660	0.112660	0.112873	–	0.013677	0.016695
M. panamense	0.213907	0.117536	0.117536	0.077443	0.123234	–	0.014860
P. hancocki	0.224814	0.143690	0.143690	0.135800	0.155865	0.129517	–

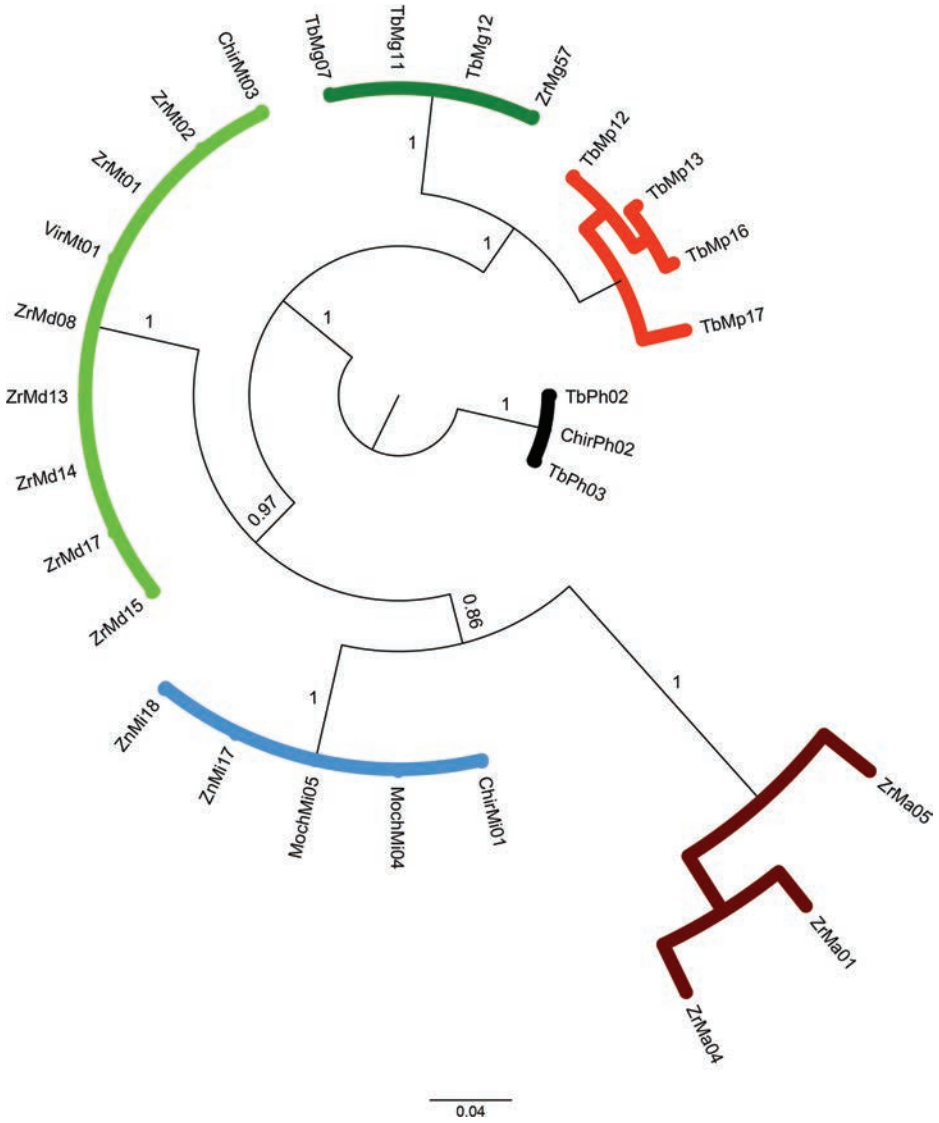

Figure 10. Phylogenetic tree based on Bayesian Inference approach generated under the GTR+I substitution model using 28 partial sequences of the nuclear 28S rRNA gene from six *Macrobrachium* species collected in Peruvian rivers of the Pacific slope. Bootstrap values and posterior probabilities ≥ 50% are shown. P*P. hancocki* was used as outgroup. GenBank accession numbers OR941575–OR9411602. Abbreviations: Mt: *M. transandicum*; Mp: *M. panamense*; Mi: *M. inca*; Mg: *M. gallus*; Ma: *M. americanum*; Md: *M. digueti*; Ph: *P. hancocki*; Chir: Chira River; Tb: Tumbes River; Zr, Zar: Zarumilla River; Vir: Virú River; Pat: Pativilca River; JR: Juana Ríos River; Chao: Chao River; Lcr: Lacramarca River; Hb: Nepeña River; For: Fortaleza River; San: Santa River; Moch: Moche River; Chic: Chicama River; Sup: Supe River; Zn: Zaña River.

Phylogenetic relationships of concatenated datasets

Overall, the phylogenetic results obtained by using the three concatenated datasets COI-16S rRNA, COI-28S rRNA, and 16S rRNA-28S rRNA (Suppl. material 1: figs S10–S12) support the results obtained with the single locus phylogenetic analyses. However, it is worth noting that we did not test if the concatenated dataset COI-16S rRNA could have resolved the two *M. panamense* sequences (TbMp16 GenBank accession OR941679 - TbMp17 GenBank accession OR941680) that were grouped within the *M. inca* clade in the phylogenetic trees of 16S rRNA gene dataset (Figs 5–7), because we could not obtain good quality COI sequences from those two *M. panamense* individuals.

Discussion

The diversity of freshwater crustacean decapods from South America is represented by seven families including Palaemonidae. In Peru, twelve Palaemonidae species occur naturally, of which eight belong to the genus *Macrobrachium* (Amaya and Guerra 1976) with only *M. inca* and *M. gallus* considered endemic to Peru (Zacarías and Yépez 2008), while *M. transandicum*, *M. digueti*, *M. panamense*, *M. americanum*, *M. tenellum*, and *M. hancocki* show a wider distribution range across the central Pacific (Holthuis 1950, 1952; Villalobos 1968; Valencia and Campos 2007; Hendrickx and Wicksten 2011; Campos 2014).

Macrobrachium presents low phenotypic variability, so species classification is usually very complicated, creating many taxonomic difficulties within the genus (Villalobos 1968; Pereira 1997; Murphy and Austin 2003, 2004; Pileggi and Mantelatto 2010). Despite this, the identification keys of Méndez (1981) and Valencia and Campos (2007) enabled morphological identification of the species.

During the morphological identification of *M. transandicum* we observed that both sexes displayed chelae of similar morphology (Suppl. material 1: figs S1–S4; Suppl. material 2: table S3). On the other hand, male individuals of *M. digueti* are characterized by having second pereiopods with unequal chelae (see Suppl. material 1: fig. S5) (Méndez 1981; Valencia and Campos 2007), which was a pivotal character for the successful morphological discrimination between both species, although the rostral formula was different from that reported by Valencia and Campos (2007) with 9–11 teeth versus 14–16/2–4. We also note that the rostrum of *M. transandicum* has more pronounced teeth than that of *M. digueti.* It has also been observed that chelae in *M. transandicum* are similar to those of the female *M. digueti* morphotype *michoacanus* Nates & Villalobos, 1990 reported by García-Velazco (2014). However, male and female individuals of *M. transandicum* identified in our study were found to have chelae of similar morphology between individuals of both sexes (Suppl. material 1: figs S1–S4). The issues found during our morphological identification are consistent with Pileggi and Mantelatto (2010) who suggested that the morphological characters frequently used in the identification of *Macrobrachium* species (rostral shape, rostral size, rostral teeth, telson spines, telson shape, morphology of the second pair of pereiopods) are not sufficient to resolve the taxonomic issues found in *Macrobrachium* species. Besides, those characters vary along the organism´s life span and are not common in both sexes.

To date, there is a lack of molecular studies of *Macrobrachium* species from Peru and most population study efforts have been focused on a single prawn species: *C.* (*C.*) *caementarius*, whose populations have been monitored periodically since 1996 by the Peruvian Marine Research Institute (IMARPE). Based on the reproductive periods determined for *C.* (*C.*) *caementarius*, a closed fishing season for all freshwater prawn species was established (Zacarías and Yépez 2008), including *C.* (*C.*) *caementarius* and *Macrobrachium* spp. (RM-312-2006-PRODUCE). In light of this, there is now an urgent need to conduct studies focused on the different *Macrobrachium* species that inhabit Peruvian ecosystems, including molecular data that can enable us to determine species delimitations and their phylogenetic relationships. An advantage of DNA sequence data is the higher taxonomic resolution over traditional systematics based on morphological characters alone (Murphy and Austin 2003, 2004; Murphy et al. 2004).

The present study represents the first effort to apply molecular data to analyze six of the eight different *Macrobrachium* species reported for Peru (Amaya and Guerra 1976), as well as contributing the first available sequences for *M. inca* and *M. gallus*, and the first sequences of *M. panamense*, *M. americanum*, *M. digueti*, and *M. transandicum* obtained from Peruvian rivers. Our genetic analyses using intra and interspecific distances and the recovered phylogenetic tree topologies based on single locus datasets corroborated the taxonomic category of species in five of the six analyzed species: *M. americanum*, *M. inca*, *M. gallus*, *M. panamense*, and *M. digueti*. On the other hand, *M. transandicum* showed very low genetic distances with *M. digueti* ranging from 0% for 28S rRNA (Table 7), 0.19% for 16S rRNA (Table 5), and 0.53% for COI (Table 3), reflected in the recovery of both species in a single clade in all phylogenetic trees obtained in this study (Figs 2–10, Suppl. material 1: figs S10–S12). Our results based on the analyses of three different molecular markers also suggest that *M. digueti* (Bouvier, 1895) and *M. transandicum* (Holthuis 1950) should be considered as a single species, with nomenclatural priority given to *M. digueti*. Similarly, Murphy and Austin (2004) using partial sequences of the mitochondrial 16S rRNA gene revealed that three different *Macrobrachium* species with considerable morphological variation were in fact only one species: *M. australiense* Holthuis, 1950. The authors reported genetic variation ranging from 0.2–1.6%, which is within the range of genetic distance detected in this study between *M. digueti* and *M. transandicum*. We also generated molecular operational taxonomic units (MOTUs) (Ramirez et al. 2023) and obtained the same results as those obtained with the sequences of the three genes in the study, i.e., *M. digueti* and *M. transandicum* form the same molecular operational unit (data not shown).

The geographic distribution of *M. transandicum* is not fully known and it has been reported that this species occurs only in three rivers in Colombia and one river in Peru (De Grave 2013). Previous studies have identified different morphotypes for *M. digueti*. For example, García-Velazco (2014) using the mitochondrial 16S rRNA gene reported a second morphotype of *M. digueti*, namely *M. michoacanus*, which was previously described as a different species habiting the Mexican Pacific slope. In the same study, a female holotype had a similar morphological appearance to *M. transandicum*. In the present work, we can rule out a misidentification of *M. transandicum* by a female of *M. digueti* because we

were able to clearly identify individuals of both sexes in *M. transandicum* by the position of the gonopores (Suppl. material 1: figs S1–S4). Rossi and Mantelatto (2013) using sequences of the nuclear gene histone H3 recovered *M. digueti*, *M. olfersii* (Wiegmann, 1836), and *M. faustinum* (de Saussury, 1857) in a single clade, suggesting the existence of an "*olfersii* complex" encompassing several subspecies. We propose that *M. transandicum* should be also included in the *olfersii* complex.

Phylogenetic relationships

The main objective of a molecular phylogenetics analysis is to infer the evolutionary history of a group of organisms and to output the results in a hierarchy branching diagram or phylogenetic tree (Palero and Crandall 2009). We chose the mitochondrial COI and 16S rRNA gene markers due to their high mutation rate (Rossi and Mantelatto 2013), and the nuclear 28S rRNA gene because it has been proven to be effective in previous studies of crustacean phylogenetics (Chen et al. 2009). The genetic distances among the different *Macrobrachium* species analyzed in our study (Tables 3, 5, 7) showed different evolutionary rates for each molecular marker, with COI being the best candidate for species discrimination and phylogenetic inferences of Peruvian *Macrobrachium* populations due to the relatively higher interspecific genetic distances observed in our results. This result agrees with previously related works. For example, Toon et al. (2009) reported that COI is highly variable among decapod species suggesting that it can be useful in resolving low-level taxonomy issues. In another work by Zhang et al. (2009), the authors used COI sequences to validate the status of species in *M. rosenbergii*, *M. nipponense* (De Haan, 1849), and *M. qilianensis* [unknown species according to WoRMS Database (2024), reporting high levels of interspecific genetic distances ranging from 19.87% to 23.84%. A more recent study by Siriwut et al. (2020) employed three molecular markers (COI, 16S rRNA, and 18S rRNA) for the phylogeny of *Macrobrachium* species from Thailand obtaining higher interspecific genetic distances with COI ranging from 9.8% to 23.3%. In the same study, the authors reported three new *Macrobrachium* species and remarked that the COI barcoding region provides the fine resolution required for the genus *Macrobrachium*.

The interspecific morphological conservation observed during the morphological identification of *Macrobrachium* is contrasted by the levels of genetic distances among species (Pileggi and Mantelatto 2010). Our phylogenetic analysis results based on the 16S rRNA gene showed a maximum interspecific genetic distance of 11.76% between *M. digueti* and *M. gallus* and a minimum of 0.1% between *M. digueti* and *M. transandicum* recovering the two latter species in a single clade. Similarly, *M. inca* and *M. panamense* were recovered in a single clade showing a low genetic distance of 0.5%. Thus, we can conclude that except for the case of *M. inca* and *M. panamense*, the 16S rRNA gene has enough resolution power and can be applied in phylogenetic studies of *Macrobrachium* species. Our results are consistent with previous crustacean phylogenetic studies based on the16S rRNA gene (Murphy and Austin 2004, 2005; Chan et al. 2008; Pileggi and Mantelatto 2010), which despite high evolutionary conservation, found interspecific divergence rates from 3.5% in decapods (Schubart 2009).

The addition of nuclear ribosomal genes for phylogeny studies of decapods has proven to be useful for different reasons including a lower evolutionary rate (Chu et al. 2009). Furthermore, previous phylogenetic studies of decapods including *Macrobrachium* based on both 28S rRNA and 16S rRNA gene markers detected some advantages of the former over the latter. Those advantages include a longer sequence length, a higher number of variable and parsimony informative sites, higher GC content, and a transition/transversion (TA/TV) rate ratio bias in favor of transitions over transversions (Crandall et al. 1999; Jarman et al. 2000; Porter et al. 2005; Chen et al. 2009). The results of the present study partially support previous findings showing that 28S rRNA sequences were 27% and 8% longer than those of the 16S rRNA and COI genes respectively, with higher GC content. However, TA/TV rate ratio was 0.99, biasing in favor of transversions over transitions. Increasing the sequence length also increases the number of informative sites, which in turn enhances the phylogenetic tree resolution (Chen et al. 2009). Furthermore, the inclusion of data from independent nuclear markers such as the 28S rRNA gene increases the possibility of recovering true phylogeny (Toon et al. 2009; Garrick et al. 2010). For example, the phylogenetic trees (MP, ML and BI) based on the 16S rRNA gene obtained in this study displayed misleading results of the true phylogenetic relationships between *M. panamense* and *M. inca*, recovering the only two *M. panamense* sequences (TbMp16 GenBank accession: OR941679 and TbMp17 GenBank accession: OR941680) within the *M. inca* clade (Figs 5–7). On the other hand, our phylogenetic analyses based on the 28S rRNA gene successfully resolved the phylogeny of *M. panamense* and *M. inca* recovering both species in separate discrete clades with high nodal support (98.3% to 100%) and posterior probabilities (100%) (Figs 8–10). We also note that the tree produced by ML and BI with 28S rRNA data (Figs 9, 10) recovered species of similar morphological characters in sister clades: *M. inca–M. americanum* (rostrum of medium size and second pair of pereiopods with unequal size), and *M. gallus–M. panamense* (long rostrum and thin and slender second pair of pereiopods); while the MP tree (Fig. 7) grouped only *M. gallus* and *M. panamense* in sister clades. These results support the hypothesis that *M. inca* and *M. gallus* are closely related to *M. americanum* and *M. panamense*, respectively. However, this hypothesis was not supported by the other two genes used in our phylogenetic inferences. We should expect a pattern of lower genetic distances between each pair of the closely related species than to the other *Macrobrachium* species considered in our analyses. Phylogenetic tree results based on partial COI gene fragments recovered this pattern only between *M. americanum* and *M. inca* but not between *M. gallus* and *M. panamense* (Figs 2–4).

Robust phylogenetic inference is achieved by using good datasets that usually depend on many sequences of long lengths. In this regard, the use of concatenated gene datasets represents a potentially powerful approach. However, this method should be used only with genes that show consistent evolutionary patterns (Palero and Crandall 2009). Our concatenated phylogenetic analysis results confirmed the results obtained with single locus datasets, determining the status of species in *M. panamense*, which was included within the *M. inca* clade in the results obtained by using the 16s rRNA gene dataset. Based on the recovered topology under both phylogenetic approaches (MP, ML and BI) using single and concatenated datasets (Figs 2–10), our results corroborated the monophyletic origin of *Macrobrachium* species from Peruvian populations

of the Pacific slope. Similar results were reported for *Macrobrachium* species from Mexico (Acuña et al. 2013) and America (Pileggi and Mantelatto 2010). Contrastingly, previous phylogenetic studies reported the polyphyletic structure of *Macrobrachium* species from Australia and East/Southeast Asia using 16S rRNA (Murphy et al. 2004; Murphy and Austin 2005) and COI (Liu et al. 2007), respectively. Anger (2013) concluded that regardless of whether monophyly or paraphyly is assumed, all Paleo- and Neotropical *Macrobrachium* species originate from the same ancestor, and further species diversification resulted as part of the evolutionary process.

Conclusions

Herein, we were able to identify and successfully recover phylogenetic relationships of six out of the eight *Macrobrachium* species reported for the Peruvian Pacific slope: *M. inca*, *M. gallus*, *M. transandicum*, *M. digueti*, *M. panamense*, and *M. americanum*. Two species, *M. tenellum* and *M. hancocki*, were not found in our field surveys and therefore not included in our study]. Based on our molecular analyses of partial fragments of COI, 16S rRNA, and 28S rRNA genes, the validity of five of these six species is supported; all our phylogenetic analyses recovered prawns morphologically identified as *M. transandicum* within the same clade as *M. digueti*, showing interspecific genetic distances near zero, and suggesting that both species belong to the same species-level lineage. Therefore, we propose that *M. transandicum* should be included in the *olfersii* complex.

Among the three molecular markers used in this study, we found that COI followed by 28S rRNA demonstrated strong resolving power for species identification and phylogenetic inferences of Peruvian *Macrobrachium* species. The 28S rRNA gene was also useful in resolving the taxonomic status of *M. panamense*. The hypothesis that *M. inca* and *M. gallus* are related to *M. americanum* and *M. panamense* respectively, was supported only by the BI phylogenetic tree based on 28S rRNA, whose topology recovered *M. inca* and *M. americanum* (rostrum of medium size and second pair of pereiopods with unequal size) and *M. gallus*–*M. panamense* (long rostrum and thin and slender second pair of pereiopods) in sister clades; while the COI trees recovered only the clade, *M. inca* and *M. americanum*. Finally, the phylogenetic approaches used in this study (MP, ML, and BI) recovered similar topologies for all the analyzed genes (COI, 16S rRNA, 28S rRNA), supporting the monophyletic origin of Peruvian *Macrobrachium* species.

Acknowledgements

We express our gratitude to the National University of Santa, for allowing us to use the facilities of the Genetics, Physiology, and Reproduction Laboratory, as well as for providing most of reagents and supplies that were used in the present study, and to the anonymous reviewers for their valuable comments and suggestions.

Additional information

Conflict of interest

The authors have declared that no competing interests exist.

Ethical statement

No ethical statement was reported.

Funding

No funding was reported.

Author contributions

Conceptualization: LDSB, EVZM. Data curation: LERF. Formal analysis: EVZM. Funding acquisition: EVZM. Investigation: EVZM. Methodology: EVZM, LERF. Validation: LERF. Writing - original draft: EVZM. Writing - review and editing: LDSB.

Author ORCIDs

Eliana Zelada-Mázmela https://orcid.org/0000-0002-5813-0954
Lorenzo E. Reyes-Flores https://orcid.org/0000-0002-1993-8010
Luis De Stefano-Beltrán https://orcid.org/0000-0002-5432-2916

Data availability

All of the data that support the findings of this study are available in the main text or Supplementary Information.

References

Acuña E, Alvarez F, Villalobos, Eguiarte L (2013) Molecular phylogeny of Mexican species of freshwater prawn genus *Macrobrachium* (Decapoda: Palaemonidae: Palaemoninae). Hidrobiologica 23(3): 276–285.

Amaya J, Guerra A (1976) Especies de Camarones de los Ríos Norteños del Perú y su Distribución. Convenio Ministerio de Pesquería – Universidad Nacional de Trujillo, 58 pp.

Anger K (2013) Neotropical *Macrobrachium* (Caridea: Palaemonidae): On the biology, origin and radiation of freshwater – invading shrimp. Journal of Crustacean Biology 33(2): 151–183. https://doi.org/10.1163/1937240X-00002124

Bate C (1868) On a new genus, with four new species, of freshwater prawns. Proceedings of the Zoological Society of London, 363–368. http://biostor.org/reference/60171

Bouvier EL (1895) Sur les palémons recueillis dans le eaux douces de la Basse-Californie par M. Diguet. Bulletin du Muséum d'Histoire Naturelle 1: 159–162.

Bowles D, Aziz K, Knight C (2000) *Macrobrachium* (Decapoda: Caridea: Palaemonidae) in the contiguous United States: A review of the species and an assessment of threats to their survival. Journal of Crustacean Biology 20(1): 158–171. https://doi.org/10.1163/20021975-99990025

Campos M (2014) New records of *Macrobrachium digueti* (Bouvier, 1895) for Colombia (Crustacea: Decapoda: Palaemonidae). Revista de la Academia Colombiana de Ciencias Exactas, Físicas y Naturales 38(147): 191–194. https://doi.org/10.18257/raccefyn.64

Chan T, Tong J, Kit Y, Chu K (2008) Phylogenetic relationships among the genera of the Penaeidae (Crustacea: Decapoda) revealed by mitochondrial 16S rRNA gene sequences. Zootaxa 1694: 38–50. [ISSN 1175-5334] https://doi.org/10.11646/zootaxa.1694.1.2

Chen R, Tsai C, Tzeng W (2009) 16S and 28S rDNA Sequences in phylogenetic analyses of freshwater prawns *Macrobrachium* Bate 1868 from Taiwan. Journal of Crustacean Biology 29(3): 400–412. https://doi.org/10.1651/08-3069.1

Chu K, Tsang L, Ma K, Chan T, Ng P (2009) Decapod Phylogeny: What Can Protein-Coding Genes Tell Us? Decapod Crustacean Phylogenetics. Department of Biology, Brigham Young University, Provo, UT 84602, U.S.A Crustacean Issues 18: 89–109. https://doi.org/10.1201/9781420092592-c6

Crandall K, Fetzner J, Lawler S, Kinnersley M, Austin Ch (1999) Phylogeneric relationships among the Australian and New Zealand genera of freshwater crayfishes. Australian Journal of Zoology 47: 199–214. https://doi.org/10.1071/ZO99011

Darriba D, Taboada G, Doallo R, Posada, D (2012) jModelTest 2: more models, new heuristics and parallel computing. Nature Methods 9(8): 772. https://doi.org/10.1038/nmeth.2109

de Bruyn M (2005) Inferring biogeography from the evolutionary history of the giant freshwater prawn (*Macrobrachium rosenbergii*). Thesis Doctor of Philosophy Degree. Queensland University of Technology.

De Grave S (2013) *Macrobrachium transandicum*. The IUCN Red List of Threatened Species 2013: eT198157A2513897.

Fuke Y, Imai H (2018) First Japanese record of *Macrobrachium ustulatum* (Crustacea: Decapoda: Palaemonidae) from Okinawa-jima Island, Japan. Fauna Ryukyuana 44: 7–15

García-Guerrero M, Becerril-Morales U, Vega-Villasante F, Espinosa-Chaurand L (2013) Los langostinos del género *Macrobrachium* con importancia económica y pesquera en América Latina: conocimiento actual, rol ecológico y conservación. Latin American Journal of Aquatic Research 41(4): 651–675. https://doi.org/10.3856/vol41-issue4-fulltext-3

García-Velazco H (2014) Filogeografía de los langostinos del género *Macrobrachium* (Decapoda: Palaemonidae) de la Península de Baja California, México. Thesis Doctorado, Universidad Autónoma de Nuevo León.

García-Velazco H, Maeda-Martínez A, Obregón-Barboza H, Campos-Torres O, Murugan G (2017) The systematics of the Mexican populations of *Macrobrachium digueti* (Bouvier, 1895) (Decapoda: Caridea: Palaemonidae). The Journal of Crustacean Biology 37(2): 168–186. https://doi.org/10.1093/jcbiol/rux008

Garrick R, Sunnuck P, Dyer R (2010) Nuclear gene phylogeography using PHASE: dealing with unresolved genotypes, lost alleles, and systematic bias in parameter estimation. BMC Evolutionary Biology (10): 17. https://doi.org/10.1186/1471-2148-10-118

Gouy M, Guindon S, Gascuel O (2010) SeaView version 4: a multiplatform graphical user interface for sequence alignment and phylogenetic tree building. Molecular Biology and Evolution 27(2): 221–224. https://doi.org/10.1093/molbev/msp259

Hendrickx M, Wicksten M (2011) New distribution and records of caridean shrimps (Crustacea: Decapoda: Caridea) from the west coast of Mexico. Hidrobiologica 21(1): 26–33. http://www.redalyc.org/articulo.oa?id=57820771003

Hernández P (2008) Efecto de la temperatura en el crecimiento y sobrevivencia del langostino *Macrobrachium occidentale* y del acocil *Cherax quadricarinatus*. Tesis para obtener el grado de Maestro en Recursos Naturales y Medio Ambientales. Instituto Politécnico Nacional.

Holthuis L (1950) Preliminary descriptions of twelve new species of Palaemonid prawns from American waters. Vol. LIII, No. 1: 93–99.

Holthuis L (1952) A general revision of the Palaemonidae (Crustacea, Decapoda, Natantia) of the Americas. II. The Subfamily Palaemonidae. Occasional Papers of the Allan Hancock Foundation 12: 1–396.

Jarman S, Nicol S, Elliot N, McMinn A (2000) 28SrDNA evolution in the Eumalacostraca and the phylogenetic position of krill. Molecular Phylogenetic and Evolution 17: 26–36. https://doi.org/10.1006/mpev.2000.0823

Kumar S, Stecher G, Tamura K (2016) MEGA7: Molecular Evolutionary Genetics Analysis version 7.0 for bigger data sets. Molecular Biology and Evolution 33: 1870–1874. https://doi.org/10.1093/molbev/msw054

Liu M, Cai Y, Tzeng C (2007) Molecular systematics of the freshwater prawn genus *Macrobrachium* Bate, 1868 (Crustacea: Decapoda: Palaemonidae) inferred from mtDNA sequences, with emphasis on East Asian species. Zoological Studies 46(3): 272–289.

López-Uriostegui F, Ponce-Palafox J, Benítez-Maldujano M, Castillo S, Rodríguez J, García-Ulloa M, Esparza H, Arredondo-Figueroa J (2013) Estudio del crecimiento del langostino *Macrobrachium tenellum* a diferentes densidades en un estanque semirústico, en un sistema de jaulas. Industria acuícola 9(3).

Luque C (2008) Estudio de la Diversidad Hidrobiológica en Tumbes. Informe Anual 2007. Instituto del Mar del Perú. Sede Regional de Tumbes.

Makombu J, Stomeo F, Oben PM, Tilly E, Stephen O, Oben B, Cheruiyot E, Tarekegn G, Zango P, Egbe AE, Ndagyong A, Mialhe E, Ngueguim JR, Mujibi F (2019) Morphological and molecular characterization of freshwater prawn of genus *Macrobrachium* in the coastal area of Cameroon. Ecology and evolution 9(24): 14217–14233. https://doi.org/10.1002/ece3.5854

McLarney W, Mafla M, Arias A, Bouchonnet D (2010) Amenazas a la biodiversidad y el funcionamiento de los ecosistemas en el sitio de patrimonio mundial la amistad por las propuestas de represas hidroeléctricas. Panamá-Costa Rica. Asociación ANAI.

Méndez M (1981) Claves de identificación y distribución de los langostinos y camarones (Crustacea: Decapoda) del mar y ríos de la Costa del Perú. Boletín Instituto del Mar del Perú 5: 142.

Munashinge D (2010) Phylogenetic positions of some species of the genus *Macrobrachium* Bate, 1868 (Crustacea, Decapoda, Palaemonidae) in Sri Lanka. Journal of the National Science Foundation of Sri Lanka 38(3): 193–199. https://doi.org/10.4038/jnsfsr.v38i3.2309

Murphy N, Austin C (2002) A preliminary study of 16S rRNA sequence variation in Australian *Macrobrachium* shrimps (Palaemonidae: Decapoda) reveals inconsistencies in their current classification. Invertebrate Systematics 16: 697–701. https://doi.org/10.1071/IT01031

Murphy N, Austin C (2003) Molecular taxonomy and phylogenetics of some species of Australian palaemonid shrimps. Journal of Crustacean Biology 23(1): 169–177. https://doi.org/10.1163/20021975-99990324

Murphy N, Austin C (2004) Multiple origins of the endemic Australian *Macrobrachium* (Decapoda: Palaemonidae) based on 16S rRNA mitochondrial sequences. Australian Journal of Zoology 52: 549–559. https://doi.org/10.1071/ZO03062

Murphy N, Austin C (2005) Phylogenetics relationships of the globally distributed freshwater prawn genus *Macrobrachium* (Crustacea: Decapoda: Palaemonidae): biogeography, taxonomy and the convergent evolution of abbreviated larval development. Journal of Crustacean Biology 23(1): 169–177. https://doi.org/10.1163/20021975-99990324

Murphy N, Short J, Austin Ch (2004) Re-examination of the taxonomy of the *Macrobrachium australiense* Holthuis (Decapoda: Palaemonidae) species-complex: molecular evidence for a single species. Invertebrate Systematics 18: 227–232. https://doi.org/10.1071/IS03003

Ndong A, Kébé K, Thiaw Ch, Diome T, Sembène M (2012) Genetic Distribution of the Cowpea (*Vigna unguiculata* (L.) Walp) Bruchid (*Callosobruchus maculatus* F., Coleoptera, Bruchidae) Populations in Different Agro-Ecological Areas of West Africa.

Journal of Animal Science Advances. 2(7): 616–630. www.grjournals.com [accessed 26 July 2014]

Nogueira C, Camargo N, Pantaleão J, R. Costa R (2023) Elucidating taxonomic problems of two closely related freshwater prawn lineages of the genus *Macrobrachium* (Caridea: Palaemonidae): A geometric morphometrics approach. Zoologischer Anzeiger 304: 73–83. https://doi.org/10.1016/j.jcz.2023.03.003

Palero F, Crandall K (2009) Phylogenetic Inference Using Molecular Data. Decapod Crustacean Phylogenetics. Department of Biology, Brigham Young University, Provo, UT 84602, U.S.A Crustacean Issues 18: 67–88. https://doi.org/10.1201/9781420092592-c5

Pereira G (1997) A cladistic analysis of the freshwater shrimps of the family Palaemonidae (Crustacea, Decapoda, Caridea). Acta Biologica Venezuelica 17, Suplemento, 1–69.

Pileggi L, Mantelatto F (2010) Molecular phylogeny of the freshwater prawn genus *Macrobrachium* (Decapoda, Palaemonidae), with emphasis on the relationships among selected American species. Invertebrate Systematics 24: 194–208. https://doi.org/10.1071/IS09043

Pileggi L, Rossi N, Wehrtmann I, Mantelatto F (2014) Molecular perspective on the American transisthmian species of *Macrobrachium* (Caridea, Palaemonidae). In: Wehrtmann IS, Bauer RT (Eds) Proceedings of the Summer Meeting of the Crustacean Society and the Latin American Association of Carcinology, Costa Rica, July 2013. ZooKeys 457: 109–131. https://doi.org/10.3897/zookeys.457.6818

Porter M, Pérez-Losada M, Crandall K (2005) Model-based multi-locus estimation of decapod phylogeny and divergence times. Molecular Phylogenetics and Evolution 37: 355–369. https://doi.org/10.1016/j.ympev.2005.06.021

PRODUCE (2023) Ministerio de la Producción. Anuario Estadístico Pesquero y Acuícola 2022. https://ogeiee.produce.gob.pe/index.php/en/shortcode/oee-documentos-publicaciones/publicaciones-anuales/item/download/1697_181879013ddb78ddc2abaf30764705a2 [accessed 26 Nov 2023]

Rambaut A (2014) Computer program and documentation distributed by the author. http://tree.bio.ed.ac.uk/ [accessed 18 Nov 2019]

Ramirez J, Valdivia P, Rosas-Puchuri U, Valdivia L (2023) SPdel: A pipeline to compare and visualize species delimitation methods for single-locus datasets. Molecular Ecology Resources. https://doi.org/10.1111/1755-0998.13864

Ronquist F, Teslenko M, van der Mark P, Ayres D, Darling A, Höhna S, Larget B, Liu L, Suchard M, Huelsenbeck J (2011) MrBayes 3.2: Efficient Bayesian phylogenetic inference and model choice across a large model space. Systematic Biology 61: 539–542. https://doi.org/10.1093/sysbio/sys029

Rossi N, Mantelatto F (2013) Molecular Analysis of the Freshwater Prawn *Macrobrachium olfersii* (Decapoda, Palaemonidae) Supports the Existence of a Single Species throughout Its Distribution. PLoS ONE 8(1): 1–13. https://doi.org/10.1371/journal.pone.0054698

Rossi N, Pantaleão JA F, Mantelatto F (2023) Integrated morphometric and molecular analyses indicate three male morphotypes in the freshwater prawn *Macrobrachium olfersii* (Decapoda, Palaemonidae) along the Brazilian neotropical region. Acta Zoologica 104(4): 538–551. https://doi.org/10.1111/azo.12437

Schubart C (2009) Mitochondrial DNA and Decapod Phylogenies: The Importance of Pseudogenes and Primer Optimization. In: Decapod Crustacean Phylogenetics, Department of Biology, Brigham Young University, Provo, UT 84602, U.S.A Crustacean Issues 18: 47–65. https://doi.org/10.1201/9781420092592-c4

Schubart S, Huber M (2006) Genetic comparisons of German populations of the stone crayfish *Austropotamobius torrentium* (Crustacea: Astacidae). Knowledge and Management of Aquatic Ecosystems 380–381: 1019–1028. https://doi.org/10.1051/kmae:2006008

Siriwut W, Jeratthitikul E, Panha S, Chanabun R, Sutcharit C (2020) Molecular phylogeny and species delimitation of the freshwater prawn *Macrobrachium pilimanus* species group, with descriptions of three new species from Thailand. PeerJ 8: e10137. https://doi.org/10.7717/peerj.10137

Stamatakis A (2014) RAxML version 8: a tool for phylogenetic analysis and post-analysis of large phylogenies, Bioinformatics 30 (9): 1312–1313. https://doi.org/10.1093/bioinformatics/btu033

Suresh P, Sasireka G, Karthikeyan K (2012) Molecular insights into the pylogenetics of spiny lobsters of Gulf of Mannar marine biosphere reserved based on 28S rDNA. Indian Journal of Biotechnology 11: 182–186.

Swofford D (2002) PAUP: Phylogenetic Analysis Using Parsimony (and other Methods). Version 4.0 Beta 10. https://doi.org/10.1111/j.0014-3820.2002.tb00191.x [accessed 18 Nov 2019]

Toon A, Finley M, Staples J, Crandall K (2009) Decapod Phylogenetics and Molecular Evolution. In: Decapod Crustacean Phylogenetics. Department of Biology, Brigham Young University, Provo, UT 84602, U.S.A Crustacean Issues 18: 9–22. https://doi.org/10.1201/9781420092592-c2

Valencia D, Campos M (2007) Freshwater prawns of the genus *Macrobrachium* Bate, 1868 (Crustacea: Decapoda: Palaemonidae) of Colombia. Zootaxa 1456: 1–44. https://doi.org/10.11646/zootaxa.1456.1.1

Villalobos A (1968) Problemas de especiación en América de un grupo de Palaemonidae del género *Macrobrachium*. FAO. Fisheries Reports 3: 1015–1073.

Werle E, Shneider C, Renner M, Völker M, Fiehn W (1994) Convenient single-step purification of PCR products for direct sequencing. Nucleic Acids Research 22 (20): 4354–4355. https://doi.org/10.1093/nar/22.20.4354

WoRMS Database (2024) DecaNet. *Macrobrachium* Spence Bate, 1868. Accessed through: World Register of Marine Species. https://www.marinespecies.org/aphia.php?p=taxdetails&id=156892 [accessed 18 July 2024]

Xia X (2017) DAMBE6: new tools for microbial genomics, phylogenetics, and molecular evolution. Journal of Heredity 108(4): 431–437. https://doi.org/10.1093/jhered/esx033

Zacarías S, Yépez V (2008) Monitoreo poblacional del camarón de río, estimación de abundancia de adultos en río de la costa centro y sur. Informe Anual 2007. Instituto del Mar del Perú, 1–34.

Zhang Q, Cheng Q, Guan W (2009) Mitochondrial COI Gene Sequence Variation and Taxonomic Status of Three *Macrobrachium* Species. Zoological Research 30(6): 613–619. https://doi.org/10.3724/SP.J.1141.2009.06613

Supplementary material 1

Morphological identification of the six *Macrobrachium* species and Phylogenetic trees based on Bayesian inference

Authors: Eliana Zelada-Mázmela, Lorenzo E. Reyes-Flores, Luis De Stefano-Beltrán
Data type: 7z

Explanation note: **fig. S1.** *Macrobrachium transandicum* Holthuis, 1950. **A** Female (collected from Zarumilla River) **B** Rostrum in close-up view. **fig. S2.** *Macrobrachium transandicum* Holthuis, 1950. Female (collected from Zarumilla River). **A** Major chela **B** Minor chela **C** Gonopore in coxae of the third pair of periopods. Note the width of the area around the fifth pair of periopods. **fig. S3.** *Macrobrachium transandicum* Holthuis, 1950. **A** Male (collected from Tumbes River) **B** Rostrum in close-up view **C** Major chela. **fig. S4.** *Macrobrachium transandicum* Holthuis, 1950. Male (collected from Tumbes River). **A** Minor chela **B** Gonopore, coxa fifth pair of periopods. Note the width of the area. **fig. S5.** *Macrobrachium digueti* (Bouvier, 1895). **A** Male (collected from Zarumilla River). **B** Rostrum in close-up view **C** Major chela. **fig. S6.** *Macrobrachium panamense* Rathbun, 1912. **A** Male (collected from Tumbes River) **B** Telson in close-up view **C** Rostrum close-up view. **fig. S7.** *Macrobrachium gallus* Holthuis, 1950. **A** Male (collected from Zarumilla River) **B** close-up view **C** Telson in close-up view. **fig. S8.** *Macrobrachium americanum* Spence Bate, 1950. **A** Male (collected from Zarumilla River) **B** Telson in close-up view. **fig. S9.** *Macrobrachium inca* Holthuis, 1950. **A** Male (collected from Chicama River) **B** Rostrum in close-up view **C** Rostrum close-up view of a female (collected from Santa River) **D** Telson in close-up view. **fig. S10.** Phylogenetic tree based on Bayesian inference approach generated under the GTR+I+G substitution model using concatenated dataset of the mitochondrial COI-16S rRNA genes from six *Macrobrachium* species collected in Peruvian rivers of the Pacific. Bootstrap values and posterior probabilities ≥ 50% are shown. *P. hancocki* was used as outgroup. Abbreviations: Mt: *M. transandicum*; Mp: *M. panamense*; Mi: *M. inca*; Mg: *M. gallus*; Ma: *M. americanum*; Md: *M. digueti*; Ph: *P. hancocki*. **fig. S11.** Phylogenetic tree based on Bayesian inference approach generated under the GTR+I+G substitution model using concatenated dataset of COI-28S rRNA genes from six *Macrobrachium* species collected in Peruvian rivers of the Pacific. Bootstrap values and posterior probabilities ≥ 50% are shown. *P. hancocki* was used as outgroup. Abbreviations: Mt: *M. transandicum*; Mp: *M. panamense*; Mi: *M. inca*; Mg: *M. gallus*; Ma: *M. americanum*; Md: *M. digueti*; Ph: *P. hancocki*. **fig. S12.** Phylogenetic tree based on Bayesian inference approach generated under the GTR+I+G substitution model using concatenated dataset of the 16S rRNA-28S rRNA genes from six *Macrobrachium* species collected in Peruvian rivers of the Pacific. Bootstrap values and posterior probabilities ≥ 50% are shown. *P. hancocki* was used as outgroup. Abbreviations: Mt: *M. transandicum*; Mp: *M. panamense*; Mi: *M. inca*; Mg: *M. gallus*; Ma: *M. americanum*; Md: *M. digueti*; Ph: *P. hancocki*.

Link: https://doi.org/10.3897/zookeys.1224.130537.suppl1

Supplementary material 2

Additional information

Authors: Eliana Zelada-Mázmela, Lorenzo E. Reyes-Flores, Luis De Stefano-Beltrán
Data type: 7z
Explanation note: **table S1.** Coordinates of collection sites of *Macrobrachium* species in rivers of the Peruvian coast. **table S2.** *Macrobrachium* species identified in this study by morphological taxonomy 230 and molecular analyses. Sampling number (n), Peruvian rivers surveyed, and GenBank 231 accession numbers for each locus are shown. **table S3.** Key to species of *Macrobrachium* from Peru (Méndez 1981; Valencia and Campos 2007). **table S4.** Substitution model results based on JModel Test 2 analysis used for Bayesian inference approach.

Link: https://doi.org/10.3897/zookeys.1224.130537.suppl2

ZooKeys 1224: 29–54 (2025)
DOI: 10.3897/zookeys.1224.135596

Research Article

Phylogeny of the planthopper genus *Megamelus* (Hemiptera, Delphacidae), with the description of two new species from South America

Nicolas A. Salinas[1,2], Roxana Mariani[3], Ana M. Marino de Remes Lenicov[2,3], Marcela S. Rodriguero[2,4,5], Alejandro J. Sosa[1,2]

1 *Fundación para el Estudio de Especies Invasivas (FuEDEI), Hurlingham, Buenos Aires, Argentina*
2 *Consejo Nacional de Investigaciones Científicas y Técnicas (CONICET), CABA, Argentina*
3 *Division Entomología, Facultad de Ciencias Naturales y Museo, Universidad Nacional de La Plata, Buenos Aires, Argentina*
4 *Instituto de Ecología, Genética y Evolución de Buenos Aires (IEGEBA), Buenos Aires, Argentina*
5 *Departamento de Ecología, Genética y Evolución, FCEN-UBA, Buenos Aires, Argentina*

Corresponding authors: Ana M. Marino de Remes Lenicov (marinoremes@gmail.com); Alejandro J. Sosa (alejsosa@fuedei.org)

Abstract

Megamelus is a genus of Delphacidae widely distributed and mostly associated with plants in freshwater environments. Despite various taxonomic revisions and thorough research, the delimitation of the genus, its diversity, and its evolutionary history need to be further explored. Moreover, features originally considered distinctive of the genus exhibit variation and should be reassessed. Here, the genus *Megamelus* in South America was examined, describing two new species, *Megamelus delticus* Remes Lenicov & Mariani, **sp. nov.** and *Megamelus serpentinus* Mariani & Remes Lenicov, **sp. nov.**, and providing information on their host plants and geographical distribution. The distribution and host range knowledge of *Megamelus iphigeniae* and *Megamelus timehri* are also expanded, the male brachypter of *M. timehri* described for the first time, and a key to distinguish the species, based on male and female genitalia and their external morphology, is provided. Moreover, the first phylogenetic analysis of the genus is presented, based on the mitochondrial COI gene to clarify the interspecific relationships among its members. Our combined findings support the monophyly of the genus and refine diagnostic features, including the importance of the pygofer's lobed appearance. This comprehensive revision highlights the need for further multidisciplinary approaches to fully understand the evolutionary history of *Megamelus* and its interactions with host plants and environments.

Key words: Distribution, host plant, phylogenetics, planthopper, species key, taxonomy

Academic editor: Mike Wilson
Received: 27 August 2024
Accepted: 20 November 2024
Published: 21 January 2025

ZooBank: https://zoobank.org/F133C995-E635-43AC-A5F0-1F778FD1F852

Citation: Salinas NA, Mariani R, Marino de Remes Lenicov AM, Rodriguero MS, Sosa AJ (2025) Phylogeny of the planthopper genus *Megamelus* (Hemiptera, Delphacidae), with the description of two new species from South America. ZooKeys 1224: 29–54. https://doi.org/10.3897/zookeys.1224.135596

Introduction

Megamelus Fieber, 1866 (Delphacinae: Delphacini) is a genus of planthoppers which includes 31 species widely distributed in the Holarctic (23 spp.) and Neotropical (7 spp.) regions and Australia (1 sp.), mostly associated with plants in freshwater environments (Mariani et al. 2013; Bartlett 2020). The genus was originally established to encompass two species from Europe, erected on the base of *Delphax notula* Germar, 1830, now *Megamelus notulus* (Germar). A few years later,

M. scutellaris Berg, 1883 was described from Argentina, being the first *Megamelus* species known in the Americas. Subsequently, several authors described a significant number of North American species and provided keys at a generic and specific level (Van Duzee 1897; Crawford 1914; Metcalf 1923; Muir and Giffard 1924; Beamer 1955). Nonetheless, most of the species were posteriorly transferred to other genera. The last revision of the genus north of Mexico was conducted by Beamer (1955), who made exhaustive taxonomic studies, described 11 new species, updated information for all the 20 recognized North American species, and proposed a new key to the genus. Moreover, he stated that the lobed appearance of the ninth segment of the male abdomen (pygofer) and other genito-anal structures were the main diagnostic features for this genus. The pygofer had already been recognized as a feature with diagnostic value, although complementary, by Muir and Giffard (1924). However, each of the structures that compose the male terminalia were described later by Muir (1926) for the South American species. Features such as color pattern and a narrow head with the vertex extending in front of the eyes, amongst others, originally defined by Fieber (1866) as distinctive of the genus, were later seen to show variations and need to be reassessed.

In South America, seven *Megamelus* species have been described to date (Berg 1883; Muir 1919, 1926; Sosa et al. 2007b; Mariani et al. 2013). One of them, *M. scutellaris*, was proposed as a biological control agent of water hyacinth, *Pontederia crassipes* Mart. (Pontederiaceae) (Sosa et al. 2004, 2007a) and was then introduced in water bodies invaded by this aquatic weed in the United States, South Africa, and Argentina (Tipping et al. 2014; Coetzee et al. 2022). Research on *M. scutellaris*, which included field surveys in wetlands of South America with laboratory and field experiments, generated knowledge on its behavior and biology, with the discovery of two new *Megamelus* species, *M. bellicus* Remes Lenicov & Sosa, 2007 and *M. nigrifasciatus* Mariani & Remes Lenicov, 2013, and the redescription of *M. scutellaris*, *M. electrae* Muir, 1926, *M. iphigeniae* Muir, 1926, *M. timehri* Muir, 1919, and *M. maculipes* (Berg, 1879) (Sosa et al. 2004, 2007b; Mariani et al. 2013). These contributions provided descriptions of adults of both sexes and wing forms of all South American species, including biological observations and specific keys for males. For the first time, these keys included diagnostic features of the female genitalia, such as the relative length of the ovipositor, shape and position of valvifer VIII, and shape and denticulation of the first and second gonopophyses.

As with many other genera of Delphacidae, *Megamelus* still lacks standard revisionary studies including morphological, genetic, and ecological information, to better understand the biology and the phylogenetic relationships among species of the genus. In this study we describe two new *Megamelus* species and provide information on their biology and distribution. Additionally, we expand the distribution and host range of *M. iphigeniae* and *M. timehri*, and describe the male brachypter of *M. timehri* for the first time. We also perform the first phylogenetic analyses of the genus based on the mitochondrial COI gene to clarify the interspecific relationships among its members. To this end, we include most of the sequences of *Megamelus* species available to date in public databases. Finally, with this set of information, we expand the existing key to include the new species and wing forms of the South American species, expanding the range of morphological characters previously established as typical of the genus.

Materials and methods

Sample collection

Field surveys were conducted in Argentina and Paraguay between 2021 and 2023 in the search of *Megamelus* specimens. Our study encompassed sites across seven Argentine provinces (Buenos Aires, Entre Ríos, Corrientes, Misiones, Chaco, Formosa, and Santa Fe) and two departments from Paraguay (Cordillera and Presidente Hayes). Insects were sought after on plants previously cited in the literature as the hosts for the South American *Megamelus* species, mainly Pontederiaceae, Alismataceae, and Apiaceae, located in water bodies of public access such as rivers, streams, lagoons, marshes, and ditches. Surrounding plants were also surveyed.

Samples were collected directly from the host plant using insect aspirators. When possible, individuals were collected from plants located at ~ 5–10 meters apart, up to a total of four or five points per site to avoid sampling sibling insects. Samples were immediately placed in absolute ethanol and stored at -20 °C for morphological studies and DNA extraction. The species of *Megamelus* found were identified by the taxonomic criteria following Beamer (1955), Sosa et al. (2007b), and Mariani et al. (2013). *Megamelus nigrifasciatus* was the only species not found in the field during our surveys. Hence, this species was studied based on the holotype and other reference specimens deposited in the Museo de Ciencias Naturales de La Plata (**MLP**). Additionally, field collected samples of two North American species, *M. toddi* Beamer, 1955 and *M. hamatus* Beamer, 1955, were used for DNA extraction and phylogenetic analyses but were not included in the morphological studies.

Data generated in this study are accessible by the GenBank accession numbers PP986913–PP986946. Information for samples used in phylogenetic analyses, including collection dates and coordinates, host plant associations and accession numbers are shown in Suppl. material 1.

Morphological studies

Males of the new species were described in detail, but only major differences were considered for females and the other winged forms. Both male and female genitalia were prepared for microscopic examination according to standard taxonomic techniques (Remes Lenicov and Virla 1993). The reported measurements come from five specimens of each sex and wing form and are given in millimeters. The male genitalia terminology mostly follows Asche (1985), but 'genital styles' is used instead of 'parameres', and 'anal segment' (segment X) and 'anal style' (segment XI) instead of 'anal tube'. For descriptive purposes, the genital styles will be referred to distal 'inner' and 'outer' angles after Bartlett 2005 (sensu Metcalf 1949). 'Genital complex' is used to illustrate the set of aedeagus, connective, genital styles, and postgenital segments when these structures are separate from the pygofer. Nomenclature of carinae of the vertex follows Yang and Yang (1986). Photographs were taken using Leica EZ5 and Leica S9 D stereoscopic microscopes and a RRID 18 HD digital camera and a Canon EOS 90D reflex camera adapted to the microscope. Specimens were deposited in the collections of the **MLP**.

Abbreviations are used as follows: **L.**, total length; **B.L.**, body length; **b.w.**, body width; **M.b.w.**, maximum body width, **t.l.**, tegmina length; **v.l.**, vertex length;

v.w., vertex width at base; **f.l.**, frons length; **M.f.w.**, maximum frons width; **m.f.w.**, minimum frons width; **a.l.I**, first antennal segment length; **a.l.II**, second antennal segment length; **p.l.**, pronotum length; **m.l.**, mesonotum length; **mti.l.**, metatibia length; **mta.l.**, metatarsi length; **mta.II.**, first hind tarsomere length; **s.l.**, metatibial spur length; and **t.n.**, number of teeth on metatibial spur; other measurements are relative.

Total length was measured from the anterior margin of vertex to the abdominal apex in brachypters, and up to the apex of the wings in macropters; body length was measured from the apex of vertex to the tip of abdomen in macropters; body width was measured in dorsal view at the external margin of tegulae. The length:width (L:W) ratio of the vertex was measured along the midline and near midlength, respectively. Averages are expressed as means ± standard error (SE).

Finally, a new key for the South American species, considering Beamer (1955), Sosa et al. (2007b), Mariani et al. (2013) and phylogenies derived from this study, is presented here to facilitate species identification. For the purposes of the proposed key only, we use the terms forewing and tegmen to refer to the first pair of wings of the macropters and brachypters, respectively.

DNA extraction

Genomic DNA was extracted from whole bodies of adults of both sexes and wing forms of *M. scutellaris*, *M. bellicus*, *M. electrae*, *M. timehri*, *M. iphigeniae*, *M. maculipes*, *M. nigrifasciatus*, *M. serpentinus* sp. nov., *M. delticus* sp. nov., *M. toddi*, and *M. hamatus* using Qiagen DNeasy Blood & Tissue Kit according to the manufacturer's instructions. After the lysis step, 2 µl of RNAse A were added and samples were incubated at 37 °C for 30 minutes. DNA concentration and quality was quantified using DS-11 Spectrophotometer/Fluorometer (Denovix) and visualized in 1% agarose gels stained with GelRed (Biotium).

PCR amplification and Sanger sequencing

A fragment of 658 bp of the cytochrome c oxidase I (COI) gene was amplified using the primers LepF2_t1 and LepR1 (Park et al. 2011), extensively used for planthopper barcoding. Under the reaction conditions used for amplification, this primer pair also amplifies a bacterial sequence belonging to the genus *Rickettsia*, revealing the presence of this bacteria in many of the samples. Thus, for samples for which the primer pair LepF2_t1/LepR1 was not useful, the universal primer pair LCO/HCO (Folmer et al. 1994) was used instead.

PCR amplification was done in a 25 µL volume containing 16.95 µL of distilled water, 2.50 µL of 10 × reaction buffer, 0.75 µL of $MgCl_2$ (50 mM), 2.50 µL dNTP mixture (4 mM), 0.6 µL of each primer (10 mM), 0.6 µL Taq DNA Polymerase and 1 µL of DNA. PCR thermocycling was performed under the following conditions: 2 min at 95 °C; 5 cycles of 40 sec at 94 °C, 40 sec at 45 °C, 1 min at 72 °C; 35 cycles of 40 sec at 94 °C, 40 sec at 51 °C, 1 min at 72 °C; 5 min at 72 °C; held at 4 °C. PCR products were checked in agarose gels and purified by adding 0.5 µL (10 u) Exonuclease I (Exo I) and 1 µL (1 u) Shrimp Alkaline Phosphatase (SAP). Samples were incubated at 37 °C for 15 min and the reaction was stopped by heating the mixture at 85 °C for 15 min. Sanger sequencing of the samples was done at Macrogen services (Korea) with the same primers used for PCR amplification. Posterior quality

check and primer trimming were performed on CodonCode Aligner v. 10.0.2 (CodonCode Corporation). Alignment of sequences was performed using the MUSCLE algorithm as implemented in MEGA11 (Tamura et al. 2021), with default settings.

Phylogenetic analyses

Phylogenetic relationships among *Megamelus* species were inferred by maximum likelihood (ML) analysis performed on W-IQ-TREE (Trifinopoulos et al. 2016) with 10,000 ultrafast Bootstrap alignments. HKY+I+R was chosen as the best-fit nucleotide substitution model for the dataset using ModelTest-NG (Darriba et al. 2020). Sequences from other genera were included as outgroups based on the positioning of *Megamelus* within the tribe Delphacini according to Urban et al. (2010). COI sequences from North American and European *Megamelus* and from other related genera were retrieved from the GenBank and BOLD databases: *M. davisi* Van Duzee, 1897 (BOLD: CNCHG1265-12, BBHMA1871-12), *M. notulus* (BOLD: ZMBN1987-21), *M. metzaria* Crawford, 1914 (KR034487.1, KR042817.1), *M. inflatus* Metcalf, 1923 (KR032845.1), *M. flavus* Crawford, 1914 (KR041514.1), *M. lunatus* Beamer, 1955 (KR034315), *M. distinctus* Metcalf, 1923 (KR033356.1, KR035000.1), *Stobaera tricarinata* (Say, 1825) (KR034279.1), *Bostaera balli* Penner, 1952 (CNCHG1224-12), *Delphax crassicornis* (Panzer, 1796) (HEMFI929-15), *Peregrinus maidis* (Ashmead, 1890) (ASIHE1417-12), *Euides basilinea* (Germar, 1821) (MZ631889.1), *Conomelus anceps* (Germar, 1821) (MZ631894.1, HEMFI926-15), and *Pissonotus paraguayensis* Bartlett, 2000 (OR523788.1). The PCR reactions performed with DNA obtained from dry specimens of *M. nigrifasciatus* failed to amplify; hence, this species was not included in the analysis.

Results

Taxonomy

***Megamelus delticus* Remes Lenicov & Mariani, sp. nov.**
https://zoobank.org/2FCBA2D6-C16D-4006-BA70-CF3ADCB898E7
Figs 1–3

Type material. ***Holotype*** male (brachypter): Argentina • Buenos Aires, Otamendi, 08-VI-2022, on *Eryngium* sp., Salinas-Sosa cols. ***Paratypes*** • same data as holotype, 7 male brachypters, 6 female brachypters (MLP).

Other material. Argentina • 6 male brachypters, 6 female brachypters, Buenos Aires, Otamendi, 08-VI-2022, on *Eryngium* sp., Salinas-Sosa cols. (MLP) • 1 male brachypters, 3 female brachypters, Buenos Aires, Dique Lujan, 19-VII-2023, on *Eryngium* sp., Salinas-Sosa cols. (MLP).

Type locality. Argentina, Buenos Aires: Otamendi, Campana, 34.1818S, 58.8706W, forested river margin, on *Eryngium* sp., 8 August 2022.

Diagnosis. Brachypter. The salient features of this new species include the following**:** dorsally overall dull dark brown color, with pale mottles on apex vertex, front disc, and a pale yellow stripe on frontoclypeal suture extending towards the base of gena. Body broadly depressed and distinctively wide at abdomen. Vertex broad, subquadrate, apical margin broadly rounded, with submedian carina forking dorsally near anterior margin of eyes, carinal branches diverging

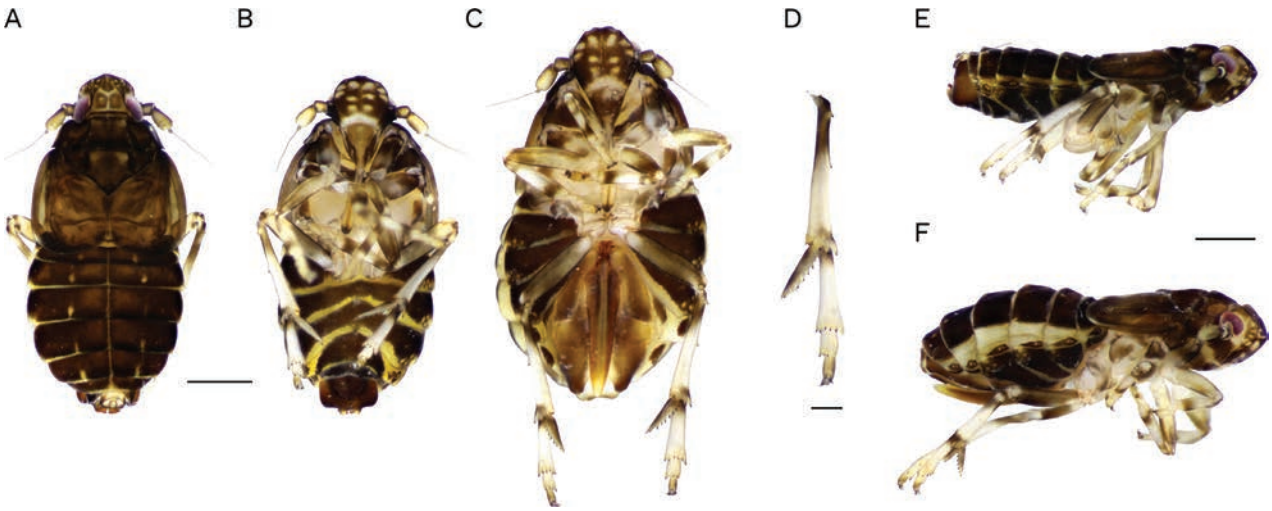

Figure 1. *Megamelus delticus* sp. nov. Habitus. Brachypterous male and female. **A** male dorsal view **B** male ventral view **C** female ventral view **D** apex of hind leg (post tibial and tarsi) **E** male lateral view **F** lateral view. Scale bars: 0.5 mm (**A–C, E, F**); 0.2 mm (**D**).

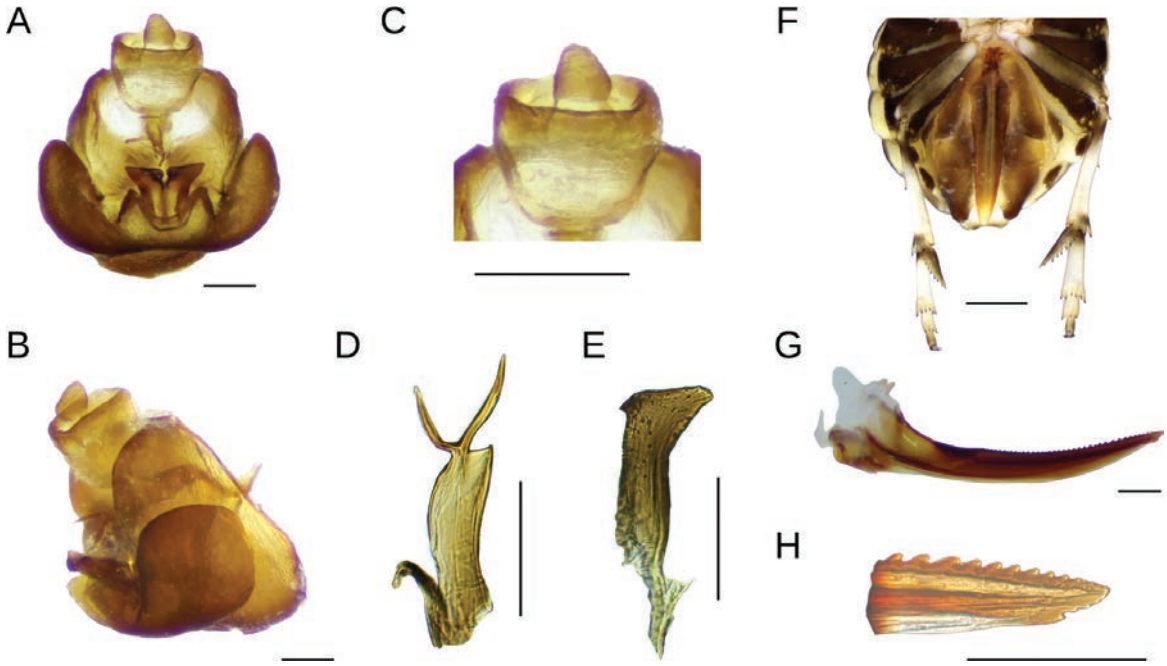

Figure 2. *Megamelus delticus* sp. nov. Terminalia. Male: pygofer **A** posterior ventral view **B** lateral view **C** anal segment **D** aedeagus, dorsal view **E** right genital style. Female **F** abdomen ventral view **G** gonapophysis IX, lateral view **H** apex of gonapophysis IX. Scale bars: 0.1 mm (**A–E, G, H**); 0.5 mm (**F**).

widely to meet anteriorly just below fastigium which is angled when viewed laterally. Eyes reduced, reddish, slightly emarginate below, barely visible in ventral view. Frons subcircular, short, about as long as wide, with lateral carinae bowed outward, converging both ventrally and dorsally; metatibial spur short and narrow, bearing eight or nine black-tipped sharp teeth on trailing margin. Male terminalia: pygofer short, with small sized outer lobes, inner lobes subtriangular in outline, with broad concavity between them; aedeagus short, bearing dorso-apical horseshoe-like process; anal segments short and wide, unarmed.

Description. Brachypterous male (Figs 1A, B, D, E, 2A–E). ***Color*** (Fig. 1) dull dark brown, with some pale marks. Reddish eyes. Vertex pale along posterior margin,

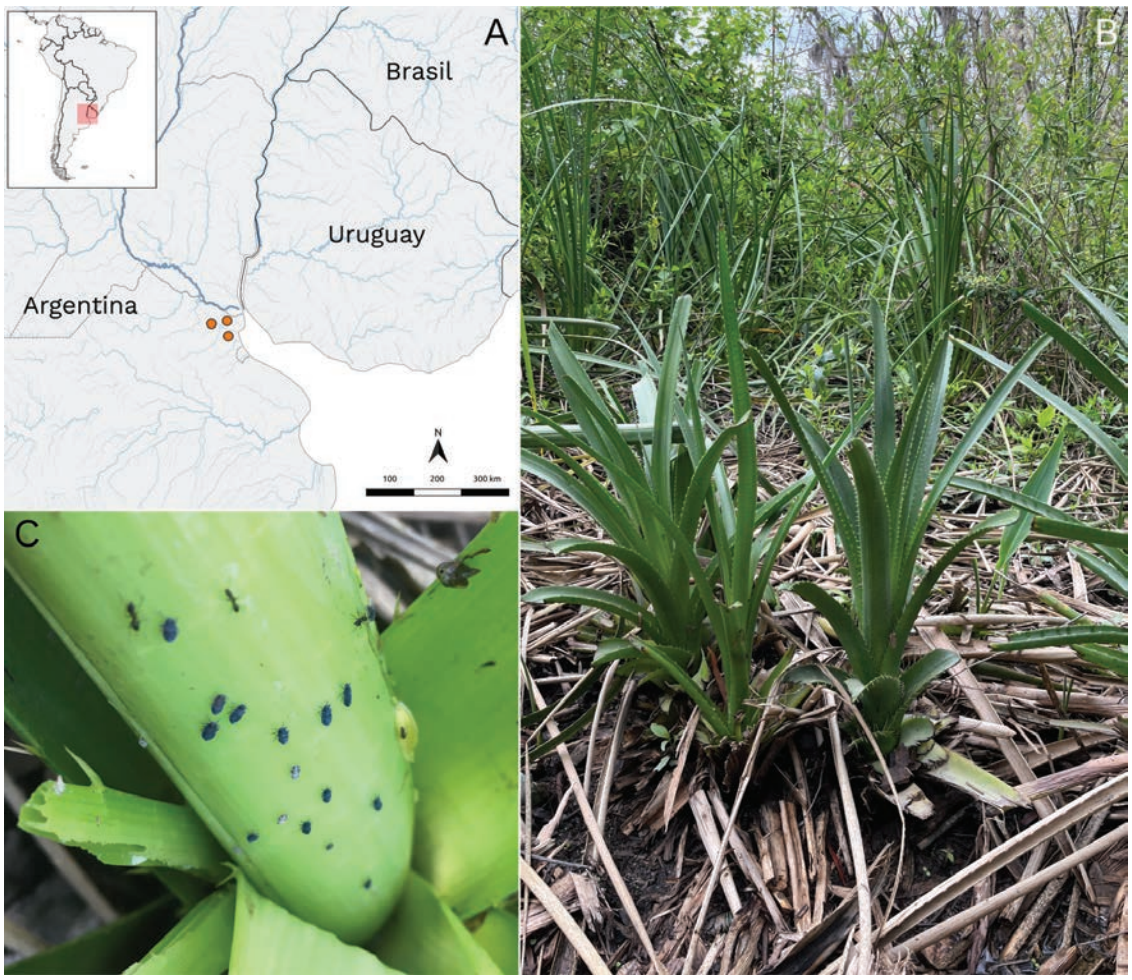

Figure 3. Geographical distribution and habitat of *Megamelus delticus* sp. nov. **A** distribution map in Argentina, orange dots represent sites where *M. delticus* was found (Suppl. material 2) **B** habitat and host plants (*Eryngium* sp.) **C** adults and nymphs on *Eryngium* sp.

median and Y-shaped carinae, with small yellowish spots on apex between submedian and lateral carina and also between lateral carina and eyes. Frons with continuous row of ~ 10 symmetrical pale dots paralleling median and lateral carinae, and transversal whitish stripe on frontoclypeal suture extending towards the base of gena. Clypeus castaneous on disc, rostrum yellowish. Antennal segments castaneous, slightly pale on anterior surface. Pronotum with pale transversal row of small spots on anterior margin between lateral carinae and several smaller spots on central disc near posterior margin; mesonotum disc with pale longitudinal spots between lateral carinae and some small spots on posterior margin. Tegmen uniformly pale brown. Legs yellowish, darker on base and apex of pro and mesocoxae, annular dark brown stripes near the base and apex of pro- and mesotibiae, apex of pro- and mesofemur, dorsal metafemur, and two annular stripes on metatibiae, one near base and the other on base of apical spines, on dorsal surface of spurs, and base of first tarsomere and apex of third. Abdomen dark brown in dorsal view, with longitudinal bilateral narrow pale stripes on tergites III–VII and ventrally on posterior margins of sternites IV–VII, and laterally around wax pores; anal segment paler, darker on apical margin as well as on anal style.

***Structure*.** Body strongly dorsoventrally flattened, suboval in outline. Head narrower than pronotum. Vertex in dorsal view almost as long as wide, rather

quadrate, broadly rounded on anterior margin; basal compartment occupying approximately more than basal half of vertex. Median carina present, forked near anterior margin of eyes, arms of fork diverging strongly (angle 170°) to meet submedian frontal carinae. Submedian frontal carinae arising from the lightly foliate lateral carinae at level of middle of eyes, meeting anteriorly just at the fastigium (Fig. 1A). In lateral view, head projected downwards in front of the eye, fastigium angled (Fig. 1E). Frons subcircular, about as long as wide, and as long as clypeus; carinae of frons distinct, evanescent toward apex, lateral carinae bowed outward, converging both ventrally and dorsally; frons widest at antenna level. Frontoclypeal suture ventrally curved. Clypeus sub-triangular with carinae evident, the laterals continuing with genal carina. Rostrum reaching metacoxae, slightly shorter than frons plus clypeus, subapical segment longer than the apical one (1.3:1). Compound eyes, very reduced, lower margin only slightly incised, barely visible in ventral view. Antennae short, first segment as long as wide, second segment 2 × the first, 2 × longer than wide (Fig. 1A, B). Pronotum with conspicuous carinae, the laterals divergent, reaching hind margin and ending slightly convex. Mesonotal disc almost as long as pronotum (1.2:1), carinae conspicuous, lateral ones slightly divergent apically reaching hind margin (Fig. 1A). Tegmen coriaceous, subquadrate, posterior margin subtruncated to slightly rounded, reaching 4th segment; veins distinct (Fig. 1A). Metatibial spur leaf-like, short, narrow apically and concave ventrally, bearing eight or nine black-tipped sharp teeth on trailing margin, almost as long as first segment of metatarsi at notch; first hind tarsomere longer than second plus third (1.7:1) (Fig. 1D). Abdomen broadest across segment V, decreasing in width towards apex (Fig. 1A).

***Terminalia*.** Pygofer trapezoidal, with laterodorsal margin slightly truncate, not projected caudad; ventrally ~ 2 × longer than dorsally; dorsally with shallow concave anal margination (Fig. 2A, B); outer lobes small-sized and rounded, slightly enfolding lateral area of pygofer, in ventral view occupying half the length of pygofer, inner lobes subtriangular in outline, broadly concave between them and with narrow notch between inner and outer lobes, partially closing ventral foramen (Fig. 2A, B); diaphragm fairly long, regularly narrowed toward middle line and caudally produced in short conical process. Aedeagus short, length-wide ratio: 2.2:1, regularly tubular and caudally downwardly directed, bearing an apical process projected on dorsal surface to left of phallotreme; this process is forked near base in two long and divergent semi-circularly curved spines (horse-shoe outline), in lateral view extending beyond genital styles (in repose); phallotreme large, near apex on dorsal surface to the right (Fig. 2D). Suspensorium sclerotized, strap-like, very short, half of aedeagus length (Fig. 2D). Genital styles (parameres) straight and flattened, widest and divergent in apical 1/3, apices truncate and enlarged, with sharp conical process on inner angle, widely expanded and rounded on outer angle, apex reaching dorsal margin of diaphragm at rest (Fig. 2E). Anal segment broad, collar-like, closely embraced by pygofer, without processes (Fig. 2C); anal style short (Fig. 2C).

Measurements (*n* = 3). L., 2.6; b.w., 0.75; M.b.w. at abdominal segment V, 1; t.l., 0.4; v.l., 0.4; v.w., 0.5; f.l., 0.4; M.f.w., 0.4; m.f.w., 0.25; a.l.I, 0.15; a.l.II, 0.2; p.l., 0.3; m.l., 0.4; mti.l., 0.8; mta.l., 0.7; mta.ll., 0.4; s.l., 0.4; t.n., 9.

Macropter unknown.

Brachypterous female (Figs 1C, F, 2F–H). ***Color*.** Body coloration pattern and structure similar to male; ovipositor brown with valvifer pale on inner margin; gonapophysis rather pale apically.

***Terminalia*.** Ovipositor short, reaching anal segment at base (Fig. 2F). Valvifer VIII regularly broad, slightly excavated on inner margin near base, with inconspicuous basal projection; separate in repose in ventral view. Gonapophysis VIII wide at base, ventrally projected between valvifers. Gonapophysis IX slightly curved, bearing numerous strong rounded teeth (~ 35) on dorsal margin on > 1/2 of its length, a few teeth smaller distally; with three or four ventral teeth (Fig. 2G, H).

Measurements (*n* = 3). L., 3; b.w., 0.83; M.b.w. at abdominal segment V, 1.265; t.l., 0.4; v.l., 0.35; v.w.,0.5; f.l., 0.4; M.f.w., 0.4; m.f.w., 0.25; a.l.I, 0.15; a.l.II, 0.2; p.l., 0.3; m.l., 0.4; mti.l., 0.85; mta.l, 0.75; mta.ll., 0.5; s.l., 0.4; t.n., 9–10.

Macropter unknown.

Etymology. The specific name comes from the Greek letter delta (Δ), which was used to refer to the triangle of fertile land that the Nile forms at its mouth (Nile Delta) and by extension, to other river deltas. In this case, the name refers to the geographical distribution of the species, which is restricted to the region of the Paraná River Delta.

Distribution. Argentina: Buenos Aires Province (Fig. 3A, Suppl. material 2).

Host plant. *Eryngium* sp. (Apiaceae).

Ecology. This planthopper was recorded in Otamendi and Dique Lujan, Paraná River Delta, in Buenos Aires Province (Argentina). It was only collected on *Eryngium* sp., a plant growing on the higher areas of river banks, where it is protected from periodical floods (Fig. 3B). Large numbers of nymphs and adults were found in the center of the plant mat (Fig. 3C), where leaves tend to accumulate water. The specimens collected had an abundant serous secretion covering their bodies, probably to repel the accumulated water. It is worth noting that *M. delticus* and *M. nigrifasciatus* were both sought after during our campaigns in search of *Megamelus* sp. and were only found in the same restricted geographical region, which suggests two possible cases of endemism.

Remarks. This new species is easily distinguished from all the other *Megamelus* species by the broadly depressed body with a broad, sub quadrate vertex, large basal compartment, fastigium angled when viewed laterally, short and subcircular frons, small compound eyes, and the male pygofer slightly enfolded by the small sized outer lobes and the aedeagus ending in a horseshoe-like bifurcation. The dull dark brown coloration with pale dots and a transversal white stripe on the face, are also distinctive. Among the South American species, *M. delticus* and *M. nigrifasciatus* share the flat frons with convex lateral margins, the short and narrow spur with a few sharp teeth, brachypterism as the only wing form, and the short gonapophysis in females. Moreover, these species share their host plant (*Eryngium* sp.), which suggests that these morphological traits are likely adaptations to their ecological niche.

***Megamelus serpentinus* Mariani & Remes Lenicov, sp. nov.**

https://zoobank.org/DDA5B411-4039-4D88-815C-B9B9E8239FCE
Figs 4–6

Type material. ***Holotype*** male (macropter): Argentina • Corrientes, Esquina, -29.99197098266, -59.52115137130, V-2022, on *Pontederia azurea*, Salinas-Sosa col. (MLP). ***Paratypes*** • same data as holotype, 3 macropterous males (1

with genitalia dissected), 5 macropterous females, 2 brachypterous females, 2 brachypterous males (MLP).

Other material. Argentina • 1 male macropter, Santa Fe, Reconquista, 26-XI-1939, Biraben-Bezzi (MLP); • 1 female macropter, Chaco, Resistencia, 20-III-1939, Denier, col. (MLP); • 1 female brachypter, Misiones, Concepción de la Sierra, 27-XI-2022, on *Pontederia azurea*, Salinas col. (MLP); • 1 male brachypter, Buenos Aires, Arroyo Botija, 10-VI-2023, on *Pontederia azurea*, Salinas col. (MLP); • 2 female macropters, Corrientes, Ramada Paso, 15-V-2022, on *Pontederia azurea*, Salinas col. (MLP); • 2 female macropters, Corrientes, Bañado Virocay, 27-XI-2022, on *Pontederia azurea*, Salinas col. (MLP); Paraguay: • 2 female macropters, Cordillera, Arroyos y Esteros, 7-IV-2022, on *Pontederia azurea*, Salinas col. (MLP).

Type locality. Argentina, Corrientes: Esquina, -29.9920S, -59.5212W, on *Pontederia azurea* floating near the bank of a stream, 12 May 2022.

Diagnosis. Macropter and brachypter. The salient features of the new species include the following: body mostly dark brown with distinctive yellowish to white marks bordering most of the sclerites of the body with legs paler and lightly marked with dark pigment. Macropters with forewings amber with pale brown veins, with strong dark marks on clavus, along Cu vein, over cross veins, and on last apical cells; brachypter with tegmen amber, brownish transverse marks in middle and claval apex, male pygofer dark brown, with dorsal surface, anal angles, and anal segment pale brown. Vertex narrow, with submedian carina forking dorsally quite far from fastigium; carinal branches closely forming a slender triangle; fastigium rounded in lateral view. Frons long, median carina prominent at or just below fastigium then fine; lateral carinae at base foliated, all carinae fine before the well-defined frontoclypeal suture. Spur large and wide, with 17 or 18 sharp, black-tipped teeth on trailing margin. Male terminalia: pygofer with relatively large lobes, the inner sharpened at apex with rounded external margin and internal sinuous; aedeagus short and tubular, with a short, slender dorso-caudally process curved at apex. Anal segment with two long, sinuous, slender caudally directed processes projecting laterally from the base.

Description. Macropterous male (Figs 4A–C, G, 5A–F). ***Color*** (Fig. 4A–C) dark brown, with distinctive marginal castaneous and yellowish white marks on head, thorax, and abdomen. Head yellowish on posterior compartments of vertex and fovea, only infuscated in concavities, and on both sides of lateral and median carinae of face below fastigium; distinctive whitish marks below the eyes and across frontoclypeal area. Thorax, whitish colored on the pronotal disc between lateral carinae, one spot behind eyes on paranotal disc, a subtriangular shaped spot on each side of postero-lateral margin of mesonotum, metanotum, and scutellum; yellowish, on lateral edges of pronotum, tegula, and a suboval longitudinal median spot on mesonotum disc. Antennal segments pale castaneous with basal segment and proximal 1/2 of second segment darkish on dorsal surface. Legs yellow with tarsi dorsally darker, with longitudinal darker spots near base and apex of pro- and mesocoxae, on dorsal surface of femora, apical region of metafemur, and base and apex of metatibiae. Forewing amber, veins pale brown, fuscous along apical veins M1+2 and M3+4 with infuscate areas on central nodal line, last apical cell, along Cu vein, on postclaval angle, and apex of clavus. Abdomen in dorsal view with contrasting white yellowish coloration on drumming segments and two lateral spots on tergites V and VIII, ventrally with most of the segment margined with yellow. Pygofer dark

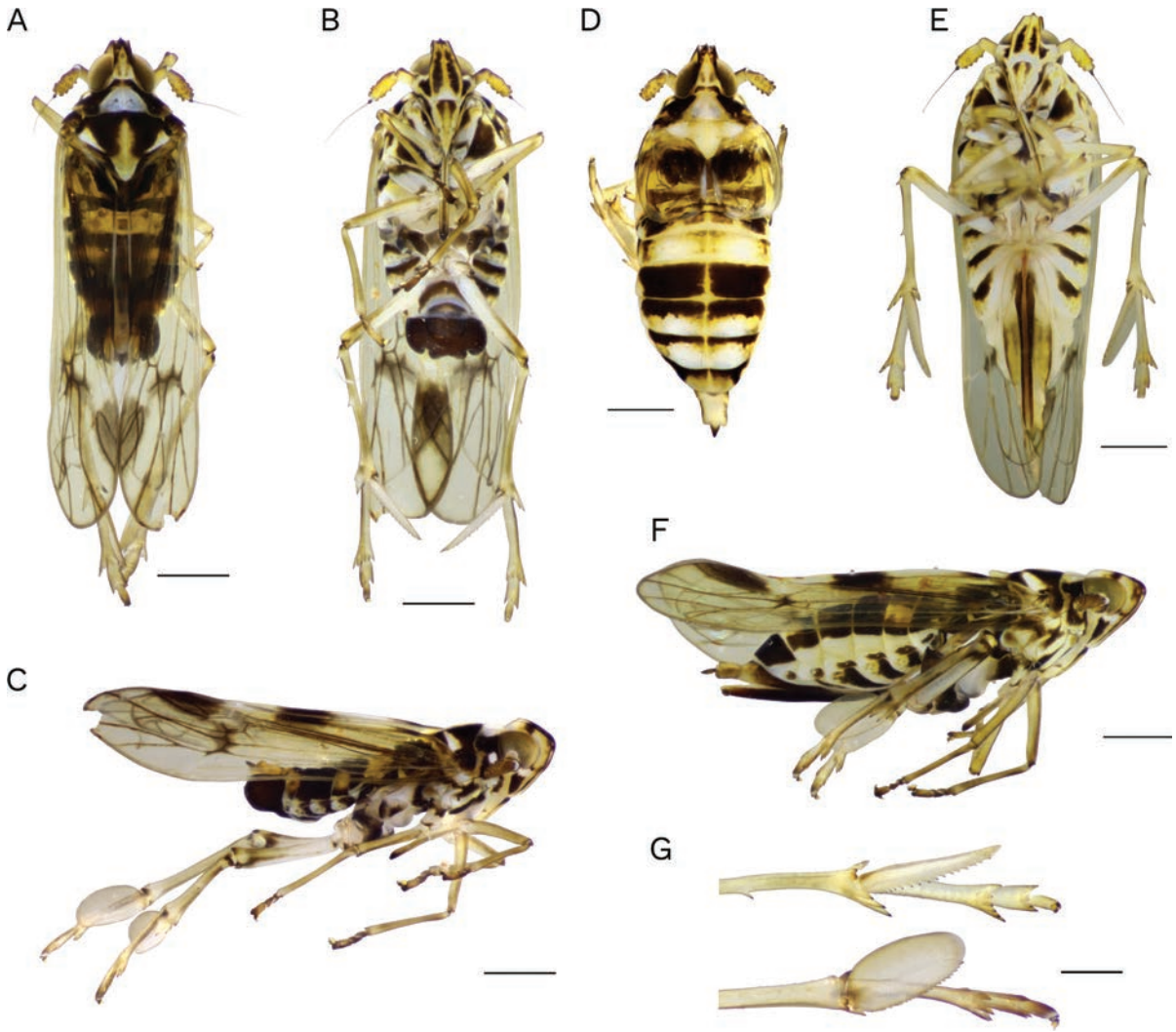

Figure 4. *Megamelus serpentinus* sp. nov. Habitus. Macropterous male and female. Male macropter **A** dorsal **B** ventral and **C** lateral view **D** female brachypter dorsal view **E** female macropter ventral and **F** lateral view **G** apex of hind leg (post tibial spur and tarsi) ventral and lateral view. Scale bars: 0.5 mm (**A–F**); 0.2 mm (**G**).

brown on outer lobes and ventral surface; pale castaneous on dorsal surface and inner lobes. Anal segment yellowish and anal style dark brown (Fig. 4A, B).

***Structure*.** Head narrower than pronotum. Vertex rectangular, longer than wide at base (2.1: 1) projecting beyond eyes > 1/3 of its length, with rounded frontal inflection; basal compartment slightly concave, occupying approximately more than basal third, stem of Y-shaped carina fine, delimiting shallow depressed areas on both sides; other carinae of head pronounced; submedian carinae forking at dorsal surface of vertex, quite far from fastigium, carinal branches forming a slender triangle, fovea, or areola little > 2 × the length; median carina strongly ridged and prominent at base at or just below fastigium then smooth; lateral carinae foliated at base, removed from eye along the length. (Fig. 4A). Frons nearly 3 × longer than wide (3:1.1), strongly narrowed between anterior margins of eyes, maximum width near basal 1/3, lateral margins slightly convex at apex; lateral and submedian carinae fine just before frontoclypeal suture, which is arched dorsally. Clypeus subtriangular, longer than wide, median carina weaker at base. Eyes globose, deeply emarginate below to receive the antennae. Rostrum reaching metacoxae, longer than frons, subapical and apical segment subequal. An-

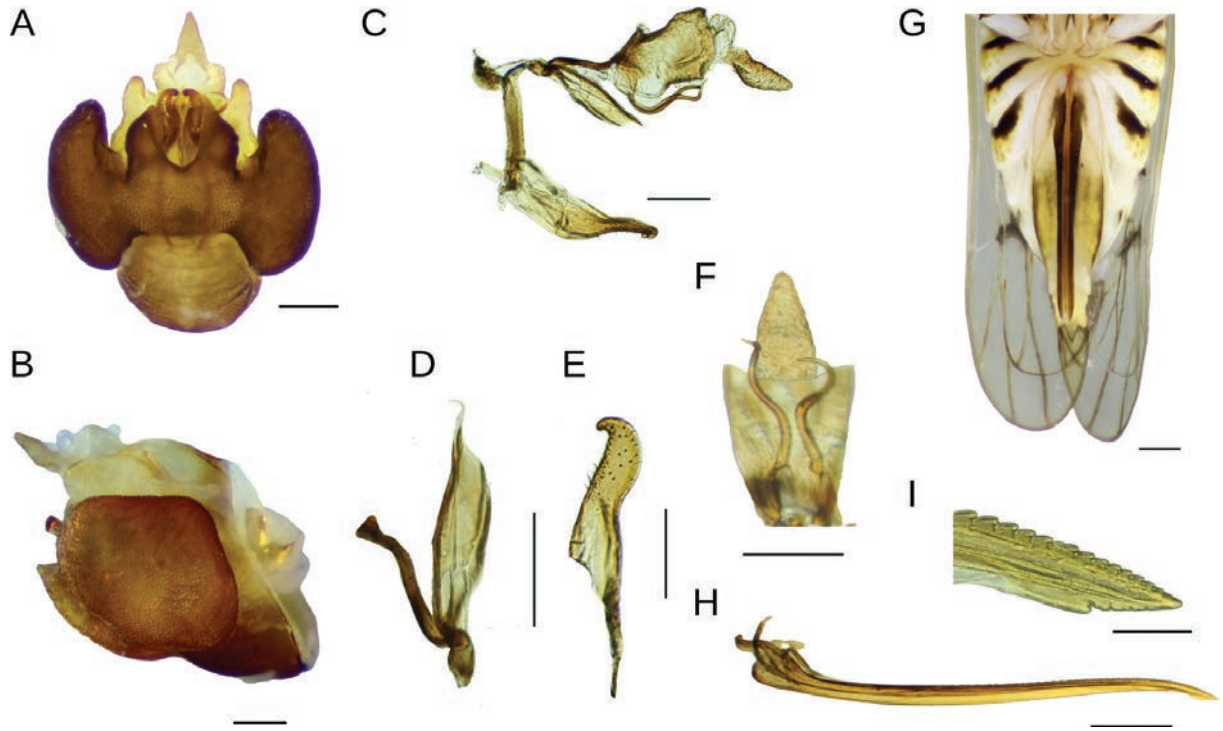

Figure 5. *Megamelus serpentinus* sp. nov. Terminalia. Male: pygofer **A** posterior ventral view **B** lateral view **C** genital complex, lateral view **D** aedeagus and suspensorium, lateral view **E** right genital style **F** anal segment, ventral view. Female **G** abdomen ventral view **H** gonapophysis IX, lateral view **I** apex of gonapophysis IX. Scale bars: 0.1 mm (**A–F, I**); 0.2 mm (**G, H**).

tennae with the first segment longer than wide, the second segment < 2 × the first, length > 2 × its width (Fig. 4A, B). Pronotum with conspicuous carinae, laterals divergent, slightly convex toward hind margin, reaching it. Mesonotum almost as long as vertex plus pronotum, fine median carina becoming obsolete at apex, lateral carinae inconspicuous, slightly divergent posteriorly, not reaching hind margin (Fig. 4A). Forewings rather long and slender, rounded at apex, length 3 × their width at subapical region, surpassing distal end of abdomen > ~ 1/3 of their length. Metatibial spur, leaf-like, long, and broad, with median rib becoming obsolete at apex which is truncated without teeth, slightly longer than metatarsomere I, with 17 or 18 regular, large, black-tipped teeth on trailing margin; first hind tarsomere longer than second plus third (1.5:1) (Fig. 4G). Abdomen regularly wide, compressed dorsoventrally (Fig. 4A).

Terminalia (Fig. 5A–F). Pygofer in dorsal view, with deeply concave anal emargination, anal angles distinctly projected caudad. In ventral view, expanded, with large, round, kidney-shaped outer lobes enfolding almost the entire lateral surface (Fig. 5A, B); inner lobes, large, wide in basal ²/₃, external margin rounded, inner margin sinuous ending apically pointed with deep and broad concavity between their bases; strong emargination between inner and outer lobes (Fig. 5A, B); diaphragm broad with dorsal margin deeply concave and medially caudad projected into lip-shaped process bearing bunch of rather short, stiff hairs. Aedeagus short, tubular, strongly narrow at base, widening up to the basal 1/3 then uniformly tubular and obliquely truncated at apex, with a single short, slender, apically curved process extending shortly beyond oval and apical phallotreme (Fig. 5C, D). Genital styles (parameres) long, narrow, convergent apically, expanded and gradually tapering basally, broadly rounded along apical 1/2 on outer margin, apex hook-like, very curved inward; in ventral view visible between the internal lobes, in almost its

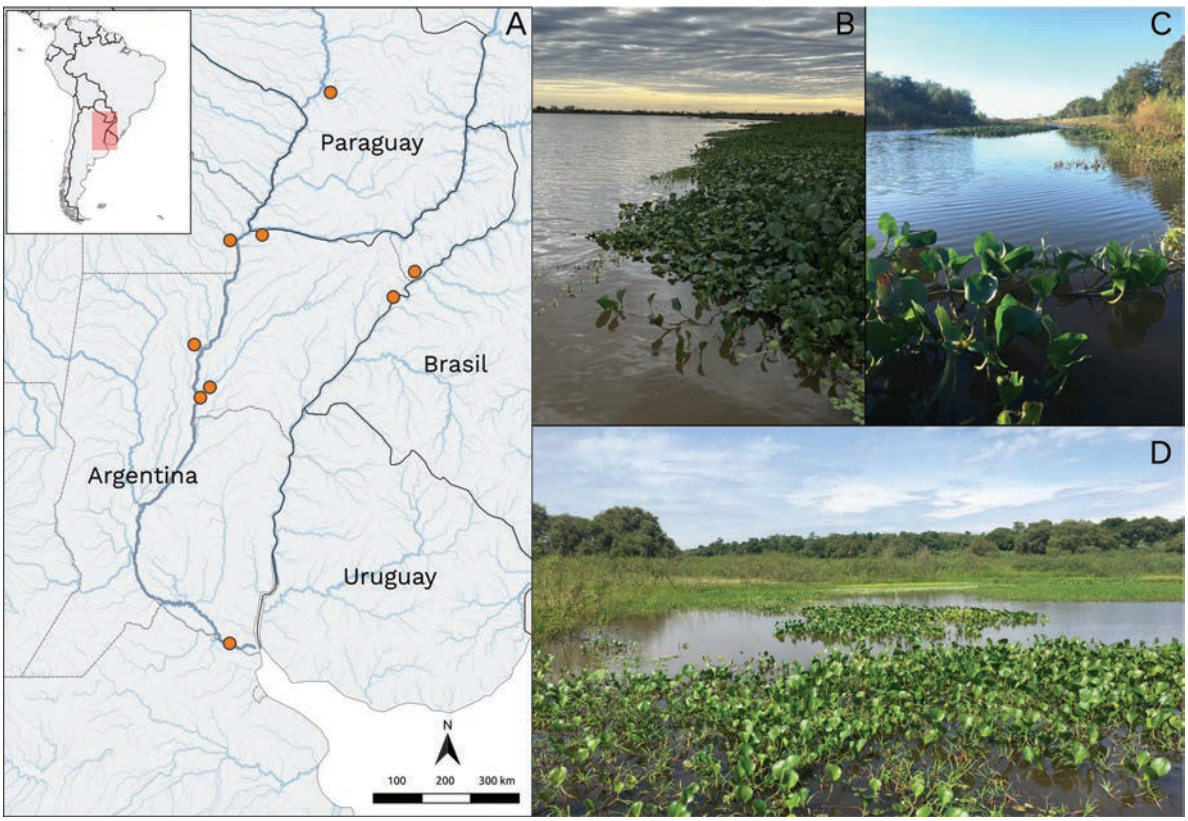

Figure 6. Geographical distribution and habitat of *Megamelus serpentinus* sp. nov. **A** distribution map in Argentina and Paraguay, orange dots represent sites where *M. serpentinus* was found (Suppl. material 2) **B–D** habitats and host plant (*P. azurea*).

entire length (Fig. 5E). Suspensorium strap-like, connected to the aedeagal base, as long as half length of aedeagus (Fig. 5C). Connective slightly compressed, almost straight (Fig. 5C). Anal segment tubular, longer than twice the width, with caudal margin deeply emarginate ventrally; with two long, sinuous, slender, caudally directed processes arising ventrolaterally just below anterior angle which is membranous; anal style slender, twice longer than broad (Fig. 5F).

Measurements (*n* = 6). L., 3.8; B.L., 2.3; b.w., 1; t.l., 3.2; v.l., 0.4; v.w., 0.2; f.l., 0.6; M.f.w., 0.3; m.f.w., 0.2; a.l.I, 0.15; a.l.II, 0.3; p.l., 0.2; m.l., 0.5; mti.l., 1.13; mta.l., 1; mta.ll., 0.7; s.l., 0.8; t.n., 17–18.

Brachypterous male. *Color* similar to macropterous form, with mesonotum paler and uniformly colored; tegmen amber with veins concolorous, with fuscous transverse marks continuous or fragmented, from base of clavus at near axillary region, and one spot at claval apex. Abdomen with similar patterns except tergites V and VI which are more uniformly dark brown contrasting with yellowish segments VII and VIII.

***Structure*.** Mesonotum shorter, > 1/2 of vertex plus pronotum length. Tegmen slightly longer than wide, rounded on external lateral margins; posterior margin truncate, covering tergite II.

Measurements (*n* = 6). L., 2.3; b.w., 0.8; t.l., 1; v.l., 0.4; v.w.,0.18; f.l., 0.6; M.f.w., 0.25; m.f.w., 0.15; a.l.I, 0.15; a.l.II, 0.3; p.l., 0.2; m.l., 0.25; mti.l., 0.9; mta.l., 0.9; mta.ll., 0.6; s.l., 0.65; t.n., 17–18.

Macropterous female (Figs 4E, F, 5G–I). ***Color*:** Head and thorax resemble male. Abdomen, in dorsal view, with contrasting yellowish marks on sides and posterior margins of sclerites, except V and VIII, which are uniformly brown. Ab-

dominal sternites with yellowish margins; pygofer and anal segment yellowish, anal style castaneous; ovipositor dark brown (Fig. 4E, F).

***Structure*.** Resembling male but abdomen is sharply tapered towards genital segments. Forewings surpassing distal end of abdomen ~ 1/6 of their length. Anal segment subrectangular; anal style slender.

Terminalia (Fig. 5G–I). Pygofer long, tubular-shaped, tapering toward the apical 1/2; in dorsal view exposed shortly beyond tergite VIII. Ovipositor long, strong, slightly sinuous in apical 1/2, as long as length of pygofer plus anal segment. Valvifer VIII regularly wide, inner margin rounded at base, separated in repose (Fig. 5G). Gonapophysis IX, long and slender, overall shape slightly sinuous, apical fifth concave ventrally, with numerous blunt small teeth on most of dorsal surface (Fig. 5H, I).

Measurements (*n* = 10). L., 4.3; B.L., 3.2; b.w: 0.9; t.l., 3.5; v.l., 0.45; v.w., 0.2; f.l., 0.7; M.f.w., 0.3; m.f.w., 0.2; a.l.I, 0.2; a.l.II, 0.3; p.l., 0.2; m.l., 0.6; mti.l., 1.1; mta.l., 1; mta.ll., 0.7; s.l., 0.6; t.n., 21–23.

Brachypterous female (Fig. 4D). ***Color*** pattern similar to that of the macropterous female, but tegmina resemble those of brachypterous male.

Measurements (*n* = 5). B.L., 2.9; b.w: 0.8; t.l., 1; v.l., 0.45; v.w.,0.2; f.l., 0.7; M.f.w., 0.3; m.f.w., 0.2; a.l.I, 0.2; a.l.II, 0.3; p.l., 0.2; m.l., 0.3; mti.l., 1; mta.l, 1; mta.ll., 0.6; s.l., 0.7; t.n., 21–23.

Etymology. The specific name comes from the Latin, *serpentinum* (serpentine), referring to the undulated shape of the long and slender male anal processes.

Distribution. Argentina: Misiones, Chaco, Corrientes, Santa Fe, and Buenos Aires provinces. Paraguay: Cordillera department (Fig. 6A, Suppl. material 2).

Host plant. *Pontederia azurea* Sw.

Ecology. In the field, *M. serpentinus* was recorded on *P. azurea* in wetlands of the La Plata Basin (Fig. 6B–D). Both adults and nymphs were observed feeding on the host plant.

Remarks. This species is distinguished from the other South American *Megamelus* species principally by their characteristic coloration and the morphology of the male genitalia. Salient features include whitish yellow marks on head, thorax and abdomen, forewings with strongly dark marks on clavus, along Cu vein, over cross veins and last apical cells; the slender vertex with submedian carinae forking at dorsal surface, quite far from fastigium; male with inner lobes of the pygofer long and sharpened at apex with a strong emargination among inner and outer lobes; the aedeagus short and tubular with a short thin apical process slightly curved apically, and the long anal segment with a long, slender and sinuous, posteriorly directed anal processes, emerging from its anterior ventral margin.

Among its congeners, *M. serpentinus* shares morphological features with *M. davisi such as* the sinuous shape and placement of the anal processes in the male, the long ovipositor in the female and the large foliaceous spur, truncated at apex. The examination of the type specimens, macropter and brachypter, in the NHNM collection, by AMRL (Fig. 7) showed that *M. davisi* has a darker coloration, almost piceous black with the carinae and fine edges on sides and posterior margin of pro and mesothorax pale, the forewings whitish with only claval area darkish, and the tegmina darker with pale veins (in the brachypter). *Megamelus davisi* also differs in the submedian carinae of vertex which is forked just on fastigium, and the flat shape of the aedeagus with a narrow twisted apex (Beamer 1955:32, plate 1, fig. 1). *Megamelus serpentinus* also shares with

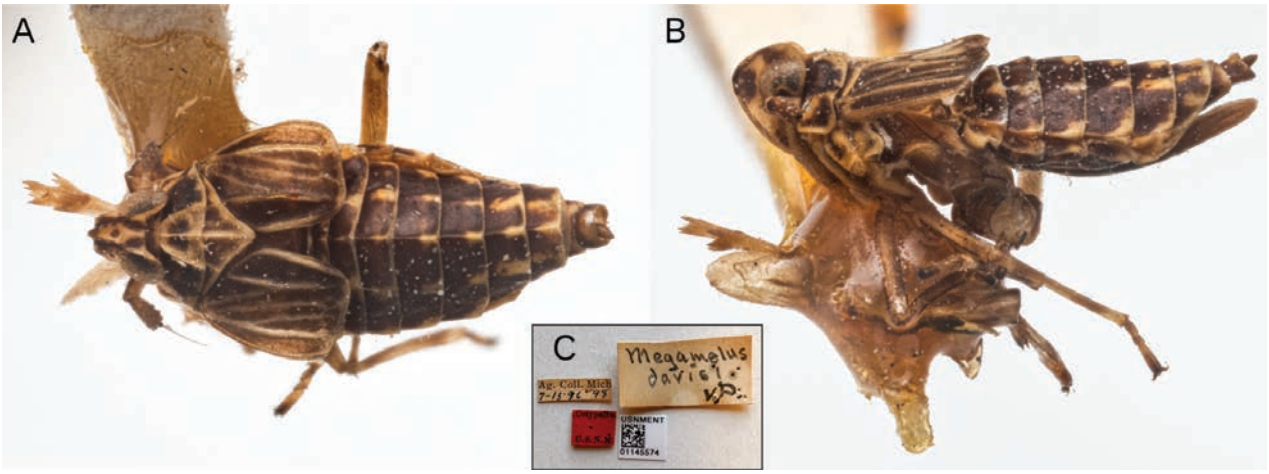

Figure 7. *Megamelus davisi* Van Duzee female brachypter. Cotype (NHNM): Habitus **A** dorsal view **B** lateral view **C** labels.

M. timehri and *M. davisi* the arrangement of the anal segment processes, caudally projected from the anterior ventral margin of the segment.

***Megamelus timehri* Muir, 1919**

Fig. 8

Material examined. Argentina • 2 male brachypters, 2 female brachypters, Corrientes, Esteros del Iberá, 30-XI-2021, on *N. indica*, Salinas-Sosa cols; Paraguay • 2 male macropter, 5 male brachypter, 2 females brachypter, Cordillera, Arroyos y Esteros, 7-IV-2022, on *N. indica*, Salinas-Sosa cols. (MLP).

Description. Brachypterous male. *Color* (Fig. 8A, B) pattern dark brown lighter on dorsal pygofer and ventrally, similar to macropterous male; tegmina, amber-colored infuscation along claval margin and longitudinal veins, with a white spot on external apical corner.

***Structure*.** Tegmen slightly longer than wide, rounded on external lateral and posterior margins, covering tergite II (Fig. 8A).

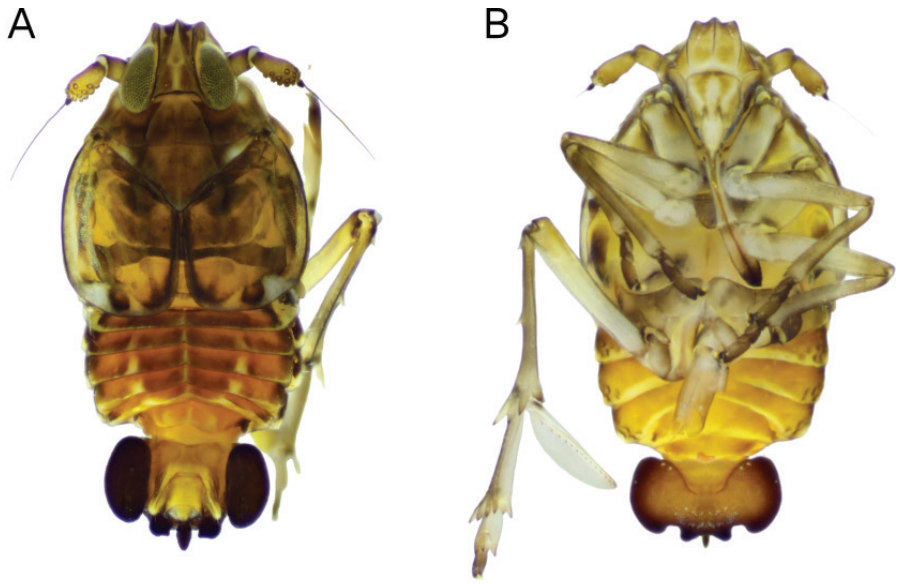

Figure 8. *Megamelus timehri Muir*. Habitus. Brachypterous male **A** dorsal view **B** ventral view. Scale bar: 0.5 mm (**A, B**).

Measurements (*n* = 3). L., 2.12; b.w., 0.72; M.b.w. at abdominal segment V, 0.90; t.l., 0.74; v.l., 0.32; v.w., 0.18; f.l., 0.44; M.f.w., 0.25; m.f.w., 0.15; a.l.I, 0.13; a.l.II, 0.17; p.l., 0.19; m.l., 0.28; mti.l., 0.73; mta.l., 0.75; mta.ll., 0.46; s.l., 0.48; t.n., 20.

Distribution. Argentina: Corrientes province (Sosa et al. 2007b). Guyana: Demerara River (Muir 1919). New record: Paraguay, Arroyos y Esteros Department.

Ecology. *Megamelus timehri* was recorded during spring 2003 on *Limnobium laevigatum* (Humb. & Bonpl. ex Willd.) Heine (Hydrocharitaceae) in northeastern Argentina (La Plata Basin, subregión Iberá System) (Sosa et al. 2007b). *Nymphoides indica* (L.) Kuntze is recorded as a new host plant. During our surveys (2021–2023) *M. timehri* was found abundantly and exclusively on this plant species across different sites. The previous record could be the result of *M. timehri* casually hopping and resting on *L. laevigatum*.

Megamelus iphigeniae **Muir, 1926**

Material examined. Argentina • 3 male macropters, 1 female macropter, Chaco, El Paranacito, 21-XII-2021, on *Pontederia rotundifolia*, Sosa-Salinas cols. (MLP); Bolivia • 1 male macropter, labeled 11.862, col. Berg (MLP).

Distribution. Argentina: Formosa, Chaco, and Corrientes provinces (Sosa et al. 2007b). BRAZIL: Pará and Mato Grosso do Sul States (Muir, 1926). New record: Bolivia.

Biological aspects. Adults and nymphs of *M. iphigeniae* were found abundantly on *P. azurea* and *P. crassipes* in northeastern Argentina (La Plata Basin, subregion Iberá System) and on *P. parviflora* Alexander in Brazil (Pantanal, subregion Paraguay River). *Pontederia rotundifolia* L.f. is a new record of host plant. Specimens were found abundantly on a small mat of *P. rotundifolia* plants stranded on the shore of a stream.

Key to *Megamelus* species from South America (modified from Mariani et al. 2013)

**M. davisi* has been included in this key because of its morphological similarity to *M. serpentinus* (Fig. 7). All the South American species here included are illustrated in Fig. 10.

1 Male anal segment with 2 processes arising ventrally near anterior margin, caudally directed **2**

– Male anal segment with 2 processes arising ventrally near posterior margin or without processes **4**

2(1) Very short anal processes, 1/5 length of segment. Aedeagus globular at base, with long, basad-directed apical process closely curved towards the left. Ovipositor short and curved, not overpassing anal segment. Mostly brown, paler on frons disc, fore wing hyaline with infuscated marks on clavus, axillar and apical cells. Submedian frontal carina forked far from fastigium. Spur broadly rounded, with 18 fine teeth (Sosa et al. 2007b: figs 45–58) ..... ***M. timehri*** **Muir**

– Long anal processes, as long as or longer than the segment. Aedeagus not globular at base. Ovipositor long, overpassing anal segment **3**

3(2) Aedeagus flat with narrow twisted apex (Beamer 1955: 32, pl. 1, fig. 1). Dark brown, with the lobes of pygofer black; carinae, veins and lined marks of abdomen usually paler; forewings whitish, pale veins with darkish pigmentation on costal and commissural area of corium; tegmina castaneous with pale veins. Submedian frontal carina forked at the apex of fastigium. Spur large, foliaceous, oblong..... ***M. davisi**** **Van Duzee**

– Aedeagus tubular, short, strongly narrow at base, with thin, short, straight process curved at apex (Fig. 5C, D). Dark brown, with distinctive yellowish to white marks bordering most of the sclerites of the body; fore wing amber, pale brown veins, with distinctive fuscous marks on central nodal and apical veins on membrane and clavus; tegmina amber, with fuscous transversal marks from axillar angle to clavus. Submedian frontal carina forked on vertex far from fastigium (Fig. 4A). Spur long and broad, apically truncated, with 17 or 18 large lateral teeth (Fig. 4G) ..... ***M. serpentinus* sp. nov.**

4(1) Anal segment with curved or folded processes near the posterior margin ...**5**

– Anal segment without processes.....**7**

5(4) Anal processes long, folded in 1/2 and parallel-sided; inner lobes of pygofer without process between them; aedeagus very long, slender, tubular; with long, thin, spine-like process closely curved to left. Ovipositor short, reaching anal segment at base. Brown, frons paler with small irregular darker spots on base, and narrow, irregular, blackish and whitish stripes toward apex; tegmina pale brown with dark spots on claval margin. Spur small, with 10–13 teeth (Mariani et al. 2013: figs 1–14)..... ..... ***M. nigrifasciatus*** **Mariani & Remes Lenicov**

– Anal processes short and curved, apically convergent or oppositely directed; inner lobes of pygofer with a process between them. Ovipositor straight and long.....**6**

6(5) Anal processes symmetrical, convergent apically; pygofer with sclerotized area bearing pair of small, sharply pointed processes between inner lobes. Brown, frons with narrow pale stripe on apex; fore wing hyaline with only 1 fuscous mark on apex of clavus. Spur long, with 15–20 teeth (Sosa et al. 2007b: figs 2–15) .....***M. bellicus*** **Remes Lenicov & Sosa**

– Anal processes asymmetrical, oppositely directed apically; pygofer with lobe-like process between inner lobes. Pale brown, frons uniformly colored; fore wing heavily infuscated on clavus and apical area. Spur large, wide, with 20–22 teeth (Sosa et al. 2007b: figs. 17–30)...***M. electrae*** **Muir**

7(4) Pygofer inner lobes truncated; aedeagus long, with 2 apical lateral processes. Ovipositor long, overpassing anal segment at base, with conspicuous truncated and dorsally denticulated teeth. Brown, frons with yellowish spots on fastigium and 2 paler transverse stripes. Spur long, with 13 or 14 small and big teeth alternated on the basal 1/2 and larger toward the apex (Sosa et al. 2004: figs 1–14) ..... ***M. scutellaris*** **Berg**

– Pygofer inner lobes rounded, sinuous or subtriangular in outline; aedeagus with a single apical process, simple or bifurcated. Ovipositor short, reaching anal segment at base **8**

8(7) Genital styles with apex wide and truncated (Fig. 2E), aedeagus with apical process forked at base (Fig. 2D), pygofer inner lobes subtriangular in outline (Fig. 2A). Body broad and flattened, with vertex broad, subquadrate, and apically rounded; submedian carina forking dorsally just at the

fastigium, which is angulated in lateral view; frons subcircular. Dull dark brown mottled with paler spots on apex of vertex and frons disc, and stripe on epistomal area extending towards base of gena (Fig. 1B). Spur small with 8 or 9 black-tipped sharp teeth (Fig. 1D) ..... ***M. delticus* sp. nov.**

– Genital styles with hook-like apex, aedeagus with single apical process, pygofer inner lobes rounded or sinuous in outline **9**

9(8) Pygofer inner lobes rounded in outline; aedeagus with long spine-like subapical process curved downwards on the left; genital styles strongly flexed inwards midway. Brown, frons with 2 paler but wide transverse stripes; forewings hyaline with veins and apical cells infuscated, tegmina amber with dark spots on apical and claval margin. Long antennal basal segment. Spur short, with 20 small teeth (Mariani et al. 2013: figs. 15–28) ..... ***M. maculipes* (Berg)**

– Pygofer inner lobes sinuous in outline; aedeagus bearing 1 long process, expanded proximally and curved upwards apically on the right; genital styles straight, curved at apex. Pale brown, uniformly colored; forewings hyaline with fuscous marks on apex of clavus, along median and cross veins, and on 2 apical cells. Short antennal basal segment. Spur long, with 19–24 regular, large teeth (Sosa et al. 2007b: figs 31–44) ..... ***M. iphigeniae* Muir**

Phylogenetic analyses

The phylogenetic relationships among several species of the genus *Megamelus* were reconstructed by means of ML based on a 658 pb fragment of the mitochondrial COI gene (Fig. 9, Suppl. material 3). We retrieved two main clades: one comprising most Holarctic species (Clade I) and one containing the South American species and three North American species: *M. davisi*, *M. hamatus*, *and M. toddi* (Clade II). Within Clade II, all species are clearly delimited, with high bootstrap values for external nodes. However, these values decrease for some older diversification events. *Megamelus scutellaris* appears as a sister group of the remainder of Clade II, which is then separated into two subclades: one comprises *M. timehri*, *M. toddi*, *M. davisi*, *M. hamatus*, and *M. serpentinus*. The other one contains the remaining South American *Megamelus* species and is subdivided into two more clades, one composed of *M. electrae* and *M. iphigeniae*, and the other one including *M. maculipes*, *M. delticus*, and *M. bellicus*.

Discussion

In the present study we describe two new species, *Megamelus delticus* sp. nov. and *Megamelus serpentinus* sp. nov., increasing to nine the number of South American *Megamelus* species known to date and to 33 worldwide (Fig. 10). The identity of these species, previously defined through the analysis of morphological characters, is now supported by genetic data, which also allowed us to investigate the phylogenetic relationships among the 18 species of the genus. Lastly, this revision of the South American species enabled us to reassess the traits considered typical of the genus and to expand the existing key.

The genus *Megamelus* was originally described mainly based on the coloration pattern, head morphology (narrow vertex and trapezoidal frons), carinae of pro- and mesothorax, and the relative length of the metatarsomeres (Fieber 1866). In addition, the lobed appearance of the pygofer and its genito-anal structures were

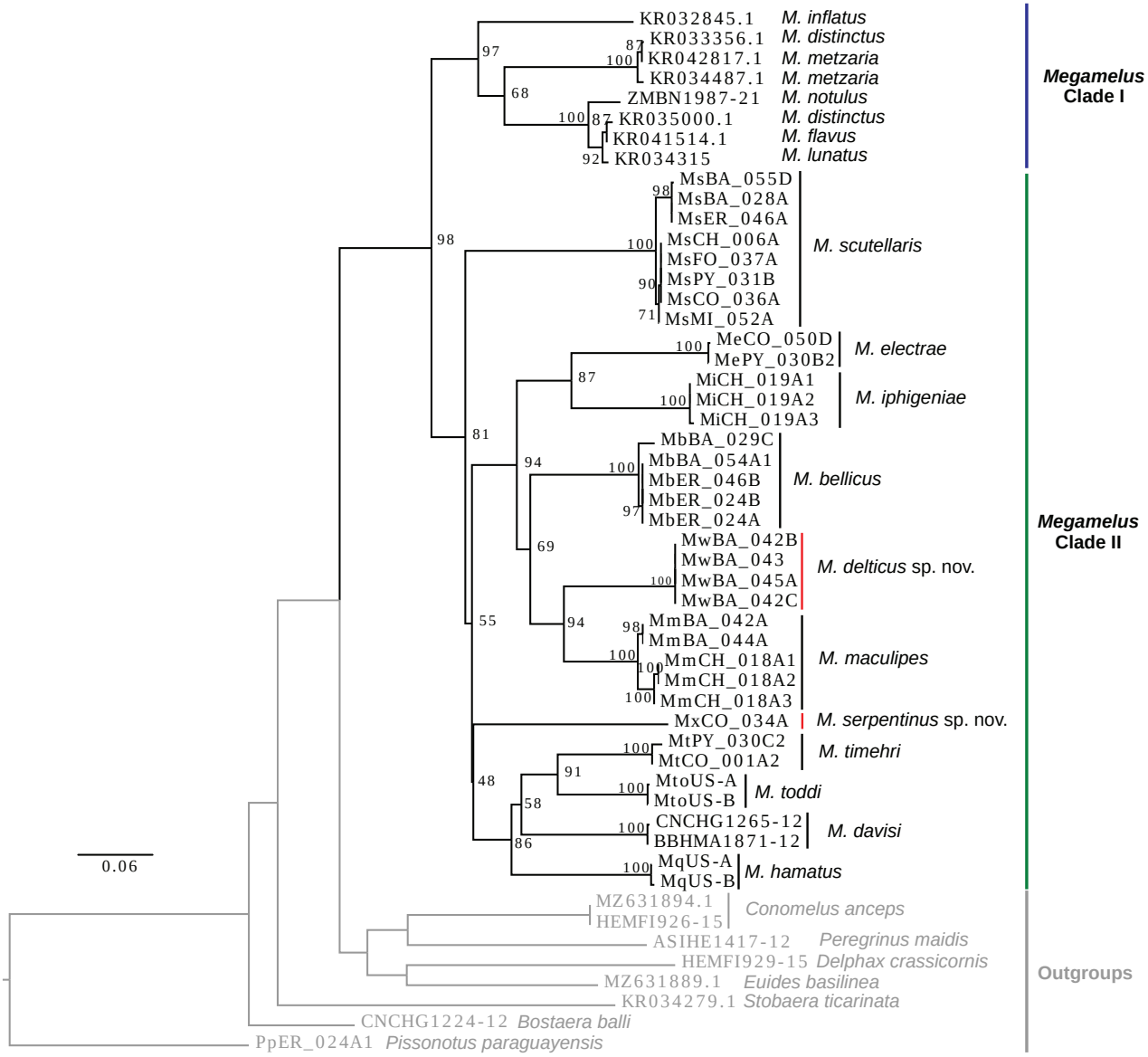

Figure 9. Maximum likelihood (ML) topology (likelihood, -6249.51) resulting from the analysis of the COI gene. UFBootstrap node support values are indicated above each node. Branch length represents the number of nucleotide substitutions per nucleotide site (scale bar = 0.06 substitutions per site). Newly described species are marked with a red line. Outgroups are shown in pale gray color.

considered by Muir (1926) and later emphasized by Beamer (1955) as the main diagnostic features for this genus. On a first approach, the case of *M. delticus* sp. nov. seems to present a contradiction. Although some attributes of this species, such as a greatly flattened and oval body, a broad and short head, angled fastigium when viewed laterally, and small eyes, are inconsistent with the ones of *Megamelus*, its pygofer and genito-anal structures do match with those of the genus. Furthermore, its classification within the genus was confirmed by our phylogenetic analysis. These combined results support the notion that the lobed appearance of the pygofer is the distinctive morphological feature for characterizing the genus, while other traits might exhibit more variation than previously thought.

Previous studies have explored the phylogenetic relationships among the Delphacidae using morphological characters (Asche 1985), genetic markers (Dijkstra et al. 2003; Huang et al. 2017; Bucher et al. 2023) or a combination of both

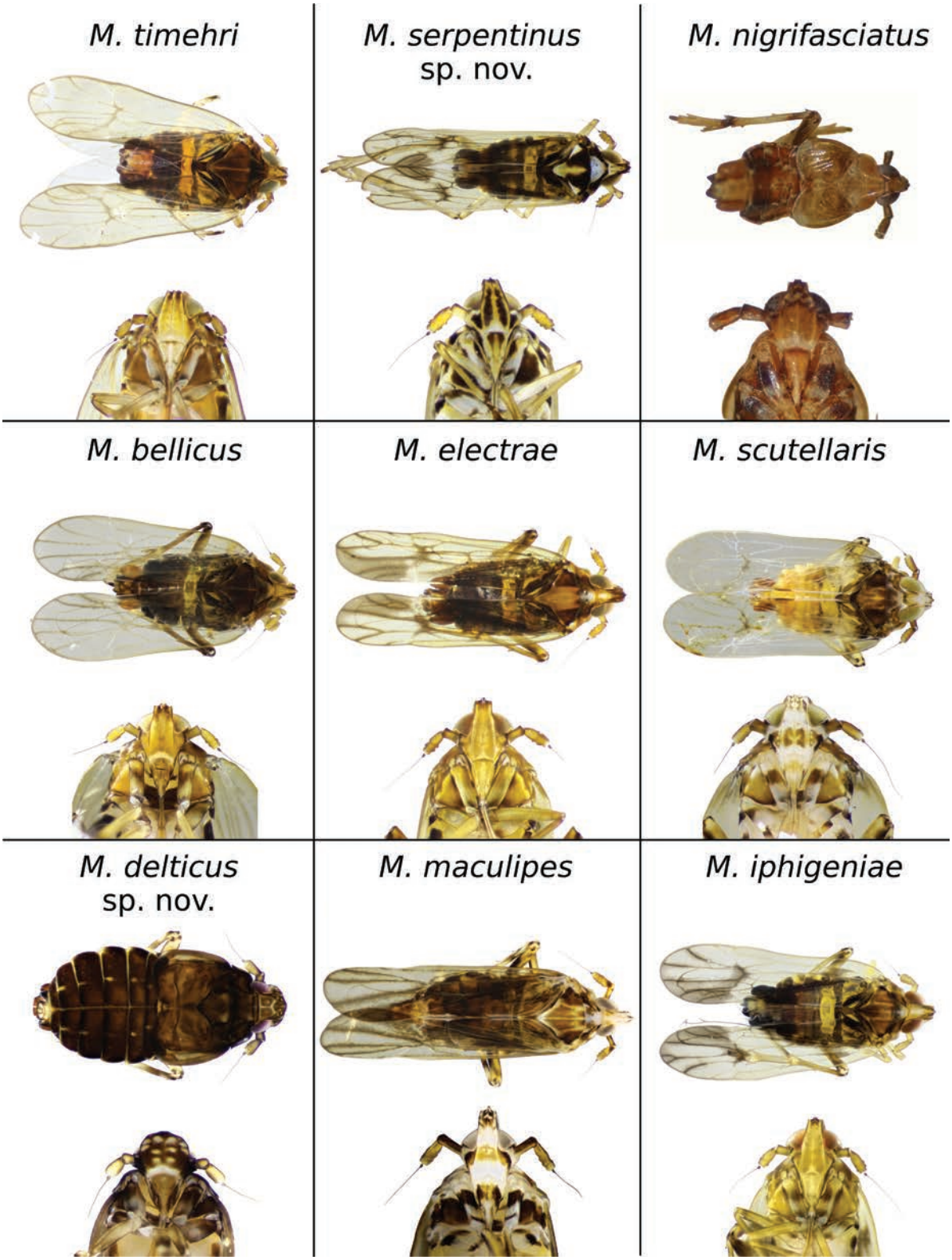

Figure 10. Dorsal and ventral view of the head of the nine South American *Megamelus* species. Macropterous males are shown for all species except for *M. delticus* sp. nov. and *M. nigrifasciatus*, for which only the brachypter is known.

(Urban et al. 2010). Some of these studies included the genus *Megamelus*, and placed it as a sister group of the genus *Conomelus*. However, phylogenetic relationships within the genus have not yet been explored. Here, newly generated COI data along with sequences retrieved from public databases were used to

reconstruct the relationship among the *Megamelus* sp. for the first time. These analyses confirm that the genus constitutes a well-supported clade and its monophyly is corroborated by the inclusion of several sequences of closely related delphacid genera. Moreover, the identity of the South American *Megamelus* species, including the two described in this article, is supported by this analysis. However, this is not the case for some sequences belonging to North American species, whose placement in the tree could be the result of a misidentification of the specimens deposited in databases and should be corroborated. Although the analysis of the COI gene sequences yielded a topology with little resolution at some diversification events, it allowed us to shed some light on the relationships among the species of the genus. Further investigation including more species and the use of more powerful genetic markers for solving deep nodes are required in order to fully clarify the relationships among the *Megamelus*.

While many delphacid genera are monophagous or oligophagous, typically feeding on hosts within the same genus or family (e.g., *Prokelisia* (Van Duzee, 1897) on *Spartina* spp. (Bartlett 2020), *Kelisia* Fieber, 1878 on Cyperaceae (Bartlett and Wheeler 2007)), the genus *Megamelus* has a much broader range of hosts, including both monocots and dicots. However, each *Megamelus* species appears to be monophagous or oligophagous, with the common trait that their hosts are found in wetland habitats. South American *Megamelus* are mostly associated with macrophytes: *M. scutellaris*, *M. electrae*, *M. bellicus*, *M. iphigeniae*, and *M. serpentinus* sp. nov. feeding on plants of the genus *Pontederia* (Pontederiaceae); *M. maculipes* on *Echinodorus* sp. (Alismataceae), and *M. timehri* on *Nymphoides indica* (Menyanthaceae). The exceptions to this seem to be *M. nigrifasciatus* (Mariani et al. 2013) and *M. delticus* sp. nov., both of which have been recorded on *Eryngium* sp. (Apiaceae), a plant that grows on the higher areas of river banks that can remain protected from floods for long periods of time. However, plants in this genus tend to accumulate rain water in the center of the mat, where both species have been found, which suggests that a close proximity to a water source is a common factor for all known species.

Host plant use seems to be one of the main forces promoting interspecific divergence in herbivorous insects (Dijkstra et al. 2003; Poveda-Martínez et al. 2020, 2022) and this should be interpreted by integrating different approaches. From a morphological standpoint, host plants have been proposed to exert a strong selective pressure in certain structures in Delphacidae, such as the ovipositor (Wallner and Bartlett 2019) and the spur (Markevich et al. 2021). For example, in this study we observed that South American *Megamelus* species with a long ovipositor and gonapophysis IX serrated in > 1/2 of its dorsal and ventral-apical margin, and with a wide foliaceous spur with numerous teeth, have the Pontederiaceae as host plants. Meanwhile, those species that live and feed on *Eryngium* sp., *M. nigrifasciatus*, and *M. delticus* sp. nov., have short gonapophysis with rounded denticulation and a spur considerably reduced in terms of size and teeth number (≤ 13), showing a notable adaptation to the microhabitat offered by their host. For *M. maculipes* and *M. timehri*, feeding on *Echinodorus* sp. and *Nymphoides indica*, respectively, the association between host plant and these morphological traits is not clear. Moreover, we also noticed that *M. timehri*, *M. toddi*, and *M. davisi*, which comprise a clade of species in the phylogenetic tree, feed on rooted aquatic plants with floating leaves, living in close proximity with the water surface. Despite the low nodal support of

this clade, we hypothesize that these species might have derived from an ancestor which fed on a macrophyte with a similar life form. In fact, these species possess a large, foliaceous spur which might allow them to walk on the water surface (Van Duzee 1897; Sosa et al. 2007b; Suppl. material 4 for *M. toddi*).

The relatively recent interest in the genus *Megamelus* due to the use of *M. scutellaris* as a biological control agent (Tipping et al. 2014; Coetzee et al. 2022) motivated field surveys and studies that contributed to the knowledge on this group of planthoppers and on its diversity in the Neotropics. Further studies including multidisciplinary approaches that combine morphological, ecological, and genetic information, will allow a better understanding of the evolutionary history of these species and their relationships with their host plants and their environment.

Acknowledgements

We are grateful to Stuart McKamey for the kind assistance allowing AMM de RL to examine the Fulgoroidea collection in 2010 and providing her with information from the database of the USNM collection. We also thank Charles Bartlett (University of Delaware, Department of Entomology and Wildlife Ecology, USA) for his assistance providing photographs of the *Megamelus davisi* type specimen from the USNM collection, taken by Solomon Hendrix. We thank Melissa Smith and Megan Reid for collecting and providing samples of *M. hamatus* and *M. toddi* from Florida, USA; and Ana Faltlhauser, Mariel Guala, Sol Bovina, and Marina Oleiro for their help during field trips in Argentina and Paraguay.

Additional information

Conflict of interest

The authors have declared that no competing interests exist.

Ethical statement

No ethical statement was reported.

Funding

This work were funded by Fundación para el Estudio de Especies Invasivas (FuEDEI) and CONICET.

Author contributions

Conceptualization: NAS, AMM, AS. Data curation: AMM, RM, MR, NAS. Formal analysis: AMM, MR, RM, NAS. Funding acquisition: AS. Investigation: AS, RM, NAS, AMM. Methodology: NAS. Project administration: AMM, AS. Resources: AS. Software: MR, NAS. Supervision: AS. Validation: RM. Writing - original draft: NAS. Writing - review and editing: AMM, RM, AS, NAS, MR.

Author ORCIDs

Nicolas A. Salinas https://orcid.org/0000-0002-1055-4475
Roxana Mariani https://orcid.org/0000-0002-0066-6692
Ana M. Marino de Remes Lenicov https://orcid.org/0000-0001-8678-5408
Marcela S. Rodriguero https://orcid.org/0000-0001-5967-2045
Alejandro J. Sosa https://orcid.org/0000-0002-1680-8712

Data availability

All of the data that support the findings of this study are available in the main text or Supplementary Information.

References

Asche M (1985) Zur Phylogenie der Delphacidae Leach, 1815 (Homoptera Cicadina Fulgoromorpha). Marburger entomologische Publikationen 2: 1–910.

Bartlett C (2005) Two new genera and species of stenocranine planthoppers (Hemiptera: Delphacidae) from North America. Entomological News 116: 291–303.

Bartlett, CR (2020) (and updates) Planthoppers of North America. https://sites.udel.edu/planthoppers/ [accessed 19 November 2024].

Bartlett CR, Wheeler AG (2007) *Kelisia* and *Stenocranus* species (Hemiptera: Fulgoromorpha: Delphacidae): new host-plant associations and distributional records of eight sedge-feeding planthoppers. Proceedings of the Entomological Society of Washington 109(2): 400–415.

Beamer RH (1955) A Revision of the genus *Megamelus* in America north of Mexico (Homoptera, Fulgoridae, Delphacinae). Journal of the Kansas Entomological Society 28: 29–40.

Berg C (1883) Hemiptera Argentina. Anales de la Sociedad Científica Entomológica Argentina 16: 235.

Bucher M, Condamine FL, Luo Y, Wang M, Bourgoin T (2023) Phylogeny and diversification of planthoppers (Hemiptera: Fulgoromorpha) based on a comprehensive molecular dataset and large taxon sampling. Molecular Phylogenetics and Evolution 186: 107862. https://doi.org/10.1016/j.ympev.2023.107862

Coetzee JA, Miller BE, Kinsler D, Sebola K, Hill MP (2022) It's a numbers game: inundative biological control of water hyacinth (*Pontederia crassipes*), using *Megamelus scutellaris* (Hemiptera: Delphacidae) yields success at a high elevation, hypertrophic reservoir in South Africa. Biocontrol Science and Technology 32: 1302–1311. https://doi.org/10.1080/09583157.2022.2109594

Crawford DL (1914) A contribution toward a monograph of the homopterous insects of the family Delphacidae of North and South America. US Government Printing Office. Proceedings of the United States National Museum 46(2041): 557–640. https://doi.org/10.5479/si.00963801.46-2041.557

Darriba D, Posada D, Kozlov AM, Stamatakis A, Morel B, Flouri T (2020) ModelTest-NG: A new and scalable tool for the selection of DNA and protein evolutionary models. Molecular Biology and Evolution 37: 291–294. https://doi.org/10.1093/molbev/msz189

Dijkstra E, Rubio JM, Post RJ (2003) Resolving relationships over a wide taxonomic range in Delphacidae (Homoptera) using the COI gene. Systematic Entomology 28: 89–100. https://doi.org/10.1046/j.1365-3113.2003.00203.x

Fieber FX (1866) Grundzüge zur generischen Theilung der Delphacini. Verhandlungen der Zoologisch-Botanischen Gesellschaft in Wien 16: 517–534.

Folmer O, Black M, Hoeh W, Lutz R, Vrijenhoek R (1994) DNA primers for amplification of mitochondrial cytochrome c oxidase subunit I from diverse metazoan invertebrates. Molecular Marine Biology and Biotechnology 3: 294–299.

Germar EF (1830) Species Cicadarium enumeratae et sub genera distributae. Thon's Entomologisches Archiv 2(2): 1–8.

Huang YX, Zheng LF, Bartlett CR, Qin DZ (2017) Resolving phylogenetic relationships of Delphacini and Tropidocephalini (Hemiptera: Delphacidae: Delphacinae) as inferred

from four genetic loci. Scientific Reports 7: 3319. https://doi.org/10.1038/s41598-017-03624-w

Mariani R, Sosa AJ, Remes Lenicov AMM de (2013) Una nueva especie neotropical del género *Megamelus* y nueva combinación para *Stenocranus maculipes* (Hemiptera: Delphacidae). Revista de la Sociedad Entomológica Argentina 72. https://www.biotaxa.org/RSEA/article/view/4198

Markevich D, Walczak M, Borodin O, Szwedo J, Brożek J (2021) Morphological reassessment of the movable calcar of delphacid planthoppers (Hemiptera: Fulgoromorpha: Delphacidae). Scientific Reports 11: 22294. https://doi.org/10.1038/s41598-021-01771-9

Metcalf ZP (1923) A key to the Fulgoridae of eastern North America with descriptions of new species. Journal of the Elisha Mitchell Scientific Society 38(3): 139–230 [32 plates]. https://doi.org/10.5962/bhl.part.7606

Metcalf ZP (1949) The redescription of twenty-one species of Areopidae described in 1923. Journal of the Elisha Mitchell Scientific Society 65(1): 48–60.

Muir F (1919) Some new American Delphacidae. The Canadian Entomologist 51: 35–39. https://doi.org/10.4039/Ent5135-2

Muir F, Giffard WM (1924) Studies in North American Delphacidae. Bulletin of the Experiment Station of the Hawaiian Sugar Planters' Association. no. 15.

Muir F (1926) Contributions to our knowledge of South American Fulgoroidea (Homoptera). Part I. The family Delphacidae. Experiment Station of the Hawaiian Sugar Planters' Association, Entomological Series, Bulletin 18: 1–51.

Park DS, Foottit R, Maw E, Hebert PDN (2011) Barcoding bugs: DNA-based identification of the true bugs (Insecta: Hemiptera: Heteroptera). PLoS ONE 6: e18749. https://doi.org/10.1371/journal.pone.0018749

Poveda-Martínez D, Aguirre MB, Logarzo G, Hight SD, Triapitsyn S, Diaz-Sotero H, Diniz Vitorino M, Hasson E (2020) Species complex diversification by host plant use in an herbivorous insect: The source of Puerto Rican cactus mealybug pest and implications for biological control. Ecology and Evolution 10: 10463–10480. https://doi.org/10.1002/ece3.6702

Poveda-Martínez D, Varone L, Fuentes Corona M, Hight S, Logarzo G, Hasson E (2022) Spatial and host related genomic variation in partially sympatric cactophagous moth species. Molecular Ecology 31: 356–371. https://doi.org/10.1111/mec.16232

Remes Lenicov AMM de, Virla EG (1993) Homópteros auquenorrincos asociados al cultivo de trigo en la República Argentina. I. Análisis preliminar de la importancia relativa de las especies. Studies on Neotropical Fauna and Environment 28: 211–222. https://doi.org/10.1080/01650529309360905

Sosa AJ, Remes Lenicov AMM de, Mariani R, Cordo HA (2004) Redescription of *Megamelus scutellaris* Berg (Hemiptera: Delphacidae), a candidate for biological control of water hyacinth. Annals of the Entomological Society of America 97: 271–275. https://doi.org/10.1603/0013-8746(2004)097[0271:ROMSBH]2.0.CO;2

Sosa AJ, Cordo HA, Sacco J (2007a) Preliminary evaluation of *Megamelus scutellaris* Berg (Hemiptera: Delphacidae), a candidate for biological control of water hyacinth. Biological Control 42: 129–138. https://doi.org/10.1016/j.biocontrol.2007.04.012

Sosa AJ, Remes Lenicov AMM de, Mariani R (2007b) Species of *Megamelus* (Hemiptera: Delphacidae) associated with Pontederiaceae in South America. Annals of the Entomological Society of America 100: 798–809. https://doi.org/10.1603/0013-8746(2007)100[798:SOMHDA]2.0.CO;2

Tamura K, Stecher G, Kumar S (2021) MEGA11: Molecular evolutionary genetics analysis Version 11. Molecular Biology and Evolution 38: 3022–3027. https://doi.org/10.1093/molbev/msab120

Tipping PW, Sosa A, Pokorny EN, Foley J, Schmitz DC, Lane JS, Rodgers L, Mccloud L, Livingston-Way P, Cole MS, Nichols G (2014) Release and establishment of *Megamelus scutellaris* (Hemiptera: Delphacidae) on water hyacinth in Florida. Florida Entomologist 97: 804–806. https://doi.org/10.1653/024.097.0264

Trifinopoulos J, Nguyen LT, von Haeseler A, Minh BQ (2016) W-IQ-TREE: a fast online phylogenetic tool for maximum likelihood analysis. Nucleic Acids Research 44: W232–W235. https://doi.org/10.1093/nar/gkw256

Urban JM, Bartlett CR, Cryan JR (2010) Evolution of Delphacidae (Hemiptera: Fulgoroidea): combined-evidence phylogenetics reveals importance of grass host shifts. Systematic Entomology 35: 678–691. https://doi.org/10.1111/j.1365-3113.2010.00539.x

Van Duzee EP (1897) Notes on Jamaican Hemiptera: A report on a collection of Hemiptera made on the island of Jamaica in the spring of 1906. Buffalo Society of Natural Sciences. https://books.google.com/books?hl=pt-PT&lr=&id=85I_AQAAMAAJ&oi=fnd&pg=PA229&dq=van+duzee+1897&ots=RTg-dz1XCE&sig=iIsBPd7NIkWv1RTy2-tmqXhQvd8 [accessed 17 July 2024]

Wallner AM, Bartlett CR (2019) Comparative morphology of female gonapophyses IX in Delphacidae (Hemiptera: Auchenorrhyncha: Fulgoromorpha) with key to tribes. Zootaxa 4564: 137–172. https://doi.org/10.11646/zootaxa.4564.1.5

Yang JT, Yang CT (1986) Delphacidae of Taiwan (I). Asiracinae and the Tribe Tropidocephalini (Homoptera: Fulgoroidea). https://www.cabidigitallibrary.org/doi/full/10.5555/19870546140 [accessed 19 November 2024]

Supplementary material 1

Collection data and accession number of genetic samples

Author: Nicolas A. Salinas

Data type: xlsx

Explanation note: Collection data and accession number of genetic samples, including geographical coordinates, collection date, host plant and GenBank accession numbers.

Link: https://doi.org/10.3897/zookeys.1224.135596.suppl1

Supplementary material 2

Collection data of two new species of *Megamelus* from South America

Author: Nicolas A. Salinas

Data type: xlsx

Explanation note: Collection data of two new species of *Megamelus* from South America, including geographical coordinates, host plants, and collection date.

Link: https://doi.org/10.3897/zookeys.1224.135596.suppl2

Supplementary material 3

Phylogenetic tree in Newick format

Author: Nicolas A. Salinas

Data type: tree

Explanation note: Phylogenetic tree of the genus *Megamelus* in Newick format.

Link: https://doi.org/10.3897/zookeys.1224.135596.suppl13

Supplementary material 4

Detail of the hind leg of *M. toddi* (specimen sample code MtoUS-A), showing the foliaceous shape of the calcar

Authors: Nicolas A. Salinas, Roxana Mariani, Ana M. Marino de Remes Lenicov, Alejandro J. Sosa

Data type: docx

Explanation note: Hind leg with detailed of spur of *Megamelus todi*.

Link: https://doi.org/10.3897/zookeys.1224.135596.suppl4

ZooKeys 1224: 55–68 (2025)
DOI: 10.3897/zookeys.1224.128761

Research Article

An eastern Congolian endemic, or widespread but secretive? New data on the recently described *Afrixalus lacustris* (Anura, Hyperoliidae) from the Democratic Republic of the Congo

Tadeáš Nečas[1], Gabriel Badjedjea[2], Janis Czurda[1,3], Václav Gvoždík[1,4]

1 *Institute of Vertebrate Biology of the Czech Academy of Sciences, Brno, Czech Republic*
2 *Biodiversity Monitoring Centre, Department of Ecology and Aquatic Biodiversity, University of Kisangani, Kisangani, Democratic Republic of the Congo*
3 *Department of Botany and Zoology, Faculty of Science, Masaryk University, Brno, Czech Republic*
4 *Department of Zoology, National Museum of the Czech Republic, Prague, Czech Republic*

Corresponding authors: Tadeáš Nečas (tad.necas@gmail.com); Václav Gvoždík (vaclav.gvozdik@gmail.com)

Abstract

The Great Lakes spiny reed frog (*Afrixalus lacustris*) was recently described from transitional (submontane) forests at mid-elevations of the Albertine Rift mountains in the eastern Congolian region. Previously, because of its similarity, it had been understood to represent eastern populations of the unrelated *A. laevis*, which is known mainly from Cameroon. Based on DNA barcoding, we document the westward extension of the known range of *A. lacustris* within lowland rainforests in the Northeastern and Central Congolian Lowland Forests. One sample was represented by a larva found in a clutch in a folded leaf, a typical oviposition type for most *Afrixalus* species, contrary to oviposition on an unfolded leaf surface in the similar *A. laevis* and closely related *A. dorsimaculatus* and *A. uluguruensis*. Comparison of the advertisement call of *A. lacustris* from Salonga National Park, Democratic Republic of the Congo, indicates similarity to its sister species from montane areas of the Albertine Rift, the ghost spiny reed frog (*A. phantasma*). Phylogeographic analysis suggests that *A. phantasma* and *A. lacustris* speciated allopatrically during the Early Pleistocene, with the former having refugia in montane forests and the latter in transitional and also lowland forests. The lowland populations of *A. lacustris* represent distinct evolutionary lineages, which diversified probably in isolated forest refugia during the Middle Pleistocene.

Key words: Afrotropics, bioacoustics, Central Africa, distribution, frogs, leaf-folding frogs, phylogeography, reproduction, spiny reed frogs, tropical rainforests

Academic editor: Johannes Penner
Received: 31 May 2024
Accepted: 6 December 2024
Published: 21 January 2025

ZooBank: https://zoobank.org/3EFC70AD-26AF-44F4-B3C2-FA69F4C6AF2F

Citation: Nečas T, Badjedjea G, Czurda J, Gvoždík V (2025) An eastern Congolian endemic, or widespread but secretive? New data on the recently described *Afrixalus lacustris* (Anura, Hyperoliidae) from the Democratic Republic of the Congo. ZooKeys 1224: 55–68. https://doi.org/10.3897/zookeys.1224.128761

Introduction

Although Central Africa has been in the viewfinder of researchers for more than a hundred years, one of its parts, the central Congo Basin located under the wide arc of the Congo River, is still a mostly 'empty spot' on a map regarding some groups of African fauna. One of these groups is amphibians, as only a single comprehensive study on the species diversity of amphibians of the Central Congolian Lowland Forests (sensu Burgess et al. 2004) has been published to

date (Badjedjea et al. 2022). Spiny reed frogs or leaf-folding frogs (*Afrixalus* Laurent, 1944) are known from 37 species from around sub-Saharan Africa, and a majority of species are characterized by a remarkable oviposition type as they use skin secretions to 'glue' edges of leaves to form a 'nest' for their eggs (Channing and Rödel 2019). One of the few exceptions is *A. laevis*, which deposits its eggs on leaf surfaces without forming the 'leaf nest' (Amiet 2012). This species had been until recently understood as having a largely disjunct distribution in western (Cameroon, Gabon, Bioko Island) and eastern Central Africa (eastern Democratic Republic of the Congo, Rwanda, Uganda) (Schiøtz 1999), although discussions about potential species-level distinction of the eastern population occurred (e.g., Amiet 2009, 2012).

The first relatively comprehensive understanding of phylogenetic relationships of *Afrixalus* was introduced by Portik et al. (2019), who showed that *Afrixalus* (beside "*Afrixalus*" *enseticola* Largen, 1974) is formed by two main clades later marked by Conradie et al. (2020) as Clade A and Clade B. Among the species studied by Portik et al. (2019) was also "*Afrixalus lacustris*" from Uganda, at that time not yet formally described and thus introduced as a *nomen nudum*. Clade B of *Afrixalus* contains the type species of the genus *A. fornasini* (Bianconi, 1849) from Southeast Africa. Otherwise Clade B contains mostly species occurring in Central and West Africa, including *A. laevis* from Cameroon (Conradie et al. 2020; Nečas et al. 2022). Clade A consists of mostly minute species primarily from East and Southeast Africa. "*Afrixalus lacustris*" from Uganda was phylogenetically re-analyzed as *A.* cf. *laevis* and *A.* sp. aff. *laevis* (Conradie et al. 2020; Nečas et al. 2022), respectively, and was confirmed as belonging to Clade A in the proximity of *A. weidholzi* (Mertens, 1938) from West to northern Central Africa and *A. dorsimaculatus* (Ahl, 1930), *A. morerei* Dubois, 1986 and *A. uluguruensis* (Barbour & Loveridge, 1928) from the Eastern Arc Mountains of Tanzania (Channing and Rödel 2019). The "eastern *A. laevis*" (*A.* cf. *laevis*, *A.* sp. aff. *laevis*) was finally formally described by Greenbaum et al. (2022) as *A. lacustris* Greenbaum, Dehling, Kusamba & Portik, 2022, who also described its sister species *A. phantasma* Dehling, Greenbaum, Kusamba & Portik, 2022 from montane areas of the central Albertine Rift in the Democratic Republic of the Congo and Rwanda (> 1700 m a.s.l.), which was previously also confused with *A. laevis*. These authors also demonstrated that another Albertine Rift montane endemic, *A. orophilus* (Laurent, 1947), belongs to a closer phylogenetic relationship with *A. lacustris*.

The Great Lakes spiny reed frog (*Afrixalus lacustris*) is presently known from the eastern Democratic Republic of the Congo (DRC) and southern Uganda, but potential distribution in Rwanda and Burundi is anticipated (Greenbaum et al. 2022). It is known mainly from transitional forests (between montane and lowland forests, mid-elevations, < 1700 m) of the Albertine Rift and more rarely from open habitats, especially near Lake Tanganyika (Greenbaum et al. 2022). The authors of the species description also reported some records along the eastern edge of the lowland Congolian rainforest (e.g., Epulu, Ituri Province, DRC) and discussed that the species might be more geographically widespread in lowland rainforests than currently recognized. In particular, they discussed a geographically isolated record from Omaniundu in the eastern Central Congolian Lowland Forests of Sankuru Province, DRC, three males collected in 1959 (approx. 500 km from the nearest locality in eastern DRC; Laurent 1982;

Greenbaum et al. 2022), which they assigned to *A. lacustris*. The authors, however, noted that due to its remote geographic origin and some morphological peculiarities, this population needs to be further investigated using molecular data. Thus, *A. lacustris* is biogeographically presently understood as an eastern Congolian species. Neither type of oviposition nor characteristics of advertisement call of *A. lacustris* have been described (Greenbaum et al. 2022).

In this study, we report a westward geographic range extension into the Congolian lowland rainforests, oviposition type, and advertisement call characteristics of this recently described, putative eastern Congolian endemic, *Afrixalus lacustris*.

Material and methods

Sampling

We obtained two genetic samples of "*Afrixalus* cf. *laevis*" during our fieldwork in the Congolian lowland rainforests in DRC in 2014 and 2023. Several individuals in a very early larval developmental stage were collected from a gelatinous mass surrounding the egg clutch on a leaf and stored in 96% ethanol (IVB-H-CD14-034; IVB-H: herpetological collection in Studenec, Institute of Vertebrate Biology of the Czech Academy of Sciences, Brno, Czech Republic). The larvae were collected in the Dalangba Forest near Lindi River, near Bafwabianga village, Tshopo Province, northeastern DRC (1.1543°N, 26.8082°E, 510 m a.s.l.) on June 16, 2014 (Fig. 1A, B). No other sightings of "*Afrixalus* cf. *laevis*" were recorded during the extensive fieldwork of our team in the lowland rainforests of DRC, until a single adult male (IVB-H-CD23-0847) was recently found calling atop a *Ficus* tree above a shallow, partially dried up swamp near Isandja-Bomongili village, Salonga National Park, Tshuapa Province, central DRC (2.0526°S, 21.3832°E, 455 m a.s.l.) on October 23, 2023 (Fig. 1C, D). The male, after recording its advertisement call, was collected, euthanized, and its muscle tissue sample was stored in 96% ethanol.

DNA barcoding

Species identities of the two samples were verified via DNA barcoding (Vences et al. 2012). Total genomic DNA was extracted using GeneJet Genomic Purification Kit (Thermo Fisher Scientific, USA). Fragments of the 16S rRNA gene (hereinafter *16S*) of mitochondrial DNA were amplified using polymerase chain reaction and the 16SL1 (forward) and 16SH1 (reverse) primers for the IVB-H-CD14-034 sample (Palumbi et al. 1991; 539 bp), and 16Sc (forward) and 16Sd (reverse) primers for the IVB-H-CD23-0847 sample (Evans et al. 2003; 871 bp) [note: 16SH1 and 16Sd bind to the same region]. Obtained *16S* sequences were compared with publicly available data (GenBank) using the BLAST search tool (Altschul et al. 1990). The most similar data were downloaded, aligned with our new data, and uncorrected *p*-distances were calculated using MEGA v. 11.0.13 (Tamura et al. 2021) after the complete deletion of gaps and missing data (Dolinay et al. 2021), resulting in 446 homologous sites. The newly generated sequences were deposited in the GenBank online database (IVB-H-CD14-034: PQ351303; IVB-H-CD23-0847: PQ351304.

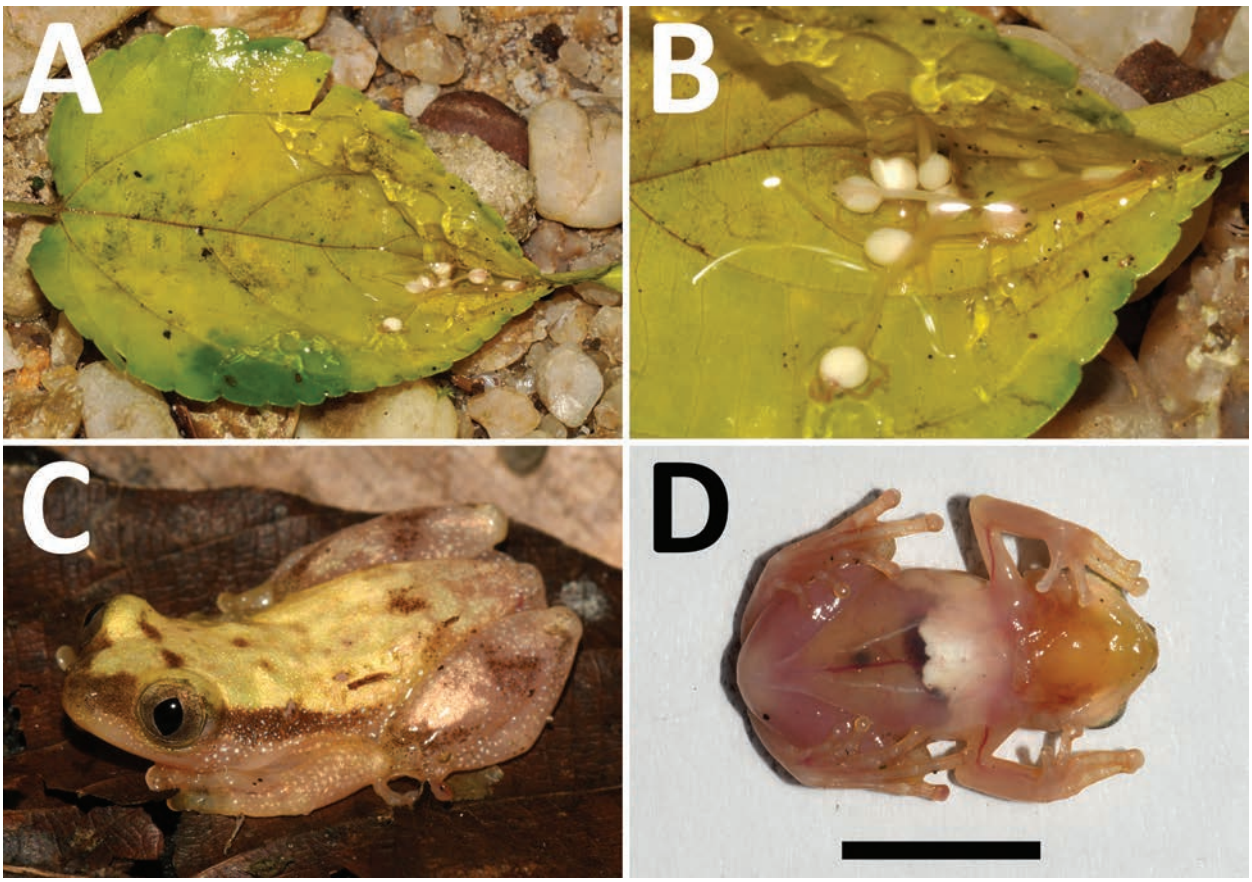

Figure 1. *Afrixalus lacustris* **A, B** clutch with developing larvae, DNA barcoded (IVB-H-CD14-034), found in a folded leaf near Bafwabianga village, Tshopo Province, DRC. The leaf was picked, opened and photographed on the ground **C, D** adult male (IVB-H-CD23-0847) from near Isandja-Bomongili village, Salonga National Park, Tshuapa Province, DRC, in day-time coloration from dorsolateral and ventral view, the black bar corresponds to 10 mm.

Phylogenetic analysis

To construct the phylogenetic tree, we used the same methodological approach as Greenbaum et al. (2022), reflecting their population-level divergence dating analysis, supplemented with our new data (Table 1). The analysis was performed on a 902 bp-long alignment using BEAST 1.10.4 (Suchard et al. 2018), GTR substitution model, coalescent tree prior, constant size growth prior, and a strict molecular clock set to 0.02 substitution/site per million years (Greenbaum et al. 2022). The analysis was run in triplicates for 10 million generations each, with sampling every 1000th generation. The first 10% were discarded as burn-in, after convergence and effective sample size values were inspected using Tracer v. 1.7.2 (Rambaut et al. 2018), and a maximum clade credibility tree with median heights was created from the remaining post-burn-in 27,000 combined trees using LogCombiner 1.10.4 and TreeAnnotator 1.10.4 (Suchard et al. 2018).

Acoustic recording and analysis

The advertisement call of the male (IVB-H-CD23-0847; snout-vent length, SVL = 21 mm) was recorded on a hand-held recorder Zoom H5 using a shotgun microphone Zoom SGH-6. The recording was obtained at 20:15 at 23.7 °C ambient temperature from a distance of 2–3 meters. The analysis of the recording was

Table 1. Origin of the *16S* sequences used in the dating analysis. Holotypes in bold. Abbreviations, collections: IVB-H (Institute of Vertebrate Biology of the Czech Academy of Sciences, Brno, herpetological collection Studenec, Czech Republic), UTEP (University of Texas at El Paso Biodiversity Collections, USA), CSB:Herp (Biodiversity Monitoring Center at University of Kisangani, herpetological collection, DRC), CAS (California Academy of Sciences, San Francisco, USA), ZFMK (Zoologisches Forschungsmuseum Alexander Koenig, Bonn, Germany); haplogroups: L (lowland), AR (Albertine Rift), N (north), S (south), C (central), NE (northeast); subgroups (a, b) of the AR-N haplogroup in parentheses.

Afrixalus	Collection No.	Locality	Haplogroup	*16S* GenBank	Reference
A. lacustris	IVB-H-CD14-034	DRC: Dalangba Forest, near Bafwabianga village	L-NE	PQ351303	This study
A. lacustris	IVB-H-CD23-0847	DRC: Isandja-Bomongili, Salonga National Park	L-C	PQ351304	This study
A. lacustris	**UTEP 20805**	DRC: Kalundu	AR-S	ON705200	Greenbaum et al. (2022)
A. lacustris	UTEP 20809	DRC: Baraka, Lake Tanganyika	AR-S	ON705201	Greenbaum et al. (2022)
A. lacustris	UTEP 22422	DRC: Baraka, Lake Tanganyika	AR-S	ON705204	Greenbaum et al. (2022)
A. lacustris	UTEP 22424	DRC: Itombwe Plateau, Mbandakila	AR-S	ON705217	Greenbaum et al. (2022)
A. lacustris	UTEP 22423	DRC: Kahuzi-Biega, Nanwa	AR-C1	PQ351598†	Greenbaum et al. (2022)
A. lacustris	UTEP 20810	DRC: Irangi	AR-C2	ON705199	Greenbaum et al. (2022)
A. lacustris	UTEP 22417	DRC: Toyokana	AR-N (a)	ON705198	Greenbaum et al. (2022)
A. lacustris	CSB:Herp:EPLU395	DRC: Epulu	AR-N (a)	ON705216	Greenbaum et al. (2022)
A. lacustris	UTEP 22416	Uganda: Bwindi, Buhoma	AR-N (a)	ON705206	Greenbaum et al. (2022)
A. lacustris	CAS 202036	Uganda: Bwindi, 2 km S of Bizenga River (by Buhoma rd.)	AR-N (a)	ON705208	Greenbaum et al. (2022)
A. lacustris	CAS 256035	Uganda: Bwindi, rd. N of Ruhija	AR-N (a)	ON705205	Greenbaum et al. (2022)
A. lacustris	DFH 1102*	Uganda: Kibale Forest, Ngogo Research Center	AR-N (b)	ON705203	Greenbaum et al. (2022)
A. lacustris	DFH 1103*	Uganda: Kibale Forest, Ngogo Research Center	AR-N (a)	ON705202	Greenbaum et al. (2022)
A. lacustris	CAS 256128	Uganda: Mabira Forest	AR-N (b)	ON705209	Greenbaum et al. (2022)
A. lacustris	CAS 256129	Uganda: Mabira Forest	AR-N (b)	ON705210	Greenbaum et al. (2022)
A. lacustris	CAS 256130	Uganda: Mabira Forest	AR-N (a)	MK509679	Portik et al. (2019)
A. lacustris	CAS 256131	Uganda: Mabira Forest	AR-N (b)	ON705207	Greenbaum et al. (2022)
A. phantasma	**ZFMK 103454**	Rwanda: Gishwati Forest	—	ON705212	Greenbaum et al. (2022)
A. phantasma	ZFMK 103455	Rwanda: Gishwati Forest	—	ON705211	Greenbaum et al. (2022)
A. phantasma	UTEP 20802	DRC: Kahuzi-Biega, ca. 4 km NW of Lwiro	—	ON705215	Greenbaum et al. (2022)
A. phantasma	UTEP 20803	DRC: Kahuzi-Biega, Mugaba	—	ON705214	Greenbaum et al. (2022)
A. phantasma	UTEP 20791	DRC: Nyakasanza Swamp near Tshibati	—	ON705213	Greenbaum et al. (2022)

†Submitted by T. Nečas, on behalf of Greenbaum et al. (2022).
*Field No. (Daniel F. Hughes), photos and tissues only (Greenbaum et al. 2022).

performed in SoundRuler v. 0.9.6 (Gridi-Papp 2007) and Raven Lite v. 2.0.5 (The Cornell Lab of Ornithology, Ithaca). The terminology of acoustic parameters is following Köhler et al. (2017). The recording was deposited in the FonoZoo online database with the reference number 14858 (https://www.fonozoo.com).

Results and discussion

Distribution and phylogeography

Due to the existence of the isolated record from Sankuru, some distribution maps of "*A. laevis*" sensu lato have shown the range as continuous from Cameroon, across the Congo, to southwestern Uganda (IUCN SSC Amphibian Specialist Group 2013; Channing and Rödel 2019). However, in reality, the range was always known as composed of two disjunct areas in the west (Cameroon, Gabon; *A. laevis* sensu stricto) and east (DRC, Rwanda, Uganda; *A. lacustris*, *A. phantasma*), with the Sankuru record located in between but closer to the eastern area (Schiøtz 1999). Greenbaum et al. (2022) assigned the Sankuru specimens to *A. lacustris*, but with a note that this population requires additional scrutiny with molecular data.

In this study, we present two new records of *A. lacustris* substantially extending its distribution in the Congo Basin westward into lowland rainforests, as the BLAST comparisons of *16S* retrieved *A. lacustris* as the most similar species for both our samples of "*Afrixalus* cf. *laevis*" (Fig. 2A, B). The IVB-H-CD14-034 sample was found to differ from the previously published *A. lacustris 16S* data by 1.5% uncorrected *p*-distance, the IVB-H-CD23-0847 sample differed by 1.9%, and the two samples differ from each other by 2.0%, which do not reach the 3% threshold suggested for identifying a potential candidate species in anurans (Vieites et al. 2009). The dated phylogenetic reconstruction performed on *16S* (Fig. 2B) shows a very similar topology to that of Greenbaum et al. (2022) although with slightly younger age estimates. The split between *A. lacustris* and its sister species *A. phantasma* is estimated to have occurred 1.11 million years ago, Mya (0.74–1.51 Mya, 95% highest posterior densities, HPD) during the Early Pleistocene (Calabrian). Six distinct mitochondrial lineages (haplogroups) with uncertain relationships are identified within *A. lacustris*, which originated during the Middle Pleistocene (Chibanian; Fig. 2B, C, Table 1). The first divergent lineage is represented by the single sample IVB-H-CD23-0847 from the Central Congolian Lowland Forests (L-C haplogroup). Its divergence is estimated to have occurred ~650 thousand years ago (hereinafter as kya; 400–970 kya) at the beginning of the Middle Pleistocene. The second diverging lineage consists of a population inhabiting the Albertine Rift in the south of the *A. lacustris* range (Itombwe Plateau, DRC, and its vicinity; AR-S haplogroup), from where the holotype originates. Diversification within the AR-S haplogroup is estimated to have occurred ~150 kya (50–280 kya), roughly corresponding with the beginning of the Late Pleistocene. The third lineage is a single sample from Kahuzi-Biega, DRC (UTEP 22423; AR-C1 haplogroup). The fourth and fifth lineages form a common clade (although with low support) and are represented by a sample from Irangi, DRC (near Kahuzi-Biega; UTEP 20810, AR-C2 haplogroup), and the sample IVB-H-CD14-034 from the lowland Dalangba Forest in northeastern Tshopo Province, DRC (L-NE haplogroup), respectively. The sixth mitochondrial lineage consists of samples from southwestern Uganda and adjacent DRC (haplogroup AR-N). Diversification within the AR-N haplogroup is estimated to have occurred ~210 kya (110–360 kya), at the end of the Middle Pleistocene. Two subgroups (a, b), with their diversifications corresponding with the beginning of the Late Pleistocene, are detectable in the AR-N haplogroup, but they have only weak supports (Fig. 2B, Table 1). The two subgroups have partially sympatric distribution in Uganda, and one subgroup (AR-N (b)) has been found only in Uganda, suggesting that a forest refugium was probably located in this area during the Late Pleistocene. The diversification into the six main mitochondrial lineages (haplogroups) of *A. lacustris* can probably be attributed to Middle Pleistocene climatic fluctuations and their impact on the suitable forest environment, which has undergone repeated fragmentations (Maley 1996; Zachos et al. 2001). However, the lack of statistical support for the relationships among the six identified mitochondrial lineages prevents further discussion on the historical biogeography of this species.

The range extensions lie in two areas (Fig. 2A). The first site is located in the north of the known *A. lacustris* range in Tshopo Province, approximately 200 km westward from the nearest locality (Epulu, Ituri Province; Greenbaum et al. 2022). The second site is situated in the south of the *A. lacustris* range, near the northern bloc of Salonga National Park in Tshuapa Province, and lies approximately 260 km to the northwest of the isolated record from Omaniundu

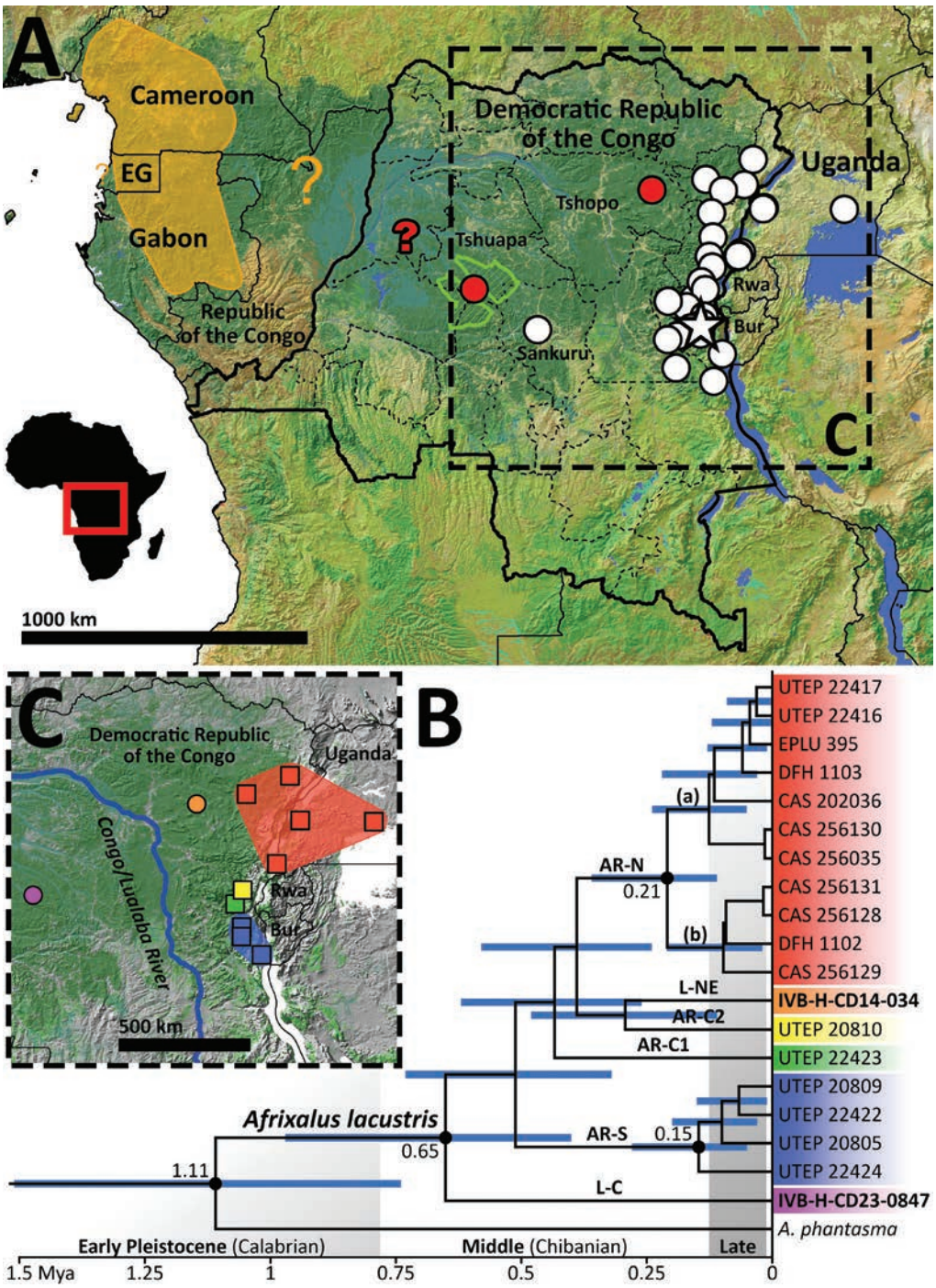

Figure 2. A map of all known distribution sites of *Afrixalus lacustris*. Red symbols mark new localities presented in this study; the red question mark denotes Boteka – a site in need of verification, where "*A. laevis*" was collected. Green polygons mark Salonga National Park. White symbols denote previously known localities of *A. lacustris* summarized by Greenbaum et al. (2022); the white star corresponds to the type locality. Orange polygons show the known distribution range of *A. laevis*, questionable areas are marked with orange question marks. EG = Equatorial Guinea, Rwa = Rwanda, Bur = Burundi **B** phylogenetic tree and **C** phylogeographic map of *A. lacustris* based on Greenbaum et al. (2022) with the addition of our new data (in bold). Black dots indicate highly supported nodes, numbers at nodes denote estimated divergence time (Mya), and blue bars denote 95% HPD intervals. A single representative of *A. phantasma* is shown as an outgroup. Haplogroups are distinguished by different colors and abbreviations placed on the branches (see Distribution and phylogeography, and Table 1). The maps were created in ArcGIS v. 10.8.1 (Esri Inc., https://www.esri.com), with land cover visualized by implementing results of the GlobCover project (Arino et al. 2012), and country and provincial boundaries and shaded relief background downloaded from https://naturalearthdata.com.

in Sankuru Province (Laurent 1982). The discussed record from Omaniundu (as "*A. laevis*" in Laurent 1982), with specimens exhibiting partly distinct morphology (Greenbaum et al. 2022), thus probably indeed represents *A. lacustris*. Our two new records suggest that *A. lacustris* is probably rather widespread in the Northeastern and Central Congolian Lowland Forests. However, the paucity of its findings in the field—we had failed to find this species during every year of fieldwork between 2015 to 2022—confirms that *A. lacustris* hides excellently in the foliage of shrubs in dense forests, which explains why this species has not been detected in many areas despite its wide geographic distribution (Laurent 1982; Greenbaum et al. 2022). *Afrixalus laevis* sensu stricto is similarly difficult to find (Greenbaum et al. 2022) and its southeastern extent is not well known. Besides Bioko Island, it is with certainty confirmed from Cameroon and Gabon (Greenbaum et al. 2022 and citations therein), but possibly extending deeper into the Congolian rainforests (Frost 2024). Unpublished data from the "Museum" database of the Royal Museum for Central Africa, which remains to be properly examined, indicate that "*A. laevis*" was also collected in 1985 in Boteka, Équateur Province, DRC (approx. 0.40°S, 19.11°E, 320 m a.s.l.). Whether this record represents an even more westward range extension of *A. lacustris*, an eastward extension of *A. laevis*, or potentially a new species, must yet be investigated.

Oviposition type

The earlier larval sample (Fig. 1A, B) provides an important view into the reproductive biology of *A. lacustris*, as it uncovers that this species folds leaves to make a nest for its egg clutch. This is in line with its phylogenetic position, which is deeply divergent from its morphological convergent, *A. laevis*, which deposits eggs on leaf surfaces without folding the leaf (e.g., Amiet 2012). However, it is not known with certainty, besides the sister species *A. phantasma*, which other species are the most closely related to *A. lacustris*, whether the East African montane species *A. dorsimaculatus*, *A. morerei* and *A. uluguruensis*, or West African to northern Central African *A. weidholzi*, or *A. orophilus* from the Albertine Rift (Portik et al. 2019; Greenbaum et al. 2022; Nečas et al. 2022). *Afrixalus dorsimaculatus* and *A. uluguruensis* do not enfold egg masses in leaves, similar to *A. laevis*; *A. weidholzi* glues leaf edges into a nest during oviposition, while it is probably not known in *A. morerei* and *A. orophilus* (Harper and Vonesh 2002; Harper et al. 2010; Channing and Rödel 2019; Dehling et al. 2023).

Advertisement call

The second sample provides DNA-based identification of the calling male (SVL = 21 mm), which was initially found on a *Ficus* tree around 1.5–2 m above the ground, then disturbed, escaped and re-found on the top of the tree about 3 m above the swampy ground (Figs 1C, D, 3D). The advertisement call consists of four to five pulsed notes (4.8 mean for 37 measured calls of the single found male; Fig. 3A–C). Each note consists of 10 or 11 pulses, but the pulsation towards the end of the note was often obscured in the waveforms. Call duration in *A. lacustris* averages at 210 ms (195–220 ms, only five-note calls measured, N = 31; 167 ms average for four-note calls, N = 6; 23.7 °C). In the sister species *A. phantasma*, Greenbaum et al. (2022) documented longer durations of five-note

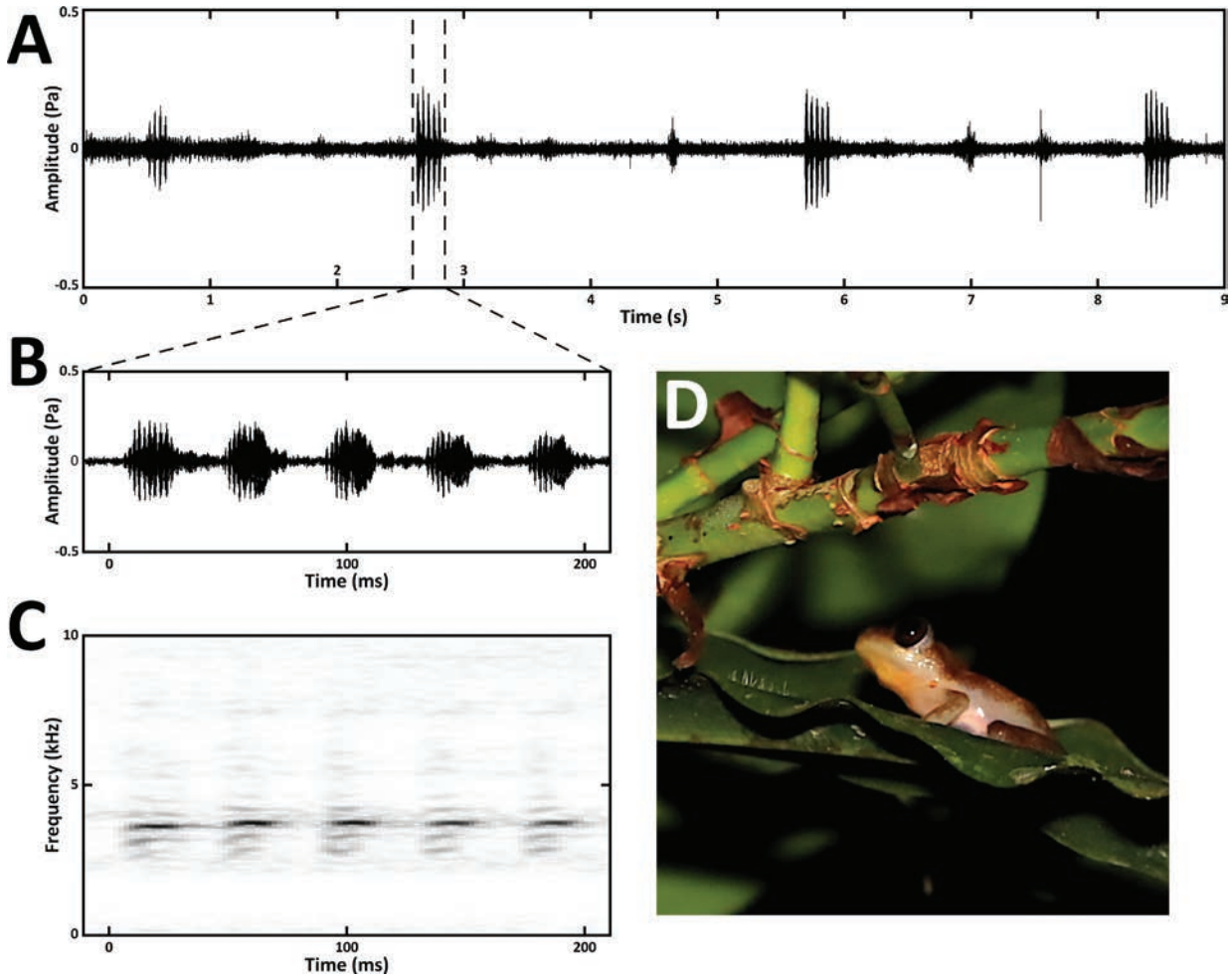

Figure 3. *Afrixalus lacustris* and its advertisement call **A** part of a call series (oscillogram, 9 s), with ambient frog chorus in the background **B** oscillogram of a five-note advertisement call **C** spectrogram of the respective call **D** the recorded male *A. lacustris* (IVB-H-CD23-0847) in nocturnal coloration in situ, perching on a leaf from where it was calling.

calls (they reported five to six, rarely four notes per call), however their recordings were made in montane habitats at substantially lower temperatures with a trend of shortening call duration with increasing temperature (from 572–620 ms at 10.9 °C to 388–397 ms at 16.2 °C, five-note calls only). If we consider this trend in *A. phantasma*, our recording of *A. lacustris* made at 23.7 °C approximately fits with the mean call duration of 210 ms to a theoretically expected value in *A. phantasma* at the same temperature. The mean dominant frequency 3720 kHz (3627–3795 kHz) of *A. lacustris* is similar to the dominant frequency of *A. phantasma*, as measured at the higher temperature (3660–3810 kHz, 16.2 °C). Greenbaum et al. (2022) also observed a similarly obscured pulsation in the rear part of notes in *A. phantasma*, discussed as probably caused by echo effects. However, as we found a similar veiling in *A. lacustris*, and a similar characteristic was found in most of the notes in *A. orophilus* (Dehling et al. 2023), it is possibly a normal characteristic of the advertisement call in these species. In general, the advertisement calls of *A. lacustris* and *A. phantasma* are very similar, which is not surprising in sister species of frogs with parapatric distribution (see e.g. Gvoždík et al. 2015).

When we compare the advertisement call of *A. lacustris* with *A. laevis* (Amiet and Goutte 2017), with which it was previously confused, the general characteristics of the calls are quite different. Thus, the morphological convergence is not

mirrored in the phonetic parameters, which might be related to partially different habitats. For example, reproduction of *A. lacustris* may occur more frequently in stagnant waters, whereas that of *A. laevis* in streams. If the advertisement call of *A. lacustris* is compared with other potentially closely related species (*A. dorsimaculatus*, *A. morerei*, *A. orophilus*, *A. uluguruensis*, *A. weidholzi*; Portik et al. 2019; Greenbaum et al. 2022; Nečas et al. 2022), none of them displays a substantial similarity of their advertisement calls; perhaps only *A. weidholzi* has partially similar call characteristics (Schiøtz 1999; Amiet and Goutte 2017; Dehling et al. 2023).

Ecology and natural history

Despite our relatively intense fieldwork in the Congolian lowland rainforests during last 10 years (especially GB), we have found *A. lacustris* only twice, in two distant areas in Tshopo and Tshuapa provinces, in both cases based on single findings – one clutch with larvae and a single calling male. In the first case (Tshopo), the habitat was dense vegetation overhanging a drying muddy place near a sandy-bottomed stream in primary forest, where also small rainwater pools and puddles were present nearby, as well as a large river (Lindi; Fig. 4A). In the second case (Tshuapa), the habitat was a small drying swamp in a forest opening, located near a forest edge (local guides informed us that the swamp is much larger, potentially connected with flooded forest, after heavy rains; Fig. 4B). In both cases, habitats were in accordance with the *A. lacustris* habitat description of Greenbaum et al. (2022). Among sympatric amphibians, we found in Tshopo: Arthroleptidae: *Arthroleptis* sp. aff. *variabilis*, *Arthroleptis tuberosus* Andersson, 1905; Hyperoliidae: *Hyperolius bolifambae* Mertens, 1938, *H. langi* Noble, 1924, *H. ocellatus* Günther, 1858; Pipidae: *Xenopus pygmaeus* Loumont, 1986, *X. ruwenzoriensis* Tymowska & Fischberg, 1973; Ptychadenidae: *Ptychadena christyi* (Boulenger, 1919); Ranidae: *Amnirana* cf. *albolabris* (Hallowell, 1856); and in Tshuapa: Arthroleptidae: *Arthroleptis* sp. aff. *variabilis*, *Leptopelis christyi* (Boulenger, 1912); Hyperoliidae: *Hyperolius* cf. *kuligae* Mertens, 1940 (eggs only), *H.* cf. *veithi* Schick, Kielgast, Rödder, Muchai, Burger & Lötters, 2010; Phrynobatrachidae: *Phrynobatrachus* sp. aff. *auritus*; Pipidae: *Hymenochirus* cf. *boettgeri* (Tornier, 1896), *Xenopus pygmaeus*; Ptychadenidae: *Ptychadena aequiplicata*

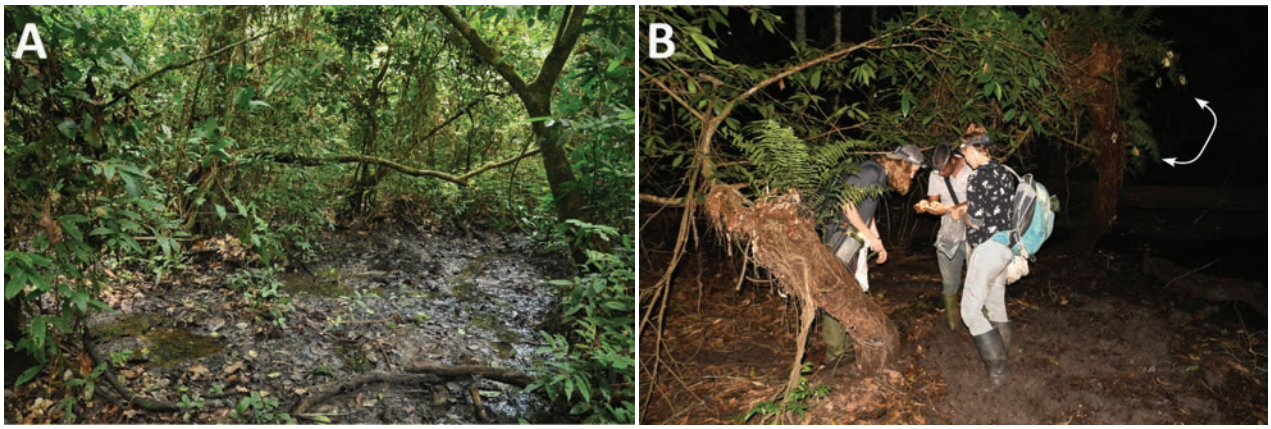

Figure 4. Habitats of *Afrixalus lacustris* in the Congolian lowland rainforests **A** Dalangba Forest, near Bafwabianga village, Tshopo Province, northeastern DRC **B** Isandja-Bomongili, Salonga National Park, Tshuapa Province, central DRC; junior authors after the finding of *A. lacustris*; note foam nests of *Chiromantis* cf. *rufescens* (white double arrow).

(Werner, 1898); Ranidae: *Amnirana* cf. *albolabris*; Rhacophoridae: *Chiromantis* cf. *rufescens* (Günther, 1869) (taxonomy and nomenclature follow Badjedjea et al. 2022). *Hyperolius* spp. at both sites and *Chiromantis* cf. *rufescens* were found with *A. lacustris* in syntopy on the same or nearby shrubs.

Conclusions

Afrixalus lacustris is more widespread in lowland rainforests than previously thought. This suggests that the eastern Congolian fauna may be more widespread in the Central Congolian Lowland Forests. The lowland populations of *A. lacustris* are representatives of distinct evolutionary lineages that probably diversified in isolated forest refugia during the Middle Pleistocene. Along with the sister species *A. phantasma*, from which *A. lacustris* diverged during the Early Pleistocene, the Tanzanian montane species *A. dorsimaculatus* and *A. uluguruensis* are probably the most closely related species (Portik et al. 2019; Greenbaum et al. 2022) but are among the few exceptions in *Afrixalus* that lay eggs on the leaf surface and do not form nests. Here, we demonstrate that *A. lacustris* oviposits in folded leaves, as is common in most species of the genus. The advertisement call of *A. lacustris* has a similar structure to that of its parapatrically distributed sister species *A. phantasma*, whereas *A. dorsimaculatus* and *A. uluguruensis* have somewhat different calls. However, to better understand the evolution of reproductive behavior with respect to leaf-nest formation, as well as the evolution of advertisement calls, it is first necessary to better understand the species diversity of *Afrixalus* and the interspecific phylogenetic relationships, which are still not sufficiently known.

Acknowledgements

We would like to thank Institut Congolais pour la Conservation de la Nature (ICCN) for the authorization of our research, the ICCN staff of Salonga National Park for help and logistical assistance, and local authorities in Bafwabianga and Isandja-Bomongili villages for allowing us access to their areas. Further, thanks belong to D. Meirte for access to unpublished data from the “Museum” database of the Royal Museum for Central Africa.

Additional information

Conflict of interest

The authors have declared that no competing interests exist.

Ethical statement

No ethical statement was reported.

Funding

This study was funded by the Czech Science Foundation (23-07331S) and the Ministry of Culture of the Czech Republic (DKRVO 2024–2028/6.I.b, National Museum of the Czech Republic, 00023272), GB was supported by the International Foundation for Science (IFS # D-6074-2), and JC by the Masaryk University (MUNI/A/1489/2023).

Author contributions

Conceptualization: VG, TN. Data curation: TN, VG. Formal analysis: TN. Funding acquisition: VG, GB, JC. Investigation: TN, GB, JC, VG. Methodology: TN, VG. Project administration: VG. Resources: VG. Supervision: VG. Validation: VG. Visualization: TN, VG. Writing - original draft: VG, TN. Writing - review and editing: TN, GB, JC, VG.

Author ORCIDs

Tadeáš Nečas https://orcid.org/0000-0002-5060-8394
Gabriel Badjedjea https://orcid.org/0000-0003-4284-4327
Janis Czurda https://orcid.org/0009-0000-9151-3482
Václav Gvoždík https://orcid.org/0000-0002-4398-4076

Data availability

All of the data that support the findings of this study are available in the main text and public databases.

References

Altschul SF, Gish W, Miller W, Myers EW, Lipman DJ (1990) Basic local alignment search tool. Journal of Molecular Biology 215: 403–410. https://doi.org/10.1016/S0022-2836(05)80360-2

Amiet J-L (2009) Observations sur les *Afrixalus* du Cameroun (Amphibia, Anura, Hyperoliidae). Revue suisse de Zoologie, 116: 53–92. https://doi.org/10.5962/bhl.part.79490

Amiet J-L (2012) Les Rainettes du Cameroun (Amphibiens Anoures). J.-L. Amiet & La Nef des Livres, Nyons-Saint-Nazaire, 591 pp.

Amiet J-L, Goutte S (2017) Chants d'Amphibiens du Cameroun. J.-L. Amiet & Editions Petit Génie, Nyons-Saint-Nazaire, 280 pp.

Arino O, Ramos Perez JJ, Kalogirou V, Bontemps S, Defourny P, Van Bogaert E (2012) Global Land Cover Map for 2009 (GlobCover 2009). European Space Agency (ESA) & Université catholique de Louvain (UCL), PANGAEA. https://doi.org/10.1594/PANGAEA.787668

Badjedjea G, Masudi FM, Dudu Akaibe B, Gvoždík V (2022) Amphibians of Kokolopori: an introduction to the amphibian fauna of the Central Congolian Lowland Forests, Democratic Republic of the Congo. Amphibian & Reptile Conservation 16: 35–70.

Burgess N, Hales JDA, Underwood E, Dinerstein E, Olson D, Itoua I, Schipper J, Ricketts T, Newman K (2004) Terrestrial Ecoregions of Africa and Madagascar. A Conservation Assessment. Island Press, Washington DC, 497 pp.

Channing A, Rödel M-O (2019) Field Guide to the Frogs and Other Amphibians of Africa. Struik Nature, Cape Town, 408 pp.

Conradie W, Keates C, Lobón-Rovira J, Vaz Pinto P, Verburgt L, Baptista NL, Harvey J, Júlio T (2020) New insights into the taxonomic status, distribution and natural history of De Witte's Clicking Frog (*Kassinula wittei* Laurent, 1940). African Zoology 55: 311–322. https://doi.org/10.1080/15627020.2020.1821771

Dehling JM, Mindje M, Dumbo B, Hinkel H, Hinkel H, Sinsch U (2023) Advertisement call and notes on the ecology of *Afrixalus orophilus* (Anura: Hyperoliidae) in Rwanda. Salamandra 59: 102–105.

Dolinay M, Nečas T, Zimkus BM, Schmitz A, Fokam EB, Lemmon EM, Lemmon AR, Gvoždík V (2021) Gene flow in phylogenomics: Sequence capture resolves species limits and

biogeography of Afromontane forest endemic frogs from the Cameroon Highlands. Molecular Phylogenetics and Evolution 163: 107258. https://doi.org/10.1016/j.ympev.2021.107258

Evans BJ, Brown RM, McGuire JA, Supriatna J, Andayani N, Diesmos A, Iskandar D, Melnick DJ, Cannatella DC (2003) Phylogenetics of Fanged Frogs: Testing Biogeographical Hypotheses at the Interface of the Asian and Australian Faunal Zones. Systematic Biology 52: 794–819. https://doi.org/10.1080/10635150390251063

Frost DR (2024) Amphibian Species of the World: an Online Reference. Version 6.2. [13th May 2024]

Greenbaum E, Portik DM, Allen KE, Vaughan ER, Badjedjea G, Barej MF, Behangana M, Conkey N, Dumbo B, Gonwouo LN, Hirschfeld M, Hughes DF, Igunzi F, Kusamba C, Lukwago W, Masudi FM, Penner J, Reyes JM, Rödel M-O, Roelke CE, Romero S, Dehling JM (2022) Systematics of the Central African Spiny Reed Frog *Afrixalus laevis* (Anura: Hyperoliidae), with description of two new species from the Albertine Rift. Zootaxa 5174: 201–232. https://doi.org/10.11646/zootaxa.5174.3.1

Gridi-Papp M (2007) SoundRuler: acoustic analysis for research and teaching. https://www.soundruler.sourceforge.net (accessed 21 February 2024). Electronic database accessible at https://amphibiansoftheworld.amnh.org/index.php. American Museum of Natural History, New York, U. S. A. https://doi.org/10.5531/db.vz.0001

Gvoždík V, Canestrelli D, García-París M, Moravec J, Nascetti G, Recuero E, Teixeira J, Kotlík P (2015) Speciation history and widespread introgression in the European short-call tree frogs (*Hyla arborea* sensu lato, *H. intermedia* and *H. sarda*). Molecular Phylogenetics and Evolution 83: 143–155. https://doi.org/10.1016/j.ympev.2014.11.012

Harper E, Vonesh JR (2002) Field Guide to the Amphibians of the East Usambara Mountains. Preliminary Draft.

Harper EB, Measey GJ, Patrick DA, Menegon M, Vonesh JR (2010) Field Guide to the Amphibians of the Eastern Arc Mountains and Coastal Forests of Tanzania and Kenya. Camerapix Publishers International, Nairobi, 320 pp.

IUCN SSC Amphibian Specialist Group (2013) *Afrixalus laevis*. The IUCN Red List of Threatened Species 2013: e.T56067A18370863. https://doi.org/10.2305/IUCN.UK.2013-2.RLTS.T56067A18370863.en [accessed 9 April 2024]

Köhler J, Jansen M, Rodríguez A, Kok PJR, Toledo LF, Emmrich M, Glaw F, Haddad CFB, Rödel M-O, Vences M (2017) The use of bioacoustics in anuran taxonomy: theory, terminology, methods and recommendations for best practice. Zootaxa 4251: 1–124. https://doi.org/10.11646/zootaxa.4251.1.1

Laurent R (1982) Le genre *Afrixalus* Laurent (Hyperoliidae) en Afrique centrale. Annales du Musée Royal de l'Afrique Centrale. Tervuren, Belgique. Série in-8°, Sciences Zoologiques 235: 1–58.

Maley J (1996) The African rain forest – main characteristics of changes in vegetation and climate from the Upper Cretaceous to the Quaternary. Proceedings of the Royal Society of Edinburgh 104B: 31–73. https://doi.org/10.1017/S0269727000006114

Nečas T, Kielgast J, Nagy ZT, Kusamba Chifundera Z, Gvoždík V (2022) Systematic position of the Clicking Frog (*Kassinula* Laurent, 1940), the problem of chimeric sequences and the revised classification of the family Hyperoliidae. Molecular Phylogenetics and Evolution 174: 107514. https://doi.org/10.1016/j.ympev.2022.107514

Palumbi SR, Martin A, Romano S, McMillan WO, Stice L, Grabowski G (1991) The Simple Fool's Guide to PCR. University of Hawaii Press, Honolulu.

Portik DM, Bell RC, Blackburn DC, Bauer AM, Barratt CD, Branch WR, Burger M, Channing A, Colston TJ, Conradie W, Dehling JM, Drewes RC, Ernst R, Greenbaum E, Gvoždík V,

Harvey J, Hillers A, Hirschfeld M, Jongsma GFM, Kielgast J, Kouete MT, Lawson LP, Leaché AD, Loader SP, Lötters S, Van Der Meijden A, Menegon M, Müller S, Nagy ZT, Ofori-Boateng C, Ohler A, Papenfuss TJ, Rößler D, Sinsch U, Rödel MO, Veith M, Vindum J, Zassi-Boulou A-G, McGuire JA (2019) Sexual dichromatism drives diversification within a major radiation of African amphibians. Systematic Biology 68: 859–875. https://doi.org/10.1093/sysbio/syz023

Rambaut A, Drummond AJ, Xie D, Baele G, Suchard MA (2018) Posterior summarisation in Bayesian phylogenetics using Tracer 1.7. Systematic Biology 67: 901–904. https://doi.org/10.1093/sysbio/syy032

Schiøtz A (1999) Treefrogs of Africa. Edition Chimaira, Frankfurt am Main, 350 pp.

Suchard MA, Lemey P, Baele G, Ayres DL, Drummond AJ, Rambaut A (2018) Bayesian phylogenetic and phylodynamic data integration using BEAST 1.10. Virus Evolution 4: vey016. https://doi.org/10.1093/ve/vey016

Tamura K, Stecher G, Kumar S (2021) MEGA11: Molecular Evolutionary Genetics Analysis version 11. Molecular Biology and Evolution 38: 3022–3027. https://doi.org/10.1093/molbev/msab120

Vences M, Nagy ZT, Sonet G, Verheyen E (2012) DNA barcoding amphibians and reptiles. In: Kress WJ, Erickson DL (Eds) DNA Barcodes: Methods and Protocols. Methods in Molecular Biology, vol. 858, Humana Press, Totowa, 79–107. https://doi.org/10.1007/978-1-61779-591-6_5

Vieites D, Wollenberg KC, Andreone F, Köhler J, Glaw F, Vences M (2009) Vast underestimation of Madagascar's biodiversity evidenced by an integrative amphibian inventory. Proceedings of the National Academy of Sciences of the United States of America 106: 8267–8272. https://doi.org/10.1073/pnas.0810821106

Zachos J, Pagani H, Sloan L, Thomas E, Billups K (2001) Trends, rhythms, and aberrations in global climate 65 Ma to present. Science (Washington) 292: 686–693. https://doi.org/10.1126/science.1059412

ZooKeys 1224: 69–85 (2025)
DOI: 10.3897/zookeys.1224.138987

Research Article

Taxonomic notes on the genus *Yunohamella* Yoshida, 2007 (Araneae, Theridiidae) from China, with two new species

Rui Zhong[1], Yang Zhong[2], He Zhang[3,4], Jie Liu[5], Changyong Liu[6], Kuai Chen[6], Changhao Hu[1,7]

1 *State Key Laboratory of Biocatalysis and Enzyme Engineering & Centre for Behavioural Ecology & Evolution, School of Life Sciences, Hubei University, Wuhan 430062, Hubei, China*
2 *School of Nuclear Technology and Chemistry & Biology, Hubei University of Science and Technology, Xianning 437100, Hubei, China*
3 *Hebei Province Sweet Potato Breeding and Application Technology Innovation Center, Xingtai 054001, Hebei, China*
4 *Guo Shoujing Innovation College, Xingtai University, Xingtai 054001, Hebei, China*
5 *Hubei Key Laboratory of Regional Development and Environmental Response, Faculty of Resources and Environmental Science, Hubei University, Wuhan 430062, Hubei, China*
6 *Qizimeishan National Nature Reserve Administration, Xuan'en 445500, Hubei, China*
7 *Hubei Broad Nature Technology Service Co., Ltd., Wuhan 430079, Hubei, China*
Corresponding author: Changhao Hu (changhaohu1998@gmail.com)

Abstract

Four *Yunohamella* species are reported from Hubei Province, China, including two new species: *Y. gutenbergi* R. Zhong, J. Liu & Hu, **sp. nov.** (♂) and *Y. mohorovicici* R. Zhong, J. Liu & Hu, **sp. nov.** (♂). *Yunohamella jiugongensis* (Liu & Zhong, 2023), **comb. nov.** is transferred from the genus *Cryptachaea* Archer, 1946, and *Y. lyrica* (Walckenaer, 1841) is newly recorded from Hubei Province and is considered as a senior synonym of *Platnickina mneon* (Bösenberg & Strand, 1906).

Key words: Biodiversity, comb-foot spiders, morphology, new combination, synonym, taxonomy

Academic editor: Francesco Ballarin
Received: 10 October 2024
Accepted: 22 December 2024
Published: 21 January 2025

ZooBank: https://zoobank.org/BE2CD401-AB28-4488-8EE8-1457F94F92FB

Citation: Zhong R, Zhong Y, Zhang H, Liu J, Liu C, Chen K, Hu C (2025) Taxonomic notes on the genus *Yunohamella* Yoshida, 2007 (Araneae, Theridiidae) from China, with two new species. ZooKeys 1224: 69–85. https://doi.org/10.3897/zookeys.1224.138987

Introduction

Yunohamella Yoshida, 2007 is a small genus within the family Theridiidae Sundevall, 1833. To date, the genus contains eight described species (World Spider Catalog 2024), which are primarily distributed across the Eurasian continent, with four species recorded from China: *Y. gibbosa* Gao & Li, 2014, *Y. lyrica* (Walckenaer, 1841), *Y. serpatusa* (Guan & Zhu, 1993), and *Y. subadulta* (Bösenberg & Strand, 1906) (Zhu et al. 1993; Guan 2002; Yoshida 2007; Gao and Li 2014; Marusik and Logunov 2017; World Spider Catalog 2024). The first reported species of *Yunohamella* were originally classified in the genus *Theridion* Walckenaer, 1805. In 2001, Yoshida revised many species of *Theridion*. He described a new genus *Takayus* Yoshida, 2001 and designated two species groups in this genus, the *takayensis* group and the *yunohamensis* group, on the difference of the following characteristics: color of body, pattern on abdomen, scapus of epigynum, embolus and tegular apophysis of male palpus, and natural history. Yoshida (2007) later established the new genus *Yunohamella*

based on the *Takayus yunohamensis* group earlier designated by him (Yoshida 2001) and transferred three species from *Takayus* to *Yunohamella*.

Yunohamella is placed in the subfamily Theridiinae Sundevall, 1833, and its phylogenetic placement shows it to be a sister group of the former *Achaearanea* Strand, 1929 sensu lato, which now is recognized as the genera *Achaearanea*, *Campanicola* Yoshida, 2015, *Cryptachaea* Archer, 1946, *Nihonhimea* Yoshida, 2016, and *Parasteatoda* Archer, 1946 (Liu et al. 2016).

The Qizimeishan National Nature Reserve, in southwestern Hubei, is characterized by a karst landscape. The reserve boasts rich forest vegetation and complex topography, providing ideal habitats that support the diversity and proliferation of the flora and fauna. Spiders of this nature reserve were surveyed from 2023 to 2024. In the current paper, we describe two new species of the genus *Yunohamella* from Qizimeishan National Nature Reserve and provide additional two taxonomic amendments.

Materials and methods

The specimens examined in this study are deposited in the Centre for Behavioral Ecology and Evolution (**CBEE**), College of Life Sciences, Hubei University in Wuhan and School of Nuclear Technology and Chemistry and Biology, Hubei University of Science and Technology (**HUST**) in Xianning. Specimens were examined using an Olympus SZX7 stereo microscope. Photographs were taken with a Leica M205 C stereo microscope, and final multifocal images were produced with Helicon Focus v. 7.7.0. The male palp was examined and photographed after dissection. The epigyne was examined after being dissected from the spider's body. The epigyne was removed and treated in a warmed 0.1 mg/ml Protease K solution before study. All morphological measurements were calculated using a Leica M205 C stereo microscope. Eye diameters were taken at the widest point. Legs measurements are given as total length (femur, patella, tibia, metatarsus, tarsus). The terminologies used in figure legends follow Agnarsson (2004) and Agnarsson et al. (2007). All measurements were in millimeters (mm).

Abbreviations: **ALE** = anterior lateral eye; **AME** = anterior median eye; **BH** = basal haematodocha; **C** = conductor; **CD** = copulatory duct; **CHd** = cymbial hood; **CO** = copulatory opening; **E** = embolus; **EB** = embolic base; **FD** = fertilization duct; **MA** = median apophysis; **PLE** = posterior lateral eye; **PME** = posterior median eye; **S** = spermatheca; **SD** = sperm duct; **ST** = subtegulum; **T** = tegulum; **TA** = tegular apophysis; **I**, **II**, **III**, **IV** = legs I–IV.

Results

Taxonomy

Family Theridiidae Sundevall, 1833

Genus *Yunohamella* Yoshida, 2007

Type species. *Theridion yunohamense* Bösenberg & Strand, 1906 (= *Yunohamella yunohamensis*) from Japan.

Diagnosis. Species of *Yunohamella* are similar to those of *Takayus* (compare Figs 2A–D, 4A–D, 5C–E, 6C, D, 7D–F, 8A, B, 9D–F; Gao and Li 2014: figs 107–109; Marusik and Logunov 2017: figs 37–39; Lee and Kim 2021: figs 3E–G, 4A,B with Zhu 1998: figs 80B–E, 83B–E, 93B–E, 94B–E, 108B–E, 114B–F, 115B–E, 116B–E, 117B–E, 118B–E, 119B–E, 120B–D, 125B, C) in having a large tegulum and a small median apophysis, a conductor conjugating with tegulum. However, *Yunohamella* can be distinguished from *Takayus* by the following: embolus thin; tegular apophysis distinct; and epigyne without a pointed scapus or with a blunt scapus (vs embolus broad, tegular apophysis invisible before expanded, epigyne with a pointed scapus in *Takayus*).

Species of *Yunohamella* can be distinguished from *Theridion* (compare Figs 2A–D, 4A–D, 5C–E, 6C, D, 7D–F, 8A, B, 9D–F; Gao and Li 2014: figs 107–109; Marusik and Logunov 2017: figs 37–39; Lee and Kim 2021: figs 3E–G, 4A, B with Zhu 1998: figs 73B–E, 76B–E, 85B–E, 88B–E, 89B–D, 90B–E, 91B, C, 97B–E, 98B–E, 106B–E, 109B–E, 110B–D 123B–E, 124B–E) by the following: embolus short and straight; tegulum large; conductor conjugating with tegulum; epigyne without depression (vs embolus long and circular; tegulum not large; conductor separated; epigyne with a distinct depression in *Takayus*) (Yoshida 2007).

Species of *Yunohamella* can be distinguished from *Cryptachaea* (compare Figs 2D, 4D, 8A, B; Levi 1957: fig. 323 with Levi 1955: fig. 82) in having a median apophysis separated from the embolus and the present tegular apophysis (vs median apophysis attached to the embolus and tegular apophysis absent in *Cryptachaea*).

Distribution. Asia, Europe, North America.

***Yunohamella gutenbergi* R. Zhong, J. Liu & Hu, sp. nov.**

https://zoobank.org/C32395E0-14D0-4BD1-8E70-56C4D298B434

Figs 1, 2, 10

Type material. ***Holotype*** • male: China, Hubei Province: Enshi Tujia and Miao Autonomous Prefecture, Xuan'en County, Qizimeishan National Nature Reserve, Changtanhe Dong Autonomous Town, Shanyangxi; 30.08°N, 109.75°E; elev. 810 m; 3 July 2023; Changhao Hu & Mian Wei leg. (CBEE, QZMS01049).

Etymology. The species is named after the geophysicist "Beno Gutenberg" who found the "core-mantle discontinuity", the boundary between the mantle and the core of Earth.

Diagnosis. Males of *Y. gutenbergi* R. Zhong, J. Liu & Hu, sp. nov. can be distinguished from all congeners in having a unique 2-shaped curved sperm duct on the tegulum and a filiform, curved embolus (Fig. 2A–C). Females are unknown.

Description. Male (holotype) measurements: total length 2.37. Carapace 1.10 long, 0.94 wide. Abdomen 1.29 long, 0.90 wide. Eyes: AME 0.10, ALE 0.08, PME 0.07, PLE 0.08, AME–AME 0.07, AME–ALE 0.04, PME–PME 0.06, PME–PLE 0.08, AME–PME 0.10, ALE–PLE 0.00. Measurements of legs [leg II missing]: I — (2.98, —, —, —, —), III 4.09 (1.38, 0.30, 0.86, 1.05, 0.50), IV 5.12 (1.79, 0.32, 1.35, 1.36, 0.30).

Carapace round, brown, and with a narrow, trapezoid, black mark between head region and median furrow; radial furrow black. Sternum shaped like an inverted triangle and brown. Chelicerae and legs orange. Abdomen oval; dorsally black, with a longitudinal mark composed of white and red spots; venter

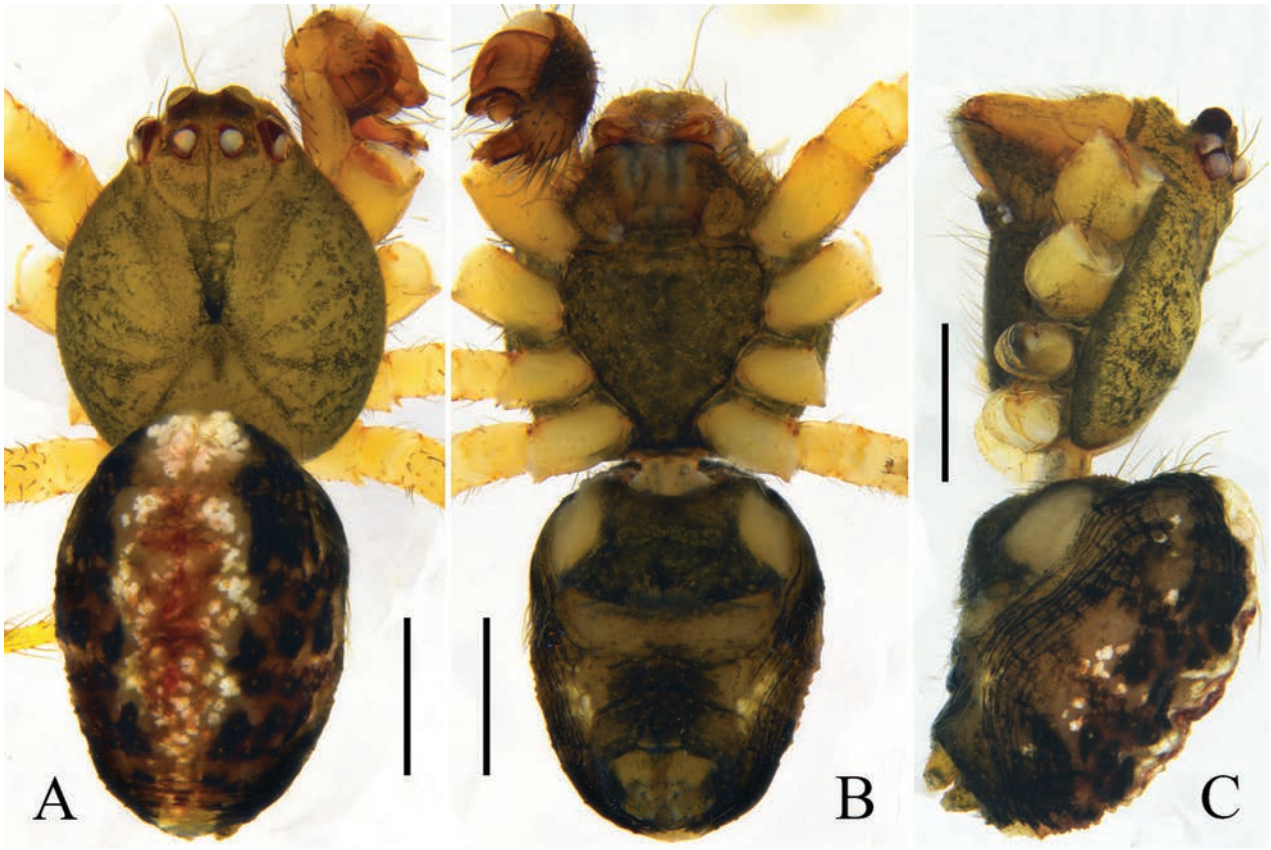

Figure 1. *Yunohamella gutenbergi* R. Zhong, J. Liu & Hu, sp. nov., male habitus. **A** dorsal view **B** ventral view **C** lateral view. Scale bars: 0.5 mm. (photos by Changhao Hu and Rui Zhong.)

dark brown; anterior part of genital groove and anterior part of spinnerets black; lateral abdomen with several white spots. Spinnerets dark brown (Fig. 1A–C).

Cymbium reniform**.** Cymbial hood longitudinal, almost ½ length of cymbium. Subtegulum bowl-shaped. Tegulum with a narrow prolateral part and a large retrolateral part; retrolateral part with a thin area that holds embolic base; sperm duct half surrounds thin area, and extends as 2-shaped, then straight down. Median apophysis lamellar. Tegular apophysis irregular. Length of median apophysis and tegular apophysis almost as long as width of bulb. Conductor sclerotized, with a triangular terminal apophysis. Embolus filiform and curved, with a lamellar base (Fig. 2A–D).

Female. Unknown.

Distribution. Known only from the type locality (Fig. 10).

***Yunohamella mohorovicici* R. Zhong, J. Liu & Hu, sp. nov.**

https://zoobank.org/8F92051B-B279-4121-AB6A-F37AD1FE3B27

Figs 3, 4, 10

Type material. ***Holotype*** • male: China, Hubei Province: Enshi Tujia and Miao Autonomous Prefecture, Xuan'en County, Qizimeishan National Nature Reserve, Changtanhe Dong Autonomous Town, Qizimeishan mountain; 30.03°N, 109.73°E; elev. 1270 m; 6 July 2023; Changhao Hu & Mian Wei leg. (CBEE, QZMS04642).

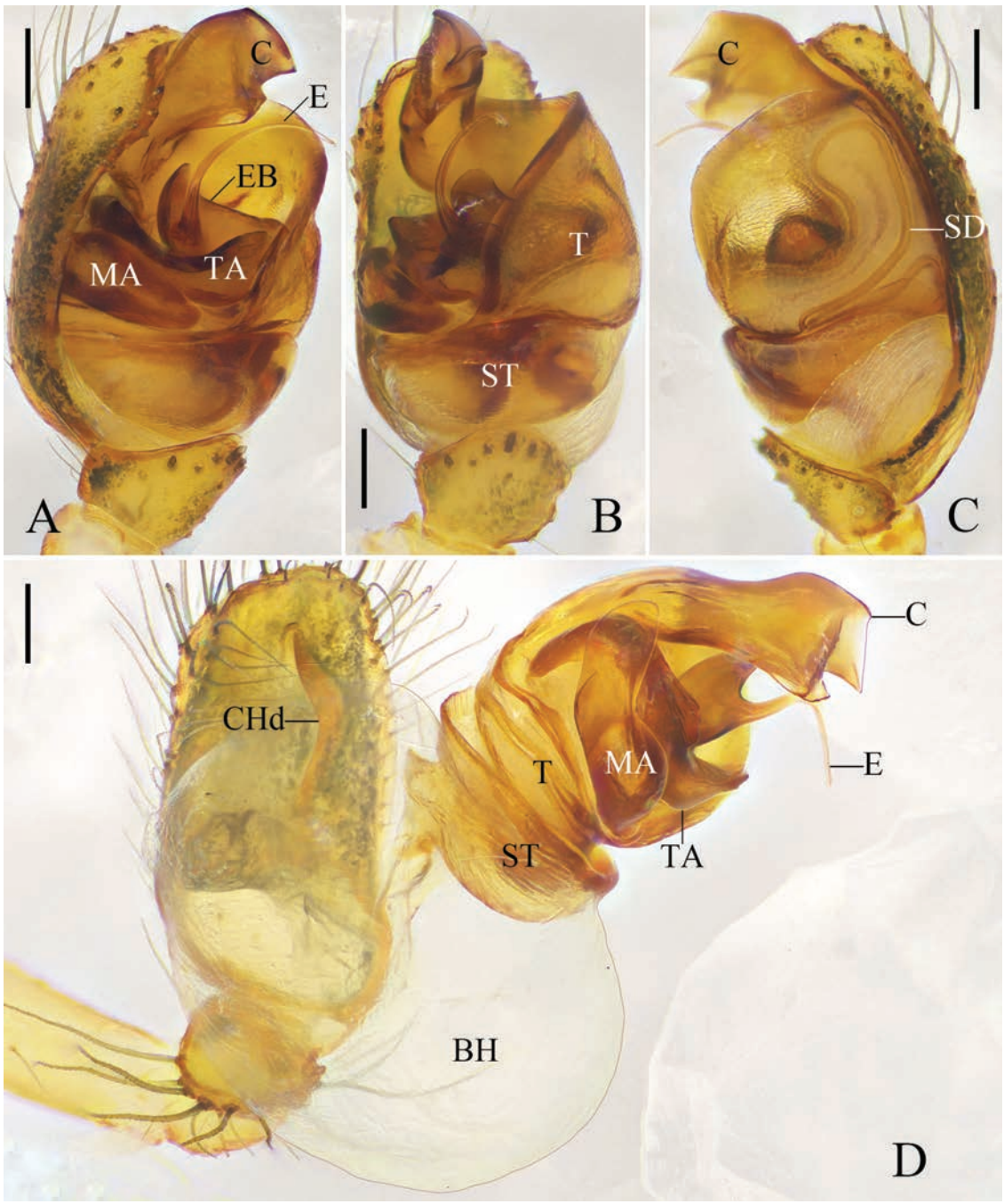

Figure 2. *Yunohamella gutenbergi* R. Zhong, J. Liu & Hu, sp. nov., left male palp. **A** prolateral view **B** ventral view **C** retrolateral view **D** expanded, ventral view. Scale bars: 0.2 mm. (Photos by Changhao Hu.)

Etymology. The species is named after the geophysicist "Andrija Mohorovičić" who found the "Moho discontinuity", the boundary between the crust and the mantle of Earth.

Diagnosis. Males of *Y. mohorovicici* sp. nov. are similar to those of *Y. jiugongensis* (Liu & Zhong, 2023) comb. nov. (compare Fig. 4A–C with Fig. 5C–E) in having an n-shaped sperm duct on the tegulum and a thick, curved embolus, but *Y. mohorovicici* can be distinguished from *Y. jiugongensis* by the following: sharp tooth-like apophysis on tegulum absent; and terminal conductor rounded (vs apophysis on tegulum present and terminal conductor knife-shaped in *Y. jiugongensis* comb. nov.). Males of *Y. mohorovicici* sp. nov. are also similar to those of *Y. palmgreni*

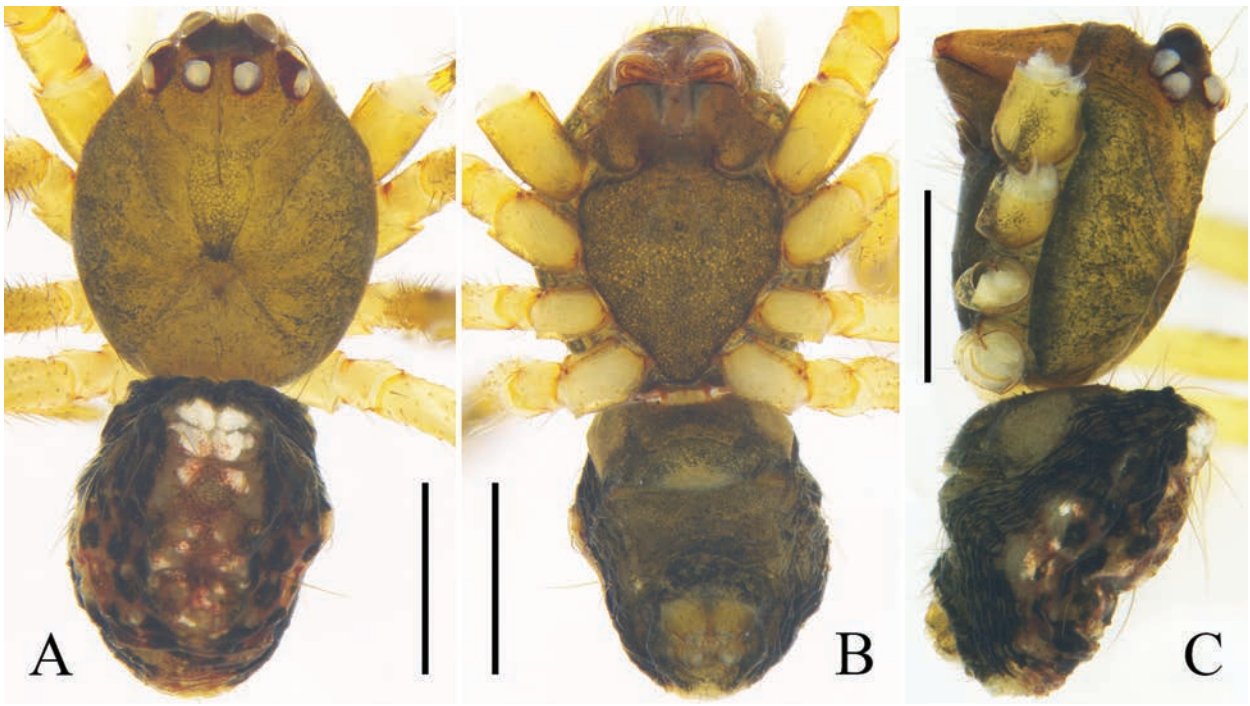

Figure 3. *Yunohamella mohorovicici* R. Zhong, J. Liu & Hu, sp. nov., male habitus. **A** dorsal view **B** ventral view **C** lateral view. Scale bars: 0.5 mm. (Photos by Changhao Hu and Rui Zhong.)

(Marusik & Tsellarius, 1986) (compare Fig. 4A–C with Marusik and Tsellarius 1986: figs 1, 2) in having an n-shaped sperm duct on the tegulum and a thick embolus, but *Y. mohorovicici* can be distinguished from *Y. palmgreni* by the following: conductor arising from the retrolateral part of the tegulum at the 2 o'clock position; and embolus curved (vs conductor arising from retrolateral part of the tegulum at the 12 o'clock position and embolus straight in *Y. palmgreni*). Females are unknown.

Description. Male (holotype), measurements: total length 1.77. Carapace 0.96 long, 0.77 wide. Abdomen 0.88 long, 0.65 wide. Eyes: AME 0.11, ALE 0.08, PME 0.07, PLE 0.07, AME–AME 0.06, AME–ALE 0.03, PME–PME 0.05, PME–PLE 0.08, AME–PME 0.05, ALE–PLE 0.01. Measurements of legs: I 6.80 (2.05, 0.37, 1.78, 1.92, 0.68), II 4.15 (1.29, 0.27, 0.99, 1.09, 0.51), III 2.70 (0.89, 0.19, 0.55, 0.67, 0.40), IV 3.66 (1.21, 0.25, 0.81, 0.95, 0.44). Leg formula: I-II-IV-III.

Carapace round, brown, with deep fovea and black radial furrow. Sternum shaped like an inverted triangle and brown. Labium brown. Chelicerae and endites orange. Legs yellow. Abdomen oval, with long hairs; dorsum black, with a longitudinal mark composed of white and red spots; venter brownish green; anterior part of spinnerets black; lateral abdomen with several white spots. Spinnerets brown (Fig. 3A–C).

Cymbium reniform**.** Cymbial hood tilted at 60°, almost ¼ length of cymbium. Subtegulum bowl-shaped. Tegulum with a narrow prolateral part and a large retrolateral part; retrolateral part with a thin area that holds embolic base; sperm duct narrowly n-shaped. Median apophysis small, almost ½ length of tegular apophysis. Tegular apophysis large, knife-shaped; length of tegular apophysis almost as long as width of bulb. Conductor sclerotized, with smooth end. Embolus corn-like, thick, and curved, with a tooth-shaped base (Fig. 4A–D).

Female. Unknown.

Distribution. Known only from the type locality (Fig. 10).

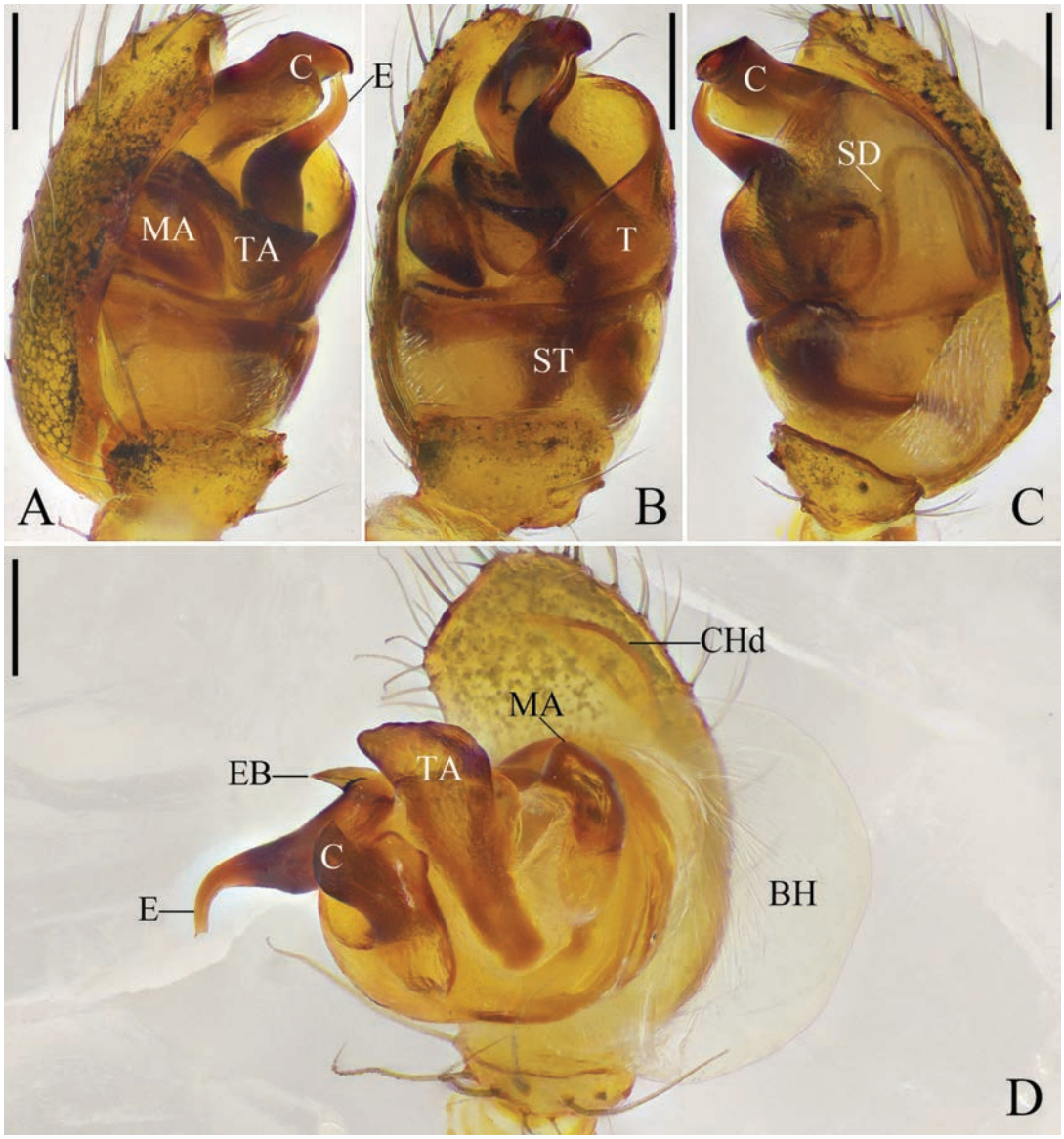

Figure 4. *Yunohamella mohorovicici* R. Zhong, J. Liu & Hu, sp. nov., left male palp. **A** prolateral view **B** ventral view **C** retrolateral view **D** expanded, ventral view. Scale bars: 0.2 mm. (Photos by Changhao Hu.)

***Yunohamella jiugongensis* (Liu & Zhong, 2023), comb. nov.**
Figs 5, 6, 10

Cryptachaea jiugongensis Liu and Zhong in Liu et al. 2023: 98, figs 1A–F, 2A–E.

Type material (examined). ***Holotype*** • male: China, Hubei Province: Xianning City, Jiugongshan National Nature Reserve, Yunzhonghu scenic spot; 29.39°N, 114.65°E; elev. 1230 m; 27 June 2021; Yang Zhong, Feng Lu, Han Dong & Jiangwei Zheng leg. (HUST, ZY2024001). ***Paratypes*** • 2 females, same data as holotype (HUST, ZY2024002).

Diagnosis. For males, see the above diagnosis under *Y. mohorovicici* sp. nov. Males of *Y. jiugongensis* comb. nov. are also similar to those of *Y. palmgreni* (compare Fig. 5C–E with Marusik and Tsellarius 1986: figs 1, 2) in having an n-shaped sperm duct on the tegulum and a thick embolus, but *Y. jiugongensis* comb. nov. can be distinguished from *Y. palmgreni* by the following: conductor

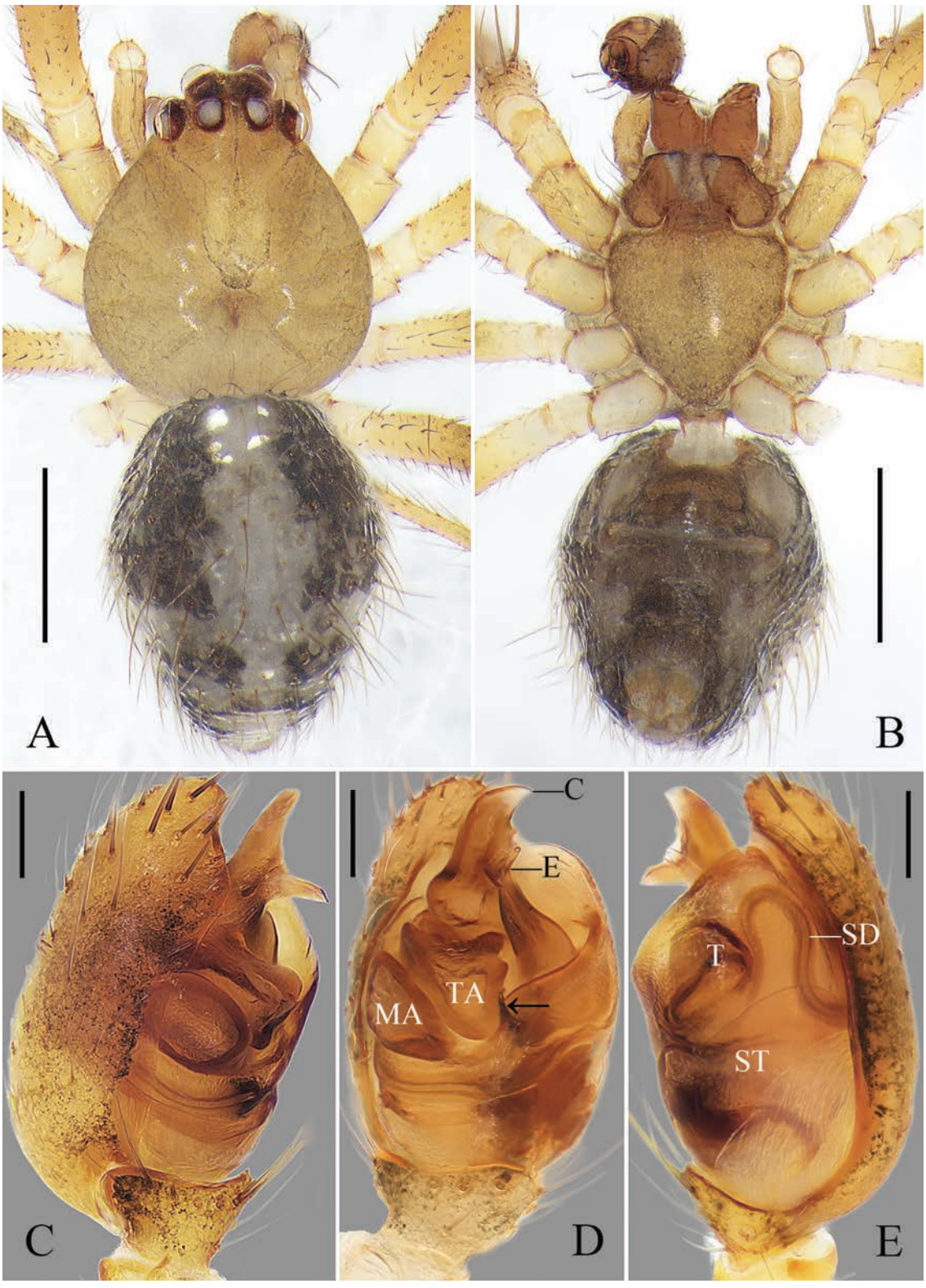

Figure 5. *Yunohamella jiugongensis* (Liu & Zhong, 2023) comb. nov., male. **A** habitus, dorsal view **B** habitus, ventral view **C** left palp, prolateral view **D** left palp, ventral view (arrow points to the sharp tooth-like apophysis on tegulum) **E** left palp, retrolateral view. Scale bars: 0.5 mm (**A, B**); 0.1 mm (**C–E**). (Photos by Yang Zhong.)

arising from the retrolateral part of the tegulum at the 2 o'clock position; and embolus curved (vs conductor arising from the retrolateral part of tegulum at the 12 o'clock position and embolus straight in *Y. palmgreni*). Females of

Y. jiugongensis comb. nov. are similar to those of *Y. serpatusa* (Guan & Zhu, 1993) (compare Fig. 6C, D with Esyunin and Efimik 1996: figs 3–5) in having a blunt scapus and the copulatory ducts almost as long as the diameter of the spermathecae, but *Y. jiugongensis* comb. nov. can be distinguished from *Y. serpatusa* by the parallel copulatory ducts (vs not parallel in *Y. serpatusa*). Females of *Y. jiugongensis* comb. nov. are also similar to those of *Y. yunohamensis* (Bösenberg & Strand, 1906) (compare Fig. 6C–D with Yoshida 2003: figs 233, 234) in having a scapus and copulatory ducts almost as long as the diameter of the spermathecae, but *Y. jiugongensis* comb. nov. can be distinguished from *Y. yunohamensis* by having an obtuse scapus and straight, parallel copulatory ducts (vs scapus with two rounded ends and copulatory ducts curved and not parallel in *Y. yunohamensis*).

Redescription. Male, measurements: total length 1.77. Carapace 0.88 long, 0.76 wide. Abdomen 0.89 long, 0.77 wide. Eyes: AME 0.10, ALE 0.06, PME 0.08, PLE 0.07, AME–AME 0.06, AME–ALE 0.03, PME–PME 0.06, PME–PLE 0.02, ALE–PLE 0.02. Measurements of legs [legs I and IV missing]: II 3.36 (0.86, 0.30, 0.79, 0.93, 0.48), III 2.14 (0.67, 0.20, 0.38, 0.55, 0.34).

Carapace light brown, with black radial furrow. Sternum shaped like an inverted triangle and light brown. Chelicerae, labium, and endites brown. Legs yellow to orange. Abdomen black, with long hairs; dorsum with a grey longitudinal mark and some white spots; posterior dorsum with grey transverse marks; median band of ventral abdomen darker than the other bands. Spinnerets orange (Fig. 5A, B).

Subtegulum bowl-shaped. Tegulum with a narrow prolateral part and a large retrolateral part; retrolateral part with a thin area that holds embolic base; sperm duct narrowly n-shaped; tegulum with a sharp, tooth-like apophysis in ventral view. Median apophysis and tegular apophysis triangular in ventral view. Conductor sclerotized, with knife-shaped end. Embolus corn-like, thick, and curved (Fig. 5C–E).

Female, measurements: total length 3.53. Carapace 1.32 long, 1.16 wide. Abdomen 2.21 long, 1.81 wide. Eyes: AME 0.11, ALE 0.11, PME 0.09, PLE 0.12, AME–AME 0.07, AME–ALE 0.06, PME–PME 0.07, PME–PLE 0.06, ALE–PLE 0.02. Measurements of legs: I 7.90 (2.30, 0.42, 2.31, 2.09, 0.78), II 4.85 (1.45, 0.38, 1.22, 1.23, 0.57), III 3.08 (0.87, 0.26, 0.75, 0.66, 0.54), IV 5.56 (1.56, 0.53, 1.29, 1.51, 0.67). Leg formula: I-IV-II-III.

Carapace brown, with median band of carapace lighter than the rest of the carapace. Sternum brown. Abdomen light grey; dorsum with irregular black marks; posterior-lateral part of genital groove with black transverse bands, a rounded and two triangular black marks located around spinnerets. Other characters of habitus as for male (Fig. 6A, B).

Epigyne with a blunt scape; copulatory openings located medially at scape. Copulatory ducts straight and parallel, almost as long as diameter of spermathecae. Spermathecae spherical. Fertilization ducts thin, long, almost ½ diameter of spermathecae, and arising posteriorly from spermathecae (Fig. 6C, D).

Natural history. This species inhabits bushes.

Comments. The justification for the removal of *Y. jiugongensis* comb. nov. from *Cryptachaea* is supported by its distinct differences from diagnostic characteristics for *Cryptachaea*, particularly the median apophysis attached to the embolus and the absence of a tegular apophysis, a defining character for the

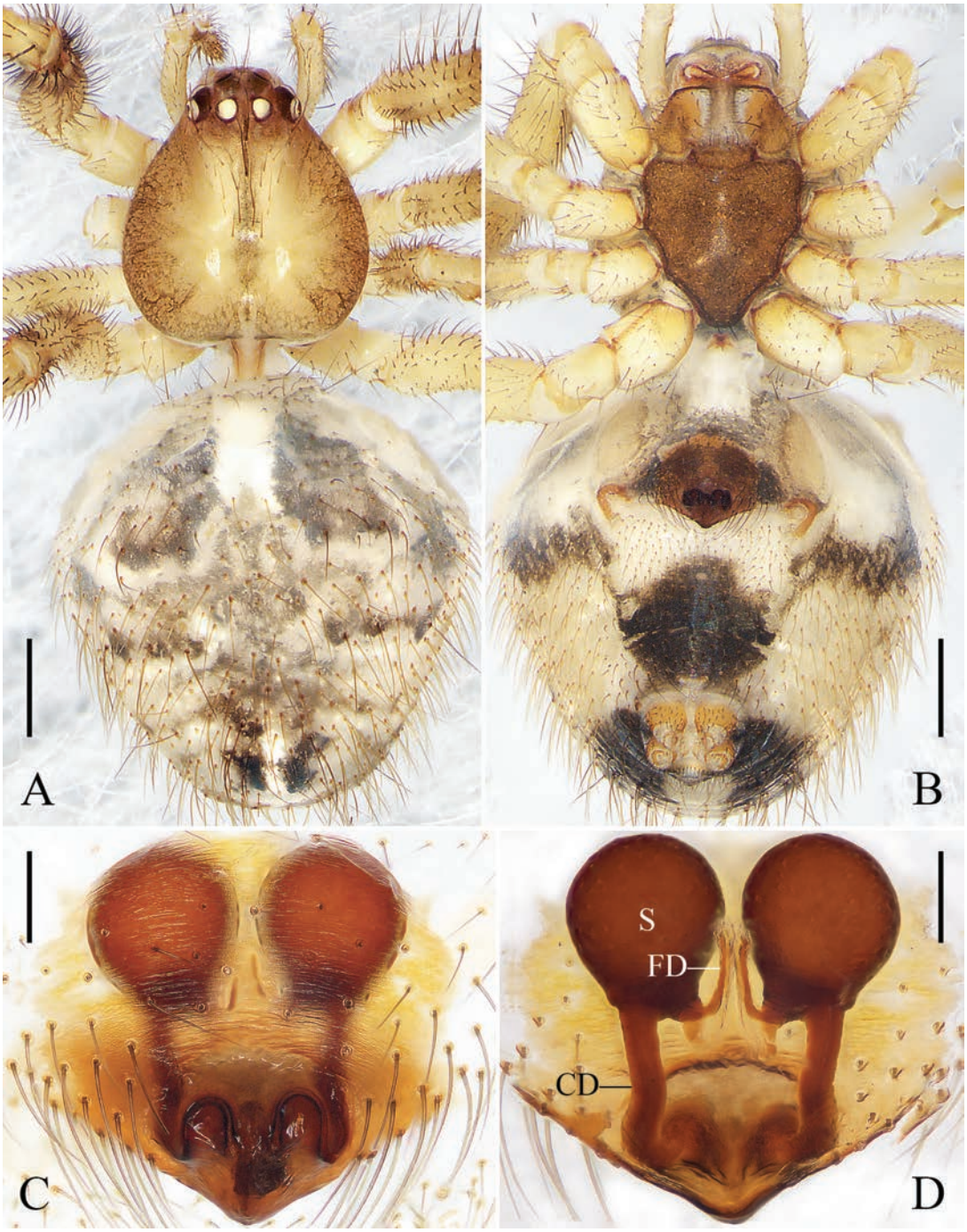

Figure 6. *Yunohamella jiugongensis* (Liu & Zhong, 2023) comb. nov., female. **A** habitus, dorsal view **B** habitus, ventral view **C** epigyne, ventral view **D** vulva, dorsal view. Scale bars: 0.5 mm (**A, B**); 0.1 mm (**C, D**). (Photos by Yang Zhong.)

genus *Cryptachaea* (Yoshida 2008; Rodrigues and Poeta 2015). In contrast, the male palp of *Y. jiugongensis* comb. nov. exhibits the presence of tegular apophysis. The species is placed into *Yunohamella* based on similarities of the palpal structures, specifically conductor conjugated with a large tegulum (Fig. 5C–E). This species also shares similarities in the epigynal structures with *Yunohamella*, specifically the presence of a blunt scapus (Fig. 6C, D), as well as similarities in the dark abdomen (Figs 5A, B, 6A, B). Consequently, we transfer *C. jiugongensis* from *Cryptachaea* to *Yunohamella* as a new combination.

Distribution. Known only from the type locality (Fig. 10).

***Yunohamella lyrica* (Walckenaer, 1841)**
Figs 7–10

Theridion lyricum Walckenaer, 1841: 288; Archer 1946: 43; Levi 1957: 89, figs 322–323, 329–331; Yoshida 1987: 13, figs 1, 2; Yoshida 1989: 318, fig. 4P–R; Chikuni 1989: 44, fig. 64; Kim and Kim 2001: 155, fig. 2A–I; Namkung 2002: 96, fig. 13.14a, b; Paquin and Dupérré 2003: 223, figs 2494–2496.
Theridion lyra Hentz, 1850: 279, pl. 9, fig. 21; Keyserling 1884: 50, pl. 2, fig. 28; Kaston 1948: 106, figs 132, 153, 154.
Theridion kentuckyense Keyserling, 1884: 78, pl. 4, fig. 47; Banks 1892: 30, pl. 5, fig. 43; Emerton 1909: 180, pl. 1, fig. 6.
Theridion mneon Bösenberg & Strand, 1906: 142, pl. 12, fig. 286.
Allotheridion lyricum: Archer 1950: 20.
Takayus lyricus: Yoshida 2001: 167; Namkung 2003: 98, fig. 13.14a, b; Yoshida 2003: 97, figs 239–242, 530.
Keijia mneon: Yoshida 2001: 172.
Yunohamella lyrica Yoshida 2007: 69; Yoshida 2009: 372, figs 149, 150; Lee and Kim 2021: 166, fig. 4A; Kim 2021: 172, fig. 75A–D.
Platnickina mneon: Koçak and Kemal 2008: 3; Ono 2011: 452; Dupérré 2023: 231, fig. 73A–C. Syn. nov.

Material examined. • 2 males, 4 females: China Hubei Province: Enshi Tujia and Miao Autonomous Prefecture, Xuan'en County, Qizimeishan National Nature Reserve, Chunmuying Town, Xiaoshui Cave; 30.02°N, 109.78°E; elev. 1777 m; 1 June 2024; Changhao Hu & Mian Wei leg. (CBEE, QZMS04713, QZMS04714, QZMS04751–QZMS04754). • 2 females: Enshi Tujia and Miao Autonomous Prefecture, Xuan'en County, Qizimeishan National Nature Reserve, Chunmuying Town, Xiaoshui Cave; 30.02°N, 109.78°E; elev. 1777 m; 12 July 2023; Changhao Hu & Mian Wei leg. (CBEE, QZMS02405, QZMS02406). • 1 female: Enshi Tujia and Miao Autonomous Prefecture, Xuan'en County, Qizimeishan National Nature Reserve, Chunmuying Town, Shaiping Village; 29.96°N, 109.76°E; elev. 1822 m; 31 July 2023; Changhao Hu & Mian Wei leg. (CBEE, QZMS01160).

Diagnosis. For males see the diagnosis under *Y. varietas* by Lee and Kim (2021). Males of *Y. lyrica* are also similar to those of *Y. subadulta* (compare Fig. 7D–F with Kim 2021: fig. 77E–G) in having a sharp terminal conductor and a sperm duct curving four times, but *Y. lyrica* can be distinguished from *Y. subadulta* in having the conductor extend beyond the cymbium (vs. conductor not exceeding the cymbium in *Y. palmgreni*). Females of *Y. lyrica* are similar to those of *Y. takasukai* Yoshida, 2012 (compare Fig. 9D–F with Yoshida 2012: figs 4, 5) in having a pair of projections on the anterlateral epigynal plate, but *Y. lyrica* can be distinguished from *Y. takasukai* by having oval, laminar projections on the anterlateral epigynal plate and long, curved copulatory ducts (vs nipple-like projections and copulatory ducts short in *Y. takasukai*).

Redescription. Male, measurements: total length 2.11. Carapace 1.16 long, 0.88 wide. Abdomen 1.10 long, 0.91 wide. Eyes: AME 0.10, ALE 0.08, PME 0.08, PLE 0.08, AME–AME 0.10, AME–ALE 0.04, PME–PME 0.07, PME–PLE 0.09, AME–PME 0.09, ALE–PLE 0.00. Measurements of legs: I 7.48 (2.27, 0.43, 1.94, 2.10, 0.74), II 4.29 (1.38, 0.30, 0.98, 1.17, 0.46), III 2.71 (1.00, 0.19, 0.52, 0.60, 0.40), IV 3.87 (1.31, 0.26, 0.88, 0.95, 0.47). Leg formula: I-II-IV-III.

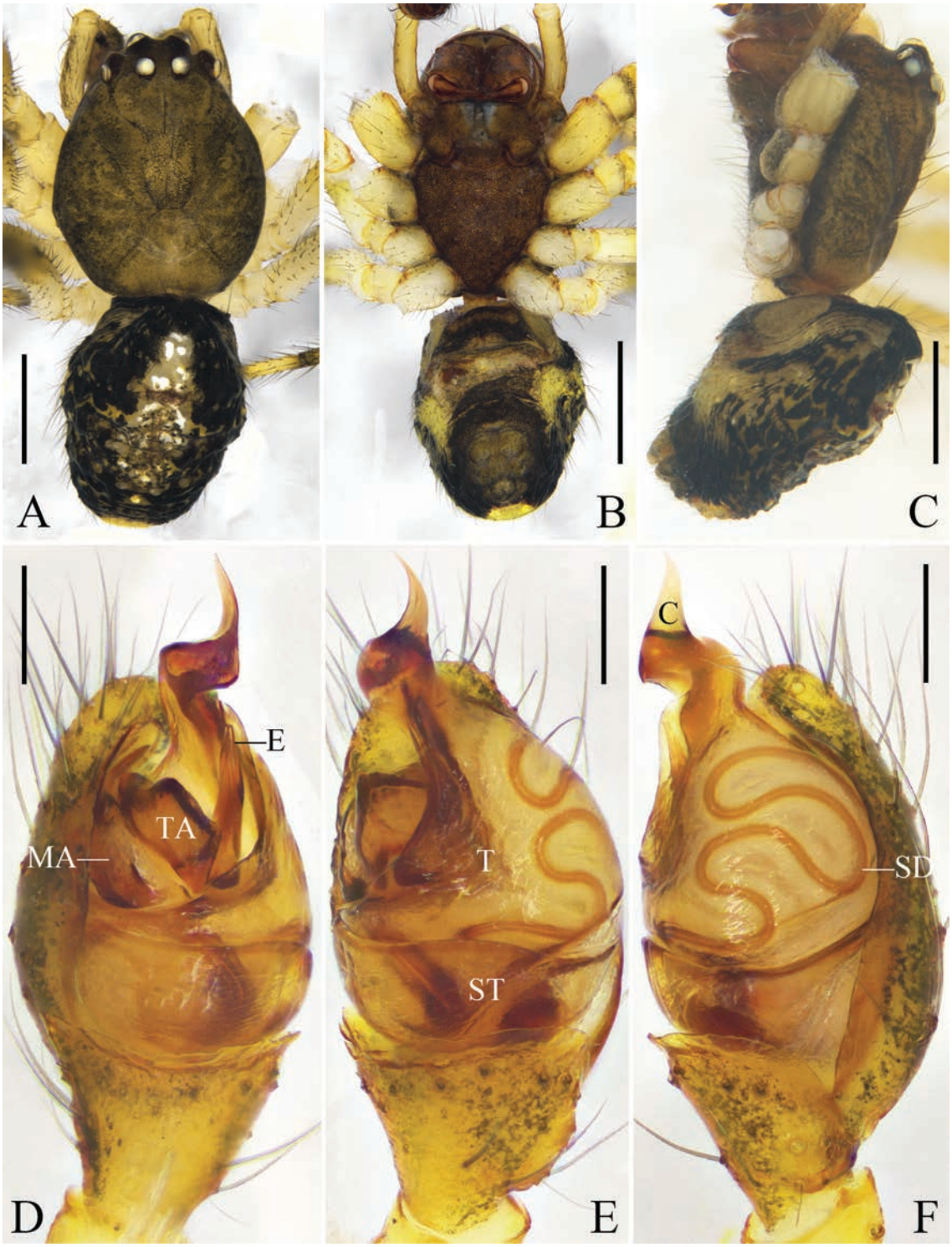

Figure 7. *Yunohamella lyrica* (Walckenaer, 1841), male. **A** habitus, dorsal view **B** habitus, ventral view **C** habitus, lateral view **D** left palp, prolateral view **E** left palp, ventral view **F** left palp, retrolateral view. Scale bars: 0.5 mm (**A–C**); 0.2 mm (**D–F**). (Photos by Changhao Hu and Rui Zhong.)

Carapace brownish green, with deep fovea and black radial furrow. Sternum shaped like an inverted triangle and dark brown. Chelicerae orange. Labium and endites dark brown. Legs yellow. Abdomen with long hairs; dorsum black, with a longitudinal mark composed of yellow base and white spots; venter yellow; anterior part of spinnerets black. Spinnerets brown (Fig. 7A–C).

Figure 8. *Yunohamella lyrica* (Walckenaer, 1841), expanded left male palp. **A** prolateral view **B** ventral view. Scale bars: 0.2 mm. (Photos by Changhao Hu.)

Cymbium oval. Cymbial hood tilted at 30°, almost 1/8 length of cymbium. Subtegulum bowl-shaped. Tegulum with a narrow prolateral part and a large retrolateral part; sperm duct curving four times. Median apophysis and tegular apophysis almost as long as the width of bulb. Conductor sclerotized, with a sharp end. Embolus straight, with a rounded base (Figs 7D–F, 8A, B).

Female, measurements: total length 2.49. Carapace 0.91 long, 0.74 wide. Abdomen 1.40 long, 1.31 wide. Eyes: AME 0.09, ALE 0.07, PME 0.09, PLE 0.09, AME–AME 0.04, AME–ALE 0.02, PME–PME 0.08, PME–PLE 0.07, AME–PME 0.05, ALE–PLE 0.00. Measurements of legs: I 5.57 (1.73, 0.32, 1.47, 1.43, 0.62),

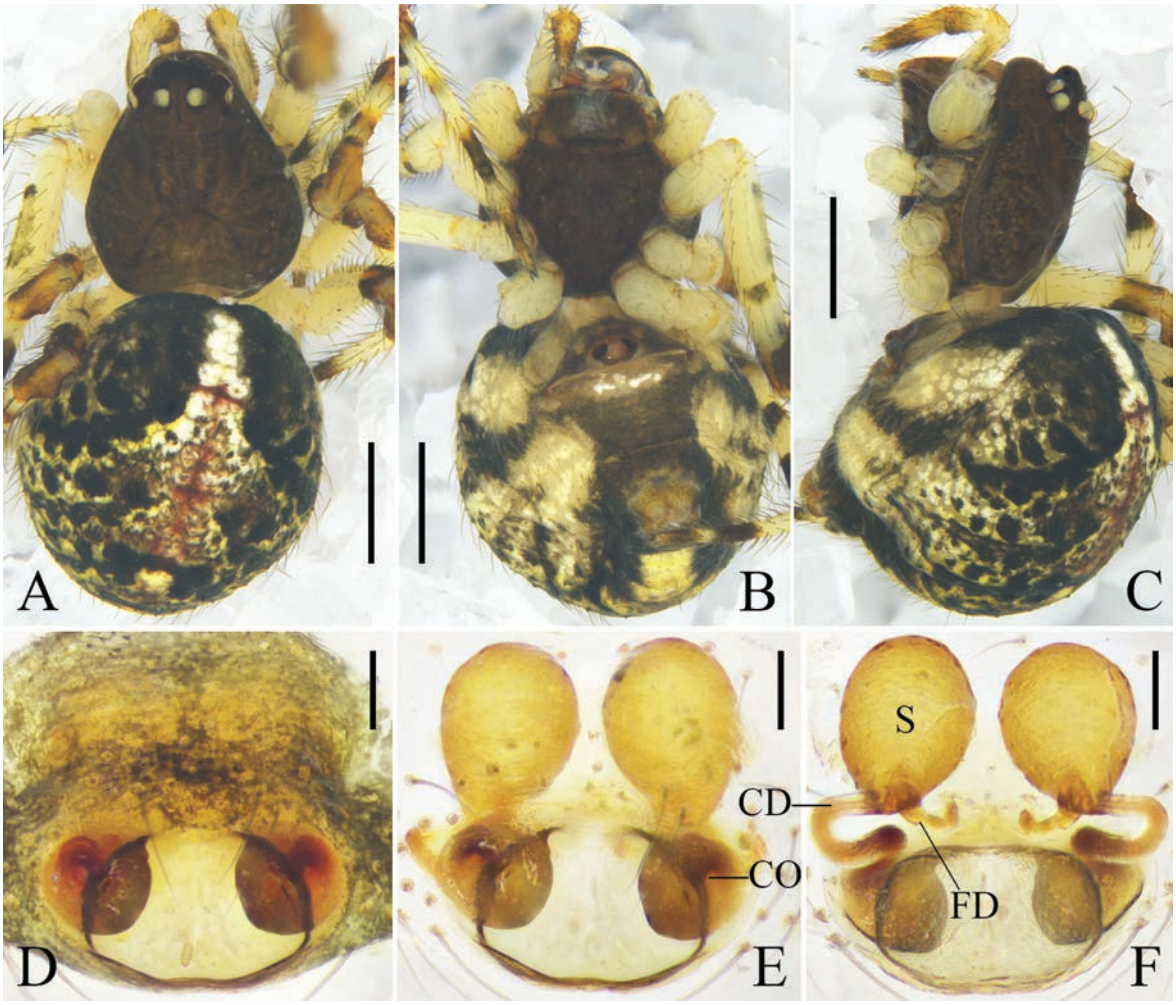

Figure 9. *Yunohamella lyrica* (Walckenaer, 1841), female. **A** habitus, dorsal view **B** habitus, ventral view **C** habitus, lateral view **D** uncleared epigyne, ventral view **E** uncleared epigyne, ventral view **F** vulva, dorsal view. Scale bars: 0.5 mm (**A–C**); 0.1 mm (**D–F**). (Photos by Changhao Hu.)

II 3.76 (1.24, 0.33, 0.83, 0.86, 0.50), III 2.71 (0.94, 0.25, 0.51, 0.61, 0.40), IV 3.84 (1.30, 0.34, 0.84, 0.91, 0.45). Leg formula: I-IV-II-III.

Carapace dark brown. Legs yellow to orange. Abdomen black; dorsum with a longitudinal mark composed of white, red, and yellow spots; posterior part of dorsum with three inverted V-shaped marks composed of yellow spots; median band of venter black, the rest yellow; posterior part of genital groove with several white spots, posterior-lateral part of genital groove with black transverse bands. Other characters of habitus as for male (Fig. 9A–C).

Epigyne with an oval atrium, two oval sclerotized plates overhanging anterolateral epigynal plate, copulatory openings located laterally on sclerotized plates. Copulatory ducts curved into a C-shape. Spermathecae spherical. Fertilization ducts arising posteriorly from spermathecae (Fig. 9D–F).

Natural history. This is one of the most widespread *Yunohamella* species. This species is found on bushes, forests, and fences, as well as inside houses (Kaston 1948; Levi 1957; Gao and Li 2014; Kim et al. 2016; Lee and Kim 2021).

Comments. *Platnickina mneon* was first described by Bösenberg and Strand (1906) based on a female specimen collected in Saga, Japan. To date, males of *P. mneon* remain unknown. Dupérré (2023) provided diagnostic characters and

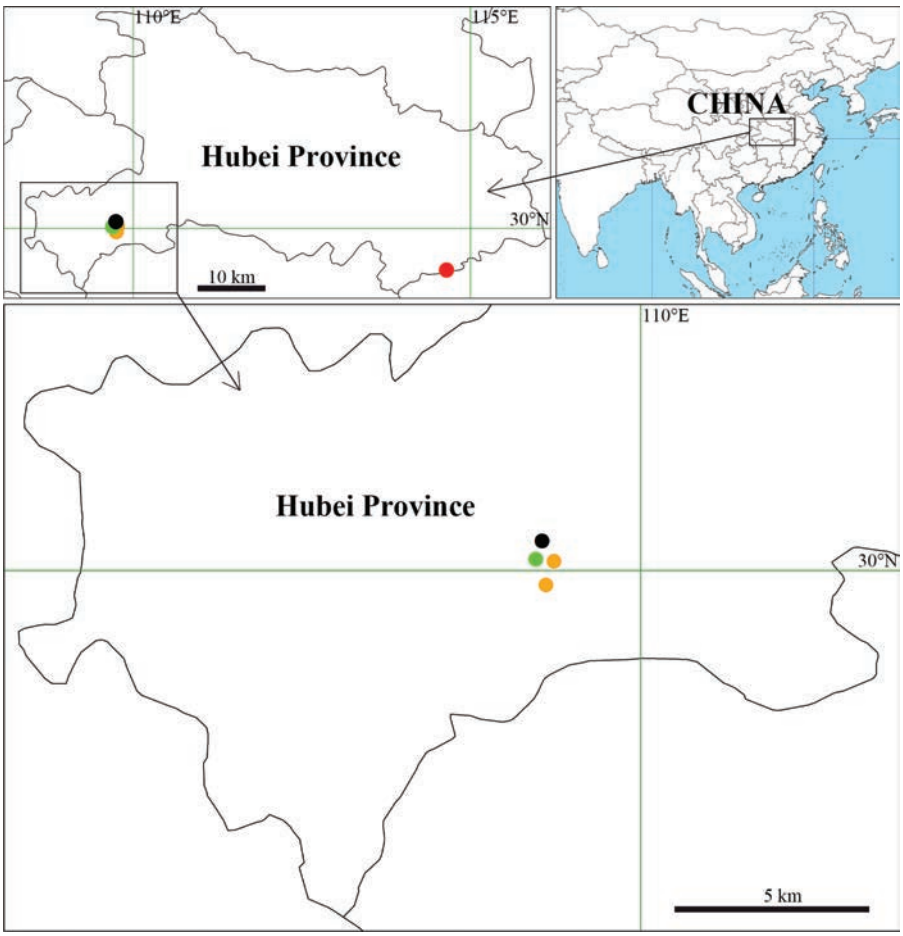

Figure 10. The collection locality of *Yunohamella* spp. from Hubei Province, China. Black circle represents *Y. gutenbergi* R. Zhong, J. Liu & Hu, sp. nov.; green circle represents *Y. mohorovicici* R. Zhong, J. Liu & Hu, sp. nov.; red circle represents *Y. jiugongensis* (Liu & Zhong, 2023) comb. nov.; orange circles represent *Y. lyrica* (Walckenaer, 1841).

illustrations of *P. mneon* after examining the female holotype and noted that this species does not conform to the characteristics of the genus *Platnickina* Koçak & Kemal, 2008 (e.g. copulatory openings located on sclerotized plates in *P. mneon* vs inside the circular depression of the epigyne in *Platnickina* spp.) and that it likely belongs to another genus. The holotype of *P. mneon* exhibits all the diagnostic features of *Y. lyrica* as provided by Levi (1957), including the two sclerotized plates, copulatory openings located on the sclerotized plates, and oval spermathecae (compare Figs 7D–F, 9D–F with Dupérré 2023: fig. 73B, C and with Levi 1957: figs 329, 330). Although the types of *Y. lyrica* and *P. mneon* were unavailable for examination, our comparison based on specimens collected in Hubei Province, China and the illustrations and descriptions provided by Levi (1957) and Dupérré (2023) allows us to consider *P. mneon* as a junior synonym of *Y. lyrica*.

Distribution. China (Hubei Province, new Province record; Yunnan Province), Japan, Korea, North America.

Acknowledgements

We thank Mian Wei (CBEE) for helping specimens' collection and identification. This manuscript benefitted greatly from the subject editor Francesco Ballarin, the copy editor Robert Forsyth, and the reviewers Ingi Agnarsson and Yejie Lin.

Additional information

Conflict of interest

The authors have declared that no competing interests exist.

Ethical statement

No ethical statement was reported.

Funding

This research was funded by the National Natural Sciences Foundation of China (NSFC-32270495/32300378/32400360), the Science & Technology Fundamental Resources Investigation Program of China (2023FY100200), the Foundation of Hubei Key Laboratory of Regional Development and Environmental Response (2022(B)004), and the China Postdoctoral Science Foundation (2023M731035).

Author contributions

Writing – original draft: RZ, CH. Writing – review and editing: RZ, YZ, JL, HZ, CL, KC, CH.

Author ORCIDs

Rui Zhong https://orcid.org/0000-0001-5910-7302
Yang Zhong https://orcid.org/0000-0002-0517-4582
He Zhang https://orcid.org/0000-0002-1478-9837
Jie Liu https://orcid.org/0000-0001-7744-9744
Changhao Hu https://orcid.org/0009-0007-5591-3121

Data availability

All of the data that support the findings of this study are available in the main text.

References

Agnarsson I (2004) Morphological phylogeny of cobweb spiders and their relatives (Araneae, Araneoidea, Theridiidae). Zoological Journal of the Linnean Society 141(4): 447–626. https://doi.org/10.1111/j.1096-3642.2004.00120.x

Agnarsson I, Coddington JA, Knoflach B (2007) Morphology and evolution of cobweb spider male genitalia (Araneae, Theridiidae). Journal of Arachnology 35(2): 334–395. https://doi.org/10.1636/SH-06-36.1

Bösenberg W, Strand E (1906) Japanische Spinnen. Abhandlungen der Senckenbergischen Naturforschenden Gesellschaft 30: 93–422.

Dupérré N (2023) New light on some historical type specimens in relation to the South American spider (Araneae) fauna. New Zealand Journal of Zoology 50(1): 118–277. https://doi.org/10.1080/03014223.2022.2123835

Esyunin SL, Efimik VE (1996) A new species of the genus *Theridion* (Aranei, Theridiidae) from the Urals. Zoologicheskiĭ Zhurnal 75: 1275–1277.

Gao CX, Li SQ (2014) Comb-footed spiders (Araneae: Theridiidae) in the tropical rainforest of Xishuangbanna, Southwest China. Zoological Systematics 39(1): 1–135.

Guan JD (2002) Description on three new records of spiders from China. Forest Pest and Disease 21(2): 4–6.

Kaston BJ (1948) Spiders of Connecticut. Bulletin of the Connecticut State Geological and Natural History Survey 70: 1–874.

Kim ST (2021) Spiders V. Arthropoda: Arachnida: Araneae: Theridiidae, Amaurobiidae, Eresidae, Zoropsidae, Anyphaenidae. Invertebrate Fauna of Korea 21(47): 1–230.

Kim ST, Lee SY, Im MS, Yoo JS (2016) Distribution of Korean Spiders. National Institute of Biological Resources, Incheon, 1624 pp.

Lee SY, Kim ST (2021) A new spider of the genus *Yunohamella* (Araneae: Theridiidae) from Korea. Species Diversity 26(2): 165–169. https://doi.org/10.12782/specdiv.26.165

Levi HW (1955) The spider genera *Coressa* and *Achaearanea* in America north of Mexico (Araneae, Theridiidae). American Museum Novitates 1718: 1–33.

Levi HW (1957) The spider genera *Enoplognatha*, *Theridion*, and *Paidisca* in America north of Mexico (Araneae, Theridiidae). Bulletin of the American Museum of Natural History 112: 1–124.

Liu J, May-Collado LJ, Pekár S, Agnarsson I (2016) A revised and dated phylogeny of cobweb spiders (Araneae, Araneoidea, Theridiidae): A predatory Cretaceous lineage diversifying in the era of the ants (Hymenoptera, Formicidae). Molecular Phylogenetics and Evolution 94: 658–675. https://doi.org/10.1016/j.ympev.2015.09.023

Liu H, Zheng MY, Cheng F, Zhong Y (2023) A new *Cryptachaea* species from Jiugong Mountains (Theridiidae: Theridiinae). Acta Arachnologica Sinica 32(2): 98–101. https://doi.org/10.3969/j.issn.1005-9628.2023.02.006

Marusik YM, Logunov DV (2017) New faunistic and taxonomic data on spiders (Arachnidae: Aranei) from the Russian Far East. Acta Arachnologica 66(2): 87–96. https://doi.org/10.2476/asjaa.66.87

Marusik YM, Tsellarius AY (1986) New species of spiders of the genus *Theridion* (Aranei, Theridiidae) from Karelia. Zoologicheskiĭ Zhurnal 65: 1736–1738.

Rodrigues ENL, Poeta MRM (2015) Twelve new Neotropical species of the spider genus *Cryptachaea* (Araneae: Theridiidae). Journal of Arachnology 43(1): 26–33. https://doi.org/10.1636/K14-47.1

World Spider Catalog (2024) World Spider Catalog. Version 25.0. Natural History Museum Bern. http://wsc.nmbe.ch [accessed on 12 June 2024]

Yoshida H (2001) A revision of the Japanese genera and species of the subfamily Theridiinae (Araneae: Theridiidae). Acta Arachnologica 50(2): 157–181. https://doi.org/10.2476/asjaa.50.157

Yoshida H (2003) The spider family Theridiidae (Arachnida: Araneae) from Japan. Arachnological Society of Japan, 224 pp.

Yoshida H (2007) A new genus of the family Theridiidae (Arachnida: Araneae). Acta Arachnologica 56(2): 67–69. https://doi.org/10.2476/asjaa.56.67

Yoshida H (2008) A revision of the genus Achaearanea (Araneae: Theridiidae). Acta Arachnologica 57(1): 37–40. https://doi.org/10.2476/asjaa.57.37

Yoshida H (2012) A new species of the genus *Yunohamella* (Araneae: Theridiidae) from Mt. Merapi, Java, Indonesia. Acta Arachnologica 61(1): 19–20. https://doi.org/10.2476/asjaa.61.19

Zhu MS (1998) Fauna Sinica: Arachnida: Araneae: Theridiidae. Science Press, Beijing, 436 pp.

Zhu MS, Gao SS, Guan JD (1993) Notes on the four new species of comb-footed spiders of the forest regions Liaoning, China (Araneae: Theridiidae). Journal of the Liaoning University (Natural Sciences Edition) 20: 89–94.

ZooKeys 1224: 87–108 (2025)
DOI: 10.3897/zookeys.1224.133244

Research Article

Two new species of *Psen* Latreille, 1796 (Hymenoptera, Apoidea, Crabronidae) from China, with a key to *Psen* species of China

Yao Deng[1], Li Ma[1], Qiang Li[1]

1 *Department of Entomology, College of Plant Protection, Yunnan Agricultural University, Kunming, Yunnan, 650201, China*
Corresponding authors: Li Ma (maliwasps@aliyun.com); Qiang Li (liqiangkm@126.com)

Abstract

Two new species of the genus *Psen* Latreille, 1796, namely *Psen fronistriatus* **sp. nov.** and *Psen scabrosus* **sp. nov.** are described and illustrated from China. A key to the Chinese species of *Psen* is also provided.

Key words: Crabronidae, digger wasps, key, taxonomy

Introduction

China encompasses 16 regions of the world's 34 biodiversity hotspots, as identified by Conservation International (Myers et al. 2000). Over the past 8 million years, China has been profoundly shaped by geological events such as continental drift, the retreat of the ancient Mediterranean Sea, and the erosion of plateau surfaces due to the uplift of the Tibetan Plateau and the development of deep rift. These events have not only shaped its geologic history and distribution pattern but have also created unique landscape, geomorphology, microhabitat differentiation, and geographic isolation. This geologic complexity has facilitated the rapid differentiation of many biological communities, making China one of the most diverse regions in the Northern Hemisphere (Boufford 2014; Price et al. 2014; Xing and Ree 2017; Fu et al. 2024). Straddling the Palearctic and Eastern Oceanic zones in the global zoogeography, China's diverse geomorphological patterns and climatic environments generate high environmental heterogeneity. This, in turn, supports a variety of habitats for insects in insects, contributing to an exceptionally rich biodiversity of species, with many species exhibiting macro- and trans-zonal distribution, with numerous endemics species, placing China in a significant and unique position within global zoogeography.

The genus *Psen* Latreille, 1796, belongs to the tribe Psenini in the subfamily Pemphredoninae and is the second-largest genus in the tribe. The genus was erected by Latreille with no species included, and Latreille (1802) later designated *Sphex ater* Fabricius, 1794 [= *Crabro ater* Olivier, 1792] as the type species of the genus. Currently, the genus *Psen* includes 95 species and 22 subspecies. These species are distributed across multiple regions: 11 species and two subspecies occur in the Palearctic, five in the Nearctic, 48 species and 17 subspecies in the Oriental, four in the Ethiopian, nine in the Neotropical, eight species and three

Academic editor: Thorleif Dörfel
Received: 27 July 2024
Accepted: 2 December 2024
Published: 22 January 2025

ZooBank: https://zoobank.org/A52CF7D1-556C-4D75-BA76-FC807EC0C3F0

Citation: Deng Y, Ma L, Li Q (2025) Two new species of *Psen* Latreille, 1796 (Hymenoptera, Apoidea, Crabronidae) from China, with a key to *Psen* species of China. ZooKeys 1224: 87–108. https://doi.org/10.3897/zookeys.1224.133244

subspecies in the Australo-Papuan, eight in each the Palearctic and Oriental, and four in each the Oriental and Australo-Papuan regions (Cameron, 1899; Turner 1912; Gussakovskij 1932; Malloch 1933; Beaumont 1937; Merisuo 1938; Tsuneki 1959, 1966, 1967, 1971, 1973, 1974, 1982, 1983; van Lith 1959, 1965, 1968, 1973, 1974, 1975, 1976, 1978; Lomholdt 1975; Bohart and Menke 1976; Kazenas 1978; Budrys 1986; Wu and Zhou 1996; Nagase 2000; Amarante 2002; Dollfuss 2004; Pulawski 2024). Of the 95 species, 26 species and six subspecies are recorded from China, comprising 27.3% of the global total, of which 20 species and one subspecies are distributed on the mainland (Yunnan, Guizhou, Sichuan, Guangdong, Guangxi, Xizang, Zhejiang, Fujian, Chongqing, Hubei, Jiangxi, Shandong, Shanxi, Henan, Beijing, Gansu, Qinghai, Inner Mongolia, Liaoning, Heilongjiang), with 11 species and five subspecies are distributed in Taiwan. Four species and one subspecies occur both in the mainland and Taiwan together (Gussakovskij 1932; Malloch 1933; Beaumont 1937; Merisuo 1938; van Lith 1968, 1974, 1975; Tsuneki 1974, 1983; Bohart and Menke 1976; Kazenas 1978; Budrys 1986; Wu and Zhou 1996; Hua 2006; Ma and Li 2006; Ma and Li 2007; Jiang et al. 2021).

The biology of *Psen* has been studied by several researchers (e.g., Girard 1879; Barth 1907; Malloch 1933; Gussakovskij 1937; Beaumont 1937, 1964; Iwata 1938; van Lith 1959, 1965, 1968; Janvier 1956; Tsuneki 1959; Steiner 1986; Woydak 1996; Kazenas 2001). Evans (1959) described the larvae of *Psen*. Members of this genus typically nests in stumps, rotten wood, hard sandy soil or mud, often with multiple nesting chambers present in decaying wood. *Psen afinis* Gussakovskii, 1937, *Psen aurifrons* Tsuneki, 1959, and *Psen betremi* van Lith, 1959 prey on species of the family Cicadellidae; *Psen ater* (Olivier, 1972), *Psen coriaceus* van Lith, 1959, *Psen curvipilosus* van Lith, 1959, *Psen erythropoda* Rohwer, 1910, *Psen richardsi* Tsuneki, 1959, and *Psen vechti* van Lith, 1959 prey on species in the family Cercopidae; and *Psen emarginatus* van Lith, 1959 preys on Membracidae.

Many researchers have conducted taxonomic studies in China in recent decades, leading to the discovery of new species. In this study, two new species of *Psen fronistriatus* sp. nov. and *Psen scabrosus* sp. nov. collected from Yunnan, Guangdong, Shaanxi, and Inner Mongolia, China, were discovered and are described in detail, and a key to the known species in China is provided, with high-quality color photographs of the two new species. Notably, *P. fronistriatus* was first collected in Ganquan County, Yan'an, Shaanxi Province, in 1971 (as a male), and 35 years later, both a female and male were obtained from Helan Mountain, Inner Mongolia. Meanwhile, *P. scabrosus* was first collected in 2007 from Guanyin Mountain, Fogang, Guangdong Province (as a female), and was later rediscovered in the same region in 2021. These findings further demonstrate the environmental complexity of China, which not only provides diverse habitat and ecological barriers for many species but also supports a wealth of micro-ecological environments that contribute to the country's extraordinary species diversity.

Materials and methods

The examined specimens are deposited in Yunnan Agricultural University, Kunming, China (**YNAU**). Specimens were photographed using a stereomicroscope (Keyence VHX-S550E) equipped with a digital microscopic system.

Plates were processed with Adobe Photoshop® 2020 software. For the terminology we mainly follow Bohart and Menke (1976). The abbreviations are as follows:

HLD head length in dorsal view (distance from the frons to the occipital margin in the middle)
HLF head length in frontal view (distance from the vertex to the clypeal margin in the middle)
HW head width (dorsal view, maximum)
AOD antenna-ocular distance (frontal view)
WAS width of antennal socket (frontal view)
IAD interantennal distance (frontal view)
POD post-ocellar distance (distance between the inner margins of the hind ocellus)
OOD ocellocular distance (distance between the outer margin of the hind ocellus and the nearest inner orbit)
OCD ocello-occipital distance (distance between the posterior margin of the hind ocellus and the occipital margin, dorsal view)
PW petiole width (dorsal view, in the middle)
PL petiole length (lateral view)
LT I maximum length of gastral tergum I (dorsal view)
WT I maximum width of gastral tergum I (dorsal view)
HFL maximum length of hind femur
HTL maximum length of hind tibia.

Taxonomic account

Psen Latreille, 1796

Psen Latreille, 1796: 122 (no included species). Type species: *Sphex ater* Fabricius, 1794 [= *Crabro ater* Olivier, 1792], designated by Latreille 1802: 338 (first included species).
Psenus Rafinesque, 1815: 124. Emendation of *Psen* Latreille, 1796.
Mesopora Wesmael, 1852: 279. Type species: *Psen ater* of Vander Linden, 1829 [= *Sphex ater* of Panzer, 1799 = *Sphex ater* Fabricius, 1794 = *Crabro ater* Olivier, 1792], by monotypy.

Diagnosis. The genus *Psen* can be identified as a member of the tribe Psenini Costa, 1858 within the subfamily Pemphredoninae based on Mandible bidentate apically; occipital carina joining hypostomal carina before midventral line of head; no genal process; scrobe sulus deep, hypoepimeral area raised; omaulus ending as it becomes ventral and turning a little posteriorly; forewing second recurrent vein ending in second or interstitial or third submarginal cell, hindwing M diverging before cu-a; propodeum usually coarsely reticulate posteriorly, sometimes multivariate; dorso-median area of petiole usually smooth, rarely with coarse punctures, without carinae but rarely with a posterior longitudinal groove, no conspicuous laterodorsal setae but abundant strong setae lateroventrally; male gastral sterna III and IV, or only III or IV, with marginal setae posteriorly, rarely without marginal setae, VIII an upturned pseudo-sting; female pygidial plate subtriangular, narrow or broad, sparsely or densely bristled (Bohart and Menke 1976).

Key to the species of *Psen* Latreille, 1796 from China

Female (females are unknown for *P. spinitibialis* Ma & Li, 2007; *P. foveicornis* Tsuneki, 1982; *P. seriatispinosus* Ma & Li, 2006; *P. assamensis* van Lith, 1965; *P. shukuzanus* Tsuneki, 1972)

1 Gastral terga with dense or sparse, long or short marginal setae posteriorly **2**
– Gastral terga without marginal setae posteriorly (Fig. 1A)..... **7**
2 Petiole cylindrical, without carina or keel, cylindrical..... **3**
– Petiole subquadrate, lateral surface with one lateral carina on each side (Figs 1B, 3B), ventral surface without or with a keel **5**
3 Propodeal enclosure with sturdy longitudinal rugae, propodeal pad narrow, impunctate, smooth, and shiny (Fig. 3F); gastral terga with long, straight marginal setae posteriorly; petiole with blue shine; clypeus with golden setae (Fig. 3C) (China: Taiwan) ..... ***P. sauteri* van Lith, 1968**
– Propodeal enclosure with slender longitudinal rugae, sometimes extending to propodeal pad (Fig. 1F); gastral terga with straight or somewhat curving, short setae, petiole without shine; clypeus with golden or silvery setae (Fig. 2C) **4**
4 All legs largely fulvous or reddish brown; gastral terga I and II, sternum II largely reddish brown to dark brown, remainder area bright reddish brown; clypeus with golden setae (Fig. 3C) (China: Zhejiang, Sichuan) ..... ***P. lacuniventris* Ma & Li, 2007**
– Legs black except gray-white tibial spur, tarsus brown; gaster black; clypeus with silvery setae (Fig. 2C) (China: Taiwan) ..... ***P. terayamai* Tsuneki, 1982**
5 Propodeal enclosure ill delimited, not impressed; second recurrent vein of forewing ending in second submarginal cell (Fig. 3A); ventral surface of petiole with a keel posteriorly, and large punctures on each side; pygidial plate with one or two rows of large punctures and setae (Fig. 3H) (China: Yunnan, Guangxi, Sichuan, Taiwan; Indonesia)..... ***P. lieftincki* van Lith, 1959**
– Propodeal enclosure well delimited by triangular or lunular carina (Fig. 1F), not or shallowly impressed; second recurrent vein of forewing ending in third submarginal cell or interstitial (Fig. 1I); ventral surface of petiole without keel, impunctate or with microscopic punctures on each side; pygidial plate with five or six rows of large punctures and setae **6**
6 Acetabular carina short, 0.7× longer than foretarsus I; gastral terga with sparse marginal setae, short and straight, silvery; gastral segments I and II, petiole ventrally bright reddish (China: Hunan, Yunnan; Nepal; India) ..... ***P. rufoannulatus* Cameron, 1907**
– Acetabular carina lacking; gastral terga with dense marginal setae, long, straight, golden; gastral segment I partly reddish brown to dark brown, gastral segment II and petiole black (China: Yunnan) ..... ***P. yunnanensis* Ma & Li, 2007**
7 Petiole cylindrical, lateral surface not carinate or with slender lateral carinae, ventral surface without keel..... **8**
– Petiole subquadrate, lateral surface with slender or sturdy lateral carinae (Fig. 3B), ventral surface without or with a keel **15**

8 Mandible much broadened **9**
– Mandible narrow or just somewhat broad medially or apically **10**
9 Propodeal pad narrow, smooth, shiny (Fig. 1F); upper frons with dense, fine punctures; ocellar area, vertex with dense, midsized punctures, without groove behind hind ocelli (Fig. 1E) (China: Hubei, Zhejiang, Guangdong, Guizhou; Japan) ..... ***P. kulingensis* van Lith, 1965**
– Propodeal pad with dense, slender, longitudinal rugae (Fig. 3E); upper frons, ocellar area, vertex with sparse, tiny punctures, shiny, with a deep transverse groove behind hind ocelli (China: Taiwan) ..... ***P. shirozui* Tsuneki, 1966**
10 Mandible somewhat broad medially or apically **11**
– Mandible narrow **13**
11 Pygidial plate broad triangular, mat, with several rows of large punctures and setae; second recurrent vein of forewing ending in interstitial of second submarginal cell (Fig. 3A) (China: Shandong; Korea; Japan) ..... ***P. aurifrons* Tsuneki, 1959**
– Pygidial plate narrow triangular, smooth, shiny, with a few midsized punctures or impunctate basally; second recurrent vein of forewing ending in third submarginal cell (Fig. 1I) **12**
12 Ocellar area, vertex slightly convex; gaster black (China: Yunnan; Nepal; India) ..... ***P. simlensis* van Lith, 1968**
– Ocellar area flat, vertex distinctly convex; gastral terga I–IV posteriorly, terga V–VI, and sternum III except median area bright yellowish brown, remainder area black (China: Sichuan; Indonesia) ..... ***P. rubicundus lawkensis* van Lith, 1959**
13 Upper frons, ocellar area, vertex with very sparse, fine punctures; scutum with sparse, tiny punctures anteriorly and laterally, remainder with sparse, fine to midsized punctures; legs largely fulvous (China: Yunnan; Philippines; India; Japan) ..... ***P. opacus* van Lith, 1959**
– Upper frons, ocellar area, vertex with dense, small to midsized punctures; scutum with dense, fine to large punctures; legs dark brown to black largely **14**
14 Scutum with dense, fine punctures (Fig. 1E); area between ocelli with longitudinal groove, behind hind ocelli with transverse groove; lateral surface of petiole with shallow groove and a slender lateral carina on each side (China: Yunnan, Sichuan, Taiwan; Japan; Korea; Russia) ..... ***P. affinis* Gussakovskij, 1937**
– Scutum with dense, midsized to large punctures; area between ocelli without groove; lateral surface of petiole without groove or carina (China: Henan, Zhejiang, Fujian, Chongqing, Yunnan, Xizang; India) ..... ***P. fuscinervis* (Cameron, 1899)**
15 Propodeal pad with sparse or dense, long, longitudinal rugae (Fig. 3E) **16**
– Propodeal pad narrow or broad, impunctate, smooth, shiny (Fig. 1F) **19**
16 Mandible narrow; interantennal tooth markedly elevated; pygidial plate broad triangular, mat, with several rows of large punctures and setae, basal 1/2 slightly convex; propodeum without bronzy shine (China: Heilongjiang, Jilin, Gansu, Beijing, Shandong, Zhejiang, Shanxi; Worldwide distribution) ..... ***P. ater* (Olivier, 1972)**
– Mandible much broadened, leaf-like medially and apically, subapical area with a virginal tooth; interantennal tooth moderately elevated; pygidial

plate narrow triangular, coriaceous, mat or somewhat shiny, with one or two rows of punctures and setae, not convex; propodeum with bronzy shine **17**

17 Lateral surface of petiole with slender lateral carinae, ventral surface with a slender keel, inconspicuously (China: Shanxi, Sichuan, Taiwan) ..... ***P. bnun* Tsuneki, 1971**

– Lateral surface of petiole with sturdy lateral carinae and deep groove, ventral surface with a strong keel **18**

18 Free margin of clypeus with a deep, semicircle depression on each side of lateral area; scutum with dense, fine punctures anteriorly, remainder with dense, midsized to large punctures (China: Henan, Zhejiang) ..... ***P. ussuriensis* van Lith, 1959**

– Free margin of clypeus without depression laterally; scutum with dense, large punctures (Fig. 3C) (China: Guangdong) ..... ***P. scabrosus* sp. nov.**

19 Propodeal pad broadly quadrate, impunctate, smooth, shiny **20**

– Propodeal pad narrow, impunctate, smooth, shiny (Fig. 1F) **21**

20 Pygidial plate coriaceous and mat, with one or two rows of large punctures and setae (Fig. 1J) (China: Beijing, Shandong, Zhejiang, Fujian, Guangdong, Guangxi, Yunnan; Indonesia; India; Sri Lanka; Malay Archipelago; Japan; Nepal) ..... ***P. nitidus* van Lith, 1959**

– Pygidial plate smooth and shiny, with a row of large punctures and setae (Fig. 3H) (China: Hainan; Indonesia) ..... ***P. amboinensis* van Lith, 1965**

21 Pygidial plate narrow triangular, smooth, shiny (Fig. 3H), without or with a few punctures **22**

– Pygidial plate elongate triangular, coriaceous, mat (Fig. 1J) or somewhat shiny, with one or two rows of fine or midsized punctures **23**

22 Interantennal tooth moderately elevated, bluntly tooth-like; second recurrent vein of forewing ending in second submarginal cell interstitial; antenna fulvous largely (China: Sichuan; Japan) ..... ***P. bettoh attenuatus* Tsuneki, 1977**

– Interantennal tooth slightly elevated, coniform; second recurrent vein of forewing ending in second submarginal cell (Fig. 3A); antenna beneath brown (China: Taiwan; Korea; Russia; Japan) ..... ***P. koreanus formosensis* Tsuneki, 1965**

23 Mandible narrow; pronotal collar with anterior-lateral corners, not forming tooth (China: Taiwan) ..... ***P. alishanus* Tsuneki, 1967**

– Mandible somewhat broad medially or apically; pronotal collar without anterior-lateral corner **24**

24 Lateral surface of petiole with a sturdy lateral carina on each side, ventral surface with a sturdy keel (China: Jilin, Inner Mongolia, Qinghai, Xizang, Sichuan, Yunnan, Taiwan; Korea; Russia; Japan) ..... ***P. seminitidus* van Lith, 1965**

– Lateral surface of petiole with a slender lateral carina on each side and a deep groove, ventral surface without keel **25**

25 Upper frons with dense, fine punctures, ocellar area, vertex with sparse, fine punctures; second recurrent vein of forewing ending in second submarginal cell; antenna beneath largely, gastral tergum I laterally, femur apically, tibia, tarsus reddish brown; head, thorax with bronzy shine (China: Taiwan) ..... ***P. tanoi* Tsuneki, 1967**

– Upper frons with dense, fine to midsized punctures and slender, longitudinal rugae (Fig. 1C), ocellar area, vertex with dense, midsized to large

punctures (Fig. 1E); second recurrent vein of forewing ending in third submarginal cell (Fig. 1I); antenna, gaster black, leg largely black; head, thorax without bronzy shine (Fig. 1B) (China: Inner Mongolia, Shaanxi, Yunnan) .. ..***P. fronistriatus* sp. nov.**

Male (males are unknown for *P. amboinensis* van Lith, 1965; *P. opacus* van Lith, 1959; *P. terayamai* Tsuneki, 1982; *P. lacuniventris* Ma & Li, 2007; *P. sauteri* van Lith, 1968; *P. scabrosus* sp. nov.)

1 Gastral sterna III and IV without marginal setae posteriorly (Fig. 2B) (China: Inner Mongolia, Shaanxi, Yunnan) .....***P. fronistriatus* sp. nov.**
– Gastral sterna III and IV with marginal setae posteriorly.....**2**
2 Only gastral sternum III or IV with marginal setae posteriorly **3**
– Gastral sterna III and IV with marginal setae posteriorly.....**6**
3 Gastral sternum III with marginal setae posteriorly, dark brown, dense, somewhat long and straight; acetabular carina lacking, mesosternum with two or three sturdy, long, longitudinal carinae on each side of ventral median carina (China: Sichuan; Indonesia).....***P. rubicundus lawkensis* van Lith, 1959**
– Gastral sternum IV with marginal setae posteriorly, fulvous or dark brown, short and straight; acetabular carina lacking or short, mesosternum without longitudinal carina **4**
4 Mandible narrow, petiole cylindrical, lateral surface not carinate or with weak lateral carina on each side (China: Taiwan)..... ***P. alishanus* Tsuneki, 1967**
– Mandible somewhat broad medially, petiole subquadrate (Fig. 2B), lateral surface with a sturdy lateral carina on each side.....**5**
5 Ventral surface of petiole without keel; upper frons, ocellar area, vertex with dense or sparse, tiny punctures, ocellar area flat; antennal joints III–XII beneath with tubercles (China: Sichuan, Taiwan; Japan)..... .....***P. bettoh attenugius* Tsuneki, 1977**
– Ventral surface of petiole with a sturdy keel; upper frons with dense, fine punctures and longitudinal rugae, ocellar area, vertex with dense, fine punctures, markedly convex; antennal joints V–VI or V–VII beneath with linear carinae (China: Jilin, Inner Mongolia, Qinghai, Xizang, Sichuan, Yunnan, Taiwan; Korea; Russia; Japan) .....***P seminitidus* van Lith, 1965**
6 Gastral terga with dense or sparse, long or short marginal setae posteriorly **7**
– Gastral terga without marginal setae posteriorly (Fig. 2A).....**10**
7 Mandible much broadened, tooth leaf-like, inner margin with a small tooth on median area and 1/3 of apex; interantennal tooth long, nail-like, sharp (Fig. 2C); antenna beneath without tyloids; petiole strongly curving to blunt angle basally, lateral surface with a median longitudinal carina medially and posteriorly, and a pair lateral carina on each side, ventral surface with a keel and large punctures (China: Yunnan, Guangxi, Sichuan, Taiwan; Indonesia) .....***P. lieftincki* van Lith, 1959**
– Mandible narrow, inner margin with a tooth subapically; interantennal tooth small tooth-like, somewhat sharp; antenna beneath without tyloids or concave; petiole slightly curving, lateral surface not carinate or with a pair lateral carina on each side, ventral surface without or with a keel, impunctate **8**

8 Gastral terga with sparse, short, straight, silvery marginal setae posteriorly; gastral segments I and II laterally bright reddish brown (China: Hunan, Yunnan; Nepal; India) ..... ***P. rufoannulatus* Cameron, 1907**

– Gastral terga with dense, long, curving or straight, golden or yellowish marginal setae posteriorly; gastral tergum I largely or wholly reddish brown, remainder black..... **9**

9 Ventral surface of petiole with a keel; second recurrent vein of forewing ending in second submarginal cell interstitial; antennal joints VI–XIII beneath with oval tubercles, black, smooth, shiny (China: Zhejiang) .... ***P. spinitibialis* Ma & Li, 2007**

– Ventral surface of petiole without keel; second recurrent vein of forewing ending in third submarginal cell (Fig. 2A); antennal joints VI–XI beneath with elliptic tubercles (China: Zhejiang)..... ***P. yunnanensis* Ma & Li, 2007**

10 Propodeal pad with longitudinal rugae or reticulation (Fig. 3E)..... **11**

– Propodeal pad narrow or broad, impunctate, smooth, shiny (Fig. 2F)..... **18**

11 Midtarsus with angular or spinous produced (Fig. 4A–E); mandible narrow or somewhat broad medially and apically..... **12**

– Midtarsus not deformed (Fig. 4F, G); mandible much broadened..... **15**

12 Petiole cylindrical, lateral surface without carina..... **13**

– Petiole subquadrate, lateral surface with a longitudinal carina on each side (Fig. 2B)..... **14**

13 Half apex of mandible broad; mid basitarsus with auriform prominence (Fig. 4D, E); second recurrent vein of forewing ending in second submarginal cell interstitial (Fig. 3A); antennal joints VI–XIII beneath with elliptic concave (China: Shandong; Korea; Japan)..... ***P. aurifrons* Tsuneki, 1959**

– Mandible narrow; each of midtarsus markedly produced posteriorly (Fig. 4C); second recurrent vein of forewing ending in third submarginal cell (Fig. 2A); antennal joints V–XIII beneath with tyloids, on joint V small, elliptic, on V–XIII large oval concave (China: Zhejiang; Guangxi; Taiwan)... ..... ***P. foveicornis* Tsuneki, 1982**

14 Inner margin of mid basitarsus with a row of 6 nail-shaped thorns basally and a long spine on 1/3 of base (Fig. 4A, B); antennal joints III–XIII beneath with tyloids (China: Guizhou) ..... ***P. seriatispinosus* Ma & Li, 2006**

– Mid basitarsus with an angular prominence medially and posteriorly; joints VI–XIII beneath with tyloids (China: Heilongjiang, Jilin, Gansu, Beijing, Shandong, Zhejiang, Shanxi; worldwide distribution) ..... ***P. ater* (Olivier, 1972)**

15 Petiole cylindrical; free margin of clypeus with broad, shallow emargination (China: Taiwan) ..... ***P. shirozui* Tsuneki, 1966**

– Petiole subquadrate (Fig. 2B); free margin of clypeus with deep, semicircular emargination **16**

16 Lateral surface of petiole with upper edge only, 1/2 apex area with dense, midsized punctures, ventral surface without keel; interantennal tooth blunt apically (China: Zhejiang; India)..... ***P. assamensis* van Lith, 1965**

– Lateral surface of petiole with a pair lateral carina on each side, without or with deep groove medially, ventral surface with a strong keel; interantennal tooth tooth-like, sharp apically **17**

17 Free margin of clypeus without depression; second recurrent vein of forewing ending in third submarginal cell (Fig. 2A) or interstitial; upper frons, ocellar area, vertex with sparse, tiny punctures; scutum with sparse, fine punctures (China: Shanxi; Sichuan; Taiwan)..... ***P. bnun* Tsuneki, 1971**

– Free margin of clypeus with a deep semicircle depression on each side; second recurrent vein of forewing ending in second submarginal cell interstitial (Fig. 3A); upper frons, ocellar area, vertex with sparse, fine punctures; scutum with dense, fine punctures anteriorly, remainder with dense, midsized to large punctures (China: Henan, Zhejiang; Russia; Sweden; Japan; Korea)..... ***P. ussuriensis* van Lith, 1959**

18 Propodeal pad broadly quadrate, impunctate, smooth, shiny; acetabular carina much longer (China: Beijing, Shandong, Zhejiang, Fujian, Guangdong, Guangxi, Yunan; Indonesia; India; Sri Lanka; Malay Archipelago; Japan; Nepal)..... ***P. nitidus* Tsuneki, 1966**

– Propodeal pad narrow or somewhat broad, impunctate, smooth, shiny (Fig. 2F); acetabular carina lacking, or short, or somewhat long..... **19**

19 Mandible broad or at least apical 1/2 somewhat broad..... **20**

– Mandible narrow..... **23**

20 Petiole subquadrate (Fig. 2B), lateral surface with a pair lateral carina on each side, without or with deep groove **21**

– Petiole cylindrical, lateral surface without carina or groove..... **22**

21 Setae on head, thorax, leg golden; upper frons with dense, fine punctures, ocellar area, vertex with sparse, fine punctures (China: Taiwan)..... ***P. tanoi* Tsuneki, 1967**

– Setae on head, thorax, leg silvery; upper frons, ocellar area, vertex with sparse, large punctures (China: Taiwan; Korea; Russia; Japan)..... ***P. koreanus formosensis* Tsuneki, 1965**

22 Scutum with sparse, tiny to fine punctures; ocellar area, vertex with sparse, tiny to fine punctures; antennal joints V–VIII beneath with linear carinae (China: Yunnan; India; Nepal)..... ***P. simlensis* van Lith, 1968**

– Scutum with dense, large punctures; ocellar area, vertex with dense, midsized punctures; antennal joints V–VIII beneath with wide cylindrical tyloids and III and XII beneath with linear carinae (China: Hubei, Zhejiang, Guangdong, Guizhou; Japan) ..... ***P. kulingensis* van Lith, 1965**

23 Petiole subquadrate (Fig. 2B), having a broad furrow on each side that is margined on both sides by carinae (China: Taiwan)..... ***P. shukuzanus* Tsuneki, 1972**

– Petiole cylindrical, lateral surface without furrow and lateral carina or with a slender lateral carina on each side or with a shallow groove.....24

24 Acetabular carina lacking; antennal joints III–XI beneath with tyloids, on joints III–X long tubercles, on joint XI short carina (China: Sichuan, Yunnan, Taiwan; Japan; Korea; Russia)..... ***P. affinis* Gussakovskii, 1937**

– Acetabular carina short, 0.3× longer than foretarsus I; antennal joints IV–XIII beneath with tyloids (China: Henan; Zhejiang; Fujian; Chongqing; Yunnan; Xizang; India) ..... ***P. fuscinervis* (Cameron, 1899)**

***Psen fronistriatus* sp. nov.**

https://zoobank.org/B1E624A9-0218-46B3-996B-BB83F7EA355C

Figs 1A–J, 2A-L

Type material. ***Holotype*.** China • ♀; Inner Mongolia, Helan Mountain; 38°57'45"N, 105°51'8"E; 24.VII.2006; 1833 m elev.; collected by Ming LUO. ***Paratypes*:** China • 1♂; same data as holotype; China • 1♀; Yunnan Province, Gaoligong Mountain, Dulong River Tunnel; 27°50'56"N, 98°28'3"E; 15.VII–2.VIII.2020; 2824 m elev.; collected by Lang YI; China • 1♂; Shaanxi Province, Yan'an City, Ganquan County, Liulimao; 36°10'3"N, 109°21'26"E; 5.VII.1971; 1077 m elev.; collected by Jikun Yang. All types deposited in YNAU.

Diagnosis. The new species is similar to *Psen seminitidus* van Lith, 1965, but differs from it and other congeners by the following characteristics (characters of *P. seminitidus* in parentheses): 1) the posterior surface of the propodeum lacks an oblique longitudinal ridge (the posterior surface of the propodeum has weakly oblique longitudinal carinae); 2) flagellomeres VII–X have linear tyloids beneath in the male (flagellomeres V–VI or V–VII beneath have linear tyloids); 3) the female POD: OOD: OCD = 12: 17: 21 (the female POD: OOD: OCD = 12: 13: 15); 4) the female PL: PW: LT I: WT I: HFL: HTL = 80: 14: 52: 64: 71: 88 (the female PL: PW: LT I: WT I: HFL: HTL = 69: 11: 41: 50: 60: 70); 5) the ocellus and vertex areas feature dense, midsized to large punctures (the ocellus and vertex area feature dense, fine punctures); 6) the scutum has dense, fine punctures anteriorly, dense and midsized to large punctures medially and posteriorly (the scutum has dense, fine punctures); 7) the petiole lacks a median longitudinal keel ventrally in the female (the petiole has median longitudinal keel); 8) the second recurrent vein ends in the third or interstitial submarginal cell (the second recurrent vein ends in the second submarginal cell).

Description. Female. Body length 11.0–11.8 mm. Black; mandible and pygidial area apically reddish brown; fore and mid tarsi dark brown. Appressed setae on clypeus golden or silvery, vertex, scutum, scutellum, and metanotum with long, dense, pale yellow pubescence. Setae on mesopleuron, legs, propodeum, and petiole mid length and silvery (Fig. 1A, B).

***Head*.** In frontal view, clypeus with dense, fine punctures except margin, mid portion prominent with arch shallow emargination medially, basal 1/2 of clypeal disk moderately convex. HW: HLF: AOD: WAS: IAD = 102: 78: 10: 8: 14. Mandible bidentate apically, broad, blunt; width basally: medially: apically = 18: 10: 3. Interantennal tooth conspicuous, high, apex obtuse or slightly acute; frontal carina weak and reaching interantennal tooth around median ocellus (Fig. 1C). Scape of antennae slightly bent, relative lengths of joints III–XII = 24–26, 16–17, 15–16, 15, 13–14, 12–13, 11–13, 11–12, 11–12, 16–17; joint III ~ 3.4–4.3× as long as wide apically, joint IV with 2.0–2.4×, joint XII with 1.8–1.9× (Fig. 1D). Frons shiny with dense, fine to midsized punctures, and below anterior ocellus with weak longitudinal ridges (Fig. 1C). In dorsal view, ocellus and vertex area shiny, with dense, midsized to large punctures, interspaces larger than frons; ocellar area not raised, behind postocelli with shallow sulcus, vertex behind postocelli region not raised, occipital carina without longitudinal ridge (Fig. 1B, E). HW: HLD: POD: OOD: OCD = 102: 36: 12: 17: 21.

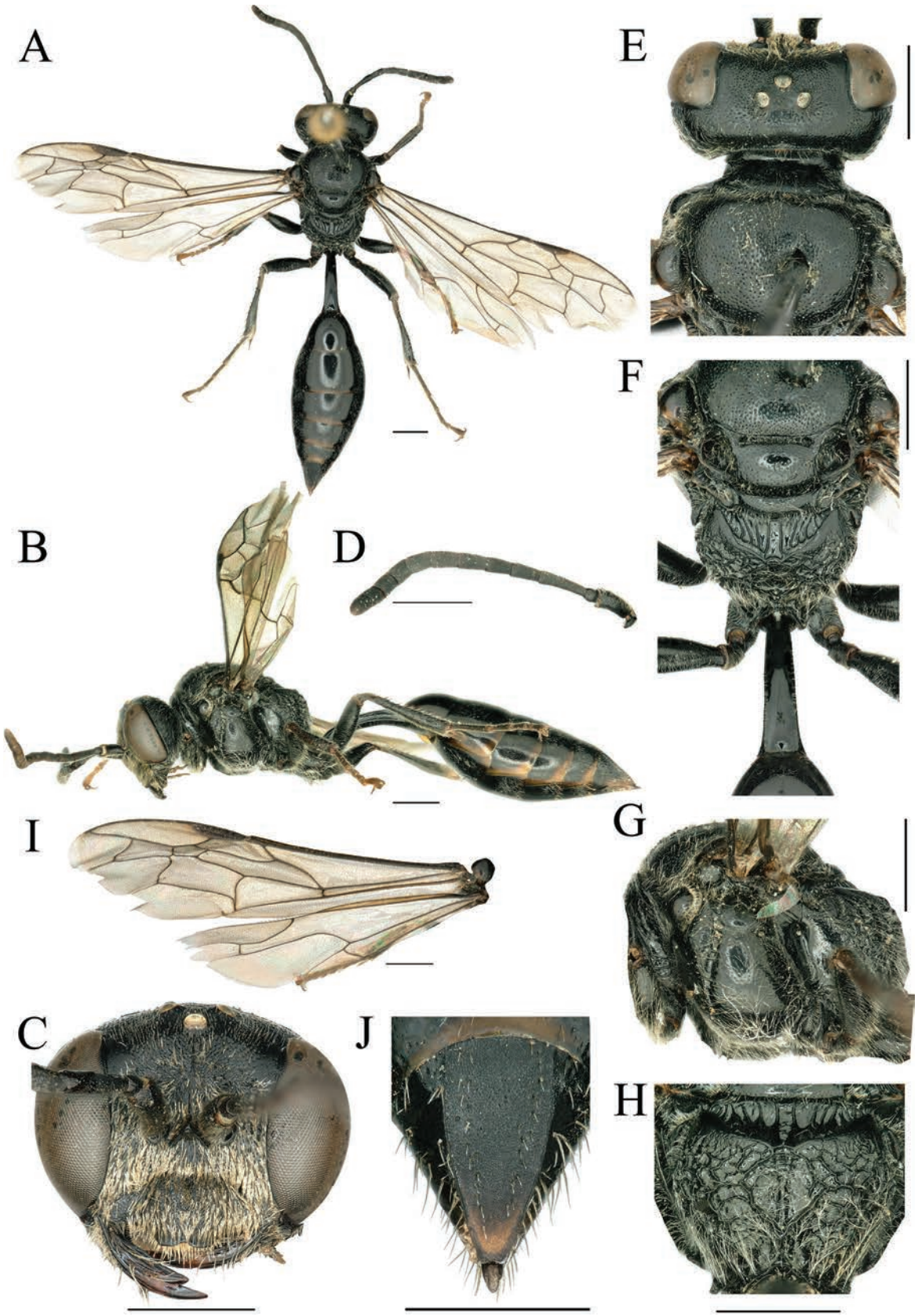

Figure 1. *Psen fronistriatus* sp. nov., holotype ♀ **A** habitus, dorsal view **B** habitus, lateral view **C** head, frontal view **D** antennae **E** head, pronotum and scutum, dorsal view **F** scutellum, metanotum and propodeum, dorsal view **G** thorax, lateral view **H** propodeum, posterior view **I** left wing **J** pygidial plate, dorsal view. Scale bars: 1 mm.

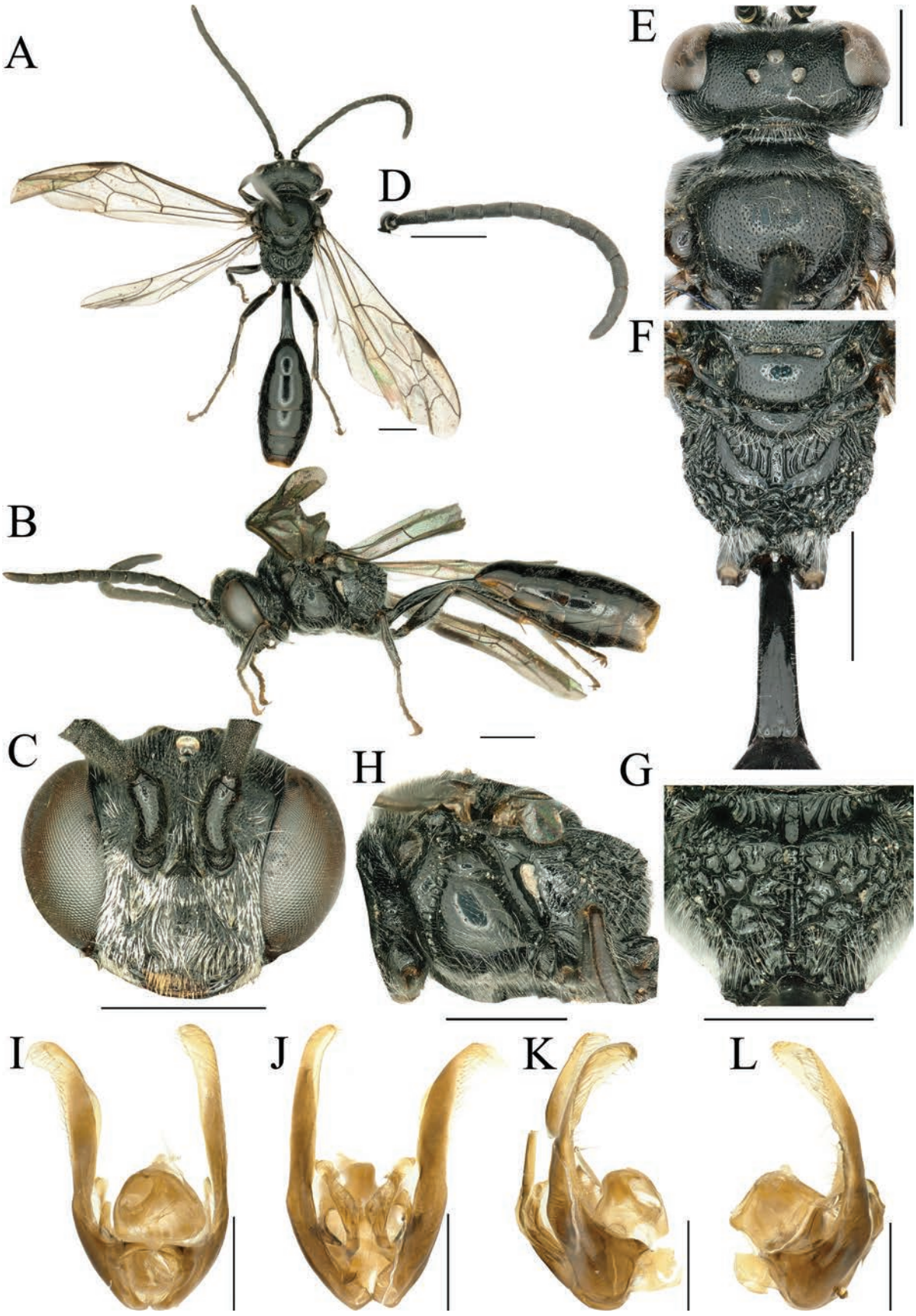

Figure 2. *Psen fronistriatus* sp. nov. ♂ **A** habitus, dorsal view **B** habitus, lateral view **C** head, frontal view **D** antennae **E** head, pronotum and scutum, dorsal view **F** scutellum, metanotum and propodeum, dorsal view **G** propodeum, posterior view **H** thorax, lateral view **I** male genitalia, dorsal view **J** male genitalia, ventral view **K, L** male genitalia, lateral view. Scale bars: 1 mm.

***Thorax*.** Scutum with dense, fine punctures anteriorly, dense, midsized to large punctures medially and posteriorly, interspaces 1–2× as wide as diameter of puncture. Admedian lines and notauluses weak, nearly parallel (Fig. 1F). Scutellum with dense, fine punctures, metanotum with sparse, microscopic punctures (Fig. 1F). Propleuron with five or six short oblique striae, epicnemial areas shiny, with sparse, microscopic punctures, omaulus ending as it becomes ventral and below normally curved backwards. Mesopleura shiny with sparse, microscopic punctures, posteriorly without longitudinal striae (Fig. 1G). Mesosternum without acetabular carina, with slightly strong, longitudinal medioventral carina, medially with one or two transverse carinae. Enclosed area of propodeum depressed, bordered by a narrow horizontal area which is distinctly separated from back of propodeum, horizontal area slightly wider on either side of sulcus, laterally with some sturdy oblique longitudinal carinae; propodeal pad with a smooth area, slightly wider on sides and narrower in middle (Fig. 1F). Posterior surface of propodeum with sturdy reticulation, medially with deep sulcus reaching enclosed area, upper of sulcus with three or four transverse carinae (Fig. 1H). In profile, dorsal surface of propodeum with posterior surface nearly obtuse angle, upper lateral surface of propodeum with oblique, short rugae (Fig. 1G). Second recurrent vein ending in third or interstitial submarginal cell (Fig. 1I). Hind tibia with a row of long, thick, brownish thorns on outer surface (Fig. 1B).

***Gaster*.** PL: PW: LT I: WT I: HFL: HTL = 80: 14: 52: 64: 71: 88. Petiole nearly quadrate in cross section, slightly bent upwards basally, slightly widened backwards, width apically 2.2× basally, dorsally completely smooth (Fig. 1B, F). Lateral side with two slender longitudinal carinae and deeply depressed (Fig. 1B); ventrally without median longitudinal keel. Gaster shiny, terga with sparse microscopic punctures. Pygidial area elongate-triangular, coriaceous, 1.8–2.1× as long as wide basally, laterally one or two rows of coarse, midsized punctures and stiff bristles, apex truncate, slightly concave in middle, basally not convex (Fig. 1J). Sterna smooth.

Male. Similar to female, but body slender, smaller, body length 9.0–11.0 mm (Fig. 2A, B). Mandible, fore and mid tibiae, and tarsi dark brown. Vertex and scutum with long, dense, palely yellow pubescence (Fig. 2C). Gastral sterna III and IV without fasciculate setae on hind margin (Fig. 2B). Clypeus mid prominent portion with arch shallow emargination in middle, two triangular protections in both sides; partially covering labrum. Frons shiny with dense, fine to midsized punctures, and below anterior ocellus with indistinct longitudinal ridges (Fig. 2C). Ocellar area slightly raised (Fig. 2A). Antennae slenderer than female, pedicel partially concealed within scape (Fig. 2A); flagellomeres VII–X beneath with linear tyloids; relative lengths of joints III–XIII = 21–24, 18–20, 17–20, 17–20, 17–19, 16–18, 15–16, 17, 16, 15–17, 20–21; joint III ~ 2.6–3.0× as long as wide apically, joint IV 2.1–2.5×, joint XII 1.6–2.0× (Fig. 2D). In frontal view, HW: HLF: AOD: WAS: IAD = 81: 61: 7: 8: 10; dorsal view, HW: HLD: POD: OOD: OCD = 81: 32: 11: 15: 16 (Fig. 2C). Hind tibia without long, thick, brownish thorns on outer surface (Fig. 2B). Petiole ventrally with median longitudinal keel medially and posteriorly, PL: PW: LT I: WT I: HFL: HTL = 70: 11: 43: 46: 53: 60. Genitalia large, yellowish brown, gonostyle slender and long, apical portion with inner (or dorsal) 1/2 turned into a semitransparent membrane, outer (or ventral) margin and apex provided with a fringe of sparse long setae (Fig. 2I–L). Volsella divided into two branches

medially, dorsal and ventral, each roundly curved and united with each other again at base of apical elongate body, cuspis flattened, hollowed ventrally, with apex gently rounded and turned ventrally, slightly produced on inner apical area.

Distribution. China (Inner Mongolia, Shaanxi, Yunnan).

Etymology. The specific name is derived from two Latin words: *froni* - (= frons) and -*striatus* (= striate), referring to the upper frons weakly striate.

***Psen scabrosus* sp. nov.**

https://zoobank.org/F238C85C-45D6-478A-B351-E8E595FEAF02

Fig. 3A–H

Type material. ***Holotype*.** China • ♀; Guangdong Province, Ruyuan County Nanling National Nature Reserve; 24°56'15"N, 113°0'40"E; 26.VI–28. IX.2021; 1278 m elev.; collected by Institute of Zoology, Guangdong Academy of Sciences. ***Paratype*:** China • 1♀; Guangdong Province, Fogan County, Guanyin Mountain; 23°58'13"N, 113°33'49"E; 15–16.IX.2007; 184 m elev.; collected by Zaifu XU. All types deposited in YNAU.

Diagnosis. The new species is similar to *Psen leclercqi* van Lith, 1974, but differs from it and other congeners by the following characteristics (characters of *P. leclercqi* in parentheses): 1) free margin of the clypeus has three teeth, middle tooth small, lateral teeth large (free margin of the clypeus has two arch-shaped teeth); 2) the frons has coarse, midsized to large punctures, which gradually increase in size from the lower frons to the mid-ocellus (the frons up to ocelli is densely striate-punctate, interstices shining, very narrow margin along the oculi with finer and sparser punctures); 3) the vertex behind the postocellus distinctly raised (not distinctly raised); 4) the mid ocellus postero-laterally has reticulate punctures with coarse interstices (with fine, sparse punctures, interstices shiny); 5) the hind tibia has a row of long, thick, brownish thorns on the outer surface only (with row of short thick thorns and thin, long, white spines); 6) the scutellum has dense, large punctures, the diameter of punctures is 2–3× as the width of the interspaces, although medially the puncture diameter as wide as interspaces (the scutellum is somewhat striate-punctate, interstices larger than punctures); 7) antennae dark brown, yellowish brown apically, while segments III–VII reddish beneath (antennae black but underside of scape and of segments II, III, and XII are reddish brown); 8) the thorax is black (the pronotum dorsally and upper part of foreside, pronotal tubercles, anterior corners of scutum, and upper 2/3 of anterior plate of the mesepisternum are reddish brown).

Description. Female. Body length 13.0–13.6 mm. Black (Fig. 3A, B); mandible apically reddish brown; palpi and antennae apically yellowish brown, antennae dark brown but joints III–VII reddish beneath (Fig. 3C, D). Fore and mid tibiae and tarsi reddish brown with subsequent parts yellowish brown and inner parts black; tarsi, tegulae, veins of wings, and stigma dark brown; margin of gastral terga yellowish brown (Fig. 3A, B). Appressed setae on clypeus golden, frons with less appressed golden pubescence and long erect setae. Long setae on vertex, occiput, collar, posterior margin of pronotum, scutum, scutellum, and metanotum golden (Fig. 3C–E). Mid-length setae on mesopleuron, legs, and propodeum palely yellow, prospectus and ventral side of petiole silvery; gaster with very dense, short, golden pubescence (Fig. 3B).

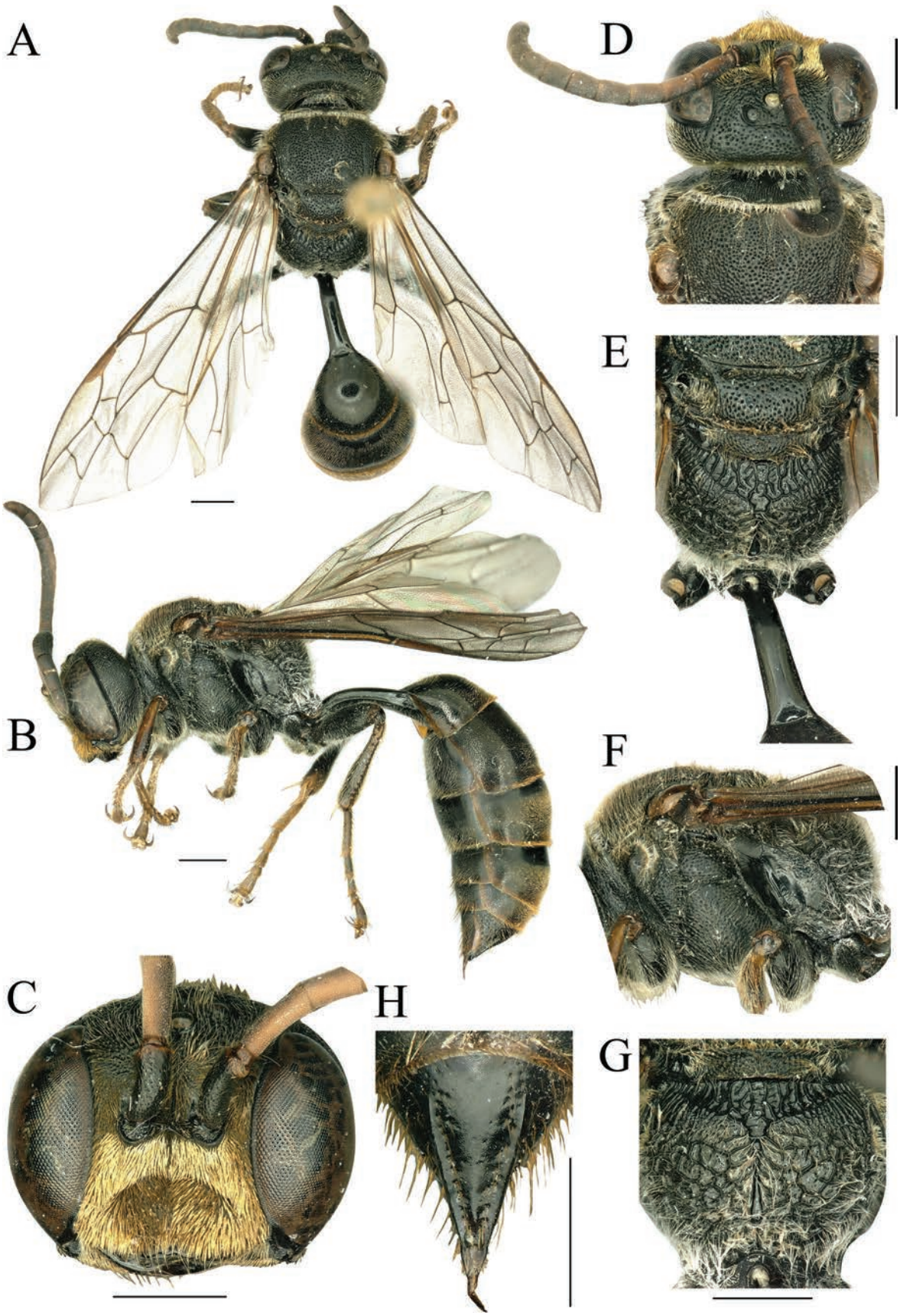

Figure 3. *Psen scabrosus* sp. nov., holotype ♀ **A** habitus, dorsal view **B** habitus, lateral view **C** head, frontal view **D** head, pronotum and scutum, dorsal view **E** scutellum, metanotum and propodeum, dorsal view **F** thorax, lateral view **G** propodeum, posterior view **H** pygidial plate, dorsal view. Scale bars: 1 mm.

***Head*.** In frontal view, clypeus with shiny margin, impunctate, free margin sinuate, with three teeth medially, middle tooth small, lateral teeth large; basal 1/2 of clypeal disk moderately convex (Fig. 3C). HW: HLF: AOD: WAS: IAD = 128: 100: 9: 12: 15. Mandible bidentate apically, broad, blunt; width basally: medially: apically = 26: 15: 5. Carina ending below antennae in low triangular tooth, connected with inner side of antennal sclerites by slender carinae, interantennal tooth distinctly high, apex straight or obtuse; frontal carina distinct and reaching interantennal tooth around median ocellus (Fig. 3C). Scape of antennae slightly bent, relative lengths of joints III–XII = 29, 21, 18, 18, 16, 16, 15, 15, 16, 23; joint III ~ 2.9× as long as wide apically, joint IV with 1.9×, joint 12 with 2.1×. Frons with coarse, midsized to large punctures, diameter of puncture 2–3× as wide as interspaces; lower 2/3 of frons slightly shiny, punctures gradually increase in size from lower frons to mid ocellus (Fig. 3C). In dorsal view, mid ocellus postero-laterally with reticulate punctures, interstices coarse; ocellar area with dense, shallow, large punctures, diameter of puncture approximately as wide as interspaces or slightly more (Fig. 3D). Vertex behind ocellus with deep, large punctures, posteriorly coarser and somewhat striate-punctate, diameter of puncture 2–3× as wide as interspaces, interspaces of vertex slightly larger than frons, barely shiny (Fig. 3D). Ocellus area not raised, behind postocellus with deep sulcus, vertex behind postocellus region distinctly raised (Fig. 3B, D). Occiput with sparse, fine punctures, occipital carina without longitudinal ridge (Fig. 3B, D). HW: HLD: POD: OOD: OCD = 128: 48: 18: 17: 36.

***Thorax*.** Scutum densely and coarsely rugose-punctate, diameter of punctures 2× as wide as interspaces, punctures on both sides arranged in longitudinal trend, interspaces slightly shiny medially; anterior 1/2 of admedian lines slightly expended, posteriorly parallel, parapsidal lines and notauluses nearly parallel (Fig. 3D). Scutellum with dense, large punctures, diameter of puncture 2–3× as wide as interspaces, but diameter of punctures medially as wide as interspaces. Metanotum with dense, oblique carinae, striate-punctate (Fig. 3E). Propleuron with dense, short striae, epicnemial areas densely and finely punctate, omaulus ending as it becomes ventral and below normally curved backwards (Fig. 3F). Mesopleura with dense, midsized to large punctures, interspaces smooth and as wide as diameter of puncture, puncture becoming smaller from top down, upper part of posterior margin of mesopleura with long striae more striking, lower part with fine punctures; subalar area with dense, large punctures, diameter of puncture 2.5× as wide as interspaces, hypo-epimeral area densely, largely striate-punctate (Fig. 3F). Metapleura shiny, with some upper transverse rugae on posterior 1/2 (Fig. 3F). Mesosternum without acetabular carina, with strong, longitudinal medioventral carina; medially with three or four strong transverse carinae. Propodeal enclosure forming a broad triangular shape, enclosed area depressed, shiny, laterally with some longitudinal carinae, medially with irregular carinae; propodeal pad with dense, slender, oblique longitudinal rugae; posterior surface of propodeum with irregular reticulate ridges reaching enclosed area (Fig. 3G). In profile, dorsal surface of propodeum together with posterior surface nearly arc-shaped, lateral surface of propodeum with oblique, short rugae and fine punctures (Fig. 3F). Second submarginal cell receiving first recurrent vein at approximately medially; second recurrent vein ending in second submarginal cell (Fig. 3A). Femora heavy, hind tibia with a row of long, thick, brownish thorns on outer surface (Fig. 3B).

Figure 4. Comparison of midtarsus features of selected species of *Psen* **A** *P. ater* (Olivier, 1792), ventral view **B** *P. ater* (Olivier, 1792), lateral view **C** *P. foveicornis* Tsuneki, 1982, lateral view **D** *P. shirozui* Tsuneki, 1966, lateral view **E** *P. shirozui* Tsuneki, 1966, lateral view **F** *P. bnun* Tsuneki, 1971, ventral view **G** *P. simlensis* van Lith, 1968, ventral view. Scale bars: 0.5 mm.

***Gaster*.** PL: PW: LT I: WT I: HFL: HTL = 80: 17: 77: 87: 82: 70. Petiole nearly quadrate in cross section, slightly bent upwards basally, widened backwards, width apically 1.8× basally, dorsally completely smooth (Fig. 3B, E). Lateral side with two slender longitudinal carinae, deeply depressed medially (Fig. 3B); ventrally with an indistinct, blunt, median longitudinal keel, two sides with dense, fine punctures. Gastral terga I and II with sparse, microscopic punctures, interspaces 2× as wide as diameter of puncture; terga III and IV with dense, fine punctures medially and posteriorly, interspaces as wide as diameter of puncture, but basally 1/3 of tergum III and basally 1/4 of tergum IV smooth, impunctate. Pygidial area elongate-triangular, polished, 1.7× as long as wide basally, laterally with one or two rows of coarse punctures and stiff bristles, apex truncate, slightly concave medially (Fig. 3H). Sterna wholly with sparse, fine punctures except sternum II with dense, fine to midsized punctures.

Male. Unknown.

Distribution. China (Guangdong).

Etymology. The specific name from Latin word: *scabrosus* (= *scabrous*), referring to the head and thorax with large, scabrous punctures.

Acknowledgements

We extend our gratitude to the subject editor and all anonymous reviewers for their valuable and constructive comments. We are grateful to Dr. Nawaz Haider Bashir for his assistance in reviewing and refining the English. We would like to express our sincere gratitude to Zaifu XU (South China Agricultural University) and Lang YI (Xishuangbanna Tropical Botanical Garden, Chinese Academy of Sciences. We also thank Mr. Jikun YANG and Ming LUO for their assistance in specimen collection.

Additional information

Conflict of interest

The authors have declared that no competing interests exist.

Ethical statement

No ethical statement was reported.

Funding

This study was supported by the National Natural Science Foundation of China under Grant number 32270485 and the Agricultural Basic Research joint project of Yunnan Province under Grant number 202101BD070001-004.

Author contributions

Yao Deng conducted the investigation, wrote and revised the manuscript; Li Ma conceived the study, acquired funding, conducted the investigation, and revised the manuscript; Qiang Li conceived the study, acquired funding, and revised the manuscript.

Author ORCIDs

Yao Deng https://orcid.org/0000-0002-0754-4647
Li Ma https://orcid.org/0000-0002-3436-1387
Qiang Li https://orcid.org/0000-0001-5950-8843

Data availability

All of the data that support the findings of this study are available in the main text.

References

Amarante STP (2002) A synonymic catalog of the Neotropical Crabronidaeand Sphecidae (Hymenoptera: Apoidea). Arquivos de Zoologia 37(1): 1–139. https://doi.org/10.11606/issn.2176-7793.v37i1p1-139

Barth (1907) On the nesting habits of *Psen barthi* Viereck. Bulletin of the Wisconsin Natural History Society (New Series) 5: 251–257. http://researcharchive.calacademy.org/research/entomology/Entomology_Resources/Hymenoptera/sphecidae/copies/Barth_1907b_*Psen_barthi*_nesting.pdf

Beaumont JD (1937) Les Psenini (Hym., Sphecid.) de la région paléarctique. Mitteilungen der Schweizerischen Entomologischen Gesellschaft 17: 33–93. http://researcharchive.calacademy.org/research/entomology/Entomology_Resources/Hymenoptera/sphecidae/copies/Beaumont-1937.pdf

Beaumont JD (1964) Insecta Helvetica, Fauna 3, Hymenoptera: Sphecidae. Musée d'Histoire naturelle, 169 pp. https://researcharchive.calacademy.org/research/entomology/Entomology_Resources/Hymenoptera/sphecidae/copies/Beaumont-1964c.pdf

Bohart RM, Menke AS (1976) Sphecid wasps of the world, a genetic revision. University of California Press, Berkeley/ Los Angeles/ London, 695 pp. https://doi.org/10.1525/9780520309548

Boufford DE (2014) Biodiversity Hotspot: China's Hengduan Mountains. Arnoldia 72: 24–35. https://doi.org/10.5962/p.253573

Budrys ER (1986) Digger wasps of the genus *Psen* Latr. (Hymenoptera, Sphecidae) of the Soviet Far East. Akademiya Nauk SSR, Dalnevostochnyi Nauchnyi Tsentr, Biologo-Pochvennyi Institute 138–147. http://researcharchive.calacademy.org/research/entomology/Entomology_Resources/Hymenoptera/sphecidae/copies/Budrys_1986.pdf

Cameron P (1899) III. Description of a new genus and some new species of Fossorial Hymenoptera from the Oriental zoological region. Journal of Natural History 4(19): 52–69. https://doi.org/10.1080/00222939908678162

Dollfuss H (2004) The Pemphredoninae wasps of "Biologiezentrum Linz" collection in Linz, Austria (Hymenoptera, Apoidea, Crabronidae). Linzer Biologische Beiträge 36: 105–129. https://www.zobodat.at/pdf/LBB_0036_2_0761-0784.pdf

Evans HE (1959) Studies on the larvae of digger wasps (Hymenoptera, Sphecidae) Part V: Conclusion. Transactions of the American Entomological Society (1890-) 85(2): 137–191. https://www.jstor.org/stable/25077709

Fu Y, Bashir NH, Li Q, Ma L (2024) A review of *Trypoxylon* Latreille, 1796 (Hymenoptera, Crabronidae) of Southwest China with descriptions of two new species. Journal of Hymenoptera Research 97: 307–347. https://doi.org/10.3897/jhr.97.121279

Girard (1879) Les insectes. Traité elémentaire d'entomologie comprenant l'histoire des espèces utiles et leurs produits, des espèces nuisibles et des moyens de les détruire, l'étude des métamorphoses et des moeurs, les procédés de chasse et de conservation. Librairie J.-B. Baillière, Paris. Vol. 2. Hyménoptères Porte-Aiguillon, 1028 pp. [Sphecodae are in volume 2, pp. 915–975]. https://www.biodiversitylibrary.org/page/33307416

Gussakovskij VV (1932) Verzeichnis der von Herrn D: r R. Malaise im Ussuri und Kamtschatka gesammelten aculeaten Hymenopteren. Arkiv Fur Zoologi, A 24(10): 1–66. https://researcharchive.calacademy.org/research/entomology/entomology_resources/hymenoptera/sphecidae/copies/Gussakovskiy_1932.pdf

Gussakovskij VV (1937) Obzor palearkticheskikh vidov rodov Didineis Wesm., *Pison* Latr. i *Psen* Latr. (Hymenoptera Sphecodea). Trudy Zoologicheskogo Instituta Akademii Nauk SSSR 4: 599–698. http://researcharchive.calacademy.org/research/entomology/Entomology_Resources/Hymenoptera/sphecidae/copies/Gussakovskij_1937.pdf

Hua (2006) Superfamily Apoidea (Sphecoidea). List of Chinese insects 4: 274–299. Vol. IV. Sun-Yat-sen University Press, Guangzhou, 539 pp.

Iwata K (1938) Habits of some Japanese pemphredonids and crabronids (Hymenoptera). Mushi 11: 20–41. [pl. 1] http://researcharchive.calacademy.org/research/entomology/Entomology_Resources/Hymenoptera/sphecidae/copies/Iwata_1938b.pdf

Janvier H (1956) Observations sur deux predateurs chasseurs d'homopteres (Hymenoptera, Sphecidae). Annales de la Société entomologique de France. Taylor & Francis 124(1): 195–208. https://www.tandfonline.com/doi/pdf/10.1080/21686351.1955.12279090

Jiang HF, Yue D, Ma L, & Li Q (2021) Four newly recorded species of the genus *Psen* Latreille from China (Hymenoptera: Crabronidae). Journal of Yunnan Agricultural University: Natural Science Edition, 39–46. [In Chinese] https://xb.ynau.edu.cn/jwk_zk/en/article/doi/10.12101/j.issn.1004-390X(n).202006038

Kazenas VL (1978) Royushchiye osy Kazakhstana i Sredney Azii (Hymenoptera, Sphecidae). Opredelitel. Izdatel'stvo Nauka Kazakhskiy SSR, Alma Ata, 172 pp. http://www.antvid.org/Kazenas/PDF/Publ/1978%20%D0%9A%D0%B0%D0%B7%D0%B5%D0%BD%D0%B0%D1%81_Ammophila,Philanthus,%20Mimesa%20-%20spp.n.%20SE%20Kaz.(1978).pdf

Kazenas VL (2001) Fauna and biology of sphecid wasps (Hymenoptera, Sphecidae) of Kazakhstan and Central Asia. Kazgos INTI, Almaty, 333 pp. https://archive.org/details/KazenasV.I.FaunaAndBiologyOfDiggerWaspshymenopteraSphecidaeOf/page/n1/mode/2up

Latreille PA (1796) Précis des caractères génériques des Insectes, disposés dans un ordre naturel. F. Bourdeaux, Brive, I–XIV + 1–201. [+ 7 unnumbered pp., 1 pl.] https://doi.org/10.5962/bhl.title.58411

Latreille PA (1802) Histoire naturelle générale et particulière des Crustacés et des Insectes. Ouvrage faisant suite à l'Histoire Naturelle générale et particulière, composée par Leclercq de Buffon, et rédigée par C.S. Sonnini, membre de plusiers Sociétés savantes. Vol. 3. Imprimerie F. Dufart, Paris. I–XII, 13–467. https://researcharchive.calacademy.org/research/entomology/Entomology_Resources/Hymenoptera/sphecidae/copies/Latreille_1802a.pdf

Lomholdt O (1975) The Sphecidae (Hymenoptera) of Fennoscandia and Denmark. Fauna Entomologica Scandinavica 4, 224 pp. https://researcharchive.calacademy.org/research/entomology/Entomology_Resources/Hymenoptera/sphecidae/copies/Lomholdt_1975_1976_Fenoscandia_1a.pdf

Ma L, Li Q (2006) A new species of the genus *Psen* (Hymenoptera: Crabronidae) from China. Entomotaxonomia 28(4): 311–314. https://researcharchive.calacademy.org/research/entomology/Entomology_Resources/Hymenoptera/sphecidae/copies/Ma_Li_2006.pdf

Ma L, Li Q (2007) Three new species and two new records of the genus *Psen* from China (Hymenoptera: Apoidea: Crabronidae). Entomological Science 10(3): 259–265. https://doi.org/10.1111/j.1479-8298.2007.00222.x

Malloch JR (1933) Review of the wasps of the subfamily Pseninae of North America (Hymenoptera: Aculeata). Proceedings of the United States National Museum 82(26): 1–60. [2 pls.] http://biodiversitylibrary.org/page/7609329

Merisuo AK (1938) Die Pseninen (Hymenoptera, Sphecidae) Finnlands. Mit einer Bestimmungstabelle der Arten. In: Annales Entomologici Fennici, Vol. 4, 248–254. http://researcharchive.calacademy.org/research/entomology/Entomology_Resources/Hymenoptera/sphecidae/copies/Merisuo_1938.pdf

Myers N, Mittermeier RA, Mittermeier CG, Da Fonse GA, Kent J (2000) Biodiversity hotspots for conservation priorities. Nature 403(6772): 853–858. https://doi.org/10.1038/35002501

Nagase H (2000) A new species of the genus *Psen* from the Ogasawara Islands, Japan (Hymenoptera, Sphecidae, Pemphredoninae). Bulletin of the National Science Museum Series A (Zoology) 26: 51–55. https://ia804505.us.archive.org/18/items/bullnatscimusazool-bnsm260203/bullnatscimusazool-bnsm260203_text.pdf

Price TD, Hooper DM, Buchanan CD, Johansson US, Tietze DT, Alström P, Olsson U, Ghosh-Harihar M, Ishtiaq F, Gupta SK, Martens J, Harr B, Singh P, Mohan D (2014) Niche filling slows the diversification of Himalayan songbirds. Nature 509(7499): 222–225. https://doi.org/10.1038/nature13272

Pulawski WJ (2024) *Psen*: Catalog of Sphecidae. https://researcharchive.calacademy.org/research/entomology/entomology_resources/hymenoptera/sphecidae/genera/*Psen*.pdf [accessed 7 July 2024]

Rafinesque CS (1815) Analyse de la nature ou tableau de l'univers et des corps organisés. Privately published, Palermo, 224 pp. https://doi.org/10.5962/bhl.title.106607

Rohwer SA (1910) Descriptions of new Psenid wasps from the United States (Hymenoptera; Psenidae). Proceedings of the Entomological Society of Washington 12: 99–104. http://biodiversitylibrary.org/page/2590135

Steiner (1986) Venoms of the Hymenoptera. Biochemical, pharmacological and behavioural aspects. Academic Press, London (Vol. 4, pp. 63–160), 570 pp. https://doi.org/10.1016/B978-0-12-554770-3.50008-5

Tsuneki K (1959) Contributions to the knowledge of the Cleptinae and Pseninae faunae of Japan and Korea (Hymenoptera, Chrysididae and Sphecidae). Memoirs

of the Faculty of Liberal Arts, Fukui University (Series II, Natural Science) 9: 1–78. http://researcharchive.calacademy.org/research/entomology/Entomology_Resources/Hymenoptera/sphecidae/copies/Tsuneki_1959g.pdf

Tsuneki K (1966) Contribution to the knowledge of the Pemphredoninae fauna of Formosa and Ryukyus (Hymenoptera, Sphecidae). Etizenia 14: 1–21. http://researcharchive.calacademy.org/research/entomology/Entomology_Resources/Hymenoptera/sphecidae/copies/Tsuneki_1966c.pdf

Tsuneki K (1967) Studies on the Formosan Sphecidae (III). The subfamily Pemphredoninae (Hymenoptera). Etizenia 24: 1–11. http://researcharchive.calacademy.org/research/entomology/Entomology_Resources/Hymenoptera/sphecidae/copies/Tsuneki_1967f.pdf

Tsuneki K (1971) Studies on the Formosan Sphecidae (XIII). A supplement to the subfamily Pemphredoninae (Hym.) with a key to the Formosan species. Etizenia 57: 1–21. http://researcharchive.calacademy.org/research/entomology/Entomology_Resources/Hymenoptera/sphecidae/copies/Tsuneki_1971j.pdf

Tsuneki K (1973) New and the first record species and subspecies of Sphecidae and Mutilidae from Japan, with taxonomic notes of some species. Etizenia 65: 1–28. http://researcharchive.calacademy.org/research/entomology/Entomology_Resources/Hymenoptera/sphecidae/copies/Tsuneki_1973a.pdf

Tsuneki K (1974) Sphecidae (Hymenoptera) from Korea. Annales Historico-Naturales Musei Nationalis Hungarici 66: 359–387. http://publication.nhmus.hu/pdf/annHNHM/Annals_HNHM_1974_Vol_66_359.pdf

Tsuneki K (1982) Studies on the new material of Sphecidae, Chrysididae and Mutillidae of Formosa and the southern Ryukyus (Hymenoptera). Special Publications of the Japan Hymenopterists Association 23: 15–45. http://researcharchive.calacademy.org/research/entomology/Entomology_Resources/Hymenoptera/sphecidae/copies/Tsuneki_1982e_23.pdf

Tsuneki K (1983) A new species of *Psen* (*Psen*) found in Japan (Hymenoptera, Sphecidae, Pemphredoninae). Special Publications of the Japan Hymenopterists Association 25, 63–65. https://researcharchive.calacademy.org/research/entomology/Entomology_Resources/Hymenoptera/sphecidae/copies/Tsuneki-1983f_SPJHA-25.pdf

Turner RE (1912) Notes on fossorial Hymenoptera. -X. The Annals and Magazine of Natural History (Series 8) 10: 361–377. https://doi.org/10.1080/00222931208693249

van Lith JP (1959) Contribution to the knowledge of theIndo-Australian Pseninae (Hymenoptera, Sphecidae). Zoologische Verhandelingen 39(1): 1–69. http://researcharchive.calacademy.org/research/entomology/Entomology_Resources/Hymenoptera/sphecidae/copies/van_Lith_1959_Indo_Australian_Pseninae.pdf

van Lith JP (1965) Contribution to the knowledge of the Indo-Australian Psenini (Hymenoptera, Sphecidae). Part III. New species of the subgenera *Psen* Latreille and Mimumesa Malloch and a review of East-Asiatic and Indo-Australian *Psen* Latreille, s.1. Zoologische Verhandelingen 73: 1–80. http://www.repository.naturalis.nl/document/148841

van Lith JP (1968) Contribution to the Knowledge of IndoAustralian. South Pacific and East Asiatic Psenini Genus *Psen* Latreille. Tijdschrift voor Entomologie 111: 89–135. http://biodiversitylibrary.org/page/28150747

van Lith JP (1973) Psenini from Nepal (Hymenoptera. Sphecidae). Tijdschrift voor Entomologie 116: 123–142. http://biodiversitylibrary.org/page/28382833

van Lith JP (1974) Revision of the Psenini of the Ethiopian Region, including Malagasy (Hymenoptera, Sphecidae, Pemphredonine). Tijdschrift voor Entomologie 117: 39–101. http://biodiversitylibrary.org/page/28200627

van Lith JP (1975) Neotropical species of *Psen* and *Pseneo* (Hymenoptera, Sphecida, Psenini). Tijdschrift voor Entomologie 118: 1–41. http://biodiversitylibrary.org/page/28195289.

van Lith JP (1976) New species and records of Indo-Australian Psenini (Hymenoptera, Sphecidae, Pemphredoninae). Tijdschrift voor Entomologie 119: 79–122. http://biodiversitylibrary.org/page/28265468

van Lith JP (1978) Psenini from Sri Lanka (Hymenoptera, Sphecidae, Pemphredoninae). Tijdschrift voor Entomologie 121: 1–12. http://biodiversitylibrary.org/page/28200231

Woydak H (1996) Hymenoptera Aculeata Westfalica Familia: Sphecidae (Grabwespen). Westfälisches Museum für Naturkunde Landschaftsverband Westfalen-Lippe. http://researcharchive.calacademy.org/research/entomology/Entomology_Resources/Hymenoptera/sphecidae/copies/Woydak_1996_Aculeata_Westfalica.pdf

Wu YR, Zhou Q (1996) Economic Insect Fauna of China, Fasc. 52. Hymenoptera: Sphecidae. Science Press, Beijing, 197 pp. (In Chinese with English Abstract) http://researcharchive.calacademy.org/research/entomology/Entomology_Resources/Hymenoptera/sphecidae/copies/Wu_Zhou_1996a.pdf

Xing Y, Ree RH (2017) Uplift-driven diversification in the Hengduan Mountains, a temperate biodiversity hotspot. Proceedings of the National Academy of Sciences 114(17): E3444-E3451. https://doi.org/10.1073/pnas.1616063114

ZooKeys 1224: 109–127 (2025)
DOI: 10.3897/zookeys.1224.141117

Research Article

First record of *Morimotobathynella* Serban, 2000 (Bathynellacea, Bathynellidae) from subterranean waters of South Korea, with the description of a new species

Su-Jung Ji[1,2], Ana Isabel Camacho[3], Gi-Sik Min[1]

1 *Department of Biological Sciences and Bioengineering, Inha University, Incheon 22212, Republic of Korea*
2 *Division of Biomedical Research, Korea Research Institute of Bioscience and Biotechnology, Daejeon 34141, Republic of Korea*
3 *Museo Nacional de Ciencias Naturales (CSIC), Dpto. Biodiversidad y Biología Evolutiva, Madrid 28006, Spain*
Corresponding author: Gi-Sik Min (mingisik@inha.ac.kr)

Abstract

This study describes *Morimotobathynella koreana* **sp. nov.**, the first new species of Bathynellidae family reported in East Asia since 2000, and it presents the first molecular analysis using CO1 and 18S gene sequences. Morphological analysis reveals that the new species and previously known *Morimotobathynella* species uniquely share key characteristics in the male and female thoracopods VIII. However, the presence or absence of the median seta on the antenna exopod, along with the length differences between the four spines in the furca, distinguish the new species from *M. miurai*, 2000. A molecular phylogenetic analysis indicates that the new species has a relatively close relationship to species from the genus *Altainella* in Mongolia and Russia.

Key words: Interstitial hyporheic zone, Korean peninsula, molecular analysis, *Morimotobathynella koreana* sp. nov., subterranean crustacea, taxonomy

Academic editor: Saskia Brix
Received: 6 November 2024
Accepted: 27 December 2024
Published: 22 January 2025

ZooBank: https://zoobank.org/7DB3E41D-28DF-4CFD-993C-29F92C600603

Citation: Ji S-J, Camacho AI, Min G-S (2025) First record of *Morimotobathynella* Serban, 2000 (Bathynellacea, Bathynellidae) from subterranean waters of South Korea, with the description of a new species. ZooKeys 1224: 109–127. https://doi.org/10.3897/zookeys.1224.141117

Introduction

The order Bathynellacea Chappuis, 1915, found exclusively in freshwater subterranean environments, currently comprises over 340 species distributed among three families: Bathynellidae Grobben, 1905, Parabathynellidae Noodt, 1965, and Leptobathynellidae Noodt, 1965 (Camacho et al. 2021). Unlike Parabathynellidae and Leptobathynellidae—with the latter often considered synonymous with the former—the family Bathynellidae is characterized by smaller, more fragile bodies and stable morphological traits (Drewes and Schminke 2011; Camacho 2015; Camacho et al. 2018a). Consequently, there is a lack of described morphospecies and limited taxonomic knowledge of Bathynellidae compared to the Parabathynellidae. Despite their global distribution, Bathynellidae are currently represented by only about 110 known species in 36 genera worldwide (Camacho et al. 2020; Ji et al. 2024; Perina et al. 2024). This family can be distinguished from other families by

several morphological characteristics: it has a pair of setae on the dorsal side of the pleotelson, the antennae possess an exopod, and the reproductive appendages in females are relatively less simplified than those in other families (Camacho 2015; Camacho et al. 2018a, 2021).

Research on the family Bathynellidae in East Asia—Korea, China, and Japan—has a relatively short history. Initial studies began in Japan in the mid-20th century and primarily focused on morphological studies using samples collected from wells (Morimoto 1959, 1970a, 1974; Uéno 1952, 1954, 1961). In Korea, research on Bathynellidae started with Morimoto (1970b), who described four species of the genus *Bathynella* Vejdovsky, 1882—*B. rufa*, *B. fodinarum*, *B. minuta*, and *B. uenoi*—from caves and wells. To date, these species remain the only known representatives of this family on the Korean Peninsula. No research has been conducted on Bathynellidae in China to date. Meanwhile, the Bathynellidae species found in East Asia have not been examined using molecular phylogenetic methods, and their phylogenetic placement relies solely on the morphological analysis provided by Serban (2000).

This study describes the first new species of Bathynellidae collected from East Asia since 2000, which was collected in South Korea. The new species was assigned to the genus *Morimotobathynella* Serban, 2000, which previously had only one species, *M. miurai* Serban, 2000, from Japan. In addition, we provide the first molecular study of East Asian Bathynellidae species, presenting a global phylogenetic analysis based on the CO1 and 18S gene sequences obtained from this new species.

Materials and methods

Sampling and morphological observation

Samples were collected from the interstitial hyporheic zone of Hongcheon-gun, South Korea (Suppl. material 1). For sampling water from the hyporheic zone, a 1 m core was driven into the points using a hammer, and water was collected using a manual pump and filtered using a 50 μm fine-mesh net (Lee and Park 2016). Specimens were immediately preserved in 95% ethanol. Specimen of *Morimotobathynella koreana* sp. nov. were dissected in glycerol under a stereomicroscope (SZX12, Olympus, Japan). Dissected appendages were mounted using Eukitt® Quick-hardening mounting medium (Sigma-Aldrich, St. Louis, MO, USA) for permanent slide. Observation and drawing were conducted using an optical microscope (DM2500, Leica, Germany). The type materials of the new species examined in this study have been deposited in the collection at the Nakdonggang National Institute of Biological Resources, Korea (**NNIBR**).

Molecular phylogenetic analysis

The genomic DNA was extracted from the tissue using the LaboPass™ Tissue Genomic DNA Isolation Kit Mini (Cosmo GENETECH, Seoul, South Korea) according to the manufacturer's instructions. Amplification by polymerase chain reaction was conducted using the following primer sets: C1-J1718 and C1-J2329 (Simon et al. 1994) for the mitochondrial CO1 gene; 1F, 5R or 3F,

9R (Giribet et al. 1996) for the nuclear 18S gene. The sequences were aligned using ClustalW (Thompson et al. 1994; Larkin et al. 2007) in Geneious Prime (v. 2024.0.2). The intraspecific genetic *p*-distances based on 18S rRNA gene sequences for the family Bathynellidae, including the new species were determined using MEGA X v. 10.1.8 (Kumar et al. 2018).

Phylogenetic analysis

Phylogenetic analyses were performed using maximum likelihood (ML) and Bayesian inference (BI) based on the concatenated sequences of mitochondrial CO1 and 18S rRNA genes. Prior to phylogenetic analysis, 18S rRNA sequences were individually trimmed using Gblocks v. 0.91b with default parameters to eliminate poorly aligned positions and divergent regions (Castresana 2000; Talavera and Castresana 2007). The resulting clean alignments of the 18S rRNA and CO1 sequences were concatenated into a single dataset for subsequent analyses. ML analysis was performed using IQ-TREE v. 1.6.8 with ModelFinder to select the best-fit substitution model. The best-fit model selected according to the Bayesian Information Criterion was GTR+F+I+G4 (Kalyaanamoorthy et al. 2017; Huang et al. 2023). Node support values were assessed using ultrafast bootstrap approximation with 1,000 replicates. Prior to the BI analysis, the best-fit nucleotide substitution model was selected using jModelTest v. 2.1.7 software based on the Akaike Information Criterion, and the GTR+I+G model was selected (Darriba et al. 2012). The BI assessment was performed using MrBayes v. 3.2.6 for 1 million generations (Ronquist et al. 2012); the first 30% of the generations were discarded as burn-ins. The final trees were displayed in FigTree v. 1.4.4 and edited using Adobe Illustrator.

Results

Order Bathynellacea Chappuis, 1915
Family Bathynellidae Grobben, 1905
Subfamily Bathynellinae Grobben, 1905

Genus *Morimotobathynella* Serban, 2000
Korean name: 모리모토옛새우속(신칭)

Amended generic diagnosis. Antennule and antenna 7-segmented. ***Pars molaris*** of the mandible formed by two teeth near the ***processus incisivus accessorius*** and two lobe with distal region covered by denticles. Endopod of thoracopods I–VII 4-segmented. Thoracopod I with coxal seta. Male thoracopod VIII with massive protopod; penial region with three formations, an anterior lobe and two formations (inner and outer) like lamella, with the distal part curved towards the median axis of the appendix, that form an "atrium"; robust endopod with elliptical transversal section, basipod without anterior prominence, small anterior lobe. Thoracopod VIII of female with well-developed epipod with only exopod; absent endopod. Uropod with few setation, with true uropodal claws on the endopod. Furcal rami with robust and short spines.

***Morimotobathynella koreana* Ji, Camacho & Min, 2024, sp. nov.**
https://zoobank.org/02D78393-4E81-4F71-B3D3-30F02D548C6C
Figs 1–6
Korean name: 한국모리모토옛새우(신칭)

Type locality. Hongcheon-gun (37°41'15.82"N, 127°41'0.53"E), South Korea; collected by G.-S. Min, C.-W. Lee, and H.-M. Yang on 4 March 2016.

Type materials. *Holotype*: male (NNIBRIV136387), dissected on six slides. ***Allotype*:** female (NNIBRIV136388), dissected on five slides. ***Paratypes*:** 3 females (NNIBRIV136389–136391).

Diagnosis. Antennule and antenna 7-segmented; antennule much longer than antenna. Antenna exopod without median seta. Mandible: mandibular palp with three articles; pars molaris with two lobes bearing small denticles distally, lacking a prominent terminal tooth. Endopod of thoracopods I–VII 4-segmented; coxa of thoracopod VII with a strong plumose seta on thoracopod I; sexually dimorphic in thoracopod VIII of males and females. Male thoracopod VIII: massive protopod with penial region forming an "atrium," inner and outer lamellae curving towards the center; basipod with a rounded crest and one distal seta; exopod elongated with a robust apex and elliptical transversal section; endopod absent. Female thoracopod VIII: coxa with a small protrusion with setules, a very large and well-developed epipod exceeding the basipod length, and an exopod with two equal long setae, lacking an endopod. Uropod: sympod with five spines; endopod with long and strong terminal setae; exopod with four setae, two barbed terminally. Furcal rami with the first spine nearly twice as long as the others.

Description. Adult male. *Total body* (Fig. 1) 0.9 mm in length. Cylindrical and elongate body with a similar diameter on thoracic and abdominal articles. Head longer than wide. Pleotelson with one small dorsal seta on each side.

Antennule (Fig. 2A) 7-segmented; the first three articles equal in length to the last four combined; the first article is the longest and the fourth is the smallest; small rectangular inner flagellum; the third article with five smooth setae; the sixth and seventh articles with three aesthetascs of different sizes; antennule much longer than antenna.

Antenna (Fig. 2B) 7-segmented; without a medial seta on exopod; the first, fourth, and sixth articles similar in length; the second and third articles similar in length and the shortest; fifth article small, measuring just over half length of first article; the last article is the longest, 1/3 longer than the first one; setal formula: 0+0/2+0/2+0/2+0/0+0/1+2/4.

Labrum (Fig. 2C). The distal smooth free edge, with central irregular protuberances.

Paragnaths (Fig. 2D) almost rectangular; having setulation on the distal half.

Mandible (Fig. 3A). Palp with three articles, the third article with two claws of different length, the first and second articles rectangular and robust, and the third article small and almost square; masticatory part: incisor process (***pars incisiva***) with two teeth; accessory incisor process (***processus incisivus accessorius***) with one tooth and one tiny spine; molar part (***pars molaris***) with two lobes having small denticles.

Maxillule (Fig. 3B). The proximal endite with four setae, all setulose; the distal endite having five teeth and the distal one with three denticles; three plumose setae of different length on the outer margin.

Figure 1. Habitus of *Morimotobathynella koreana* sp. nov. (female, NNIBRIV136391). Scale bar: 0.5 mm

Maxilla (Fig. 3C) 4-segmented; setal formula 6, 4, 6, and 4.

Thoracopods I–VII (Figs 3D, E, 4A–D, 5A). Well developed; thoracopod I–III (Figs 3D, E, 4A) progressively longer; thoracopod IV–VI (Fig. 4B–D) of similar length; thoracopod VII (Fig. 5A) longer than the others; thoracopod I–VII with epipod a little longer than half the basipod; coxa with long strong plumose seta on thoracopod I; rectangular basipod with two smooth setae on thoracopods I–IV, with only one seta on thoracopod V–VII.

Exopods of thoracopods I–VII (Figs 3D, E, 4A–D, 5A) 1-segmented with barbed setae (two terminal, one dorsal and two ventral) and shorter than endopods of thoracopods I–VII; as long as the first two articles combined in thoracopods I–III and VI–VII, reaching the middle of the third endopodal article in thoracopods IV and V.

Endopods thoracopods I–VII (Figs 3D, E, 4A–D, 5A) 4-segmented; the first two articles similar in length in thoracopod I; second article longer than the first article, equal in length to the third article in thoracopods II and VII; the second article very long in thoracopods VI and VII; the fourth article small in all thoracopods. Setal formula of endopods (the number of setae on basipod in brackets):

Thoracopod I: (2) 2+0/2+1/2+0/3

Thoracopods II, III: (2) 2+0/2+1/2+0/3

Thoracopod IV: (2) 2+0/2+1/2+0/3

Thoracopod V: (1) 2+0/1+1/1+0/3

Thoracopods VI, VII: (1) 0+0/0+1/0+0/2(1)

Thoracopod VIII (Fig. 5B) with a massive protopod; penial region with the distal prolongation similar in size to the three other formations: an anterior lobe and two formations (inner and outer) resembling lamellae rather than lobes, with the distal part curved towards the median axis of the appendix, forming an "atrium"; basipod with a rounded crest with a small seta at the base; robust exopod with elliptic transversal section and four setae; endopod absent.

Pleopods (Fig. 5D) 2-segmented; the first article with very long smooth seta; the second article with five setae: four smooth setae and one barbed seta of different lengths.

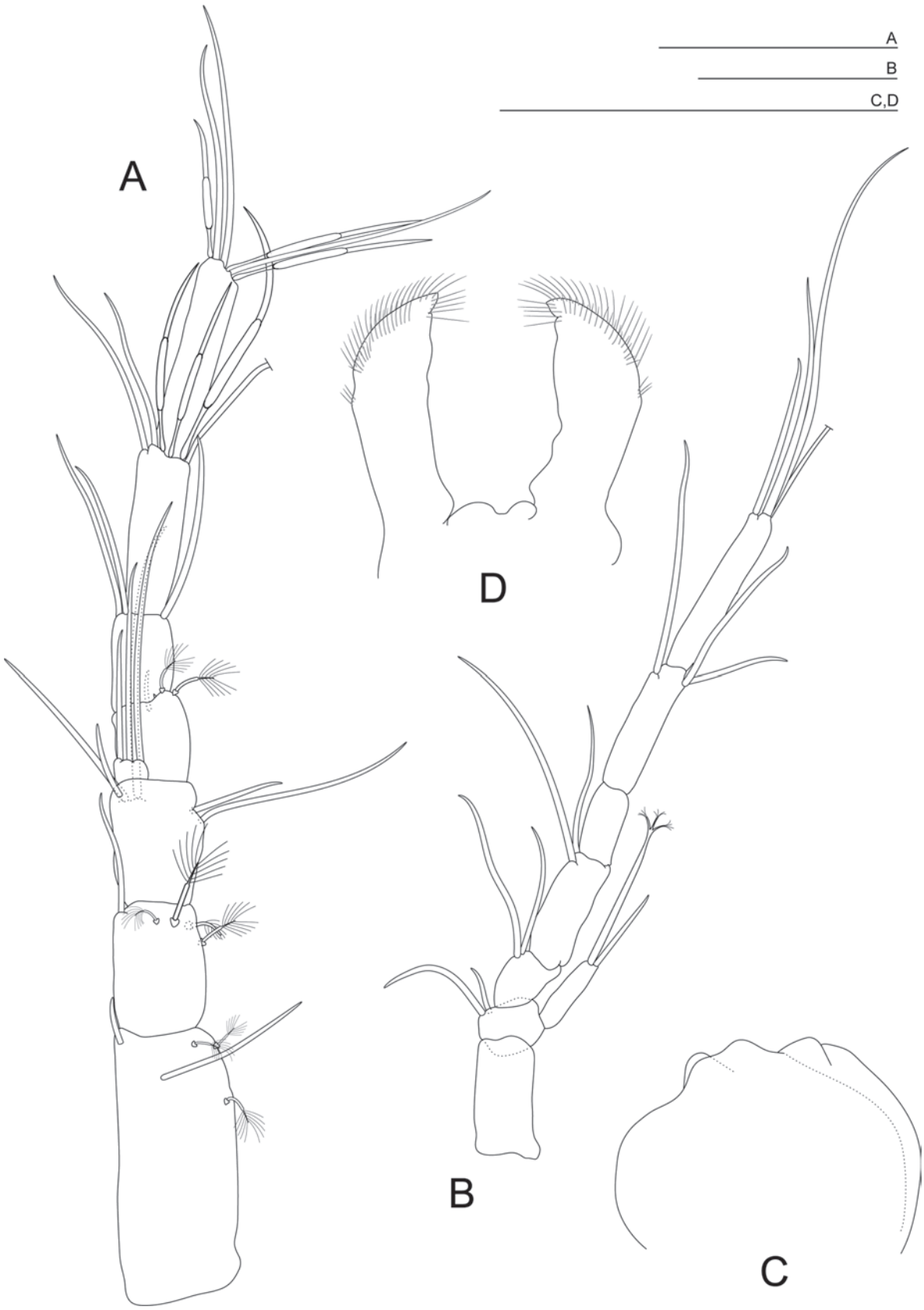

Figure 2. *Morimotobathynella koreana* sp. nov., holotype male **A** antennule **B** antenna **C** labrum **D** paragnath. Scale bars: 0.05 mm.

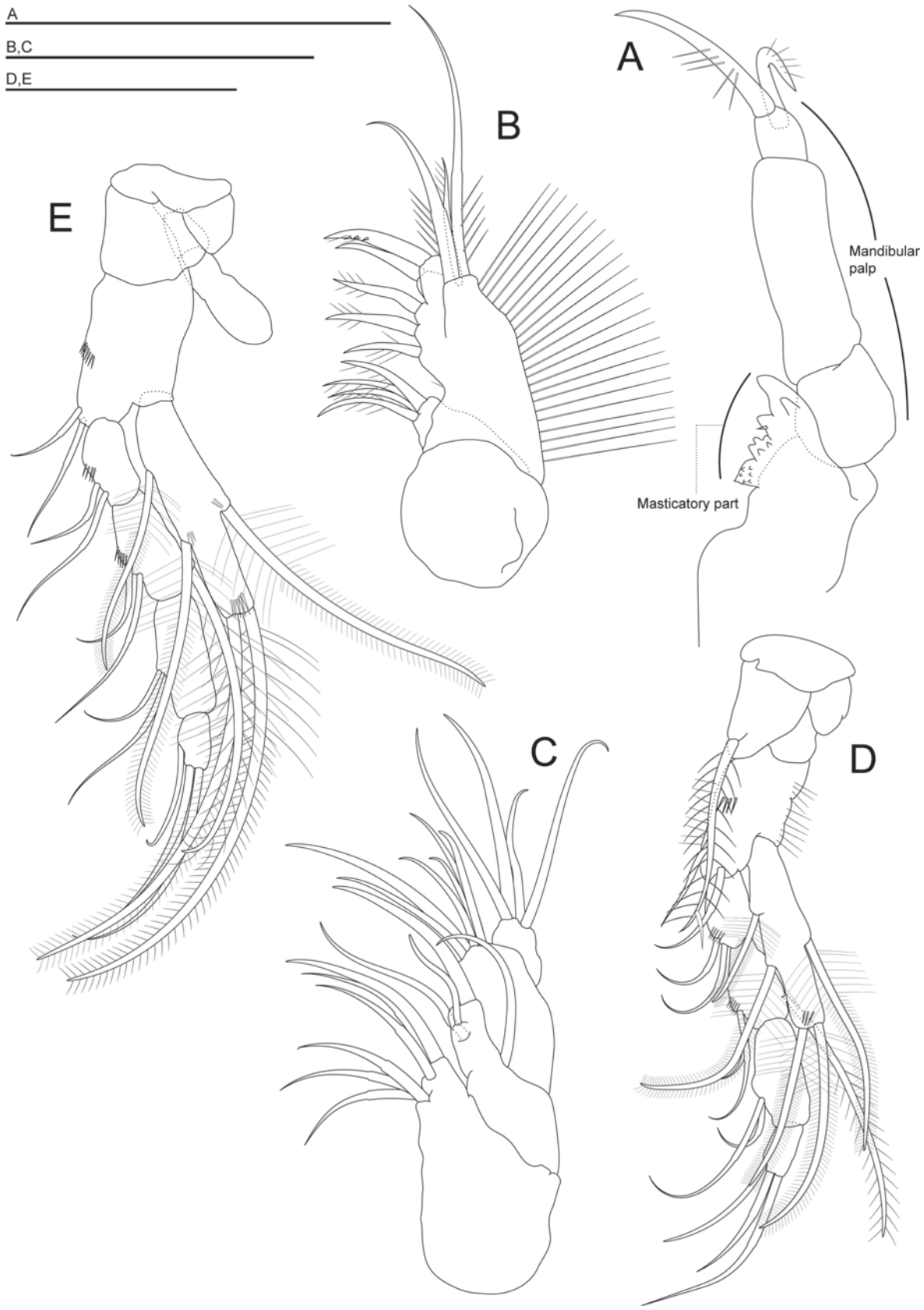

Figure 3. *Morimotobathynella koreana* sp. nov., holotype male **A** mandible **B** maxillule **C** maxilla **D** thoracopod I **E** thoracopod II. Scale bars: 0.05 mm.

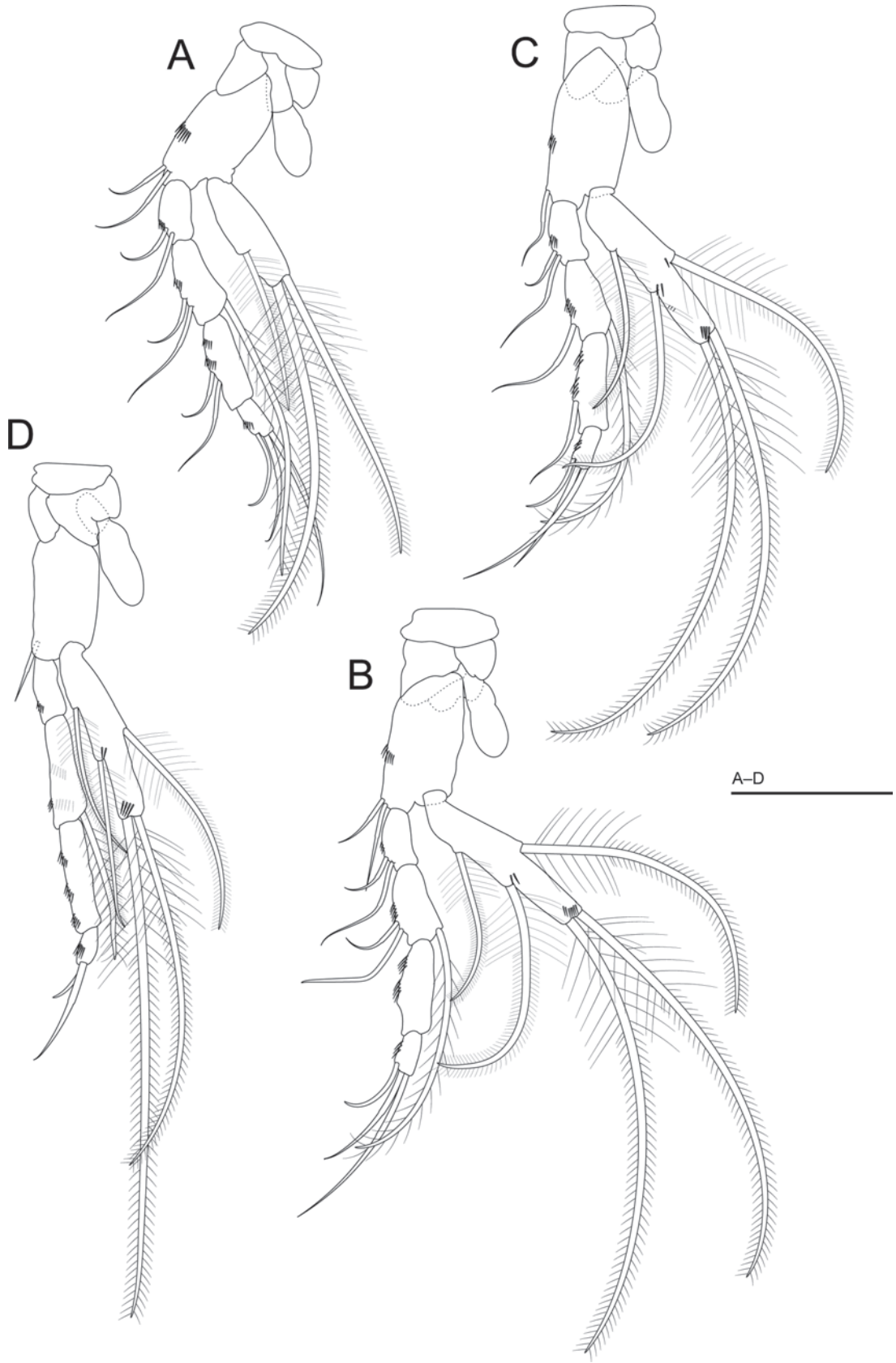

Figure 4. *Morimotobathynella koreana* sp. nov., holotype male **A** thoracopod III **B** thoracopod IV **C** thoracopod V **D** thoracopod VI. Scale bars: 0.05 mm.

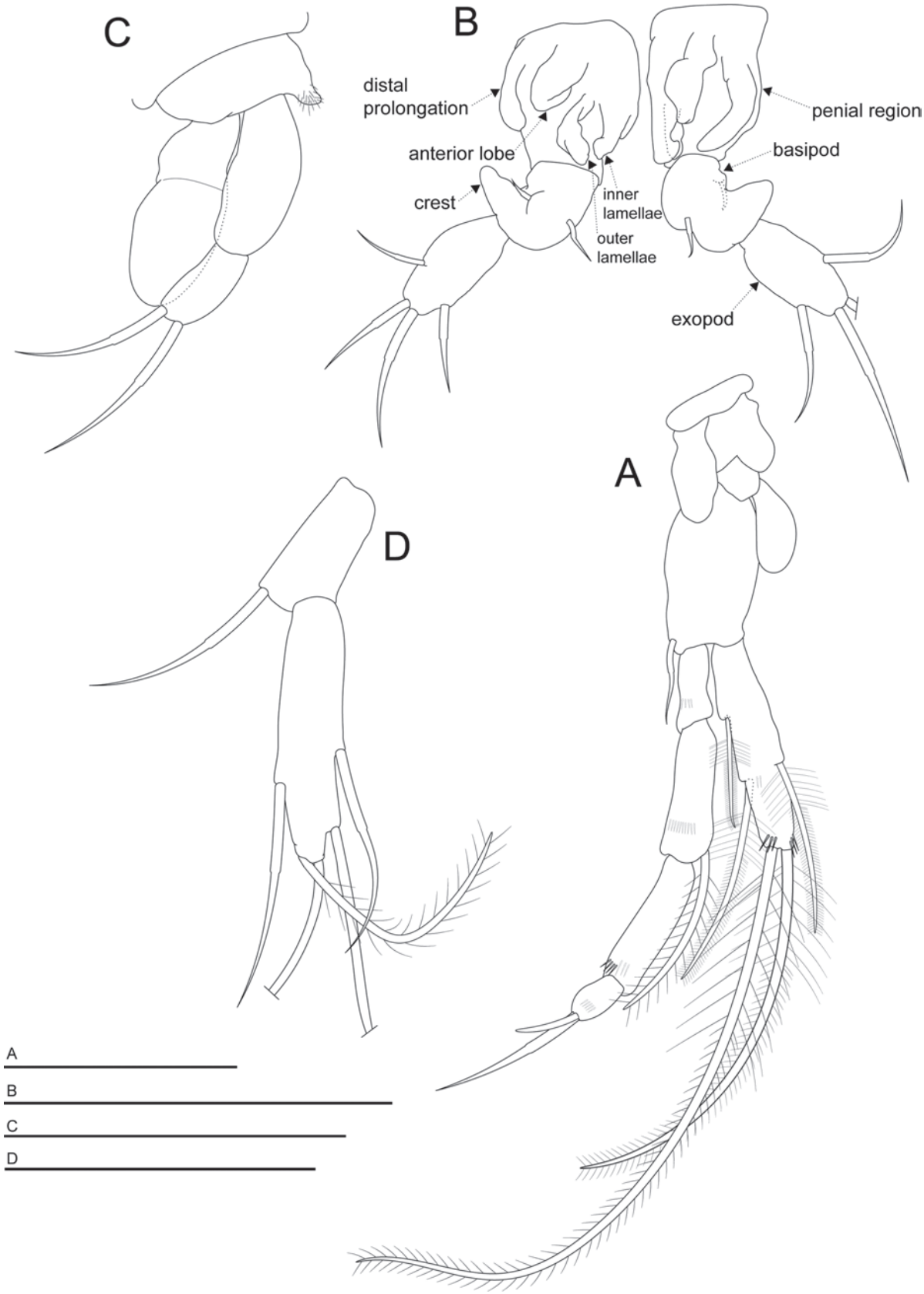

Figure 5. *Morimotobathynella koreana* sp. nov., (**A, B, D**) holotype male, (**C**) allotype female **A** thoracopod VII **B** thoracopod VIII **C** thoracopod VIII **D** pleopod. Scale bars: 0.05 mm.

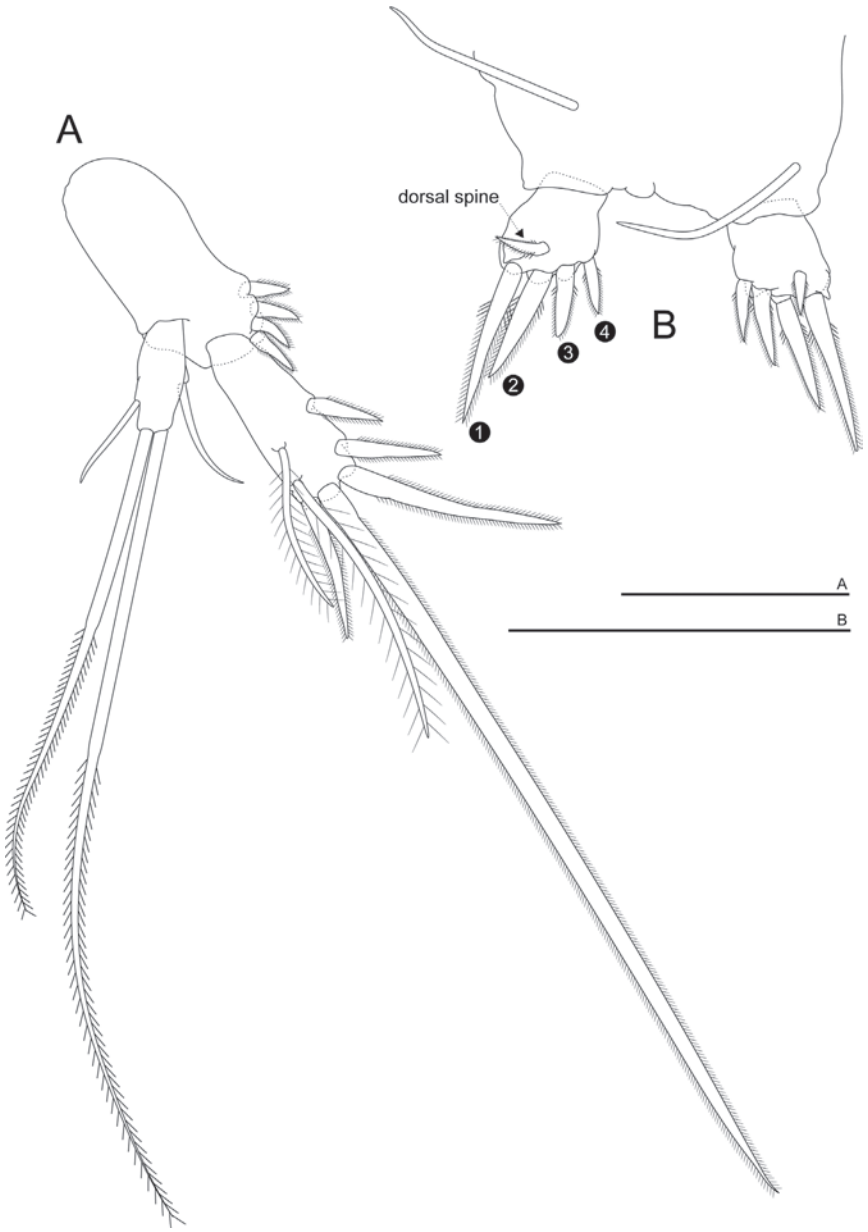

Figure 6. *Morimotobathynella koreana* n. sp., holotype male **A** uropod **B** pleotelson and furcal rami. Scale bars: 0.05 mm.

Uropods (Fig. 6A). Sympod 50% longer than wide and as long as the endopod, with four equal distal spines; endopod almost 50% longer than exopod, with three strong spines, the distal one being two times longer than second which is longer than the first, and one fourth terminal spine thinner than the other three, and on distal end there are a long and strong special seta, and two plumose setae located dorso-laterally; exopod with four setae, two terminal barbed, of different length, and two short medial setae.

Pleotelson (Fig. 6B) with one barbed dorsal seta on each side near the base of furca, each extending beyond furcal rami

Furcal rami (Fig. 6B) almost square, bearing five spines; the first spine almost twice as long as the fourth and slightly longer than the second, which itself a bit longer than the third; the fourth spine about the same length as the dorsal spine.

Adult female. The female is similar to the male in all its features except for thoracopod VIII.

Thoracopod VIII (Fig. 5C). Coxa with a small protrusion with setules; having a very well-developed epipod exceeding the length of the basipod, reaches the distal end of the exopod; with only one ramus, the exopod with two equal long setae, absent endopod.

Morphological remarks. Morphological comparisons of the new species with the three subfamilies within Bathynellidae, as well as comparisons between the two species of the genus *Morimotobathynella*, are listed in the tables (Suppl. material 2: table S1, Table 1). This section presents a detailed examination of the morphological characteristics of the appendages of these two *Morimotobathynella* species.

Table 1. Morphological differences among *Morimotobathynella miurai* Serban, 2000 and *M. koreana* sp. nov.

	M. miurai	***M. koreana* sp. nov.**
Country	Japan	South Korea
Antennule		
Aesthetacs on sixth article	3	3
Aesthetacs on seventh	3	3
Antenna		
Medial seta on exopod	Present	Absent
Setal formula	0+0/2+0/2+0/2+0/0+0/0+0/5	0+0/2+0/2+0/2+0/0+0/1+2/4
AI vs. AII	AI < AII	AI > AII
Mandible		
Teeth	5+small lobe with denticles	7+denticles
Paragnath	with setules and strong tooth	with setules
Maxillule		
Setules on outer margin	Absent	Present
Maxilla		
Setal formula	—	6, 4, 6, 4
Thoracopod I-VII		
Epipod on thoracopod I	Absent	Absent
Number of setae on thoracopods I-VII exopod	5-5-5-5-5-5-5	5-5-5-5-5-5-5
(Basipod setae) Setal formula of thoracopod I-VII endopod	(4) 4+0/3+1/3+0/4	(2) 2+0/2+1/2+0/3
	(3) 3+0/3+1/3+0/4	(2) 2+0/2+1/2+0/3
	(3) 3+0/3+1/3+0/4	(2) 2+0/2+1/2+0/3
	(3) 3+0/3+1/2+0/3	(2) 2+0/2+1/2+0/3
	(1) 1+0/0+1/0+0/2	(1) 2+0/1+1/1+0/3
	(1) 1+0/0+1/0+0/2	(1) 0+0/0+1/0+0/2(1)
	(1) 1+0/0+1/0+0/2	(1) 0+0/0+1/0+0/2(1)
Thoracopod VIII of female		
Coxa	With setulated protuberance on inner margin	With setulated protuberance on inner margin
Basipod	With 2 setae on inner margin	Without setae
Endopod	absent	Absent
Exopod	With 2 terminal setae of similar length	With 2 terminal setae of similar length
Epipod	Exceeding the length of basipod and exopod combined	Similar in length to the basipod and exopod combined
Thoracopod VIII of male		
Distal prolongation	Present	Present

	M. miurai	***M. koreana* sp. nov.**
Anterior lobe	Present	Present
Inner lamella vs. outer lamella	Inner < outer, two lamellae completely closed, forming a small inner space	Inner = outer, two lobes not completely closed, Forming a small inner space.
Basipod axis	Vertical	Inclined
Crest (anterior prominence) on basipod	Absent	Blunt-tipped conical shape
Endopod	Present; fused with basipod	Absent
Exopod	Like exopod of thoracopods	Like exopod of thoracopods
Pleopod		
First article	1 seta	1 seta
Second article	3 setae	5 setae
Uropod		
Number of spines on sympod	4	4
Sympod vs. endopod	Sympod > endopod	Sympod = endopod
Length of endopod	Slightly longer than exopod	Twice longer than exopod
Furca		
Spines length comparison	Dorsal spine <4<1<3<2	Dorsal spine = 4<3<2<1
Dorsal spines	Very small	Similar to the fourth spine
Dorsal seta of pleotelson	Absent	Exceeding the furcal rami

1. The size proportions of antennule articles differ between the two species. In the new species, the first three articles are approximately the same length as the last four articles, with the first being the longest and the fourth being the shortest. In *M. miurai*, the combined lengths of the first three articles were greater than those of the last four articles. In addition, the second and third articles are twice as long as the fourth and fifth articles, which are the shortest and equally long, respectively.
2. In the new species, the length of antennule is greater than that of antenna, whereas in *M. miurai*, antennule is shorter than antenna.
3. In both species, the longest article is the last article, followed by the first, fourth, and sixth articles of the same length. The second, third, and fifth articles are the shortest and very similar in length in the new species. In contrast, in *M. miurai*, the fifth article is twice as long as the second and third articles, which are similar in size and are the smallest.
4. In the new species, the pars molaris of the mandible does not have a terminal tooth larger than the denticles on the two lobes, as observed in *M. miurai*.
5. The new species has dense setules on the outer margin of the maxillule, which are absent in *M. miurai*.
6. The setal formula of the thoracopods differs between the two species (see Discussion and Table 1). However, we cannot compare the proportions of the articles because the thoracopods were not illustrated in the original description of *M. miurai*.
7. Thoracopod VIII in males differs significantly between the two species; *M. miurai* has an endopod with two setae, that are absent in the new species.
8. In thoracopod VIII of female, *M. miurai* has a large epipod that extends beyond the exopod, whereas in the new species, the epipod does not exceed the length of the exopod. *Morimotobathynella miurai* has two setae on the basipod, that are absent in the new species.

9. In the uropod, *M. miurai* has four spines on the sympod that are similar in pairs, with the two distal spines being longer than the two proximal spines. In the new species, all four spines on the sympod are similar in length and shorter than those of the type species of the genus. Additionally, in *M. miurai*, the exopod and endopod are equal in length, whereas in the new species, the endopod is twice as long as the exopod.
10. In the furcal rami, the longest spine in *M. miurai* is the second, which has nearly the same length as the third, while the first and fourth spines are similar in size and slightly smaller, and the dorsal spine is very small. In the new species, the longest spine is the first, with the spines gradually decreasing in length; the fourth is one-third the length of the first and similar in size to the dorsal spine.

Etymology. The specific epithet "*koreana*" is derived from South Korea, the country where the new species was discovered.

***Morimotobathynella* sp.**

Material examined. Pocheon-si (38°6'56.21"N, 127°15'46.38"E), South Korea. Collected by S. -J. Ji and C. -W. Lee on 31 May 2020.

Remarks. This specimen was included in the phylogenetic analysis to mitigate potential long-branch attraction issues that could affect the phylogenetic placement of *M. koreana* sp. nov. The inclusion of this closely related species provides a more robust phylogenetic framework for the genus *Morimotobathynella* in East Asia. Although a detailed morphological examination suggests that this specimen represents another potentially new species, a formal description requires additional material.

CO1 and 18S rRNA gene sequencing

In this study, 597 bp of CO1 (PQ790059–PQ790061) and 1,713 bp of 18S sequences (PQ789943, PQ789944) were obtained from *M. koreana* sp. nov. The three CO1 and two 18S sequences obtained from *M. koreana* sp. nov. showed no intraspecific variation. Additionally, 597 bp of CO1 (PQ790062) and 1,210 bp of 18S sequences (PQ789945) were obtained from *Morimotobathynella* sp. collected in Pocheon, South Korea. Genetic divergence analysis revealed that the two Korean *Morimotobathynella* species had *p*-distances of 10.4% for CO1 and 1.2% for 18S sequences.

Phylogenetic analysis

ML and BI analyses were performed using a concatenated 1,002 bp dataset comprising CO1 (615 bp) and 18S rRNA (387 bp) sequences from the new species and 18 other Bathynellidae species available in GenBank (Fig. 7, Suppl. material 2: table S2). *Allobathynella danyangensis* Ji & Min, 2023 from South Korea (Family Parabathynellidae) was used as outgroup, and the analysis confirmed the monophyly of Bathynellidae. Both the ML and BI analyses produced congruent tree topologies. Our results also support the separation of three distinct subfamilies within Bathynellidae, corroborating previous studies (Camacho

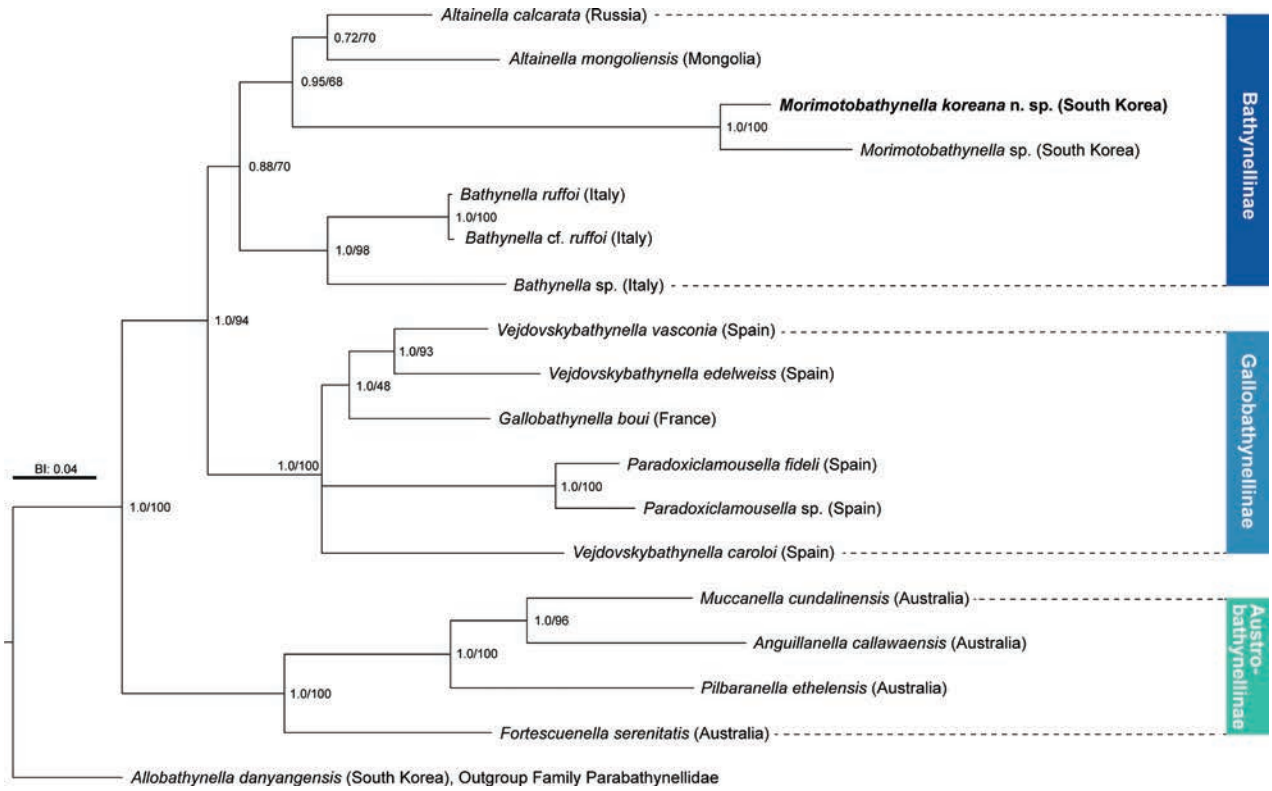

Figure 7. Maximum likelihood and Bayesian inference analyses based on nuclear 18S and mitochondrial CO1 sequences (1,002 bp). Numbers on nodes represent bootstrap values for maximum likelihood and Bayesian posterior probabilities.

et al. 2013, 2020). Phylogenetic trees revealed that *M. koreana* sp. nov. and *Morimotobathynella* sp. from South Korea formed a distinct monophyletic lineage within the subfamily Bathynellinae, with strong support (bootstrap support: 100%, posterior probability: 1.0). They showed a close relationship with species of the genus *Altainella* from Mongolia and Russia (bootstrap support: 68%, posterior probability: 0.95). This phylogenetic relationship may suggest a historical biogeographic connection among bathynellid taxa in Northeast Asia.

Discussion

Six genera within the family Bathynellidae have been identified in East Asia: *Bathynella* Vejdovsky, 1882; *Uenobathynella* Serban, 2000; *Parauenobathynella* Serban, 2000; *Nihobathynella* Serban, 2000; *Paradoxibathynella* Serban, 2000; and *Morimotobathynella* Serban, 2000 (Morimoto 1970b; Serban 2000). Of these, five genera, except *Bathynella*, were all found and recorded only in Japan (Serban 2000). The only known species belonging to the genus *Morimotobathynella*, *M. miurai* Serban, 2000, and *M. koreana* sp. nov., share the following phylogenetically significant morphological characteristics: the female thoracopod VIII has only the exopod without the endopod; the female thoracopod VIII has a small projection with ctenidia on the inner margin and a large epipod; and the inner and outer lamellae located on the inner side of the penial region of the male thoracopod VIII curve towards the center, forming a narrow space—referred to as the "atrium" (see Description and Fig. 5). Based on this morphological evidence, we assigned a new species from South Korea to the genus *Morimotobathynella*. Serban's (2000) description of *M. miurai* is relatively detailed, and the morphological comparison of the two species within the

genus *Morimotobathynella*, presented in Table 1, confirms that they are clearly distinct despite sharing evolutionary important characteristics. However, no molecular support currently exists to distinguish species within the family Bathynellidae from East Asia, including the genus *Morimotobathynella*.

The molecular phylogenetic analysis of the Bathynellidae revealed several key findings (Fig. 7). Our results placed the two *Morimotobathynella* species collected from South Korea within the subfamily Bathynellinae, one of the three recognized subfamilies within Bathynellidae. Despite its relatively long branch, the genus *Morimotobathynella* showed a closer phylogenetic relationship with the Asian clade represented by *Altainella* species from Mongolia and Russia than with the European or Australian taxa (Fig. 7). Meanwhile, phylogenetic analyses of the families Bathynellidae and Parabathynellidae, revealed similar biogeographic patterns, with separation into Eurasian and Australian clades (Camacho et al. 2018b; Ji and Min 2023a, 2023b). These results indicate that the two families, although independently evolved, may have responded similarly to shared paleogeographic events such as tectonic events or faults, owing to their exclusive presence in continental groundwater environments. This phylogeographical aspect has been relatively well documented in the family Parabathynellidae but remains understudied in Bathynellidae.

Serban (2000) assigned the genus *Morimotobathynella* to the subfamily Bathynellinae, which is consistent with the results of the molecular phylogenetic analysis presented in this study. However, morphological examination revealed that *M. koreana* sp. nov. did not match the currently recognized diagnostic characteristics of the three subfamilies (Suppl. material 2: table S1). The inability to place the new species within existing subfamilies based on morphology suggests that the current morphological diagnosis for subfamily classification within Bathynellidae may be insufficient or require revision. While this study points to the need for refinement of morphological diagnoses to better reflect phylogenetic relationships, such revisions require broader comparative studies across diverse bathynellid taxa. To resolve this issue, prioritizing morphological and molecular phylogenetic studies on bathynellid samples from underrepresented regions, such as Asia, South Africa, and South America, is needed.

Hereby, five species within the family Bathynellidae are present in South Korea, including the newly described *M. koreana* sp. nov. and four species of the genus *Bathynella* recorded in 1970 (Morimoto 1970b). As noted in several studies (Camacho et al. 2018a, 2020; Perina et al. 2018), a taxonomic revision and possible reassignment to new genera of these *Bathynella* species may be necessary, although this falls outside the scope of the current research. Considering that 40 species of the family Parabathynellidae, another well-known group of Bathynellacea in South Korea, have been documented, and given their similar evolutionary histories in subterranean freshwater environments, it is likely that the true diversity of Bathynellidae in South Korea is much higher than that currently recognized.

This study is significant because it presents a starting point for new research on Bathynellidae in the East Asian region by describing a newly discovered Bathynellidae species in South Korea through morphological and molecular analyses. Future research should focus on conducting comprehensive field surveys, detailed morphological assessments, and molecular phylogenetic analyses of the family Bathynellidae in this region to uncover hidden species diversity and enhance our understanding of their evolutionary and biogeographical patterns on a global scale.

Acknowledgements

Additional support was provided by Inha University, Korea Research Institute of Bioscience and Biotechnology (KRIBB) Research Initiative Program, and the Ministry of Science and ICT [충남대WISET경복제2024-가08호].

Additional information

Conflict of interest

The authors have declared that no competing interests exist.

Ethical statement

No ethical statement was reported.

Funding

This study was supported by a grant from the Nakdonggang National Institute of Biological Resources (NNIBR), funded by the Ministry of Environment (MOE) of the Republic of Korea (NNIBR20252102).

Author contributions

Conceptualization: SJJ. Data curation: SJJ. Formal analysis: SJJ. Funding acquisition: GSM. Investigation: GSM. Methodology: SJJ. Project administration: GSM. Resources: GSM. Software: SJJ. Supervision: GSM. Visualization: SJJ. Writing - original draft: SJJ, AIIC. Writing - review and editing: SJJ, GSM, AIIC.

Author ORCIDs

Su-Jung Ji https://orcid.org/0000-0003-3132-2021
Ana Isabel Camacho https://orcid.org/0000-0003-0596-7678
Gi-Sik Min https://orcid.org/0000-0003-2739-3978

Data availability

All of the data that support the findings of this study are available in the main text or Supplementary Information.

References

Camacho AI (2015) Class: Malacostraca. Orden Bathynellacea. Revista Electronica IDE@-SEA 79: 1–17.

Camacho AI, Dorda BA, Rey I (2013) Integrating DNA and morphological taxonomy to describe a new species of the family Bathynellidae (Crustacea, Syncarida) from Spain. Graellsia 69: 179–200. https://doi.org/10.3989/graellsia.2013.v69.086

Camacho AI, Mas-Peinado P, Dorda BA, Casado A, Brancelj A, Knight LR, Hutchins B, Bou C, Perina G, Rey I (2018a) Molecular tools unveil an underestimated diversity in a stygofauna family: a preliminary world phylogeny and an updated morphology of Bathynellidae (Crustacea: Bathynellacea). Zoological Journal of the Linnean Society 183: 70–96. https://doi.org/10.1093/zoolinnean/zlx063

Camacho AI, Mas-Peinado P, Watiroyram S, Brancelj A, Bandari E, Dorda BA, Casado A, Rey I (2018b) Molecular phylogeny of Parabathynellidae (Crustacea, Bathynellacea),

and three new species from Thai caves. Contributions to Zoology 87: 227–260. https://doi.org/10.1163/18759866-08704002

Camacho AI, Mas-Peinado P, Iepure S, Perina G, Dorda BA, Casado A, Rey I (2020) Novel sexual dimorphism in a new genus of Bathynellidae from Russia, with a revision of phylogenetic relationships. Zoologica Scripta 49: 47–63. https://doi.org/10.1111/zsc.12387

Camacho AI, Mas-Peinado P, Reddy YR, Bandari E, Shaik S, Perina G, Dorda BA, Casado A, Rey I (2021) An integrated approach to re-evaluate the validity of the family Leptobathynellidae (Crustacea: Bathynellacea. Zoological Journal of the Linnean Society 192: 853–895. https://doi.org/10.1093/zoolinnean/zlaa121

Castresana J (2000) Selection of conserved blocks from multiple alignments for their use in phylogenetic analysis. Molecular Biology and Evolution 17: 540–552. https://doi.org/10.1093/oxfordjournals.molbev.a026334

Darriba D, Taboada GL, Doallo R, Posada D (2012) jModelTest 2: more models, new heuristics and parallel computing. Nature Methods 9: 772–772. https://doi.org/10.1038/nmeth.2109

Drewes J, Schminke HK (2011) Number of families within Bathynellacea (Malacostraca) and year of publication of their names, with redescription of *Baicalobathynella magna* (Bazikalova, 1954) from Lake Baikal. Crustaceana 84: 1377–1401. https://doi.org/10.1163/001121611X590120

Giribet G, Carranza S, Baguñà J, Riutort M, Ribera C (1996) First molecular evidence for the existence of a Tardigrada+Arthropoda clade. Molecular Biology and Evolution 13: 76–84. https://doi.org/10.1093/oxfordjournals.molbev.a025573

Huang Z, Yuan X, Sun S, Leng G, Tang Q (2023) Groundwater depletion rate over China during 1965–2016: the long-term trend and inter-annual variation. Journal of Geophysical Research, Atmospheres 128: e2022JD038109. https://doi.org/10.1029/2022JD038109

Ji SJ, Min GS (2023a) A new subterranean species of *Arisubathynella* Park & Eun, 2012 (Crustacea: Bathynellacea: Parabathynellidae) from South Korea, with remarks on the phylogenetic relationships among 15 parabathynellid genera. Journal of Crustacean Biology 43: ruad022. https://doi.org/10.1093/jcbiol/ruad022

Ji SJ, Min GS (2023b) Two new species of *Nipponbathynella* Schminke, 1973 from South Korea, with a brief discussion on Korean parabathynellid genera (Crustacea, Bathynellacea). Diversity 15(10): 1052. https://doi.org/10.3390/d15101052

Ji SJ, Camacho AI, Lee CW, Min GS (2024) The first report of Bathynellacea in the subterranean water of Mongolia: a new species of *Altainella* Camacho, 2020 (Crustacea, Bathynellidae). Biodiversity Data Journal 12: e130024. https://doi.org/10.3897/BDJ.12.e130024

Kalyaanamoorthy S, Minh BQ, Wong TK, Von Haeseler A, Jermiin LS (2017) ModelFinder: fast model selection for accurate phylogenetic estimates. Nature Methods 14: 587–589. https://doi.org/10.1038/nmeth.4285

Kumar S, Stecher G, Li M, Knyaz C, Tamura K (2018) MEGA X: molecular evolutionary genetics analysis across computing platforms. Molecular Biology and Evolution 35: 1547–1549. https://doi.org/10.1093/molbev/msy096

Larkin MA, Blackshields G, Brown NP, Chenna R, McGettigan PA, McWilliam H, Valentin F, Wallace IM, Wilm A, Lopez R, Thompson JD, Gibson TJ, Higgins DG (2007) Clustal W and Clustal X version 2.0. Bioinformatics 23: 2947–2948. https://doi.org/10.1093/bioinformatics/btm404

Lee CW, Park JG (2016) Distribution of meiobenthic arthropod communities in the hyporheic zone of Nakdonggang. Journal of Species Research 5: 157–165. https://doi.org/10.12651/JSR.2016.5.1.157

Morimoto Y (1959) A new bathynellid from the southwestern coast of Shikoku, Japan. Memoirs of the College of Sciences, Kyoto, Series B 26(3): 281–284.

Morimoto Y (1970a) Bathynellid crustaceans from the islands of Tsuhisma. Bulletin of the National Science Museum, Tokyo 13: 219–230.

Morimoto Y (1970b) Results of the speleological survey in South Korea 1966. XXI Bathynellid crustaceans (Syncarida) from South Korea. Bulletin of the National Science Museum, Tokyo 13(2): 149–184.

Morimoto Y (1974) Bathynellid crustaceans from the islands of Okinawa and Ishigaki-jima in the Ryukyus. Memoirs of the National Science Museum, Tokyo 7: 135–143.

Perina G, Camacho AI, Huey J, Horwitz P, Koenders A (2018) Understanding subterranean variability: the first genus of Bathynellidae (Bathynellacea, Crustacea) from Western Australia described through a morphological and multigene approach. Invertebrate Systematics 32: 423–447. https://doi.org/10.1071/IS17004

Perina G, Camacho AI, White NE, Morgan L, Lawrie A, Floeckner S, Guzik MT (2024) Unveiling hidden Bathynellidae (Crustacea: Bathynellacea) diversity in Australia: an integrated study reveals remarkable diversity and a new subfamily from Queensland. Zoological Journal of the Linnean Society 202(4): zlae151. https://doi.org/10.1093/zoolinnean/zlae151

Ronquist F, Teslenko M, Van Der Mark P, Ayres DL, Darling A, Höhna S, Larget B, Liu BL, Suchard MA, Huelsenbeck JP (2012) MrBayes 3.2: efficient Bayesian phylogenetic inference and model choice across a large model space. Systematic Biology 61: 539–542. https://doi.org/10.1093/sysbio/sys029

Serban E (1989) Le système des Gallobathynellines et sur certains rapports entre les péréiopodes 8 des Bathynellidés (Bathynellacea, Podophallocarida, Malacostraca). Miscellanea Speologica Romanica. 1: 121–168.

Serban E (2000) *Uenobathynella* ng, *Parauenobathynella* ng, *Morimotobathynella* ng, *Nihobathynella* ng, et *Paradoxibathynella* ng Bathynellinae du Japon (Bathynellidae, Bathynellacea, Podophallocarida). Trav. Inst. Speol. E. Racovitza 36: 3–61.

Simon CI, Frati F, Beckenbach A, Crespi B, Liu H, Flook P (1994) Evolution, weighting, and phylogenetic utility of mitochondrial gene sequences and a compilation of conserved PCR primers. Annals of the Entomological Society of America 87 (6): 651–701. https://doi.org/10.1093/aesa/87.6.651

Talavera G, Castresana J (2007) Improvement of phylogenies after removing divergent and ambiguously aligned blocks from protein sequence alignments. Systematic Biology 56: 564–577. https://doi.org/10.1080/10635150701472164

Thompson JD, Higgins DG, Gibson TJ (1994) CLUSTAL W: improving the sensitivity of progressive multiple sequence alignment through sequence weighting, position-specific gap penalties and weight matrix choice. Nucleic Acids Research 22: 4673–4680. https://doi.org/10.1093/nar/22.22.4673

Uéno M (1952) Three new species of Bathynellidae (Syncarida) found in subterranean waters of Japan. Annotationes Zoologicae Japonenses 25: 317–328.

Uéno M (1954) The Bathynellidae of Japan (Syncarida, Bathynellacea). Archiv für Hydrobiologie 49: 519–538.

Uéno M (1961) A new Japanese bathynellid. Crustaceana 2: 85–88. https://doi.org/10.1163/156854061X00266

Supplementary material 1

Distribution map of the two species of *Morimotobathynella* Serban, 2000, and photographs of interstitial groundwater sampling in the type locality of *M. koreana* sp. nov.

Authors: Su-Jung Ji, Ana Isabel Camacho, Gi-Sik Min

Data type: tif

Link: https://doi.org/10.3897/zookeys.1224.141117.suppl1

Supplementary material 2

Aditional information

Authors: Su-Jung Ji, Ana Isabel Camacho, Gi-Sik Min

Data type: xlsx

Explanation note: **table S1.** Differences amongst the three subfamilies and Korean new species of the family Bathynellidae (modified from Serban, 1989; Camacho et al. 2018b). **table S2.** CO1 and 18S GenBank numbers used in the molecular phylogenetic study. Bold type indicates sequences newly generated in this study.

Link: https://doi.org/10.3897/zookeys.1224.141117.suppl2

ZooKeys 1224: 129–140 (2025)
DOI: 10.3897/zookeys.1224.141248

Research Article

Cirrhimuraena taiwanensis sp. nov., a new species of cirri-bearing eel (Anguilliformes, Ophichthidae) from Yilan, northeastern Taiwan

Yen-Ting Lin[1], Yu-Hsiang Lin[1], Yu-San Han[1]

1 *Institute of Fisheries Science, College of Life Science, National Taiwan University, Taipei, Taiwan*
Corresponding author: Yu-San Han (yshan@ntu.edu.tw)

Abstract

A new species of cirri-bearing eel, *Cirrhimuraena taiwanensis* **sp. nov.** (Anguilliformes, Ophichthidae), is described based on a specimen collected from the estuary of the Langyang River (Yilan County), northeastern Taiwan. The new species is distinct from all congeners, except *C. odishaensis* and *C. orientalis*, in possessing a single row of mandibular teeth. *Cirrhimuraena taiwanensis* **sp. nov.** differs from *C. odishaensis* in having significantly shorter pectoral fins and fewer vertebrae, and it is distinguished from *C. orientalis* by its larger head, notably more total vertebrae, and a dorsal fin that originates well behind the gill opening. In the neighbor-joining tree based on COI sequences, the new species forms a distinct monophyletic group; thus, it is clearly separable from congeners both morphologically and genetically. With this addition, there are now 13 species in the genus *Cirrhimuraena*.

Key words: Biodiversity, brackish water, COI analysis, Taiwanese fringe-lip eel, taxonomy

OPEN ACCESS

Academic editor: Yahui Zhao
Received: 7 November 2024
Accepted: 11 December 2024
Published: 24 January 2025

ZooBank: https://zoobank.org/60197A0C-E82B-486A-ACAE-A8698E6CCAAE

Citation: Lin Y-T, Lin Y-H, Han Y-S (2025) *Cirrhimuraena taiwanensis* sp. nov., a new species of cirri-bearing eel (Anguilliformes, Ophichthidae) from Yilan, northeastern Taiwan. ZooKeys 1224: 129–140. https://doi.org/10.3897/zookeys.1224.141248

Introduction

The family Ophichthidae, commonly known as snake eels, represents the most varied group within the order Anguilliformes, containing two subfamilies (Myrophinae and Ophichthinae), with 62 genera and 361 species recorded (Fricke et al. 2024). In Taiwan, there have been reported of 19 genera and 60 species of snake eels identified (Chiu et al. 2018).

The genus *Cirrhimuraena* Kaup, 1856 belongs to the subfamily Ophichthinae and is known as cirri-bearing eels. This genus is notable for its unique morphological traits, particularly the presence of cirri, which are small, fleshy projections located on the upper jaw (Mohapatra et al. 2021). Cirri-bearing eels typically inhabit sandy or muddy substrates in coastal and estuaries waters (Mohapatra et al. 2021; Mohanty et al. 2023). Currently, 12 valid species are known, including *Cirrhimuraena chinensis* (Kaup, 1856), *C. tapeinoptera* (Bleeker, 1863), *C. cheilopogon* (Bleeker, 1860), *C. calamus* (Günther, 1870), *C. playfairii* (Günther, 1870), *C. oliveri* (Seale, 1910), *C. paucidens* (Herre & Myers, 1931), *C. inhacae* (Smith, 1962), *C. orientalis* (Nguyen, 1993), *C. yuanding* (Tang & Zhang, 2003), *C. indica* (Mohapatra, Mohanty, Ray, Mishra & Seth, 2021), and *C. odishaensis* (Mohanty, Behera, Patro & Mohapatra, 2023). Of these 12 species, only one, *C. chinensis*, has been recorded in Taiwan, and research on this genus remains scarce (Ho et al. 2015).

We conducted a survey of freshwater glass eels (juveniles of *Anguilla* spp.) in the the Langyang River estuary in northeastern Taiwan (24.7162°N, 121.8352°E) twice a month since 2010. Notably, this survey has yielded both a new species of Ophichthidae (*Lamnostoma taiwanense* Chiu, Huang & Shao, 2018) and new records of *Anguilla borneensis* Popta, 1924 and *A. interioris* Whitley 1938 (Chiu et al. 2018; Lin and Han 2024). In December 2023, a single *Cirrhimuraena* specimen was collected. A morphological analysis and molecular evidence indicated that this specimen represents an undescribed species. Although only a single specimen was obtained, its distinct morphology and genetic characteristics underscore its importance in advancing our understanding of *Cirrhimuraena* species in Taiwan. Furthermore, the discovery of new species and fish records highlights the need for conservation efforts to protect fish biodiversity in the Langyang River, one of the most critical habitats for Anguilliformes in Taiwan (Han et al. 2016).

Materials and methods

Sample collection

The specimen was collected from the estuary of the Langyang River in Yilan County, Taiwan (24.7162°N, 121.8352°E) on December 22, 2023. The environmental conditions of the collection site at the time of collection were as follows: substrate sandy, water depth 1 m, salinity 7‰, and water temperature 18 °C. A single, undescribed specimen of *Cirrhimuraena* was captured using a fyke net. Once collection, the specimen was photographed and radiographed, measured, and subsequently preserved in 95% ethanol. The specimen was deceased at the time of collection, and no live animals were included in this study.

Measurement and comparisons

The morphometrics were measured with digital calipers with an accuracy of 0.1 mm, and the meristic analysis and counting of head pores followed the protocol used by McCosker et al. (1989). The identified specimen was deposited in the collection of Biodiversity Research Museum of the Academia Sinica of Taiwan (**ASIZP**) under registration code ASIZP0082637. The specimen was compared with records of all congeners documented from Taiwan, *Cirrhimuraena chinensis*, and nearby waters, including *C. yuanding* from Pingtan, China (Tang and Zhang 2003), and *C. playfairii* from Okinawa, Japan (Hibino et al. 2021).

Molecular analysis

The dorsal muscle was dissected for the total genomic DNA extraction using the EasyPure Genomic DNA Spin Kit (Bioman Scientific, Taiwan). A polymerase chain reaction (PCR) was carried out to amplify the partial segment of the cytochrome c oxidase subunit I (COI) by using the forward primer FishF1+2 (5'-TCR ACY AAY CAY AAA GAY ATY GGC AC-3') and the reverse primers FishR1 (5'-TAG ACT TCT GGG TGG CCA AAG AAT CA-3') and FishR2 (5'-ACT TCA GGG TGA CCG AAG AAT CAG AA-3') following the protocol adjusted from Chang et al. (2016). The final PCR product was sequenced using the primer FishF1+2 by Genomics Scientific, Taiwan.

The COI sequences were aligned and trimmed using BioEdit v. 7.7.1, resulting in partial sequences of 562 base pairs. Once aligned, the sequences were saved in FASTA format and imported into MEGA v. 11 (Tamura et al. 2021) for phylogenetic analysis. A neighbor-joining (NJ) tree was constructed using the Kimura 2-parameter (K2P) distance model, with 10,000 bootstrap replicates to assess the reliability of the branches. Among all congeners, only two valid species of *Cirrhimuraena*, *C. chinensis* and *C. indica*, were available in the NCBI GenBank. In total, 16 sequences were used to construct the NJ tree. In the ingroup, *C. chinensis* (GenBank numbers KY472820.1, KX215192.1, KX215193.1, KX215194.1, MK264639.1, MK264640.1, MK264641.1, GU674221.1, and GU674224.1), *C. indica* (GenBank number MT019886.1), and *C. taiwanensis* sp. nov. (GenBank number PQ558516.1) were included. In the outgroup, and following the study by Mohapatra et al. (2021) were *Ophichthus lithinus* Jordan & Richardson, 1908 (GenBank number KU94289.1), *O. zophochir* Jordan & Gilbert, 1882 (GenBank number GU440436.1), *O. olivaceus* McCosker & Bogorodsky, 2020 (GenBank number MN480448.1), and *Pisodonophis cancrivorus* Richardson, 1848 (GenBank number KU942788.1, and MK777102.1). The details of all COI sequences used are listed in Table 1.

Table 1. The detail of the sequences used in the phylogenetic analysis.

Species	NCBI Accession number	Source	Voucher Number	Sampling Locality
Cirrhimuraena taiwanensis sp. nov.	PQ524198.1	This study	ASIZP0082637	Yilan, Taiwan
Cirrhimuraena chinensis	KY472820.1	GenBank	PT011	China
Cirrhimuraena chinensis	KX215192.1	GenBank	JLJ050	China
Cirrhimuraena chinensis	KX215193.1	GenBank	JLJ051	China
Cirrhimuraena chinensis	KX215194.1	GenBank	JLJ052	China
Cirrhimuraena chinensis	MK264639.1	GenBank	PTD055	China
Cirrhimuraena chinensis	MK264640.1	GenBank	PT055	China
Cirrhimuraena chinensis	MK264641.1	GenBank	QZ053	China
Cirrhimuraena chinensis	GU674221.1	GenBank	BWA6863	Indonesia
Cirrhimuraena chinensis	GU674224.1	GenBank	BWA6862	Indonesia
Cirrhimuraena indica	MT019886.1	GenBank	EBRC/ZSI/11811	India
Ophichthus lithinus	KU942789.1	GenBank	ASIZP0801626	Taiwan
Ophichthus olivaceus	MN480448.1	GenBank	KAU17-80	Saudi Arabia
Ophichthus zophochir	GU440436.1	GenBank	MFC132	California, USA
Pisodonophis cancrivorus	MK777102.1	GenBank	DOS05154	Vietnam
Pisodonophis cancrivorus	KU942788.1	GenBank	ASIZP0800053	Taiwan

Results

Family Ophichthidae

***Cirrhimuraena taiwanensis* sp. nov.**
https://zoobank.org/3214769E-E179-46DD-B800-CE12D2A318B0
Figs 1–4, Table 2

Material examined. *Holotype*: Taiwan • ASIZP0082637, 178.1 mm total length (TL); Yilan; 24.7162°N, 121.8352°E; 22 Dec. 2023; caught by fyke net, ca 1 m, Yu-San Han & Yen-Ting Lin leg.

Diagnosis. A new *Cirrhimuraena* species with the combination of following characteristics: pectoral fin very small, only 15.2% of head length (HL) (in congeners > 21% HL); HK 9.7% of TL dorsal fin originates 1½ pectoral-fin length behind gill opening; tooth pattern unique, with only a single row of mandibular teeth; cirri on upper jaw 11; vertebrae 150, vertebral formula 13-53-150.

Description. The morphometric and meristic measurements of the holotype are shown in Table 2. Body very elongate, cylindrical; body height is almost consistent from gill opening to anus, with depth at gill opening of 2.2% of TL and depth at anus of 2.3% of TL. Head moderate, with head length (HL) 9.7% of TL. Tail longer than trunk, 63.6% of TL. Anal fin low, situated right after anus, with pre-anal length 36.8% of TL. Dorsal fin also low, originating far behind gill opening and pectoral fin; pre-dorsal length 13.2% of TL. Pectoral fin very small, 15.2% of HL, 1.5% of TL; pectoral-fin base positioned at same vertical as gill opening; gill opening positioned on latero-ventral side, length 16.4% of HL.

Eye relatively large, positioned nearer to snout tip than rictus; eye diameter 8.9% of HL; interorbital space slightly wider; interorbital length 6.1% of HL. Anterior nostril tubular, positioned at snout tip, while posterior nostril lies slightly behind orbit. Snout long, pointed, 19.1% of HL. Upper jaw longer than lower jaw, 35.7% and 26.9% of HL, respectively.

Five small cirri on edge of upper jaw between anterior and posterior nostrils; 6 cirri behind posterior nostril. No cirri on lower jaw and tip of jaw in front of nostrils. Dentition pattern illustrated in Fig. 3. Teeth numerous, closely arranged in a band, and primarily small and pointed, with slightly larger teeth at ends. Vomerine teeth in 1–3 rows, extending to posterior of maxilla; 5 teeth form a small patch at prevomer. Maxillary teeth in 2–6 rows of small, conical teeth; mandibular teeth band in only a single row on both sides. Pre-dorsal vertebrae 13, pre-anal vertebrae 53, and total vertebral 150.

Head pores tiny and indistinct, with supraorbital pores 1 + 3, infraorbital pores 3 + 2, preoperculomandibular pores 7 + 4, and supra-temporal pores 1 (Fig. 4). Lateral line pores before pectoral fin/gill opening 12, before dorsal-fin origin 16, and before anus 48.

Dorsal surface of body grayish, with numerous tiny black spots; some melanophores concentrated at tip of snout. Ventral side whitish. Dorsal and anal fins translucent; pectoral fin whitish.

Distribution. Currently only known from the type locality, with sandy substrate.

Etymology. The specific epithet *taiwanensis* refers to the location of the type locality, which recently only known in Taiwan; it is used as an adjective.

Remarks. Compared to all 12 congeners, *C. taiwanensis* sp. nov. can be easily distinguished from 10 species, except *C. odishaensis* and *C. orientalis*, in having only a single row of mandibular teeth (Fig. 4). However, *C. taiwanensis* sp. nov. can be separated from these two species morphologically, with comparative details shown in Table 3. The new species differs from *C. odishaensis* in having a shorter pectoral fin, only 15.2% of HL (compared to 21.3–25.0% HL in *C. odishaensis*); fewer vertebrae, with 13 pre-dorsal, 53 pre-anal, and 150 total vertebrae (vs 10 pre-dorsal, 46–47 pre-anal, and 160–162 total vertebrae in *C. odishaensis*); and fewer rows of maxillary teeth (2–6 rows in *C. taiwanensis* sp. nov. vs 3–7 rows in *C. odishaensis*). Compared to *C. orientalis*, *C. taiwanensis* sp. nov. has a larger head at 9.7% of TL (vs 5.5–6.2% of TL in *C. orientalis*), significantly more vertebrae (150 vs 131–136 in *C. orientalis*),

Figure 1. *Cirrhimuraena taiwanensis* sp. nov., ASIZP0082637, 178.1 mm total length. Scale bar: 30 mm.

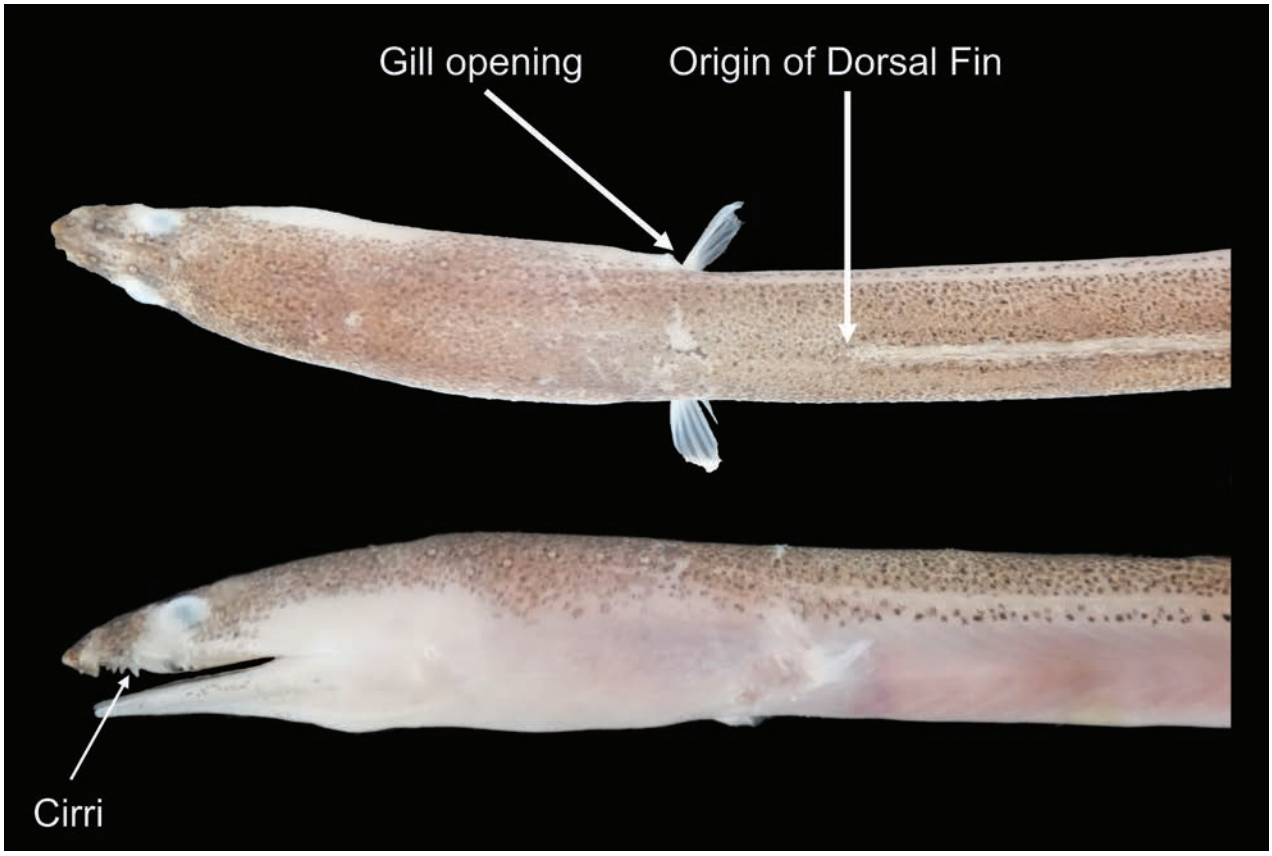

Figure 2. Head profile of *Cirrhimuraena taiwanensis* sp. nov. **A** origin of dorsal fin well behind gill opening **B** arrow indicates cirri on upper jaw.

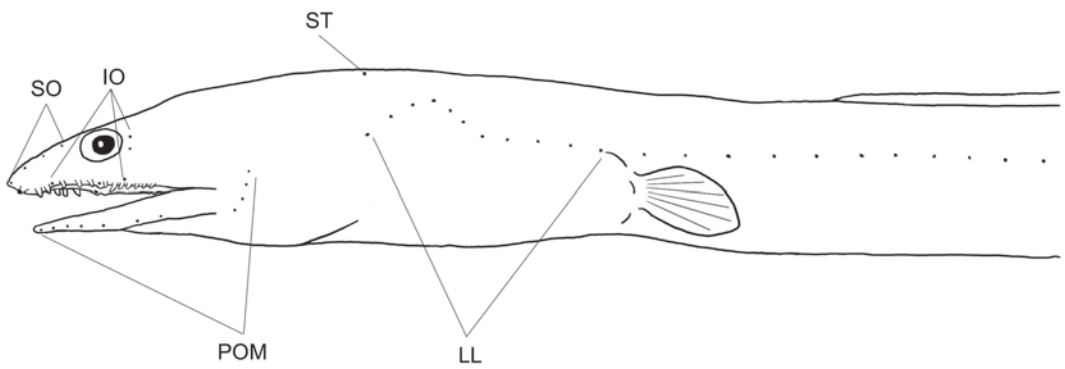

Figure 3. Head and lateral line pores in *Cirrhimuraena taiwanensis* sp. nov. Abbreviaitons: IO: infraorbital pores; LL: lateral-line pores; POM: preoperculomandibular pores; SO: supraorbital pores; ST: supra-temporal pores.

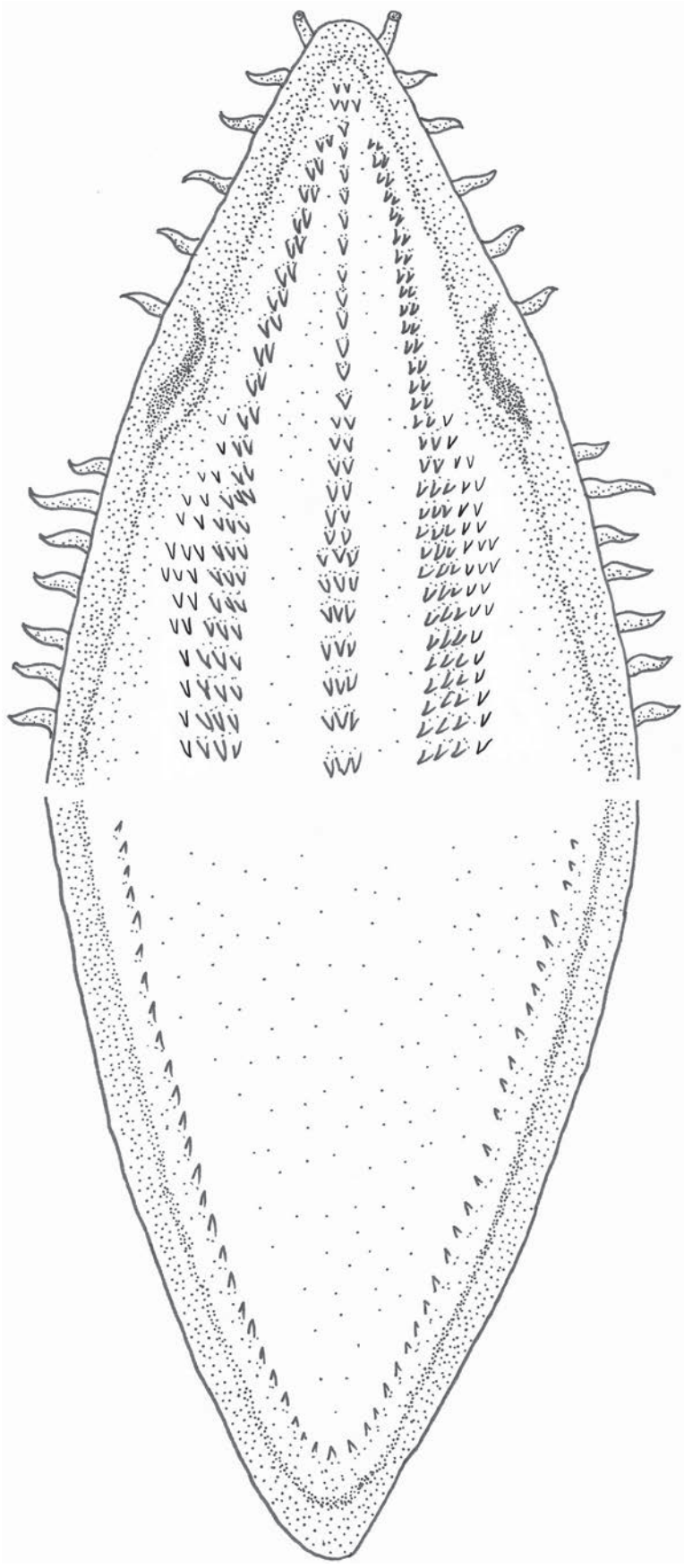

Figure 4. Tooth dentition pattern in upper and lower jaws of *Cirrhimuraena taiwanensis* sp. nov. (holotype, ASIZP0082637, 178.1 mm total length).

Table 2. Morphometric and meristic data of *Cirrhimuraena taiwanensis* sp. nov.

	Cirrhimuraena taiwanensis* sp. nov. Holotype, *ASIZP0082637
Total length (SL, mm)	178.1
Head length (HL, mm)	17.4
Pre-anal length (PAL, mm)	65.6
Pre-dorsal length (PDL, mm)	23.6
% in HL	
Snout length	19.1
Eye diameter	8.9
Interorbital length	6.1
Upper jaw length	35.7
Lower jaw length	26.9
Gill opening length	16.4
Pectoral-fin length	15.2
% in TL	
Head length	9.7
Pre-anal length	36.8
Pre-dorsal length	13.2
Trunk length	27.1
Tail length	63.6
Depth at gill opening	2.2
Depth at anus	2.3
Pores	
Supraorbital	1 + 3
Infraorbital	3 + 2
Preoperculomandibular	7 + 4
Pores before pectoral fin	11
Pores before dorsal fin	16
Pores before anus	48
Vertebrae	
Pre-dorsal	13
Pre-anal	53
Total	150

and more rows of maxillary teeth (2–6 rows in *C. taiwanensis* sp. nov. vs 2–3 rows in *C. orientalis*).

Molecular results. Sixteen COI sequences from three taxa were analyzed, revealing nine unique haplotypes across 562 aligned base pairs, which included 196 variable sites and 151 parsimony-informative sites. The NJ tree analysis identified *C. taiwanensis* sp. nov. in a well-supported clade (bootstrap values 99%) with all other *Cirrhimuraena* species included in NCBI (Fig. 5). The av-

Table 3. Morphometric comparisons of *Cirrhimuraena taiwanensis* sp. nov. with congeners with only a single row of mandibular teeth.

	***Cirrhimuraena taiwanensis* sp. nov. (This study)**	***C. odishaensis* (Mohanty et al., 2023)**	***C. orientalis* (Nguyen., 1993)**
HL % in TL	9.7	9.1–10.6	5.5–6.2
Pectoral fin % in HL	15.2	21.3–25.0	—
Mandibular teeth	1 row	1 row	1 row
Maxillary teeth	2–6 rows	3–7 rows	2–3 rows
Total vertebrate	150	160–162	131–136

— No data available.

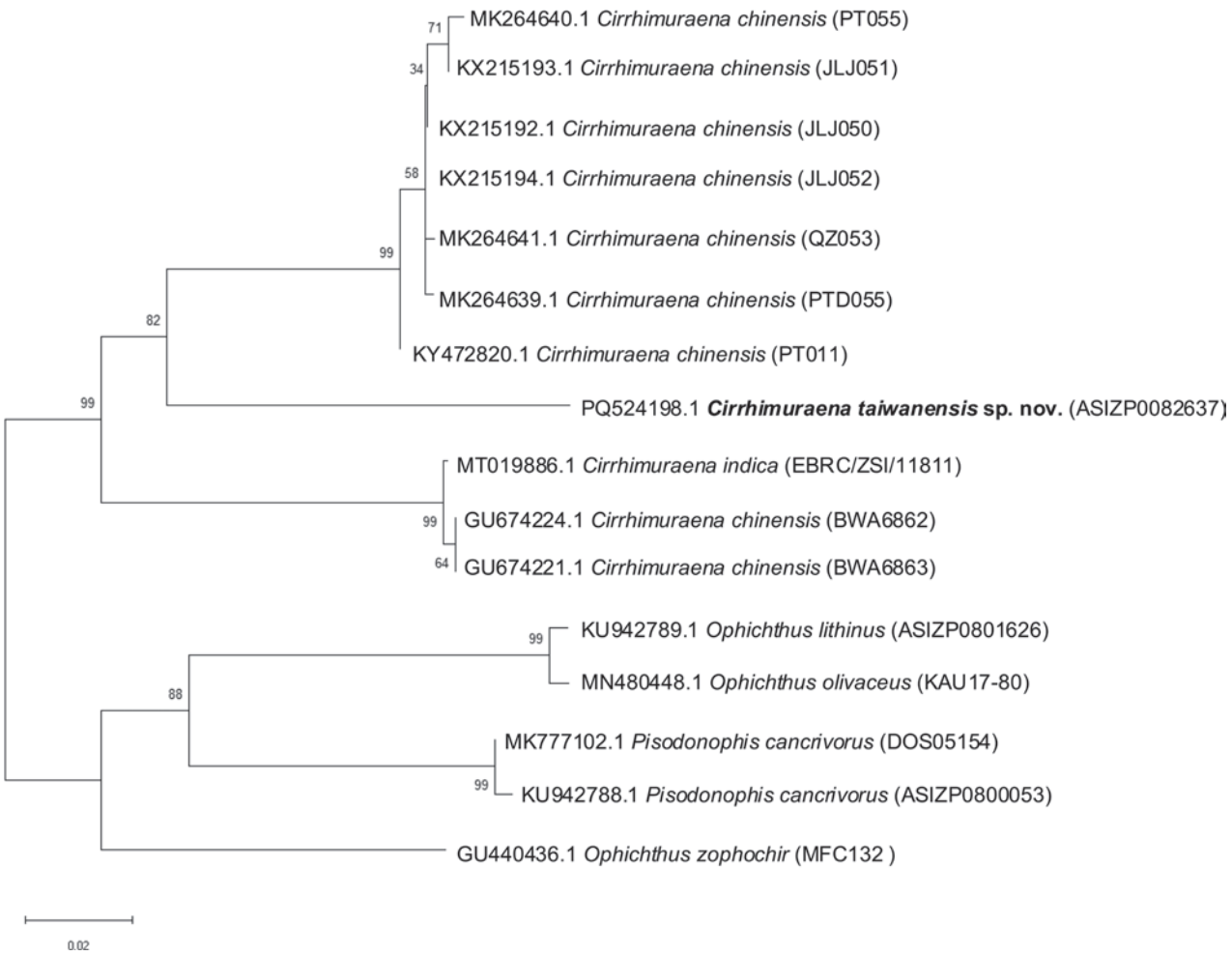

Figure 5. The neighbor-joining tree based on COI sequences of *Cirrhimuraena taiwanensis* sp. nov. and all the valid congeners in NCBI.

erage pairwise K2P genetic distance between *C. taiwanensis* sp. nov. and its congeners is 0.124, aligning with the average genetic distance typically found among congeneric fish species, as reported by Ward et al. (2005). Within the *Cirrhimuraena* group, *C. taiwanensis* sp. nov. and most *C. chinensis* specimens are clearly separated (bootstrap value 99%) from *C. indica* and two *C. chinensis* specimens collected in Indonesia (GU674221.1 and GU674224.1), which are suspected misidentifications of *C. indica* (Mohapatra et al. 2021). *Cirrhimuraena taiwanensis* sp. nov. also demonstrates a distinct separation from *C. chinensis*, with high bootstrap support of 82% and forming a unique monophyletic group. The distinct morphological characteristics and NJ tree results further support the separation of *C. taiwanensis* sp. nov. as a distinct species.

Discussion

Currently, there are 12 valid species in the genus *Cirrhimuraena*, and the distribution in the northwestern Pacific Ocean is primarily centered around the South China and Java Seas (Mohapatra et al. 2021; Mohanty et al. 2023). Only one species, *C. chinensis*, has been recorded from Taiwanese waters, from along the coast of Pingtung in southwestern Taiwan and Kinmen Island (Shao et al. 2008; Ho et al. 2015). Additional to *C. chinensis* recorded in Taiwanese waters, in the subtropical

North Pacific there are two additional species: *C. playfairii*, recorded from Makiya, Okinawa Island, Japan (Hibino et al. 2021: fig. 6b, c), and *C. yuanding*, recorded from Pingtan County, Fujian Province, China (Tang and Zhang 2003) (Fig. 6).

In Table 4, we compare the new species, which exhibits distinct morphological differences from congeners found in Taiwanese waters (*C. chinensis*) and nearby regions (*C. yuanding* and *C. playfairii*). The two species recorded from China (*C. yuanding*) and Japan (*C. playfairii*) can be clearly distinguished from *C. taiwanensis* sp. nov. by the position of the dorsal fin, which originates in front of the gill opening in both *C. playfairii* and *C. yuanding*, with a pre-dorsal length (PDL) shorter than the HL (Table 4). Compared to the *C. chinensis*, *C. taiwanensis* sp. nov. has a significantly shorter pectoral fin at 15.2% of HL (vs 45.2–51.6% HL in *C. chinensis*); a smaller gill opening length at 16.4% of HL (vs 25.4–30.1% HL in *C. chinensis*); dorsal fin that originates well behind the gill opening, with a PDL of 13.2% TL (vs 9.6–11.2% TL in *C. chinensis*); and a slightly smaller head, at 9.7% TL (vs 10.9–11.8% TL in *C. chinensis*) (Table 4). Furthermore, molecular data confirm the distinction between *C. chinensis* and *C. taiwanensis* sp. nov., with a high bootstrap value (82%) supporting their separation (Fig. 5).

There are also notable morphological differences between *Cirrhimuraena taiwanensis* sp. nov. and other Indo-West-Pacific congeners. *Cirrhimuraena calamus* and *C. oliveri* both have significantly smaller heads, measuring 16.6% pre-anal length (PAL) in *C. calamus* (Günther 1870) and 16.4% of PAL in *C. oliveri* (Seale 1910), compared to 26.5% PAL in *C. taiwanensis* sp. nov.; *C. tapeinoptera*, *C. cheilopogon*, and *C. inhacae* have significantly larger pectoral fins, approximately 40–50% HL

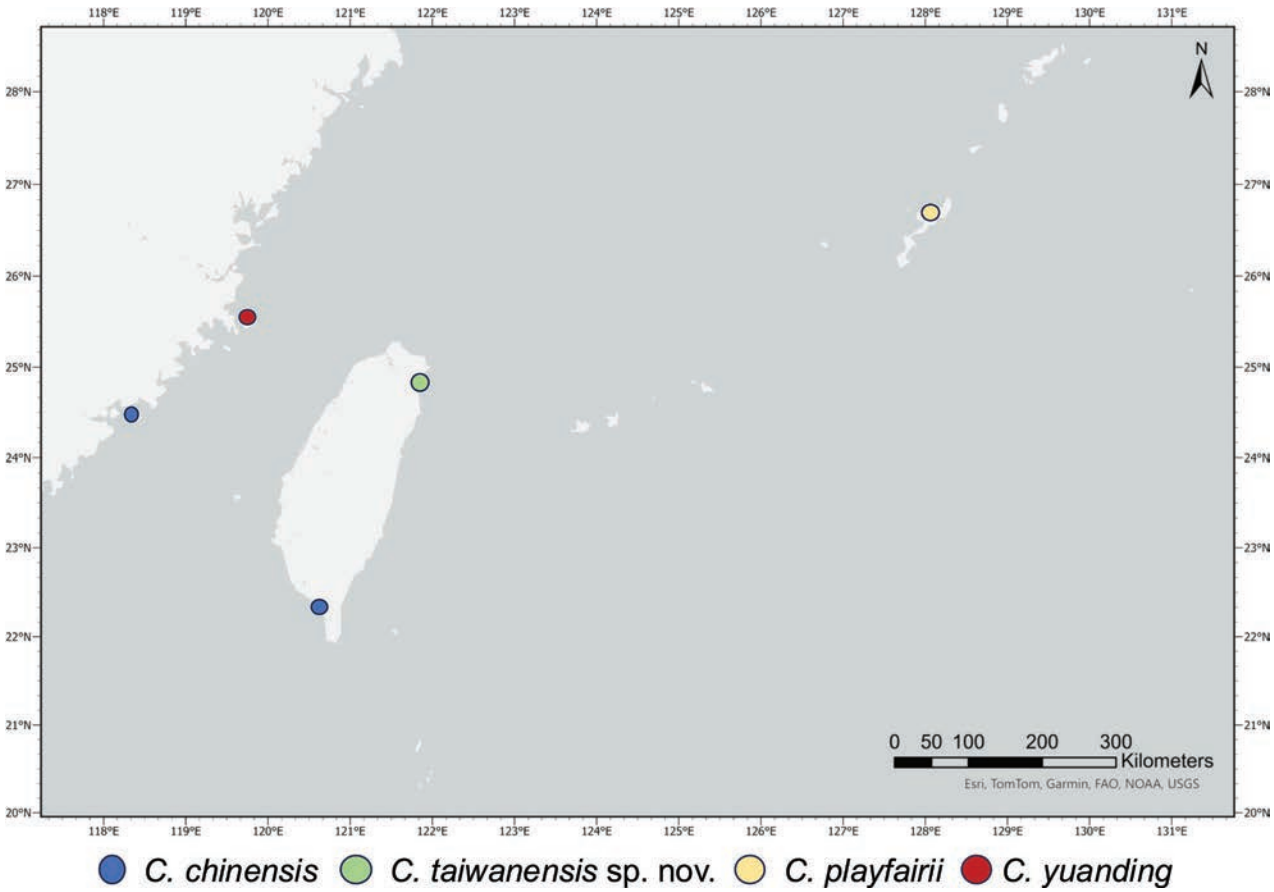

Figure 6. Distribution map of *Cirrhimuraena* species found in Taiwanese waters and nearby regions.

Table 4. Comparisons of *Cirrhimuraena taiwanensis* sp. nov. and *C. chinensis* in Taiwan, and two other congeners recorded from nearby waters.

	***Cirrhimuraena taiwanensis* sp. nov. Holotype**	***C. chinensis n = 10***	***C. yuanding n* = 1 (Tang and Zhang 2003)**	***C. playfairii n* = 1 (Hibino et al. 2021)**
Collection site	Taiwan	Taiwan	China	Japan (Okinawa)
Total length (SL, mm)	178.1	227–293	520.5	229
Head length (HL, mm)	17.4	23.5–28.9	30.0	—
Pre-anal length (PAL, mm)	65.6	89.3–94.2	161.3	—
Pre-dorsal length (PDL, mm)	23.6	25.5–28.2	20.5	—
% in HL				
Snout length	19.1	18.9–22.7	16.0	15.3
Upper jaw length	35.7	37.1–40.0	24.0	31.3
Lower jaw length	26.9	34.5–43.5	—	—
Gill opening length	16.4	25.4–30.1	12.7	8.6
Pectoral-fin length	15.2	45.2–51.6	28.3	23.3
% in TL				
Head length	9.7	10.9–11.8	5.8	7.1
Pre-anal length	36.8	32.1–39.4	31.0	33.6
Pre-dorsal length	13.2	9.6–11.2	3.9	4.6
Depth at gill opening	2.2	2.5–3.3	1.8	2.0
Depth at anus	2.3	2.8–3.7	2.2	2.1
Vertebrate				
Pre-dorsal	13	11	—	4
Pre-anal	53	49	—	60
Total	150	154	—	183

— No data available.

(Weber and de Beaufort 1916; Smith 1962; Smith and Heemstra 1986) vs 15.2% in *C. taiwanensis* sp. nov.; *C. taiwanensis* sp. nov. also has a shorter pre-anal length, at 36.8% TL, compared to 41.8% in *C. paucidens* (Catania and Fong 2020; Mohapatra et al. 2021). The combined morphological and molecular differences between the new species and all 12 congeners strongly support that the specimen we collected represents a distinct new species, *Cirrhimuraena taiwanensis* sp. nov.

The habitat of the *Cirrhimuraena taiwanensis* sp. nov. is at the estuary of the Langyang River, where the water is brackish year round and has an abundance plankton. The river estuary serves as an important habitat for the Anguilliformes and other brackish and freshwater fish species (Shih et al. 2008; Dahms et al. 2012; Han et al. 2016). The substrate is sandy, and the brackish-water environment is typical habitat for the *Cirrhimuraena* species (Mohanty et al. 2023). With the description of the new species, the ecological importance of the Langyang River estuary is enhanced; this estuary already serves as the type locality of *Lamnostoma taiwanensis* and habitat for other anguillid species in Taiwan (Chiu et al. 2018; Lin and Han 2024). In addition, the these new and recently described species suggests that many more unidentified species may be present in brackish waters, which highlight the importance of these environments for biodiversity.

Acknowledgements

We thank Zhen-Hui Chen (local fisherman) for assisting us in setting the fyke net and providing various sampling support, Chien-Hsiang Lin and Hsin-Wei Liu (Biodiversity Research Center, Academia Sinica) for photographing specimen and

offering curatorial insights for this research, and Hong-Ji Veterinary Hospital for helping taking the radiograph for the specimen. We sincerely thank the academic editor, Dr. Yahui Zhao, two anonymous reviewers, and Dr. Mohapatra for their invaluable comments and suggestions to improve the quality of this manuscript.

Additional information

Conflict of interest

The authors have declared that no competing interests exist.

Ethical statement

No ethical statement was reported.

Funding

The authors extend our gratitude to the National Science and Technology Council, Executive Yuan, Taiwan (MOST 111-2313-B-002-016-MY3) for funding this project.

Author contributions

The sample collecting was performed by Yu-San Han and Yen-Ting Lin. Yen-Ting Lin conducted the measurement and write the manuscript; Yu-Hsiang Lin for the head profile and dentition drafting; Yu-San Han designed and supervised the experiments. All authors participated in manuscript writing and interpretation of results. All authors read and approved the final manuscript.

Data availability

All data that support the findings of this study are available in the main text, and the holotype is deposited in the collection of Biodiversity Research Museum of the Academia Sinica of Taiwan, under registration code ASIZP0082637.

References

Catania D, Fong J (2020) CAS Ichthyology (ICH). Version 150.227. California Academy of Sciences. https://doi.org/10.15468/efh2ib

Chang CH, Lin HY, Ren Q, Lin YS, Shao KT (2016) DNA barcode identification of fish products in Taiwan: government-commissioned authentication cases. Food Control 66: 38–43. https://doi.org/10.1016/j.foodcont.2016.01.034

Chiu YC, Shao KT, Huang SP, Chen HM (2018) The freshwater snake eel genus *Lamnostoma* (Anguilliformes: Ophichthidae) in Taiwan, with description of a new species. Zootaxa 4454(1): 18–32. https://doi.org/10.11646/zootaxa.4454.1.4

Dahms HU, Tseng LC, Hsiao SH, Chen QC, Kim BR, Hwang JS (2012) Biodiversity of planktonic copepods in the Lanyang River (northeastern Taiwan), a typical watershed of Oceania. Zoological Studies 51(2): 60–174.

Fricke R, Eschmeyer WN, Van der Laan R (2024) Eschmeyer's Catalog of Fishes: Genera, Species, References. [Accessed on 2024-5-11]

Günther A (1870) Catalogue of the Fishes in the British Museum. Vol. 8. Trustees of the British Museum, London, [xxv +] 549 pp.

Han YS, Wu CR, Iizuka Y (2016) Batch-like arrival waves of glass eels of *Anguilla japonica* in offshore waters of Taiwan. Zoological Studies 55: e36. https://doi.org/10.6620/ZS.2016.55-36

Hibino Y, Miyamoto K, Sakurai Y, Kimura S (2021) Annotated checklist of marine eels (Actinopterygii: Anguilliformes) stranded by a serious cold wave in January 2016 in Ryukyu Islands, Japan, including two newly recorded species of Japan. Bulletin of the Kitakyushu Museum of Natural History, Series A 19: 13–26. https://doi.org/10.34522/kmnh.19.0_13

Ho HC, Smith DG, McCosker JE, Hibino Y, Loh KH, Tighe KA, Shao KT (2015) Annotated checklist of eels (orders Anguilliformes and Saccopharyngiformes) from Taiwan. Zootaxa 4060(1): 140–189. https://doi.org/10.11646/zootaxa.4060.1.16

Lin YT, Han YS (2024) Species diversity of freshwater glass eel (Anguilliformes, Anguillidae) of Yilan, Taiwan, with remark on two new records. In: Ho HC, Russell B, Hibino Y, Lee MY (Eds) Biodiversity and taxonomy of fishes in Taiwan and adjacent waters. ZooKeys 1220: 5–14. https://doi.org/10.3897/zookeys.1220.125590

McCosker JE, Böhlke EB, Böhlke JE (1989) Family Ophichthidae. In: Böhlke EB (Ed.) Fishes of the Western North Atlantic, Number 1 Part 9. Sears Foundation for Marine Research, Yale University, New Haven, Connecticut, 254–412.

Mohanty SR, Behera RK, Patro S, Mohapatra A (2023) A new species of cirri-bearing eel of the genus *Cirrhimuraena* (Anguilliformes: Ophichthidae) from the coastal Bay of Bengal, India. Zootaxa 5315(6): 575–583. https://doi.org/10.11646/zootaxa.5315.6.5

Mohapatra A, Mohanty SR, Ray D, Mishra SS, Seth JK (2021) A new species of the genus *Cirrhimuraena* (Anguilliformes: Ophichthidae) from the Bay of Bengal, India. Journal of Fish Biology 98(5): 1363–1370. https://doi.org/10.1111/jfb.14671

Nguyen KH (1993) Cá biên Viêt nam [Marine Fishes of Vietnam]. Vol. 2. Part 2. (Anguillomorpha, Cyprinomorpha, Atherinomorpha). Science & Technology Publishers, Hanoi and Ho Chi Minh City, 176 pp. [In Vietnamese]

Seale A (1910) New species of Philippine fishes. The Philippine Journal of Science. Section A, General Science 4(6): 491–543.

Shao KT, Ho HC, Lin PL, Lee PF, Lee MY, Tsai CY, Liao YC, Lin, YC (2008) A checklist of the fishes of southern Taiwan, northern South China Sea. Raffles Bulletin of Zoology Supplement 19: 233–271.

Shih SS, Lee HY, Chen CC (2008) Model-based evaluations of spur dikes for fish habitat improvement: A case study of endemic species *Varicorhinus barbatulus* (Cyprinidae) and *Hemimyzon formosanum* (Homalopteridae) in Lanyang River, Taiwan. Ecological engineering 34(2): 127–136. https://doi.org/10.1016/j.ecoleng.2008.07.016

Smith JLB (1962) Sand-dwelling eels of the western Indian Ocean and the Red Sea. Ichthyological Bulletin 24: 447–466.

Smith MM, Heemstra PC (1986) Smiths' Sea Fishes. Macmillan South Africa, Johannesburg, 1047 pp. https://doi.org/10.1007/978-3-642-82858-4

Tamura K, Stecher G, Kumar S (2021) MEGA 11: Molecular Evolutionary Genetics Analysis version 11. Molecular Biology and Evolution 38(7): 3022–3027. https://doi.org/10.1093/molbev/msab120

Tang WQ, Zhang CG (2003) A new species of the genus *Cirrhimuraena* from the East China Sea (Pisces, Anguilliformes, Ophichthidae). Acta Zootaxonomica Sinica 28(3): 551–553.

Ward RD, Zemlak TS, Innes BH, Last PR, Hebert PD (2005) DNA barcoding Australia's fish species. Philosophical Transactions of the Royal Society B: Biological Sciences 360(1462): 1847–1857. https://doi.org/10.1098/rstb.2005.1716

Weber M, de Beaufort LF (1916) The Fishes of the Indo-Australian Archipelago. Vol. 3. E.J. Brill, Leiden, 455 pp. https://doi.org/10.1163/9789004590434

ZooKeys 1224: 141–164 (2025)
DOI: 10.3897/zookeys.1224.129618

Research Article

First records of *Oxychilus alliarius* and *O. cellarius* (Gastropoda, Stylommatophora, Oxychilidae) in Mexico: mtDNA identification and potential distributions

Ali Gabrielle Trujillo-Díaz[1], Victoria Araiza-Gómez[1,2], Jazmín García-Román[3], José Luis Hernández-Domínguez[4], Gerardo Zúñiga[1], Edna Naranjo-García[5]

1 *Laboratorio de Variación Biológica y Evolución, Escuela Nacional de Ciencias Biológicas, Instituto Politécnico Nacional, Prolongación de Carpio y Plan de Ayala, Col. Santo Tomas, Alc. Miguel Hidalgo, Ciudad de México CP 11340, Mexico*
2 *Centro de Investigación en Alimentación y Desarrollo, Unidad Mazatlán, Av. Sábalo-Cerritos S/N, Sinaloa, C.P. 82100, Mexico*
3 *Universidad Autónoma de Nuevo León, Facultad de Ciencias Forestales, Kilómetro 145, Nacional 85, 67700 Linares, N.L, Mexico*
4 *Agencia digital de Innovación Pública, Dirección Ejecutiva de Inteligencia de Datos, Plaza de las Vizcaínas No.30, Col. Centro, Alc. Cuauhtémoc, Ciudad de México CP 06080, Mexico*
5 *Departamento de Zoología, Instituto de Biología, Universidad Nacional Autónoma de México, Apartado postal 70-153, 04510 México, D. F., Mexico*
Corresponding author: Victoria Araiza-Gómez (varaiza9693@gmail.com)

Abstract

This paper reports the first Mexican records of *Oxychilus alliarius* (Puebla, State of Mexico, Mexico City) and *O. cellarius* (Mexico City), and expands the Mexican distribution of *O. draparnaudi* to Querétaro, Tlaxcala, and State of Mexico. These three introduced land snail species were identified by combining their genital anatomy and mitochondrial COI DNA sequence data. A two-dimensional geometric morphometric analysis of shell shape variation based on both apertural and apical views showed that there were no significant conchological differences between the three species except, to some degree, size. Using locality data of newly collected specimens, information from previous studies, and data retrieved from GBIF and iNaturalist, an analysis of the potential distributions of *Oxychilus* species in Mexico was conducted with an R implementation of Maxent. This showed that *Oxychilus* tends to occupy principally the Southern Highlands and the Transmexican Volcanic Belt Province.

Key words: COI, distribution, introduced species, land snail, Mollusca, taxonomy

OPEN ACCESS

Academic editor: Thierry Backeljau
Received: 10 July 2024
Accepted: 1 December 2024
Published: 28 January 2025

ZooBank: https://zoobank.org/E2D2023A-E1E6-4103-90DD-B28FBF26976E

Citation: Trujillo-Díaz AG, Araiza-Gómez V, García-Román J, Hernández-Domínguez JL, Zúñiga G, Naranjo-García E (2025) First records of *Oxychilus alliarius* and *O. cellarius* (Gastropoda, Stylommatophora, Oxychilidae) in Mexico: mtDNA identification and potential distributions. ZooKeys 1224: 141–164. https://doi.org/10.3897/zookeys.1224.129618

Introduction

Biological invasions modify native diversity, ecosystem functioning and species interactions (Lankau 2013). Non-native species invasions often negatively affect community structure, although positive effects can sometimes occur (Geerts and Pauw 2009; Simberloff et al. 2013). These outcomes depend on whether species compete for single or multiple factors (Case 1990; Godoy 2019). The detrimental impacts of introduced species on native biodiversity have been extensively discussed worldwide (McNeely 2001; Meyer and Cowie 2010). Research has focused on identifying common patterns in invasion events, examining the intrinsic characteristics of invaders, the vulnerability of

natural communities to invasion, and the relationship between invader distribution and environmental factors (Kappes et al. 2009; Stoll et al. 2012). However, studies addressing the impacts and distribution of introduced land snails in Mexico remain scarce (Naranjo-García and Castillo-Rodríguez, 2017). Land snails are a highly diverse group of animals that have received relatively little attention in Mexico, despite their important roles in ecosystem functioning (Correa et al. 2012). One widely distributed and increasingly expanding land snail genus is *Oxychilus* Fitzinger, 1833 (Curry et al. 2016; Ali and Robinson 2020). The genus *Oxychilus* (family Oxychilidae Hesse, 1927) includes species that are usually found in humid habitats, under rocks, among moss, and near water bodies. The genus comprises 103 species (MolluscaBase 2021), characterized by thin shells that are either depressed, discoidal, or slightly elevated with a rounded periphery. The shells have an umbilicus and a semilunar aperture, and their coloration ranges from yellowish to brown or even whitish (Correa-Sandoval et al. 2017). However, species identification and generic assignment are challenging because of the extreme conchological similarities between both species and genera (Falkner 2008; Bronne and Delcourt 2022).

Oxychilus cellarius (O.F. Müller 1774) and *O. draparnaudi* (H. Beck, 1837) are native in Europe and have been introduced in many other parts of the world. As such, *O. draparnaudi* has also been recorded in the Canary Islands, the Azores, and numerous parts of North and South America (Virgillito and Miquel 2013), South Africa and New Zealand (Brook 1999; MacDonald et al. 2004), among others. In Mexico, Naranjo-García and Castillo-Rodríguez (2017) reported *O. draparnaudi* from Coyoacán, Mixcoac, Bosque de Chapultepec, Bosque de Tlalpan, and Pedregal de San Ángel in Mexico City (CDMX). *Oxychilus cellarius*, in turn, has been reported from Asia Minor, North Africa, the United States, and Chile, including Juan Fernández Islands and Santiago (Stuardo and Vega 1985). Valdovinos (1999) situated its distribution between latitudes 30°S and 40°S. *Oxychilus alliarius* (J.S. Miller, 1822) is a third *Oxychilus* species that has been recorded outside its native European range. It occurs in Colombia, North America, Greenland, St. Helena, South Africa, Sri Lanka, Australia, New Zealand, Hawaii, and the Juan Fernández Islands (Stuardo and Vega 1985). This species selectively preys on other snails smaller than 3 mm (Frömming 1954; Meyer 2005) and Stone and Scott (1985) claimed that it is an invasive species that occurs in higher densities than other snail species, by which it contributes to the decline of these other species (Meyer 2005).

In this paper we report for the first time the presence in Mexico of *O. cellarius* and *O. alliarius* using anatomical and mtDNA data. Additionally, we assess the potential future spread of these invasive species in new habitats by analyzing their distribution patterns in Mexico through habitat suitability modeling.

Materials and methods

We used *Oxychilus* samples deposited in the National Collection of Mollusks (**CNMO**) at the Institute of Biology (**IB-UNAM)**, specimens stored in the laboratory of Biological Variation and Evolution at the National School of Biological Sciences (**ENCB-IPN**), and recent collections made from July to November 2021 and in November 2022 (Suppl. material 1: table S1). The collected specimens were relaxed by immersing them in a container filled with boiled cold water. They were preserved in 95% ethanol for anatomical and DNA analysis.

To recognize the conchological attributes of the genus *Oxychilus*, we employed specialized literature (Giusti and Manganelli 1997, 2002; Sysoev and Schileyko 2009; Thompson 2011). Characteristic attributes such as the number of whorls, color, shape, and ornamentation were compared with descriptions in the literature. Furthermore, shell diameter, shell height, and umbilicus diameter were measured using a caliper. Snails were dissected (15 *O. draparnaudi*, two *O. alliarius*, and two *O. cellarius*) under a Nikon SMZ800 stereomicroscope and diagnostic anatomical structures were photographed.

mtDNA identification

DNA was extracted from a fragment of the foot using the DNeasy Tissue kit according to the manufacturer's specifications (QIAGEN, California, USA). A 600-bp fragment of the mitochondrial cytochrome oxidase subunit 1 (COI) gene was amplified by PCR using the universal primers LCO1490 and HCO2198 (Folmer et al. 1994). PCR amplifications were performed with a thermocycler (Techne TC-5000) on 25 µl reaction volume containing 2.5 µl of 10X PCR buffer, 2.5 mM $MgCl_2$ 10 mM dNTPs, 13 pmol of primers, 1U Taq DNA polymerase (Invitrogen) and 2 µl of template DNA. Cycling conditions were an initial 5 min denaturation step at 94 °C, followed by 35 cycles: 94 °C for 30 s, 50 °C for 30 s, and 72 °C for 45 s; and a final step at 72 °C for 7 min. The PCR products were purified using the GFXTM PCR DNA and GelBand Purification Kit (GE Healthcare, Buckinghamshire, UK) and sequenced by Macrogen, Korea.

The nucleotide sequences of the COI fragment were compared with sequences deposited in GenBank (http://www.ncbi.nlm.nih.gov) using BLASTn. Sequences were aligned and manually edited using CHROMAS v. 2.33 (http://www.technelysium.com.au/chromas.html) and SEAVIEW v. 4.0 (Gouy et al. 2010) software programs. After editing the sequences, a 450-bp fragment was used for phylogenetic analysis.

Phylogenetic analysis was performed by Bayesian inference with BEAST v. 2.7.3 (Drummond and Rambaut 2007) under the HKY substitution model. Tree runs were performed independently with four Markov chains that went for 10,000,000 generations, resampling every 10,000 states and a Burn-in of 10%. The new sequences were deposited in GenBank under the accession numbers PP431570, PP431571, PP431572, PP431573, PP431574, PP658222, PP658223, PP658224, and PP942456.

Geometric morphometrics analysis

We examined shell shape variation with a two-dimensional geometric morphometric analysis, under the hypothesis that *O. draparnaudi*, *O. cellarius*, and *O. alliarius* represent three shell morphotypes that were defined by their genital anatomy. Shell shape variation was analyzed both in apertural and apical views, quantified through landmarks and semi-landmarks placed on photographs of the individual shells (Bookstein 1982; Zelditch et al. 2004). Shell images were captured using a camera attached to a stereomicroscope Nikon SMZ800, ensuring that the suture of the spire (in apical view) or the shell aperture (in apertural view) were observed in the same plane in all shells of either series.

A total of 22 apertural view photographs (eight *O. cellarius*, seven *O. alliarius*, and seven *O. draparnaudi*) and 39 apical view photographs (five *O. cellarius*, 17 *O. alliarius*, and 17 *O. draparnaudi*) were obtained. For the apical view, 50 semi-landmarks were used, while for the apertural view, 30 semi-landmarks were used (Fig. 1a, b). The x, y coordinates of the landmarks and semi-landmarks were digitized in the program TPSDIG2 v. 2.32 (Rohlf 2004), using the 'draw background curves' function, placing equidistant semi-landmarks along curves. In the apical view, two curves were used, one corresponding to the outer curvature of the shell starting at the distal point of the shell aperture and ending at the proximal point of the same aperture, and the other corresponding to the spire sutures (Fig. 2a); for the apertural view, only one curve that runs along the entire shell aperture, passing through the body whorl to the embryonic spire, was used (Fig. 2b).

To minimize the tangential variation of the semi-landmarks, a coordinate adjustment was performed using the SEMILAND6 program from the IMP suite (Sheets 2014). To superimpose the specimen coordinates and extract relevant shape data for comparison, a Generalized Procrustes Analysis (GPA) was performed using the SEMILAND6 program from the IMP suite, in which all sets of landmarks were translated around a common origin to remove the effect of position, scale, and orientation (Masonick and Weirauch 2020).

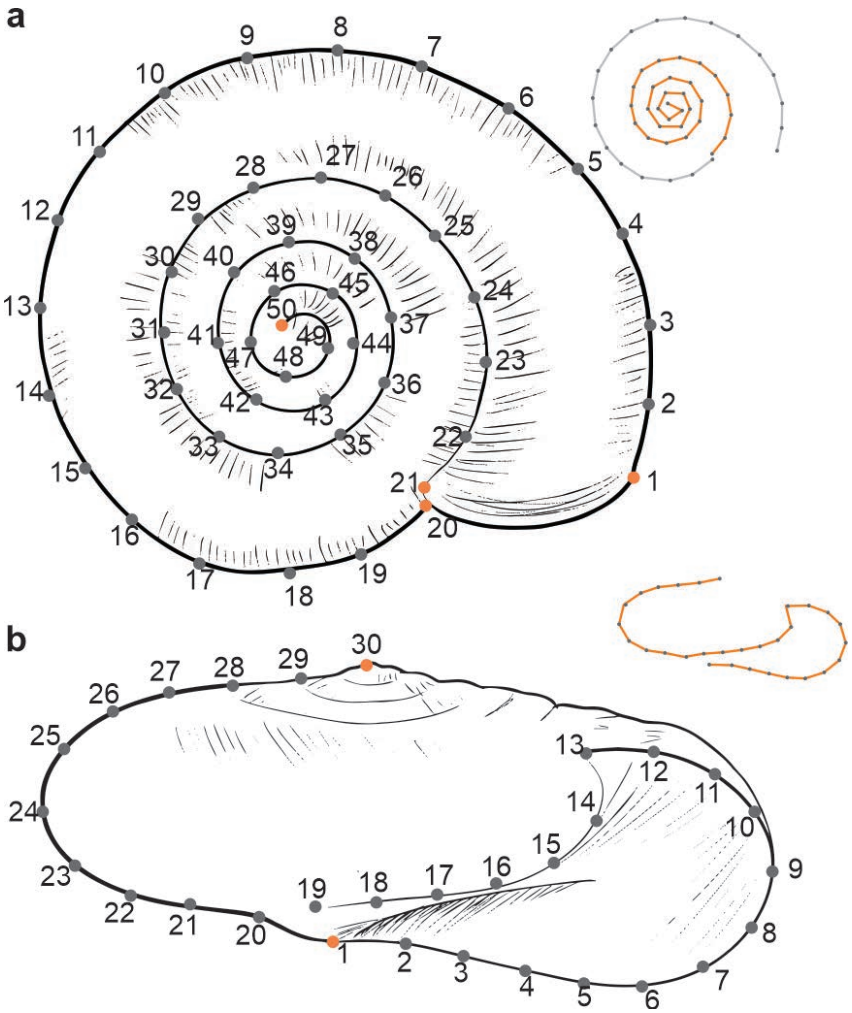

Figure 1. Landmarsks *sensu stricto* (orange dots) and semi-landmarks placed on *Oxychilus* shells **a** apical view **b** apertural view.

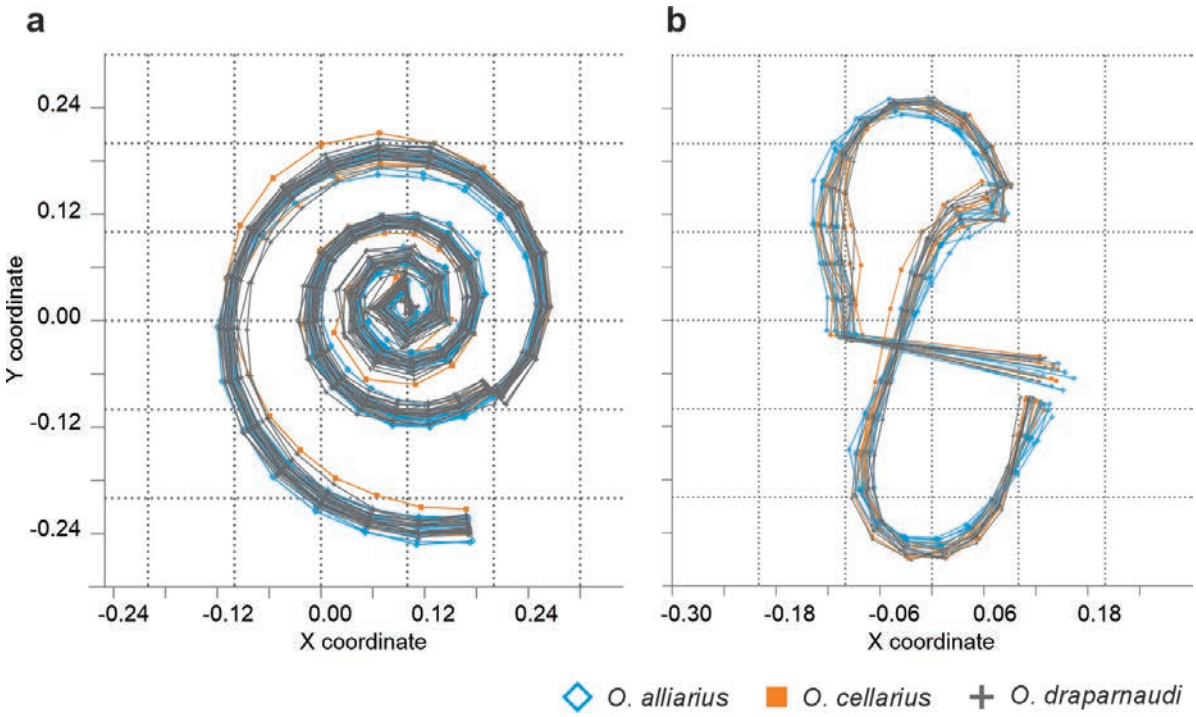

Figure 2. Superimposition of landmark coordinates for the three morphotypes hypothesis **a** apical view **b** apertural view.

Shell shape variation was evaluated using a Principal Coordinates Analysis (PCoA) in the PAST program v. 4.08 (Hammer and Harper 2006), based on the covariance matrix of individuals, obtaining a scatterplot with the two components that accounted for the highest percentage of variation. To represent the overall shape modification of each component, thin-plate spline deformation grids were calculated from the variability of the average shape along each PCoA.

Distribution data

Species distribution data were obtained from (1) the information on the labels of the specimens deposited in the IB-UNAM CNMO, (2) the Global Biodiversity Information Facility database (Hammer and Harper 2006), and (3) iNaturalist-MX (https://mexico.inaturalist.org/). The citizen observations in iNaturalistMX were reviewed by VAG, considering only those that matched the characteristics of the genus. Blurry photos and erroneous identifications (two records involved *Succinea* sp., two records to family Polygyridae, one to family Euconulidae, and one was an insect larva) were removed. These corrections were documented on the iNaturalistMX observation platform. With these records, a data table was built with the following attributes: 1) latitude, 2) longitude, 3) source from which the record was obtained and 4) locality (Suppl. material 1: table S2). Records with incomplete locality data that did not allow locating the collection site were excluded from the analysis.

Potential distribution

The model was created utilizing an R implementation (R Core Team 2024) of Maxent from the Maxnet library (Phillips 2021) and SDMtune (Vignali et al. 2022) for the training and evaluation of distribution models. Maxent employs the

principle of maximum entropy to estimate the probability distribution of a species using presence and absence data. The species habitat modeling was done with 142 *Oxychilus* spp. occurrence locations in Mexico: 26 from our collections and the CNMO records, one from GBIF (a specimen in the Carnegie Museum of Natural History) (GBIFa 2022; GBIFb 2023) and 115 from iNaturalistMX. We employed 19 bioclimatic variables downloaded from the WorldClim v. 2.1 (http://worldclim.org/version2) with a spatial resolution of 30 s. The model establishes a statistical connection between the environmental factors found at the locations where a species is observed and data indicating the species presence. It is commonly used for habitat modeling, even when there is limited information about the species occurrences (Phillips et al. 2006). The model randomly selects background points across the study area, representing locations where the species is considered to be either truly absent or likely absent (pseudo-absent). The relative significance of the environmental variable was calculated using Jackknife analysis inbuilt in the model. Using jackknife and Spearman correlation analysis we included the variables which were not highly correlated ($r < 0.7$) (Fig. 3). The model was evaluated with the help of AUC (Area under curve) of the ROC (Receiver operating characteristics) plot and true skill statistics (TSS) (Allouche et al. 2006). AUC in percentages measures model performance and varies from random to perfect discrimination (Swets 1988; Fawcett 2006).

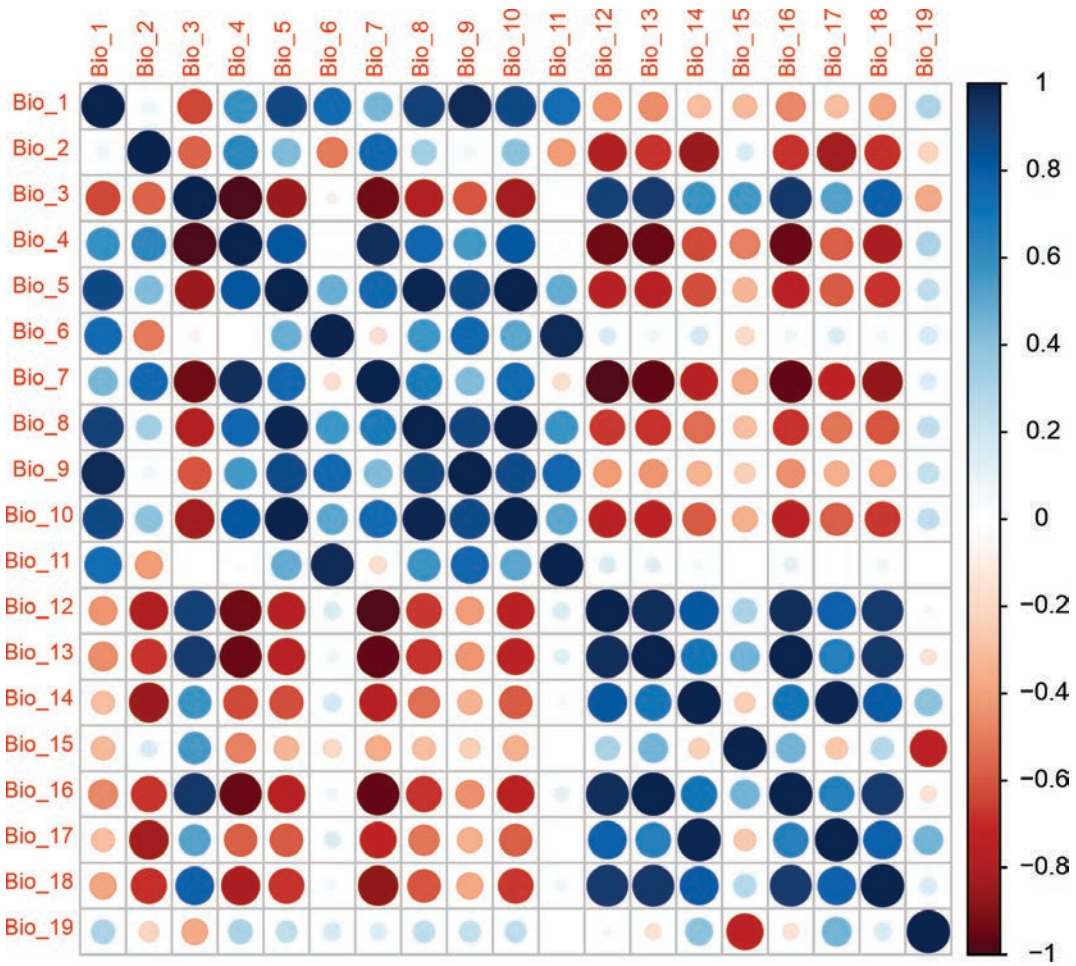

Figure 3. Spearman pairwise correlation coefficients between predictive variables. Variables selected for the final model were not highly correlated ($r < 0.7$).

Results

Collections and morphological identifications

We analyzed 50 specimens (Suppl. material 1: table S1) and 74 shells from four states of Mexico in two biogeographical provinces (Fig. 12). The live snails were found under logs and damp wood in (1) Tlaxcala (Atlihuetzia) where they lived in sympatry with *Deroceras laeve* (O.F. Müller), 1774, *D. reticulatum* (O.F. Müller 1774), *Arion intermedius* Normand, 1852, and *Boettgerilla pallens* (Simroth, 1912), (2) Querétaro where they were found in sympatry with *D. laeve*, (3) CDMX (Bosque de Tlalpan) where they co-occurred with *D. laeve* and *B. pallens*, and (4) Puebla (Teopancingo) where they were found in sympatry with *B. pallens* and *Pallifera* sp. The newly collected specimens were deposited at the **CNMO** (Suppl. material 1: table S1).

Systematics

Superfamily Gastrodontoidea Tryon, 1866
Family Oxychilidae Hesse, 1927
Subfamily Oxychilinae Hesse, 1927

Genus *Oxychilus* Fitzinger, 1833

Type species. *Helix cellaria* O.F. Müller, 1774 (type designation: Herrmannsen 1847).

Oxychilus draparnaudi (H. Beck, 1837)

Fig. 4

Worldwide distribution. Originally described from France, probably in the Montpellier area (Giusti and Manganelli 1997). Its native range includes western Europe and the western Mediterranean region (Barker 1999). It has spread to other parts of the world, including North America (Forsyth 2004) Russia, North and South Africa, Asia, Australia, and New Zealand (Barker 1999), Madeira (Seddon 2008), and Argentina (Virgillito and Miquel 2013).

Distribution in Mexico. Querétaro (Cadereyta de Montes), Tlaxcala (Atlihuetzia), State of Mexico (Tlalnepantla), CDMX (Álvaro Obregón, Benito Juárez, Tlalpan). According to Morrone (2019), localities belong to the Sierra Madre Oriental and Transmexican Volcanic Belt Province.

Diagnostic features. 15 specimens were dissected. Anatomically, all of them displayed the genital features typical of *O. draparnaudi* as described by Giusti and Manganelli (1997): a penis with a very slender proximal portion and a wider distal portion, both separated by a "bottle-neck" (= BS, i.e., a twisted duct or constriction) covered by a thin translucent sheath (Fig. 4D, G). Internally the proximal penis shows prominent papillae (Fig. 4F, I), while the distal penis shows four to five thin longitudinal internal folds (Fig. 4E, H).

Shell discoidal (Fig. 4B, C) with a depressed spire (Burch 1962), thin, yellowish, shiny; shell surface generally smooth with fine growth lines most evident near the suture and few very fine spiral lines (Fig. 4A). Shell whorls: 5 ½ to

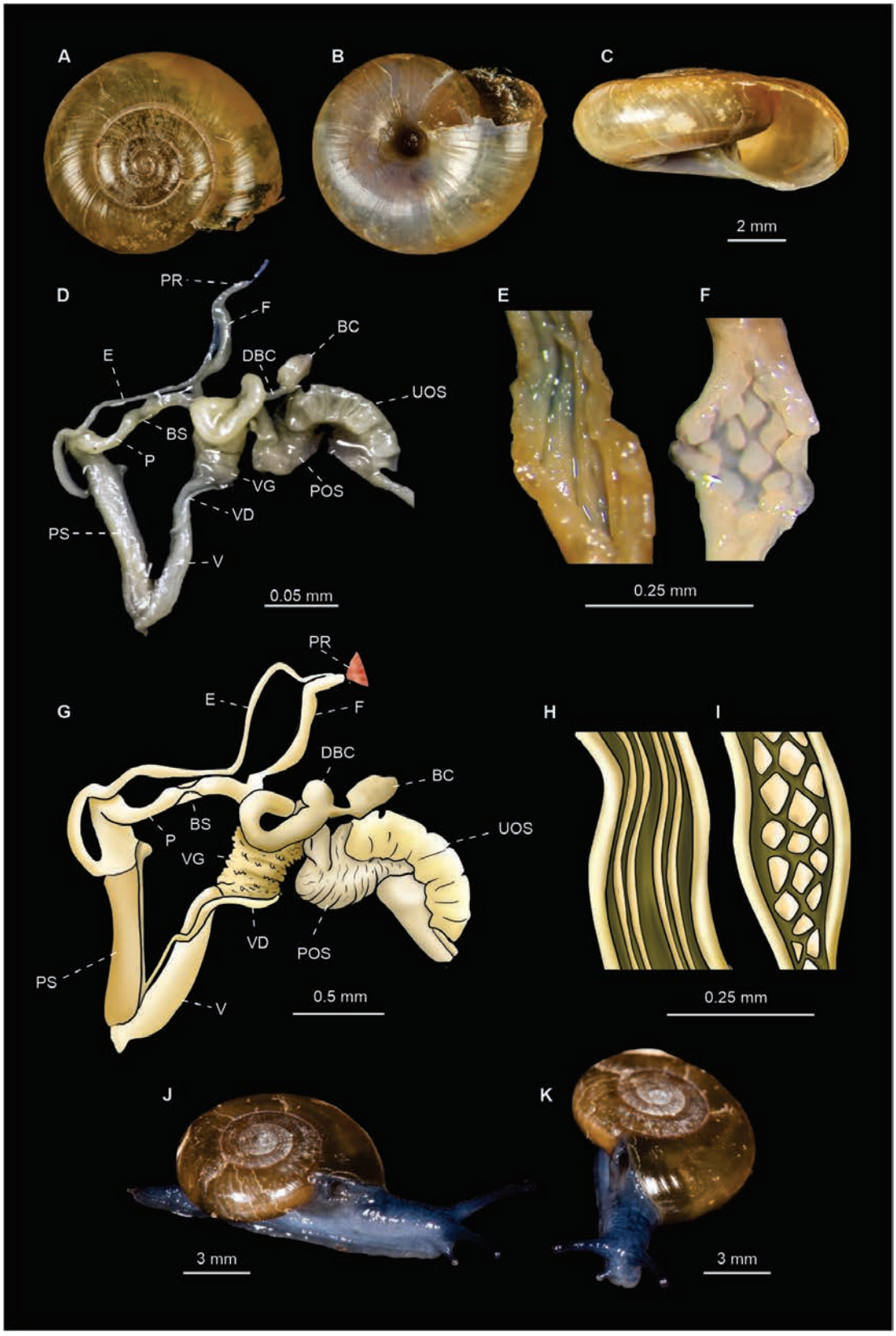

Figure 4. *Oxychilus draparnaudi* (CNMO 8470 Cadereyta, Querétaro). **A–C** shell in apical, ventral, and apertural view **D, G** genitalia of *O. draparnaudi* **F, I** internal ornamentation of the proximal penis **E, H** internal ornamentation of distal penis **J, K** live specimens. Abbreviations: BS bottleneck region, BC bursa copulatrix, DBC bursa duct, E epiphalus, F flagellum, P penis, POS prostatic portion of ovospermiduct, PR penial retractor, PS penial sheath, UOS uterine portion of ovospermiduct, V vagina, VD vas deferens, VG vaginal gland.

6. Umbilicus moderately wide, 1⁄6 of maximum shell diameter. Shell diameter 9–13 mm, shell height 3–6 mm (Fig. 7). Aperture width: 3.00–4.95 mm.

Radula (*n* = 5) composed of 30 rows with ~ 25 teeth/row (Fig. 8A). Radular formula: C/3 + 2–3 L/3 + 0–1 LM/2 + 9–12 M/1.

Oxychilus alliarius (J.S. Miller, 1822)

Fig. 5

Worldwide distribution. Originally described from the "Environs of Bristol", England (Miller 1822). Its native distribution includes Iceland, Greenland (Roth and Sadeghian 2003), and Central and Western Europe (Horáčková and Juřičková 2009). It has been reported as introduced in Austria, Belgium, Denmark, Estonia, Finland, France, Germany, Great Britain, Greece, Czech Republic, Spain, and Portugal (Horáčková and Juřičková 2009; Borges et al. 2010; De Oliveira and Altonaga 2010; IUCN Red List 2017), and spread to Hawaii (Cowie 1997), Tasmania (Kershaw 1991), South Atlantic (Preece 2001), North America (Forsyth 2004), Colorado, the Pacific coast states (Roth and Sadeghian 2003), South America (Hausdorf 2002), Chile (Cádiz et al. 2013), Sri Lanka (Naggs et al. 2003), Madeira (Seddon 2008), and the Philippines (Tañan and Sumaya 2024).

Distribution in Mexico. Puebla (Teopancingo), Transmexican Volcanic Belt Province.

Diagnostic features. Two specimens were dissected. The proximal part of the penis is initially wider and then gradually becomes distally narrower as described by Giusti and Manganelli (2002) (Fig. 5D, G). Internally the proximal (Fig. 5E, H) and distal penis show 2–4, thin, slightly undulating, longitudinal folds that seem to be a continuation of one another, but never showing lateral branching or assuming a papilla-like shape (Fig. 5F, I).

Shell discoidal, depressed, slightly convex above, compressed below, thin, semitransparent, variably shiny, yellowish to yellowish-brown, opalescent below (Fig. 5B, C); surface fairly smooth, with fainter growth lines more pronounced at sutures and very fine, wavy, spiral lines (Fig. 5A); aperture oval, oblique. Shell whorls: 4–4½. Umbilicus is rather broad, ~ 1⁄6 of maximum shell diameter. Shell dimensions: 6–9 mm diameter, 3–4 mm height (Fig. 7). Aperture width: 2–4 mm.

Radula (*n* = 3) composed of~ 35 rows with 25–31 teeth/row (Fig. 8B). Radular formula: C/3 + 2–3 L/3 + 0–1 LM/2 + 9–13 M/1.

Oxychilus cellarius (O.F. Müller, 1774)

Fig. 6

Worldwide distribution. Originally described from a wine cellar in Copenhagen (Müller 1774). Its native range includes northern and western Europe (Horáčková and Juřičková 2009), Asia Minor, and North Africa (Roth and Sadeghian 2003). It has been introduced into Tasmania (Kershaw 1991), Greenland, North America (Forsyth 2004), St Helena, South Africa, Chile (Stuardo and Vega 1985), Hawaii (Cowie 1997), Australia and New Zealand (Barker 1999).

Distribution in Mexico. CDMX (Tlalpan).

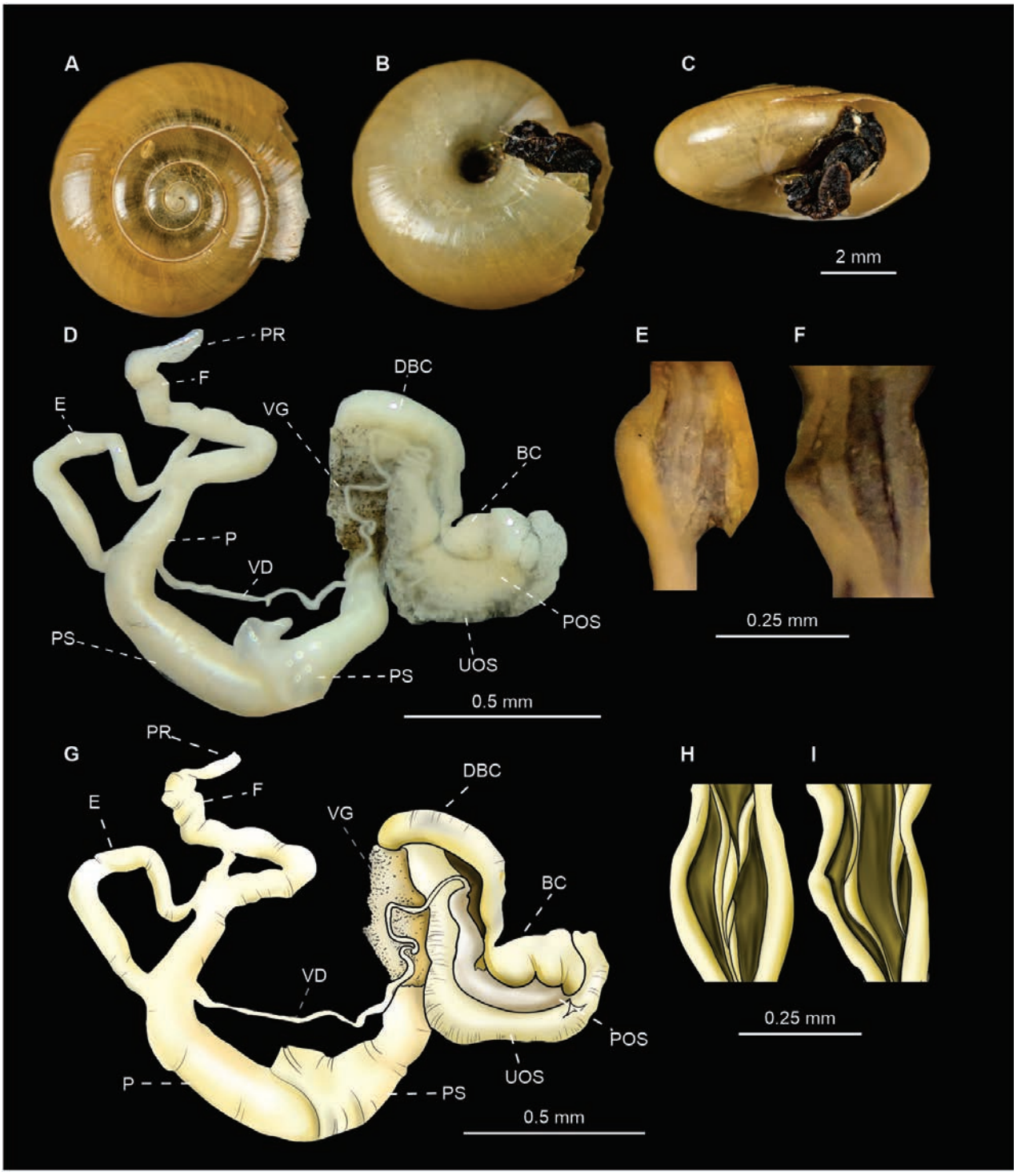

Figure 5. *Oxychilus alliarius* (CNMO 8464 Teopancingo, Puebla). **A–C** shell in apical, ventral and apertural view **D**, **G** genitalia of *O. alliarius* **E, H** internal ornamentation of the proximal penis **F, I** internal ornamentation of the distal penis. Abbreviations: BC bursa copulatrix, DBC bursa duct, E epiphalus, F flagellum, P penis, POS prostatic portion of the ovospermiduct, PR penial retractor muscle, PS penial sheath, UOS uterine portion of the ovospermiduct, VG vaginal gland, VD vas deferens.

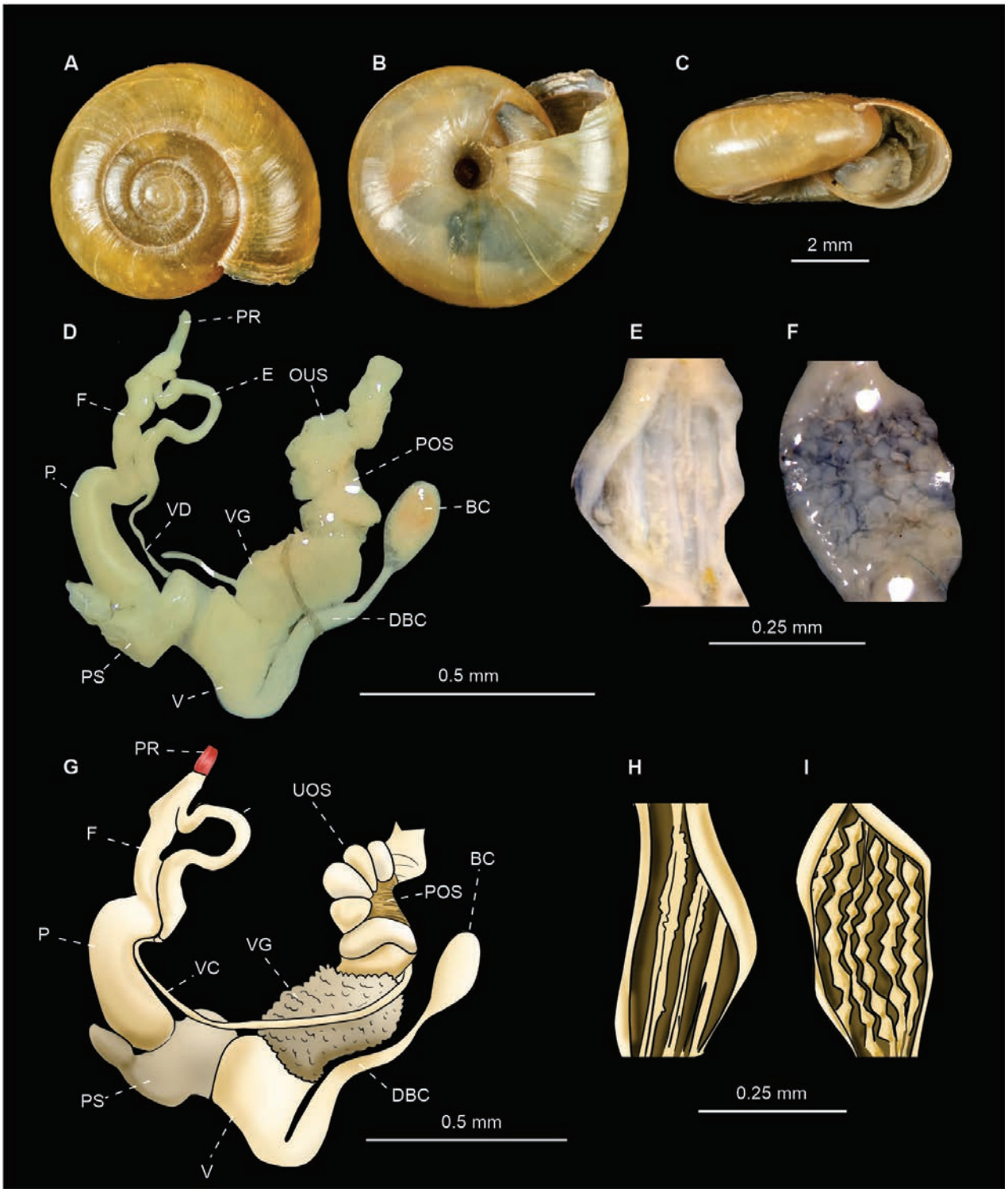

Figure 6. *Oxychilus cellarius* (CNMO 3858 Tlalpan, CDMX). **A–C** shell in apical, ventral and apertural view **D, G** genitalia of *O. cellarius* **E, H** internal ornamentation of the distal penis **F, I** internal ornamentation of proximal penis. Abbreviations: BC bursa copulatrix, DBC bursa duct, E epiphalus, F flagellum, P penis, POS prostatic portion of the ovospermiduct, PR penial retractor muscle, PS penial sheath, UOS uterine portion of the ovospermiduct, V vagina, VD vas deferens, VG vaginal glands.

Diagnostic features. Two specimens were dissected. The penis is cylindrical with a relatively constant width in the middle portion (Fig. 6D, G). Internally the proximal penis shows small, evenly distributed papillae that tend to be joined together in rows which occasionally form undulating folds (Fig. 6F, I). The distal penis presents four, thin, internal folds (Fig. 6E, H).

Shell discoidal, flattened, convex (Fig. 6C), light yellowish in color with fine lines of radial growth (Fig. 6A). Shell whorls: 4½–5. Umbilicus slightly flared, ~ 1/12 of maximum shell diameter (Fig. 6B). Shell dimensions: 8–10 mm diameter, 4 mm height (Fig. 7). Aperture width 3–4 mm.

Radula (*n* = 2) composed of 35 rows with ~ 25 teeth/row (Fig. 8C). Radular formula: C/3+ 2–3 L/3+ 0–1 LM/2 + 9–14 M/1.

mtDNA analysis

The COI tree recovered three clades corresponding to the three species studied in this study (Fig. 9), each with a posterior probability of 0.99–1.00. The sequence of the specimen from Teopancingo Puebla (TEN) was associated with GenBank sequences of *O. alliarius* from the United Kingdom and New Zealand,

Figure 7. Shells of Mexican (from left to right) *Oxychilus alliarius* (CNMO 8464 Teopancingo, Puebla, *O. cellarius* (CNMO 3858 Tlalpan, CDMX), and *O. draparnaudi* (CNMO 8470 Cadereyta, Querétaro). **A** apical view **B** ventral view **C** apertural view.

whose morphology agrees with that of the Mexican specimens. The other eight sequences from Querétaro, Tlaxcala, CDMX and Edo. Mex. (Suppl. material 1: table S3) formed a group with the GenBank sequences of *O. draparnaudi* from France, Canada, and the USA. Attempts to amplify the COI gene fragment for *O. cellarius* were unsuccessful due to insufficient DNA quality. However, the sequences reported in GenBank for this species were included in the analysis and formed a distinct group.

Geometric morphometric analyses

The superimposition of shell shape configuration in the apertural view for each individual did not exhibit regions with differences among the species. However, in the apical view, slight variations in the width of the shell aperture were observed (Fig. 9). The first two principal coordinates of the PCoA in the apertural view accounted for 70.96% of the variation (PCo1 = 53.39%, PCo2 = 17.57%), while in the apical view, they accounted for 60.80% of the variation (PCo1 = 42.13%, PCo2 = 18.67%). The scatterplots of the first two PCoA coordinates did not separate the species in either of the two evaluated views (Figs 10, 11).

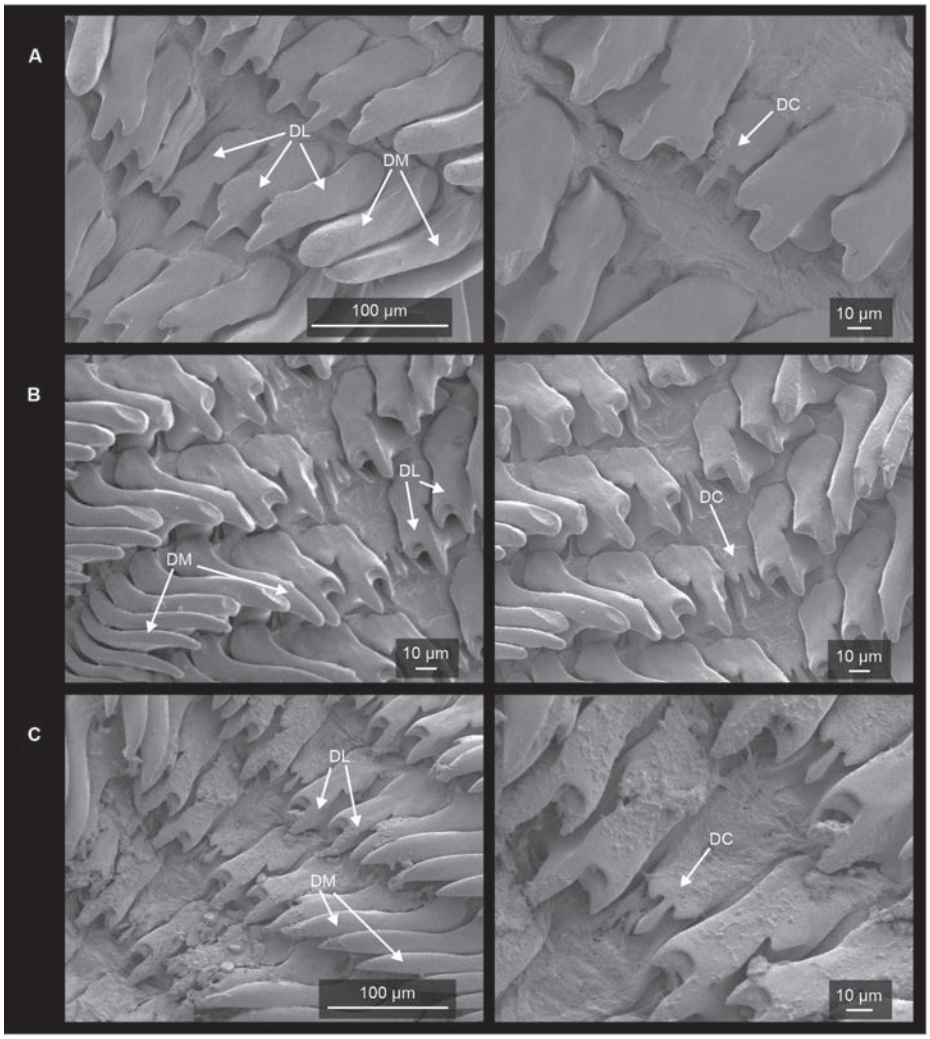

Figure 8. Radulae of Mexican. **A** *O. draparnaudi* (CNMO 8470 Cadereyta, Querétaro), **B** *O. alliarius* (CNMO 8464 Teopancingo, Puebla), and **C.** *O. cellarius* (CNMO 3858 Tlalpan, CDMX). Abbreviations: DC central tooth, DL lateral teeth, DM marginal teeth.

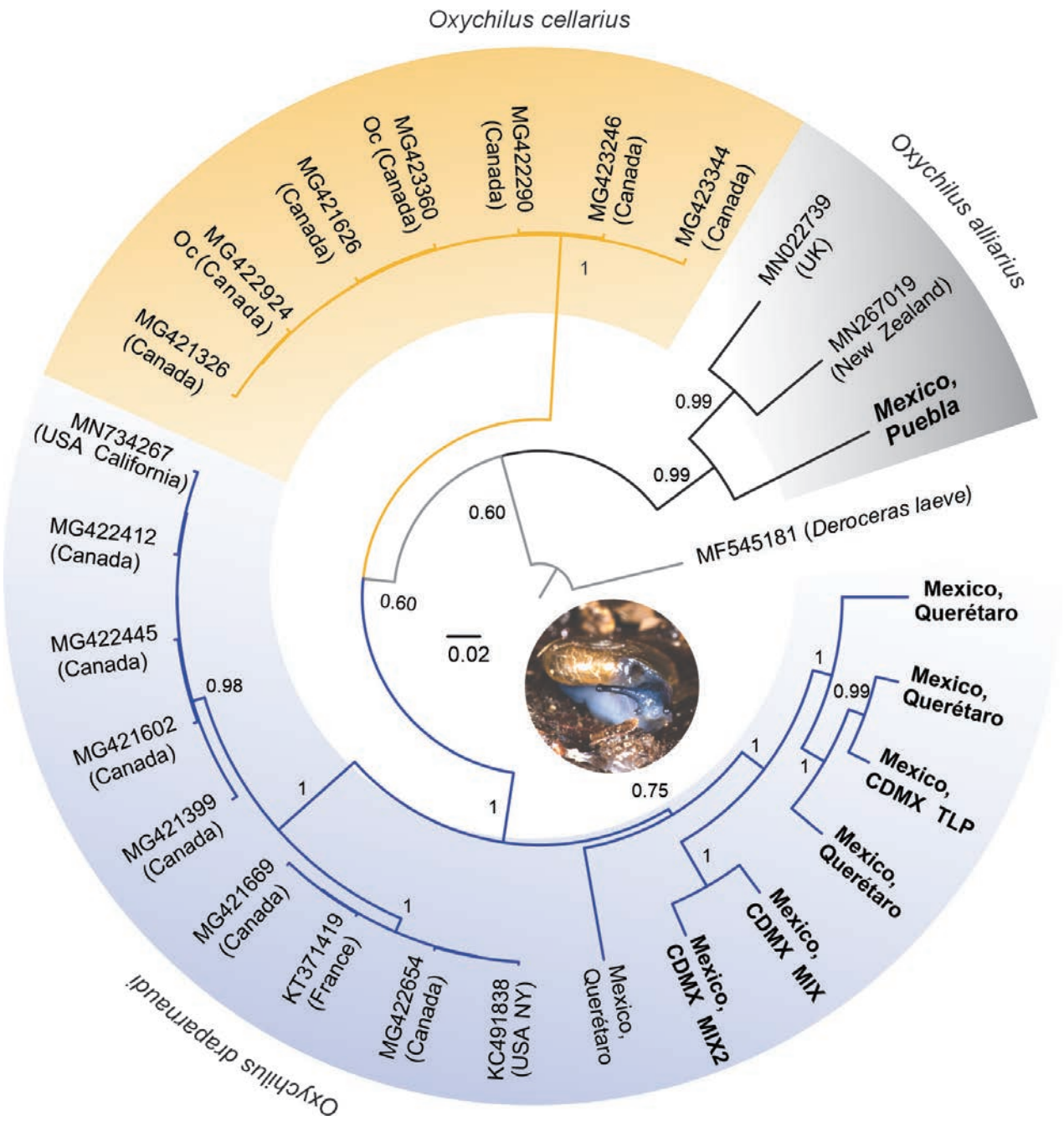

Figure 9. Bayesian phylogenetic tree of Mexican *Oxychilus alliarius*, *O. cellarius*, and *O. draparnaudi* based on the COI gene fragment (450 bp).

Distribution analysis

A map was obtained using data from Mexican specimens of *O. alliarius*, *O. cellarius*, and *O. draparnaudi*, showing that *O. draparnaudi* is the most widespread of the three species. Most records are in the Transmexican Volcanic Belt Province, including the states of Querétaro, Puebla, CDMX, and the State of Mexico (Fig. 12). The potential distribution map for the genus *Oxychilus* shows a tendency towards locations in the Volcanic Axis, a part of the Eastern Sierra Madre, and a part of the Southern Sierra Madre (Fig. 13). The variables that contributed most for predicting potential areas according to correlation and

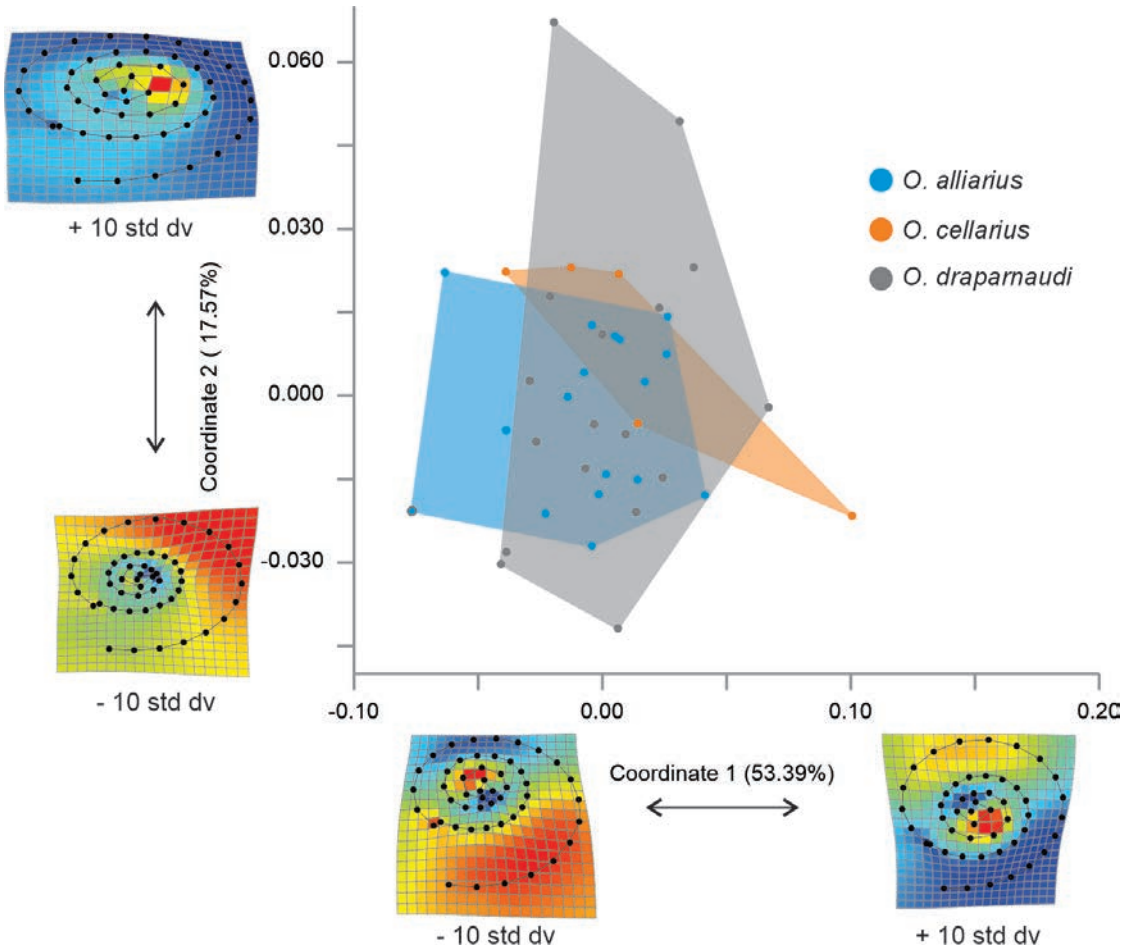

Figure 10. Geometric morphometric variation among shells of Mexican *Oxychilus alliarius*, *O. cellarius*, and *O. draparnaudi* in apical view.

jackknife analysis (Suppl. material 1: fig. S1) were BIO_5 (maximum temperature of warmest month), BIO_14 (precipitation of driest month (mm), BIO_11 (mean temperature of coldest quarter), BIO15 (precipitation seasonality (coefficient of variation)), BIO_3 (isothermality), BIO_7 (temperature annual range) and BIO_2 (mean diurnal range). The max temperature of the warmest month (BIO_5) of potential areas was 20–25 °C, and the precipitation during the driest month (Bio_ 14) was 5–15 mm (Suppl. material 1: fig. S2). The model performed well with an AUC of 0.958 (Suppl. material 1: fig. S3) and a TSS of 0.86.

Discussion

The anatomical and DNA analyses unequivocally confirm the identification of *O. draparnaudi* and *O. alliarius*, and provide the first documentation of the invasive species *O. alliarius* in Mexico, while expanding the Mexican distribution range of *O. draparnaudi*. However, the potential distribution model indicates that the genus *Oxychilus* can be established not only in urban areas, but also in mountain regions, where *Oxychilus* species may potentially threaten native biodiversity. This was already observed with *O. alliarius* in natural areas like Hawaiian islands (Curry et al. 2016). Its presence is limited to temperate and humid regions, where temperatures are neither excessively high nor low, and where there is moderate water availability throughout the year. Sensitivity to

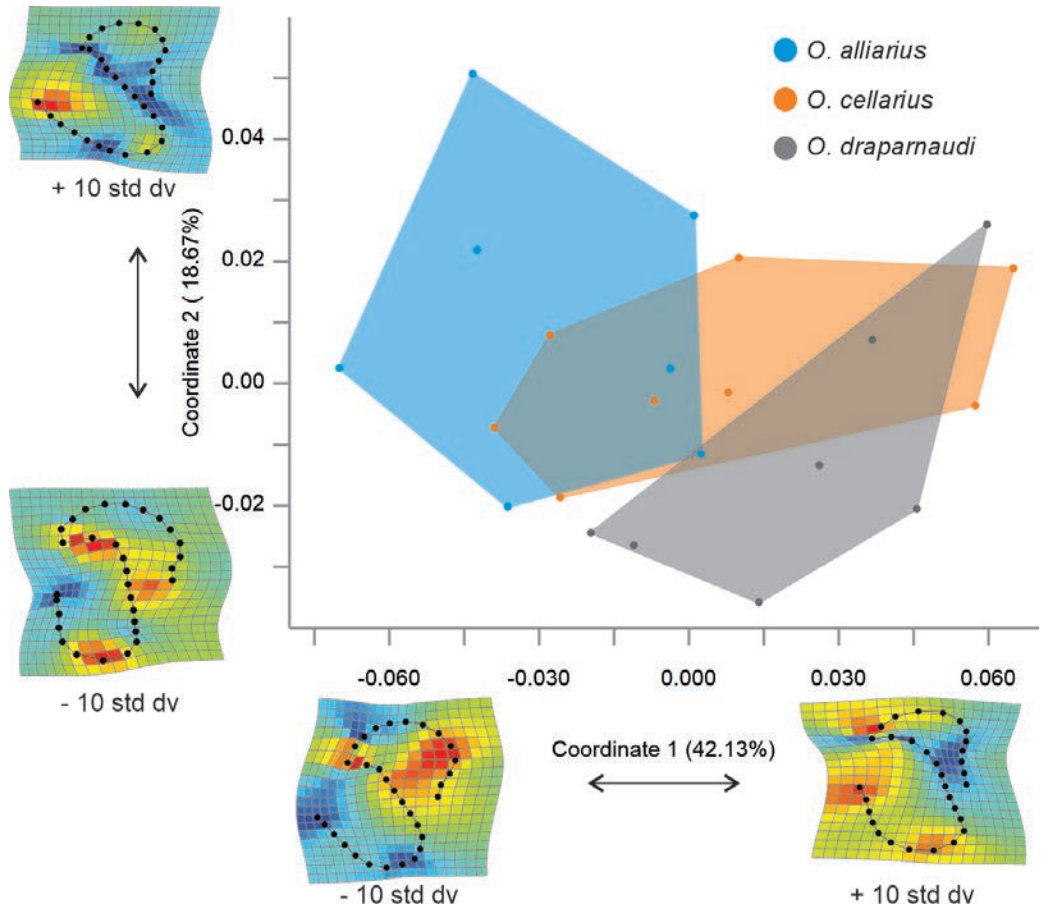

Figure 11. Geometric morphometric variation among shells of Mexican *Oxychilus alliarius*, *O. cellarius*, and *O. draparnaudi* in apertural view.

desiccation and extreme temperatures are limiting factors to all the land snails (Nicolai and Ansart 2017). As such, isothermality (BIO_3) is an important climate variable that is commonly shared with other potential distribution models for land snails (Vogler et al. 2013; Adhikari et al. 2020; Horsák et al. 2022).

Although COI is an effective marker to identify *Oxychilus* species (Dahirel et al. 2015; Salvador et al. 2019), we could not apply it to Mexican *O. cellarius* because of the poor quality of the extracted DNA. However, the anatomical data were sufficiently evident to confirm the presence of this species in Mexico.

Given that in field conditions one may often find more empty shells than live animals, it is tempting to identify the three *Oxychilus* species by their shells only. However, our geometric morphometric analyses have shown that it is very tricky, if not impossible, to distinguish the three species conchologically. Hence, more accurate identification techniques are required. Usually, live *O. alliarius* are easily recognized by its characteristic garlic smell (Cádiz et al. 2013); however, we don´t detect that smell in the specimens reported in this study. Shell morphology did not show any identifiable pattern of variability, the three identified species show similarities, the only difference being size. *O. alliarius* is the species with the smallest size, ranging from 6 to 9 mm, followed by *O. cellarius* with a diameter between 8 and 10 mm, while *O. draparnaudi* is the largest, ranging from 9 mm to 13 mm in diameter. However, shell size is an unreliable diagnostic feature since it shows some overlap among the three species (Giusti and Manganelli 1997; Cádiz et al. 2013), particularly when immature specimens are

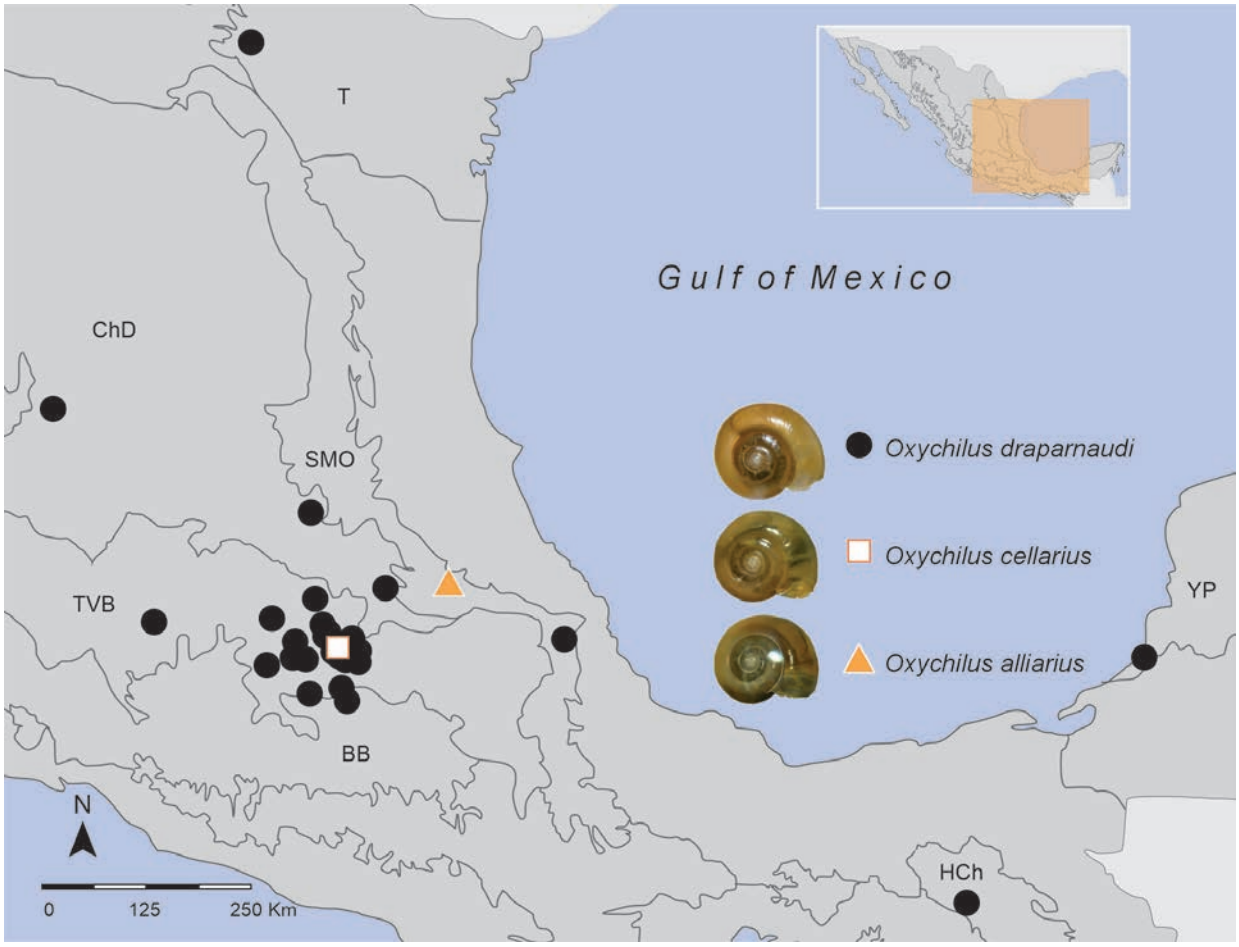

Figure 12. Actual distributions of *O. draparnaudi* (circle), *O. cellarius* (square), and *O. alliarius* (triangle) in Mexico. Biogeographic provinces (Morrone et al. 2017): T. Tamaulipas Province, ChD. Chihuahuan Desert Province SMO. Sierra Madre Oriental Province, TVB. Transmexican Volcanic Belt Province, BB. Balsas Basin Province, HCh. Chiapas Highlands Province, YP. Yucatan Peninsula Province.

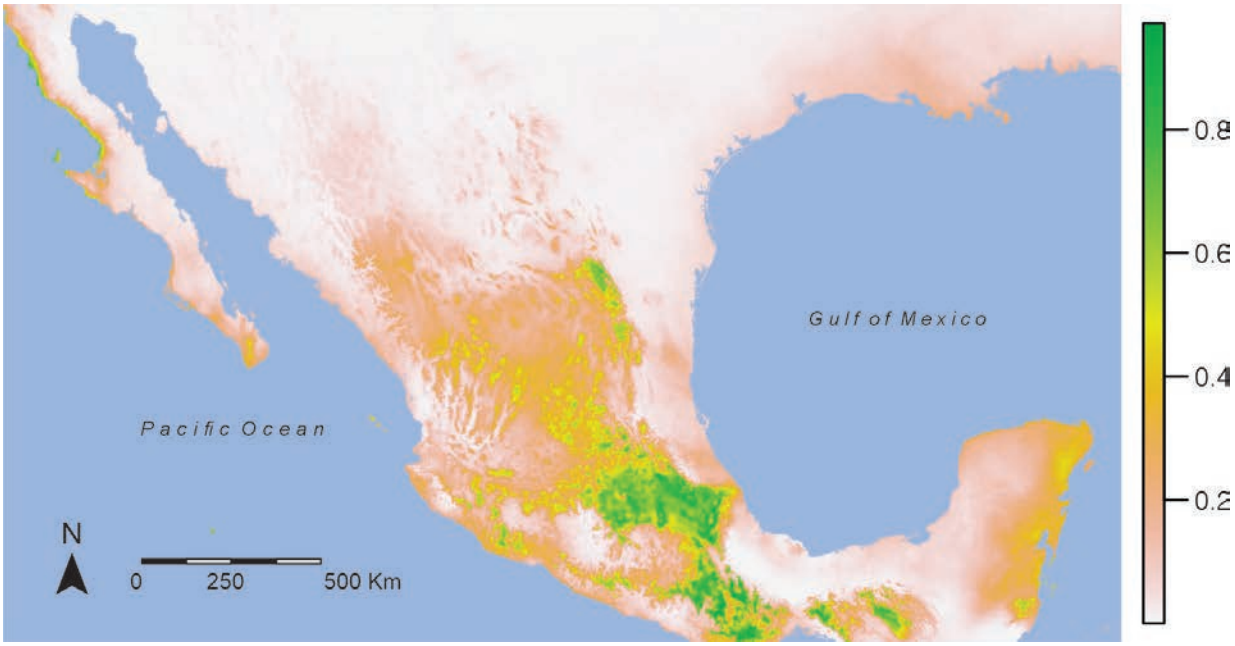

Figure 13. Potential distribution of the genus *Oxychilus* in Mexico. Green areas indicate high suitability areas.

involved. Hence, because of the conchological similarity between O. *alliarius*, *O. cellarius*, and *O. draparnaudi*, their identification should as much as possible be based on both their genital features and COI sequence data. Our results show that *O. draparnaudi* is already widespread in the central part of Mexico and may spread further southward. More research is required to determine to what extent local native faunas are impacted by *Oxychilus* species, since the three *Oxychilus* species reported here are partially carnivorous (Speiser 2001).

Acknowledgements

We are grateful to Dra. Flor Nohemí Rivera Orduño for the facilities to access scanning electron microscopy and Dr. Hugo Martínez Gutiérrez from Centro de Nanociencias Micro y Nanotecnologias for his help in taking micrographs.

Additional information

Conflict of interest

The authors have declared that no competing interests exist.

Ethical statement

No ethical statement was reported.

Funding

This work formed part of the bachelor dissertation of Ali Trujillo, who received a scholarship from Instituto Politecnico Nacional (BEIFI-IPN).

Author contributions

Conceptualization: VAG. Data curation: VAG, ENG. Formal analysis: AGTD, VAG. Funding acquisition: GZ, VAG. Investigation: AGTD. Methodology: JGR, JLHD. Project administration: GZ, VAG. Resources: GZ. Software: JLHD, JGR. Supervision: VAG. Validation: ENG. Writing – original draft: AGTD. Writing – review and editing: VAG, ENG.

Author ORCIDs

Ali Gabrielle Trujillo-Díaz https://orcid.org/0009-0002-2120-6414
Victoria Araiza-Gómez https://orcid.org/0000-0001-5583-1918
Jazmín García-Román https://orcid.org/0000-0003-0044-339X
Gerardo Zúñiga https://orcid.org/0000-0002-5041-4258
Edna Naranjo-García https://orcid.org/0000-0001-9015-1758

Data availability

All of the data that support the findings of this study are available in the main text or Supplementary Information.

References

Adhikari S, Sharma HP, Rimal B, Belant JL, Katuwal HB (2020) Road as a major driver for potential distribution of the invasive giant African land snail in Nepal. Tropical Ecology 61: 583–588.https://doi.org/10.1007/s42965-020-00115-4

Ali RF, Robinson DG (2020) Four records of new to Egypt gastropod species including the first reported Tropical Leatherleaf slug *Laevicaulis alte* (d'A. de Férussac, 1822) (Pulmonata: Veronicellidae). Zoology and Ecology 30: 138–156. https://doi.org/10.35513/21658005.2020.2.8

Allouche O, Tsoar A, Kadmon R (2006) Assessing the accuracy of species distribution models: prevalence, kappa and the true skill statistic (TSS). Journal of Applied Ecology 43:1223–1232. https://doi.org/10.1111/j.1365-2664.2006.01214.x

Barker GM (1999) Naturalised terrestrial Stylommatophora (Mollusca: Gastropoda). Fauna of New Zealand, Manaaki Whenua Press, Lincoln-New Zealand, 253 pp. https://doi.org/10.7931/J2/FNZ.38

Beck H (1837) Index molluscorum praesentis aevi musei principis augustissimi Christiani Frederici. Hafniae, Copenhagen, 101–124. https://doi.org/10.5962/bhl.title.77331

Bookstein FL (1982) Foundations of Morphometrics. Annual Review of Ecology and Systematics 13: 451–470. https://doi.org/10.1146/annurev.es.13.110182.002315

Borges PAV, Bried J, Costa A, Cunha R, Gabriel R, Gonçalves V, Martins AF, Melo I, Parente M, Raposeiro P, Rodrigues P, Santos RS, Silva L, Vieira P, Vieira V, Mendonça E, Boieiro M (2010) Description of the terrestrial and marine Azorean biodiversity. In: Borges PAV, Costa A, Cunha R, Gabriel R, Gonçalves V, Martins AF, Melo I, Parente M, Raposeiro P, Rodrigues P, Santos RS, Silva L, Vieira P, Vieira V (Eds) List of molluscs (Mollusca). Princípia, Cascais, 169–177. https://islandlab.uac.pt/fotos/publicacoes/publicacoes_Listagem_ml.pdf

Bronne L, Delcourt J (2022) The snail *Morlina glabra* (Gastropoda: Oxychilidae), although previously unrecognized, is widespread throughout Belgium and at least present in the Netherlands and Luxembourg. Journal of Conchology 44: 267–275. https://conchsoc.org/sites/default/files/jconch/44/3/2022-44306.pdf

Brook FJ (1999) Distribution and conservation status of the dune snail *Succinea archeyi* Powell (Stylommatophora: Succineidae) in northern New Zealand. Science for Conservation: Department of Conservation, Wellington New Zealand, 28 pp. https://www.doc.govt.nz/globalassets/documents/science-and-technical/sfc129.pdf

Burch JB (1962) How to Know the Eastern Land Snails: Pictured-keys for Determining the Land Snails of the United States Occurring East of the Rocky Mountain Divide. Wm. C. Brown Company Publishers, Dubuque-Iowa, 214 pp. https://babel.hathitrust.org/cgi/pt?id=mdp.39076006431519&seq=5

Cádiz F, Cádiz D, Grau J (2013) An invasive predatory snail *Oxychilus alliarius* (Miller, 1822) (Stylommatophora: Zonitidae) threatens the native malacofauna of continental Chile: a morphological and molecular confirmation. Studies on Neotropical Fauna and Environment 48: 119–124. https://doi.org/10.1080/01650521.2013.843910

Case TJ (1990) Invasion resistance arises in strongly interacting species-rich model competition communities. Proceedings of the National Academy of Sciences of the USA 87: 9610–9614. https://doi.org/10.1073/pnas.87.24.9610

Correa A, Martínez V, Horta J, Castro I (2012) Zoogeografía de los gasterópodos terrestres del sur de Tamaulipas, México. Revista de Biología Tropical 60: 317–331. https://doi.org/10.15517/rbt.v60i1.2764

Correa-Sandoval A, Rodríguez-Castro R, Venegas-Barrera C, Horta-Vega J, Barrientos-Lozano L, Rodríguez-Castro J (2017) Diversidad y zoogeografía de los moluscos terrestres de la sierra de Tamaulipas, México. Acta Zoológica Mexicana 33: 76–88. https://doi.org/10.21829/azm.2017.3311015

Cowie RH (1997) Catalog and bibliography of the nonindigenous nonmarine snails and slugs of the Hawaiian Islands. Bishop Museum Occasional Papers 50: 1–66. https://www.cabidigitallibrary.org/doi/full/10.5555/19971109211

Curry PA, Yeung NW, Hayes KA, Meyer III WM, Taylor AD, Cowie RH (2016) Rapid range expansion of an invasive predatory snail, *Oxychilus alliarius* (Miller 1822), and its impact on endemic Hawaiian land snails. Biological Invasions 18: 1769–1780. https://doi.org/10.1007/s10530-016-1119-0

Dahirel M, Olivier E, Guiller A, Martin MC, Madec L, Ansart A (2015) Movement propensity and ability correlate with ecological specialization in European land snails: comparative analysis of a dispersal syndrome. Journal of Animal Ecology 84: 228–238. https://doi.org/10.1111/1365-2656.12276

De Oliveira A, Altonaga K (2010) Materiais para o estudo da malacofauna não-marinha de Portugal. 10. *Oxychilus* (*Ortizius*) *alliarius* (Miller, 1822) e *Oxychilus* (*Oxychilus*) *cellarius* (Müller O.F., 1774) Pulmonata, Oxychilidae). Noticiario de la Sociedad Española de Malacología 54: 46–47.

Drummond AJ, Rambaut A (2007) BEAST: Bayesian evolutionary analysis by sampling trees. BMC Evolutionary Biology 7: 1–8. https://doi.org/10.1186/1471-2148-7-214

Falkner G (2008) *Oxychilus* (*Ortizius*) *edmundi* spec. nov. – a new narrow range endemic from Corsica (Gastropoda, Pulmonata, Oxychilidae). Basteria 72: 135–141. https://natuurtijdschriften.nl/pub/643854/BAST2008072004008.pdf

Fawcett T (2006) Introduction to ROC analysis. Pattern Recognition Letters 27: 861–874. https://doi.org/10.1016/j.patrec.2005.10.010

Folmer O, Black M, Hoeh W, Lutz R, Vrijenhoek R (1994) DNA primers for amplification of mitochondrial cytochrome c oxidase subunit I from diverse metazoan invertebrates. Molecular Marine Biology and Biotechnology 3: 294–299. https://www.mbari.org/wp-content/uploads/2016/01/Folmer_94MMBB.pdf

Forsyth RG (2004) Land snails of British Columbia. Royal British Columbia Museum, Victoria, British Columbia.

Frömming E (1954) Biologie der mitteleuropäischen Land Gastropoden. Duncker et Humblot, Berlin, 404 pp. https://openlibrary.org/works/OL7377270W/Biologie_der_mitteleuropa%CC%88ischen_Landgastropoden

Geerts S, Pauw A (2009) African sunbirds hover to pollinate an invasive hummingbird-pollinated plant. Oikos 118: 573–579. https://doi.org/10.1111/j.1600-0706.2008.17167.x

Giusti F, Manganelli G (1997) How to distinguish *Oxychilus cellarius* (Müller, 1774) easily from *Oxychilus draparnaudi* (Beck, 1837) (Gastropoda, Stylommatophora, Zonitidae). Basteria 61: 43–56. https://natuurtijdschriften.nl/pub/597112

Giusti F, Manganelli G (2002) Redescription of two west European *Oxychilus* species: *O. alliarius* (Miller, 1822) and *O. helveticus* (Blum, 1881), and notes on the systematics of, *Oxychilus* Fitzinger, 1833 (Gastropoda: Pulmonata: Zonitidae). Journal of Conchology 37: 455–476. https://doi.org/10.5962/p.408196

GBIFa (2022) GBIF Occurrence. https://doi.org/10.15468/dl.dbjnfm [accessed 18 November 2022]

GBIFb (2023) GBIF Occurrence. https://doi.org/10.15468/dl.en8cxd [accessed 9 October 2023]

Godoy O (2019) Coexistence theory as a tool to understand biological invasions in species interaction networks: Implications for the study of novel ecosystems. Functional Ecology 33: 1190–1201. https://doi.org/10.1111/1365-2435.13343

Gouy M, Guindon S, Gascuel O (2010) SeaView Version 4: A Multiplatform Graphical User Interface for Sequence Alignment and Phylogenetic Tree Building. Molecular Biology and Evolution 27: 221–224. https://doi.org/10.1093/molbev/msp259

Hammer Ø, Harper D (2006) Paleontological Data Analysis. Blackwell Publishing 6: 186–197. https://doi.org/10.1002/9780470750711

Hausdorf B (2002) Introduced land snails and slugs in Columbia. Journal of Molluscan Studies 68: 127–131. https://doi.org/10.1093/mollus/68.2.127

Herrmannsen AN (1847) Indicis Generum Malacozoorum Primordia. Cassellis: Theodoria Fischeri, 717 pp.

Horáčková J, Juřičková L (2009) A new record of *Oxychilus alliarius* (Gastropoda: Zonitidae) with the species distribution in the Czech Republic. Malacologica Bohemoslovaca 8: 63–65. https://doi.org/10.5817/MaB2009-8-63

Horsák M, Horsáková V, Divíšek J, Nekola JC (2022) Ecological niche divergence between extant and glacial land snail populations explained. Scientific Reports 12: 806. https://doi.org/10.1038/s41598-021-04645-2

Kappes H, Delgado JD, Alonso MR, Ibáñez M (2009) Native and introduced gastropods in laurel forests on Tenerife, Canary Islands. Acta Oecologica 35: 581–589. https://doi.org/10.1016/j.actao.2009.05.004

Kershaw RC (1991) Snail and slug pests of Tasmania. Queen Victoria Museum and Art Gallery, Launceston, 67 pp.

Lankau RA (2013). Species invasion alters local adaptation to soil communities in a native plant. Ecology 94: 32–40. https://doi.org/10.1890/12-0675.1

MacDonald I, Reaser JK, Bright C, Neville L, Murphy S, Preston G (2004) Invasive alien species in Southern Africa. National Reports and Directory of Resources, Cape Town, 125 pp. https://wis.orasecom.org/content/study/Data%20still%20to%20be%20sorted/InvasiveAlienVegetation_refs/MacDonald%20et%20al%202003.pdf

Masonick P, Weirauch C (2020) Integrative species delimitation in Nearctic ambush bugs (Heteroptera: Reduviidae: Phymatinae): insights from molecules, geometric morphometrics and ecological associations. Systematic Entomology 45: 205–223. https://doi.org/10.1111/syen.12388

McNeely J (2001) Invasive species: a costly catastrophe for native biodiversity. Land Use and Water Resources Research 1: 1–10. https://ageconsearch.umn.edu/record/47850?v=pdf

Meyer III WM (2005) Potential impact of an abundant introduced omnivorous land snail, *Oxychilus alliarius* on native land snails on the Island of Hawaii. Tentacle 13: 16–17. https://www.cabidigitallibrary.org/doi/full/10.1079/cabicompendium.119076

Meyer III WM, Cowie RH (2010) Invasive temperate species are a threat to tropical island biodiversity. Biotropica, 42: 732–738. https://doi.org/10.1111/j.1744-7429.2010.00629.x

Miller JS (1822) A list of the freshwater and land shells occurring in the environment of Bristol, with observations. Annals of Philosophy 3: 376–381. https://www.biodiversitylibrary.org/page/2498134

MolluscaBase [Eds] (2021) MolluscaBase *Oxychilus* Fitzinger, 1833. http://molluscabase.org/aphia.php?p=taxdetails&id=818444 [accessed 15 November 2023]

Morrone JJ, Escalante T, Rodríguez-Tapia G (2017) Mexican biogeographic provinces: map and shapefiles. Zootaxa 4277: 277–279. https://doi.org/10.11646/zootaxa.4277.2.8

Morrone JJ (2019) Regionalización biogeográfica y evolución biótica de México: encrucijada de la biodiversidad del Nuevo Mundo. Revista Mexicana de Biodiversidad, 90: 1–67. https://doi.org/10.22201/ib.20078706e.2019.90.2980

Müller OF (1774) Vermium terrestrium et fluviatilium, seu animalium infusorium, Helminthicorum, et testaceorum, non marinorum, succincta historia. 2: 1–214. https://doi.org/10.5962/bhl.title.46299

Naggs F, Raheem DC, Mordan PB, Grimm B, Ranawana KB, Kumburegama NPS (2003) Ancient relicts and contemporary exotics: faunal change and survivorship in Sri Lanka's snail fauna. In Slugs and snails: agricultural, veterinary and environmental perspectives, 103–108.

Naranjo-García E, Castillo-Rodríguez G (2017) First inventory of the introduced and invasive mollusks in Mexico. The Nautilus 131: 107–126. https://www.biodiversitylibrary.org/item/276658#page/5/mode/1up

Nicolai A, Ansart A (2017) Conservation at a slow pace: terrestrial gastropods facing fast-changing climate. Conservation Physiology 5: cox007. https://doi.org/10.1093/conphys/cox007

Phillips S (2021) Maxnet: Fitting 'Maxent' Species Distribution Models with 'glmnet'. R package version 0.1.4, https://CRAN.R-project.org/package=maxnet [accessed 19 November 2023]

Phillips SJ, Anderson RP, Schapire RE (2006) Maximum entropy modeling of species geographic distributions. Ecological Modelling 190: 231–259. https://doi.org/10.1016/j.ecolmodel.2005.03.026

Preece RC (2001) Introduced land molluscs on the islands of the Tristan da Cunha—Gough group (South Atlantic). Journal of Conchology 37: 253–259. https://doi.org/10.5962/p.408084

R Core Team (2024) R: A Language and Environment for Statistical Computing. R Foundation for Statistical Computing, Vienna, Austria. https://www.R-project.org/ [accessed 19 November 2023]

IUCN (2017) IUCN Red List, *Oxychilus alliarius*. The IUCN Red List of Threatened Species 2017: e.T171258A1323544.

Rohlf FJ (2004) TpsDig Version 1.4. Department of Ecology and Evolution. State University of New York at Stony Brook, New York. http://life.bio.sunysb.edu/morph/index.html [accessed 19 December 2022]

Roth B, Sadeghian PS (2003) Checklist of the land snails and slugs of California. Santa Barbara Museum of Natural History, Santa Barbara, CA, 81.

Salvador RB, Birmingham CMR, Kilduff LA, Bliss T, Green J (2019) First records of the exotic garlic snail *Oxychilus alliarius* on Takapourewa and a reassessment of its distribution in New Zealand. Tuhinga 31: 120–128.

Seddon M (2008) The landsnails of Madeira. An illustrated compendium of the landsnails and slugs of the Madeiran archipelago. Studies in the biodiversity and systematics of terrestrial organisms from the National Museum of Wales. Biotir Reports 2: 1–204.

Sheets HD (2014) Integrated Morphometrics Package (IMP) 8, 2014. https://www.animal-behaviour.de/imp/ [accessed 18 December 2022]

Simberloff D, Martin JL, Genovesi P, Maris V, Wardle DA, Aronson J, Courchamp F, Galil B, García-Berthou E, Pascal M, Pyšek P, Sousa R, Tabcchi E, Vilà M (2013) Impacts of biological invasions: what's what and the way forward. Trends in Ecology and Evolution 28: 58–66. https://doi.org/10.1016/j.tree.2012.07.013

Simroth H (1912) Neue Beiträge zur Kenntnis der kaukasischen Nacktschneckenfauna. Mitteilungen des Kaukasischen Museums, 6: 1–140. https://www.biodiversitylibrary.org/page/58474211

Speiser B (2001) Food and feeding behaviour. In: Barker GM (Ed.) The biology of terrestrial mollusks. CABI publishing. New York, USA, 259–288. https://doi.org/10.1079/9780851993188.0001

Stoll P, Gatzsch K, Rusterholz HP, Baur B (2012) Response of plant and gastropod species to knotweed invasion. Basic and Applied Ecology 13: 232–240. https://doi.org/10.1016/j.baae.2012.03.004

Stone CP, Scott JM (1985) Hawaii's terrestrial ecosystems: preservation and management. Honolulu (Hawaii). In: Cooperative National Park Resources Studies Unit, University of Hawai'i. Proceedings of a Symposium held. Hawai'i Volcanoes National Park, 149–179. https://pcsuhawaii.org/books-1985/book_all_1985.pdf

Stuardo J, Vega R (1985) Synopsis of the land mollusca of Chile. Studies on Neotropical Fauna and Environment 20: 125–146. https://doi.org/10.1080/01650528509360682

Swets JA (1988) Measuring the Accuracy of Diagnostic Systems. Science 240: 1285–1293. https://doi.org/10.1126/science.3287615

Sysoev AV, Schileyko AA (2009) Land snails of Russia and adjacent countries. Pensoft Publishers, Sofia/Moskva, 47–50.

Tañan VB, Sumaya NHN (2024) Bio-inventory of terrestrial gastropod species in Northern Mindanao, Philippines. Biodiversitas, 25: 3391–3402. https://doi.org/10.13057/biodiv/d251001

Thompson F (2011) An annotated checklist and bibliography of the land and freshwater snails of México and Central America. Bulletin of the Florida Museum of Natural History 50: 1–299. https://doi.org/10.58782/flmnh.bnej7351

Valdovinos C (1999) Biodiversidad de moluscos chilenos: Base de datos taxonómica y distribucional. Gayana 63: 111–164. https://ia801304.us.archive.org/33/items/biostor-118235/biostor-118235.pdf

Vignali S, Barras AG, Arlettaz R, Braunisch V (2022) SDMtune: An R package to tune and evaluate species distribution models. Ecology and Evololution 10: 11488–11506. https://doi.org/10.1002/ece3.6786

Virgillito M, Miquel S (2013) New records of exotic land snails and slugs in Argentina. Revista del Museo Argentino de Ciencias Naturales 15: 295–303. http://www.scielo.org.ar/scielo.php?script=sci_arttext&pid=S1853-04002013000200011&lng=es&tlng=. https://doi.org/10.22179/REVMACN.15.186

Vogler RE, Beltramino AA, Sede MM, Gregoric DEG, Núñez V, Rumi A (2013) The Giant African Snail, *Achatina fulica* (Gastropoda: Achatinidae): Using Bioclimatic Models to Identify South American Areas Susceptible to Invasion. American Malacological Bulletin 31: 39–50. https://doi.org/10.4003/006.031.0115

Zelditch M, Swiderski D, David H, Fink W (2004) Geometric Morphometrics for Biologists: A Primer. Elsevier Academic Press, New York, 416 pp. https://books.google.com.mx/books?id=VJiuHQXlMb4C&lpg=PP1&pg=PA228#v=onepage&q&f=false

Supplementary material 1

Supplementary data

Authors: Ali Gabrielle Trujillo-Díaz, Victoria Araiza-Gómez, Jazmín García-Román, José Luis Hernández-Domínguez, Gerardo Zúñiga, Edna Naranjo-García

Data type: docx

Explanation note: Distribution data obtained in this study and consulted in databases used for potential distribution analysis are attached, in addition to the accession numbers of the COI gene sequences generated in this study.

Link: https://doi.org/10.3897/zookeys.1224.129618.suppl1

ZooKeys 1224: 165–174 (2025)
DOI: 10.3897/zookeys.1224.142859

Research Article

Two new species of the genus *Veraphis* Casey (Coleoptera, Staphylinidae, Scydmaeninae) from Korea

Ui-Joung Byeon[1], Jong-Seok Park[1]

1 *Department of Biological Sciences and Biotechnology, Chungbuk National University, 1 Chungdae-ro, Seowon-gu, Cheongju-si, Chungbuk-do, 28644, Republic of Korea*
Corresponding author: Jong-Seok Park (jpark16@chungbuk.ac.kr)

Abstract

Two new species, *Veraphis odaesanensis* **sp. nov.** and *Veraphis myeonggiensis* **sp. nov.**, of the ant-like stone beetle, are described from the Korean Peninsula. The Korean fauna of *Veraphis* Casey now comprises three species, including *V. engelmarki koreanus*. This study provides habitus images and aedeagus illustrations of the new species.

Key words: Ant-like stone beetles, distribution map, Eutheiini, morphology, taxonomy

OPEN ACCESS

Academic editor: Adam Brunke
Received: 27 November 2024
Accepted: 17 December 2024
Published: 28 January 2025

ZooBank: https://zoobank.org/5793D52C-81D9-40A7-B544-DEAED1E62F34

Citation: Byeon U-J, Park J-S (2025) Two new species of the genus *Veraphis* Casey (Coleoptera, Staphylinidae, Scydmaeninae) from Korea. ZooKeys 1224: 165–174. https://doi.org/10.3897/zookeys.1224.142859

Introduction

The genus *Veraphis* Casey, 1897 (Staphylinidae: Scydmaeninae: Eutheiini) is exclusively distributed in the Northern Hemisphere, comprising 35 species (including three subspecies). Eight species occur in the Nearctic region, one species in Scandinavia, and the remaining species are found in Far East Russia, Japan, North Korea, Siberia, Mongolia, and China (Sawada 1962; Franz 1971; Hisamatsu 1985; Kurbatov 1995, 2006; Jałoszyński and Hoshina 2005; Jałoszyński 2009, 2012, 2013, 2014a, 2019, 2024). According to Jałoszyński and Hoshina (2005), the Japanese *Veraphis* species are grouped into three distinct species groups, except for *V. engelmarki* Franz and *V. ishikawai* Hisamatsu. Some species, *Veraphis spinosus* Jałoszyński, *V. qinghaiensis* Jałoszyński, *V. calcarifer* Jałoszyński, *V. gansuanus* Jałoszyński, *V. shaanxiana* Jałoszyński, and *V. dabashana* Jałoszyński, recorded in China have morphological characters similar to those of the Japanese species groups but do not perfectly align with their characteristics. Therefore, it is difficult to assign these species to any specific group (Jałoszyński 2009, 2012, 2013, 2024).

The genus *Veraphis* was first recorded from the Korean Peninsula in 2005, with the description of *V. engelmarki koreanus* Jałoszyński & Hoshina, 2005 from Pyongyang, North Korea. Since then, no additional species of *Veraphis* have been documented from the Korean Peninsula. This study reports two new species of *Veraphis* from South Korea, marking the first record in approximately 20 years. The present study provides images of the habitus, aedeagus, and a distribution map.

Material and methods

A total of 14 dry and alcohol-preserved specimens were examined in this study. Male specimens were relaxed in warm water before being mounted on sticky tabs for imaging. Subsequently, the specimens were point-mounted and preserved as dry specimens. Observations were conducted using a Leica S8APO. Images of the habitus, diagnostic characters, and aedeagus were produced using a Sony ILCE-7RM3 mirrorless camera with a Mitutoyo M Plan Apo 20X objective lens. The aedeagus was imaged after the internal organs were removed using Proteinase K. The images were stacked using Helicon Focus 8, and line drawings were created with Adobe Illustrator 2024. Morphological terminology followed Jałoszyński (2014b) and Jałoszyński and Hoshina (2005). Distribution maps were generated using SimpleMappr (Shorthouse 2010). The figure plates used in this study were edited and produced using Adobe Photoshop 2024. Data labels of holotypes were transcribed verbatim, while those of paratypes were standardized for consistency. Body length was measured from the anterior margin of the head to the posterior margin of the elytra.

All examined specimens were deposited in the following collections.

CBNUIC Chungbuk National University Insect Collection, Cheongju, South Korea;

NIBR National Institute of Biological Resources, Incheon, South Korea.

Taxonomy

Genus *Veraphis* Casey, 1897

Veraphis Casey, 1897: 509. Type species: *Eutheia impressa* LeConte, 1879 (designated by Franz in Newton and Franz 1998).

Diagnosis. This genus is distinguished from other genera of Scydmaeninae by the following combination characteristics: body flattened and elongated (Figs 1A, 2A); procoxal cavities broadly open (Fig. 1E); prosternum with a narrow intercoxal carina (Fig. 1E); each elytron with a setose basal fovea (Figs 1B, 2B). For more detailed diagnostic characters and phylogenetic information on this genus, refer to Jałoszyński (2014b).

Distribution. Northern Hemisphere (China, Japan, Korea, USA, Finland, Sweden, Mongolia, Russia (Far East, East Siberia)).

Remarks. According to Jałoszyński 2024, this genus is primarily found in leaf litter and soil, and all species discovered in China inhabit alpine regions at altitudes above 2000 m. Additionally, species found in Japan are also thought to be distributed in cooler climates. These species are very similar in external morphology, making examination of the aedeagus crucial for species identification. In some species, modifications of the male legs are present, which can be useful for distinguishing species.

***Veraphis odaesanensis* sp. nov.**
https://zoobank.org/99E3D6D4-1540-4CA5-81F9-FA16CD4DC18F
Figs 1, 3A–D, 4

Type material designated. ***Holotype*** • ♂ NIBR: "**Korea:** Gangwon Prov. Mt. Odae, Dongsan-ri, Jinbu-myeon, Pyeongchang-gun, 17.VIII.2022, 37°47'14.2"N, 128°33'56.2"E, 897 m, sifting leaf & soil litter, J.-W. Seo, J.-I. Shin" ***Paratypes*** **Korea:** Gangwon Prov. • 1♂1♀ (1♂ genitalia dissected; CBNUIC), Pyeongchang-gun, Jinbu-myeon, Dongsan-ri, 21.IX–02.XI.2022, 37°47'14.2"N, 128°33'56.2"E, 897 m, F.I.T, J.-W. Kang, J-I. Shin • 1♀ (CBNUIC), 02.XI.2022, 37°47'14.2"N, 128°33'56.2"E, 897 m, F.I.T, J.-W. Kang, J-I. Shin • 1♀ (CBNUIC), 17.VIII.2022, 37°47'14.2"N, 128°33'56.2"E, 897 m, sifting soil & leaf litter, J.-W. Seo, J-I. Shin • 8♀♀ (7♀♀ 95% EtOH in tube; CBNUIC), Odaesan-ro 1211-14, Mt. Odae, Sangwonsa, 17.VIII–21.IX.2022, 37°47'14.2"N, 128°33'56.2"E, 897 m, F.I.T, J-I. Shin U.-J. Hwang.

Diagnosis. Vertex with two shallow longitudinal grooves extending from posterior margin to posterior 1/2; area between grooves relatively flattened and impressed (Fig. 1B). Protibiae of male with small subapical pin-like projection (Fig. 1D). Metaventrite with shallow longitudinal impression (Fig. 1E). Aedeagus (Fig. 3A–D) strongly elongated and symmetrical, length 0.24 mm. In ventral view, lateral margins of median lobe somewhat parallel, middle of apex weakly protruding, with small shallow punctures in subapical region in ventral view; in lateral view, slightly curved near base and subapical region with strong ventral indentation. Endophallus symmetrical, U-shaped structured. Parameres slender, reaching middle of median lobe; each paramere with two short apical setae and one subapical seta.

Male description. Body length 1.27–1.32 mm; reddish-brown, appendages lighter; flattened and elongated; surface covered yellow hairs (Fig. 1A). Head wider than long, widest across eyes; punctures of surface inconspicuous; hairs short and sparse (Fig. 1B). Temples nearly 1/4 length of eyes, with shorter hairs than those on surface (Fig. 1B). Vertex with small pits on medioposterior margin; two shallow longitudinal grooves extending from posterior margin to posterior 1/2 present; area between grooves relatively flattened and impressed (Fig. 1B). Antennae with distinct distal three-segmented club; antennomere 1 strongly elongate, 2 elongate but weaker than 1, 3 slightly wider than long, 4–6 as long as wide, 5 slightly larger than 4, 6 slightly smaller than 5, 7 subpentagonal, 8 distinctly wider than long, 9–11 forming club (Fig. 1A). Pronotum distinctly wider than head, as long as wide, widest near middle; anterior margin somewhat rounded, lateral margins strongly rounded in anterior 1/3, somewhat parallel in posterior 1/3, posterior angles somewhat right-angled, posterior margin weakly sinuate; pronotal base with shallow median pits and transverse impression, lateral pits distinct; punctures of surface inconspicuous; hairs short and sparse (Fig. 1B). Elytra slightly wider than pronotum, distinctly longer than wide, widest near middle; lateral margins and posterior margin relatively rounded; punctures of surface inconspicuous; hairs short and sparse; each elytron with distinct humeral denticle (Fig. 1A, B). Hind wings well-developed. Metaventrite with shallow longitudinal impression (Fig. 1E). Legs moderately long and

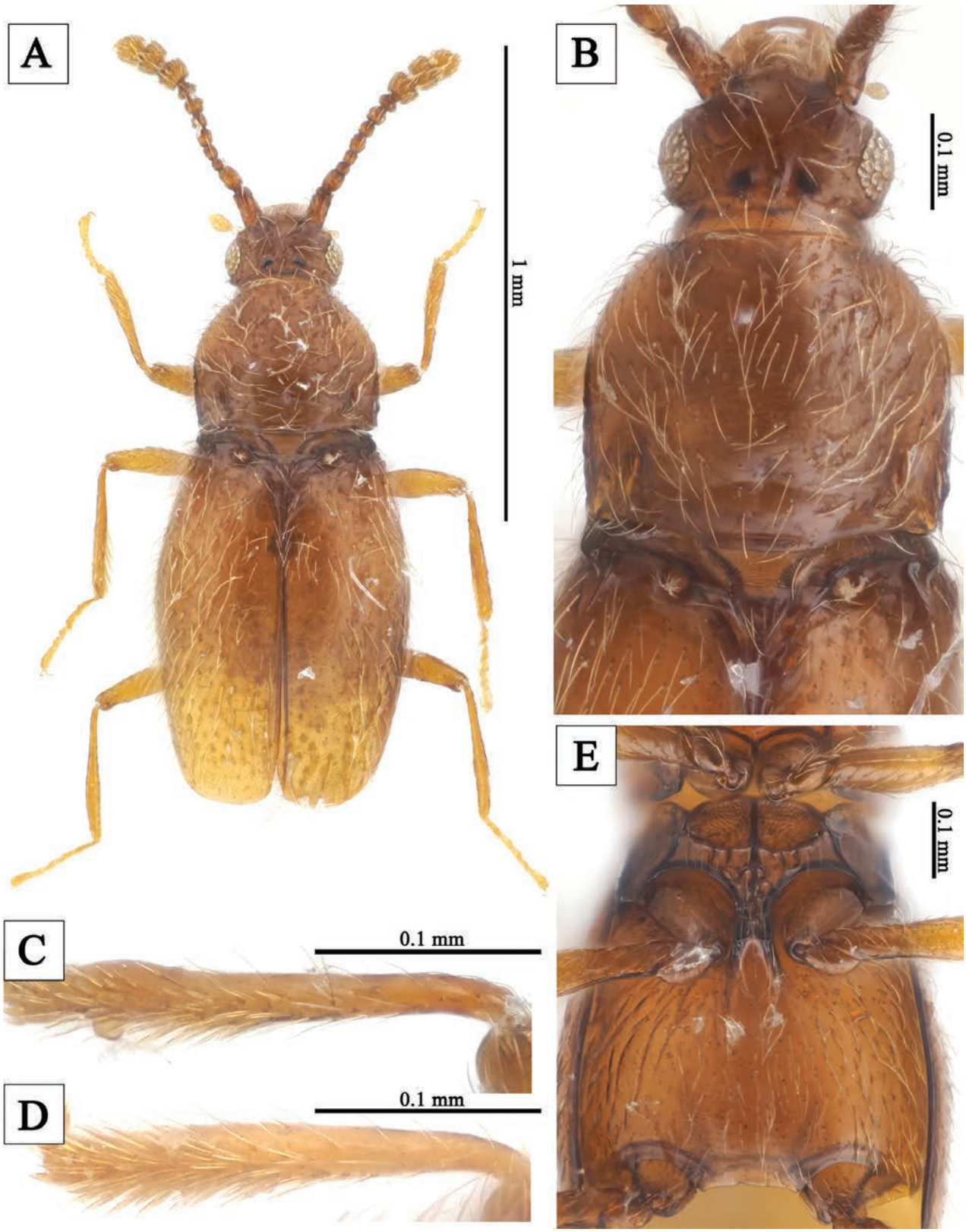

Figure 1. *Veraphis odaesanensis* sp. nov. **A** male habitus, dorsal view **B** male head and pronotum, dorsal view **C** male protibia **D** female protibia **E** meso-, metaventrite.

slender. Protibiae with small subapical pin-like projection (Fig. 1C). Aedeagus (Fig. 3A–D) strongly elongated and symmetrical, length 0.24 mm. In ventral view, lateral margins of median lobe somewhat parallel, middle of apex weakly

protruding, with small shallow punctures in subapical region in ventral view; in lateral view, slightly curved near base and subapical region with strong ventral indentation. Endophallus symmetrical, U-shaped. Parameres slender, reaching middle of median lobe; each paramere with two short apical setae and one subapical seta.

Sexual dimorphism. Protibiae without subapical pin-like projection (Fig. 1D).

Distribution. South Korea (Fig. 4).

Etymology. The specific epithet is an adjective derived from the type locality 'Mt. Odae'.

Habitat. This species was collected from relatively high-altitude mountains in South Korea, at elevations above 800 m. It was frequently captured using flight intercept traps, indicating its ability to fly with well-developed wings. Additionally, it was also collected from soil and leaf litter.

Remarks. *Veraphis odaesanensis* can be classified within the *japonicus* species group based on the characteristics of the male leg, antennae, and aedeagus (Jałoszyński and Hoshina 2005). This species shows clear differences in the aedeagus from the Japanese species. In China, it shares a similar aedeagus with *V. assingi* Jałoszyński, but the apex of the median lobe is more pointed, and there are significant differences in the morphology of the endophallus and the median lobe in lateral view.

***Veraphis myeonggiensis* sp. nov.**

https://zoobank.org/352AF5C9-41F3-43D4-8835-2A12E1807574

Figs 2, 3E–H, 4

Type material designated. ***Holotype*** • ♂ NIBR: "**Korea:** Gyeonggi Prov. Mt. Myeonggi, 520, Nonnamgi-gil, Buk-myeon, Gapyeong-gun, 5.X.2023, 37°58'12.2"N, 127°24'18.7"E, 402 m, sifting leaf litter & soil, J.-W. Kang, J.-I. Shin".

Diagnosis. Vertex with two shallow longitudinal grooves extending from posterior margin to posterior 1/2; area between grooves relatively flattened and impressed (Fig. 2B). Protibiae of male with small subapical pin-like projection (Fig. 2C). Metaventrite with shallow longitudinal impression (Fig. 2D). Aedeagus (Fig. 3E–H) strongly elongated and symmetrical, length 0.23 mm. In ventral view, median lobe gradually widening from base to apical 1/4, widest at apical 1/4, then slightly narrowing; sides from base to middle somewhat parallel; apex rounded; in lateral view, slightly curved near base and subapical region with strong ventral indentation. Endophallus symmetrical, structure complex. Parameres slender, reaching middle of median lobe; each paramere with two short apical setae and one subapical seta.

Male description. Body length 1.14 mm; reddish-brown, appendages lighter; flattened and elongated; surface covered yellow hairs (Fig. 2A). Head wider than long, widest across eyes; punctures of surface inconspicuous; hairs short and sparse (Fig. 2B). Temples nearly 1/4 length of eyes (Fig. 2B). Vertex with small pits on medioposterior margin; two shallow longitudinal grooves extending from posterior margin to posterior 1/2 present; area between grooves relatively flattened and impressed (Fig. 2B). Antennae with distinct distal three-segmented club; antennomere 1 strongly elongate, 2 elongate but less so than 1, 3 slightly wider than long, 4–6 as long as wide, 5 slightly larger than 4, 6 slightly

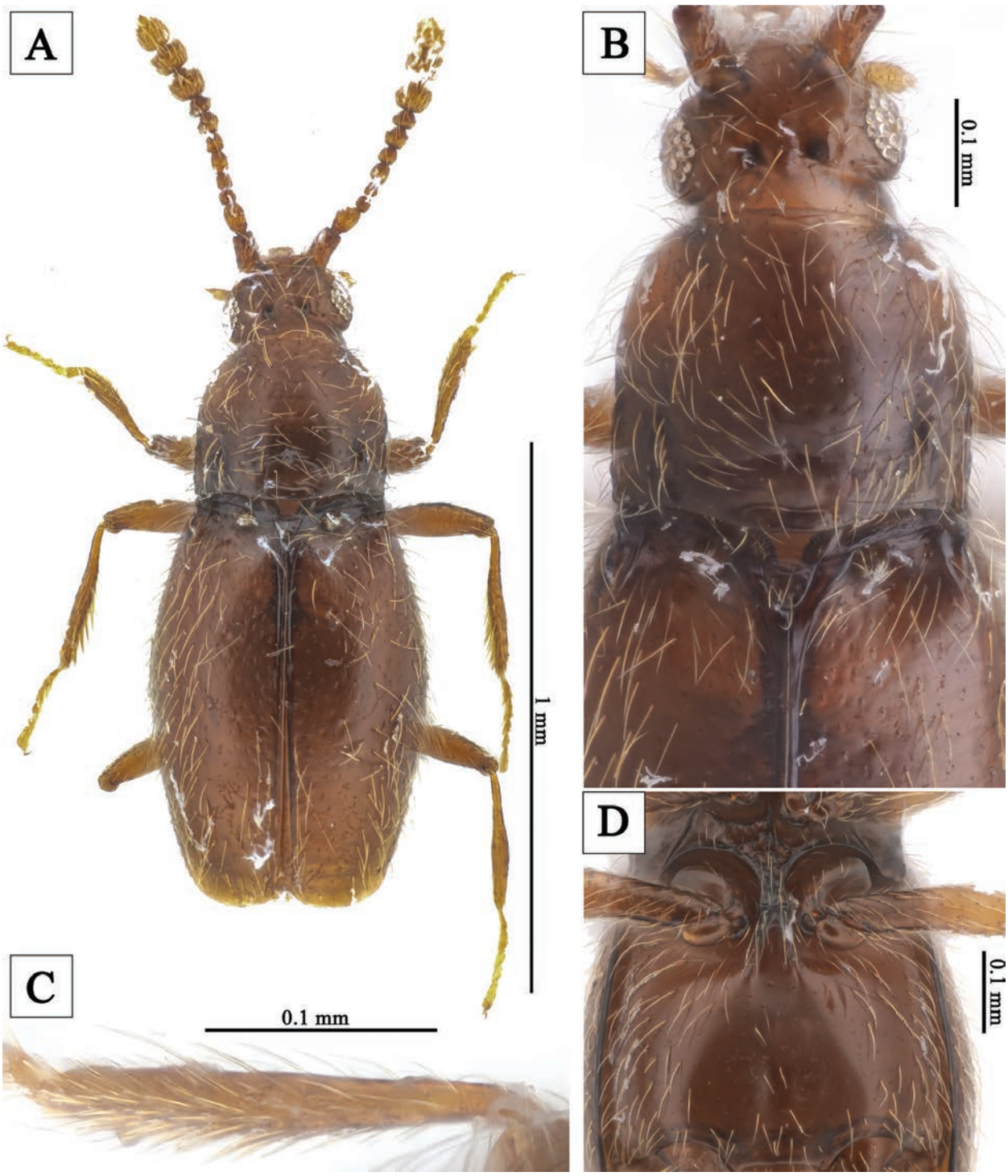

Figure 2. *Veraphis myeonggiensis* sp. nov. **A** male habitus, dorsal view **B** male head and pronotum, dorsal view **C** male protibia **D** meso-, metaventrite.

smaller than 5, 7 subpentagonal, 8 distinctly wider than long, 9–11 forming a club (Fig. 2A). Pronotum distinctly wider than head, as long as wide, widest near middle; anterior margin somewhat rounded, lateral margins strongly rounded in anterior 1/3, somewhat parallel in posterior 1/3, posterior angles somewhat right-angled, posterior margin weakly sinuate; pronotal base with shallow median pits and transverse impression, lateral pits distinct; punctures

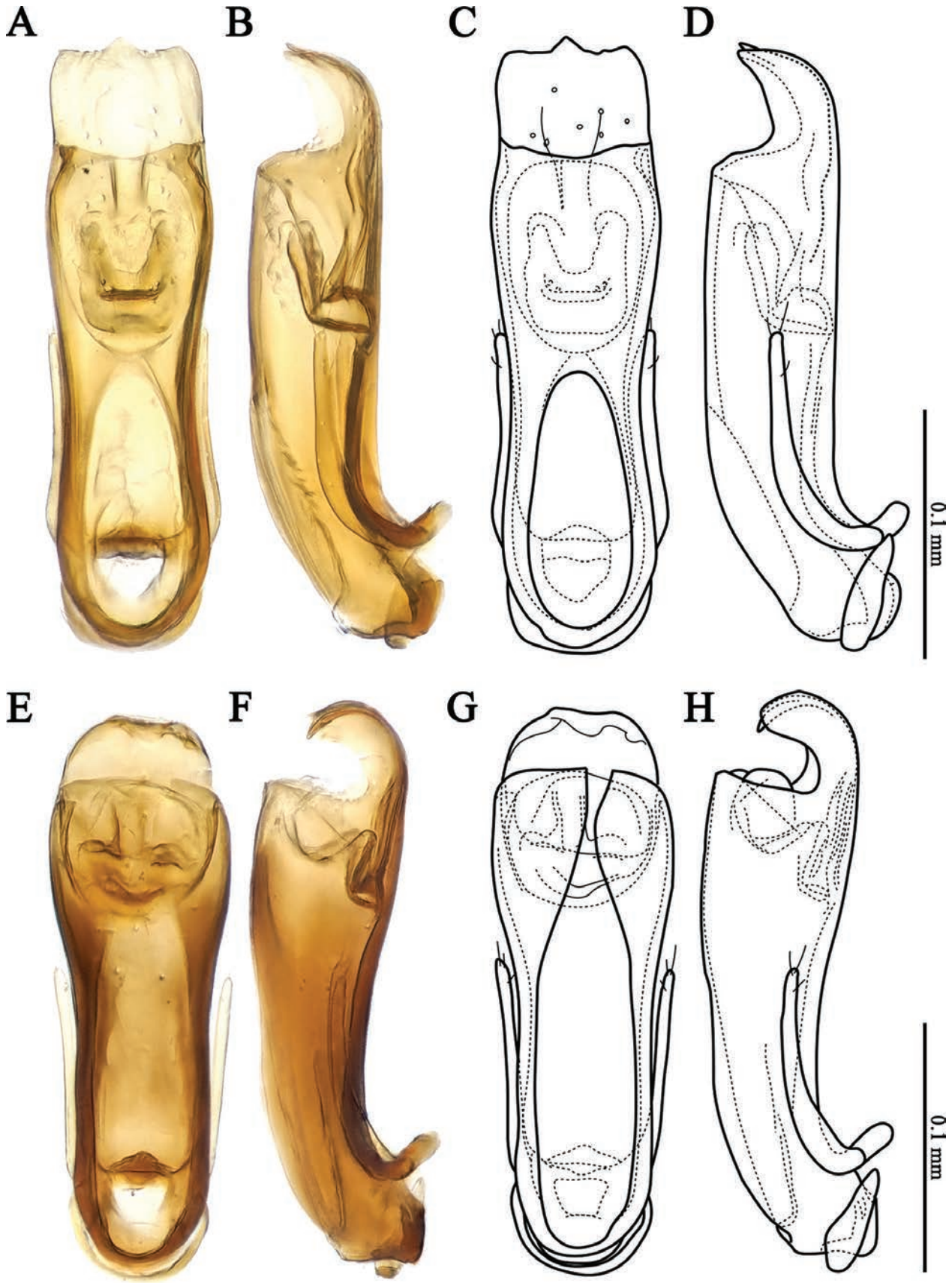

Figure 3. Aedeagus of *Veraphis odaesanensis* sp. nov. (**A–D**) and *V. myeonggiensis* sp. nov. (**E–H**) **A, C, E, G** ventral view **B, D, F, H** lateral view.

of surface inconspicuous; hairs short and sparse (Fig. 2B). Elytra slightly wider than pronotum, distinctly longer than wide, widest near middle; lateral margins and posterior margin relatively rounded; punctures of surface inconspicuous; hairs short and sparse; each elytron with distinct humeral denticle (Fig. 2A, B). Hind wings well-developed. Metaventrite with shallow longitudinal impression (Fig. 2D). Legs moderately long and slender. Protibiae with small subapical pin-like projection (Fig. 2C). Aedeagus (Fig. 3E–H) strongly elongated and symmetrical, length 0.23 mm. In ventral view, median lobe gradually widening from base to apical 1/4, widest at apical 1/4, then slightly narrowing; sides from base to middle somewhat parallel; apex rounded; in lateral view, slightly curved near base and subapical region with strong ventral indentation. Endophallus symmetrical, complex structured. Parameres slender, reaching middle of median lobe; each paramere with two short apical setae and one subapical seta.

Sexual dimorphism. Unknown.

Distribution. South Korea (Fig. 4).

Etymology. The specific epithet is an adjective derived from the type locality 'Mt. Myeonggi'.

Habitat. This species was collected from soil and leaf litter in mixed forest at relatively low altitudes, unlike other previously known species.

Remarks. *Veraphis myeonggiensis* can be classified within the *japonicus* species group based on the characteristics of the male leg, antennae, and aedeagus (Jałoszyński and Hoshina 2005). The aedeagus of this species is similar to that of *V. tottoriensis* Jałoszyński & Hoshina from Japan. However,

Figure 4. Distribution map.

the apex of the median lobe is more strongly curved ventrally, and the central structure of the endophallus is absent. Additionally, the parameres are slightly shorter. It also shares a similar aedeagus with *V. modestus* Jałoszyński but differs in the apex of the median lobe and the structure of the endophallus. Moreover, the overall morphology in lateral view is clearly distinct. Also, this species is externally very similar to *E. odaesanensis*, but it is smaller in size and clearly differed in the aedeagus.

Acknowledgments

We thank the CBNUIC members who joined us in the field to collect specimens for this study.

Additional information

Conflict of interest

The authors have declared that no competing interests exist.

Ethical statement

No ethical statement was reported.

Funding

This work was supported by a grant from the National Institute of Biological Resources (NIBR), funded by the Ministry of Environment (MOE) of South Korea (NIBR202304105) and the National Research Foundation of Korea (NRF) grant funded by the Korean government (MSIT) (RS-2024-00334183).

Author contributions

Supervision: JSP. Visualization: UJB. Writing – original draft: UJB. Writing – review & editing: JSP.

Author ORCIDs

Ui-Joung Byeon https://orcid.org/0009-0000-0512-2312
Jong-Seok Park https://orcid.org/0000-0003-2063-2534

Data availability

All of the data that support the findings of this study are available in the main text.

References

Casey TL (1897) Coleopterological notices. VII. Annals of the New York Academy of Sciences 9(1): 285–684. https://doi.org/10.1111/j.1749-6632.1896.tb55435.x

Franz H (1971) Untersuchungen über die paläarktischen Arten der Gattungen *Euthia* Steph. und *Veraphis* Casey (Col. Scydmaenidae). Eos, Revista Española de Entomología 46: 57–83.

Hisamatsu S (1985) Notes on some Japanese Coleoptera, I. Transactions of the Shikoku Entomological Society 17: 5–13.

Jałoszyński P (2009) Two new species of *Veraphis* Casey from China (Coleoptera, Scydmaenidae). Genus 20(1): 43–48.

Jałoszyński P (2012) Two new species of *Veraphis* Casey (Coleoptera, Staphylinidae, Scydmaeninae) from China. Zootaxa 3322(1): 63–68. https://doi.org/10.11646/zootaxa.3322.1.4

Jałoszyński P (2013) Three new species of Eutheiini (Coleoptera, Staphylinidae, Scydmaeninae) from China. Zootaxa 3609(5): 495–503. https://doi.org/10.11646/zootaxa.3609.5.5

Jałoszyński P (2014a) *Veraphis yoshitomii* sp. n. (Coleoptera, Staphylinidae, Scydmaeninae) from Japan. Zootaxa 3860(6): 589–595. https://doi.org/10.11646/zootaxa.3860.6.7

Jałoszyński P (2014b) Phylogeny of a new supertribe Cephenniitae with generic review of Eutheiini and description of a new tribe Marcepaniini (Coleoptera: Staphylinidae: Scydmaeninae). Systematic Entomology 39(1): 159–189. https://doi.org/10.1111/syen.12044

Jałoszyński P (2019) Four new species and new records of *Veraphis* Casey in Japan (Coleoptera, Staphylinidae, Scydmaeninae). Zootaxa 4701(1): 54–64. https://doi.org/10.11646/zootaxa.4701.1.4

Jałoszyński P (2024) Two new *Veraphis* species in China (Coleoptera, Staphylinidae, Scydmaeninae). Zootaxa 5507(1): 194–200. https://doi.org/10.11646/zootaxa.5507.1.11

Jałoszyński P, Hoshina H (2005) Revision of Palearctic species of *Veraphis* Casey (Coleoptera: Scydmaenidae). Entomological Reviews of Japan 60(2): 101–136.

Kurbatov SA (1995) Sur les Euthiini et Cephenniini (Coleoptera, Scydmaenidae) de l'extrême-est de la Russie et du Japon. Revue suisse de Zoologie 102(4): 943–960. https://doi.org/10.5962/bhl.part.80485

Kurbatov SA (2006) Description de quelques Scydménides et Psélaphines nouveaux russes (Coleoptera: Scydmaenidae et Staphylinidae, Pselaphinae). Russian Entomological Journal 15(1): 25–31.

LeConte JL (1879) The Coleoptera of the alpine Rocky Mountain regions. Part II. Bulletin of the United States Geological and Geographical Survey of the Territories 5(3): 331–520.

Newton A, Franz H (1998) World catalog of the genera of Scydmaenidae. Koleopterologische Rundschau 68: 137–165.

Sawada K (1962) Sur deux formes nouvelles des Cephenniini du Japan (Coléopt. Scydmaenidae). The Entomological Review of Japan 14(1): 19–20.

Shorthouse DP (2010) SimpleMappr, an online tool to produce publication-quality point maps. https://www.simplemappr.net/ [Accessed on 25.11.2024]

ZooKeys 1224: 175–186 (2025)
DOI: 10.3897/zookeys.1224.135572

Review Article

Two new species of the *Clubiona corticalis* group (Araneae, Clubionidae) from Yunnan, China

Minghao Guo[1], Zhaoyi Li[2,3], Feng Zhang[2,3]

1 *Hebei Vocational University of Industry and Technology, Shijiazhuang, Hebei 050091, China*
2 *Key Laboratory of Zoological Systematics and Application, College of Life Sciences, Hebei University, Baoding, Hebei 071002, China*
3 *Hebei Basic Science Center for Biotic Interaction, Hebei University, Baoding, Hebei 071002, China*
Corresponding author: Feng Zhang (dudu06042001@163.com)

Abstract

Two new species belonging to the *corticalis* group of the sac spider genus *Clubiona* Latreille, 1804 are described from both males and females: *Clubiona longyangensis* **sp. nov.** and *Clubiona multiprocessa* **sp. nov.** The two species are currently known to occur in Baoshan City and Dali Bai Autonomous Prefecture, Yunnan, China, respectively. Detailed descriptions, diagnoses, and photographs of the two species are provided.

Key words: Clubionids, diversity, sac spiders, taxonomy

Academic editor: Gergin Blagoev
Received: 26 August 2024
Accepted: 9 December 2024
Published: 28 January 2025

ZooBank: https://zoobank.org/45FAE35A-4E17-4D75-8FAF-B43A3390AC8A

Citation: Guo M, Li Z, Zhang F (2025) Two new species of the *Clubiona corticalis* group (Araneae, Clubionidae) from Yunnan, China. ZooKeys 1224: 175–186. https://doi.org/10.3897/zookeys.1224.135572

Introduction

The genus *Clubiona* Latreille, 1804 is widely known and distributed worldwide except for the polar regions (World Spider Catalog 2024). This genus comprises 79% of the total number of species of the family (528 of 665 described species) (WSC 2024). Due to the high species diversity of *Clubiona*, several infrageneric classifications have been proposed, and therefore *Clubiona* species have been assigned to a series of species groups and/or subgenera (e.g. Simon 1932; Dondale and Redner 1982; Deeleman-Reinhold 2001; Jäger and Dankittipakul 2010; Mikhailov 2012; Liu et al. 2016; Zhang et al. 2021; Wu et al. 2023).

There are at least 16 species groups of *Clubiona* discussed or frequently used in recent publications (Zhang et al. 2021). One of the most diverse groups is the *C. corticalis* group, which was first recognized by Simon (1932) and later by Mikhailov (1995), Deeleman-Reinhold (2001), and Yu and Li (2019). Until now, 86 *Clubiona* species have been assigned to the *C. corticalis* group, and they are mainly distributed in Eurasia and Australia (Zhang et al. 2021; Zhong et al. 2022; Li et al. 2023; Wu et al. 2023). Currently, 175 species of *Clubiona* have been recorded from China (WSC 2024), and 72 of them belong to the *corticalis* group (Zhang et al. 2021; Zhong et al. 2022; Li et al. 2023; Wu et al. 2023), making this group one of the most well-known clubionid groups in China.

While examining clubionid spiders collected from Yunnan Province, China, we encountered specimens of two undescribed species, *Clubiona longyangensis* sp. nov. and *Clubiona multiprocessa* sp. nov. These two species possess characters associated with the *corticalis*-group, but they can be easily distinguished from the other species in the group.

Materials and methods

All measurements are given in millimeters. Leg measurements are shown as: total length (femur, patella, tibia, metatarsus, tarsus). Eye diameters as AME, ALE, PME, PLE and interdistances as AME–AME, AME–ALE, PME–PME, PME–PLE. Epigynes were removed and cleared in a pancreatin solution and then transferred to 75% ethanol for images captured. Photographs were taken using Leica M205A and Olympus BX51 microscope. All photographs were imported into Helicon Focus v. 7 for stacking. Final figures were retouched using Adobe Photoshop 2020. All specimens examined were deposited in Museum of Hebei University, Baoding, China (**MHBU**). The following abbreviations are used:

A	atrium
AER	anterior eye row
ALE	anterior lateral eyes
AME	anterior median eyes
AME–ALE	distance between AME and ALE
AME–AME	distance between AMEs
B	bursa
C	conductor
CD	copulatory duct
CO	copulatory opening
E	embolus
FD	fertilisation duct
LTA	lateral tibial apophysis
MOA	median ocular area
PER	posterior eye row
PLE	posterior lateral eyes
PME	posterior median eyes
PME–PLE	distance between PME and PLE
PME–PME	distance between PMEs
PPA	prolateral patellar apophysis
RFA	retrolateral femoral apophysis
RPA	retrolateral patellar apophysis
RTA	retrolateral tibial apophysis
S	spermatheca
SA	spermathecal appendage
SB	spermathecal base
SH	spermathecal head
VTA	ventral tibial apophysis

Taxonomy

Clubiona corticalis group

Atalia Thorell, 1887: 54 (type species *Atalia concinna* Thorell, 1887).
Clubiona corticalis group: Simon 1932: 905; Mikhailov 1990: 142; Mikhailov 1995: 38, 42; Deeleman-Reinhold 2001: 90; Yu and Li 2019: 153.
Paraclubiona Lohmander, 1944: 19 (type species *Aranea corticalis* Walckenaer, 1802).

Diagnosis. See Mikhailov (1995), Deeleman-Reinhold (2001), and Yu and Li (2019).

Clubiona longyangensis sp. nov.

https://zoobank.org/E78D0880-A34C-404E-9D59-5B15FD1A75C6
Figs 1–3
Chinese name: 隆阳管巢蛛

Type material. ***Holotype*** • ♂ (CLU847-1); China: Yunnan Province, Baoshan City, Longyang District, Lujiang Town, Baihua Ling Village; 25.3016°N, 98.7994°E; 1669 m elev.; 24.XI.2017; leg. Zhaoyi Li. ***Paratypes*** • 3♂2♀ (CLU847-2–CLU847-6); same data as holotype.

Other material examined. 3♂1♀ (CLU845-1–CLU845-4); Baihua Ling Village; 25.2981°N, 98.7863°E; 1983 m elev.; 24.XI.2017; leg. Zhaoyi Li.

Etymology. The specific name is derived from the type locality; an adjective.

Diagnosis. Among the species of the *Clubiona corticalis* group, the male (Fig. 2) of this new species resembles *C. multiprocessa* sp. nov. (Fig. 5) by having a long (more than 1/2 of femur length), finger-shaped RFA (vs RFA absent or, if present, not finger-shaped in all other species in the grouper; e.g. tongue-shaped in *C. lamellaris* as shown by Zhang et al. 2018: figs 3C, 4C). However, the new species can be distinguished by the following: (1) VTA triangular, apex sharp (Fig. 2B, C) (vs papilliform; Fig. 5A, C); (2) LTA shaped like an inverted trapezoid, distal tip truncated in retrolateral view (Fig. 2C) (vs ridge-like; Fig. 5C); (3) conductor extends at a 45° angle towards the base of the embolus (Fig. 2A) (vs extends in a more or less 7-shaped; Fig. 5A); (4) embolus claw-shaped, with a curved apex in ventral view (Fig. 2A) (vs shaped like an equicrural triangle, embolic tip not curved; Fig. 5A). The female is similar to *C. falciforma* Liu, Peng & Yan, 2016 (Liu et al. 2016: 567, figs 30, 31, 35, 36) in the general shape of vulva (Fig. 3), but the new species can be distinguished by the following: (1) atrium umbelliform, with arched hood (vs elliptical and hood lacking); (2) bursae spherical (vs elongate-oval).

Description. Male (holotype) (Fig. 1A, B): total length 4.50. Carapace 2.14 long, 1.52 wide; abdomen 2.36 long, 1.24 wide. Carapace yellowish brown, narrowed in pars cephalica, widest between coxae II and III, clothed with short fine hairs along the ridge of the thoracic region, forming a V-shaped region. Fovea longitudinal. AER slightly recurved, PER wider than AER, almost straight in dorsal view. Eye sizes and interdistances: AME 0.06, ALE 0.10, PME 0.08, PLE 0.10;

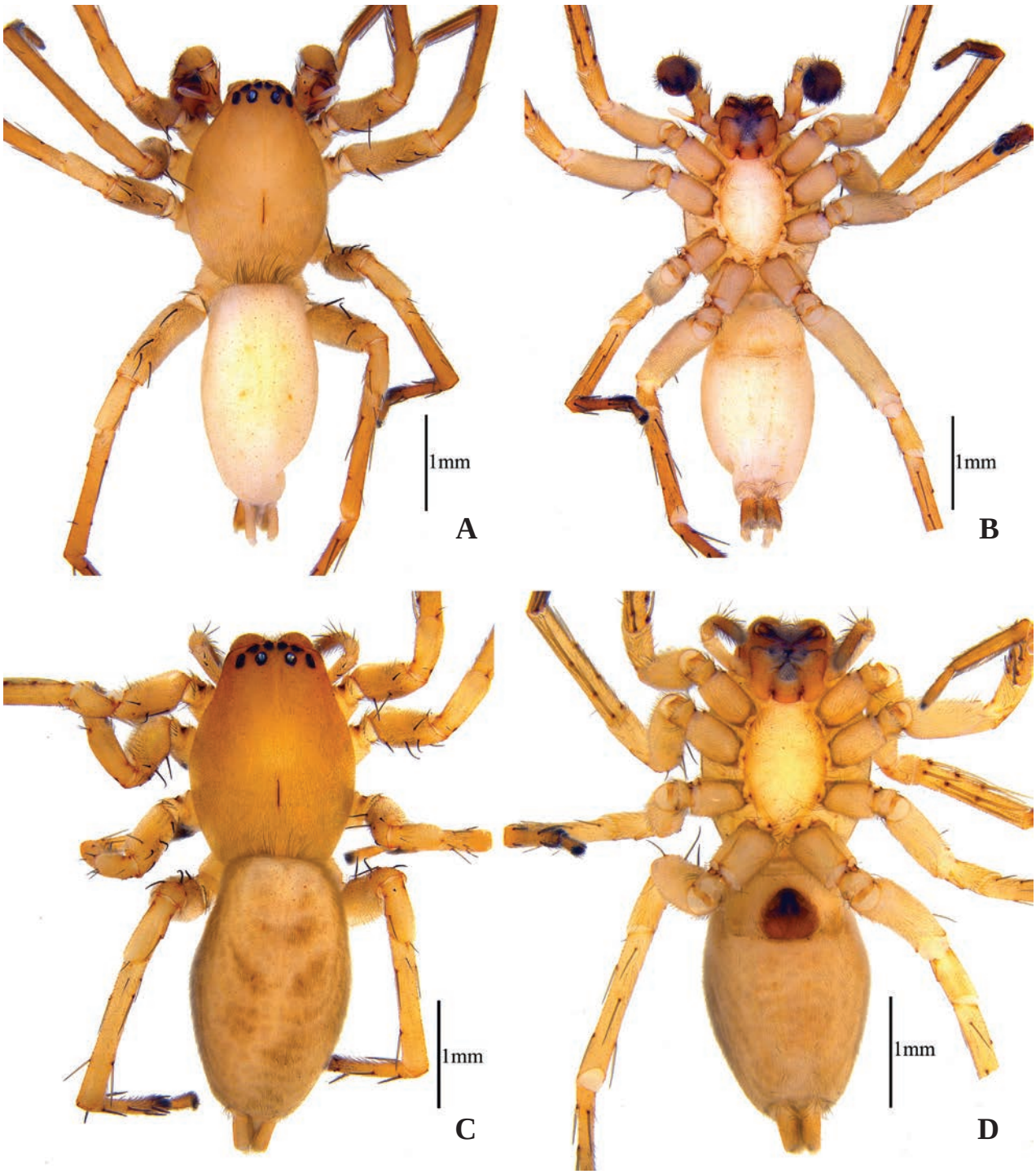

Figure 1. Habitus of *Clubiona longyangensis* sp. nov. **A** male (holotype), dorsal view **B** same, ventral view **C** female (paratype), dorsal view **D** same, ventral view.

AME–AME 0.05, AME–ALE 0.03, PME–PME 0.17, PME–PLE 0.11. MOA 0.28 long, front width 0.21, back width 0.36. Chelicerae reddish brown, with seven promarginal and five retromarginal teeth, with dense scopula in both margins. Clypeus height 0.05. Sternum light orange, 1.14 long, 0.71 wide. Labium and endites coloured as chelicerae, anterior edge with dark scopula, longer than wide. Legs yellowish brown, without distinct colour markings. Leg measurements: I 4.17 (1.13, 0.62, 1.35, 0.62, 0.45), II 4.24 (1.19, 0.63, 1.45, 0.52, 0.45), III 3.58

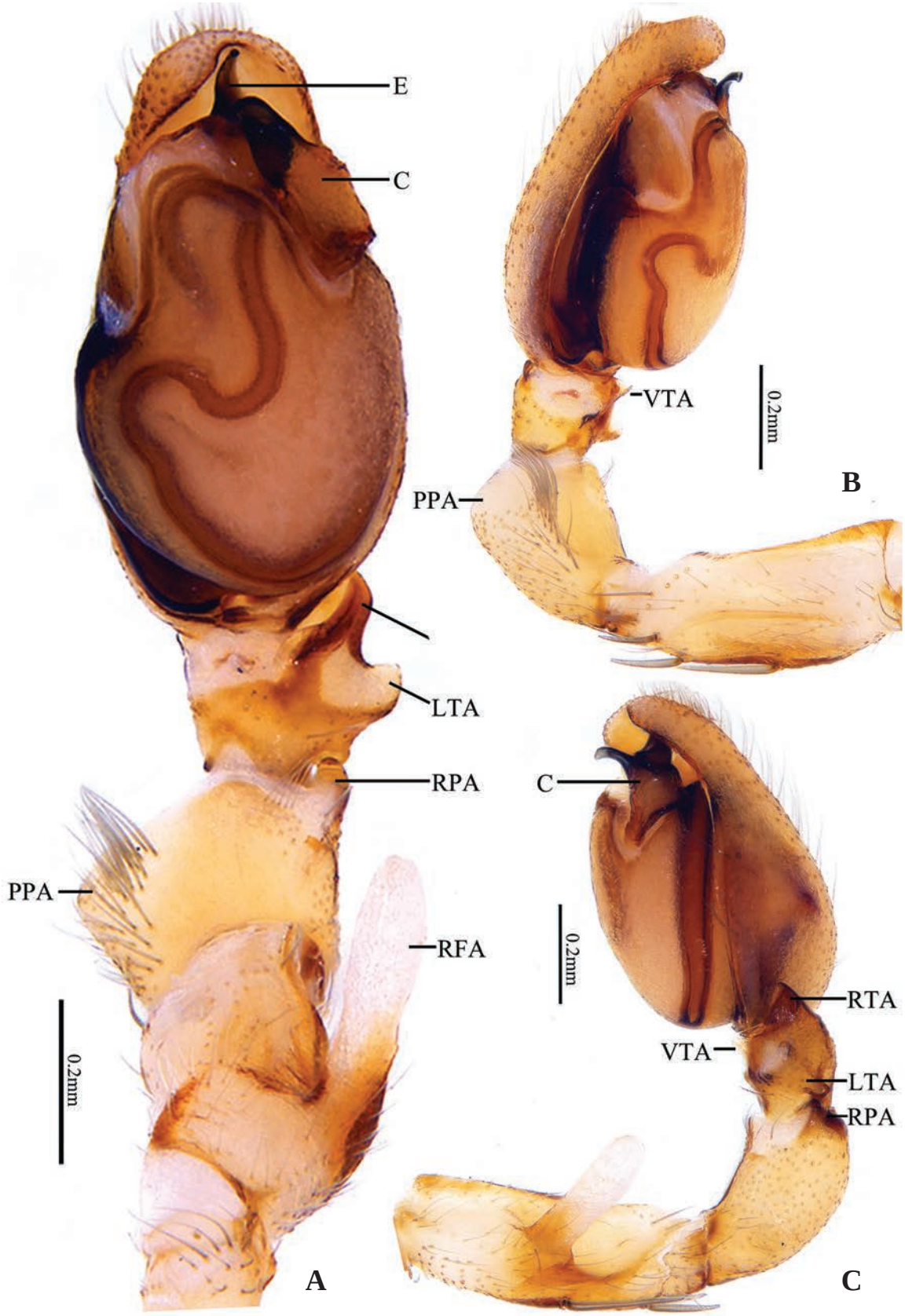

Figure 2. *Clubiona longyangensis* sp. nov., holotype male **A** left palp, ventral view **B** same, prolateral view **C** same, retrolateral view. Abbreviations: C = conductor; E = embolus; LTA = lateral tibial apophysis; PPA = prolateral patellar apophysis; RFA = retrolateral femoral apophysis; RPA = retrolateral patellar apophysis; RTA = retrolateral tibial apophysis; VTA = ventral tibial apophysis.

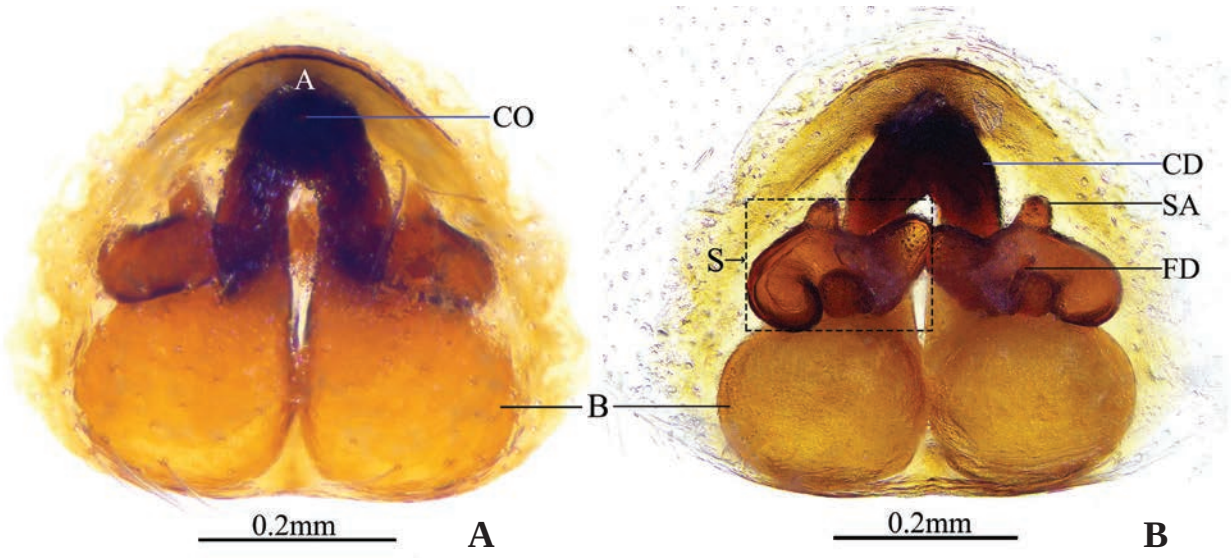

Figure 3. *Clubiona longyangensis* sp. nov., paratype female **A** epigyne, ventral view **B** vulva, dorsal view. Abbreviations: A = atrium; B = bursa; CD = copulatory duct; CO = copulatory opening; FD = fertilisation duct; S = spermatheca; SA = spermathecal appendage.

(1.01, 0.59, 1.02, 0.57, 0.39), IV 4.32 (1.25, 0.59, 1.49, 0.53, 0.46). Abdomen elongate-oval, dorsum pale yellow, with conspicuous anterior tufts of hairs, and two pairs of inconspicuous muscular depressions; venter pale yellow, with numerous yellowish spots.

Palp (Fig. 2). Femur retrolaterally with a slanting finger-like apophysis (RFA), more than 1/2 of femur's length. RFA partly membranous, arising mesially from femur, directing retrolatero-dorsally. Patella approximately twice as long as the tibia, with two apophyses: PPA large, broad, and blunt, located medially, represented by an enlarged tubercle; RPA short, almost thumb-shaped in ventral view, more or less inverted V-shaped in retrolateral view, located distally. Tibia short, with three apophyses: RTA short, with beak-shaped tip in ventral view, broad, flat, nearly triangular in retrolateral view, apex sclerotized; VTA short and membranous, almost triangular in lateral view; LTA shaped like an inverted trapezoid, distal tip truncated in retrolateral view. Cymbium almost 1.8 × longer than wide. Tegulum elongated oval, ca 1.6 × longer than wide; subtegulum visible prolaterally. Sperm duct long and sinuated, running an irregular course in the prolateral part of the tegulum. Embolus (E) originating at distal portion of tegulum, claw-shaped, apex curved ventrally. Conductor (C) large, originating from retrolateral side of tegulum, about 2 o'clock position, widest in the mid part, terminal part heavily sclerotized, beak-shaped, apex directing prolaterally.

Female (paratype) (Fig. 1C, D): one specimen body length 4.39. Carapace 2.10 long, 1.55 wide; abdomen 2.29 long, 1.53 wide. Carapace reddish brown, clothed with short fine hairs. Eye sizes and interdistances: AME 0.08, ALE 0.12, PME 0.09, PLE 0.10; AME–AME 0.06, AME–ALE 0.06, PME–PME 0.19, PME–PLE 0.15. MOA 0.30 long, front width 0.23, back width 0.39. Clypeus height 0.04. Sternum 1.24 long, 0.74 wide. Chelicerae, labium, and endites coloured as carapace. Leg measurements: I 3.76 (1.24, 0.41, 1.16, 0.56, 0.39), II 3.92 (1.20, 0.49, 1.12, 0.65, 0.46), III 3.47 (1.26, 0.47, 0.92, 0.56, 0.26), IV 4.15 (1.45, 0.58, 1.07, 0.68, 0.37). Abdomen oval, dorsum yellowish brown, with numerous, short fine hairs and two pairs of inconspicuous muscular depressions.

Epigyne (Fig. 3). Epigynal plate slightly longer than wide. Atrium (A) distinctly large, umbelliform, with a delimited, arched anterior margin (hood) and nearly invisble postterior margin, located at anterior portion of epigynal plate. Copulatory openings (CO) indistinct, tiny, located centrally in atrium. Copulatory ducts (CD), heavily sclerotised, relatively long and thick, ca 1/2 length of epigynal plate, descend obliquely, forming a ∧-shaped course. Spermathecae (S) longer laterally juxtaposed at the tip represented by two ∼-shaped tubes, anterior surface with a papilliform spermathecal appendage (SA), respectively. Fertilisation ducts (FD) acicular, located terminally on spermathecae. Bursae (B) close together, spherical, weakly sclerotized, surface smooth.

Distribution. Presently known only from Yunnan, China.

***Clubiona multiprocessa* sp. nov.**

https://zoobank.org/86311755-A356-458D-8AA8-672B437D6514

Figs 4–6

Chinese name: 多突管巢蛛

Type material. ***Holotype*** • ♂ (CLU1440-1), China: Yunnan Province, Dali Bai Autonomous Prefecture, Cang Shan; 2500 m elev.; 11.IX.2011; leg. Qiuju Wei. ***Paratypes*** • 2♂4♀ (CLU1440-2–CLU1440-7); same data as holotype.

Other material examined. • 1♂9♀ (CLU1439-1–CLU1439-10), Cang Shan, 2500 m elev.; 11.VIII.2008; leg. Tingbang Yang • 1♂7♀ (CLU1441-1–CLU1441-8); Cang Shan; 2600 m elev.; 9.VIII.2011; leg. Qiuju Wei.

Etymology. The specific name comes from the combination of "multi-" and "processus", referring to the multiple (six) apophysis on the male palp; an adjective.

Diagnosis. The male of *C. multiprocessa* sp. nov. can be distinguished from all other members of the *C. corticalis* group except for *C. longyangensis* sp. nov. (Fig. 2). Refer to the detailed diagnosis above for the similarities and differences between the two. The females of the new species (Fig. 6) resembles *C. applanata* Liu, Yan, Griswold & Ubick, 2007 (Liu et al. 2007: 64, figs 1, 2), *C. dichotoma* Wang, Chen & Zhang, 2018 (Wang et al. 2018: 319, figs 2C, D, 3F, G), *C. subapplanata* Wang, Chen, Zhang, 2018 (Wang et al. 2018: 327, figs 14C, D, 15E, F), and *C. lamellaris* Zhang, Yu, Zhong, 2018 (Zhang et al. 2018: 396, figs 3F, G, 4D, E) in the general shape of vulva, but the new species can be distinguished by the following: (1) epigynal plate wider than long (vs longer than wide in the other four species); (2) anterior surface of spermathecae with a papilliform appendage (vs absent in the other four species).

Description. Male (holotype) (Fig. 4A, B): total length 3.34. Carapace 1.67 long, 1.21 wide; abdomen 1.67 long, 0.98 wide. Carapace uniformly orange-yellow, with indistinct radial striae. Fovea longitudinal, dark. AER slightly recurved, PER wider than AER, almost straight in dorsal view. Eye sizes and interdistances: AME 0.07, ALE 0.10, PME 0.08, PLE 0.11; AME–AME 0.03, AME–ALE 0.01, PME–PME 0.14, PME–PLE 0.10. MOA 0.26 long, front width 0.18, back width 0.31. Chelicerae yellow-brown, with four promarginal and five retromarginal teeth, with dense scopula in both margins. Clypeus height 0.02. Sternum pale yellow, 0.95 long, 0.63 wide. Labium coloured as chelicerae, anterior edge with dark scopula. Endites reddish brown. Legs pale yellow, tibia, metatarsus, and tarsus slightly darker in colour. Leg measurements: I 3.15 (0.85, 0.48, 0.72, 0.69, 0.41), II 3.69

Figure 4. Habitus of *Clubiona multiprocessa* sp. nov. **A** male (holotype), dorsal view **B** same, ventral view **C** female (paratype), dorsal view **D** same, ventral view.

(0.95, 0.45, 1.08, 0.78, 0.43), III 3.06 (1.07, 0.32, 0.64, 0.68, 0.35), IV 4.48 (1.46, 0.45, 0.84, 1.22, 0.51). Abdomen elongate-oval, dorsum yellowish brown, with conspicuous anterior tufts of hairs and many scattered darker spots.

Palp (Fig. 5). Femur with a slanting finger-like retrolateral apophysis (RFA), ca 3/4 of femur's length. RFA partly membranous, arising mesially from femur, directing retrolatero-dorsally. Patella with two apophyses: PPA broad and blunt, located medially, shaped like an equilateral triangle in ventral view; RPA short, ca 1/3 of patella's length, slightly curved at apex in ventral view, more or less inverted V-shaped in retrolateral view, located distally. Tibia slightly shorter than patella, with three apophyses: RTA short and blunt, ca 1/2 of tibia's length in

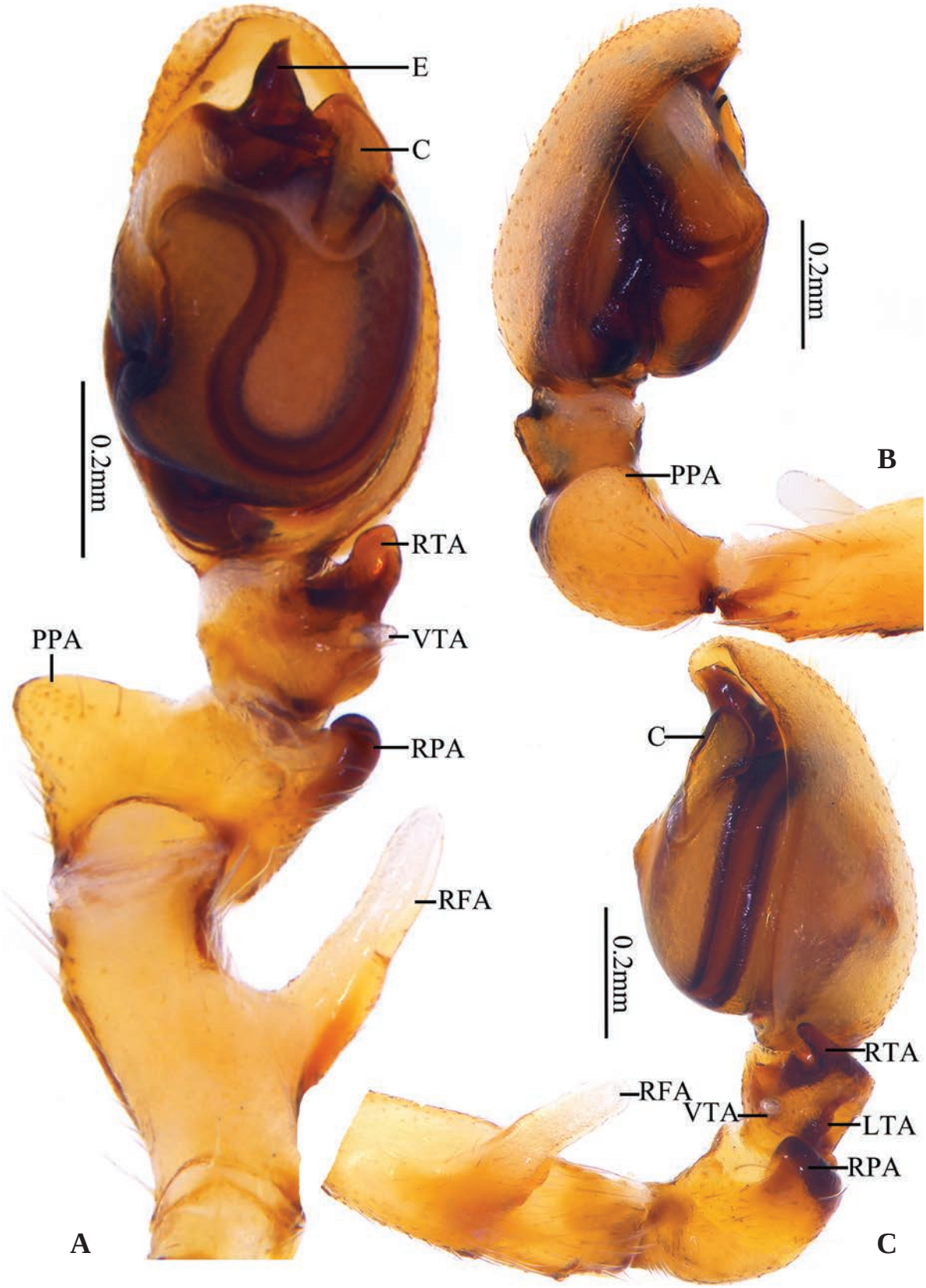

Figure 5. *Clubiona multiprocessa* sp. nov., holotype male **A** left palp, ventral view **B** same, prolateral view **C** same, retrolateral view. Abbreviations: C = conductor; E = embolus; LTA = lateral tibial apophysis; PPA = prolateral patellar apophysis; RFA = retrolateral femoral apophysis; RPA = retrolateral patellar apophysis; RTA = retrolateral tibial apophysis; VTA = ventral tibial apophysis.

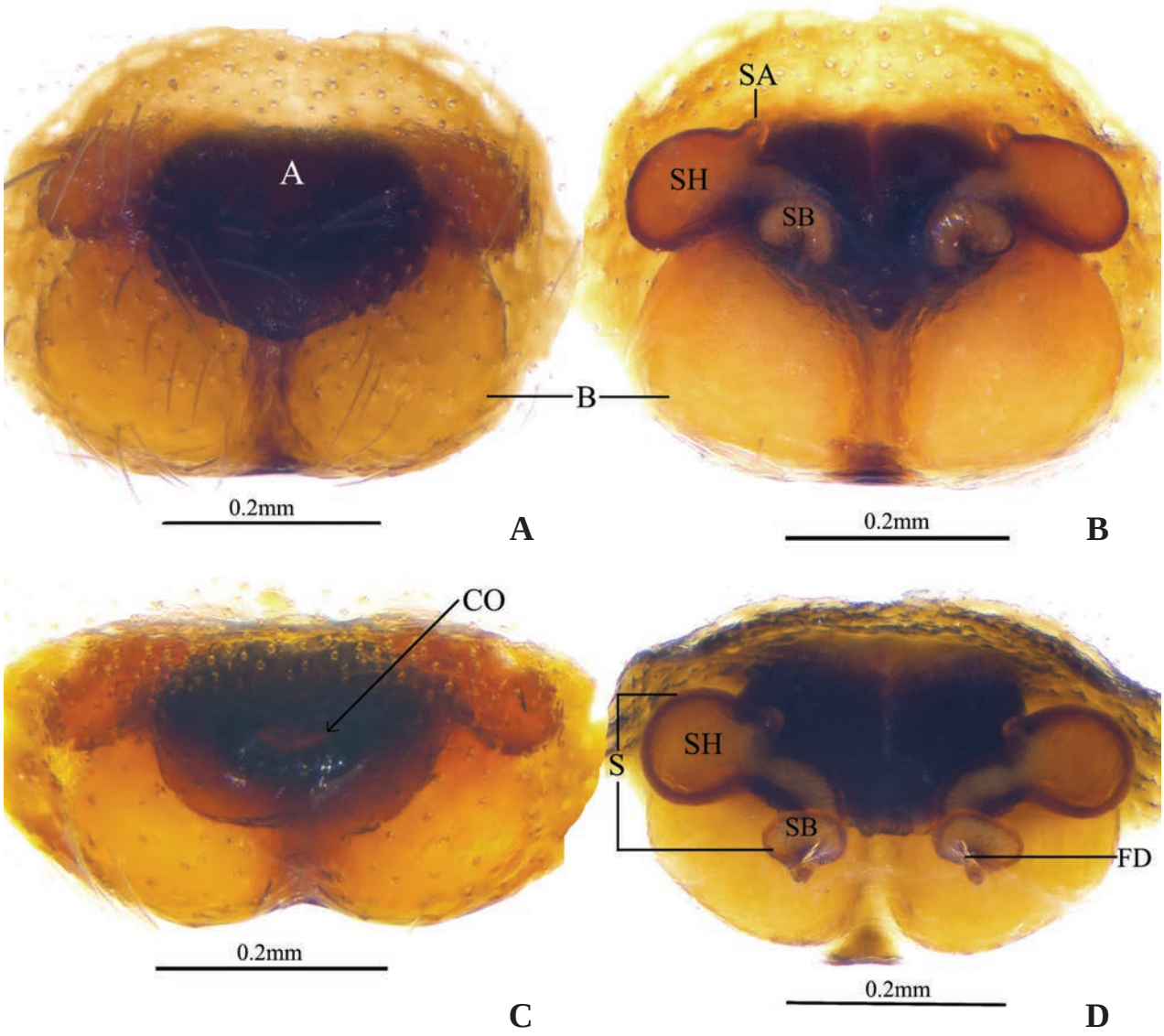

Figure 6. *Clubiona multiprocessa* sp. nov., paratype female **A** epigyne, ventral view **B** vulva, dorsal view **C** epigyne, anterior view **D** vulva, anterior view. Abbreviations: A = atrium; B = bursa; CO = copulatory opening; FD = fertilisation duct; S = spermatheca; SA = spermathecal appendage; SB = spermathecal base; SH = spermathecal head.

ventral view, broad, flat, and with blunt apex in retrolateral view; VTA papilliform, short and transparent; LTA ridge-like, near the base of tibia. Cymbium almost 1.6 × longer than wide. Tegulum elongated oval, ca 1.4 × longer than wide; subtegulum visible prolaterally. Sperm duct sinuate, nearly U-shaped in ventral view. Embolus (E) arising from distal portion of tegulum, shaped like an isosceles triangle in ventral view, broad at base, gradually tapering toward apex. Conductor (C) large, originating from retrolateral side of tegulum, about 2 o'clock position, approximately 7-shaped in ventral view, distal part gradually tapering, extended transversely to the base of embolus.

Female (paratype) (Fig. 4C, D): one specimen body length 3.75. Carapace 1.68 long, 1.33 wide; abdomen 2.07 long, 1.47 wide. Carapace orange, clothed with short fine hairs. Eye sizes and interdistances: AME 0.08, ALE 0.09, PME 0.09, PLE 0.09; AME–AME 0.05, AME–ALE 0.04, PME–PME 0.18, PME–PLE 0.11. MOA 0.26 long, front width 0.21, back width 0.37. Clypeus height 0.02. Sternum

1.01 long, 0.64 wide. Chelicerae, labium, and endites coloured as carapace. Leg measurements: I 3.29 (0.96, 0.51, 0.88, 0.54, 0.40), II 3.45 (0.94, 0.53, 0.96, 0.63, 0.39), III 3.03 (0.74, 0.33, 0.85, 0.73, 0.38), IV 4.42 (1.29, 0.59, 1.14, 1.06, 0.34). Abdomen oval, dorsum greyish white, with a narrow longitudinal band in middle.

Epigyne (Fig. 6). Epigynal plate slightly wider than long. Atrium (A) nearly heart-shaped, located at anterior portion of epigynal plate. Copulatory openings (CO) tiny, located centrally in atrium. Copulatory ducts (CD) invisible. Spermathecae (S) long, located at the anterior position of bursae, spermathecal heads (SH) ovate, with a papilliform spermathecal appendage (SA), spermathecal bases (SB) tubular, with small fertilisation ducts terminally (FD). Bursae (B) close together, nearly spherical, situated posteriorly.

Distribution. Presently known only from Yunnan, China.

Acknowledgements

We are grateful to the subject editor and reviewers for providing their comments on the manuscript. We thank Kun Yu (Hebei University) for assistance in photographing of copulatory organs of the new species.

Additional information

Conflict of interest

The authors have declared that no competing interests exist.

Ethical statement

No ethical statement was reported.

Funding

This work was supported by the National Natural Science Foundation of China (No. 32170468), and by the Science and Technology Fundamental Resources Investigation Program (Grant No. 2022FY202100).

Author contributions

Writing-original draft: Minghao Guo. Writing – review and editing: Minghao Guo, Zhaoyi Li, Feng Zhang.

Author ORCIDs

Zhaoyi Li https://orcid.org/0000-0001-6303-6041
Feng Zhang https://orcid.org/0000-0002-3347-1031

Data availability

All of the data that support the findings of this study are available in the main text.

References

Deeleman-Reinhold CL (2001) Forest spiders of South East Asia: with a revision of the sac and ground spiders (Araneae: Clubionidae, Corinnidae, Liocranidae, Gnaphosidae, Prodidomidae and Trochanterriidae). Brill, Leiden, 591 pp. https://doi.org/10.1163/9789004475588

Dondale CD, Redner JH (1982) The insects and arachnids of Canada, Part 9. The sac spiders of Canada and Alaska, Araneae: Clubionidae and Anyphaenidae. Research Branch Agriculture Canada Publication 1724: 1–194.

Jäger P, Dankittipakul P (2010) Clubionidae from Laos and Thailand (Arachnida: Araneae). Zootaxa 2730: 23–43. https://doi.org/10.11646/zootaxa.2730.1.2

Li LF, Liu P, Li B, Peng XJ (2023) Two new species of the sac-spider genus *Clubiona* Latreille, 1804 (Araneae, Clubionidae) and the female of *C. subcylindrata* from China. Zootaxa 5263 (4): 520–530. https://doi.org/10.11646/zootaxa.5263.4.3

Liu P, Yan HM, Griswold C, Ubick D (2007) Three new species of the genus *Clubiona* from China (Araneae: Clubionidae). Zootaxa 1456: 63–68. https://doi.org/10.11646/zootaxa.1456.1.3

Liu P, Peng XJ, Yan HM (2016) Five new species of the *Clubiona corticalis* species group (Araneae, Clubionidae) from China. Zootaxa 4184(3): 561–575. https://doi.org/10.11646/zootaxa.4184.3.10

Lohmander H (1944) Vorläufige Spinnennotisen. Arkiv för Zoologi 35(A, 16): 1–21.

Mikhailov KG (1990) The spider genus *Clubiona* Latreille 1804 in the Soviet Far East, 1 (Arachnida, Aranei, Clubionidae). Korean Arachnology 5: 139–175.

Mikhailov KG (1995) Erection of infrageneric groupings within the spider genus *Clubiona* Latreille, 1804 (Aranei Clubionidae): a typological approach. Arthropoda Selecta 4(2): 33–48.

Mikhailov KG (2012) Reassesment of the spider genus *Clubiona* (Aranei, Clubionidae). Vestnik Zoologii 46: 177–180. https://doi.org/10.2478/v10058-012-0015-z

Simon E (1932) Les arachnides de France. Tome VI. Synopsis générale et catalogue des espèces françaises de l'ordre des Araneae; 4e partie. Roret, Paris, 773–978.

Thorell T (1887) Viaggio di L. Fea in Birmania e regioni vicine. II. Primo saggio sui ragni birmani. Annali del Museo Civico di Storia Naturale di Genova 25: 5–417.

Wang LY, Chen HM, Wu PL, Zhang F, Zhang ZS (2018) Spider diversity in Fanjing Mountain Nature Reserve, Guizhou, China, II: Clubionidae (Araneae). Zoological Systematics 43(4): 317–333. https://doi.org/10.11865/zs.201827

World Spider Catalog (2024) World Spider Catalog. Version 25.5. Natural History Museum Bern. https://doi.org/10.24436/2 [Accessed on 24 August 2024]

Wu PL, Chen Y, Zhang F (2023) Three new species of the *Clubiona corticalis* group (Araneae, Clubionidae) from China. ZooKeys 1157: 163–176. https://doi.org/10.3897/zookeys.1157.99674

Yu H, Li SQ (2019) Eight new species of the genus *Clubiona* Latreille, 1804 from Xishuangbanna Rainforest, southwestern China (Araneae, Clubionidae). Zootaxa 4545(2): 151–178. https://doi.org/10.11646/zootaxa.4545.2.1

Zhang JS, Yu H, Zhong Y (2018) Two new species of the *Clubiona corticalis*-group from Guizhou Province, China (Araneae: Clubionidae). Zootaxa 4415(2): 393–400. https://doi.org/10.11646/zootaxa.4415.2.10

Zhang JS, Yu H, Li SQ (2021) Taxonomic studies on the sac spider genus *Clubiona* (Araneae, Clubionidae) from Xishuangbanna Rainforest, China. ZooKeys 1034: 1–163. https://doi.org/10.3897/zookeys.1034.59413

Zhong Y, Gong XS, Yu H (2022) A new species of the *Clubiona corticalis*-group (Araneae, Clubionidae) from Jiugong Mountains, Hubei Province, central China. Biodiversity Data Journal 10: e94735. https://doi.org/10.3897/BDJ.10.e94735

ZooKeys 1224: 187–209 (2025)
DOI: 10.3897/zookeys.1224.140549

Research Article

An integrative approach to a revision of the freshwater mussel genus *Songkhlanaia* (Bivalvia, Unionidae), with the description of a new species

Ekgachai Jeratthitikul[1], Chirasak Sutcharit[2], Pongpun Prasankok[3]

1 *Animal Systematics and Molecular Ecology Laboratory, Department of Biology, Faculty of Science, Mahidol University, Bangkok 10400, Thailand*
2 *Animal Systematics Research Unit, Department of Biology, Faculty of Science, Chulalongkorn University, Bangkok 10330, Thailand*
3 *School of Biology, Institute of Science, Suranaree University of Technology, Nakhon Ratchasima 30000, Thailand*
Corresponding author: Ekgachai Jeratthitikul (Ekgachai.jer@mahidol.ac.th)

Abstract

Mainland Southeast Asia, also known as Indochina, is recognized as a global biodiversity hotspot for freshwater mussels, hosting a significant number of species and exhibiting high levels of endemism. Recently, the monotypic genus *Songkhlanaia* was described from the Songkhla Lake Basin in southern Thailand. In this study, two additional lineages are revealed, *S. moreleti* **comb. nov.** and *S. songkhramensis* **sp. nov.**, from the Mekong Basin through an integrative taxonomic approach combining morphological characters and molecular phylogenetic analyses. The multi-locus phylogenetic inference supported the monophyly of the genus and further elucidated the sister relationship between *S. moreleti* and the new species, and with *S. tamodienica* positioned as a basal lineage. Pairwise uncorrected COI p-distances among these three species also supported the species validity and ranged from 4.2% to 8.24%. Notably, *S. songkhramensis* **sp. nov.** and *S. moreleti* exhibit similarities in shell morphology; however, the new species can be differentiated by more robust pseudocardinal teeth. Both species are distinguishable from *S. tamodienica* by their approximately twice larger size, more inflated shells, and more prominent, roughened, irregular growth lines on the shell surface. Furthermore, based on the current data, these three species are recognized as endemic and are restricted to disjunct biogeographic areas in Indochina: *S. tamodienica* in the Songkhla Lake Basin in southern Thailand, *S. moreleti* in the Tonle Sap and Lower Mekong basins, and *S. songkhramensis* **sp. nov.** in the Songkhram Basin and its nearby tributaries of the Middle Mekong Basin.

Key words: Freshwater mussels, Indochina, Mekong Basin, multi-locus phylogeny, new taxa, Pseudodontini, taxonomic revision, Thailand

Academic editor: Ruiqi Li
Received: 29 October 2024
Accepted: 26 December 2024
Published: 28 January 2025

ZooBank: https://zoobank.org/8F8AAC17-7284-46F8-A2B5-1BA03FDB54E1

Citation: Jeratthitikul E, Sutcharit C, Prasankok P (2025) An integrative approach to a revision of the freshwater mussel genus *Songkhlanaia* (Bivalvia, Unionidae), with the description of a new species. ZooKeys 1224: 187–209. https://doi.org/10.3897/zookeys.1224.140549

Introduction

Mainland Southeast Asia, also known as Indochina, is recognized as a world biodiversity hotspot for freshwater mussels (Unionoida), hosting a significant number of species and high levels of endemism (Graf and Cummings 2021), and thus has been hypothesized to be one of the origins for freshwater mussel radiation (Bolotov et al. 2017a). Indochina is characterized by its complex hydrological systems, which include at least three major freshwater catchments:

the Salween in the west, the Chao Phraya in the middle, and the Mekong in the east, alongside several tributary systems in the coastal areas (Abell et al. 2008). These catchments are critical for the distribution and diversity of freshwater mussels, as they provide a variety of ecological niches and facilitate the evolution of endemic species (Konopleva et al. 2019b; Bolotov et al. 2020, 2022).

Two families of freshwater mussels are reported from Indochina. The Margaritiferidae, which are represented by only two species, are distributed exclusively in the northern part of the region (Brandt 1974; Lopes-Lima et al. 2018). In contrast, the Unionidae exhibit a vast distribution range that encompasses the entire region, contributing to a notable richness in biodiversity with 144 species from 40 genera being recognized and approximately 80% of these species being considered endemic to this region (i.e., MUSSELp; Graf and Cummings 2024). Several of them have been recently described based on advancements in integrative taxonomy, combining morphological revisions, molecular data, and biogeographical history (Bolotov et al. 2017b, 2020; Konopleva et al. 2019b, 2021, 2023; Pfeiffer et al. 2021; Jeratthitikul et al. 2022, 2024; Jeratthitikul and Sutcharit 2023).

Recently, Konopleva et al. (2023) conducted a comprehensive phylogenetic investigation of the freshwater mussels in the Malay Peninsula Eastern Slope (southern Thailand), an area that has received less study compared to others, i.e., Chao Phraya and Mekong basins (Jeratthitikul et al. 2019a, 2019b, 2022; Konopleva et al. 2021; Pfeiffer et al. 2021). This study reveals several new taxa, including a monotypic genus, *Songkhlanaia* Konopleva et al., 2023, that was described based on a single specimen of the type species from Klong Tamod of the Songkhla Lake Basin (Konopleva et al. 2023: fig. 2c–h). The genus is characterized by a shell that is rectangular, rather compressed, posterior slope possessing distinct prominent folds, one pseudocardinal tooth on each valve, and lateral teeth absent (Konopleva et al. 2023). Apart from these conchological characteristics, the multi-locus phylogenetic analysis also revealed the genus as a distinct phylogenetic lineage, which is distantly related to other genera of the tribe Pseudodontini (Konopleva et al. 2023).

Songkhlanaia is considered to be restricted to the Songkhla Lake Basin (Bolotov et al. 2023; Konopleva et al. 2023), the largest lake in Thailand, which serves as an important ecological and economic resource for the surrounding communities (Cookey et al. 2016). However, the investigation of additional samples from the Mekong Basin, based on a combination of morphological characters and molecular phylogenetic analysis, has revealed two additional lineages within the genus. One of these coincides with a previously recognized species, while the other cannot be attributed to any known taxon; therefore, it is described herein as a new species. The diagnosis of the genus is also revised here to encompass the variation in shell morphology of the newly added species.

Material and methods

Specimen sampling

The animal use protocol in this study was approved by the Faculty of Science, Mahidol University Animal Care and Use Committee under approval number MUSC65-013-606 and MUSC66-016-646. Freshwater mussel specimens were collected by hand and euthanized at the collection site using the two-step

method outlined by the AVMA (2020). Live specimens were initially placed in a container with freshwater. Then 95% (v/v) ethanol was gradually added to the container, starting at a concentration of approximately 5% (v/v) until the foot and adductor muscles relaxed completely. The anesthetized specimens were moved to another container with 70% (v/v) ethanol for fixation. Small pieces of foot tissues were snipped, preserved in 95% (v/v) ethanol, and stored at -20 °C for subsequent DNA extraction. The remaining specimens were dissected into soft body parts and shells. The soft body parts were stored in 70% (v/v) ethanol and used in anatomical study. The shells were kept as dry specimens. All specimens, including the type series of the new taxon, were deposited into the Mahidol University Museum of Natural History, Department of Biology, Faculty of Science, Mahidol University, Bangkok, Thailand (**MUMNH**).

Morphological analysis

Species identification was based on shell characteristics following descriptions in the taxonomic literature (i.e., Crosse and Fischer 1876; Deshayes and Jullien 1876; Morlet 1884; Simpson 1914; Haas 1920, 1924, 1969; Konopleva et al. 2023) or by comparing with photographs of type series available on the online database of the Muséum national d'Histoire naturelle, Paris (**MNHN**; https://science.mnhn.fr). Various shell morphological characteristics were examined, including the outline, size, thickness, surface sculpture, shape and position of the umbo, hinge teeth structure, and muscle attachment scars. Shell dimensions were measured using a digital vernier caliper (±0.01 mm) for shell length, height, and width. Anatomical features of the soft body parts were also observed under a stereomicroscope.

Molecular analysis

Genomic DNA was extracted from foot tissues using the NucleoSpin Tissue Extraction Kit (Macherey-Nagel, Germany) and stored at -20 °C for subsequent analysis. Partial fragments of the mitochondrial cytochrome c oxidase subunit I (COI), mitochondrial large ribosomal subunit rRNA (16S rRNA), and nuclear 28S large ribosomal subunit rRNA (28S rRNA) genes were amplified using polymerase chain reaction (PCR) and employed as genetic markers for phylogenetic analyses and genetic distance calculations (COI only). PCR primers, cycling conditions, and DNA sequencing were conducted following protocols established in our previous studies (Jeratthitikul et al. 2024). All newly generated sequences were deposited in the GenBank nucleotide sequence database under accession numbers PQ231666–PQ231681, PQ764574, and PQ764575 for COI; PQ236701–PQ236716, PQ776233, and PQ776234 for 16S rRNA; and PQ236717–PQ236732, PQ764576, and PQ764577 for 28S rRNA.

Phylogenetic analysis

Phylogenetic trees were estimated using a concatenated dataset of the three aforementioned gene fragments generated from 70 mussel specimens (Suppl. material 1). The ingroup included 18 newly sequenced *Songkhlanaia* specimens from this study and the holotype of *Songkhlanaia tamodienica*, the type species

(Konopleva et al. 2023). The outgroup was selected from previously published sequences of phylogenetic studies in the Unionidae (Huang et al. 2013; Pfeiffer and Graf 2015; Zieritz et al. 2016, 2021b; Bolotov et al. 2017a, 2017b, 2020, 2023; Lopes-Lima et al. 2017; Froufe et al. 2020; Jeratthitikul et al. 2021b, 2022, 2024; Konopleva et al. 2021, 2023; Jeratthitikul and Sutcharit 2023). These included single representative specimens of all available Pseudodontini taxa from GenBank (in total 44 species/subspecies), with representative species from other more distantly related unionid tribes (Schepmaniini, Gonideini, and Lamprotulini).

Separate multiple alignments for each gene were performed by the MUSCLE algorithm using MEGA11 v. 11.0.13 (Tamura et al. 2021), and later all three gene alignments were joined into one concatenated data matrix. The final concatenated data set was partitioned into five partitions (3 codons of COI + 16S rRNA + 28S rRNA). The optimal nucleotide substitution model for each partition was identified using PartitionFinder2 v. 2.3.4 (Lanfear et al. 2017) under the corrected Akaike Information Criterion (AICc). The program suggested GTR+I+G as the best nucleotide substitution model for the first codon of COI, 16S rRNA, and 28S rRNA partitions; F81+I for the second codon of COI partition; and GTR+G for the third codon of COI partition. These nucleotide substitution models were used in the subsequent phylogenetic analyses.

Phylogenetic analyses were conducted using Maximum Likelihood (ML) and Bayesian Inference (BI) methods on the online CIPRES Science Gateway (Miller et al. 2010). ML analysis was performed using IQ-TREE v. 2.2.2.7 (Minh et al. 2020) with 10,000 ultrafast bootstrap replicates to assess node support (Hoang et al. 2018). Bayesian Inference was conducted using MrBayes v. 3.2.7 (Ronquist et al. 2012) with four Markov Chain Monte Carlo (MCMC) chains run simultaneously for 10,000,000 generations. Tree samples were taken every 1,000 generations. The initial 25% of samples were discarded as burn-in. The average effective sample size (ESS) from the MCMC analysis was > 200 for all parameters. The resulting phylogenetic trees were visualized and edited using FigTree v. 1.4.4 (http://tree.bio.ed.ac.uk/software/figtree/). Nodes with ultrafast bootstrap support values (BS) ≥ 95% and Bayesian posterior probabilities (BPP) ≥ 0.95 were considered well-supported (San Mauro and Agorreta 2010; Hoang et al. 2018).

Genetic distance analysis

Intraspecific and interspecific genetic distances were assessed using uncorrected p-distances calculated in MEGA11 v. 11.0.13 (Tamura et al. 2021) based on the mitochondrial COI gene dataset. The results are expressed as a percentage of the mean with standard deviation.

Results

Phylogenetic analysis and genetic distances

Sequencing the target gene fragments from 19 specimens of *Songkhlanaia* produced 660 bp of COI, 481 bp of 16S rRNA, and 763–764 bp of 28S rRNA. After concatenated alignment of these three genes with outgroups,

the final 1,959-bp matrix was generated and used for phylogenetic tree reconstruction. The ML and BI trees exhibited almost identical topologies; therefore, only the ML tree is depicted in Fig. 1. *Songkhlanaia* specimens form a single clade within the tribe Pseudodontini with significant supports for this relationship from both analyses (BS = 96%, BPP = 1). The genus is further divided into three strongly supported species-level clades (BS = 100%, BPP = 1), consisting of a clade of *S. tamodienica*, the type species of the genus, and two other novel clades recognized in this study. One clade,

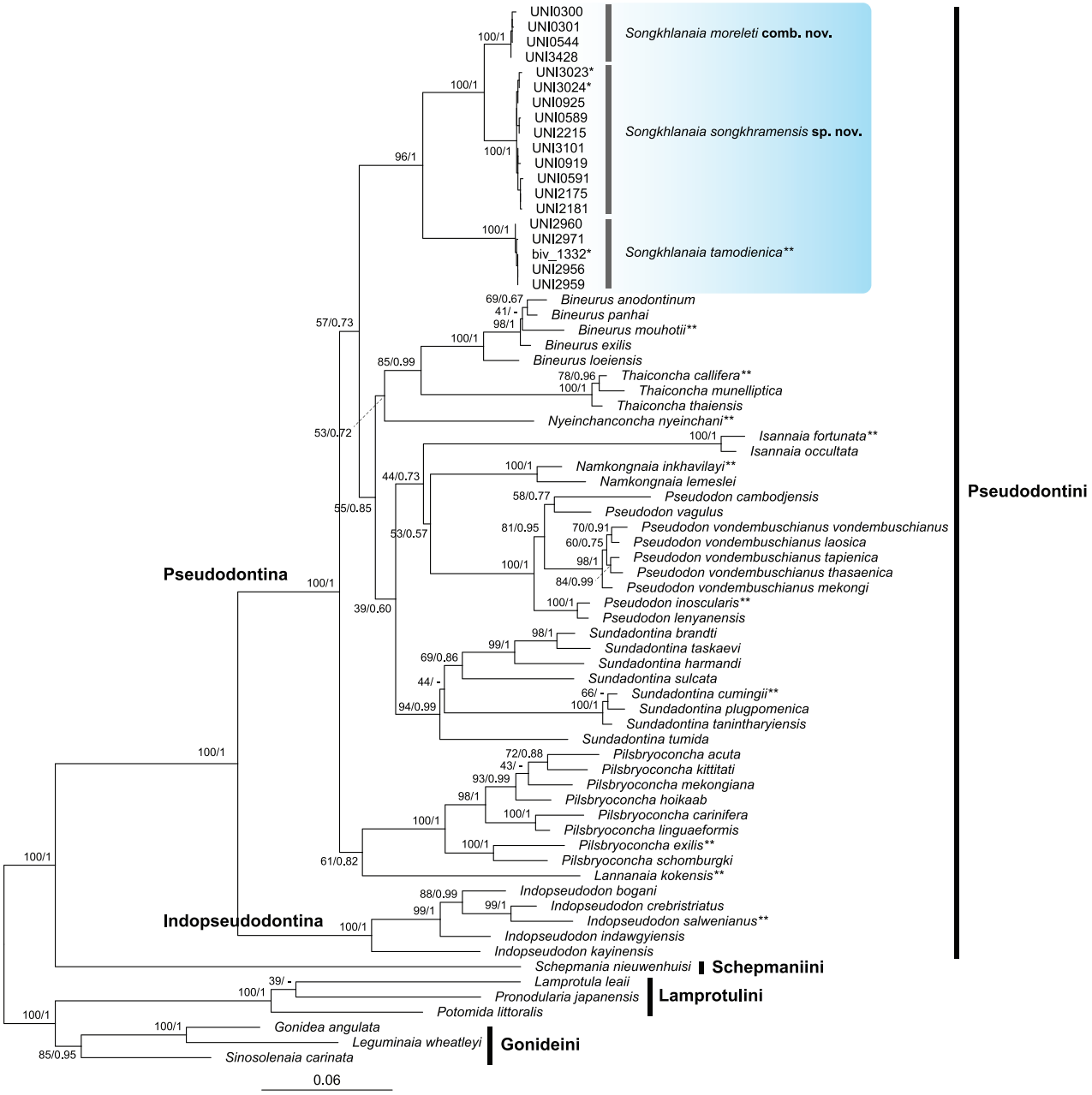

Figure 1. Maximum likelihood (ML) phylogenetic tree of freshwater mussels within the subfamily Gonideinae based on a combined DNA sequence dataset of COI, 16S rRNA, and 28S rRNA genes (1,959 bp). Branch support values are indicated on nodes as bootstrap percentages from ML analysis and Bayesian posterior probabilities from BI analysis, and shown as ML/BI. The scale bar represents the estimated evolutionary distance between taxa. The clade of the genus *Songkhlanaia* is highlighted in blue, and type specimens are indicated by an asterisk (*). Type species of Pseudodontini genera are marked with two asterisks (**).

Table 1. Comparison of conchological characteristics among *Songkhlanaia* species.

Conchological feature	*S. tamodienica* (*n* = 7)	*S. moreleti* (*n* = 3)	*S. songkhramensis* sp. nov. (*n* = 4; types)
Shell length (mm)	50.8–67.6	95.4–121.7	104.7–120.5
Shell height (mm)	32.9–43.7	62.0–78.7	73.8–78.5
Shell width (mm)	16.5–28.1	39.3–48.2	46.2–55.3
Shell shape	rectangular	subrhomboidal to ovate	subrhomboidal to ovate
Shell inflatedness	rather compressed	rather inflated	rather inflated
Shell thickness	not thick	moderate thick	thick
Shell color (adult specimens)	rusty brown to dark brown	dark brown to black	dark brown to black
Shell surface	fine growth lines, moderately roughened on the posterior slope	with irregular growth lines, roughened on the posterior slope and border of the shell	with irregular growth lines, roughened on the posterior slope and border of the shell
Folds on posterior slope	two fine folds	one or two faint folds	one or two faint folds
Umbo shape	tiny, slightly elevated	rounded, moderately elevated	rounded, wide, moderately elevated
Dorsal margin	straight, anterior low, posterior end high	slightly curved, anterior low, posterior end high	curved to slightly curved, anterior low, posterior end high
Ventral margin	slightly curved to almost straight	slightly curved to straight	slightly curved to straight
Right valve pseudocardinal tooth	tubercular to hill-like	tubercular or knob-like	triangular or high tubercular
Left valve pseudocardinal tooth	hill-like or lingula-shaped subcompressed	hill-like or triangulate, subcompressed	well-developed, rectangular, rather broad and high
V-shaped furrow on posterior end of the hinge structure	weak, not prominent	wide	wide
Anterior adductor muscle scar	shallow, somewhat droplet-like, contiguous with anterior protractor muscle scar	impressed, ovate, separated from anterior protractor muscle scar	impressed, somewhat drop-like, separated from anterior protractor muscle scar
Posterior adductor muscle scar	somewhat rounded, shallow to very shallow	drop-like to ovate, shallow	drop-like to ovate, shallow
Umbo cavity	shallow	moderate deep	deep, wide

consisting of specimens collected from the Tonle Sap Basin, conchologically matches well with the previously recognized taxon, *Pseudodon moreleti* Crosse & Fischer, 1876 (currently recognized as *Sundadontina moreleti* by Bolotov et al. 2023). We thus recognize this clade as *Songkhlanaia moreleti* comb. nov. Another clade consists of specimens collected from the Songkhram Basin and tributaries of the Mekong River in northeastern Thailand. This clade is conchologically similar to *S. moreleti* but possesses several diagnostic characteristics sufficient to separate them as distinct species (Table 1). It is thus described herein as *Songkhlanaia songkhramensis* sp. nov.

The phylogenetic relationship between *S. moreleti* and the new species is significantly supported as sister taxa (BS = 100%, BPP = 1). Meanwhile, *S. tamodienica* was placed at the basal position within *Songkhlanaia*. Phylogenetic analyses further confirm *Songkhlanaia* as a member of the subtribe Pseudodontina with strong support (BS = 100%, BPP = 1). However, the phylogenetic position of this genus in relation to other genera is not significantly supported.

Interspecific divergence among *Songkhlanaia* species ranged from 4.17 to 8.26% uncorrected p-distance of the COI gene (Table 2), while intraspecific divergences were low, ranging from 0 to 0.34%.

Table 2. Mean genetic distances (uncorrected p-distance: %±SD) based on 660-bp COI fragment sequences among *Songkhlanaia* species (below diagonal), and within each species (in bold).

Taxon	1.	2.	3.
1. *S. tamodienica*	**0**		
2. *S. moreleti*	8.26 ± 0.07	**0.23 ± 0.02**	
3. *S. songkhramensis* sp. nov.	8.04 ± 0.18	4.17 ± 0.23	**0.34 ± 0.02**

Taxonomic account

Family Unionidae Rafinesque, 1820
Subfamily Gonideinae Ortmann, 1916
Tribe Pseudodontini Frierson, 1927
Subtribe Pseudodontina Frierson, 1927

Genus *Songkhlanaia* Konopleva, Lheknim, Sriwoon, Kondakov, Vikhrev & Bolotov, 2023

Songkhlanaia Konopleva et al., 2023: 13, 14. Bolotov et al. 2023: 12.

Type species. *Songkhlanaia tamodienica* Konopleva, Lheknim, Sriwoon, Kondakov, Vikhrev & Bolotov in Konopleva et al. 2023 (by original designation).

Species included. *Songkhlanaia* currently consists of three species: *S. tamodienica* (type species), *S. moreleti* comb. nov., and *S. songkhramensis* sp. nov.

Diagnosis. Shell medium to large, rectangular or subrhomboidal, rather compressed to inflated. Anteriorly constricted, dorsal margin straight or slightly curved, slightly elevated posteriorly. One or two folds on posterior slope. Shell surface with fine or irregular growth lines, roughened on posterior slope or border of shell. One pseudocardinal tooth on each valve; lateral teeth obsolete.

Distribution. Endemic to Indochina, including Songkhla Lake Basin, Tonle Sap Basin, and Middle to Lower Mekong basins.

Comments. *Songkhlanaia* is represented in multi-locus phylogenetic analyses as a distinct clade among the Pseudodontini genera (Fig. 1). Morphologically, its rectangular or overall subrhomboidal shape outline also makes *Songkhlanaia* easily distinguishable from other genera that have somewhat narrow and elongate shells: *Bineurus* Simpson, 1900, *Isannaia* Jeratthitikul et al., 2024, *Namkongnaia* Jeratthitikul et al., 2021, and *Pilsbryoconcha* Simpson, 1900 (Jeratthitikul et al. 2021b, 2024; Konopleva et al. 2021; Bolotov et al. 2023). Although members of *Songkhlanaia* possess rather short and high shell outlines which resemble those of the genera *Indopseudodon* Prashad, 1922, *Lannanaia* Jeratthitikul et al., 2024, *Nyeinchanconcha* Bolotov et al., 2020, *Pseudodon* Gould, 1844, *Sundadontina* Bolotov et al., 2020, and *Thaiconcha* Bolotov et al., 2020, the unique roughened and irregular growth lines on the outer shell surface (which are fine or less developed growth lines in *S. tamodienica*) make it easily distinguishable from these genera (Bolotov et al. 2020, 2023; Konopleva et al. 2021; Jeratthitikul et al. 2024).

Members of *Songkhlanaia* are likely the largest freshwater mussels in the tribe Pseudodontini recorded to date. The largest specimen examined herein is *S. moreleti* (MUMNH-UNI0301; shell length 121.7 mm) from Srakeo, Thailand. The syntype has a shell length of 123 mm (Crosse and Fischer 1876) and a specimen from Cambodia examined by Simpson (1914) reached 124 mm.

***Songkhlanaia tamodienica* Konopleva, Lheknim, Sriwoon, Kondakov, Vikhrev & Bolotov, 2023**

Figs 2A, B, 5A, Table 1

Songkhlanaia tamodienica Konopleva et al., 2023: 14, fig. 2c–h. Type Locality: "Southern Thailand: Klong Plug Pom, middle reach of Klong Tamod, Songkhla Lake Basin, Ban Kok Sai, Tambon Mae Kree, Tamod District, Phatthalung Province, 7.3324°N, 100.0917°E". Bolotov et al. 2023: 12.

Material examined. Thailand – **Phatthalung Province** • 7 shells; Tamot District, Mae Khari Subdistrict, Songkhla Lake Basin, Tamot Stream; 7.3302°N, 100.0873°E; 17 May 2023; E. Jeratthitikul leg.; MUMNH-UNI2956 to 2960, UNI2971 to 2972.

Diagnosis. Shell medium, rectangular, thin, rather compressed. Anteriorly constricted, dorsal margin straight, slightly elevated posteriorly. Posterior slope with two prominent folds. Umbo tiny, slightly elevated. Shell surface with fine irregular growth lines, roughened on posterior slope. Right valve with one smooth tubercular or triangular pseudocardinal tooth, left valve with somewhat lingula-shaped tooth. V-shaped furrow on posterior end of hinge structure weak, not prominent. Anterior adductor muscle scar shallow, somewhat drop-like, contiguous with anterior protractor muscle scar. Umbo cavity shallow.

Differential diagnosis. This species can be distinguished from the other two congeners by its much smaller (about half size) and thin shell, rectangular shape, and rather compressed lateral profile. It can also be distinguished by 39 fixed nucleotide substitutions in the COI gene fragment (Table 3).

Distribution. So far, known only from the type locality in Songkhla Lake Basin, southern Thailand (Fig. 3).

Comments. *Songkhlanaia tamodienica* was described based on a single specimen. The holotype has a relatively small (shell length 44.2 mm), thin, lighter colored shell with shallow adductor muscle scar, and slightly elevated posterior wing (Konopleva et al. 2023: fig. 2c–h). This specimen appeared to be small and young individual. Recently, we revisited the type locality and collected seven more specimens; two of these shells are larger in size and probably from fully grown specimens. They exhibit a thickened and inflated shell, rounded posterior end, dark periostracum, deep adductor muscle scar, and less pronounced posterior wing (Fig. 2A). The largest specimen measured is 67.3 mm in shell length. In addition, the outer shell surface is sculpted by irregular growth lines, which are pronounced on the posterior slope and border of the shell (Fig. 2A). This feature is present in younger specimens but is less prominent (Fig. 2B).

Table 3. Fixed nucleotide differences of COI sequences among *Songkhlanaia* species useful for species diagnosis. Nucleotide position based on the sequence alignment in this study.

Taxon	Fixed nucleotide differences
1. *S. tamodienica*	39G, 48A, 57A, 72A, 90C, 93G, 97T, 99G, 112C, 123G, 126C, 132A, 147A, 159C, 174G, 204C, 243A, 244T, 246G, 249C, 267G, 279C, 288A, 289T, 312A, 318C, 345T, 348A, 366C, 408T, 414G, 453A, 462G, 480A, 483A, 498T, 510A, 558A, 654T
2. *S. moreleti*	63A, 69A, 84A, 195C, 225G, 264A, 342C, 345A, 429C, 486C, 555A, 561G, 618T, 627T
3. *S. songkhramensis* sp. nov.	12C, 42C, 214G, 282A, 345G, 531T, 546T, 559C, 580C, 597C, 603C, 657A

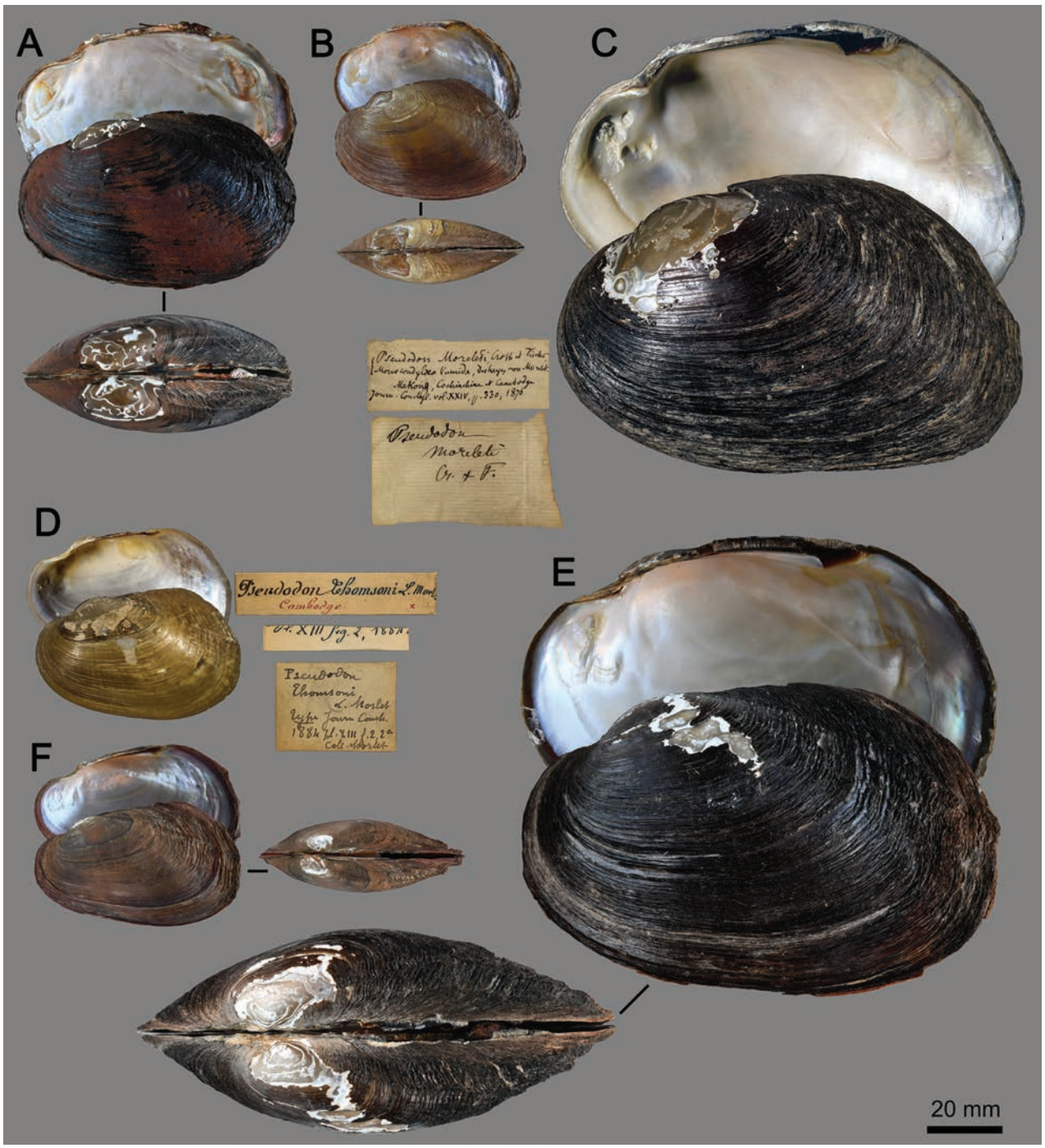

Figure 2. Shells of *Songkhlanaia* species **A, B** topotype of *S. tamodienica* from Tamot Stream, Songkhla Lake Basin, Thailand **A** adult specimen MUMNH-UNI2956 and **B** young specimen MUMNH-UNI2971 **C–F** *S. moreleti* **C** syntype MNHN-IM-2000–34623 from Mekong Basin, Cambodia, with original labels **D** syntype of *Pseudodon thomsoni* Morlet, 1884, MNHN-IM-2000-1800 from Mekong Basin, Cambodia, with original labels **E** adult specimen MUMNH-UNI0301, and **F** young specimen MUMNH-UNI3428 from Phrom Hot Stream, Tonle Sap Basin, Thailand. Photographs **C, D** M. Caballer (2019, MNHN Project: RECOLNAT No. ANR-11-INBS-0004).

***Songkhlanaia moreleti* (Crosse & Fischer, 1876), comb. nov.**
Figs 2C–F, 5B, Table 1

Monocondylea [sic] *tumida* Deshayes & Jullien, 1876: 117–120, pl. 5, figs 1–3 [in part; non *Monocondylus tumidus* Morelet, 1866].

Pseudodon moreleti Crosse & Fischer, 1876: 330. Type Locality: "les marécages qui avoisinent les rives du Mékong; dans un lac, à Préai-Bac, arroyo de Peam-Chelang; d'eau de la province de Compong-Soai" [= Peam Chileang and Kampong Svay, Cambodia]. Fischer 1891: 221. Fischer and Dautzenberg 1904: 436. Dautzenberg and Fischer 1905: 452, 453.

Pseudodon (*Pseudodon*) *moreleti*—Simpson 1900: 838. Simpson 1914: 1094, 1095. Haas 1924: 137, 138. Haas 1969: 130.

Sundadontina moreleti—Bolotov et al. 2020: 10, fig. 4e. Graf and Cummings 2021: 22. Bolotov et al. 2023: 13.

Pseudodon thomsoni Morlet, 1884: 401, 402, pl. 13, figs 2, 2a. Type Locality: "Cambodge" [= Cambodia]. Morlet 1889: 166. Fischer 1891: 221. Fischer-Piette 1950: 154. Zieritz et al. 2018: supplementary material 1. Bolotov et al. 2023: 11. Syn. nov.

Margaritana thomsoni—Paetel 1890: 174.

Pseudodon (*Pseudodon*) *thomsoni*—Simpson 1900: 838. Simpson 1914: 1092, 1093.

Pseudodon (*Bineurus*) *thomsoni*—Haas 1920: 336–337. Haas 1924: 144. Graf and Cummings 2007: 311.

?Pseudodon thomsoni—Konopleva et al. 2021: 11, fig. 3h.

Type material. ***Syntypes*** MNHN-IM-2000–34623 (2 shells). ***Syntype*** MNHN-IM-2000-1800 (1 shell) of *Pseudodon thomsoni* Morlet, 1884, (inadvertently stated as holotype by Fischer-Piette, 1950).

Other material examined. Thailand – **Sa Kaeo Province** • 1 shell; Aranyaprathet District, Aranyaprathet Subdistrict, Tonle Sap Basin, Phrom Hot Stream; 13.6694°N, 102.5210°E; 31 Jan. 2015; E. Jeratthitikul leg.; MUMNH-UNI0544 • 1 shell; Aranyaprathet District, Aranyaprathet Subdistrict, Tonle Sap

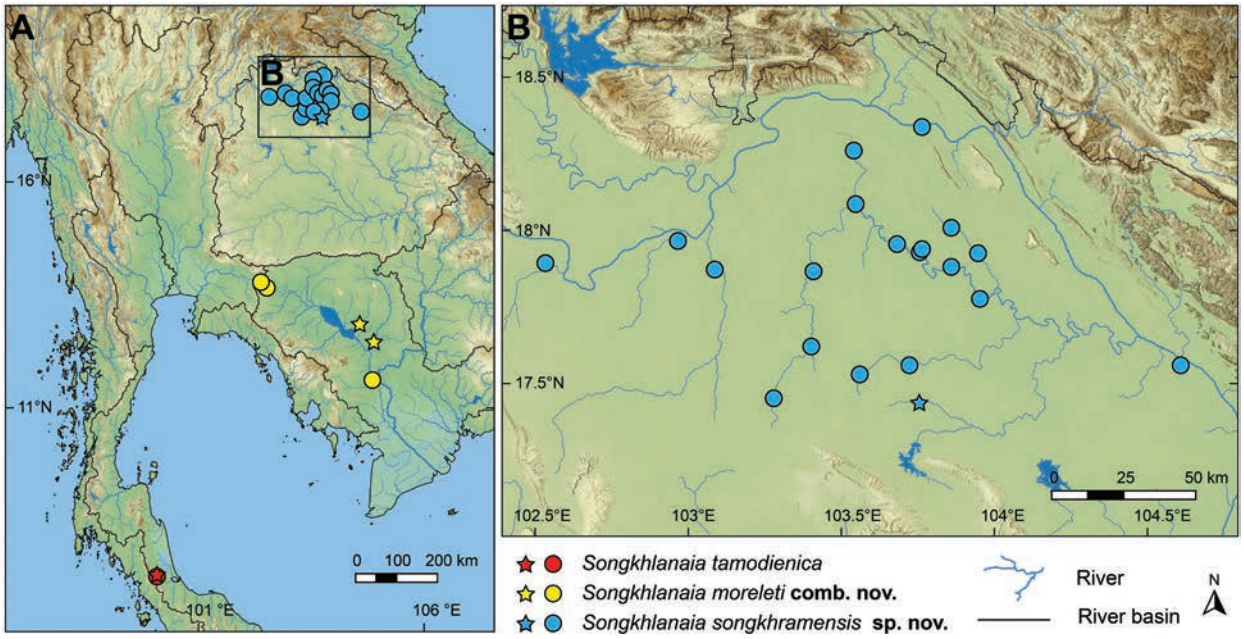

Figure 3. A, B map showing the geographical distribution of all known *Songkhlanaia* species (circles) and their type locality (stars). Map was generated using QGIS v. 3.36.0 with the outline of major river basins from the Freshwater Ecoregions of the World (Abell et al. 2008), river and lake topology from the HydroSHEDS database (https://www.hydrosheds.org), and the map raster data from the NASA EARTHDATA (https://www.earthdata.nasa.gov/).

Basin, Phrom Hot Stream; 13.6718°N, 102.5166°E; MUMNH-UNI3428 • 2 shells; Watthana Nakhon District, Phak Kha Subdistrict, Tonle Sap Basin, Phrom Hot Stream; 13.7490°N, 102.4271°E; 5 May 2015; P. Prasankok leg.; MUMNH-UNI0300 to 0301.

Diagnosis. Shell large, subrhomboidal to ovate, moderately thickened, rather inflated. Anteriorly constricted, dorsal slightly curved, slightly elevated posteriorly. Posterior slope with one or two faint folds. Umbo rounded, moderately elevated. Shell surface with irregular growth lines, roughened on posterior slope and border of shell. Right valve with one smooth tubercular pseudocardinal tooth, left valve with hill-like or triangulate pseudocardinal tooth, subcompressed. V-shaped furrow on posterior end of hinge structure prominent, wide. Anterior adductor muscle scar impressed, ovate, separated from anterior protractor muscle scar. Umbo cavity moderately deep.

Differential diagnosis. This species is much larger and more inflated than the type species. Irregular growth lines on the shell surface are rougher, especially on the posterior slope and along the shell border. This species is also distinct from congenerics due to 14 fixed nucleotide substitutions in the COI gene fragment (Table 2).

Distribution. Tonle Sap Basin in Thailand and Cambodia (Crosse and Fischer 1876; Deshayes and Jullien 1876; this study), and the Lower Mekong Basin in Cambodia (Morlet 1884) (Fig. 3).

Comments. Originally, *Songkhlanaia moreleti* was described based on a partially misidentified specimen from Cambodia as *Monocondylus tumidus* Morelet, 1866 by Deshayes and Jullien (1876). Crosse and Fischer (1876) reexamined the specimens and provided it with a new name, *Pseudodon moreleti*. This nominal species had been recognized as valid by subsequent studies for more than a hundred years (e.g., Fischer 1891; Fischer and Dautzenberg 1904; Dautzenberg and Fischer 1905; Simpson 1900, 1914; Haas 1924, 1969). Later, Brandt (1974: 271) and Graf and Cummings (2007: 311) listed this taxon as a junior synonym of either species or subspecies of '*tumidus* Morelet, 1866'. Recently, Bolotov et al. (2020) raised this species as valid and placed it in their new genus, *Sundadontina*. However, this resurrection and generic placement seemed provisionally based on conchological characters alone. Fortunately, specimens collected from Sa Kaeo Province in Thailand (Fig. 2E), the location of the headwaters of the Tonle Sap Basin and the type locality for this species, have been found to match well with the syntypes (Fig. 2C). Furthermore, these specimens cluster within the phylogenetic position of the *Songkhlanaia* (Fig. 1). Therefore, we propose transferring this species to the more appropriate genus *Songkhlanaia*.

Pseudodon thomsoni Morlet, 1884 was described based on specimens collected from Cambodia by Auguste Jean-Marie Pavie. Later, Morlet (1889: 166) detailed and specified the type locality as "Etang de Pnom-Penh (Cambodge)" [= pond in Phnom Penh, Cambodia]. It was recognized as a distinct species for more than a century, until it was recently treated as a junior synonym of *Thaiconcha callifera* (von Martens, 1860) by some authors (Bolotov et al. 2020: 10; Graf and Cummings 2021: 22). The following year, it was resurrected as a valid species by Konopleva et al. (2021) and again by Bolotov et al. (2023). However, the syntype of *Pseudodon thomsoni* Morlet, 1884 is relatively small (Fig. 2D; shell length 53 mm), and its shell characteristics generally resemble those of

young specimens of *S. moreleti* (Fig. 2F), such as the long obovate shell that is constricted anteriorly, moderately elevated umbo, and a bean-shaped anterior protractor scar. Furthermore, the type locality in 'Phnom Penh, Cambodia' is in the lower Mekong Basin (Fig. 3), the same basin as the type locality of *S. moreleti*. Based on this conchological and biogeographic evidence, we thus synonymise this species with *S. moreleti*.

The molecular data examined in this study included individuals of *S. moreleti* solely collected from the headwater areas of the Tonle Sap Basin in Thailand. In fact, previous freshwater mollusk surveys of areas surrounding the Tonle Sap Lake in Cambodia by Ng et al. (2020) did not recover any specimens identified as *S. moreleti* from over 40 sampling localities. This possibly suggests a low abundance or local disappearance from the area. Further intensive surveys throughout the basin, including the headwater area and its tributaries, may encounter more specimens, which would be beneficial for assessing the genetic viability and conservation status of this species.

***Songkhlanaia songkhramensis* sp. nov.**

https://zoobank.org/B44C6882-92FD-460F-B904-CAD25A2222D6

Figs 4, 5C Tables 1, 4

Type material. ***Holotype*** Thailand – **Sakon Nakhon Province** • Phang Khon District, Hai Yong Subdistrict, Songkhram Basin, Prahang River; 17.4376°N, 103.7569°E; 7 Apr. 2023; E. Jeratthitikul and W. Siriwut leg.; MUMNH-UNI3024 (shell length 120.5 mm, shell height 78.5 mm, shell width 55.3 mm). ***Paratype*** • 3 shells; same collection data as for holotype; MUMNH-UNI3022, 3023, 3025.

Other material. Thailand – **Nong Khai Province** • 5 shells; Si Chiang Mai District, Nong Pla Pak Subdistrict, Mekong Basin, Nam Mong River; 17.8914°N, 102.5341°E; 7 Apr. 2015; E. Jeratthitikul, K. Wisittikoson, and P. Prasankok leg.; MUMNH-UNI2174 to 2178 • 2 shells; Phon Phisai District, Thung Luang Subdistrict, Mekong Basin, Nam Suai Stream; 17.9640°N, 102.9659°E; 8 Apr. 2015; E. Jeratthitikul, K. Wisittikoson, and P. Prasankok leg.; MUMNH-UNI2214, 2215. **Udon Thani Province** • 2 shells; Ban Dung District, Ban Dung Subdistrict, Songkhram Basin, Songkhram River; 17.8666°N, 103.4034°E; 5 Apr. 2023; E. Jeratthitikul and W. Siriwut leg.; MUMNH-UNI2978, 2979 • 2 shells; Ban Dung District, Ban Muang Subdistrict, Songkhram Basin, Songkhram River; 17.7293°N, 103.4101°E; 5 Apr. 2023; E. Jeratthitikul and W. Siriwut leg.; MUMNH-UNI2981, 2982 • 7 shells; Thung Fon District, Thung Fon Subdistrict, Songkhram Basin, Songkhram River; 17.4521°N, 103.2808°E; 8 Apr. 2015; E. Jeratthitikul, K. Wisittikoson, and P. Prasankok leg.; MUMNH-UNI919, 0925 to 0927, 3003 to 3005 • 3 shells; Sang Khom District, Chiang Da Subdistrict, Mekong Basin, Huai Luang River; 17.8730°N, 103.0875°E; 8 Apr. 2015; E. Jeratthitikul, K. Wisittikoson, and P. Prasankok leg.; MUMNH-UNI2179 to 2181. **Bueng Kan Province** • 6 shells; Mueang District, Khok Kong Subdistrict, Mekong Basin, Huay Kam Paeng. 18.3381°N, 103.7625°E; 5 Apr. 2015; E. Jeratthitikul, K. Wisittikoson, and P. Prasankok leg.; MUMNH-UNI0586 to 0591 • 3 shells; Seka District, Nong Thum Subdistrict, Songkhram Basin, Songkhram River; 17.8822°N, 103.8609°E; 4 Apr. 2023; E. Jeratthitikul and W. Siriwut leg.; MUMNH-UNI3051 to 3053 • 1 shell; Seka District, Pong Hai Subdistrict, Songkhram Basin, Nam Hee Stream,

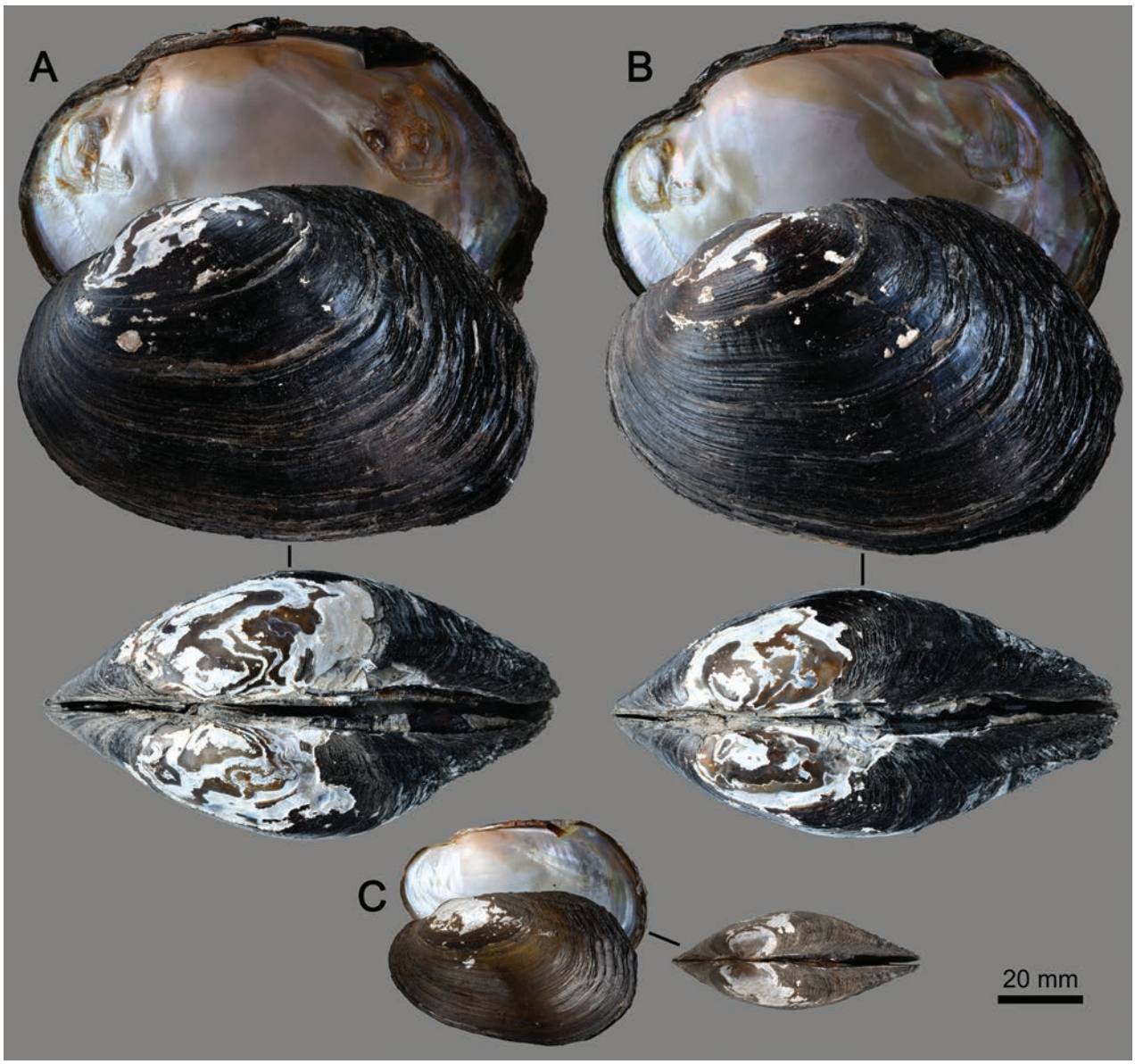

Figure 4. Shells of *Songkhlanaia songkhramensis* sp. nov. **A** holotype MUMNH-UNI3024 and **B** paratype MUMNH-UNI3023 from Prahang River, Songkhram Basin, Thailand **C** specimen MUMNH-UNI0925 from Songkhram River, Songkhram Basin, Thailand.

Unnamed Check Dam; 18.0117°N, 103.8585°E; 4 Apr. 2023; E. Jeratthitikul and W. Siriwut leg.; MUMNH-UNI3069 • 1 shell; Phon Charoen District, Wang Chomphu Subdistrict, Songkhram Basin, Songkhram River; 17.9557°N, 103.6802°E; 4 Apr. 2023; E. Jeratthitikul and W. Siriwut leg.; MUMNH-UNI3107 • 2 shells; Mueang District, Na Sawan Subdistrict, Songkhram Basin, Huay Pak Kong Stream, Ban Na Waeng Cheek Dam; 18.2603°N, 103.5425°E; 4 Apr. 2023; E. Jeratthitikul and W. Siriwut leg.; MUMNH-UNI3088, 3089 • 3 shells; Phon Charoen District, Nong Hua Chang Subdistrict, Songkhram Basin, Huay Pak Kong Stream, Unnamed Cheek Dam; 18.0863°N, 103.5462°E; 5 Apr. 2023; E. Jeratthitikul and W. Siriwut leg.; MUMNH-UNI3048 to 3050 • 9 shells; Seka District, Seka Subdistrict, Market (collected from Nam Hee Stream); 17.9265°N, 103.9455°E; 19 Jan 2023; K. Macharoenboon leg.; MUMNH-UNI2855 to 2863 • 9 shells; Seka District, Tha Sa-at Subdistrict, Songkhram Basin, Songkhram

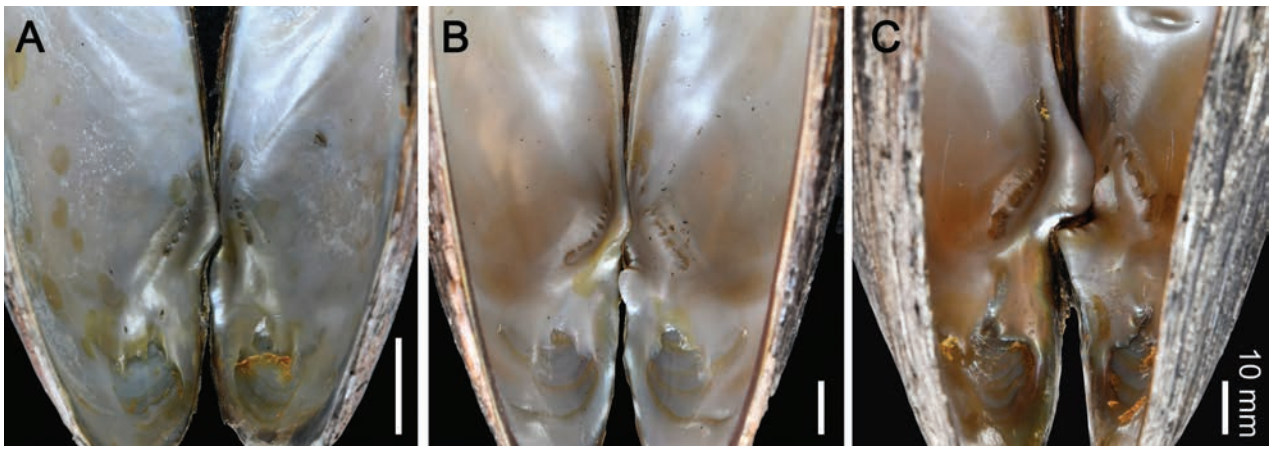

Figure 5. Pseudocardinal teeth, left valve on the left-hand side, and right valve on the right-hand side **A** *S. tamodienica*, topotype MUMNH-UNI2956 from Tamot Stream, Songkhla Lake Basin, Thailand **B** *S. moreleti*, specimen MUMNH-UNI0301 from Phrom Hot Stream, Tonle Sap Basin, Thailand **C** *S. songkhramensis* sp. nov., holotype MUMNH-UNI3024 from Prahang River, Songkhram Basin, Thailand. Scale bars: 10 mm.

Table 4. Shell measurements and GenBank accession numbers for the type series of *Songkhlanaia songkhramensis* sp. nov. Measurements in millimeters (mm).

Status of specimen	Specimen voucher	Shell dimensions (mm)			Genbank accession		
		length	height	width	COI	16S rRNA	28S rRNA
Holotype	MUMNH-UNI3024	120.5	78.5	55.3	PQ231674	PQ236709	PQ236725
Paratype	MUMNH-UNI3022	116.4	76.2	47.9	-	-	-
Paratype	MUMNH-UNI3023	109.8	76.3	53.5	PQ231673	PQ236708	PQ236724
Paratype	MUMNH-UNI3025	104.7	73.8	46.2	-	-	-

River; 17.9318°N, 103.7600°E; 5 Apr. 2015; E. Jeratthitikul, K. Wisittikoson, and P. Prasankok leg.; MUMNH-UNI0667, 0668. **Nakhon Phanom Province** • 2 shells; Tha Uthen District, Non Tan Subdistrict, Mekong Basin, Thuai River; 17.5621°N, 104.6096°E; 2 Apr. 2023; E. Jeratthitikul and W. Siriwut leg.; MUMNH-UNI3101, 3102. **Sakon Nakhon Province** • 2 shells; Sawang Daen Din District, Khok Si Subdistrict, Songkhram Basin, Songkhram River; 17.6205°N, 103.4020°E; 6 Apr. 2023; E. Jeratthitikul and W. Siriwut leg.; MUMNH-UNI3077, 3078 • 4 shells; Wanon Niwat District, Khon Sawan Subdistrict, Songkhram Basin, Yam Stream, Huai Kho Check Dam; 17.5637°N, 103.7203°E; 7 Apr. 2023; E. Jeratthitikul and W. Siriwut leg.; MUMNH-UNI3013 to 3016 • 7 shells; Charoen Sin District, Khok Sila Subdistrict, Songkhram Basin, Yam Stream; 17.5322°N, 103.5608°E; 3 May 2015; E. Jeratthitikul, K. Wisittikoson, and P. Prasankok leg.; MUMNH-UNI0344 to 0350 • 1 shell; Kham Ta Kla District, Kham Ta Kla Subdistrict, Songkhram Basin, Songkhram River; 17.9307°N, 103.7572°E; 18 Jan. 2023; K. Macharoenboon leg.; MUMNH-UNI2853 • 1 shell; Akat Amnuai District, Tha Kon Subdistrict, Songkhram Basin, Songkhram River; 17.7786°N, 103.9528°E; 9 Jan. 2023; local people leg.; MUMNH-UNI2198.

Diagnosis. Shell large, subrhomboidal to ovate, thick, rather inflated. Anteriorly constricted, dorsal slightly curved, slightly elevated posteriorly. Posterior slope with one or two faint folds. Umbo rounded, wide, moderately elevated. Shell surface with irregular growth lines, roughened on posterior slope and border of shell. Right valve with one smooth triangular or high tubercular pseudocardinal tooth, left valve with well-developed, rectangular, rather broad and

high pseudocardinal tooth. V-shaped furrow on posterior end of hinge structure prominent and wide. Anterior adductor muscle scar impressed, somewhat droplet-like, separated from anterior protractor muscle scar. Umbo cavity moderately deep and wide.

Differential diagnosis. This new species can be distinguished from *S. moreleti* by having well-developed pseudocardinal teeth (Fig. 5), particularly the one on the left valve, which is characterized as a rectangular, rather broad, and high tooth (vs subcompressed, hill-like, or triangulate in *S. moreleti*); a wider V-shaped furrow at the posterior end of the hinge structure; and a deeper umbo cavity. The new species also possesses a set of unique fixed nucleotide substitutions in the COI gene fragment that make it genetically distinct from its congeners (Table 3). The new species is genetically closely related to *S. moreleti*, with a 4.17% uncorrected p-distance in the COI gene. They also form a sister clade in the phylogenetic analysis (Fig. 1).

Description. Shell large-sized (shell length 104.7–120.5 mm, shell height 73.8–78.5 mm, shell width 46.2–55.3 mm; Table 4), thick, rather high (H/L ratio = 0.65–0.70), inequilateral, subrhomboidal to ovate shape, rather inflated. Anterior margin rounded; posterior margin oblique above, subtruncate below; ventral margin slightly curved to straight. Dorsal margin curved to slightly curved; anterior low, rather constricted, slightly elevated to posterior end; posterior end high, resembling posterior wing in young specimens (Fig. 4C). Umbo rounded, wide, moderately elevated, usually eroded. Posterior ridge wide and obtuse, not prominent; posterior slope with one or two faint folds running as curved line from umbo to posterior margin; lower one more prominent, ending at approximately middle of posterior margin, forming angulate point. Periostracum moderately thick, dark brown to black, eroded part white to coppery-brown. Shell surface with irregular growth lines, roughened on posterior slope and border of shell.

Inner side of shell: ligament long, narrow, dark brown in color. Pseudocadinal teeth one on each valve; smooth, triangular or high tubercular shape on right valve; well-developed, smooth, rectangular shape, rather broad and high on left valve; in shell coupling position, pseudocadinal tooth on right valve situated well anteriorly. Lateral teeth obsolete. Posterior end of hinge structure with wide V-shaped furrow. Anterior muscle scars impressed; anterior adductor muscle scar somewhat droplet-like, contiguous with anterior pedal retractor, but separated from anterior protractor muscle scars; pedal retractor muscle scar rounded, protractor muscle scar bean-shaped. Posterior adductor muscle scar large, drop-like to ovate, shallow. Pallial line well-marked and continuous. Umbo cavity deep, wide, with one row of 5–10 muscle scars. Nacre whitish blue to yellowish.

Siphon apertures with strip of dark pigmentation running along aperture edge. Exhalant aperture smooth, shorter than inhalant. Inhalant aperture with one row of conical papillae, varying in length, with more of the longer papillae near ventral edge. Small epithelial fold divides exhalant and inhalant aperture. Gills elongated and slightly ribbed; outer gills narrower than inner gills; anterior margin of inner gills slightly longer than outer gills. Labial palps elongate, somewhat pointed at tip. Glochidia unknown.

Etymology. The species name *songkhramensis* refers to the Songkhram Basin, a sub-river basin of the Middle Mekong Basin in northeastern Thailand, in which this species is highly abundant. The type locality of the species is also situated in the Songkhram Basin.

Distribution. The new species occurs in the Songkhram Basin and tributaries of the Mekong River in northeastern Thailand. It is a common freshwater mussel in the middle to upper part of Songkhram Basin (Fig. 3) and is usually found in high abundance.

Comments. Among the mussel species commonly found sympatrically with *S. songkhramensis* sp. nov., *Thaiconcha callifera* is the most similar in overall shell features, and thus may confuse the identification. However, the new species can be easily distinguished from *T. callifera* by its thick shell (vs moderately thick), subrhomboidal to ovate shape (vs elliptical or rounded shape), higher shell (vs somewhat elongate), wider and more elevated umbo (vs narrow and slightly elevated), less shiny shell (vs somewhat shiny shell), shell surface sculptured with irregular growth lines, heavily roughened on the posterior slope (vs shell surface rather smooth, with fine growth lines, slightly roughened on the posterior slope), and rectangular and rather broad pseudocardinal teeth (vs tubercular pseudocardinal teeth) (Bolotov et al. 2020; Konopleva et al. 2021).

Discussion

This study integrated molecular evidence, shell morphology, and biogeography into the identification of two additional species in the *Songkhlanaia*. One is a new combination of the previously recognized nominal taxon, *S. moreleti*, while the other is a new species from the Middle Mekong Basin, namely *S. songkhramensis* sp. nov. The discovery of the new species adds to the known diversity of the tribe Pseudodontini, making it the most speciose tribe of the Unionidae in Southeast Asia, with a total of 51 species across eleven genera, more than the 35 species in Contradentini and the 28 species in Gonideini (Graf and Cummings 2021, 2024; Bolotov et al. 2023; Jeratthitikul et al. 2024). Moreover, the discovery of this new species further emphasizes the remarkable diversity and endemism of the freshwater mussel fauna in the Mekong Basin, and particularly in the Songkhram Basin, the recently listed Ramsar site in Thailand. The Songkhram Basin houses a diverse assemblage of unionid mussels accounting for 12 species from 12 genera; nine of these species (75%) are considered as endemic to the basin (Jeratthitikul et al. 2019a, 2019b, 2021a, 2021b, 2024; Muanta et al. 2019; Konopleva et al. 2021; Pfeiffer et al. 2021; Bolotov et al. 2023). Unfortunately, the high levels of endemism in this area are threatened by anthropogenic impacts, including pollution and habitat destruction (Saluja and Piman 2022), which may result in significant habitat loss for the mussels, thereby threatening their survival (Lopes-Lima et al. 2018; Aldridge et al. 2023).

Members of the Pseudodontini share common characteristics of the obsolete lateral teeth and the single pseudocardinal tooth on each valve, which can be represented as either weakly or well-developed knob-like pseudocardinal teeth. Meanwhile, other conchological traits exhibit a broad range of variability, and species in the taxon range from having thin and ultra-elongate shells to rather thick and rounded shells (Bolotov et al. 2023). Species in each genus of the Pseudodontini also exhibit high levels of cryptic diversity, rendering it challenging to distinguish them based solely on morphological characteristics (Jeratthitikul et al. 2022; Bolotov et al. 2023). This challenge is particularly evident in the comparison between two sister species, *S. moreleti* and *S. songkhramensis* sp. nov. Although these species can be differentiated by their pseudocardinal

teeth, they are very similar in overall shell features (Table 1). However, we found that fragments of the COI gene, the common DNA barcoding gene marker used in freshwater mussels (e.g., Pfeiffer et al. 2021; Jeratthitikul et al. 2022, 2024; Jeratthitikul and Sutcharit 2023), remains an effective tool for distinguishing between them. They are genetically different by 4.17% uncorrected p-distance of the COI gene (Table 2) and have several fixed nucleotide differences (Table 3). This genetic divergence is comparable to established thresholds for species delimitation in other Indochinese freshwater mussels ranging from 2.32 to 12.3% (Jeratthitikul et al. 2019a, 2019b, 2021a, 2021b, 2022, 2024; Konopleva et al. 2019a; Jeratthitikul and Sutcharit 2023). This study thus has once again highlighted the importance of utilizing an integrative approach of combining morphology and molecular data in species delimitation of freshwater mussels.

Multi-locus phylogenetic analysis (COI + 16S rRNA + 28S rRNA) in this study recovered members of *Songkhlanaia* as a well-supported clade (Fig. 1), confirming the identity of the genus among the Pseudodontini genera. Furthermore, the genus was placed in the subtribe Pseudodontina with significant support from both ML and BI analyses (BS = 100%, BPP = 1). However, the phylogenetic position of this genus in relation to other genera in the Pseudodontina remains unstable among studies that use similar genetic markers. The Bayesian time-calibrated phylogenetic tree in Bolotov et al. (2023) suggested a separation of *Pilsbryoconcha* from other genera in the Pseudodontina, including *Songkhlanaia*, although the relationships among the genera within this clade were uncertain. Jeratthitikul et al. (2024) revealed a supported sister relationship between *Songkhlanaia* and *Lannanaia*. In contrast, the phylogenetic results in Konopleva et al. (2023) and this study fail to recover a supported phylogenetic position for *Songkhlanaia*. This incongruent phylogenetic relationship suggests that using these three genetic markers may not be sufficient to recover strong support for the deep nodes within Pseudodontina. To enhance phylogenetic resolution, further studies should incorporate longer sequences (i.e., the whole 28S rRNA gene), add more genes such as ND1, histone 3, or 18s rRNA (Ortiz-Sepulveda et al. 2020; Zieritz et al. 2024), or utilize complete mitochondrial genomes (Froufe et al. 2020; Zieritz et al. 2021a), as well as employ more comprehensive phylogenomic datasets (Pfeiffer et al. 2019).

Alternatively, the unclear relationships among genera within the Pseudodontina might be attributed to rapid radiation within the group, where lineages may have undergone a series of speciation events in a relatively short period of time. This phenomenon could result in a complex evolutionary history that complicates the resolution of phylogenetic trees with certain features such as short internal branches and poorly supported nodes, as evidenced in other groups of animals (e.g., Grummer et al. 2018; Duan et al. 2023). The time estimation of rapid radiation events of the Pseudodontina genera has been suggested to occur during the Late Cretaceous to Eocene times (approximately 75–50 million years; Jeratthitikul et al. 2021b; Bolotov et al. 2023).

Acknowledgements

We thank S. Klomthong, K. Wisittikoson, members of Animal Systematics and Molecular Ecology Laboratory Mahidol University (ASME lab), and members of Animal Systematic Research Unit (ASRU), Chulalongkorn University for their

assistance in collecting samples, and extend our thanks to D.J. Anderson for grammar checking and comments. The CIPRES Science Gateway V3.3 provided access to computational analysis.

Additional information

Conflict of interest

The authors have declared that no competing interests exist.

Ethical statement

The animal uses in this study have been approved by the Faculty of Science, Mahidol University Animal Care and Use Committee, SCMU-ACUC (MUSC65-013-606 and MUSC66-016-646).

Funding

This study has been supported by the Centre of Excellence on Biodiversity (BDC), Office of Higher Education Commission (BDC-PG1-166001) and the National Research Council of Thailand (NRCT) (N34E670115).

Author contributions

EJ and CS developed the concept of the study. EJ and PP collected specimens and conducted molecular analyses. EJ performed phylogenetic analyses and prepared taxonomic accounts with input from CS. CS prepared shell images. EJ prepared the manuscript and all illustrations. All authors discussed, gave input and acknowledged the final version of the manuscript.

Author ORCIDs

Ekgachai Jeratthitikul https://orcid.org/0000-0002-3477-9548
Chirasak Sutcharit https://orcid.org/0000-0001-7670-9540
Pongpun Prasankok https://orcid.org/0000-0001-5967-223X

Data availability

All of the data that support the findings of this study are available in the main text or Supplementary Information.

References

Abell R, Thieme ML, Revenga C, Bryer M, Kottelat M, Bogutskaya N, Coad B, Mandrak N, Balderas SC, Bussing W, Stiassny MLJ, Skelton P, Allen GR, Unmack P, Naseka A, Ng R, Sindorf N, Robertson J, Armijo E, Higgins JV, Heibel TJ, Wikramanayake E, Olson D, López HL, Reis RE, Lundberg JG, Sabaj Pérez MH, Petry P (2008) Freshwater ecoregions of the World: A new map of biogeographic units for freshwater biodiversity conservation. BioScience 58: 403–414. https://doi.org/10.1641/B580507

Aldridge DC, Ollard IS, Bespalaya YV, Bolotov IN, Douda K, Geist J, Haag WR, Klunzinger MW, Lopes-Lima M, Mlambo MC, Riccardi N, Sousa R, Strayer DL, Torres SH, Vaughn CC, Zając T, Zieritz A (2023) Freshwater mussel conservation: A global horizon scan of emerging threats and opportunities. Global Change Biology 29: 575–589. https://doi.org/10.1111/gcb.16510

AVMA (2020) AVMA guidelines for the euthanasia of animals. American Veterinary Medical Association. https://www.avma.org/sites/default/files/2020-02/Guidelines-on-Euthanasia-2020.pdf [30 September 2024, date last accessed]

Bolotov IN, Kondakov AV, Vikhrev IV, Aksenova OV, Bespalaya YV, Gofarov MY, Kolosova YS, Konopleva ES, Spitsyn VM, Tanmuangpak K, Tumpeesuwan S (2017a) Ancient river inference explains exceptional oriental freshwater mussel radiations. Scientific Reports 7: 2135. https://doi.org/10.1038/s41598-017-02312-z

Bolotov IN, Vikhrev IV, Kondakov AV, Konopleva ES, Gofarov MY, Aksenova OV, Tumpeesuwan S (2017b) New taxa of freshwater mussels (Unionidae) from a species-rich but overlooked evolutionary hotspot in Southeast Asia. Scientific Reports 7: 11573. https://doi.org/10.1038/s41598-017-11957-9

Bolotov IN, Konopleva ES, Vikhrev IV, Gofarov MY, Lopes-Lima M, Bogan AE, Lunn Z, Chan N, Win T, Aksenova OV, Tomilova AA, Tanmuangpak K, Tumpeesuwan S, Kondakov AV (2020) New freshwater mussel taxa discoveries clarify biogeographic division of Southeast Asia. Scientific Reports 10: 6616. https://doi.org/10.1038/s41598-020-63612-5

Bolotov IN, Konopleva ES, Chan N, Lunn Z, Win T, Gofarov MY, Kondakov AV, Tomilova AA, Vikhrev IV (2022) A riverine biodiversity hotspot in northern Myanmar supports three new and narrowly endemic freshwater mussel species. Aquatic Conservation: Marine and Freshwater Ecosystems 32: 1490–1508. https://doi.org/10.1002/aqc.3850

Bolotov IN, Konopleva ES, Vikhrev IV, Gofarov MY, Kondakov AV, Lyubas AA, Soboleva AA, Chan N, Lunn Z, Win T, Inkhavilay K (2023) Integrative taxonomic reappraisal and evolutionary biogeography of the most diverse freshwater mussel clade from Southeast Asia (Pseudodontini). Water 15: 3117. https://doi.org/10.3390/w15173117

Brandt RAM (1974) The non-marine aquatic Mollusca of Thailand. Archiv für Molluskenkunde 105: 1–423.

Cookey PE, Darnsawasdi R, Ratanachai C (2016) A conceptual framework for assessment of governance performance of lake basins: Towards transformation to adaptive and integrative governance. Hydrology 3: 12. https://doi.org/10.3390/hydrology3010012

Crosse H, Fischer P (1876) Mollusques fluviatiles, recueillis au Cambodge, par la mission scientifique francaise de 1873. Journal de Conchyliologie 24: 313–342.

Dautzenberg P, Fischer H (1905) Liste des mollusques récoltés par M.H. Mansuy en Indo-chine et au Yunnan et description d'especes nouvelles. Journal de Conchyliologie 53: 343–471.

Deshayes G-P, Jullien J (1876) Mémoire sur les mollusques nouveaux du Cambodge: Envoyés au muséum par M. le docteur Jullien. Bulletin des Nouvelles Archives du Muséum d'Histoire Naturelle 10: 115–163. https://doi.org/10.5962/bhl.title.10273

Duan Y, Fu S, Ye Z, Bu W (2023) Phylogeny of Urostylididae (Heteroptera: Pentatomoidea) reveals rapid radiation and challenges traditional classification. Zoologica Scripta 52: 264–278. https://doi.org/10.1111/zsc.12582

Fischer P (1891) Catalogue et distribution géographique des mollusques terrestres, fluviatiles & marins d'une partie de l'Indo-chine (Siam, Laos, Cambodge, Cochinchine, Annam, Tonkin). Bulletin de la Société d'Histoire Naturelle d'Autun 4: 87–276. https://doi.org/10.5962/bhl.title.14809

Fischer H, Dautzenberg P (1904) Catalogue des mollusques terrestres et fluviatiles de l'Indo-Chine orientale cites jusqu'à ce jour. Mission Pavie, Etudes diverses 3: 390–442.

Fischer-Piette E (1950) Liste des types décrits dans le Journal de Conchyliologie et conservés dans la collection de ce journal (avec planches) (suite). Journal de Conchyliologie 90: 149–180.

Froufe E, Bolotov I, Aldridge DC, Bogan AE, Breton S, Gan HM, Kovitvadhi U, Kovitvadhi S, Riccardi N, Secci-Petretto G, Sousa R, Teixeira A, Varandas S, Zanatta D, Zieritz A, Fonseca MM, Lopes-Lima M (2020) Mesozoic mitogenome rearrangements and freshwater mussel (Bivalvia: Unionoidea) macroevolution. Heredity 124: 182–196. https://doi.org/10.1038/s41437-019-0242-y

Graf DL, Cummings KS (2007) Review of the systematics and global diversity of freshwater mussel species (Bivalvia: Unionoida). Journal of Molluscan Studies 73: 291–314. https://doi.org/10.1093/mollus/eym029

Graf DL, Cummings KS (2021) A 'big data' approach to global freshwater mussel diversity (Bivalvia: Unionoida), with an updated checklist of genera and species. Journal of Molluscan Studies 87: eyaa034. https://doi.org/10.1093/mollus/eyaa034

Graf DL, Cummings KS (2024) The freshwater mussels (Unionoida) of the World (and other less consequential bivalves). https://mussel-project.uwsp.edu/ [accessed 30 Sept 2024]

Grummer JA, Morando MM, Avila LJ, Sites JW, Leaché AD (2018) Phylogenomic evidence for a recent and rapid radiation of lizards in the Patagonian *Liolaemus fitzingerii* species group. Molecular Phylogenetics and Evolution 125: 243–254. https://doi.org/10.1016/j.ympev.2018.03.023

Haas F (1920) Die Unioniden. In: Küster HC (Ed) Systematisches Conchylien-Cabinet von Martini und Chemnitz 9. pt. 2, h. 53. 305–344, pls. 369–373. https://doi.org/10.5962/bhl.title.120018

Haas F (1924) Beiträge zu einer Monographie der asiatischen Unioniden. Abhandlungen der Senckenbergischen Naturforschenden Gesellschaft 38: 129–203.

Haas F (1969) Superfamilia Unionacea. In: Martens R, Hennig W (Eds) Das Tierrich, Lieferung Vol 88. Walter de Gruyter, Berlin, 1–663.

Hoang DT, Chernomor O, von Haeseler A, Minh BQ, Vinh LS (2018) UFBoot2: Improving the Ultrafast Bootstrap Approximation. Molecular Biology and Evolution 35: 518–522. https://doi.org/10.1093/molbev/msx281

Huang X-C, Rong J, Liu Y, Zhang M-H, Wan Y, Ouyang S, Zhou C-H, Wu X-P (2013) The complete maternally and paternally inherited mitochondrial genomes of the endangered freshwater mussel *Solenaia carinatus* (Bivalvia: Unionidae) and implications for Unionidae taxonomy. PLoS ONE 8: e84352. https://doi.org/10.1371/journal.pone.0084352

Jeratthitikul E, Sutcharit C (2023) Multi-locus phylogeny reveals a new freshwater mussel in the genus *Bineurus* Simpson, 1900 (Unionidae: Pseudodontini) from Thailand. Tropical Natural History Supplement 7: 173–180.

Jeratthitikul E, Phuangphong S, Sutcharit C, Prasankok P, Kongim B, Panha S (2019a) Integrative taxonomy reveals phenotypic plasticity in the freshwater mussel *Contradens contradens* (Bivalvia: Unionidae) in Thailand, with a description of a new species. Systematics and Biodiversity 17: 134–147. https://doi.org/10.1080/14772000.2018.1554607

Jeratthitikul E, Sucharit C, Prasankok P (2019b) Molecular phylogeny of the Indochinese freshwater mussel genus *Scabies* Haas, 1911 (Bivalvia: Unionidae). Tropical Natural History 19: 21–36.

Jeratthitikul E, Paphatmethin S, Zieritz A, Lopes-Lima M, Ngor PB (2021a) *Hyriopsis panhai*, a new species of freshwater mussel from Thailand (Bivalvia: Unionidae). Raffles Bulletin of Zoology 69: 124–136. https://doi.org/10.26107/RBZ-2021-0011

Jeratthitikul E, Sutcharit C, Ngor PB, Prasankok P (2021b) Molecular phylogeny reveals a new genus of freshwater mussels from the Mekong River Basin (Bivalvia: Unionidae). European Journal of Taxonomy 775: 119–142. https://doi.org/10.5852/ejt.2021.775.1553

Jeratthitikul E, Paphatmethin S, Sutcharit C, Ngor PB, Inkhavilay K, Prasankok P (2022) Phylogeny and biogeography of Indochinese freshwater mussels in the genus *Pilsbryoconcha* Simpson, 1900 (Bivalvia: Unionidae) with descriptions of four new species. Scientific Reports 12: 20458. https://doi.org/10.1038/s41598-022-24844-9

Jeratthitikul E, Sutcharit C, Prasankok P (2024) Two new genera and three new species of exceptionally rare and endemic freshwater mussels (Bivalvia: Unionidae) from the Mekong Basin. Zoosystematics and Evolution 100: 1333–1345. https://doi.org/10.3897/zse.100.130929

Konopleva ES, Bolotov IN, Spitsyn VM, Kondakov AV, Gofarov MY, Vikhrev IV (2019a) A new *Contradens* from Laos (Bivalvia: Unionidae: Contradentini). Ecologica Montenegrina 24: 25–31. https://doi.org/10.37828/em.2019.24.5

Konopleva ES, Pfeiffer JM, Vikhrev IV, Kondakov AV, Gofarov MY, Aksenova OV, Lunn Z, Chan N, Bolotov IN (2019b) A new genus and two new species of freshwater mussels (Unionidae) from western Indochina. Scientific Reports 9: 4106. https://doi.org/10.1038/s41598-019-39365-1

Konopleva ES, Bolotov IN, Pfeiffer JM, Vikhrev IV, Kondakov AV, Gofarov MY, Tomilova AA, Tanmuangpak K, Tumpeesuwan S (2021) New freshwater mussels from two Southeast Asian genera *Bineurus* and *Thaiconcha* (Pseudodontini, Gonideinae, Unionidae). Scientific Reports 11: 8244. https://doi.org/10.1038/s41598-021-87633-w

Konopleva ES, Lheknim V, Sriwoon R, Kondakov AV, Tomilova AA, Gofarov MY, Vikhrev IV, Bolotov IN (2023) Diversity and phylogenetics of freshwater mussels (Unionidae) from southern Thailand with the description of one new genus and five new species-group taxa. Diversity 15: 10. https://doi.org/10.3390/d15010010

Lanfear R, Frandsen PB, Wright AM, Senfeld T, Calcott B (2017) PartitionFinder 2: New methods for selecting partitioned models of evolution for molecular and morphological phylogenetic analyses. Molecular Biology and Evolution 34: 772–773. https://doi.org/10.1093/molbev/msw260

Lopes-Lima M, Froufe E, Do VT, Ghamizi M, Mock KE, Kebapçı Ü, Klishko O, Kovitvadhi S, Kovitvadhi U, Paulo OS, Pfeiffer JM, Raley M, Riccardi N, Şereflişan H, Sousa R, Teixeira A, Varandas S, Wu X, Zanatta DT, Zieritz A, Bogan AE (2017) Phylogeny of the most species-rich freshwater bivalve family (Bivalvia: Unionida: Unionidae): Defining modern subfamilies and tribes. Molecular Phylogenetics and Evolution 106: 174–191. https://doi.org/10.1016/j.ympev.2016.08.021

Lopes-Lima M, Burlakova LE, Karatayev AY, Mehler K, Seddon M, Sousa R (2018) Conservation of freshwater bivalves at the global scale: Diversity, threats and research needs. Hydrobiologia 810: 1–14. https://doi.org/10.1007/s10750-017-3486-7

Lopes-Lima M, Bolotov IN, Tu V, Aldridge DC, Fonseca MM, Gan HM, Gofarov MY, Kondakov AV, Prié V, Sousa R, Varandas S, Vikhrev IV, Teixeira A, Wü R, Wu X, Zieritz A, Froufe E, Bogan AE (2018) Expansion and systematics redefinition of the most threatened freshwater mussel family, the Margaritiferidae. Molecular Phylogenetics and Evolution 127: 98–118. https://doi.org/10.1016/j.ympev.2018.04.041

Miller MA, Pfeiffer W, Schwartz T (2010) Creating the CIPRES Science Gateway for inference of large phylogenetic trees. 2010 Gateway Computing Environments Workshop (GCE), 1–8. https://doi.org/10.1109/GCE.2010.5676129

Minh BQ, Schmidt HA, Chernomor O, Schrempf D, Woodhams MD, von Haeseler A, Lanfear R (2020) IQ-TREE 2: New models and efficient methods for phylogenetic inference in the genomic era. Molecular Biology and Evolution 37: 1530–1534. https://doi.org/10.1093/molbev/msaa015

Morelet A (1866) Description d'espèces appartenant à la faune malacologique de l'Indo-Chine. Journal de Conchyliologie 14: 62–64.

Morlet L (1884) Description d'espèce nouvelles de coquilles, recueillies par M. Pavie, au Cambodge. Journal de Conchyliologie 32: 386–403.

Morlet L (1889) Catalogue des coquilles recueillies, par M. Pavie, dans le Cambodge et le Royaume de Siam, et description d'espèces nouvelles. Journal de Conchyliologie 37: 121–199.

Muanta S, Jeratthitikul E, Panha S, Prasankok P (2019) Phylogeography of the freshwater bivalve genus *Ensidens* (Unionidae) in Thailand. Journal of Molluscan Studies 85, 224–231. https://doi.org/10.1093/mollus/eyz013

Ng TH, Jeratthitikul E, Sutcharit C, Chhuoy S, Pin K, Pholyotha A, Siriwut W, Srisonchai R, Hogan ZS, Ngor PB (2020) Annotated checklist of freshwater molluscs from the largest freshwater lake in Southeast Asia. ZooKeys 958: 107–141. https://doi.org/10.3897/zookeys.958.53865

Ortiz-Sepulveda CM, Stelbrink B, Vekemans X, Albrecht C, Riedel F, Todd JA, Van Bocxlaer B (2020) Diversification dynamics of freshwater bivalves (Unionidae: Parreysiinae: Coelaturini) indicate historic hydrographic connections throughout the East African Rift System. Molecular Phylogenetics and Evolution 148: 106816. https://doi.org/10.1016/j.ympev.2020.106816

Paetel F (1890) Catalog der Conchylien-Sammlung. Vol. 3, 256 pp.

Pfeiffer JM, Graf DL (2015) Evolution of bilaterally asymmetrical larvae in freshwater mussels (Bivalvia: Unionoida: Unionidae). Zoological Journal of the Linnean Society 175: 307–318. https://doi.org/10.1111/zoj.12282

Pfeiffer JM, Breinholt JW, Page LM (2019) Unioverse: A phylogenomic resource for reconstructing the evolution of freshwater mussels (Bivalvia, Unionoida). Molecular Phylogenetics and Evolution 137: 114–126. https://doi.org/10.1016/j.ympev.2019.02.016

Pfeiffer JM, Graf DL, Cummings KS, Page LM (2021) Taxonomic revision of a radiation of Southeast Asian freshwater mussels (Unionidae: Gonideinae: Contradentini+Rectidentini). Invertebrate Systematics 35: 394–470. https://doi.org/10.1071/IS20044

Ronquist F, Teslenko M, van der Mark P, Ayres DL, Darling A, Höhna S, Larget B, Liu L, Suchard MA, Huelsenbeck JP (2012) MrBayes 3.2: Efficient Bayesian phylogenetic inference and model choice across a large model space. Systematic Biology 61: 539–542. https://doi.org/10.1093/sysbio/sys029

Saluja R, Piman T (2022) The wetlands of the lower Songkhram River basin need collaborative conservation. Policy Brief. Stockholm Environment Institute.https://doi.org/10.51414/sei2022.029

San Mauro D, Agorreta A (2010) Molecular systematics: A synthesis of the common methods and the state of knowledge. Cellular and Molecular Biology Letters 15: 311–341. https://doi.org/10.2478/s11658-010-0010-8

Simpson CT (1900) Synopsis of the naiades, or pearly fresh-water mussels. Proceedings of the United States National Museum 22: 501–1044. https://doi.org/10.5479/si.00963801.22-1205.501

Simpson CT (1914) A descriptive catalogue of the naiades, or pearly fresh-water mussels. Parts I–III. Bryant Walker, Detroit, Michigan, 1540 pp. https://doi.org/10.5962/bhl.title.10910

Tamura K, Stecher G, Kumar S (2021) MEGA11: Molecular Evolutionary Genetics Analysis Version 11. Molecular Biology and Evolution 38: 3022–3027. https://doi.org/10.1093/molbev/msab120

von Martens EV (1860) On the mollusca of Siam. Proceedings of the Zoological Society of London 1860: 6–18.

Zieritz A, Lopes-Lima M, Bogan AE, Sousa R, Walton S, Rahim KAA, Wilson J-J, Ng P-Y, Froufe E, McGowan S (2016) Factors driving changes in freshwater mussel (Bivalvia, Unionida) diversity and distribution in Peninsular Malaysia. Science of The Total Environment 571: 1069–1078. https://doi.org/10.1016/j.scitotenv.2016.07.098

Zieritz A, Bogan AE, Froufe E, Klishko O, Kondo T, Kovitvadhi U, Kovitvadhi S, Lee JH, Lopes-Lima M, Pfeiffer JM, Sousa R, Van Do T, Vikhrev I, Zanatta DT (2018) Diversity, biogeography and conservation of freshwater mussels (Bivalvia: Unionida) in East and Southeast Asia. Hydrobiologia 810: 29–44. https://doi.org/10.1007/s10750-017-3104-8

Zieritz A, Froufe E, Bolotov I, Gonçalves DV, Aldridge DC, Bogan AE, Gan HM, Gomes-Dos-Santos A, Sousa R, Teixeira A, Varandas S, Zanatta D, Lopes-Lima M (2021a) Mitogenomic phylogeny and fossil-calibrated mutation rates for all F- and M-type mtDNA genes of the largest freshwater mussel family, the Unionidae (Bivalvia). Zoological Journal of the Linnean Society 193: 1088–1107. https://doi.org/10.1093/zoolinnean/zlaa153

Zieritz A, Jainih L, Pfeiffer J, Rahim KAA, Prayogo H, Anwari MS, Fikri AH, Diba F, Taha H, Sulaiman Z, Froufe E, Lopes-Lima M (2021b) A new genus and two new, rare freshwater mussel (Bivalvia: Unionidae) species endemic to Borneo are threatened by ongoing habitat destruction. Aquatic Conservation: Marine and Freshwater Ecosystems 31: 3169–3183. https://doi.org/10.1002/aqc.3695

Zieritz A, Pfeiffer J, Rahim KAA, Prayogo H, Anwari MS, Diba F, Froufe E, Blackwell T, Hartikainen H, Lopes-Lima M (2024) High endemic freshwater mussel (Bivalvia: Unionida) diversity in western Borneo, with description of three new species. Zoological Journal of the Linnean Society 201: zlae076. https://doi.org/10.1093/zoolinnean/zlae076

Supplementary material 1

List of voucher specimens with GenBank accession numbers used in phylogenetic analysis

Authors: Ekgachai Jeratthitikul, Chirasak Sutcharit, Pongpun Prasankok

Data type: docx

Link: https://doi.org/10.3897/zookeys.1224.140549.suppl1

ZooKeys 1224: 211–252 (2025)
DOI: 10.3897/zookeys.1224.137972

Research Article

Sounds of the northern Andes: the calls of a diverse and endangered frog community (Amphibia, Anura) from Ecuador

Diego Batallas[1,2,3], Rafael Márquez[4], Juan M. Guayasamin[2]

1 *Departamento de Biodiversidad, Ecología y Evolución, Facultad de Ciencias Biológicas, Universidad Complutense de Madrid, Calle J.A. Nováis 12, 28040, Madrid, Spain*
2 *Laboratorio de Biología Evolutiva, Colegio de Ciencias Biológicas y Ambientales COCIBA, Universidad San Francisco de Quito USFQ, vía Interoceánica y Diego de Robles 17-1200-841, Quito, Ecuador*
3 *Instituto Nacional de Biodiversidad (INABIO), Calle Rumipamba 341 y Av. de Los Shyris, Casilla Postal 17-07-8976, Quito, Ecuador*
4 *Fonoteca Zoológica, Departamento de Biodiversidad y Biología Evolutiva, Museo Nacional de Ciencias Naturales (CSIC), 28006, Madrid, Spain*
Corresponding author: Diego Batallas (bioandino_kakaram@hotmail.com)

Abstract

The emission of calls is one of the most distinctive and important reproductive traits in anurans. Given the biological significance of vocalizations, this trait is also useful for identification proposes and is key in recognizing cryptic diversity. However, the majority of the calls from tropical ecosystems, especially in the high Andean mountains, are unknown. Between 2016 and 2021, a total of 14 expeditions were conducted to the forests and moorlands of the eastern and western Andean Mountain range of the province of Carchi-Ecuador, at elevations ranging from 2694 to 3848 m a.s.l. The objective of these expeditions was to record the calls of the anuran fauna present in these ecosystems. In total, 30 anuran species were recorded, and calls of 20 species were described, 15 of which are described and reported for the first time in the present study. The call of *Hyloxalus delatorreae*, a critically endangered species, is described with a remarkable recording of the call of *Niceforonia brunnea*, a species considered mute. In addition, nine are candidate species, including the first record of *Pristimantis farisorum* for Ecuador. This study represents the most comprehensive and accurate acoustic documentation of a highland community, which will facilitate taxonomic and conservation work in the area.

Key words: Andean mountains, anurofauna, bioacoustics, Carchi province, conservation

Academic editor: Luis Ceríaco
Received: 27 September 2024
Accepted: 21 December 2024
Published: 30 January 2025

ZooBank: https://zoobank.org/4E773D7F-0DBE-4268-B6DB-91FDB90B8DAF

Citation: Batallas D, Márquez R, Guayasamin JM (2025) Sounds of the northern Andes: the calls of a diverse and endangered frog community (Amphibia, Anura) from Ecuador. ZooKeys 1224: 211–252. https://doi.org/10.3897/zookeys.1224.137972

Introduction

Acoustic communication is one of the most varied communication systems that animals use to transmit information and interact with each other (Redondo 1994; Bradbury and Vehrencamp 1998; Simmons 2003). This type of communication is one of the most distinctive, important, and conspicuous ethological traits of anurans (Zelick et al. 1999; Colafrancesco and Gridi-Papp 2016). They emit different types of calls, which are associated with a specific social context and function (Wells and Schwartz 2007; Toledo et al. 2015; Köhler et al. 2017). Given the evolutionary role of vocalization in conspecific recognition, the knowledge and analysis of anuran calls represent a relevant tool for species identification, especially

in sympatry. The analysis and determination of call variations, in conjunction with the use of molecular and morphometric tools, has enabled the resolution of phylogenetic and taxonomic inconsistencies in certain groups of species. (e.g., Páez-Vacas et al. 2010; Hutter and Guayasamin 2015; Caminer et al. 2017; Ron et al. 2018; Páez and Ron 2019; Yánez-Muñoz et al. 2021). The study of species using integrative approaches has led to a more comprehensive understanding of diversity in taxonomic, phylogeographic, evolutionary, and conservation terms (Angulo and Reichle. 2008; Gill et al. 2016; Mendoza-Henao et al. 2020, 2023).

This study focuses on the acoustic description of several localities in the Andes of northern Ecuador, part of the tropical Andes, one of the most biodiverse regions on Earth (Duellman 1999; Hutter et al. 2017; Hazzi et al. 2018). The northern Andes exhibit the highest levels of endemism among ecosystems (Armesto and Señaris 2017; Guayasamin et al. 2020; Yánez-Muñoz et al. 2020). However, the region is threatened by the constant destruction of its habitat (Guayasamin et al. 2022). As a consequence, a significant part of the biodiversity present in these ecosystems being in critical danger of extinction (Ojala-Barbour et al. 2019; Yánez-Muñoz et al. 2020).

In this study, we characterized and described the acoustic parameters of anurans calls present in the high Andean ecosystems of northern Ecuador, Carchi province. We highlight the utility of vocalizations to identify species and to discover new taxa.

Materials and methods

Study area

A total of 13 localities were selected in the northern Andes of Ecuador, Carchi province, at elevations ranging from 2694 to 3848 m a.s.l. (Table 1). The habitats and microhabitats of the different high Andean ecosystems were examined, encompassing the western and eastern slopes of the Andes (Figs 1, 2).

Field techniques

A total of 14 expeditions were conducted across two distinct phases. The initial phase of the study was conducted between December 2016 and May 2017 and comprised of a total of six expeditions, with ten sampling days per month. The second phase between 2020–2021 comprised eight field expeditions (five in 2020 and three in 2021), each of which lasted 12 days (limited by the restrictions imposed by the Covid-19 pandemic). The rainfall regime of the northern zone of Ecuador, from October to May, was considered in the context of the fieldwork. At the selected localities, individualized recordings were made utilizing direct visual encounters and auditive bands transects (Heyer et al. 2014; Rueda-Almondacid et al. 2006) between 18:00 and 23:00 h; similarly, recordings were made between 5:00 and 10:00 h and 15:00 and 17:00 h, in order to record anurans exhibiting nocturnal, diurnal, and crepuscular activities, respectively.

The calls were recorded using an Olympus LS-100 digital recorder, which was coupled to a Sennheiser K6-C modular system and ME 66 shotgun microphone head, or to a Rode NTG3 shotgun microphone. All recordings were made at a sampling rate of 44.1 kHz and 16 “bits” resolution, saving the audio files in the

Table 1. Details of the 11 localities and ecosystems of the province of Carchi (Ecuador) that were sampled in this study. The abbreviations used in the ecosystem correspond to: Northeastern Andean High Mountain Evergreen Forest (**BsAn01**); Northwestern Andean High Mountain Evergreen Forest (**BsAn03**); Northwestern Andean Montane Evergreen Forest (**BsMn03**); Northeastern Andean Montane Evergreen Forest (**BsMn01**); Paramo Evergreen Forest (**BsSn01**); Caulescent Rosette and Páramo Grassland (frailejones) (**RsSn01**). The classification system proposed by the Ministerio del Ambiente (2013) is followed.

Locality	Coordinates	Altitude	Ecosystem
Moran	0°46'07.10"N, 78°03'20.00"W	2785	BsMn03
Bosque de los Arrayanes	0°33'03.44"N, 77°47'14.68"W	2870	BsMn01
Las canoas	0°48'55.2"N, 77°43'34.4"W	2877	BsMn03
Loma San Francisco	0°31'20.7"N, 77°46'38.1"W	2922	BsAn01
Cascadas de Cartagena	0°41'25.3"N, 77°38'14.1"W	3068	BsAn01
Loma la Esperanza	0°30'57.6"N, 77°46'09.5"W	3118	BsAn01
Cerro la Bretaña	0°34'07.92"N, 77°42'53.00"W	3226	BsAn01
Camino Tufiño-Maldonado	0°48'10.0"N, 78°00'16.8"W	3362	BsMn03
San Francisco de Pioter	0°40'16.1"N, 77°47'43.9"W	3416	BsAn03
Aguas hediondas	0°48'38.01"N, 77°54'15.5"W	3595	BsSn01
Potrerillos	0°48'15.5"N, 77°58'03.1"W	3785	BsSn01
Páramo del Ángel	0°44'29.3"N, 78°01'49.3"W	3848	RsSn01
Virgen Negra	0°39'17.57"N, 77°36'21.13"W; 0°39'54.2"N, 77°38'42.1"W	2994 3627	BsAn01 RsSn01

uncompressed WAV format. Air temperature and humidity data for each of the recordings were taken with a Taylor 1523 digital thermohydrometer. After recording, specimens were manually located and collected. Specimens were sacrificed according to the recommendations of Chen and Combs (1999) and preserved according to the protocols of Simmons (2015), with liver samples extracted for genetic analyses and preserved in 99% ethanol. The handling and collection of specimens was conducted under permits granted by The Ministerio del Ambiente y Agua de Ecuador: MAE-DNB-CM-2016-0045 y MAE-DNB-CM-2018-0105.

The specimens were deposited at the División de Herpetología del Instituto Nacional de Biodiversidad (**DHMECN**), Quito, Ecuador and at the Museo de Zoología de la Universidad San Francisco de Quito (**ZSFQ**). Tissues for molecular analyses are deposited at the Laboratorio de Biología Evolutiva de la Universidad San Francisco de Quito (**LBE**) and acoustic recordings are deposited at the Fonoteca Zoológica (www.fonozoo.com) del Museo Nacional de Ciencias Naturales (**CSIC**), Madrid, Spain.

Bioacoustic analysis

The spectral and temporal parameters of calls were analyzed using the software Raven 1.6 (K. Lisa Yang Center for Conservation Bioacoustics 2024), using for the spectrograms Hann window with 256 samples of the Fast Fourier Transformation (FFT), and time grids with a hop size of 26 samples, with 90% of overlap and a frequency grid with 512 samples of the Discrete Fourier Transformation (DFT), and a 3 dB filter bandwidth of 248 Hz. The parameters analyzed were: (**CD**) Call duration: Total time elapsed from the beginning to the end of a call. (**IC**) Interval between calls: Duration of the interval of silence between

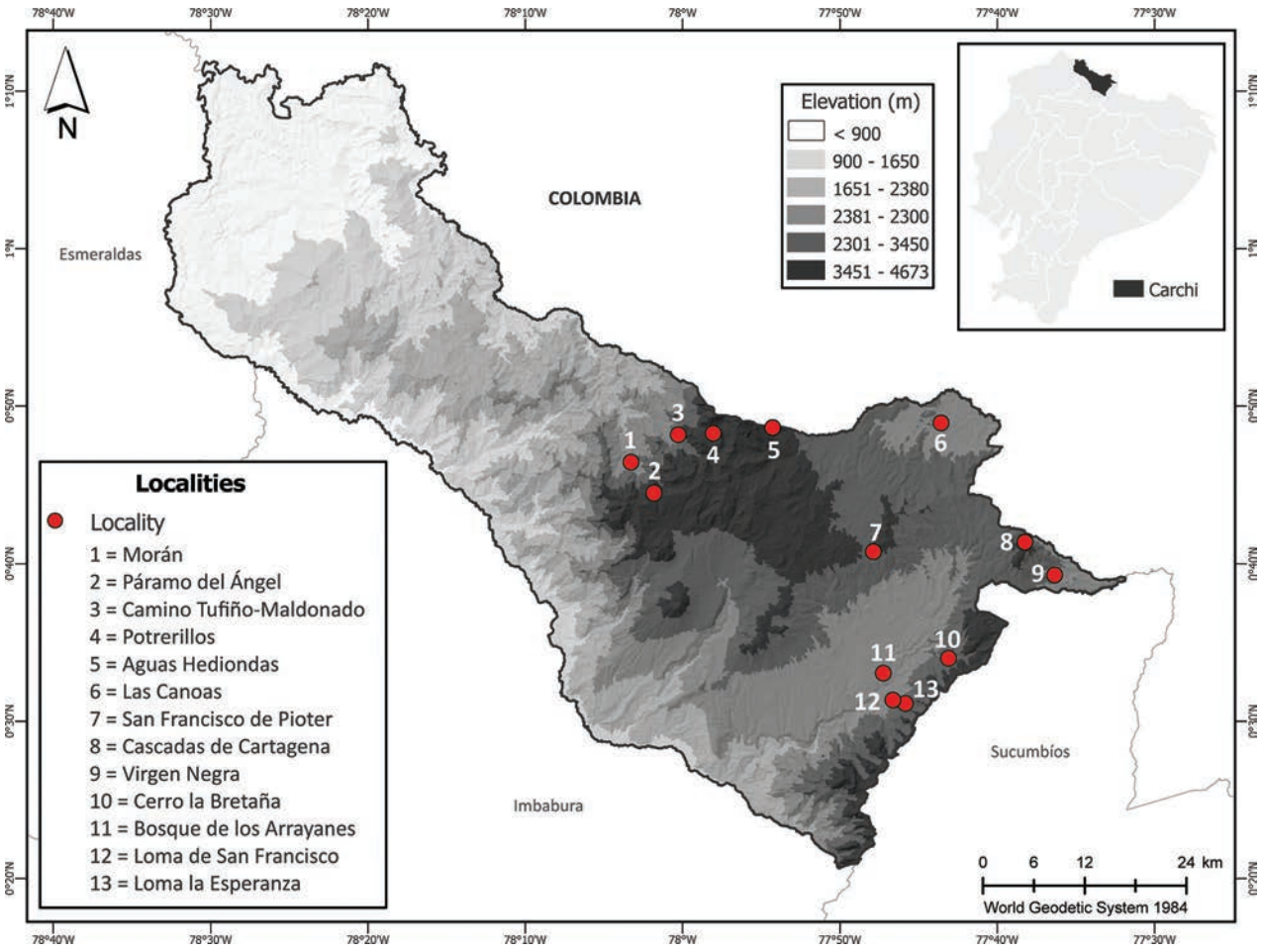

Figure 1. Map of Carchi province, Ecuador, showing the exact locations of the sampled localities.

two consecutive calls. (**CR**) Call rate: Total number of calls emitted in a specific period of time, calculated as calls per minute. In this study, the call rate was determined by analyzing the entire recording, which contained regular sequences of calls while avoiding intervals with very prolonged silences. **(NC)** Notes/call: Number of notes in a call, where a note is a subunit of a call separated from other notes by intervals of silence. (**ND**) Note Duration: Total time elapsed from the beginning to the end of a note. (**IN**) Intervals between notes: Duration of the interval of silence between two consecutive notes. (**NR**) Note rate: Total number of notes emitted in a specific period of time, calculated as notes per second. (**PN**) Pulse/note: Number of pulses in a call or note, where a pulse is the shortest indivisible subunit of a call. (**PD**) Pulse duration: Total time elapsed from the beginning to the end of a pulse. (**IP**) Intervals between pulses: Duration of the interval of silence between two consecutive pulses. (**PR**) Pulse rate: Total number of pulses emitted in a specific period of time, calculated as pulses per second. (**FF**) Fundamental frequency: The lowest frequency or first harmonic of a harmonic series, which frequently coincides with the dominant frequency. (**DF**) Dominant frequency: The frequency that contains the highest energy within the call or the peak of the frequency spectrum with the highest amplitude value. (**MinF**) Minimum frequency: Minimum or lower limit of the frequency, with consideration given to the frequency at 5% for this value. (**MaxF**) Maximum frequency: Maximum or upper limit of the frequency, with consideration

Figure 2. Characteristic habitats of the high-altitude Andean ecosystems of northern Ecuador, Carchi Province. **A** reserva ecológica del Ángel **B** Páramo San francisco de Pioter **C** Laguna cerro la Bretaña **D** Morán **E** Virgen Negra **F** San Francisco de Pioter **G** Cerro la Bretaña **H** La Changadera-Morán; **I**) San francisco de Pioter; Bosque de los Arrayanes. The upper part shows the Páramo ecosystems, the middle part a general overview, and the lower part the Andean montane forests.

given to the frequency at 95% for this value. (**FM**) Frequency modulation: Variation of the dominant frequency that increases or decreases in comparison to the initial and final frequencies of the call. (**NH**) Number of visible harmonics: Definitions, terminology, and measurements of acoustic parameters have been reviewed and adapted from the works of Cocroft and Ryan (1995), Köhler et al. (2017), and Sueur (2018). The definition of call structure (note-pulse) and the calculation of frequency modulation were based on Emmrich et al. (2020). In the measurement of the minimum and maximum frequencies we followed the recommendations of Forti et al. (2019). The variability of the calls generated different types of interpretations and values for their temporal and spectral parameters (see Figs 3, 4). The oscillogram and spectrogram figures were processed and constructed in the R software (R Development Core Team 2024), through the Seewave package v. 2.1.4 (Sueur et al. 2008), using a Hann window at 99% overlap with a size of 256 samples of the fast Fourier transform (FFT). The audio files in WAV format were imported with the tuneR package v. 1.4.7 (Ligges et al. 2018). With the values of the analyzed parameters, the measures of central tendency (means) and dispersion (maximum, minimum, and standard deviation) were calculated. A Principal Component Analysis (PCA) was

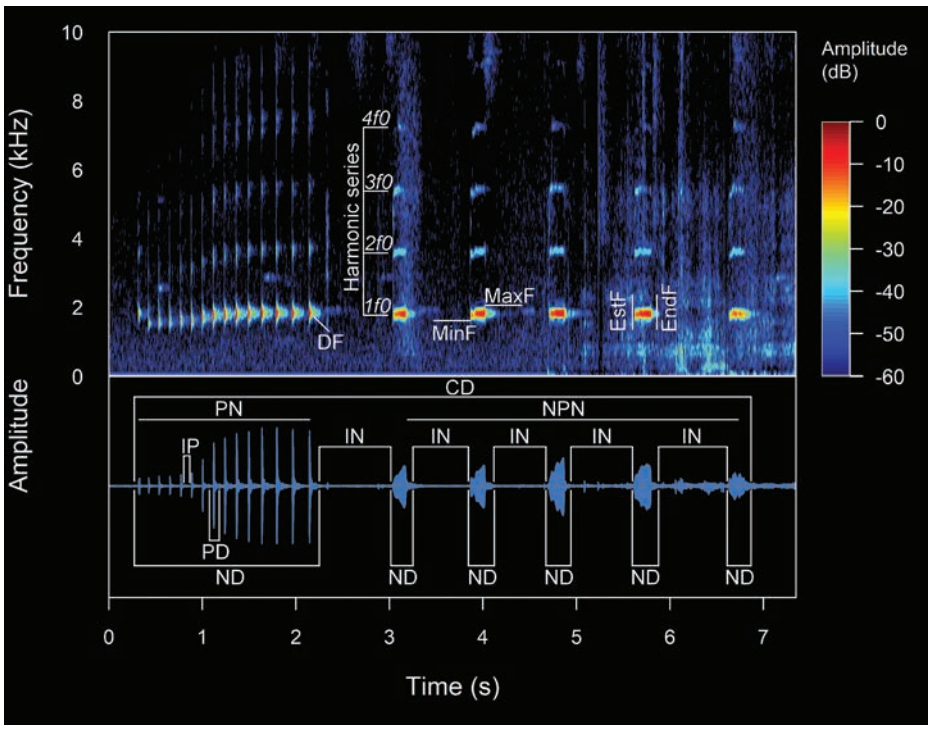

Figure 3. The spectral (above) and temporal (bellow) parameters used in the analyses performed in this study. Abbreviations: **CD** Call duration; **ND** Note Duration; **PN** Pulsed note; **NPN** Non-Pulsed Notes **IN** Intervals between notes; **PD** Pulse duration; **IP** Intervals between pulses; **DF** Dominant frequency; **MinF** Minimum frequency; **MaxF** Maximum frequency; **Estf** Start-frequency; **Endf** End-frequency; **Harmonic Series** series of harmonics visible in the frequency spectrum (1f0 = first harmonic, 2f0 = second harmonic, 3f0 = third harmonic, 4f0 = fourth harmonic)

conducted using the prcomp function in R software (R Development Core Team 2024) leveraging the mean values of eight acoustic variables from the analyzed calls to preliminarily and prospectively determine the acoustic differentiation among the species under study. The results of the PCA were subsequently visualized using the ggplot2 package in R (Wickham 2016).

Taxonomic identification and candidate species

Taxonomic nomenclature follows Frost (2024). The identification of the collected males was conducted using a combination of specialist keys, reference materials, taxonomic reviews, museum collections, and input from subject matter experts (e.g., Coloma 1995; Lynch and Duellman 1997; Duellman and Lehr 2009; Duellman 2015; Guayasamin et al. 2020). In regard to the candidate species, we have adhered to the terminology and designations set forth by Franco-Mena et al. (2023). These authors, in turn, followed Vieites et al. (2009) and Padial et al. (2010), particularly in the case of the *Pristimantis myersi* group. The molecular revisions and sequencing of this group were conducted using genetic material derived from the collections generated in the present study. The remaining species, for which no specific identity has been determined, are regarded as unconfirmed candidates based on their morphological and bioacoustical characteristics.

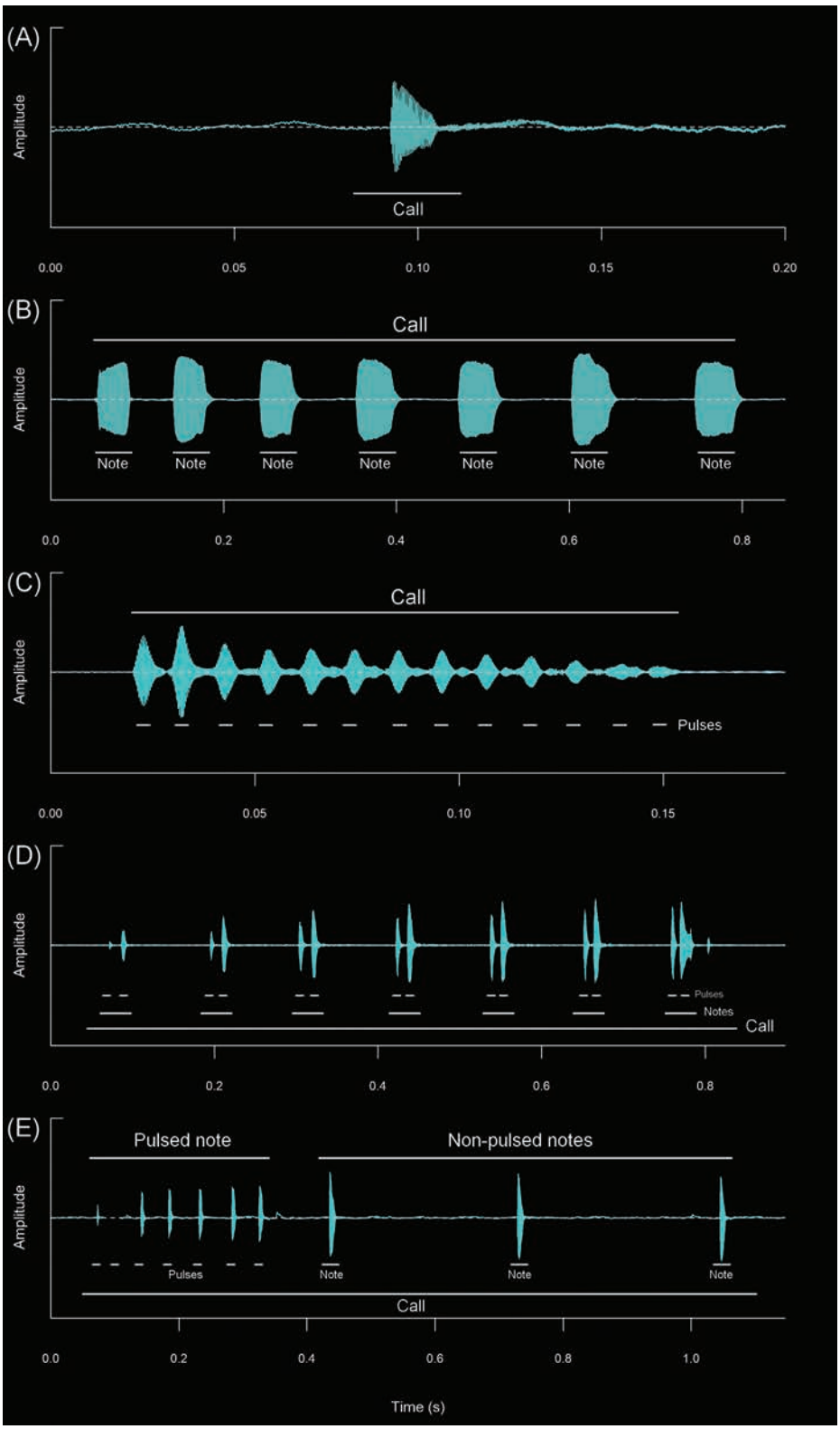

Figure 4. Types of calls analyzed in this study, classified based on their temporal characteristics and note-centered focus (Köhler et al. 2017; Emmrich et al. 2020). **A** non-pulsed simple call (*Pristimantis* sp. 4; *Pristimantis myersi*; ZSFQ 4427) **B** call with uniform non-pulsed notes (*Hyloxalus* sp.**;** ZSFQ 4442) **C** call with one pulsed note (*Centrolene buckleyi*; DHMECN 13375) **D** call with uniform pulsed notes (*Pristimantis* sp. 5; *Pristimantis myersi* group; DHMECN 13334) **E** complex call (*Pristimantis* sp. 3; *Pristimantis myersi*; ZSFQ 4554).

Results

A total of 30 species belonging to six families have been documented in the high-altitude Andean ecosystems of northern Ecuador, Carchi province (Plates 1, 2). From this diversity, recordings of 20 species were obtained by analyzing 1197 calls from 88 males (Suppl. material 2). Nine are candidate species, with the first record for Ecuador of *Pristimantis farisorum* (Suppl. material 1, Table 2). The PCA of the calls of 88 males from 20 species showed eigenvalues > 1.0 in the first two components, which collectively account for 84.7% of the total variance. The first component (PC1) exhibits notable positive loadings on the spectral variables, including Dominant Frequency, Minimum Frequency, Maximum Frequency, Start Frequency, and End Frequency accounting for 64% of the variance. The second component (PC2) has significant negative loadings on the temporal variables, such as Call Duration, Interval Between Calls, and Call Rate (/min), accounting for 20.7% of the variance. The bioacoustics PCA demonstrates exploratory differences between the calls, manifesting as groupings and segregations among the various species, with some overlap observed in certain species groups (Table 3, Fig. 5). Below, we present detailed acoustic descriptions, organized by family:

The first component (PC1) exhibits notable positive loadings on the spectral variables, including Dominant Frequency, Minimum Frequency, Maximum Frequency, Start Frequency, and End Frequency, accounting for 64% of the variance. The second component (PC2) has significant negative loadings on the temporal variables, such as Call Duration, Interval Between Calls, and Call Rate (/min), accounting for 20.7% of the variance. The bioacoustics PCA demonstrates exploratory differences between the calls, manifesting as groupings and segregations among the various species, with some overlap observed in certain species groups (Table 3, Fig. 5). Below, we present detailed acoustic descriptions, organized by family.

CENTROLENIDAE

Centrolene buckleyi (Boulenger, 1882)

We recorded four males (Suppl. material 2, Table 2). The call (Fig. 6) is characterized by emission of a pulsed "Tri" type note (sensu Duarte-Marín et al. 2022). The recorded males were calling perched on herbaceous and shrubby vegetation in a marshy area ~ 50–150 cm above the ground. The calls are loud and can be clearly audible at distances of up to ca 200 m. *Centrolene buckleyi* is a nocturnal species with moderate vocal activity, which intensifies following a drizzle. The mean call duration is 140.18 ± 16.35 ms (range 119–183), emitted at mean intervals of 20.88 ± 6.19 s (range 11.96–32.7 s), with a mean rate of 3.1 ± 0.92 calls/minute (range 1.83–4.96 calls/minute). The calls are composed of a mean of 12.32 ± 1.13 pulses (range 11–15 pulses). The mean pulses duration is 7.76 ± 2.09 ms (range 4–18 ms), emitted at mean intervals of 4.13 ± 1.58 ms (range 1–11 ms), with a mean rate of 87.94 ± 12.54 pulses/second (range 55.56–166.67 pulses/second). The calls are upward frequency modulated, with a mean frequency modulation of 2 ± 0.65 Hz/ms (range 1.15–3.69 Hz/ms). The mean dominant frequency (coincides with the fundamental) is 3.12 ± 0.13 kHz (range 2.58–3.27 kHz). The mean minimum frequency is 2.92 ± 0.13 kHz (range 2.41–3.1 kHz), while the mean maximum frequency of 3.31 ± 0.14 kHz (range 2.84–3.53 kHz). Up to six harmonics are visible.

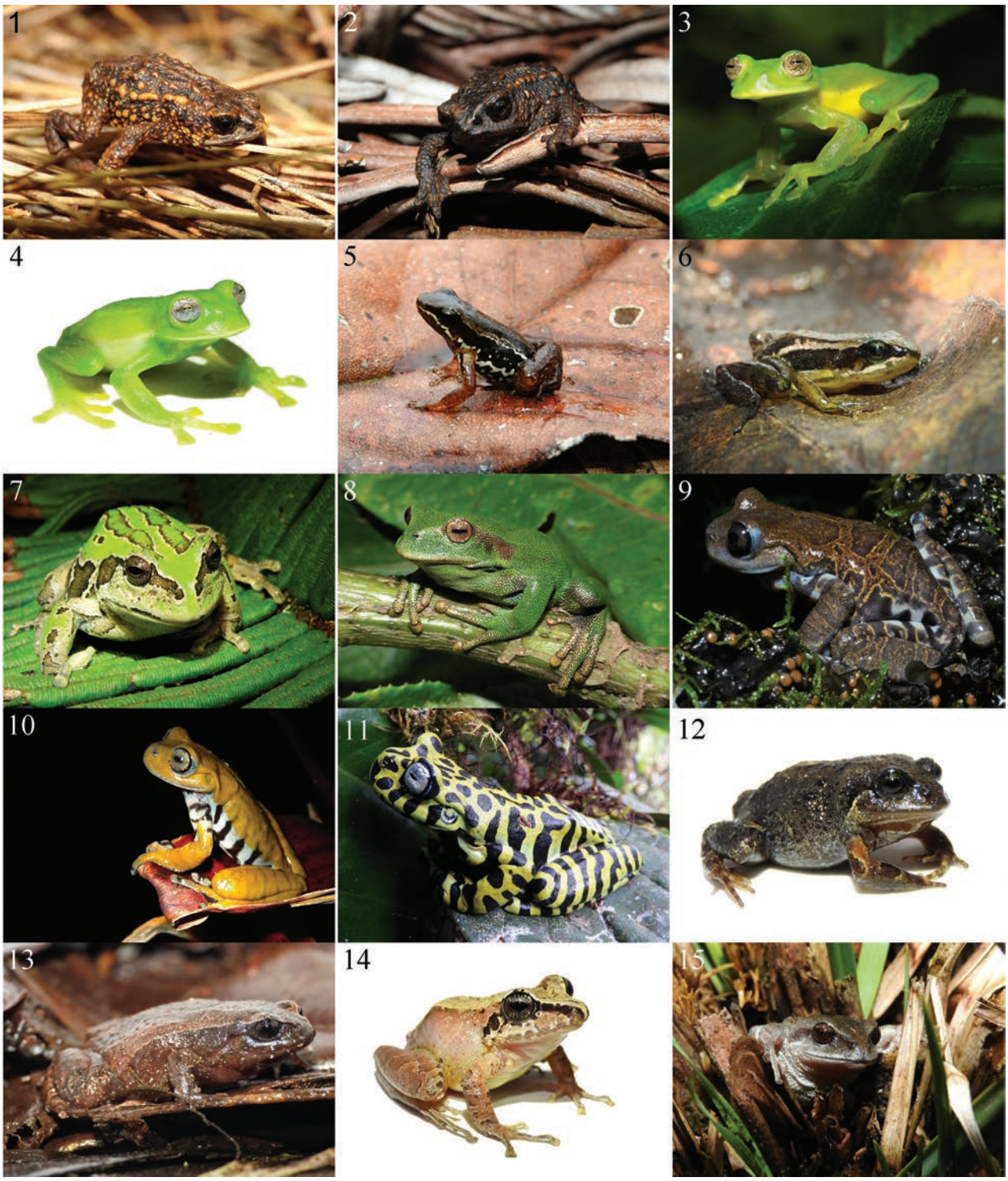

Plate 1. The anurans of the high Andean ecosystems of the Carchi province in Ecuador. **1** *Osornophryne angel* DHMECN 13783 **2** *Osornophryne bufoniformis* DHMECN 13763 **3** *Centrolene buckleyi* ZSFQ 4421 **4** *Nymphargus* sp. ZSFQ 6778 **5** *Hyloxalus delatorrae* (not_collected) **6** *Hyloxalus* sp. ZSFQ 4442 **7** *Gastrotheca espeletia* DHMECN 13758 **8** *Gastrotheca orophylax* DHMECN 13761 **9** *Hyloscirtus criptico* (not collected Photo: Mario Yánez-Muñoz) **10** *Hyloscirtus larinopygion* DHMECN 3799 Photo Mario Yánez-Muñoz) **11** *Hyloscirtus tigrinus* (not collected Photo: Libardo Tello) **12** *Niceforonia brunnea* ZSFQ 4470 **13** *Noblella* sp. ZSFQ 4543 **14** *Pristimantis actites* ZSFQ 4487 **15** *Pristimantis buckleyi* DHMECN 13670.

Plate 2. The anurans of the high Andean ecosystems of the Carchi province in Ecuador. **16** *Pristimantis Chloronotus* DSCN6763 **17** *Pristimantis farisorum* DHMECN 13760 **18** *Pristimantis festae* ZSFQ 4438 **19** *Pristimantis huicundo* DHMECN 13777 **20** *Pristimantis ocreatus* DHMECN 13650 **21** *Pristimantis pteridophilus* ZSFQ 4490 **22** *Pristimantis supernatis* DHMECN 13759 **23** *Pristimantis thymelensis* DHMECN 13787 **24** *Pristimantis unistrigatus* DHMECN 13351 **25** *Pristimantis* sp. (not collected) **26** *Pristimantis* sp. 1 *ridens* group DHMECN 13753 **27** *Pristimantis* sp. 2 *myersi* group DHMECN 13643 **28** *Pristimantis* sp. 3 *myersi* group DHMECN 13775 **29** *Pristimantis* sp. 4 *myersi* group DHMECN 13638 **30** *Pristimantis* sp. 5 *myersi* group ZSFQ 4486.

Table 2. Anurofauna recorded in the high Andean ecosystems of northern Ecuador (Carchi province), with previous information on the knowledge of their calls. *Candidates species.

Family	Species	Sample analyzed		Advertisement call
		Males	Calls	
Bufonidae	*Osornophryne angel*	–	–	Not described
Bufonidae	*Osornophryne bufoniformis*	–	–	Not described
Centrolenidae	*Centrolene buckleyi*	4	22	Bolívar et al. 1999; Guayasamin et al. 2006; Almendáriz and Batallas 2012; Guayasamin et al. 2020; Duarte-Marín et al. 2022; Cuellar-Valencia et al. 2023; Present study
Centrolenidae	*Nymphargus* sp.*	1	15	Present study
Dendrobatidae	*Hyloxalus delatorrae*	1	10	Present study
Dendrobatidae	*Hyloxalus* sp.*	4	49	Present study
Hemiphactidae	*Gastrotheca espeletia*	–	–	Sinsch and Juraske 2006
Hemiphactidae	*Gastrotheca orophylax*	4	28	Sinsch and Juraske 2006; Present study
Hylidae	*Hyloscirtus criptico*	–	–	Not described
Hylidae	*Hyloscirtus larinopygion*	–	–	Rivera-Correa et al. 2017; Cuellar-Valencia et al. 2023
Hylidae	*Hyloscirtus tigrinus*	–	–	Not described
Strabomantidae	*Niceforonia brunnea*	2	5	Present study
Strabomantidae	*Noblella* sp.*	1	3	Present study
Strabomantidae	*Pristimantis actites*	–	–	Not described
Strabomantidae	*Pristimantis buckleyi*	4	35	Cuellar-Valencia et al. 2023; Present study
Strabomantidae	*Pristimantis chloronotus*	–	–	Not described
Strabomantidae	*Pristimantis farisorum*	3	12	Present study
Strabomantidae	*Pristimantis festae*	8	96	Holzheuser and Merino-Viteri 2019; Present study
Strabomantidae	*Pristimantis huicundo*	5	47	Present study
Strabomantidae	*Pristimantis ocreatus*	6	103	Present study
Strabomantidae	*Pristimantis pteridophilus*	–	–	Not described
Strabomantidae	*Pristimantis supernatis*	2	3	Present study
Strabomantidae	*Pristimantis thymelensis*	2	57	Present study
Strabomantidae	*Pristimantis unistrigatus*	4	22	Chaves-Acuña et al. 2023; Present study
Strabomantidae	*Pristimantis* sp. 1*	–	–	Not described
Strabomantidae	*Pristimantis* sp. 2 *ridens* group*	4	25	Present study
Strabomantidae	*Pristimantis* sp. 3 *myersi* group*	12	295	Present study
Strabomantidae	*Pristimantis* sp. 4 *myersi* group*	9	181	Present study
Strabomantidae	*Pristimantis* sp. 5 *myersi* group*	6	127	Present study
Strabomantidae	*Pristimantis* sp. 6 *myersi* group*	6	62	Present study

Table 3. Results obtained from Principal Component Analysis (PCA) of eight acoustic call variables from 20 frog species in Carchi, Ecuador.

	PC1	PC2
Dominant frequency	**0.992**	0.094
Minimum frequency	**0.99**	0.108
Maximum frequency	**0.987**	0.132
Start-frequency	**0.981**	0.066
End-frequency	**0.971**	0.178
Call duration	-0.45	**0.633**
Interval between calls	-0.251	**0.812**
Call Rate (/min)	0.107	**-0.721**
Eigenvalue	5.121	1.654
% Variance	64.009	20.676
% cumulative	64.009	84.685

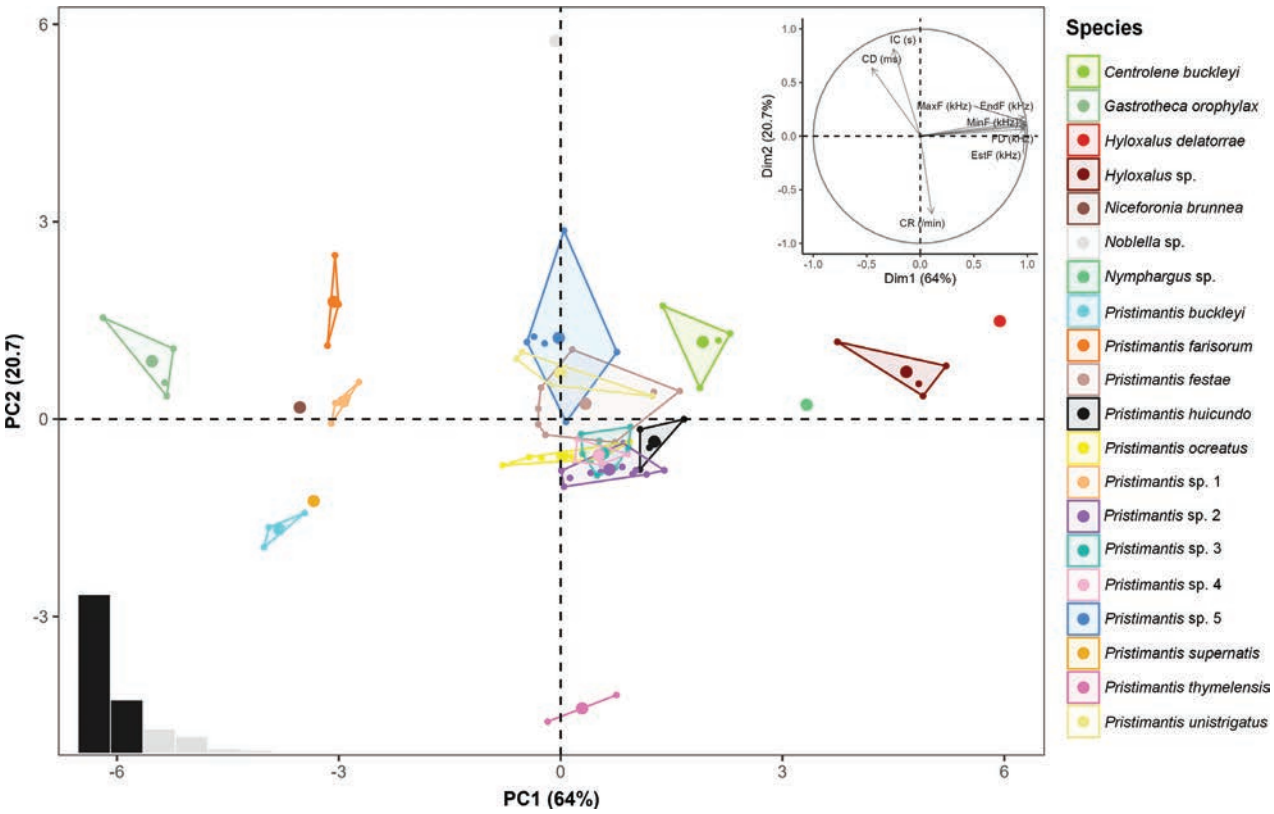

Figure 5. Principal Component Analysis (PCA) based on eight acoustic parameters of 20 Anuran species (Suppl. material 2, Table 2). The figure displays the number of principal components in the lower left-hand corner and the loading of each variable on the components in the upper right-hand corner.

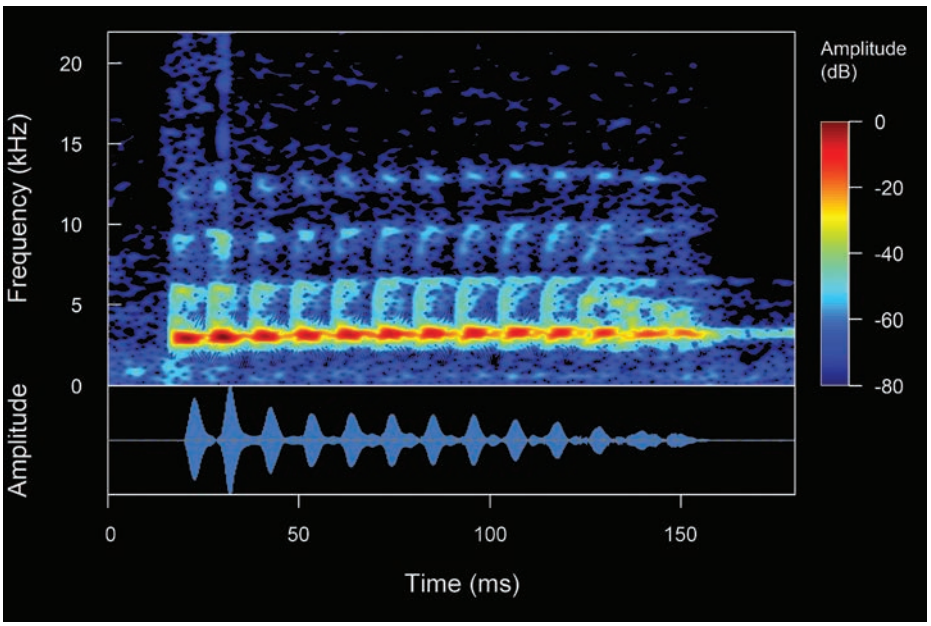

Figure 6. Spectrogram and oscillogram of the advertisement call of *Centrolene buckleyi* (DHMECN 13375, SVL 29.37 mm, 10 °C air temperature, 86% relative humidity). Spectrogram obtained using the Hann window at 99% overlap, 256 samples of FFT size and 3 dB filter bandwidth of 248 Hz.

Nymphargus sp.

We recorded one male (Suppl. material 2, Table 2). The call (Fig. 7) is characterized by the emission of a non-pulsed "Tic" type note (*sensu* Duarte-Marín et al. 2022). The recorded males were calling perched on the branches of bushes in the middle of a river ~ 180 cm above the ground. The calls are loud and audible at distances of up to ca 100 m, even in the presence of a high noise level generated by the river. *Nymphargus* sp. is a nocturnal species with low to moderate vocal activity, which intensifies in the presence of light rain. The mean call duration is 23.56 ± 7.37 ms (range 15–41 ms), emitted at mean intervals of 7.94 ± 3.43 s (range 2–13.95 s) with a mean rate of 10.31 ± 7.72 calls/minute (range 4.29–29.7 calls/minute). These are upward frequency modulated calls, with a mean frequency modulation of 6.36 ± 4.6 Hz/ms (range 0–14.33 Hz/ms). The mean dominant frequency (coincides with the fundamental) is 3.41 ± 0.05 kHz (range 3.36–3.45 kHz). The mean minimum frequency is 3.27 ± 0.04 kHz (range 3.19–3.27), while the mean maximum frequency of 3.6 ± 0.04 kHz (range 3.53–3.62 kHz). Harmonics are not visible and are attributable to loud environmental background noise (recorded in the middle of a river).

DENDROBATIDAE

Hyloxalus delatorrae (Coloma, 1995)

We recorded one male (Suppl. material 2, Table 2). The call (Fig. 8). The call is a continuous emission of pulsed notes that onomatopoeically resembles a "tri-tri-tri". The recorded male was calling from a swamp densely covered with grassland. It is a diurnal species with high vocal activity, which intensifies between 11:00–12:00 h of the day. The calls are very loud and clearly audible at distances of up to ca 800 m. It is worth mentioning that a single individual was the only frog that we were able to listen to and record (not collected) in an area of ca 5 ha. The mean call duration is 2.29 ± 0.51 s (range 0.96–2.78 s), emitted at mean intervals of 3.62 ± 0.38 s (range 2.99–4.08 s) with a mean rate of 10.88 ± 2.34 calls/minute (range 9.15–16.95 calls/minute). The calls are composed of a mean of 6.1 ± 1.2 notes (range 3–7). The mean note duration is 1.46 ± 2.47 ms (range 66–77 ms), emitted at mean intervals of 363.34 ± 24.11 ms (range 324–416 ms), with a mean rate of 2.31 ± 0.13 notes/second (range 2.04–2.54 notes/second). The notes are composed of a mean of 6.72 ± 0.81 pulses (range 6–10 pulses). The mean pulses duration is 7.99 ± 5.36 ms (range 2–26 ms). The initial pulses are the longest in each note, with a mean duration of 19.88 ± 3.89 ms (range 8–26 ms). The pulses are emitted at mean intervals of 3.22 ± 1.4 ms (range 0.6–13 ms), with a mean rate of 100.04 ± 36.57 pulses/second (range 33.48–333.33 pulses/second). The calls are upward frequency modulated, with a mean frequency modulation of 2.93 ± 3.09 Hz/ms (range 0–19.28 Hz/ms). The dominant frequency is in the second harmonic, with a mean value of 4.24 ± 0.23 kHz (range 3.19–5.0 kHz), with a mean fundamental frequency of 2.12 ± 0.1 kHz (range 1.64–2.5 kHz). The mean minimum frequency is 4.04 ± 0.18 kHz (range 2.67–4.31), and the mean maximum frequency is 4.54 ± 0.2 kHz (range 3.45–5.25 kHz). Up to eight harmonics are visible, the third one having a mean frequency of 6.37 ± 0.35 kHz (range 5–7.92 kHz) and the eighth having a mean frequency of 16.66 ± 0.61 kHz (range 13.09–17.23 kHz). There might be one or two subharmonics between the first harmonic.

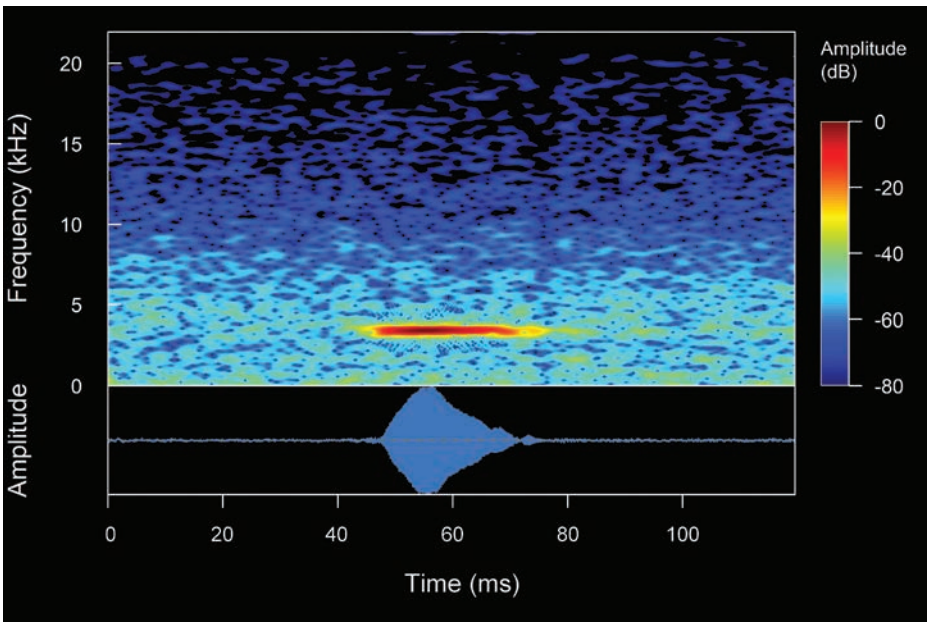

Figure 7. Spectrogram and oscillogram of the advertisement call of *Nymphargus* sp. (ZSFQ 6778, SVL 25. 68 mm, 10.3 °C air temperature, 96% relative humidity). Spectrogram obtained using the Hann window at 99% overlap, 256 samples of FFT size and 3 dB filter bandwidth of 248 Hz.

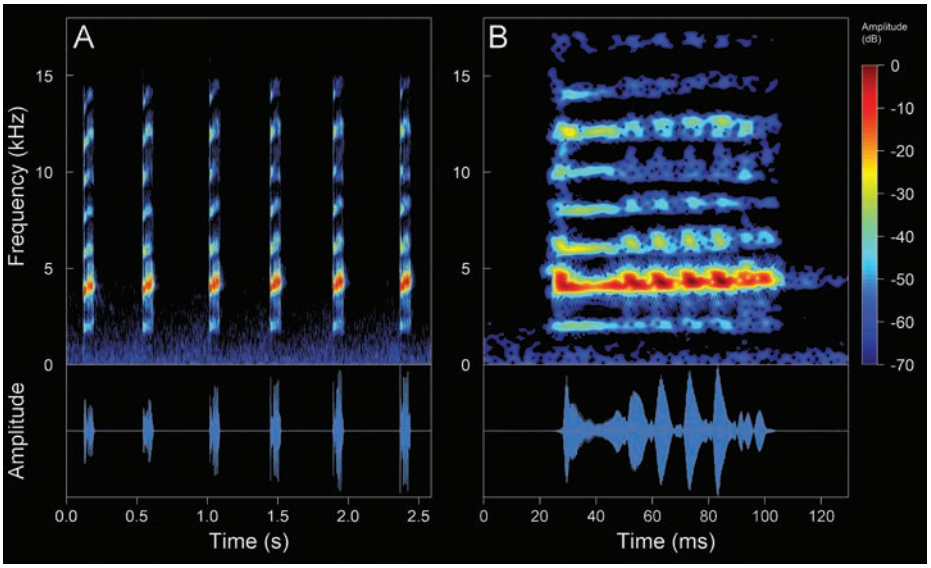

Figure 8. Spectrograms and oscillograms of the advertisement call of *Hyloxalus delatorrae*. (Not collected, 17 °C air temperature, 61% relative humidity). **A** complete advertisement call **B** detail of a note with its pulses. Spectrogram obtained using the Hann window at 99% overlap, 256 samples of FFT size and 3 dB filter bandwidth of 248 Hz.

Hyloxalus sp.

We recorded four males (Suppl. material 2, Table 2). The call (Fig. 9). The call is a continuous emission of non-pulsed notes that onomatopoeically resembles a “ti-ti-ti”. The recorded male was calling from a swamp on the banks of a river. The area contained several springs of water from old wells that were

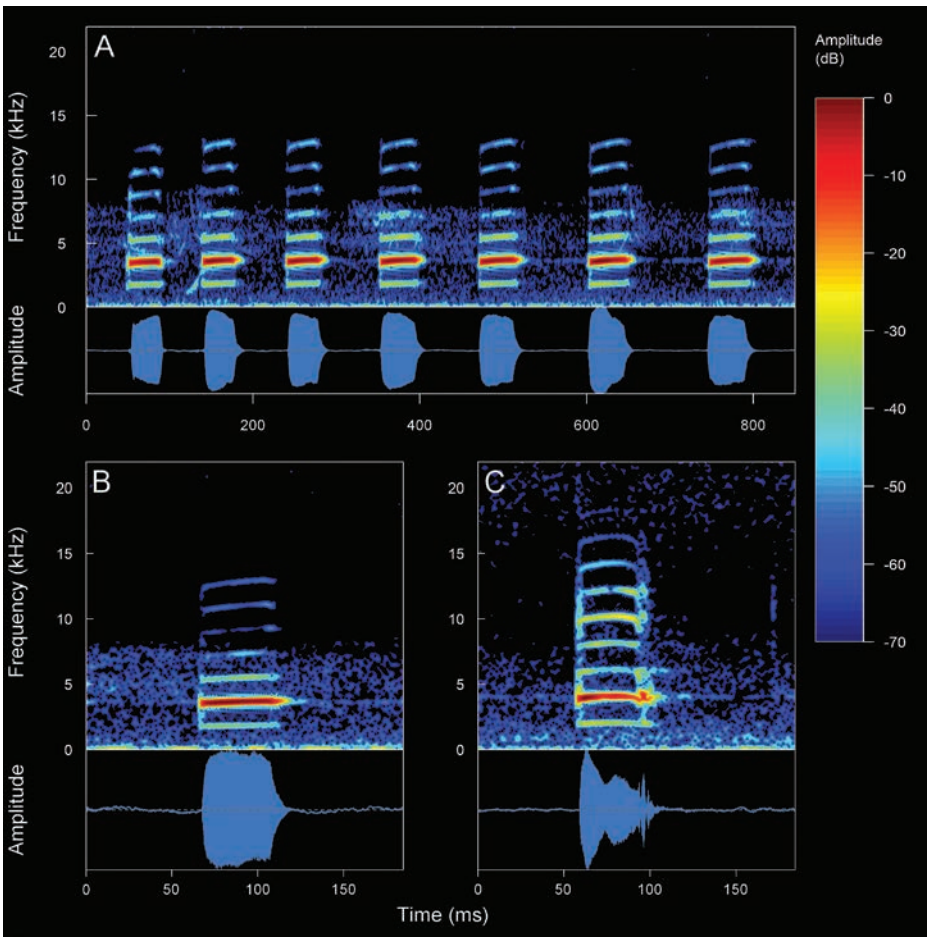

Figure 9. Spectrograms and oscillograms of the advertisement call of *Hyloxalus* sp. (ZSFQ 4442, SVL 15.45 mm, 16.5 °C air temperature, 66% relative humidity). **A** complete advertisement call **B** detail of a note with upward modulation **C** detail of a note with downward modulation. Spectrogram obtained using the Hann window at 99% overlap, 256 samples of FFT size and 3 dB filter bandwidth of 248 Hz.

used for human consumption. The calls are very loud and clearly audible at distances of up to ca 500 m. *Hyloxalus* sp. is a diurnal species with high vocal activity, which intensifies between 9:00–1:00 h, especially on sunny days. The mean call duration is 610.24 ± 167.58 ms (range 368–888 ms), emitted at mean intervals of 6.2 ± 5.41s (range 2.05–37.85 s) with a mean rate of 11.21 ± 4.59 calls/minute (range 1.58–24.59 calls/minute). The calls are composed of a mean of 6.27 ± 0.91 notes (range 5–8). The mean note duration is 34.66 ± 6.28 ms (range 17–51 ms), emitted at mean intervals of 75.18 ± 16.28 ms (range 48–122 ms), with a mean rate of 9.45 ± 1.76 notes/second (range 6.25–13.7 notes/second). The calls are upward frequency modulated (except for one recording that features downward modulation calls), with a mean frequency modulation of 6.22 ± 4.28 Hz/ms (range 0–29.85 Hz/ms). The dominant frequency is in the second harmonic, with a mean value of 3.91 ± 0.18 kHz (range 3.27–4.13 kHz), with a mean fundamental frequency of 1.95 ± 0.09 kHz (range 1.64–2.07 kHz). The mean minimum frequency is 3.72 ± 0.16 kHz (range 3.19–3.96 kHz), while the mean maximum frequency is 3.36 ± 0.13 kHz (range 2.9–3.63 kHz). Up to nine harmonics are visible

HEMIPHRACTIDAE

Gastrotheca orophylax Duellman & Pyles, 1980

We recorded four males (Suppl. material 2, Table 2). The call (Fig. 10) consists of the continuous emission of pulsed and non-pulsed notes. Their sounds are like a kind of knocking on wood that onomatopoeically resembles a " toc, toc, troc". The recorded males were calling perched on branches of trees and leafy shrubs ~ 2–6 m above the ground. The calls are of high intensity and clearly audible at long distances of up to ca 600 m. *Gastrotheca orophylax* is a nocturnal species with low to moderate vocal activity, which intensifies in a drizzle. The mean call duration is 3.01 ± 1.47 s (range 1.11–7.66 s), emitted at mean intervals of 18.46 ± 15.99 s (range 5.69–87.84 s), with a mean rate of 3.52 ± 1.35 calls/minute (range 0.67–6.44 calls/minute). The calls are composed of a mean of 4 ± 1.34 notes (range 1–7 notes). The mean note duration is 34.87 ± 45.98 ms (range 6–265 ms), emitted at mean intervals of 915.58 ± 256.57 ms (range 160–1421 ms), with a mean rate of 1.19 ± 0.65 notes/second (range 0.68–5.92 notes/second). The final notes consist of 1–4 pulses and are the longest in the call (range 20–219 ms). One of the distinctive characteristics of the call is the presence of two introductory notes or elements that break with the temporal uniformity of the intervals between notes. The calls are non-frequency modulated, with a mean dominant frequency (coincides with the fundamental) of 0.98 ± 0.12 kHz (range 0.78–1.21 kHz). The mean minimum frequency is 0.78 ± 0.12 kHz (range 0.52–1.12), while the mean maximum frequency is 1.16 ± 0.1 kHz (range 0.86–1.29 kHz). Up to eight harmonic partials are visible.

STRABOMANTIDAE

Niceforonia brunnea (Lynch, 1975)

We recorded two males (Suppl. material 2, Table 2). The call (Fig. 11) consists of the emission of pulsed notes. Their sounds are reminiscent of the quacking of a duck that onomatopoeically resembles a "quack, quack, quack". The recorded males were calling from stony ground at a depth of ~ 50–150 cm below the ground surface (i.e., species of fossorial habits). The calls are of low intensity and, given the fossorial habits of the species, are unlikely to be audible even at relatively short distances. *Niceforonia brunnea* is a crepuscular and nocturnal species with low vocal activity. The mean call duration is 1.39 ± 0.4 s (range 0.8–1.7 s), emitted at mean intervals of 18.21 ± 21.76 s (range 2.63–43.07 s), with a mean rate of 9.71 ± 10.98 calls/minute (range 1.34–22.14 calls/minute). The calls are composed of a mean of 3.2 ± 1.1 notes (range 2–4 notes). The mean note duration is 94.69 ± 11.96 ms (range 79–122 ms), emitted at mean intervals of 495.27 ± 158.54 ms (range 375–916 ms), with a mean rate of 1.77 ± 0.36 notes/second (range 0.96–2.12 notes/second). The notes are composed of a mean of 20.6 ± 2.67 pulses (range 14–24 pulses). The mean pulse duration is 2.69 ± 0.95 ms (range 1–9 ms), emitted at mean intervals of 2 ± 3.53 ms (range 0.3–21 ms), with a mean rate of 289.96 ± 91.47 pulses/second (range 41.67–500 pulses/second). In general, the intervals between pulses are almost indistinguishable. However, the

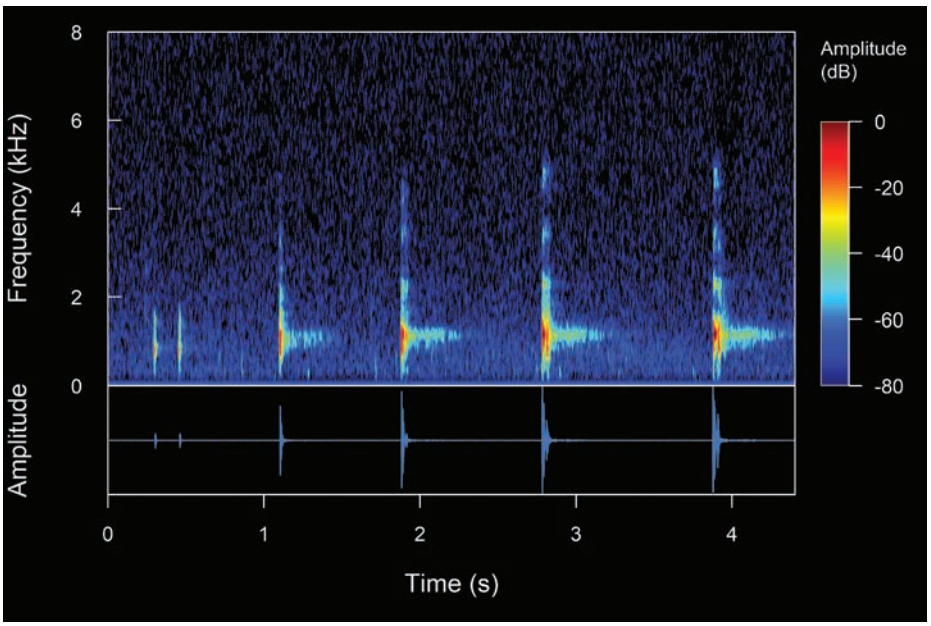

Figure 10. Spectrogram and oscillogram of the advertisement call of *Gastrotheca espeletia*. (DHMECN 13761, SVL 57.65 mm, 12.3 °C air temperature, 93% relative humidity). Spectrogram obtained using the Hann window at 99% overlap, 512 samples of FFT size and 3 dB filter bandwidth of 124 Hz.

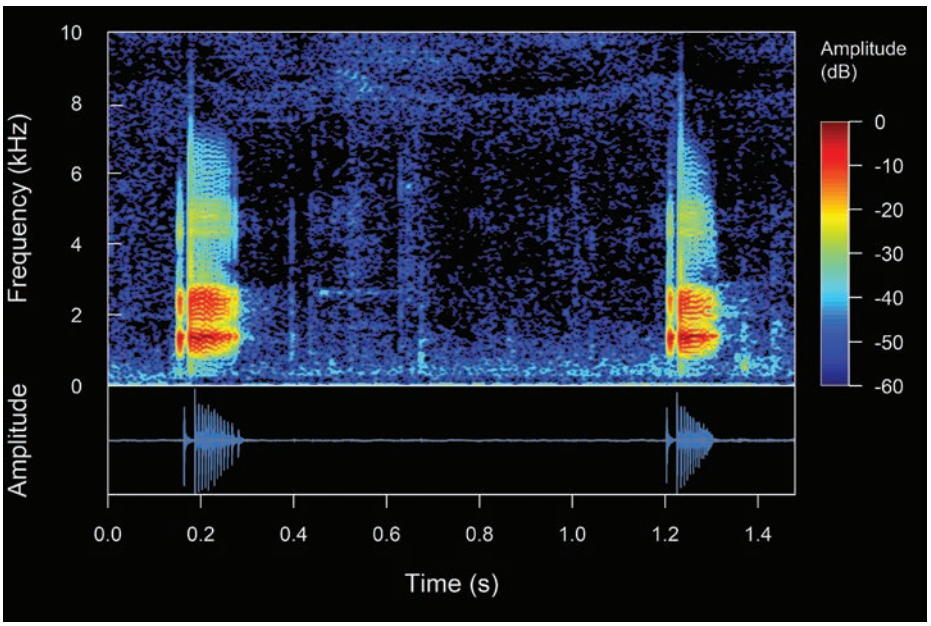

Figure 11. Spectrogram and oscillogram of the advertisement call of *Niceforonia brunnea*. (ZSFQ 4507, SVL 19.8 mm, 8.2 °C air temperature, 91% relative humidity). Spectrogram obtained using the Hann window at 99% overlap, 1024 samples of FFT size and 3 dB filter bandwidth of 61.9 Hz.

introductory pulses of each note are emitted at clearly differentiated intervals (range 14–18 ms), in addition to being the longest lasting pulses (range 4–9 ms). The calls are upward frequency modulated, with a mean frequency modulation of 1.23 ± 1.25 Hz/ms (range 0–3.67 Hz/ms). The dominant frequency is between the fourth and seventh harmonic partial, with a mean value of 1.47

± 0.11 kHz (range 1.03–1.89 kHz), while the mean fundamental frequency is 0.35 ± 0.07 kHz (range 0.22–0.56 kHz). The mean minimum frequency is 1.33 ± 0.11 kHz (range 0.95–1.72), with a mean maximum frequency of 1.59 ± 0.13 kHz (range 1.16–2.11 kHz). The harmonic series exhibits a wide frequency distribution, with a considerable number of partials visible (range 25–47 harmonics, including sidebands). In this context, the partial with the maximum frequency has a mean of 7.83 ± 0.83 kHz (range 6.91–9.72 kHz).

Noblella sp.

We recorded 1 male (Suppl. material 2, Table 2). The call (Fig. 12) consists of the continuous emission of non-pulsed notes. Their sounds are low-intensity whistles that may be confused for the calls of a dendrobatid. The males were recorded calling from leaf litter in a mountainous area traversed by deep ravines. The calls are of moderate intensity and can be audible at distances of up to ca 50 m. *Noblella* sp. is a diurnal species with low to moderate vocal activity, which intensifies until the early afternoon (between 13:00–15:00 h). The mean call duration is 6.49 ± 0.29 s (range 6.29–6.83 s), emitted at intervals range 31.7–69.79 s, with a mean rate of 0.86–1.89 calls/minute. The calls are composed of ten notes, with a mean duration of 160.97 ± 16.42 ms (range 130–196 ms). The notes are emitted at mean intervals of 542.89 ± 131.52 ms (range 375–916 ms), with a mean rate of 1.45 ± 0.2 notes/second (range 0.84–1.77 notes/second). The calls are upward frequency modulated, with a mean frequency modulation of 2.14 ± 0.71 Hz/ms (range 0.93–3.84 Hz/ms). The mean dominant frequency (coincides with the fundamental) is 2.9 ± 0.04 kHz (range 2.84–2.93 kHz). The mean minimum frequency is 2.69 ± 0.03 kHz (range 2.67–2.76 kHz) while the mean maximum frequency is 3.1 ± 0.02 kHz (range 3.01–3.1 kHz).

Pristimantis buckleyi (Boulenger, 1882)

We recorded four males (Suppl. material 2, Table 2). The call (Fig. 13) consists of the emission of a non-pulsed single note that onomatopoeically resembles a “bop”. The recorded males were calling from grasslands, swamps, and shrubby vegetation 50 to 80 cm above the ground. The calls are of low to medium intensity and can be audible at distances of up to ca 20 m. *Pristimantis buckleyi* is a nocturnal species with low to moderate vocal activity, which intensifies until approximately 20:00 h. The mean call duration is 51.46 ± 4.77 ms (range 45–61 ms), emitted at mean intervals of 4.23 ± 0.96 s (range 1.44–5.83 s), with a mean rate of 15.12 ± 5.63 calls/minute (range 10.22–40.27 calls/minute). Normally, the call of *P. buckleyi* is composed of a single note. However, after a long call train, they emit calls that are unusually and sporadic, composed of multiple notes (in the present study, we recorded a call with 12 notes). These notes are emitted at mean intervals of 240.64 ± 34.75 ms (range 209–335 ms), with a mean rate of 3.36 ± 0.32 notes/second (range 2.56–3.64 notes/second). The calls are upward frequency modulated, with a mean frequency modulation of 1.22 ± 1.47 Hz/ms (range 0–4.78 Hz/ms). The mean dominant frequency (coin-

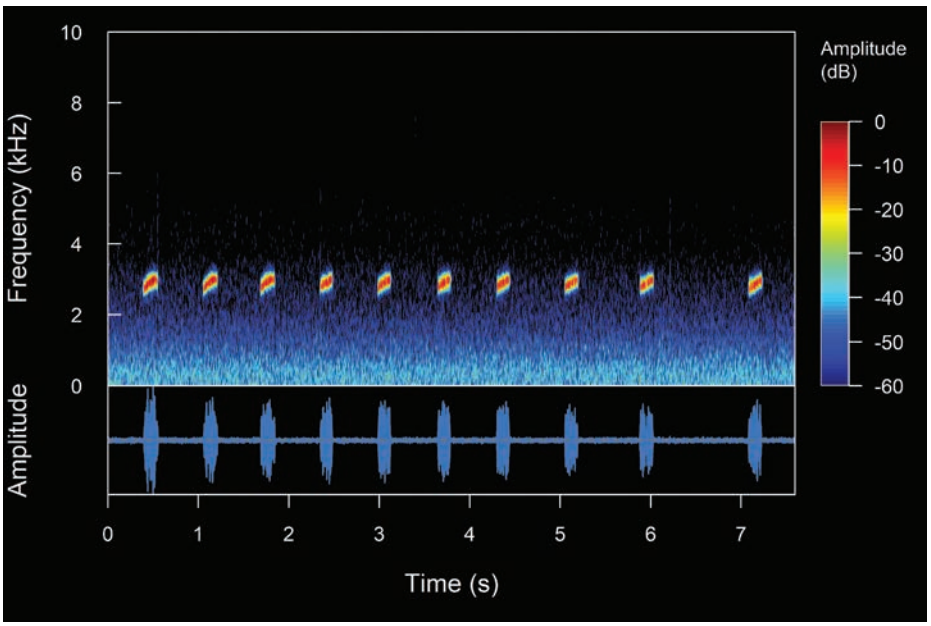

Figure 12. Spectrogram and oscillogram of the advertisement call of *Noblella* sp. (ZSFQ 4543, SVL 22.8 mm, 12.6 °C air temperature, 94% relative humidity). Spectrogram obtained using the Hann window at 99% overlap, 512 samples of FFT size and 3 dB filter bandwidth of 124 Hz.

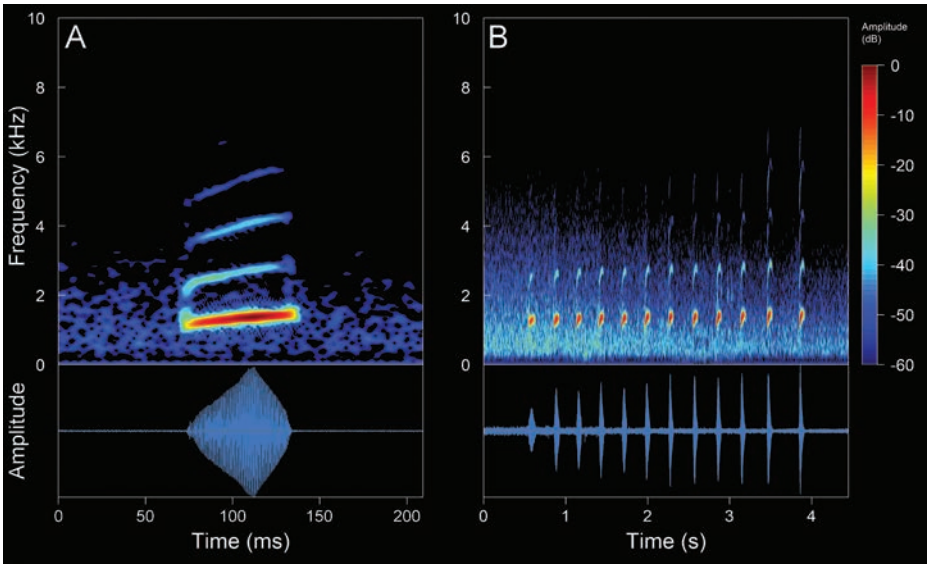

Figure 13. Spectrograms and oscillograms of the advertisement call of *Pristimantis buckleyi*. **A** single call (DHMECN 13785, SVL 26.62 mm, 8.7 °C air temperature, 73% relative humidity) **B** call with continuous notes (DHMECN 13670, SVL 28.27 mm, 7.2 °C air temperature, 73% relative humidity). Spectrograms obtained using the Hann window at 99% overlap, 512 samples of FFT size and 3 dB filter bandwidth of 124 Hz.

cides with the fundamental) is 1.26 ± 0.07 kHz (range 1.12–1.38 kHz). The mean minimum frequency is 1.08 ± 0.07 kHz (range 1.03–1.21 kHz) while the mean maximum frequency is 1.42 ± 0.09 kHz (range 1.29–1.55 kHz). Up to seven harmonics are visible.

Pristimantis farisorum Mueses-Cisneros, Perdomo-Castillo & Cepeda-Quilindo, 2013

We recorded three males (Suppl. material 2, Table 2). This is a complex call (Fig. 14) consisting of the emission of a pulsed note followed by several non-pulsed notes. Their sounds are like a metallic tapping that onomatopoeically resembles a "tic", followed by characteristic and peculiar whistling sounds that can become a high-pitched moaning. The recorded males were calling perched on branches of trees and leafy shrubs ~ 1.5–4 m above the ground. The calls are high intensity, particularly evident in the non-pulsed notes which can be audible over considerable distances. It is a crepuscular and nocturnal species with moderate vocal activity, which intensifies after a light rain or in response to the calls of nearby males. The mean call duration is 2.51 ± 1.48 s (range 1.45–6.48 s), emitted at mean intervals of 25.17 ± 5.8 s (range 17.04–33.74 s) with a mean rate of 2.27 ± 0.57 calls/minute (range 1.57–3.15 calls/minute). The calls are composed of a mean of 1.67 ± 1.61 notes (range 1–6 notes). The mean duration of the first note is 1.65 ± 0.16 s (range 1.45–1.85 s). The first note is pulsed, composed of a mean of 16.7 ± 1.64 pulses (range 15–19 pulses). The mean pulse duration is 9.16 ± 3.9 ms (range 4–24 ms), emitted at mean intervals of 109.72 ± 16.93 ms (range 64–164 ms), with a mean rate of 8.66 ± 1.35 pulses/second (range 5.59–14.49 pulses/second). The pulsed note is followed by 3–5 non-pulsed notes, which are separated by intervals of 779–875 ms. The mean non-pulsed notes duration is 173.63 ± 17.94 ms (range 141–199 ms), emitted at mean intervals of 765.5 ± 72.15 ms (range 682–848 ms), with a mean rate of 1.08 ± 0.11 notes/second (range 0.97–1.21 notes/second). The calls are non-frequency modulated. However, an upward gradual increase in frequency can be noted in the two types of notes. This upward increase is more evident in the pulsed notes, without being considered a modulated frequency (pulsed note: 0.12 ± 0.56 Hz/ms; non-pulsed note 0.91 ± 0.35 Hz/ms; *sensu* Emmrich et al. 2020). In certain calls, the frequency of the first pulse is usually higher and breaks the upward hegemony of the frequency of the other elements of the call. The mean dominant frequency (coincides with the fundamental) is 1.64 ± 0.15 kHz (range 1.38–1.89 kHz). The mean minimum frequency is 1.48 ± 0.15 kHz (range 1.21–1.72 kHz) with a mean maximum frequency of 1.83 ± 0.14 kHz (range 1.55–2.07 kHz). Up to eight harmonics are visible.

Pristimantis festae (Peracca, 1904)

We recorded eight males (Suppl. material 2, Table 2). The call (Fig. 15) consists of the emission of non-pulsed and pulsed notes (mostly non-pulsed). The calls are melodious whistles, emitted from inside hollow logs, leaf litter, pajonal (a group of tall herbaceous plants of the genera *Calamagrostis* and *Agrostis*), and ferns. The calls are of medium to high intensity, with sounds that can be audible at distances of up to ca 50 m. *Pristimantis festae* is a diurnal and nocturnal species, with low to moderate vocal activity, which intensifies in the presence of light rain. The mean call duration is 0.98 ± 0.71 s (range 0.15–3.2 s), emitted at mean intervals of 8.66 ± 2.52 s (range 4.95–19.37 s)

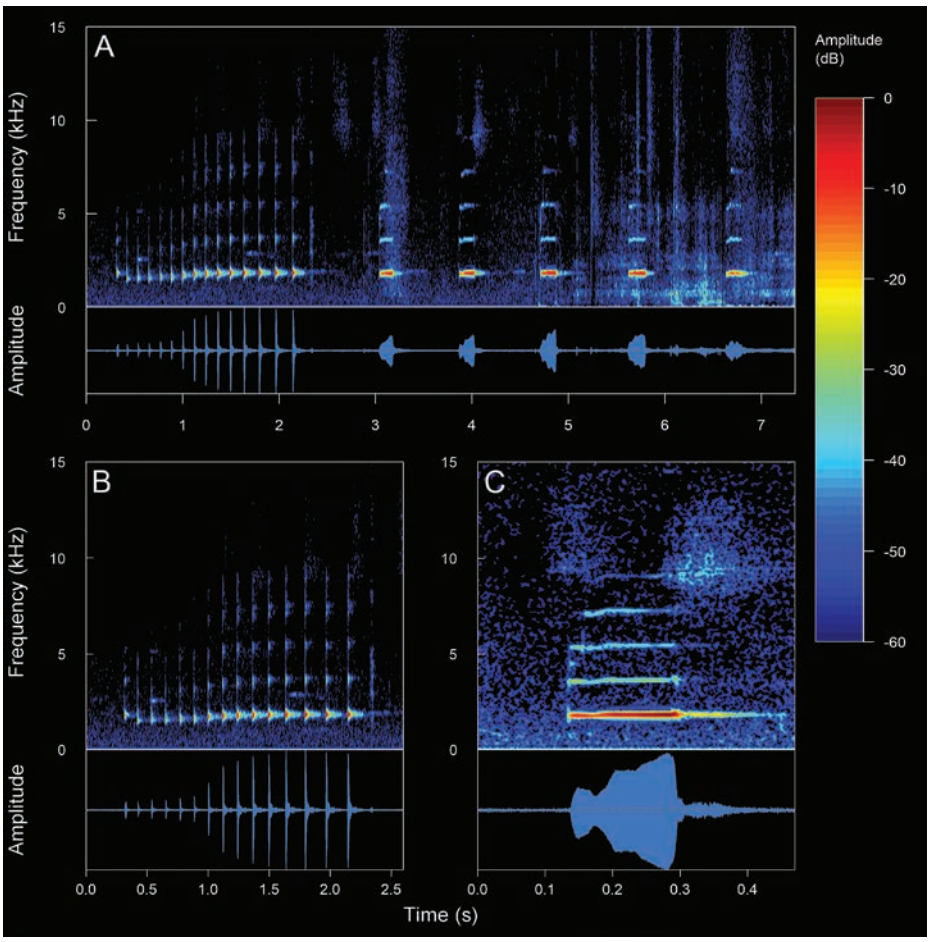

Figure 14. Spectrograms and oscillograms of the advertisement call of *Pristimantis farisorum* (DHMECN 13762, SVL 32.4 mm, 10.8 °C air temperature, 98% relative humidity). **A** complete advertisement call. **B** detail of pulsed note. **C** detail of a non-pulsed note. Spectrograms obtained using the Hann window at 99% overlap, 256 samples of FFT size and 3 dB filter bandwidth of 248 Hz.

with a mean rate of 6.73 ± 1.85 calls/minute (range 3.06–11.7 calls/minute). The calls are composed of a mean of 1.72 ± 0.58 notes (range 1–3 notes). The mean note duration is 249.29 ± 29.61 ms (range 191–320 ms), emitted at mean intervals of 782.96 ± 215.01 ms (range 480–1497 ms), with a mean rate of 1 ± 0.18 notes/second (range 0.58–1.41 notes/second). Some notes have the peculiarity of being composed of a mean of 3.47 ± 2.75 pulses (range 1–10 pulses). The mean pulse duration is 12.34 ± 10.7 ms (range 2–55 ms), emitted at mean intervals of 5.98 ± 4.51 ms (range 1–21 ms), with a mean rate of 94.5 ± 64.8 pulses/second (range 16.13–250 pulses/second). The calls are upward frequency modulated, with a mean frequency modulation of 1.05 ± 0.49 Hz/ms (range 0–3.05 Hz/ms). The mean dominant frequency (coincides with the fundamental) is 2.58 ± 0.22 kHz (range 2.33–3.01 kHz). The mean minimum frequency is 2.41 ± 0.21 kHz (range 2.15–2.76 kHz), while the mean maximum frequency is 2.75 ± 0.2 kHz (range 2.5–3.1 kHz). Up to eight harmonics are discernible, with two to four subharmonics evident between each harmonic. These subharmonics are observable in certain calls and specific individuals, and do not occur throughout the entire call.

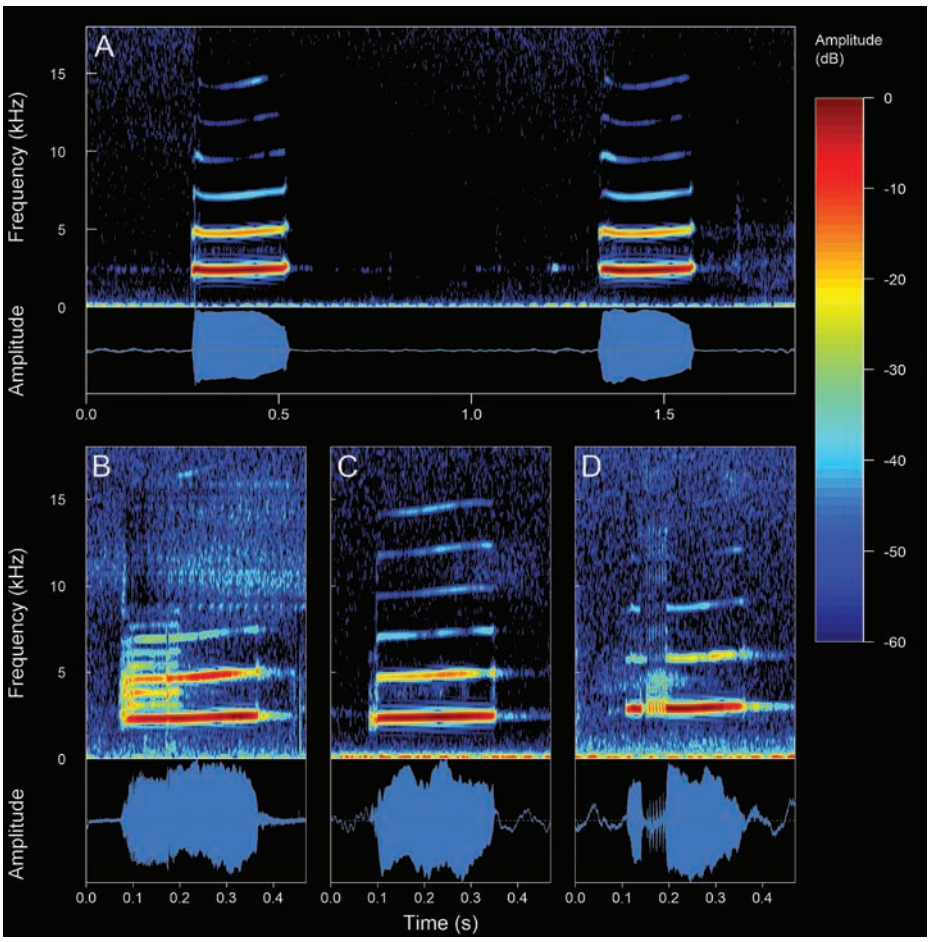

Figure 15. Spectrograms and oscillograms of the advertisement call of *Pristimantis festae*. **A** detail of a complete advertisement call with two notes (ZSFQ 4440, SVL 18.7 mm, 7.7 °C air temperature, 85% relative humidity) **B** call with visible side bands (ZSFQ 4525, SVL 15.73 mm, 8.1 °C air temperature, 93% relative humidity) **C** single call with its characteristic harmonics (ZSFQ 4516, SVL 16.75 mm, 10.2 °C air temperature, 76% relative humidity) **D** detail of pulsed note (ZSFQ 4528, SVL 13.25 mm, 11.6 °C air temperature, 82% relative humidity). Spectrograms obtained using the Hann window at 99% overlap, 512 samples of FFT size and 3 dB filter bandwidth of 124 Hz.

Pristimantis huicundo (Guayasamin, Almeida-Reinoso & Nogales-Sornosa, 2004)

We recorded five males (Suppl. material 2, Table 2). The call (Fig. 16) consists of the emission of a non-pulsed note. Their sounds are like a kind of a slight snoring mixed with a metallic tapping that onomatopoeically resembles a "tuic". The recorded males were calling from inside bromeliads (commonly referred to as huicundos) or perching on branches of trees, ~ 1–5 m above the ground. The calls are of medium intensity and can be audible over long distances due to the arboreal habits. *Pristimantis huicundo* is a nocturnal species with low vocal activity. The mean call duration is 76.06 ± 26.04 ms (range 41–175 ms), emitted at mean intervals of 5.82 ± 1.97 s (range 2.87–9.32 s) with a mean rate of 11.49 ± 4.24 calls/minute (range 6.36–20.27 calls/minute). The calls are frequency modulated between upward

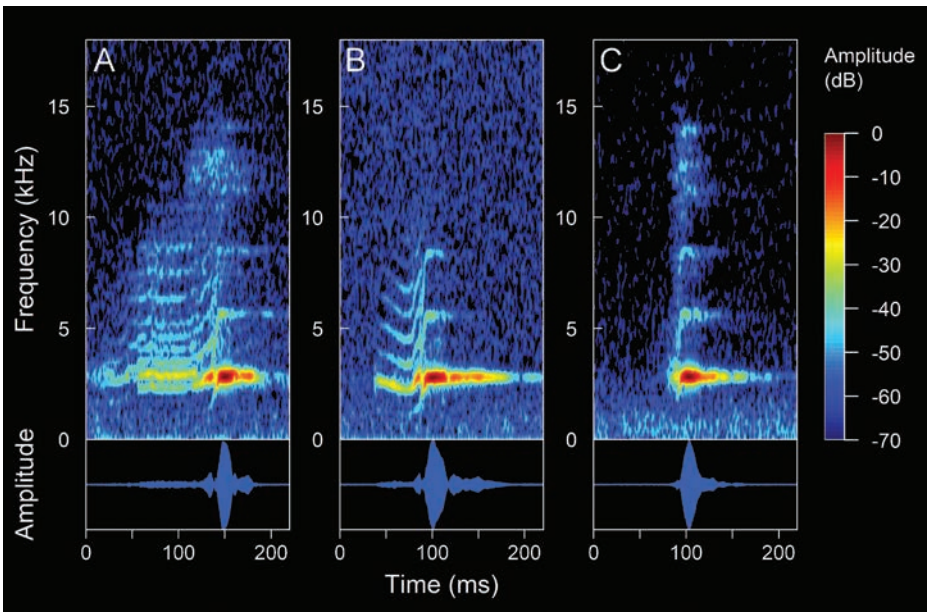

Figure 16. Spectrograms and oscillograms of the different types of advertisement calls present in *Pristimantis huicundo*. **A** inharmonic call (Not collected, 10 °C air temperature, 61% relative humidity) **B** downward call (DHMECN 13777, SVL 17.7 mm, 9.8 °C air temperature, 96% relative humidity) **C** single call (DHMECN 13791, SVL 22.4 mm, 9.7 °C air temperature, 77% relative humidity). Spectrograms obtained using the Hann window at 99% overlap, 256 samples of FFT size and 3 dB filter bandwidth of 248 Hz.

and downward (mostly upward), with a mean frequency modulation of 2.65 ± 1.86 Hz/ms (range 0–6.29 Hz/ms). The mean dominant frequency (coincides with the fundamental) is 2.8 ± 0.07 kHz (range 2.76–2.93 kHz). The mean minimum frequency is 2.63 ± 0.07 kHz (range 2.58–2.76 kHz), with a mean maximum frequency of 2.98 ± 0.07 kHz (range 2.93–3.1 kHz). Up to five harmonics are visible, with one sideband between each harmonic. The second harmonic partial has a mean frequency of 5.59 ± 0.14 kHz (range 5.51–5.86 kHz) and the fifth a mean frequency of 13.92 ± 0.28 kHz (range 13.78–14.64 kHz). In addition, two elements are observed in the call of *P. huicundo*. An introductory element of low intensity, almost imperceptible, which generates a sound similar to a slight snoring. A final element of high intensity, which generates a sound similar to a metallic tapping. These elements, particularly the introductory one, indicate a variability in the spectral and temporal characteristics. From these variations, three different types of calls can be identified: inharmonic calls. These types of calls are characterized by upward frequency modulation, with sidebands present between each harmonic. ***Downward calls***. These types of calls are characterized by downward frequency modulation, upward in the final element of the call. There are several visible harmonics, without the presence of sidebands. ***Single calls***. They are characterized by the absence of an introductory element and the presence of several harmonics. It is important to note that the distinctive feature of the *P. huicundo* call is the difference in the sequence of the harmonic series between the introductory and final element. This marks a tonal difference in the same emission.

***Pristimantis ocreatus* (Lynch, 1981)**

We recorded six males (Suppl. material 2, Table 2). The call (Fig. 17) consists of the emission of a non-pulsed note. Their sounds are like a kind of metallic tapping that onomatopoeically resembles a "tic". The recorded males were calling from within the inside adventitious tree roots, leaf litter, pajonal (a group of tall herbaceous plants of the genera *Calamagrostis* and *Agrostis*), and from inside spiny bromeliads of the genus *Puya* (commonly referred to as achupallas). The calls are of low to medium intensity and can be audible at distances of up to ca 10 m. *Pristimantis ocreatus* is a diurnal and nocturnal species with low to moderate vocal activity, which intensifies in the middle or after rain. The mean call duration is 18.12 ± 2.49 ms (range 15–23 ms), emitted at mean intervals of 528.62 ± 163.8 ms (range 393–916 ms), with a mean rate of 1.95 ± 0.44 calls/minute (range 1.07–2.44 calls/minute). The calls are downward frequency modulated, with a mean frequency modulation of 14.15 ± 4.45 Hz/ms (range 3.78–23.89 Hz/ms). The mean dominant frequency (coincides with the fundamental) is 2.4 ± 0.17 kHz (range 2.15–2.76 kHz). The mean minimum frequency is 2.2 ± 0.17 kHz (range 1.98–2.5 kHz), while the mean maximum frequency is 2.58 ± 0.18 kHz (range 2.33–2.84 kHz). Up to eight harmonics are visible.

***Pristimantis supernatis* (Lynch, 1979)**

We recorded two males (Suppl. material 2, Table 2). The call (Fig. 18) consists of the continuous emission of non-pulsed notes. Their sounds are like a kind of throaty chuckle, reminiscent of the cackling of a bird. The recorded males were calling perched on trees and shrub branches, ~ 0.8–3 m above the ground. The calls are of medium intensity and clearly audible, even over considerable distances. *Pristimantis supernatis* is a nocturnal species with low vocal activity, which emits calls fortuitously and without following a constant pattern. The mean call duration is 1359.35 ± 1273.35 ms (range 621–2830 ms), emitted at intervals of 3.92 s, with a rate of 13.19 calls/minute. The calls are composed of a mean of 8.67 ± 6.35 notes (range 5–16 notes), with a mean note duration of 44.54 ± 12.56 ms (range 22–66 ms). It should be noted that the call composed of 16 notes, is a sporadic and untimely call that usually follows a call train of short calls (composed of ≤ 5 notes). The mean intervals between notes are 127.13 ± 30.57 ms (range 74–167 ms), with a mean rate of 6.06 ± 1.12 notes/second (range 4.61–8.62 notes/second). The notes are composed of a mean of 3.32 ± 1.04 pulses (range 2–5 pulses). The mean pulse duration is 10.96 ± 8.13 ms (range 2–28 ms), emitted at mean intervals of 2.38 ± 1.71 ms (range 1–10 ms), with a mean rate of 146.14 ± 83.52 pulses/second (range 45.45–333.33 pulses/second). The dominant frequency is in the second harmonic partial, with a mean value of 1.43 ± 0.08 kHz (range 1.29–1.55 kHz). The mean fundamental frequency is 0.71 ± 0.04 kHz (range 0.6–0.78 kHz), with up to 15 harmonic partials visible. The mean minimum frequency is 1.21 ± 0.08 kHz (range 1.03–1.38 kHz), while the mean maximum frequency is 1.71 ± 0.1 kHz (range 1.46–1.98 kHz). This is a complex call at both the temporal and spectral levels. It has different tonalities and intensities throughout its emission. From this perspective, the call of *P. supernatis* call presents different elements (clarifying that they are not notes or pulses). The introductory element, composed

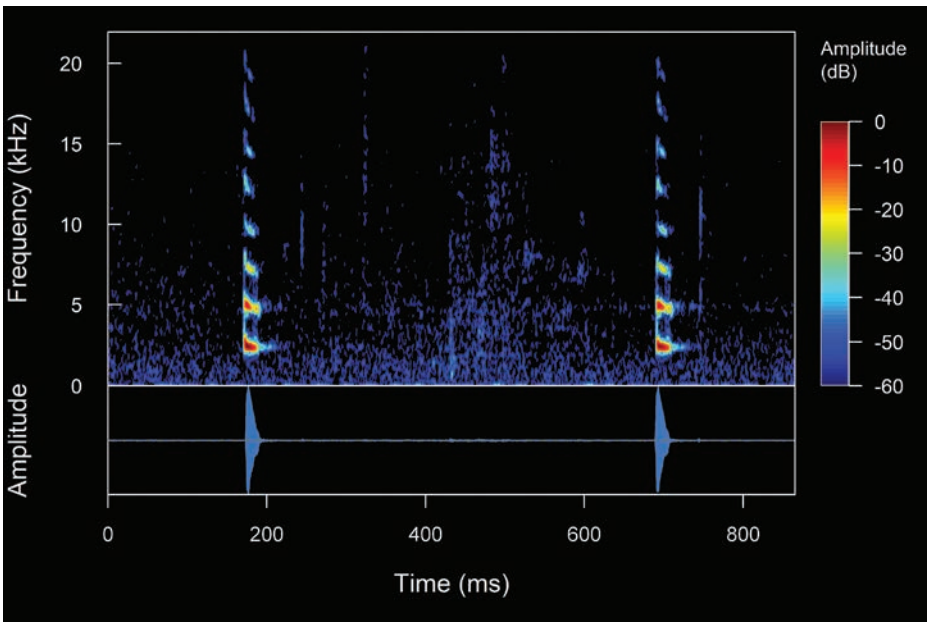

Figure 17. Spectrogram and oscillogram of the advertisement call of *Pristimantis ocreatus*. (DHMECN 13654, SVL 13.35 mm, 8.2 °C air temperature, 88% relative humidity). Spectrogram obtained using the Hann window at 99% overlap, 256 samples of FFT size and 3 dB filter bandwidth of 248 Hz.

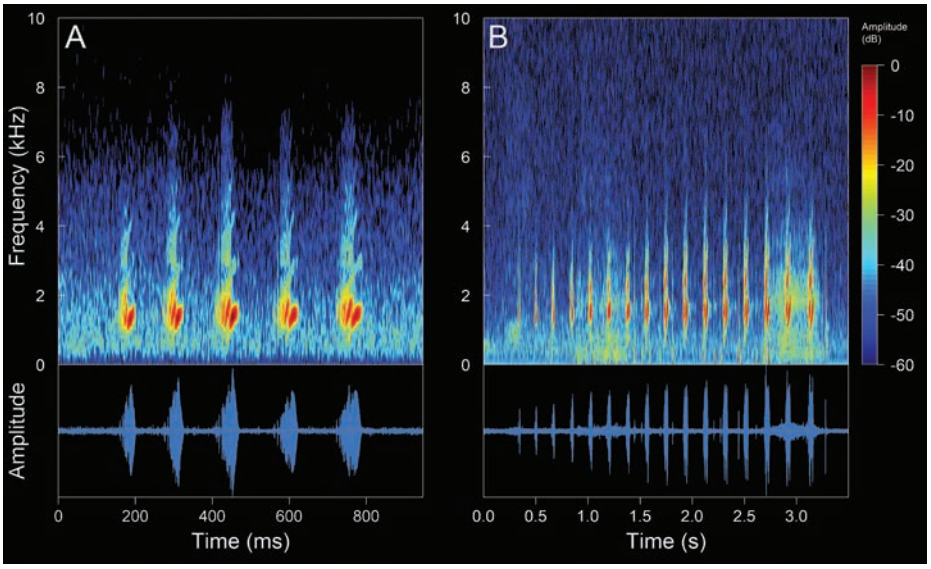

Figure 18. Spectrograms and oscillograms of the advertisement call of *Pristimantis supernatis*. **A** advertisement call, common and characteristic (DHMECN 13658, SVL 27.25 mm, 6.7 °C air temperature, 83% relative humidity) **B** unusual, explosive and sporadic advertisement call (DHMECN 13820, SVL 25.65 mm, 10 °C air temperature, 79% relative humidity). Spectrograms obtained using the Hann window at 99% overlap, 256 samples of FFT size and 3 dB filter bandwidth of 248 Hz.

of pulses of short duration, with harmonic partials that are not very distinguishable. The middle element, which has an upward frequency modulation, numerous harmonic partials, and visible sidebands. The final element, which has an upward frequency modulation, lacks visible sidebands and harmonics with different frequency values. This indicates that the values of the dominant

frequency and harmonics differ from those of the other elements, which results in a distinct tonality within the same emission. Furthermore, the unique tonality differentiation observed in the vocalizations of *Pristimantis supernatis* can be described as a call with biphonation segments, augmenting both temporal and spectral variability. This phenomenon has been documented in other species (e.g., Brito et al. 2017; Zhang et al. 2017; Hepp et al. 2019).

***Pristimantis thymelensis* (Lynch, 1972)**

We recorded two males (Suppl. material 2, Table 2). The call (Fig. 19) consists of the emission of non-pulsed and pulsed notes. Their sounds are very varied and usually resemble a hoarse squeal or moan range low- to high-pitched. The recorded males were calling from within inside the tall grasses of the genus *Cortaderia*, ferns, bromeliads of the genus *Puya* (achupallas), and perched on branches of shrubs and among the leaves of frailejones of the genus *Espeletia* ~ 20–60 cm from above the ground. The calls are of medium to high intensity and can be audible over long distances. *Pristimantis thymelensis* is a diurnal, crepuscular, and nocturnal species, with low vocal activity. It is important to note that calls are emitted in a solitary and sporadic manner, except when between 84 and 386 consecutive calls are emitted within a period of between two and three minutes. In such cases, continuous emissions would be regarded as a complete call train. The calls of *P. thymelensis* show variability and differences in their spectral and temporal values, which makes it difficult to generalize the call of this species under a single pattern. However, considering these differences, *P. thymelensis* has three distinct different call types. ***Complex calls***. The mean duration of this type is 158.8 ± 41.73 ms (range 93–204 ms), emitted at mean intervals of 7.38 ± 9.7 s (range 1.24–24.53 s), with a mean rate of 19.5 ± 15.98 calls/minute (range 2.43–45.11 calls/minute). The calls are composed of a mean of 2.83 ± 0.41 pulses (range 2–3 pulses), with a mean pulse duration of 14.04 ± 14.59 ms (range 3–114 ms). The dominant frequency is in the second harmonic partial, with a mean value of 2.63 ± 0.09 kHz (range 2.5–2.76 kHz). They are upward frequency modulated, with a mean fundamental frequency of 1.38 kHz. The mean minimum frequency is 2.37 ± 0.11 kHz (range 2.15–2.5 kHz), while the mean maximum frequency is 2.8 ± 0.09 kHz (range 2.58–2.93 kHz). The complex call is divided into an introductory, middle, and final element. Each of these elements has different spectral characteristics. In this context, this type of call has up to six harmonics, which are only visible in the middle element. It should be noted that this type of call marks the beginning of the call train. ***Single calls***. They are unusual, uncommon calls, which have no division of elements and are composed of a single note. The mean duration of this type is146.25 ± 55.42 ms (range 64–185 ms), emitted at mean intervals of 2.27 ± 1.99 s (range 0.62–4.84 s) with a mean rate of 45.82 ± 35.89 calls/minute (range 11.98–86.96 calls/minute). The dominant frequency is in the second harmonic, with a value of 2.41 kHz. The calls are downward and upward frequency modulated, with a fundamental frequency of 1.21 kHz. The mean minimum frequency is 2.08 ± 0.07 kHz (range 1.98–2.15 kHz), while the maximum frequency is 2.5 kHz. Up to eight harmonics are visible, the third having a frequency of 3.62 kHz and the eighth

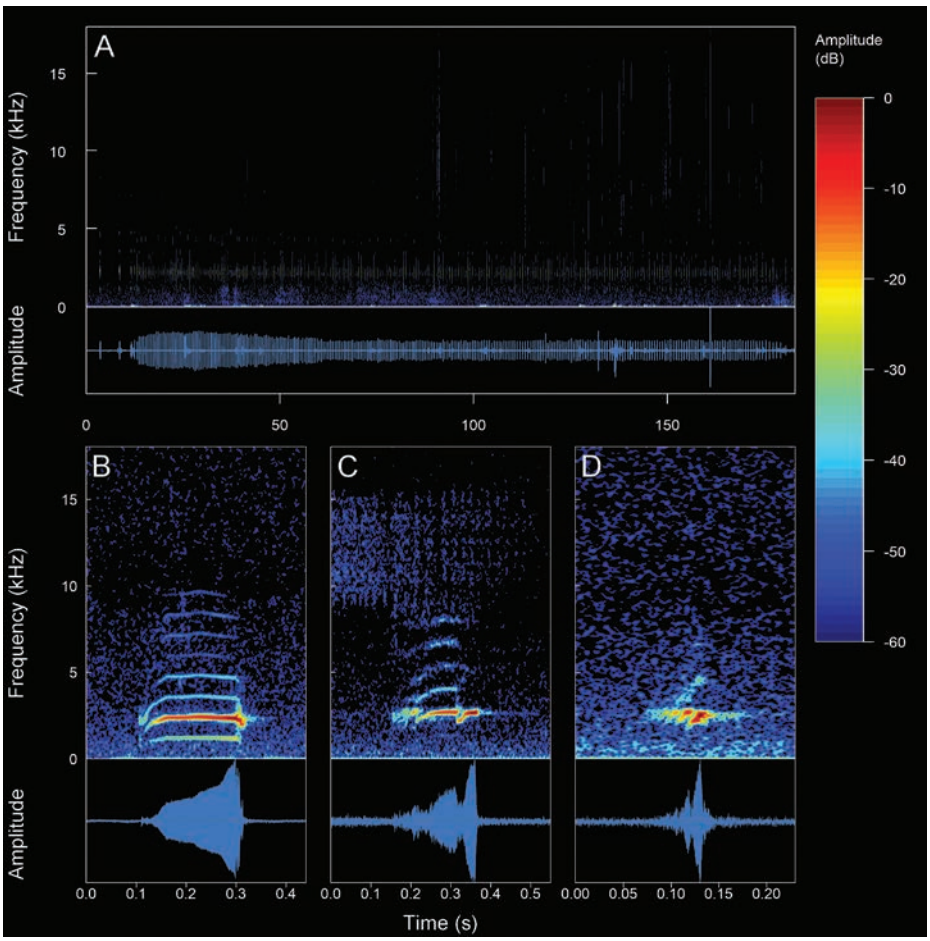

Figure 19. Spectrograms and oscillograms of the different types of advertisement calls present in *Pristimantis thymelensis*. **A** complete call train of 84 calls **B** single calls (**A, B** not collected individual) **C** complex calls **D** pulsed calls (C, D DHMECN 13786, SVL 19.98 mm, 4 °C air temperature, 90% relative humidity). Spectrograms obtained using the Hann window at 99% overlap, 512 samples of FFT size and 3 dB filter bandwidth of 124 Hz.

a frequency of 9.65 kHz. They are unusual, uncommon calls, which have no division of elements and are composed of a single note. ***Pulsed calls***. The mean call duration is 47.79 ± 9.36 ms (range 31–67 ms), emitted at intervals of 0.57 ± 0.13 s (range 0.41–0.99 s), with a rate of 99.65 ± 18.99 calls/minute (range 58.25–130.43 calls/minute). The calls are composed of a mean of 3.53 ± 1.3 pulses (range 2–6 pulses). The mean pulse duration is 10.67 ± 5.07 ms (range 3–27 ms), the last pulses being the longest of the call, with a mean duration of 16.57 ± 5.11 ms (range 11–27 ms). Calls downward frequency modulated, with a gradual and continuous decrease in frequency over the course of the call. The dominant frequency is in the second harmonic, with a mean value of 2.63 ± 0.09 kHz (range 2.24–2.76 kHz), while the mean fundamental frequency is 1.2 ± 0.02 kHz (range 1.12–1.21 kHz). The mean minimum frequency is 2.26 ± 0.1 kHz (range 2.07–2.5 kHz), with a mean maximum frequency of 2.77 ± 0.12 kHz (range 2.58–2.84 kHz). Up to six harmonics are visible, The pulsed call is not emitted as an isolated call (i.e., without being part of a call train). This type represents the most intense part of the call train, with intervals between calls becoming shorter as the call train progresses.

Pristimantis unistrigatus (Günther, 1859)

We recorded four males (Suppl. material 2, Table 2). The call (Fig. 20) consists of the continuous emission of non-pulsed notes. Their sounds are like a kind of metallic tapping that onomatopoeically resembles a "tic-tic-tic". The recorded males were calling from grasslands, leaf litter and in cultivated areas (this species does not inhabit forests), or perching on shrubby vegetation ~ 20–60 cm above the ground. The calls are of medium to high intensities and may be audible over long distances, particularly in open fields. *Pristimantis unistrigatus* is a diurnal, crepuscular, and nocturnal species, with moderate to high vocal activity, which intensifies during or after a drizzle. The mean call duration is 1.54 ± 0.47 ms (range 0.67–2.13 ms), emitted at mean intervals of 9.18 ± 3.49 s (range 4.87–16.27 s) with a mean rate of 6.31 ± 2.16 calls/minute (range 3.35–10.6 calls/minute). The calls are composed of a mean of 5.48 ± 1.57 notes (range 3–8 notes). The mean note duration is 7.47 ± 2.7 ms (range 4–15 ms), emitted at mean intervals of 343.48 ± 53.58 ms (range 250–459 ms), with a mean rate of 2.92 ± 0.47 notes/second (range 2.13–3.91 notes/second). The calls are non-frequency modulated, with downward frequency modulated notes. The mean dominant frequency (coincides with the fundamental) is 2.51 ± 0.2 kHz (range 1.98–2.93 kHz). The mean minimum frequency is 2.26 ± 0.19 kHz (range 1.81–2.15 kHz), while the mean maximum frequency is 2.86 ± 0.27 kHz (range 2.33–3.36 kHz). Up to six harmonics are visible.

Pristimantis sp. (*Pristimantis ridens* species group)

We recorded four males (Suppl. material 2, Table 2). This is a complex call (Fig. 21) consisting of a pulsed note followed by several non-pulsed notes. The call of this species is very similar to that of *P. farisorum* in both structure and sound (these 2 species are cryptic). That is, metallic tapping that onomatopoeically resembles a "tic", followed by characteristic and peculiar whistling sounds that can become a high-pitched moaning. The recorded males were calling perched on branches of trees and leafy shrubs ~ 1–4 m above the ground. The calls are high intensity, particularly evident in the non-pulsed notes which can be audible over long distances. This is a crepuscular and nocturnal species with moderate vocal activity, which intensifies after a light rain or in response to the calls of nearby males. The mean call duration is 1.91 ± 0.68 s (range 0.6–3.35 s), emitted at mean intervals of 11.81 ± 4.07 s (range 3.31–22.66 s), with a mean rate of 4.79 ± 2.05 calls/minute (range 2.39–12.3 calls/minute). The calls are composed of a mean of 1.84 ± 0.69 notes (range 1–4 notes). The mean duration of the first note is 1241.94 ± 306.06 s (range 679–1603 s). The first note is pulsed, composed of a mean of 11.68 ± 2.24 pulses (range 7–15 pulses). The mean pulse duration is 8.33 ± 7.57 ms (range 3–50 ms), emitted at mean intervals of 91.11 ± 10.4 ms (range 82–140 ms), with a mean rate of 10.3 ± 1.02 pulses/second (range 6.33–11.36 pulses/second). The pulsed note is followed by 1–4 non-pulsed notes, which are separated by intervals of 414–960 ms. The mean non-pulsed notes duration is 338.91 ± 131.04 ms (range 141–199 ms), emitted at mean intervals of 631.2 ± 137.61 ms (range 414–960 ms), with a mean rate of 0.69 ± 0.23 notes/second (range 0.39–1.14

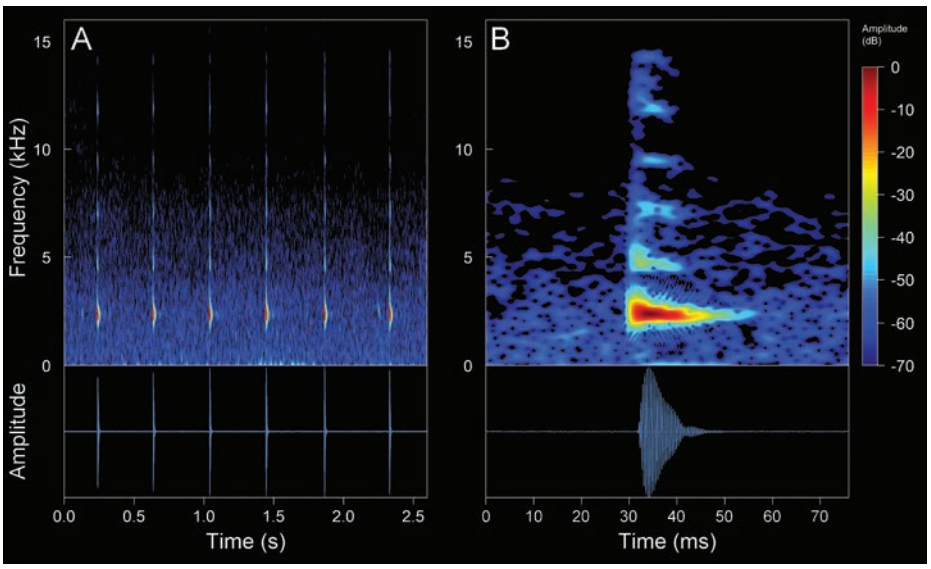

Figure 20. Spectrograms and oscillograms of the advertisement call of *Pristimantis unistrigatus* (ZSFQ 4549, SVL 20.25 mm, 9.8 °C air temperature, 62% relative humidity). **A** complete advertisement call **B** detail of a note. Spectrogram obtained using the Hann window at 99% overlap, 256 samples of FFT size and 3 dB filter bandwidth of 248 Hz.

notes/second). Some secondary notes (i.e., those that followed the first note) are composed of a mean of 11.5 ± 4.95 pulses (range 8–15 pulses). Secondary note pulses have a mean duration of 41.72 ± 49.12 ms (range 9–184 ms), emitted at mean intervals of 8.24 ± 4.07 ms (range 2–17 ms), with a mean rate of 37.11 ± 19.6 pulses/second (range 2.76–71.43 pulses/second). The calls are non-frequency modulated. However, an upward gradual increase in frequency can be noted in the two types of notes. This upward increase is more evident in the pulsed notes but is not considered a modulated frequency (pulsed note: 0.22 ± 0.17 Hz/ms; secondary notes 0.62 ± 0.58 Hz/ms; *sensu* Emmrich et al. 2020). The mean dominant frequency (coincides with the fundamental) is 1.64 ± 0.11 kHz (range 1.38–1.81 kHz), The mean minimum frequency is 1.44 ± 0.12 kHz (range 1.03–1.64 kHz), while the mean maximum frequency is 1.85 ± 0.1 kHz (range 1.55–1.98 kHz). Up to seven harmonics are visible.

Pristimantis sp. 2 (*Pristimantis myersi* species group)

We recorded 12 males (Suppl. material 2, Table 2). The call (Fig. 22) consists of the emission of a non-pulsed note. Their sounds are like a kind of metallic tapping that onomatopoeically resembles a “tic”. The recorded males were calling from dense undergrowth with abundant bryophytes, leaf litter, within hollow trunks, and the base and interior of adventitious tree roots. The calls are of medium to high intensities and they can be audible at distances of up to ca 150 m. This species is active during the day and night, with moderate to high vocal activity, which intensifies during or after rain and in response to the calls of nearby males. The mean call duration is 225.79 ± 263.9 ms (range 8–1042 ms), emitted at mean intervals of 3.8 ± 1.71 s (range 2.15–21.45 s), with a mean rate of 16.23 ± 3.96 calls/minute (range 2.79–27.03 calls/minute). The calls are composed of a mean of 1.6 ± 0.63 notes (range 1–3 notes).

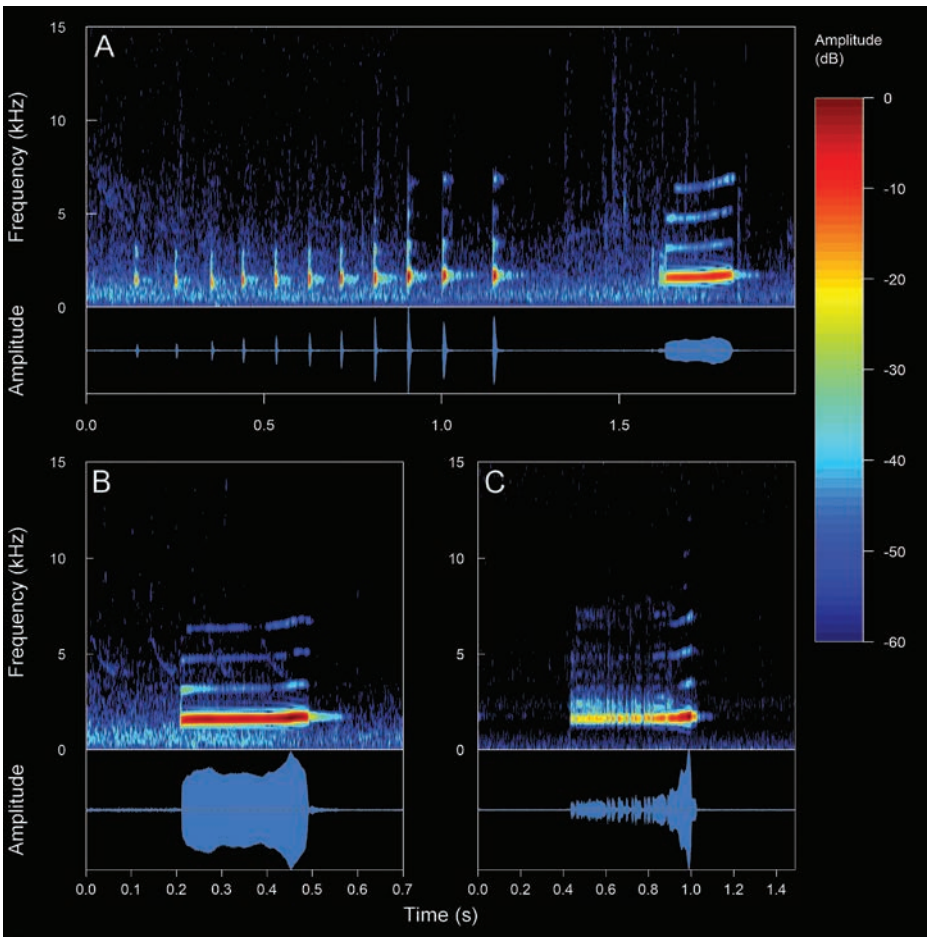

Figure 21. Spectrograms and oscillograms of the advertisement call of *Pristimantis* sp. 1 *ridens* group **A** Complete advertisement call **B** detail of a non-pulsed note (**A, B** DH-MECN 13752, SVL 34.4 mm, 11 °C air temperature, 85% relative humidity) **C** detail of a pulsed secondary note (**A, B** ZSFQ 4499, SVL 39.1 mm, 11.6 °C air temperature, 90% relative humidity). Spectrograms obtained using the Hann window at 99% overlap, 256 samples of FFT size and 3 dB filter bandwidth of 248 Hz.

The mean note duration is 14.01 ± 4.89 ms (range 9–39 ms), emitted at mean intervals of 407.51 ± 91.52 ms (range 302–798 ms), with a mean rate of 2.46 ± 0.41 notes/second (range 1.24–3.18 notes/second). The calls are downward frequency modulated (upward in some calls), with a mean frequency modulation of 6.23 ± 6.4 Hz/ms (range 0–34.4 Hz/ms). The mean dominant frequency (coincides with the fundamental) is 2.63 ± 0.13 kHz (range 2.33–2.84 kHz). The mean minimum frequency is 2.42 ± 0.12 kHz (range 2.15–2.67 kHz), while the mean maximum frequency is 2.78 ± 0.13 kHz (range 2.5–3.01 kHz). Up to eight harmonics are visible.

Pristimantis sp. 3 (*Pristimantis myersi* species group)

We recorded nine males (Suppl. material 2, Table 2). This is a complex call (Fig. 23) consisting of a pulsed note seconded by several non-pulsed notes. Their sounds are like a constant metallic tapping that onomatopoeically resembles a “tic”. The recorded males were calling from leaf litter,

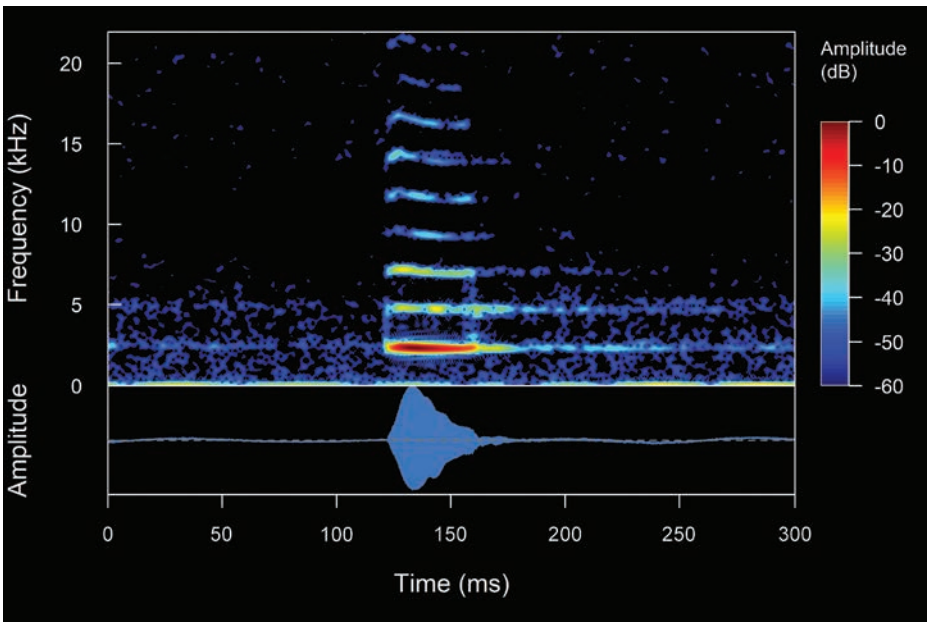

Figure 22. Spectrogram and oscillogram of the advertisement call of *Pristimantis* sp. 2 *myersi* group (ZSFQ 4565, SVL 18.86 mm, 11.5 °C air temperature, 89% relative humidity). Spectrogram obtained using the Hann window at 99% overlap, 256 samples of FFT size and 3 dB filter bandwidth of 248 Hz.

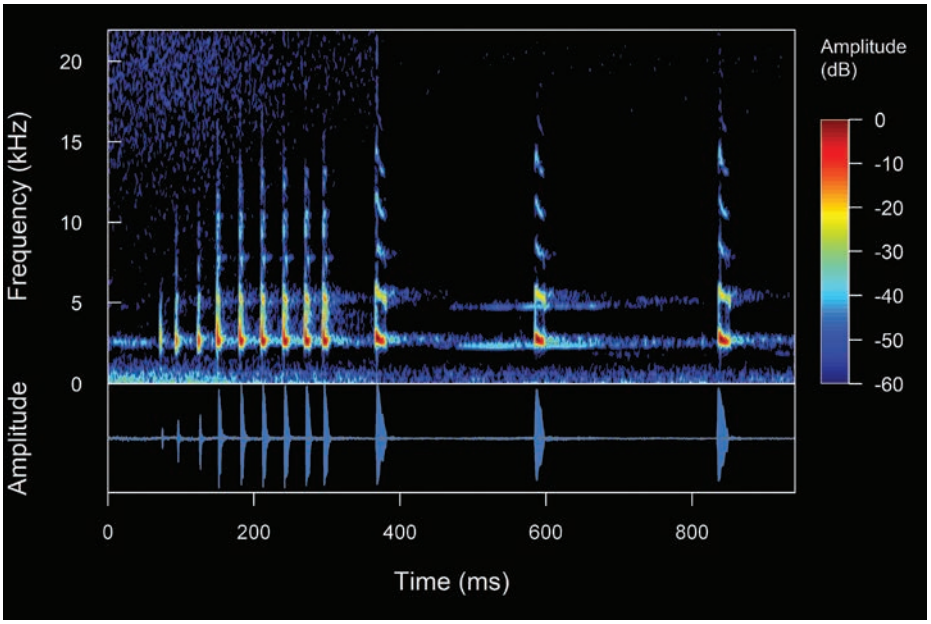

Figure 23. Spectrogram and oscillogram of the advertisement call of *Pristimantis* sp. 3 *myersi* group (ZSFQ 4512, SVL 13.35 mm, 9.9 °C air temperature, 76% relative humidity). Spectrogram obtained using the Hann window at 99% overlap, 256 samples of FFT size and 3 dB filter bandwidth of 248 Hz.

inside hollow trunks, the base and interior of trees, frailejones of the genus *Espeletia*, and ferns. The calls are of low to high intensity, with sounds that can be audible at distances of up to ca 30 m. This is a crepuscular and nocturnal species (with little diurnal activity), with moderate to high vocal activity,

which intensifies after a rain. The mean call duration is 630.17 ± 281.68 ms (range 207–1294 ms), emitted at mean intervals of 3.89 ± 1.2 s (range 2.29–12.92 s), with a mean rate of 14.21 ± 3.28 calls/minute (range 7.03–20.62 calls/minute). The calls are composed of a mean of 3.01 ± 1.11 notes (range 1–5 notes). The mean duration of the first note is 239.18 ± 79.5 ms (range 104–490 s). The first note is pulsed, composed of a mean of 6.5 ± 1.88 pulses (range 2–12 pulses), The mean pulse duration is 6.08 ± 2.41 ms (range 1–19 ms), emitted at mean intervals of 39.33 ± 14.21 ms (range 4–93 ms), with a mean rate of 24.58 ± 8.68 pulses/second (range 10.2–111.11 pulses/second). The first note is followed by 1–4 non-pulsed notes, which are separated by a mean interval of 95.88 ± 30.08 (range 53–258 ms). The mean non-pulsed notes duration is 13.02 ± 3.71 ms (range 6–29 ms), emitted at mean intervals of 254.13 ± 44.82 ms (range 191–644 ms), with a mean rate of 3.54 ± 0.8 notes/second (range 1.34–9.62 notes/second. The calls are non-frequency modulated, exhibiting downward modulation in their notes (Pulsed note: 1.31 ± 0.77 Hz/ms; non-pulsed notes 22.42 ± 8.07 Hz/ms). The mean dominant frequency (coincides with the fundamental) is 2.55 ± 0.09 kHz (range 2.33–2.84 kHz). The mean minimum frequency is 2.34 ± 0.09 kHz (range 2.07–3.19 kHz), while the mean maximum frequency is 2.85 ± 0.18 kHz (range 2.58–3.79 kHz). Up to eight harmonics are visible. In the pulsed note, the presence of one or two sidebands between harmonics is observed.

Pristimantis sp. 4 (*Pristimantis myersi* species group)

We recorded six males (Suppl. material 2, Table 2). The call (Fig. 24) consists of the emission of a non-pulsed note. Their sounds are like a kind of metallic tapping that onomatopoeically resembles a “tic”. The recorded males were calling from dense undergrowth, leaf litter, within hollow trunks, and the base and interior of adventitious tree roots. The calls are of medium to high intensities and they can be audible at distances of up to ca 100 m. This is a crepuscular and nocturnal species (with little diurnal activity), with moderate to high vocal activity, which intensifies after a rain and in response to the calls of nearby males. The mean call duration is 149.16 ± 251.15 ms (range 9–903 ms), emitted at mean intervals of 5.21 ± 0.87 s (range 3.85–9.15 s), with a mean rate of 11.45 ± 1.91 calls/minute (range 5.91–15.54 calls/minute). The calls are composed of a mean of 1.24 ± 0.43 notes (range 1–2 notes). The mean note duration is 11.88 ± 1.07 ms (range 10–13 ms), emitted at mean intervals of 567.93 ± 94.17 ms (range 467–877 ms), with a mean rate of 1.76 ± 0.23 notes/second (range 1.12–2.08 notes/second). The calls are downward frequency modulated (upward in some calls), with a mean frequency modulation of 14.68 ± 8.7 Hz/ms (range 0–35.83 Hz/ms). The mean dominant frequency (coincides with the fundamental) is 2.57 ± 0.08 kHz (range 2.33–2.76 kHz). The mean minimum frequency is 2.36 ± 0.09 kHz (range 2.15–2.5 kHz), while the mean maximum frequency is 2.76 ± 0.08 kHz (range 2.58–2.93 kHz). Up to eight harmonics are visible, the second having a mean frequency of 5.13 ± 0.19 kHz (range 4.65–5.51 kHz) and the eighth having a mean frequency of 20.07 ± 0.5 kHz (range 19.29–20.76 kHz).

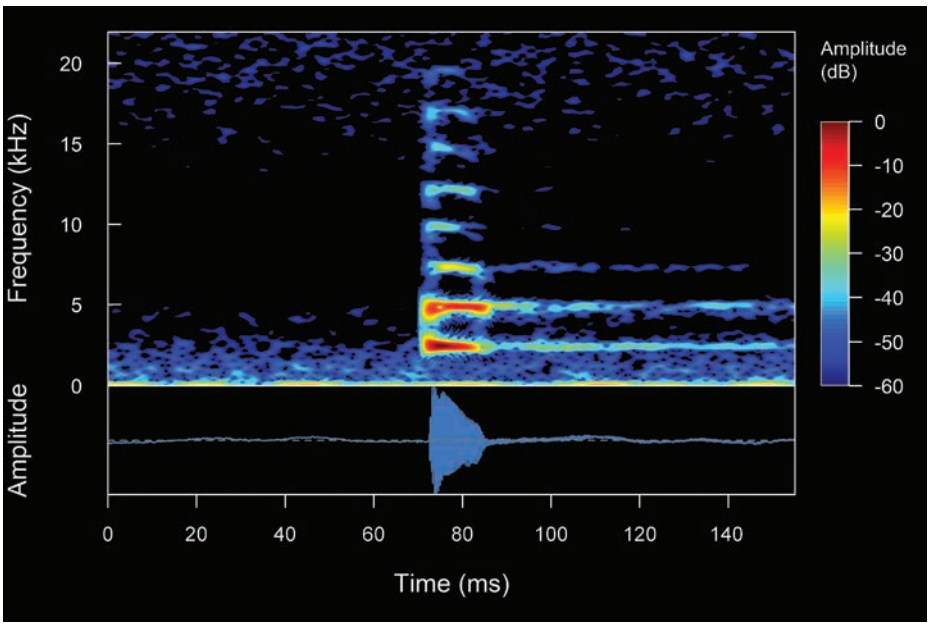

Figure 24. Spectrogram and oscillogram of the advertisement call of *Pristimantis* sp. 4 *myersi* group (ZSFQ 4427, SVL 15.28 mm, 7.9 °C air temperature, 82% relative humidity). Spectrogram obtained using the Hann window at 99% overlap, 256 samples of FFT size and 3 dB filter bandwidth of 248 Hz.

Pristimantis sp. 5 (*Pristimantis myersi* species group)

We recorded six males (Suppl. material 2, Table 2). The call (Fig. 25) consists of the continuous emission of pulsed notes. The recorded males were calling from grassland, leaf litter, and shrubby vegetation between 40 and 80 cm above the ground. The calls are of medium intensity and can be audible at distances particularly in open fields. This species is crepuscular and nocturnal, with moderate vocal activity, which intensifies after a rain and in response to the calls of nearby males. The mean call duration is 357–827 s (range 502.45 ± 123.07 s), emitted at mean intervals of 22.26 ± 13.55 s (range 2.89–57.66 s) with a mean rate of 3.96 ± 3.18 calls/minute (range 1.03–18.13 calls/minute). This species usually emits two to three consecutive calls grouped in series, at mean intervals of 538.33 ± 50.8 ms (range 429–616 ms). The calls are composed of a mean of 6.85 ± 0.96 notes (range 5–9 notes). The mean note duration is 20.88 ± 7.29 ms (range 2–48 ms), emitted at mean intervals of 61.34 ± 12.7 ms (range 40–108 ms), with a mean rate of 12.58 ± 1.76 notes/second (range 8.13–19.23 notes/second). The notes are composed of a mean of 3.02 ± 1.06 pulses (range 1–7 pulses). The mean pulse duration is 5 ± 2.61 ms (range 1–21 ms), the last pulse being the longest of the call, with a mean duration of 12.79 ± 3.83 ms (range 7–21 ms). The pulses are emitted at mean intervals of 3.45 ± 3.01 ms (range 0.5–25 ms), with a mean rate of 185.46 ± 100.59 pulses/second (range 14.08–500 pulses/second). The calls are non-frequency modulated, exhibiting upward-downward modulation in their notes (8.01 ± 5.7 Hz/ms). The mean dominant frequency (coincides with the fundamental) is 2.48 ± 0.14 kHz (range 2.15–2.84 kHz). The mean minimum frequency is 2.22 ± 0.16 kHz (range 1.72–2.58 kHz), while the mean maximum frequency is 2.77 ± 0.19 kHz (range 2.41–3.62 kHz). Up to eight harmonics are visible.

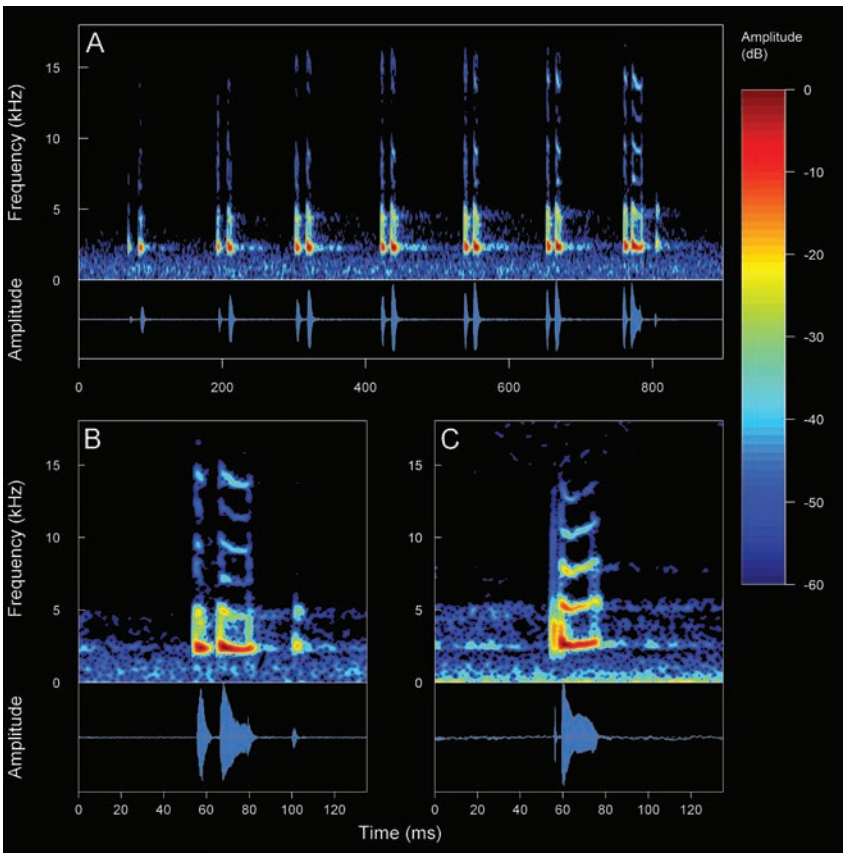

Figure 25. Spectrograms and oscillograms of the advertisement call of *Pristimantis* sp. 5 *myersi* group. **A** complete advertisement call **B** detail of a pulsed note with downward frequency modulation (**A, B** DHMECN 13334, SVL 17.1 mm, 8.3 °C air temperature, 78% relative humidity) **C** detail of a pulsed note with upward frequency modulation (ZSFQ 4500, SVL 18.27 mm, 11.8 °C air temperature, 93% relative humidity). Spectrograms obtained using the Hann window at 99% overlap, 256 samples of FFT size and 3 dB filter bandwidth of 248 Hz.

Discussion

The present study describes the spectral and temporal parameters of advertisement calls of 20 anurans from the high Andean ecosystems of northern Ecuador, Carchi province. Only the calls of five of these species have already been reported in previous studies (Table 1). Sinsch and Juraske (2006) describe the call of *Gastrotheca orophylax*, reported from a locality in the high Andean ecosystems of northern Ecuador (San Gabriel, Carchi). The authors mention that the calls of *G. orophylax* are pulsed, with a mean duration of 2.47 ± 0.42 s (3.01 ± 1.47 s in this study) and a mean dominant frequency of 0.99 ± 0.1 kHz (0.98 ± 0.12 kHz in this study). This indicates spectral values that are similar to those described in the present study, although with different temporal values. In this regard, the variation of temporal parameters in anuran calls may be associated with environmental and social factors, such as temperature, specific habitats, and behavioral strategies (Zimmerman 1983; Jansen et al. 2016; Muñoz et al. 2020; Gillard and Rowley 2023; Mendoza-Henao et al. 2023). *Centrolene buckleyi* is the species with the highest number of call descriptions in Ecuador and Colombia. Consequently, it is the best studied species in the northern Andes (e.g., Guayasamin et al. 2006; Almendáriz and Batallas 2012; Duarte-Marín et al. 2022). It has been proposed that *C. buckleyi*

is a species complex, as evidenced by molecular data (Amador et al. 2018; Guayasamin et al. 2020; Cisneros-Heredia et al. 2023; Cuellar-Valencia et al. 2023; Franco-Mena et al. 2024). However, the calls exhibit structural similarities, characterized by short pulses, upward frequency modulation, and a dominant frequency not exceeding 3.3 kHz. Despite these similarities, the complex has yet to be evaluated with acoustic evidence at the level of its variation.

The call characteristics of *Pristimantis festae* are consistent with those presented by Holzheuser and Merino-Viteri (2019) and recorded at Hacienda Zuleta, Imbabura province, Ecuador. They agree that the calls are high-pitched whistles composed of one or two notes. Holzheuser and Merino-Viteri (2019) reported that calls of *P. festae* are composed of one or two short auxiliary notes that second a main note. The present study, the call of *P. festae* contains more than two auxiliary elements, which we interpret and consider to be structural pulses of a note. In addition to the designation of these elements as notes or pulses, we concur that a correlation may exist between these elements and a potential behavioral or environmental context that could result in variation in the structure of the call. In terms of activity, the recordings obtained by Holzheuser and Merino-Viteri (2019), were made during the day, with no nocturnal recordings. This contrasts with the data obtained in the present study, where the highest vocal activity was nocturnal and all recordings of *P. festae* were obtained at night.

Another previously reported call is that of *P. buckleyi*, as described by Cuellar-Valencia et al. (2023), from individuals recorded in southwestern Colombia. The mean duration of the call was reported to be 56 ± 4 ms (51.46 ± 4.77 ms in the present study), with a mean call rate of 15.007 ± 0.652 calls/minute (15.12 ± 5.63 calls/minute in the present study), while the mean dominant frequency is 1.01 ± 0.02 kHz (1.26 ± 0.07 kHz in the present study). As with *Centrolene buckleyi*, the calls of *Pristimantis festae* and *Pristimantis buckleyi* described in this study are similar to those previously documented. The subtle spectral and temporal variations in their calls may have taxonomic implications, aligning with molecular evidence that suggests these species form a species complex (Franco-Mena et al. 2023; Reyes-Puig et al. 2023).

The major contribution of the current study is the first description of vocalizations from 15 species, ten of which belong to the genus *Pristimantis*, a genus with an outstanding richness (613 species described so far; Frost 2024), but whose the bioacoustic, ecological, and ethological information remain scarce (Batallas and Brito 2016; Hutter et al. 2016). It is likely that this limited knowledge is a consequence of short-term studies based only on direct visual encounters (Batallas and Brito 2023), as well as the difficulties associated obtaining high-quality recording in harsh environments such as the Andean highlands at night. It is also important to note that the lack of bioacoustical information is a wide reality for most anuran species (De la Riva et al. 1995; Márquez et al. 1995; Köhler et al. 2017).

Notably, in the present study we describe the call of *Niceforonia brunnea*, a species that is characterized by the absence of vocal slits and sacs. The description of this call contributes to the growing body of evidence indicating that species that lack these structures and have historically been considered mute may in fact possess the capacity to vocalize (see Duellman 1978; Batallas and Brito 2022).

This study also presents the first description of the call of *Hyloxalus delatorreae*, a species endemic to the province of Carchi-Ecuador and critically endangered (Coloma et al. 2022). In a study conducted by Yánez-Muñoz et al. (2010),

the population status of *H.delatorreae* was evaluated in the same area where the call of this study was recorded (Moran-Carchi). The study estimated there to be a number of 52 individuals in an area of ca 5 ha. The population was found to be facing a number of critical problems, and the possibility of extinction is predicted. It is noteworthy that *H. delatorreae* has not been recorded again since February 2017, suggesting the local, and most likely global, extinction of this endemic species.

This is the first study to provide a general view of the acoustic diversity of anurans inhabiting the high Andean ecosystems of northern Ecuador. These ecosystems remain poorly understood and are significantly impacted by human activities (Yánez-Muñoz et al. 2020). The confirmation of nine candidate species and the southernmost record of *Pristimantis farisorum* underscores the necessity of implementing supplementary studies employing both active and passive methodologies (e.g., passive acoustic monitoring with programmable audio recorders) in these fragile and vulnerable ecosystems. In addition, the groupings obtained in the results of the Principal Component Analysis (PCA), according to the parameters analyzed, demonstrate the diversity and acoustic identity. Therefore, the importance of the use of acoustic parameters in the classification and identification of anuran species is supported and confirmed in a preliminary and prospective way Complementing acoustic data with molecular phylogenies and morphology will leads us to a better and deeper understanding of the anurofauna, with the aim of conserving the invaluable high Andean ecosystems.

Acknowledgements

Special thanks to Luis Batallas and Julia Revelo, illustrious Carchenses for their invaluable assistance and unwavering support throughout the research process. We thank Libardo Tello, Marcelo Oliva, Carlos Castro, Franklin Rodríguez, Jaime Rosero, Fernando Paguay, Roque Cerón, Luis Cuasquer, Daniel Rivadeneira, Daniel Padilla, and Valeria Ayo, for their assistance in the field work. We are very grateful to Daniela Franco and Gabriela Gavilánez from the Laboratorio de Biología Evolutiva de la Universidad San Francisco de Quito USFQ for their invaluable assistance in the molecular processing of the samples. We thank Laura González of the Fonoteca Zoológica de Madrid, for her invaluable help and patience with the sound bank. To Carolina Reyes and David Brito, of the Museo de Zoologia de la Universidad San Francisco de Quito USFQ, grateful thanks for advice and assistance in depositing specimens. We would like to express our gratitude to all the families of Carchi who welcomed us into their homes during the fieldwork and made us feel at home. We special thanks to Jorge Brito, Mario H. Yanez-Muñoz, Diego Inclán, and Francisco Prieto of INABIO, for their assistance in facilitating access to the institution and for allowing us to conduct laboratory work. We would like to express our gratitude to Luis Ceríaco, Fabio Hepp, Nathalie Yonow and an anonymous reviewer for their valuable comments that significantly improved the quality of this manuscript. We thank the prefectura del Carchi, especially Guillermo Herrera, for providing us with the necessary facilities at the tourist complex “Aguas Hediondas”. We thank Mateo Vega-Yanez for his contribution to the map design. Thanks to José Luis Tellería who provided useful comments on the first version of the manuscript. This work is dedicated to the memory of Luis Fernando Batallas Revelo.

Additional information

Conflict of interest

The authors have declared that no competing interests exist.

Ethical statement

No ethical statement was reported.

Funding

No funding was reported.

Author contributions

All authors have contributed equally.

Author ORCIDs

Diego Batallas https://orcid.org/0000-0002-0068-8146
Rafael Márquez https://orcid.org/0000-0002-2070-860X
Juan M. Guayasamin https://orcid.org/0000-0003-0098-978X

Data availability

All of the data that support the findings of this study are available in the main text or Supplementary Information.

References

Almendáriz A, Batallas D (2012) Nuevos datos sobre la distribución, historia natural y el canto de *Centrolene condor* Cisneros-Heredia y Morales-Mite 2008 (Amphibia: Anura: Centrolenidae). Revista Politécnica 30(3): 42–53.

Amador L, Parada A, D'Elía G, Guayasamin JM (2018) Uncovering hidden specific diversity of Andean glassfrogs of the *Centrolene buckleyi* species complex (Anura: Centrolenidae) PeerJ 6: e5856 https://doi.org/10.7717/peerj.5856

Angulo A, Reichle S (2008) Acoustic signals, species diagnosis, and species concepts: the case of a new cryptic species of *Leptodactylus* (Amphibia, Anura, Leptodactylidae) from the Chapare region, Bolivia. Zoological Journal of the Linnean Society 152: 59–77. https://doi.org/10.1111/j.1096-3642.2007.00338.x

Armesto LO, Señaris JC (2017) Anuros del norte de los Andes: riqueza de especies y estado de conservación. Papéis Avulsos de Zoologia 57(39): 491–526. https://doi.org/10.11606/0031-1049.2017.57.39

Batallas D, Brito J (2016) Descripción de las vocalizaciones de *Pristimantis ganonotus* (Anura: Craugastoridae) de Ecuador. Cuadernos de Herpetología 30(1): 31–34.

Batallas D, Brito J (2022) The call of *Rhinella festae* (Peracca, 1904) (Anura: Bufonidae) from Morona Santiago, Ecuador. Neotropical Biodiversity 8(1): 31–34. https://doi.org/10.1080/23766808.2022.2029320

Batallas D, Brito J (2023) The advertisement calls of *Pristimantis galdi* Jiménez de la Espada, 1870 and *Pristimantis katoptroides* (Flores, 1988) (Anura, Strabomantidae). Herpetozoa 36: 59–64. https://doi.org/10.3897/herpetozoa.36.e97705

Bolívar GW, Grant T, Osorio LA (1999) Combat behavior in *Centrolene buckleyi* and other centrolenid frogs. Alytes 16(3–4): 77–83.

Bradbury JH, Vehrencamp SL (1998) Principles of animal communication, 2nd edn. Sinauer Associates, Sunderland, 697 pp.

Brito R, Ojala-Barbour R, Brito DM, Brito JR, Brito MS (2017) New species of arboreal rat of the genus *Rhipidomys* (Cricetidae, Sigmodontinae) from Sangay National Park, Ecuador. Neotropical Biodiversity 3(1): 65–79. https://doi.org/10.1080/23766808.2017.1292755

Caminer MA, Mila B, Jansen M., Fouquet A, Venegas PJ, Chávez G, Lougheed SC, Ron SR (2017) Systematics of the *Dendropsophus leucophyllatus* species complex (Anura: Hylidae): Cryptic diversity and the description of two new species. PLoS ONE 12(3): e0171785. https://doi.org/10.1371/journal.pone.0171785

Chaves-Acuña W, Moreno EA, Yánez-Muñoz MH (2023) The advertisement call of *Pristimantis unistrigatus* (Anura: Strabomantidae) from the Ecuadorian Andes. Phyllomedusa 22(1): 49–55. https://doi.org/10.11606/issn.2316-9079.v22i1p49-55

Chen HM, Combs CA (1999) An alternative anesthesia for amphibians: ventral application of benzocaine. Herpetological Review 30: 34

Cisneros-Heredia DF, Yánez-Muñoz MH, Sánchez-Nivicela JC, Ron SR (2023) Two new syntopic species of glassfrogs (Amphibia, Centrolenidae, *Centrolene*) from the southwestern Andes of Ecuador. PeerJ 11: e15195. https://doi.org/10.7717/peerj.15195

Cocroft RB, Ryan MJ (1995) Patterns of advertisement call evolution in toads and chorus frogs. Animal Behaviour 49(2): 283–303. https://doi.org/10.1006/anbe.1995.0043

Colafrancesco KC, Gridi-Papp M (2016) Vocal Sound Production and Acoustic Communication in Amphibians and Reptiles. In: Suthers RA, Fitch WT, Fay RR, Popper AN (Eds) Vertebrate Sound Production and Acoustic Communication. Springer International Publishing, Switzerland, 51–82. https://doi.org/10.1007/978-3-319-27721-9_3

Coloma LA (1995) Ecuadorian frogs of the genus *Colostethus* (Anura: Dendrobatidae). Miscellaneous Publications of the Museum of Natural History (University of Kansas) 87: 1–72. https://doi.org/10.5962/bhl.title.16171

Coloma LA, Ortiz DA, Frenkel C (2022). *Hyloxalus delatorreae* In: Ron S, Merino-Viteri A, Ortiz D (Eds) Anfibios del Ecuador. Version 2022.0. Museo de Zoología, Pontificia Universidad Católica del Ecuador. https://bioweb.bio/faunaweb/amphibiaweb/FichaEspecie/Hyloxalus%20delatorreae [accessed 20 May 2024]

Cuellar-Valencia OM, Bolaños-Molina BE, Bolívar-García W (2023) Exploring the acoustic diversity of Andean frogs in the Farallones de Cali National Natural Park, southwestern Colombia. Studies on Neotropical Fauna and Environment, 1–19. https://doi.org/10.1080/01650521.2023.2266187

De la Riva I, Márquez Rafael, Bosch J (1995) Advertisement calls of eight Bolivian hylids (Amphibia, Anura). Journal of herpetology 29(1): 113–118. https://doi.org/10.2307/1565094

Duarte-Marín S, Rada M, Rivera-Correa M, Caorsi V, Barona E, González-Durán G, Vargas-Salinas F (2022) Tic, Tii and Trii calls: Advertisement call descriptions for eight glass frogs from Colombia and analysis of the structure of auditory signals in Centrolenidae. Bioacoustics 32(3): 143–180. https://doi.org/10.1080/09524622.2022.2077833

Duellman WE (1978) The biology of an equatorial herpetofauna in Amazonian Ecuador. Miscellaneous Publications of the University of Kansas 65: 1–352.

Duellman WE (1999) Distribution patterns of amphibians in South America. In: Duellman WE (Ed.) Patterns of distribution of amphibians, a global perspective. Johns Hopkins University Press, London, 255–328. https://doi.org/10.56021/9780801861154

Duellman WE (2015) Marsupial Frogs: *Gastrotheca* & Allied Genera. Johns Hopkins University Press, Baltimore, 407 pp. https://doi.org/10.1353/book.40894

Duellman WE, Lehr E (2009) Terrestrial-Breeding Frogs (Strabomantidae) in Peru. Nature und Tiere Verlag, Naturwissenschaft, Münster, 382 pp.

Emmrich M, Vences M, Ernst R, Köhler J, Barej MF, Glaw F, Jansen M, Rödel MO (2020) A guild classification system proposed for anuran advertisement calls. Zoosystematics and Evolution 96(2): 515–525. https://doi.org/10.3897/zse.96.38770

Forti LR, Haddad CFB, Leite F, Drummond LO, de Assis C, Crivellari LB, Mello CM, Garcia PCA, Zornosa-Torres C, Toledo LF (2019) Notes on vocalizations of Brazilian amphibians IV: Advertisement calls of 20 Atlantic Forest frog species. PeerJ 7: e7612. https://doi.org/10.7717/peerj.7612

Franco-Mena D, Guayasamin JM, Andrade-Brito D, Yánez-Muñoz MH, Rojas-Runjaic FJM (2023) Unveiling the evolutionary relationships and the high cryptic diversity in Andean rain frogs (Craugastoridae: *Pristimantis myersi* group). PeerJ 11: e14715. https://doi.org/10.7717/peerj.14715

Franco-Mena D, De la Riva I, Vega-Yánez MA, Székely P, Amador L, Batallas D, Reyes-Puig JP, Cisneros-Heredia DF, Venegas-Valencia K, Galeano SP, Culebras J, Guayasamin JM. 2024. Simplifying the *Centrolene buckleyi* complex (Amphibia: Anura: Centrolenidae): a taxonomic review and description of two new species. PeerJ 12: e17712. https://doi.org/10.7717/peerj.17712

Frost DR (2024) Amphibian Species of the World: an Online Reference. Version 6.2. Electronic Database. American Museum of Natural History, New York, USA. https://doi.org/10.5531/db.vz.0001 [accessed 16 December 2024]

Gill BA, Kondratieff BC, Casner KL, Encalada AC, Flecker AS, Gannon DG, Funk WC (2016) Cryptic species diversity reveals biogeographic support for the 'mountain passes are higher in the tropics' hypothesis. Proceedings of the Royal Society B 283: 20160553. https://doi.org/10.1098/rspb.2016.0553

Gillard GL, Rowley JJL (2023) Assessment of the acoustic adaptation hypothesis in frogs using large-scale citizen science data. Journal of Zoology 310(2): 123–135. https://doi.org/10.1111/jzo.13088

Guayasamin JM, Bustamante MR, Almeida-Reinoso D, Funk WC (2006) Glass frogs (Centrolenidae) of Yanayacu Biological Station, Ecuador, with the description of a new species and comments on centrolenid systematics. Zoological Journal of the Linnean Society 147(4): 489–513. https://doi.org/10.1111/j.1096-3642.2006.00223.x

Guayasamin JM, Cisneros-Heredia DF, McDiarmid RW, Peña P, Hutter CR (2020) Glassfrogs of Ecuador: diversity, evolution, and conservation. Diversity 12(6): 222. https://doi.org/10.3390/d12060222

Guayasamin JM, Brunner RM, Valencia-Aguilar A, Franco-Mena D, Ringler E, Medina Armijos A, Morochz C, Bustamante L, Maynard RJ, Culebras J (2022) Two new glassfrogs (Centrolenidae: *Hyalinobatrachium*) from Ecuador, with comments on the endangered biodiversity of the Andes. PeerJ 10: e13109. https://doi.org/10.7717/peerj.13109

Hazzi NA, Moreno JS, Ortiz-Movliav C, Palacio RD (2018) Biogeographic regions and events of isolation and diversification of the endemic biota of the tropical Andes. Proceedings of the National Academy of Sciences 115(31): 7985–7990. https://doi.org/10.1073/pnas.1803908115

Hepp F, Bezerra AM, Botero JP (2019) First description of sound emission of *Rhaphiptera affinis* Thomson, 1868 (Cerambycidae: Lamiinae: Pteropliini). Zootaxa 4567(3): 580–582. https://doi.org/10.11646/zootaxa.4567.3.9

Heyer R, Donnelly, MA, Foster, M, Mcdiarmid R [Eds] (2014) Measuring and monitoring biological diversity: standard methods for amphibians. Smithsonian Institution Press. Washington, D.C, 364 pp.

Holzheuser C, Merino-Viteri A (2019) Call structure and activity period of *Pristimantis festae* a high-elevation anuran in Ecuador. Herpetological Review 50(3): 479–483.

Hutter CR, Guayasamin JM (2015) Cryptic diversity concealed in the Andean cloud forests: two new species of rainfrogs (*Pristimantis*) uncovered by molecular and bioacoustic data. Neotropical Biodiversity 1: 36–59. https://doi.org/10.1080/23766808.2015.1100376

Hutter CR, Liu V, Kell T, Lyons JA, Guayasamin JM (2016) The Natural History, Distribution, and Conservation of Lonely Rainfrogs, *Pristimantis eremitus*. Herpetologica 72(1): 13–22. https://doi.org/10.1655/Herpetologica-D-14-00020

Hutter CR, Lambert SM, Wiens JJ (2017) Rapid diversification and time explain amphibian richness at different scales in the tropical Andes, earth's most biodiverse hotspot. The American Naturalist 190(6): 828–843. https://doi.org/10.1086/694319

Jansen M, Masurowa A, O'Hara RB (2016) Temporal variation, duty cycle, and absolute calling effort during sustained calling of *Leptodactylus mystacinus* (Anura: Leptodactylidae). Salamandra 52: 328–336.

K. Lisa Yang Center for Conservation Bioacoustics (2024) Raven Pro: Interactive Sound Analysis Software (Version 1.6.5). Computer software. The Cornell Lab of Ornithology. Ithaca, NY. https://ravensoundsoftware.com/

Köhler J, Jansen M, Rodríguez A, Kok PJR, Toledo LF, Emmrich M, Glaw F, Haddad CFB, Rödel M, Vences M (2017) The use of bioacoustics in anuran taxonomy: theory, terminology, methods and recommendations for best practice. Zootaxa 4251: 1–124. https://doi.org/10.11646/zootaxa.4251.1.1

Ligges U, Krey S, Mersmann O, Schnackenberg S (2018) TuneR: Analysis of music. R package version 2.2.3. https://CRAN.Rproject.org/package=tuner

Lynch JD, Duellman WE (1997) Frogs of the genus *Eleutherodactylus* in western Ecuador: systematics, ecology, and biogeography. Special Publication Natural History Museum University of Kansas 23: 1–236.

Márquez R, De la Riva I, Bosch, J (1995) Advertisement calls of Bolivian Leptodactylidae (Amphibia, Anura). Journal of Zoology 237(2): 313–336. https://doi.org/10.1111/j.1469-7998.1995.tb02765.x

Mendoza-Henao AM, Arias E, Townsend JH, Parra-Olea G (2020) Phylogeny-based species delimitation and integrative taxonomic revision of the *Hyalinobatrachium fleischmanni* species complex, with resurrection of *H. viridissimum* (Taylor, 1942). Systematics and Biodiversity 18(5): 464–484. https://doi.org/10.1080/14772000.2020.1776781

Mendoza-Henao AM, Zamudio KR, Guayasamin JM, Escalona M, Parra-Olea G (2023) Environment rather than character displacement explains call evolution in glassfrogs. Evolution 77(2): 355–369. https://doi.org/10.1093/evolut/qpac041

Muñoz MI, Goutte S, Ellers J, Halfwerk W (2020) Environmental and morphological constraints interact to drive the evolution of communication signals in frogs. Journal of Evolutionary Biology 33(12): 1749–1757. https://doi.org/10.1111/jeb.13713

Ojala-Barbour R, Brito J, Teska WR (2019) A comparison of small mammal communities in two High-Andean *Polylepis* woodlands in Ecuador. Avances en Ciencias e Ingenierías 11(2): 208–221. https://doi.org/10.18272/aci.v11i2.516

Padial JM, Miralles A, De la Riva I, Vences M (2010) The integrative future of taxonomy. Frontiers in Zoology 7: 16. https://doi.org/10.1186/1742-9994-7-16

Páez NB, Ron SR (2019) Systematics of *Huicundomantis*, a new subgenus of *Pristimantis* (Anura, Strabomantidae) with extraordinary cryptic diversity and eleven new species. ZooKeys 868: 1–112. https://doi.org/10.3897/zookeys.868.26766

Páez-Vacas MI, Coloma LA, Santos JC (2010) Systematics of the *Hyloxalus bocagei* complex (Anura: Dendrobatidae), description of two new cryptic species, and recognition of *H. maculosus*. Zootaxa 2711: 1–75. https://doi.org/10.11646/zootaxa.2711.1.1

R Development Core Team (2024) R: A language and environment for statistical computing. R Foundation for Statistical Computing. Vienna, Austria. http://www.R-project.org

Redondo T (1994) Comunicación: teoría y evolución de las señales. In: Carranza J (Ed.) Etología: Introducción a la ciencia del comportamiento. Publicaciones de la Universidad de Extremadura, Cáceres, 255–298.

Reyes-Puig JP, Urgilés-Merchán M, Franco-Mena D, Guayasamin JM, Batallas D, Reyes-Puig C (2023) Two new species of terrestrial frogs of the *Pristimantis* gladiator complex (Anura, Strabomantidae) from the Ecuadorian Andes, with insights on their biogeography and skull morphology. ZooKeys 1180: 257–293. https://doi.org/10.3897/zookeys.1180.107333

Rivera-Correa M, Vargas-Salinas F, Grant T (2017) Statistical differences and biological implications: a comparative analysis of the advertisement calls of two Andean stream treefrogs (Hylidae: *Hyloscirtus*) and the evolution of acoustic characters. Salamandra 53(2): 237–244.

Ron SR, Duellman WE, Caminer, MA, Pazmiño D (2018) Advertisement calls and DNA sequences reveal a new species of *Scinax* (Anura: Hylidae) on the Pacific Lowlands of Ecuador. PLoS ONE 13(9): e0203169. https://doi.org/10.1371/journal.pone.0203169

Rueda-Almondacid JV, Castro F, Cortez C (2006) Técnicas para el inventario y muestreo de anfibios: Una compilación. In: Angulo A, Rueda-Almondacid JV, Rodriguez-Mahecha JV, La Marca E (Eds) Técnicas de inventario y monitoreo para los anfibios de la Región Tropical Andina. Conservación Internacional, Serie Manuales para la conservación N2, Panamericana Formas e Impresos S.A, Bogotá, 135–171.

Simmons AM (2003) Perspectives and progress in animal acoustic communication. In: Simmons AM, Fay RR, Popper AN (Eds) Acoustic communication. Springer-Verlag, New York, 1–14. https://doi.org/10.1007/0-387-22762-8_1

Simmons JE (2015) Herpetological Collecting and Collections Management, 3rd edn. Society for the Study of Amphibians and Reptiles Herpetological Circular No. 42. Salt Lake City, UT, 191 pp.

Sinsch U, Juraske N (2006) Advertisement calls of hemiphractine marsupial frogs: II. *Gastrotheca plumbea* group. In: Vences M, Köhler T, Ziegler T, Böhme W (Eds) Herpetologia Bonnensis 2: Proceedings of the 13th Congress of the Societas Europaea Herpetologica. Societas Europaea Herpetologica, Bonn, 149–152.

Sueur J (2018) Sound Analysis and Synthesis with R. Springer International Publishing, Switzerland, 637 pp. https://doi.org/10.1007/978-3-319-77647-7

Sueur J, Aubin T, Simonis C (2008) Seewave: a free modular tool for sound analysis and synthesis. Bioacoustics 18: 213–226. https://doi.org/10.1080/09524622.2008.9753600

Toledo LF, Martins IA, Bruschi DP, Passos MA, Alexandre C, Haddad CFB (2015) The anuran calling repertoire in the light of social context. Acta Ethologica 18(2): 87–99. https://doi.org/10.1007/s10211-014-0194-4

Vieites DR, Wollenberg KC, Andreone F, Kohler J, Glaw F, Vences M (2009) Vast underestimation of Madagascar's biodiversity evidenced by an integrative amphibian inventory. Proceedings of the National Academy of Sciences 106(20): 8267–8272. https://doi.org/10.1073/pnas.0810821106

Wells KD, Schwartz JJ (2007) The behavioral ecology of anuran communication. In: Narins PM, Feng AS, Fay RR, Popper AN (Eds) Hearing and sound communication in amphibians. Springer, New York, 44–86. https://doi.org/10.1007/978-0-387-47796-1_3

Wickham H (2016) Ggplot2: Elegant Graphics for Data Analysis. Springer-Verlag New York. [ISBN 978-3-319-24277-4] https://doi.org/10.1007/978-3-319-24277-4

Yánez-Muñoz MH, Meza-Ramos P, Altamirano M, Castro C (2010) Estado poblacional de una de rana nodriza (Anura: Dendrobatidae: *Hyloxalus delatorreae*),

críticamente amenazada, en los Andes Norte de Ecuador. Boletín Técnico, Serie Zoológica 9(6): 38–64.

Yánez-Muñoz MH, Batallas D, Franco-Mena D, Meza-Ramos PA, Oyagata LA, Padilla D, Paucar C, Reyes-Puig JP, Rodríguez A, Urgilés-Merchán MA, Vega-Yánez M (2020) Anfibios en los Ecosistemas Andino-Tropicales de la provincia del Carchi. Publicación Miscelanea No 14, Instituto Nacional de Biodiversidad. Quito, 339 pp.

Yánez-Muñoz, MH, Reyes-Puig, JP, Batallas D, Broaddus C, Urgilés-Merchán M, Cisneros-Heredia DF, Guayasamin JM (2021) A new Andean treefrog (Amphibia: *Hyloscirtus bogotensis* group) from Ecuador: an example of community involvement for conservation. PeerJ 9: e11914. https://doi.org/10.7717/peerj.11914

Zelick R, Mann D, Popper A (1999) Acoustic Communication in Fishes and Frogs. In: Fay R, Popper A (Eds) Comparative Hearing: Fish and Amphibians. Springer, Heidelberg, Germany, 363–411. https://doi.org/10.1007/978-1-4612-0533-3_9

Zhang F, Zhao J, Feng AS (2017) Vocalizations of female frogs contain nonlinear characteristics and individual signatures. PLoS ONE 12(3): e0174815. https://doi.org/10.1371/journal.pone.0174815

Zimmerman BL (1983) A comparison of structural features of calls of open and forest habitat frog species in the Central Amazon. Herpetologica 39(3): 235–246.

Supplementary material 1

Anurans of Carchi-Ecuador

Authors: Diego Batallas, Rafael Márquez, Juan M. Guayasamin

Data type: xlsx

Explanation note: This database contains collection data and recordings of anurans from the high Andean ecosystems of Carchi, Ecuador (2016–2021).

Link: https://doi.org/10.3897/zookeys.1224.137972.suppl1

Supplementary material 2

Bioacoustics of Anurans from Carchi, Ecuador

Authors: Diego Batallas, Rafael Márquez, Juan M. Guayasamin

Data type: xlsx

Explanation note: This database contains the acoustic measurements obtained from the calls of the various specimens collected and not collected in the study. It details the sample number in relation to each specimen, the calls, the notes, and the pulses.

Link: https://doi.org/10.3897/zookeys.1224.137972.suppl2

ZooKeys 1224: 253–260 (2025)
DOI: 10.3897/zookeys.1224.136863

Short Communication

Complete mitochondrial genome and phylogenetic analysis of the Atrato slider, *Trachemys medemi* (Testudines, Emydidae)

Sebastián Cuadrado-Ríos[1,2], Mario Vargas-Ramírez[1,2], Christian Kehlmaier[2], Uwe Fritz[2]

1 *Grupo de Biodiversidad y Conservación Genética, Instituto de Genética, Universidad Nacional de Colombia, Bogotá, Colombia*
2 *Museum of Zoology, Senckenberg Natural History Collections Dresden, 01109 Dresden, Germany*
Corresponding author: Uwe Fritz (uwe.fritz@senckenberg.de)

Abstract

The mitochondrial genome of three *Trachemys medemi* was sequenced and annotated for the first time. The mitochondrial genome is a circular DNA molecule of 16,711–16,810 bp in size, with 60.9% AT content. It includes 13 protein-coding genes, two rRNA genes, 22 tRNA genes, and the non-coding control region. The genome composition is characterized by a positive AT skew (0.123) and a negative GC skew (-0.342). Phylogenetic analyses based on complete mitogenomes, which lack some *Trachemys* species, placed *T. medemi* as sister to *T. venusta*. Phylogenies from the same dataset, but including available shorter mtDNA information for most *Trachemys* species, recovered *T. medemi* as sister to *T. dorbigni*, and this clade was sister to *T. venusta*, *T. yaquia*, and *T. ornata*. The newly obtained data are valuable for future mitogenomic investigations on *Trachemys*. Furthermore, our results underline the impact of incomplete taxon sampling.

Key words: Chocó, Colombia, mitogenome, phylogeny, primer walking, turtle

Academic editor: Scott A. Thomson
Received: 11 September 2024
Accepted: 23 December 2024
Published: 31 January 2025

ZooBank: https://zoobank.org/8F93590D-3B0C-4E13-AA54-72D4CCC1DD74

Citation: Cuadrado-Ríos S, Vargas-Ramírez M, Kehlmaier C, Fritz U (2025) Complete mitochondrial genome and phylogenetic analysis of the Atrato slider, *Trachemys medemi* (Testudines, Emydidae). ZooKeys 1224: 253–260. https://doi.org/10.3897/zookeys.1224.136863

Introduction

The Atrato slider (*Trachemys medemi* Vargas-Ramírez, del Valle, Ceballos & Fritz, 2017) is a species of freshwater turtle with a narrow distribution. It is restricted to the Atrato Basin of northwestern Colombia (Vargas-Ramírez et al. 2017; TTWG 2021) and one of the four endemic turtle species of the country (Páez et al. 2022). Only described in 2017, *Trachemys* individuals from the Atrato Basin were previously misidentified as various other taxa, including *Trachemys venusta uhrigi* McCord, Joseph-Ouni & Blanck, 2010, a Central American taxon (TTWG 2017, 2021; see also the review in Vargas-Ramírez et al. 2017). Other slider turtle populations in Colombia and Venezuela actually represent *T. venusta* (Gray, 1856), the species with which the Atrato sliders were associated before. However, phylogenetic analyses using mitochondrial and nuclear DNA sequences (Vargas-Ramírez et al. 2017; Fritz et al. 2023, 2024) recovered *T. medemi* as sister to *T. dorbigni* (Duméril & Bibron, 1835), a species which occurs far away in Brazil, Uruguay and Argentina. To expand our knowledge of *T. medemi*, we sequenced its entire mitogenome for the present study. In the context of taxonomic uncertainties and introgression

in *Trachemys* (Fritz et al. 2023, 2024), these data can be critical for further taxonomic and phylogenetic studies, and also provide a valuable resource for mitogenomic studies in turtles.

Material and methods

We used ethanol-preserved blood samples from three *Trachemys medemi* from the Banco de Tejidos de la Biodiversidad Colombiana (BTBC), Instituto de Genética, Universidad Nacional de Colombia, Bogotá. To maximize the utility of these data for future analyses, we selected three individuals from different localities (BTBC12643: between Las Brisas and Llano Rico, Riosucio, Chocó, 7.3267, -76.8129; BTBC13199: Reserva Natural Surikí, Turbo, Antioquia, 7.7704, -76.8838; BTBC13207: Ciénaga de Napipí, Bojayá, Chocó, 6.6277, -76.9489).

DNA was extracted using the innuPREP DNA Mini Kit 2.0 (Analytik Jena), with a final elution of 80 µl milliQ water. The complete mitochondrial genome was amplified using long-range PCR followed by primer-walking procedures. Using primers from Fritz et al. (2012, 2023), two long-range PCR reactions (LR1 and LR2) were performed, yielding amplicons with lengths of 11,824 bp and 6797 bp, which overlap by more than 1000 bp. Long-range PCR products were purified using the ExoSAP-IT enzymatic clean-up (USB Europe, Staufen, Germany). These amplicons cover most of the mitochondrial genome, except for the first part of the tRNA-Phe and the final 3'-end of the control region. These regions were amplified using standard PCR procedures and custom primers designed from the consensus sequence of the primer-walking PCR products. The cleaned products were Sanger sequenced using a set of primers compatible with the mitochondrial genome of *Trachemys scripta elegans* (GenBank accession number MW019443; Suppl. material 1: table S1). The initial batch of sequences was mapped onto the same mitogenome sequence from *T. s. elegans* (MW019443) and curated using GENEIOUS R7 (http://geneious.com). From this assembly, new sequencing primers were designed to close the gaps between the sequences. This process was repeated twice, resulting in a total of 14 newly designed primers (Suppl. material 1: table S1). Detailed laboratory procedures are provided in the Suppl. material. Mitogenomes were annotated with MITOS v. 2.1.7 (Bernt et al. 2013) through the Proksee server (Grant et al. 2023; Suppl. material 1: table S2). Initiation and termination codons were identified using ORFFINDER (https://www.ncbi.nlm.nih.gov/orffinder). AT skew and GC skew were calculated to describe the base composition (Perna and Kocher 1995). The new mitogenomes have been deposited in the European Nucleotide Archive (ENA) under accession numbers OZ183365–OZ183367.

Phylogenetic analyses using maximum likelihood (ML) and Bayesian inference (BI) were performed with a complete mitogenome dataset, which included all available complete mitogenomes for *Trachemys* (Suppl. material 1: table S3). However, no mitogenomes have been published for the two taxa (*T. d. dorbigni*, *T. d. adiutrix*) previously identified as sister to *T. medemi* (Vargas-Ramírez et al. 2017; Fritz et al. 2023, 2024). Therefore, we re-analyzed the mitogenomes from our initial dataset together with the 3221-bp-long mtDNA dataset from Fritz et al. (2024), with missing information coded as Ns. For further details, see Suppl. material 1.

Results

We obtained three complete mitogenomes of *Trachemys medemi*, ranging from 16,711 bp to 16,810 bp. The length variation was due to the absence of a 92-bp-long repetitive sequence in the control region of one mitogenome (ENA accession number OZ183367) and some minor indels in the terminal repetitive part of the control region.

The mitogenome consists of 13 protein-coding genes, 2 ribosomal RNA (rRNA) genes, 22 transfer RNA (tRNA) genes and the non-coding control region (Fig. 1, Suppl. material 1: table S2), as in other *Trachemys* and related emydid species (Fritz et al. 2023, 2024; Ren et al. 2024). Nine of the 37 genes are encoded on the light strand; the remaining genes are on the heavy strand. The three mitogenomes differ in two mutations in the ND1 gene, one mutation in the ND2 gene, two mutations in the ND4L gene, two mutations in the ND4

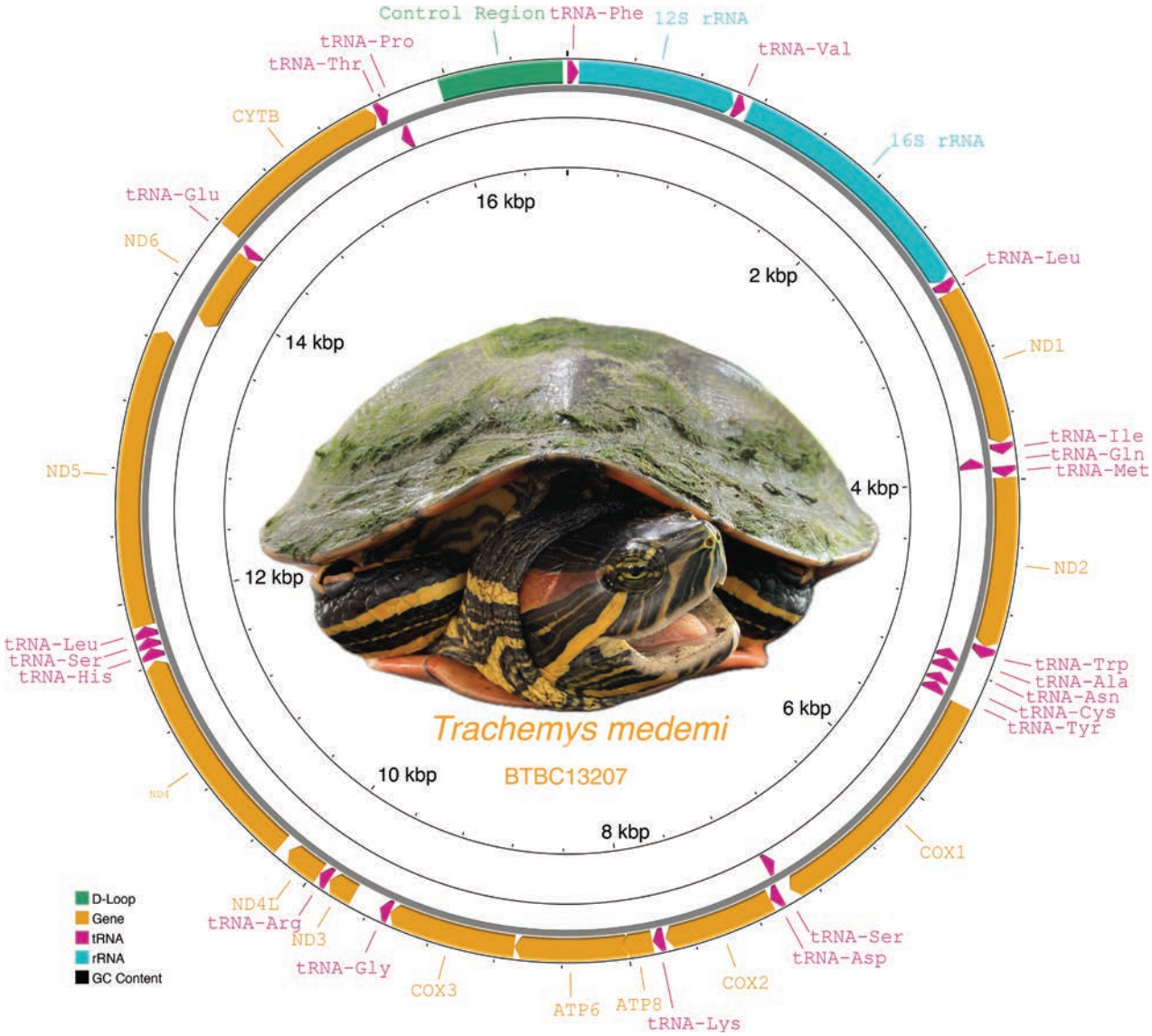

Figure 1. Circular view of the complete annotated mitogenome of the Atrato slider (*Trachemys medemi*), displaying 13 protein-coding genes, two rRNA genes, 22 tRNA genes, and the control region (ENA accession number OZ183365). Inset photo: *T. medemi*, adult female from Ciénaga de Napipí, Bojayá, Chocó, Colombia. Photo: Sebastián Cuadrado-Ríos.

Figure 2. Part of the alignment of the three *Trachemys medemi* mitogenomes obtained in the present study illustrating the absence of a 92-bp-long duplicated sequence in the control region of BTBC13207, spanning from position 15,861 to 15,952.

gene, one mutation in the ND5 gene, one mutation in the ND6 gene, and one mutation and the absence/presence of a duplicated part of the control region (92 bp) and a few minor indels in the terminal repetitive part of the control region (Fig. 2). The genome composition is A: 34.3%, C: 26.1%, G: 12.8%, T: 26.6%, with a slight AT bias (60.9%), a positive AT skew (0.123), and a negative GC skew (-0.342). The AT skew falls within the range of other *Trachemys* species, but is higher than in most previously sequenced emydid mitogenomes. The GC skew is also higher than in most of the other emydid mitogenomes (Ren et al. 2024). As in other *Trachemys* species, the GC content was consistent across the mitogenome, ranging from 38.1% to 39.5%, except for the control region with a GC content of 32.7% (Suppl. material 1: table S3).

Of the 22 tRNA genes in the mitogenome of *T. medemi*, 14 are encoded on the heavy strand and eight on the light strand (Fig. 1). The tRNA genes ranged between 67 and 75 bp in length and exhibited a positive AT skew (0.128) and A+T bias (61.7%; Suppl. material 1: table S3). The 12S rRNA gene is located between the initial tRNA-Phe and tRNA-Val; the 16S rRNA is between tRNA-Val and tRNA-Leu (Fig. 1). The rRNA genes are 976 bp and 1635 bp long, respectively, and show an A+T bias (60.2%), a positive AT skew (0.282) and a negative GC skew (-0.161; Suppl. material 1: table S3). The control region is located between the tRNA-Pro and tRNA-Phe genes. In one mitogenome (BTBC13207), the control region is distinctly shorter due to the absence of a repetitive sequence of 92 bp length (Fig. 2). The control region has only a very slightly positive AT skew (0.002) and a negative GC skew (-0.266). The mitogenomic characteristics of *T. medemi* and other species are detailed in Suppl. material 1: table S3.

Phylogenetic analyses using complete mitogenomes resulted in similar topologies with robust support for the major clades (Fig. 3A). Both analyses placed *T. medemi* as sister to *T. venusta* sensu lato, with both species forming a clade that is sister to *T. grayi*. When the mitogenomes were aligned with the 3221-bp-long mtDNA dataset from Fritz et al. (2024), the resulting phylogenies showed similar topologies, also with robust support for the main clades (Fig. 3B). However, these phylogenies placed *T. medemi* as sister species to *T. dorbigni*, with this clade being sister to a clade composed of *T. venusta* sensu lato, *T. yaquia*, and *T. ornata* (Fig. 3B). The phylogenetic position of the West Indian species *T. terrapen*, *T. decorata*, *T. stejnegeri*, and *T. decussata* was weakly resolved (Fig. 3B).

Discussion and conclusion

In this study, we sequenced, assembled and characterized three mitogenomes of *Trachemys medemi*, representing the first complete mitogenomes for the species. One mitogenome (BTBC13207) lacks a duplicated sequence between positions 15,861 and 15,952 (Fig. 2) in the right domain of the control region according to Bernacki and Kilpatrick (2020). The turtle was captured in the Ciénaga de Napipí, Bojayá, Chocó, Colombia, at the southernmost edge of the distri-

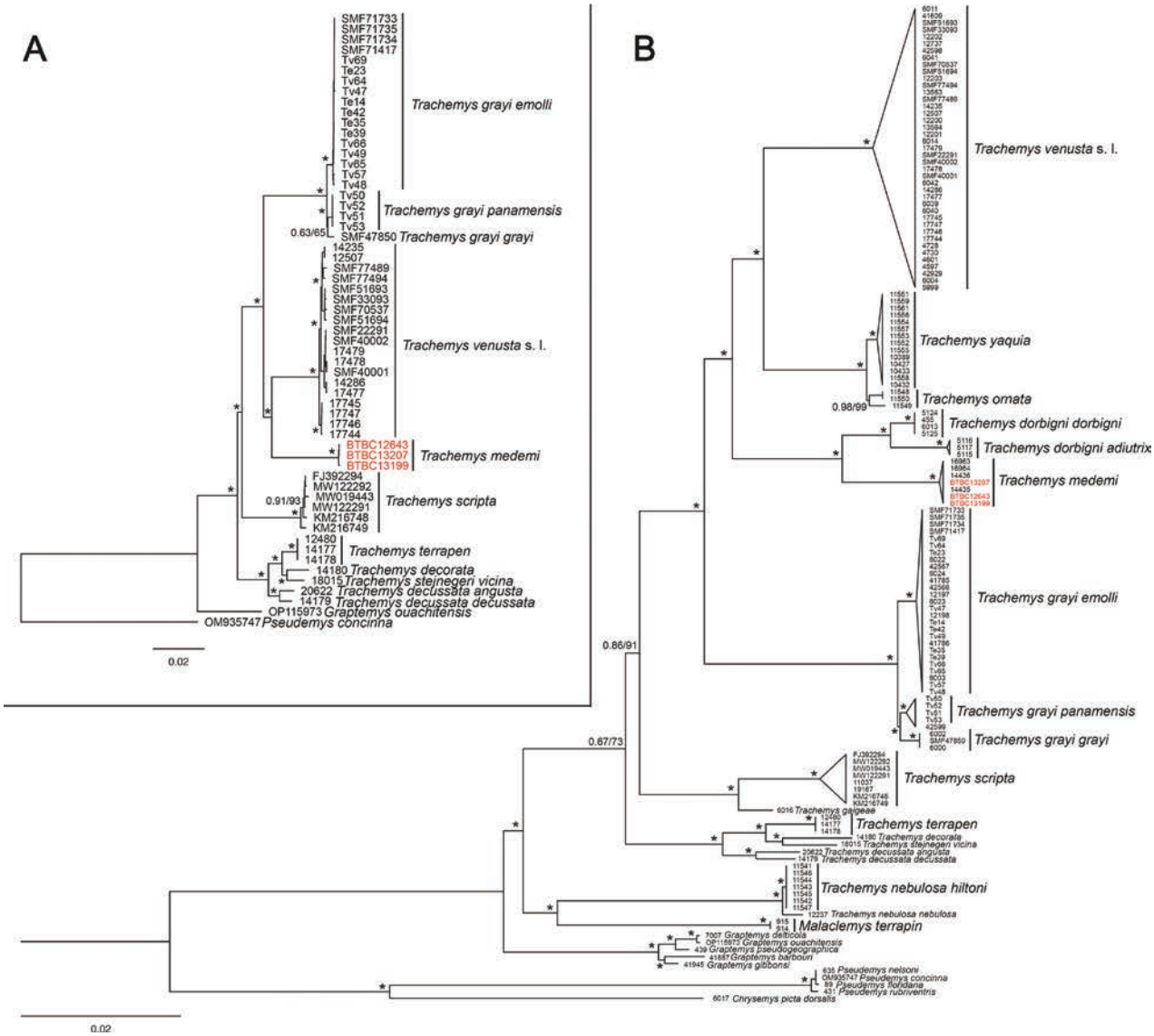

Figure 3. Maximum likelihood trees estimated with (**A**) mitogenomes and (**B**) mitogenomes combined with data from Fritz et al. (2024), representing nearly all *Trachemys* taxa. Outgroup (*Deirochelys reticularia*) removed for clarity in (**B**). The newly sequenced *T. medemi* mitogenomes are highlighted in red. Numbers at nodes represent posterior probabilities from a Bayesian phylogeny (left) and bootstrap values from the ML tree (right). Asterisks indicate maximum support from both approaches.

bution range (see Vargas-Ramírez et al. 2017). Furthermore, an examination of the mitogenome alignment revealed that this phenomenon also occurs in *T. venusta*: the only mitogenome published for *T. v. iversoni* (OZ038161), which does not significantly differ from the mitogenomes of *T. v. venusta* and *T. v. uhrigi* (Fritz et al. 2024), misses the same duplicated region as BTBC13207. It remains to be tested whether this has population genetic implications or merely represents individual variation.

Our phylogenetic analyses based on complete mitogenomes (Fig. 3A) recovered *T. medemi* as sister to *T. venusta* sensu lato in a maximally supported clade. However, when additional mtDNA sequences were included, *T. medemi* was sister to *T. dorbigni*, with these two species together representing the sister clade of another clade composed of *T. venusta* sensu lato, *T. yaquia*, and *T. ornata* (Fig. 3B). Thus, our results underline the impact of incomplete taxon sampling when the mitogenome data are considered alone and confirm previous phylogenetic analyses

based on shorter mtDNA sequences (Vargas-Ramírez et al. 2017; Fritz et al. 2023, 2024). Furthermore, the mitochondrial genomes of the narrow-endemic *T. medemi* are a valuable resource for future mitogenomic investigations.

Acknowledgements

We thank Anke Müller and Andrea Criado-Flórez (Senckenberg Natural History Collections Dresden) for their guidance and assistance with laboratory work. Scott Thomson and an anonymous reviewer made helpful comments on an earlier version of this study.

Additional information

Conflict of interest

The authors have declared that no competing interests exist.

Ethical statement

No turtles were collected or sampled for the present study.

Funding

This research was supported by the Turtle Conservation Fund (TCF). SC-R is supported by the "Convocatoria del Fondo de Ciencia, Tecnología e Innovación del Sistema General de Regalías, en el marco del Programa de Becas de Excelencia Doctoral del Bicentenario – Corte II", Department of Chocó, Universidad Nacional de Colombia and Ministerio de Ciencia, Tecnología e Innovación de Colombia and by a "Research Grant (bi-nationally supervised Doctoral Degree/Cotutelle, 2023/24)" from the German Academic Exchange Service (DAAD).

Author contributions

Conceptualization: SC-R, MV-R, CK, UF. Data curation: SC-R, CK. Formal analysis: SC-R. Funding acquisition: SC-R, MV-R. Investigation: SC-R. Methodology: SC-R, CK. Project administration: UF. Resources: SC-R, MV-R, UF. Supervision: MV-R, CK, UF. Visualization: SC-R. Writing – original draft: SC-R. Writing– review and editing: SC-R, MV-R, CK, UF.

Author ORCIDs

Sebastián Cuadrado-Ríos https://orcid.org/0000-0002-1060-820X
Mario Vargas-Ramírez https://orcid.org/0000-0001-8974-3430
Christian Kehlmaier https://orcid.org/0000-0001-9622-0566
Uwe Fritz https://orcid.org/0000-0002-6740-7214

Data availability

The mitochondrial genome sequences are openly available from the European Nucleotide Archive (ENA) at https://www.ebi.ac.uk/ena/browser/home under the accession numbers OZ183365-OZ183367 (BioProject number PRJEB79932).

References

Bernacki LE, Kilpatrick CW (2020) Structural variation of the turtle mitochondrial control region. Journal of Molecular Evolution 88: 618–640. https://doi.org/10.1007/s00239-020-09962-0

Bernt M, Donath A, Jühling F, Externbrink F, Florentz C, Fritzsch G, Pütz J, Middendorf M, Stadler PF (2013) MITOS: Improved de novo metazoan mitochondrial genome annotation. Molecular Phylogenetics and Evolution 69: 313–319. https://doi.org/10.1016/j.ympev.2012.08.023

Fritz U, Stuckas H, Vargas-Ramírez M, Hundsdörfer AK, Maran J, Päckert M (2012) Molecular phylogeny of Central and South American slider turtles: Implications for biogeography and systematics (Testudines: Emydidae: *Trachemys*). Journal of Zoological Systematics and Evolutionary Research 50: 125–136. https://doi.org/10.1111/j.1439-0469.2011.00647.x

Fritz U, Kehlmaier C, Scott RJ, Fournier R, McCranie JR, Gallego-García N (2023) Central American *Trachemys* revisited: New sampling questions current understanding of taxonomy and distribution (Testudines: Emydidae). Vertebrate Zoology 73: 513–523. https://doi.org/10.3897/vz.73.e104438

Fritz U, Herrmann HW, Rosen PC, Auer M, Vargas-Ramírez M, Kehlmaier C (2024) *Trachemys* in Mexico and beyond: Beautiful turtles, taxonomic nightmare, and a mitochondrial poltergeist (Testudines: Emydidae). Vertebrate Zoology 74: 435–452. https://doi.org/10.3897/vz.74.e125958

Grant JR, Enns E, Marinier E, Mandal A, Herman EK, Chen CY, Graham M, Van Domselaar G, Stothard P (2023) Proksee: In-depth characterization and visualization of bacterial genomes. Nucleic Acids Research 51: W484–W492. https://doi.org/10.1093/nar/gkad326

Páez VP, Bock BC, Alzate-Estrada DA, Barrientos-Muñoz KG, Cartagena-Otálvaro VM, Echeverry-Alcendra A, Gómez-Rincón MT, Ramírez-Gallego C, del Río JS, Vallejo-Betancur MM (2022) Turtles of Colombia: An annotated analysis of their diversity, distribution, and conservation status. Amphibian & Reptile Conservation 16: 106–135 [e306].

Perna NT, Kocher TD (1995) Patterns of nucleotide composition at fourfold degenerate sites of animal mitochondrial genomes. Journal of Molecular Evolution 41: 353–358. https://doi.org/10.1007/BF01215182

Ren Y, Zuo Z, Xing X, Zhai X, Wang T, Ma G (2024) The characterization of the mitochondrial genome of *Graptemys ouachitensis*. Mitochondrial DNA B 9: 563–567. https://doi.org/10.1080/23802359.2024.2347506

TTWG [Turtle Taxonomy Working Group] (2017) Turtles of the world. Annotated checklist and atlas of taxonomy, synonymy, distribution, and conservation status (8th edn.). Chelonian Research Monographs 7: 1–292. https://doi.org/10.3854/crm.7.checklist.atlas.v8.2017

TTWG [Turtle Taxonomy Working Group] (2021) Turtles of the world. Annotated checklist and atlas of taxonomy, synonymy, distribution, and conservation status (9th edn.). Chelonian Research Monographs 8: 1–472. https://doi.org/10.3854/crm.8.checklist.atlas.v9.2021

Vargas-Ramírez M, del Valle C, Ceballos CP, Fritz U (2017) *Trachemys medemi* n. sp. from northwestern Colombia turns the biogeography of South American slider turtles upside down. Journal of Zoological Systematics and Evolutionary Research 55: 326–339. https://doi.org/10.1111/jzs.12179

Supplementary material 1

Supplementary information

Authors: Sebastián Cuadrado-Ríos, Mario Vargas-Ramírez, Christian Kehlmaier, Uwe Fritz
Data type: pdf
Explanation note: Details for long-range PCR, primer walking and phylogenetic analyses.

Link: https://doi.org/10.3897/zookeys.1224.136863.suppl1

ZooKeys 1224: 261–282 (2025)
DOI: 10.3897/zookeys.1224.137935

Research Article

Soil campodeids (Diplura, Campodeidae) of Eastern Europe, in Romanian and Bulgarian reliefs

Alberto Sendra[1,2], Cristina Fiera[3], Jesús Selfa[4], Pavel Stoev[5,6]

1 *Departament de Didàctica de les Ciències Experimentals i Socials, Facultat de Magisteri, Universitat de València, València, Spain*
2 *Research Team on Soil Biology and Subterranean Ecosystems, Department of Life Sciences, Faculty of Science, Campus Universitario Crta, Universidad de Alcalá, A-2 Km. 33.6, 28805, Alcalá de Henares, Madrid, Spain*
3 *Institute of Biology Bucharest, Romanian Academy, 296 Splaiul Independenţei, 060031, Bucharest, Romania*
4 *Laboratori d'Investigació d'Entomologia, Departament de Zoologia, Universitat de València, Burjassot, València, Spain*
5 *National Museum of Natural History at the Bulgarian Academy of Sciences, Tsar Osvoboditel Blvd. 1, 1000 Sofia, Bulgaria*
6 *Pensoft Publishers, Prof. G. Zlatarski Str. 12, Sofia, Bulgaria*
Corresponding author: Cristina Fiera (cristina.ivanescu@ibiol.ro, cfiera2013@gmail.com)

Abstract

This study presents data on soil campodeids collected in Romania and Bulgaria in recent years. The collection comprises 12 species of genus *Campodea* Westwood, 1842 in total. A new species, *Campodea* (*Dicampa*) *transylvanica* Sendra, **sp. nov.** is described from Zarand and Făgăraș mountains in Romania. *Campodea* (*Campodea*) *plusiochaeta* Silvestri, 1912 is newly recorded for the Romanian fauna, while *Campodea* (*Paurocampa*) *ruseki* Condé, 1966 represents a new record for Bulgaria. New distributional data are also provided for the remaining ten species.

Key words: *Campodea*, *Dicampa*, new records, new species, *Paurocampa*, taxonomy

Academic editor: Louis Deharveng
Received: 26 September 2024
Accepted: 22 December 2024
Published: 31 January 2025

ZooBank: https://zoobank.org/F7854302-D5B4-4E43-91AA-7271BAD9BE4B

Citation: Sendra A, Fiera C, Selfa J, Stoev P (2025) Soil campodeids (Diplura, Campodeidae) of Eastern Europe, in Romanian and Bulgarian reliefs. ZooKeys 1224: 261–282. https://doi.org/10.3897/zookeys.1224.137935

Introduction

The first records of Campodeidae species (*Campodea staphylinus* Westwood, 1842 and *Campodea fragilis* Meinert, 1865) from Romania were published by Vellay (1900) and later cited by Stach (1929). However, both species are now considered misidentifications (Sendra et al. 2012). Years later, in Bulgaria, Silvestri (1931) described three species of campodeids from cave habitats: *Campodea* (*Dicampa*) *frenata* Silvestri, 1931, *Plusiocampa bulgarica* Silvestri, 1931, and *Plusiocampa bureschi* Silvestri, 1931. Later, Drĕnovski (1937) reported three species from soil habitats in Bulgaria: *Campodea* (*Dicampa*) *malpighii bulgarica* Drĕnovski, 1937, *Campodea witoschensis* Drĕnovski, 1937, and *Plusiocampa montana* Drĕnovski, 1937. However, Paclt (1957, 1969) considered each a nomen nudum, and the first two were respectively assigned to *Campodea* (*Dicampa*) *frenata* Silvesti, 1931 and *Campodea* (*Paurocampa*) *suensoni* Tuxen, 1930 while the third remained without assignation. During 1950s and 1960s, several contributions significantly improved our understanding of the soil and cave Campodeidae of the Carpathians (Romania) and the mountains in Bulgaria (Ionescu 1951, 1955; Rusek 1965a;

Paclt 1969). In the 21st century, the diversity of soil species increased to 18 species in Romania (Sendra et al. 2012) and seven species in Bulgaria (Sendra and Georgiev 2021). In addition to the soil-dwelling Campodeidae fauna, nine cave-adapted species have been described or reported: five species from caves in the southern Carpathians (Ionescu 1955; Condé 1991, 1993, 1996; Sendra et al. 2012) and six species from caves in Bulgaria (Silvestri 1931; Bareth and Condé 2001).

The aim of this study is to enhance the understanding of the family Campodeidae within the basal hexapod class Diplura in the Carpathians and Balkan Mountains in Romania and Bulgaria by providing new records and distributional data, describing a new species, and publishing taxonomic and distributional remarks on certain taxa.

In total, 222 specimens from 44 sampling sites in Romania and one site in Bulgaria were examined, based on a collection provided by C. Fiera collected between 2018 and 2021. Additional material from six localities in Bulgaria was collected by Boyan Petrov, Petar Beron, and Pavel Stoev, zoologists at the National Museum of Natural History, Bulgarian Academy of Sciences.

Materials and methods

Most of the Diplura specimens were extracted from samples of leaf litter, soil, and mosses using Berlese funnels. The material has been deposited in the private collection of Alberto Sendra, València, Spain (Coll. AS) and most of specimens were mounted on slides using Marc André II medium. These were observed and identified using a phase-contrast microscope, and measurements were taken with an ocular micrometre.

Photomicrography was performed with a stereo microscope (Leica M165C) with an integrated capture system image (LAS v. 4.13) and software LCS Lite, and a compound microscope with a photographic camera K3 C/M and the software LCS Lite. We used the software Helicon Focus to combine photos of a specimen at different levels of focal planes, which helped achieve a more accurate and complete illustration. Several specimens for SEM photography (Hitachi S-4900) were coated with palladium-gold.

The type and studied material are kept at the following institutions:

Coll. AS	private collection of Alberto Sendra, València, Spain
IBB	Institute of Biology Bucharest, Romanian Academy
NMNHS	National Museum of Natural History at the Bulgarian Academy of Sciences.

Results

Campodea (*Campodea*) *magna* Ionescu, 1955

Material examined. **Romania** • 1 ex., Bârgău Mountains: Leșu, Bistrița-Năsăud County, 47.289248°N, 24.756708°E, 749 m a.s.l., beach, rarely fir, litter, 02.11.2021, C. Fiera leg.; • 1 ex., RO, Bârgău Mountains: Lunca Ilvei, near Pepiniera Silhoasa, Bistrița-Năsăud County, 47.346245°N, 25.015375°E, 749 m a.s.l.,

mixed forest (fir and beach), soil, 04.11.2021, C. Fiera leg.; • 2 ex., Doftana Valley: Șotriile, 45.227694°N, 25.729119°E, 609 m a.s.l., beech forest, soil, 18.11.2016, C. Fiera leg.; • 7 ex., Bârgău Mountains: Tureac, site 1, Bistrița-Năsăud County, 47.257408°N, 24.856696°E, 862 m a.s.l., beech forest, soil, 18.08.2018, C. Fiera leg.; • 1 ex., Suceava County: Zamostea-Lunca forest, 47.870137°N, 26.252775°E, 290 m a.s.l., old oak (120 years old, rarely 180 years old), in association with ash, aspen, maple, hornbeam, litter, 08.08.2019, C. Fiera leg.

Habitat and distribution. Soil-dwelling species found in several localities from the southern Carpathians (Ionescu 1955; Sendra et al. 2012) and recently in Bulgaria (Sendra and Georgiev 2021). The species is also known from the northern Anatolia (Sendra et al. 2010).

Campodea (*Campodea*) *plusiochaeta* Silvestri, 1912

Material examined. **Romania** • 1 ex., Alba County: Cenade, 46.036341°N, 24.007781°E, 436 m a.s.l., vineyards, soil, 10.09.2020, M. Șandor leg.; • 1 ex., Suceava County: Iacobeni, 47.446179°N, 25.311171°E, 895 m a.s.l., mixed forest (fir, larch, hornbeam), soil and litter, C. Fiera leg.

Habitat and distribution. A soil-dwelling species, living under stones or among the alluvial debris (Condé 1960) which is common under barks or moss. It is also found in dry environments, burrows of mammals or gardens, sometimes reaches high altitude in mountains. It is one of the most widespread species collected at many sites of the Euro-Mediterranean region: British Isles (Condé 1961), southern Jutland and southern Scandinavian peninsulas (Silvestri 1912; Arevad 1957; Olsen 1996), North Africa (Condé 1947a, 1953), throughout the Iberian Peninsula (Sendra and Moreno 2004), throughout continental Europe including west, central, and eastern Europe (Silvestri 1912; Pagés 1951; Rusek 1964; Stach 1964; Wygodzinsky 1941; Paclt 1965), Apennine Peninsula (Silvestri 1912; Ramellini 1995; 2000), Balkan Peninsula (Condé 1984), and Anatolia (Sendra et al. 2010). The easternmost localities are in western Russia (Silvestri 1912; Rusek 1965b) close to the 60° parallel.

Remarks. New record for the Romanian fauna.

Campodea (*Campodea*) *taunica* Marten, 1939

Material examined. **Romania** • 1 ex., Dâmbovița County: Springs Complex of Corbii Ciungi, near Corbii Mari County, 44.524361°N, 25.512138°E, 122 m a.s.l., scrubs, soil, M. Manu leg.

Habitat and distribution. A soil-dwelling species that is distributed throughout Central Europe, including France (Husson 1946; Pagés 1951), Central Germany (Paclt 1961), Swiss Alps (Orelli 1956), and reaching as far as the Romanian Carpathians (Ionescu 1951, 1955; Sendra et al. 2012) and Serbia (Blesić 2000a). Surprisingly, it has not been found yet in the Czech Republic or Slovakia. Outside Central Europe, it has been quoted in the Pontic Mountains and the northern part of Anatolia (Sendra et al. 2010).

Campodea (*Campodea*) *wallacei* Bagnall, 1918

Material examined. **Romania** • 4 ex., Bucegi Massif: Sinaia, Prahova County, 45.333328°N, 25.549175°E, 858 m a.s.l., in the city of Sinaia, park, under *Larix* sp., 23.09.2019, C. Fiera and M.W. Weiner leg.

Habitat and distribution. A soil-dwelling species, which is also found in cave habitats (Condé 1956, 1962; Sendra et al. 2013). It is distributed in England (Bagnall 1918), southern Scandinavian Peninsula (Agrell 1944), Maritime Alps (Bareth and Condé 1985; Ramellini 2000), France (Condé 1947b, 1947c, 1950; Pagés 1951), Germany (Christian 2003) and the Dinaric Mountains (Blesić 1998a, 1998b, 2000a, 2001). The species has been recorded from Romania by Ionescu (1951, 1955) and Sendra et al. (2012).

Campodea (*Dicampa*) *apula* Silvestri, 1912

Material examined. **Romania** • 1 ex., Făgăraș Mountains: Nucșoara, Argeș County, 45.417893°N, 24.733326°E, 1196 m a.s.l., mixed forest (*Fagus sylvatica*, *Betula pendula*, *Alnus viridis*, *Sambucus* sp.), litter, 10.11.2021, C. Fiera and I. Vicol leg.

Habitat and distribution. A soil-dwelling species known from Foggia, Italy (Silvestri 1912), the Carpathian Mountains across Slovakia, Poland, and Romania (Ionescu 1951, 1955; Paclt 1961; Szeptycki 1974), and extending to the western border of the Caucasus.

Campodea (*Dicampa*) *campestris* Ionescu, 1955

Material examined. **Romania** • 5 ex., Făgăraș Mountains: Sâmbăta de Sus, Brașov County, 45.681608°N, 24.791662°E, 746 m a.s.l., mixed forest (fir and beach), soil, 11.11.2021, C. Fiera and I. Vicol leg.; 1 ex. Doftana Valley: Voila, 45.166241°N, 25.753028°E, 600 m a.s.l., sessile oak and beech, soil, 14.07.2018, C. Fiera leg.

Habitat and distribution. A soil-dwelling species distributed from the southern Carpathians to the Balkan Mountains (Rusek 1965a; Blesić 1984, 1998a, 2000a; Sendra et al. 2012).

Campodea (*Dicampa*) *frenata* Silvestri, 1931

Fig. 1a–f

Material examined. **Bulgaria** • 3 ex., Vrachanski Balkan Nature Park, hut Purshevitza, 1400 m a.s.l., forest, 12.07.1993, B. Petrov leg.; • 5 ex. Central Balkan National Park, hut Rai, 1250 m a.s.l., foliage, 08.12.1992, B. Petrov leg.; • 5 ex., Western Rhodopes Mts., village Mostovo, under stones, 14.03.1992, B. Petrov leg.; • 2 ex., Western Rila Mts., near Popovski ezera Lakes, 2350 m a.s.l., 25.07.1993, B. Petrov leg.

Taxonomic notes. Specific observations using scanning electron microscopy reveal short and slightly thick gouge sensilla on the antennomeres (Fig. 1a); tergites: dense microdenticles with rosette glands along with well-barbed

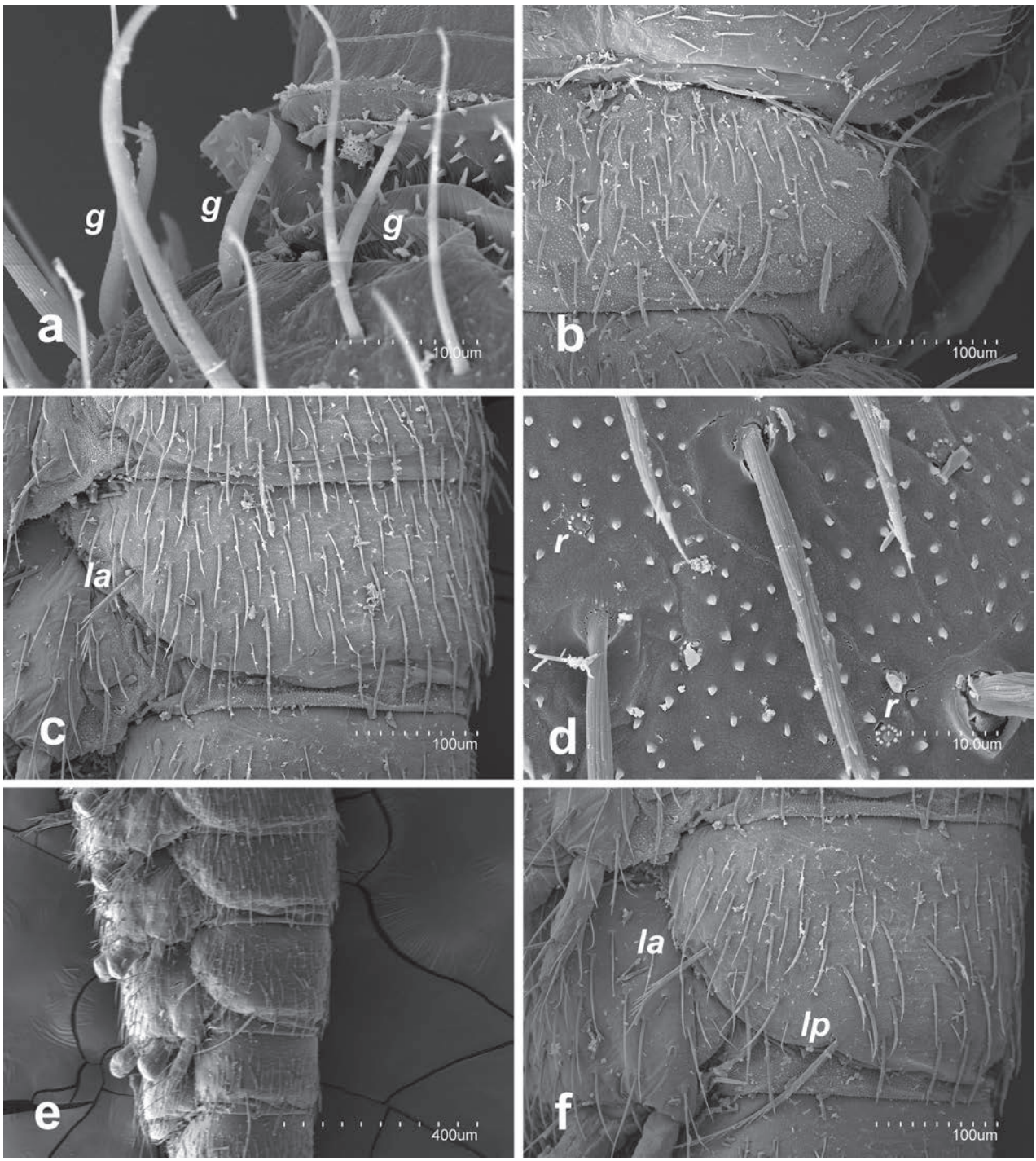

Figure 1. *Campodea* (*Dicampa*) *frenata* Silvestri, 1931, specimen in Coll. AS. **a** lateral anterior view of a medial antennomere **b** pronotum **c** lateral view of abdominal segment 6 **d** detail of pronotum **e** lateral view of abdominal segments 6–8 **f** lateral view abdominal segment 7. Abbreviations: ***g*** gouge sensillum, ***la*** lateral anterior macrosetae, ***r*** rosette gland, *lp* lateral posterior macrosetae.

macrosetae; thick and well-barbed marginal setae, in addition to clothing setae with one or two distal barbs (Fig. 1b–f).

Habitat and distribution. A soil-dwelling species that is only occasionally found in caves (Silvestri 1931; Bareth and Condé 2001). It is distributed throughout the Carpathians Mountains (Ionescu 1955; Rusek 1964), and extends southward into the Balkan Mountains (Paclt 1969; Blesić 1984; 2000a).

***Campodea* (*Dicampa*) *propinqua* Silvestri, 1932**
Figs 2a–f, 3a–c

Material examined. Romania • 1 ex., Bârgău Mountains: Valea Mare, Bistrița-Năsăud County, 47.481778°N, 24.999045°E, 762 m a.s.l., spruce forest, soil, 04.11.2021, C. Fiera leg.; • 1 ex., Bârgău Mountains: Șanț, Bistrița-Năsăud County, 47.50723°N, 24.970762°E, 826 m a.s.l., cutted spruce forest, litter, 04.11.2021, C. Fiera leg.; • 15 ex., Brașov County: Pârâul Rece, 45.512108°N, 25.507398°E, 1073 m a.s.l., spruce forest, litter, 12.11.2021, C. Fiera and I. Vicol leg.; • 5 ex., Făgăraș Mountains: Cârtișoara, Sibiu county, 45.670567°N, 24.590975°E, 927 m a.s.l., beech forest, soil, 10.10.2020, C. Fiera and I. Vicol leg.; • 5 ex., Făgăraș Mountains: Turnu Roșu, Sibiu county, 45.616342°N, 24.323312°E, 704 m a.s.l., mixed forest (spruce, fir, beech), predominantly spruce. litter, 11.11.2021, C. Fiera and I. Vicol leg.; • 1 ex., Făgăraș Mountains: Cârtișoara, Sibiu county, 45.671965°N, 24.791662°E, 808 m a.s.l., beach forest, litter, 11.11.2021, C. Fiera and I. Vicol leg.; • 1 ex., Făgăraș Mountains: near Berivoi Monastery, Brașov County, 45.687445°N, 24.970958°E, 709 m a.s.l., beech forest, rarely fir, litter, 12.11.2021, C. Fiera and I. Vicol leg.; • 3 ex., Suceava County: Iacobeni, 47.446179°N, 25.311171°E, 895 m a.s.l., mixed forest (fir, larch, hornbeam), soil and litter, C. Fiera leg.; • 2 ex., Gorj County: Rânca locality, 45.301415°N, 23.680959°E, 1622 m a.s.l., spruce forest, soil and litter, 17.06.2021, C. Fiera leg.; • 1 ex., Zarand Mountains, site 1, Căsoaia, near Arăneag, Arad county, 46.225324°N, 21.764489°E, 226 m a.s.l., mixed forest (*Abies alba*, *Fagus sylvatica*, *Quercus frainetto*, *Carpinus betulus*, *Acer campestre*), soil, 10.11.2020, C. Fiera and I. Vicol leg.; • 1 ex., Zarand Mountains, site 4, Milova, Arad county, 46.124375°N, 21.801121°E, 191 m a.s.l., mixed forest (*Picea abies*, *Fagus sylvatica*, *Pinus nigra*, *Acer campestre*, *Quercus* sp., *Aces pseudoplatanus*), soil, 11.11.2020, C. Fiera leg. and I. Vicol; • 2 ex., Zarand Mountains, site 5, Bârzava, Arad county, 46.127396°N, 21.986602°E, 168 m a.s.l., mixed forest (*Fagus sylvatica*, *Quercus petraea*, *Avium cerasus*), soil, 11.11.2020, C. Fiera and I. Vicol leg.; • 1 ex., Zarand Mountains, site 6, Conop, Arad county, 46.098845°N, 21.903658°E, 165 m a.s.l., mixed forest (*Quercus cerris*, *Q. frainetto*, *Acer campestre*, *Fagus sylvatica*, *Ligustrum vulgare*, *Robinia pseudocacia*, *Sorbus* sp., *Carpinus betulus*, *Sorbus terminalis*), soil, 11.11.2020, C. Fiera and I. Vicol leg. **Bulgaria** • 1 ♂, 1 ♀, Pirin Mts., 6 km of Predela, MSS trap, alt. 676 m a.s.l., 16.06.2006, P. Stoev, B. Petrov leg.

Taxonomic notes. The morphological taxonomic features observed in the studied specimens under an optical microscope show no differences from the Iberian specimens. However, a molecular analysis should be conducted to confirm whether these geographically distant populations belong to the same species.

Specific observations using scanning electron microscopy reveal large embase of antennal trichobothria (Fig. 2a), dense microdenticles (Fig. 2b, d) including rosette-type glands on all tergites (Fig. 2f), well-barbed macrosetae (Fig. 2b), and clothing setae with a single distal barb (Fig. 3a, b). Additionally, the stylus setae are smooth, with the apical one featuring two long basal denticles (Fig. 3c). Claws are simple, with a protuberance between them (Fig. 2c, e).

Habitat and distribution. A soil-dwelling species known from a single locality in the western Subbaetic Mountains, southern Iberian Peninsula (Silvestri 1932a), and inhabiting colluvial scree slopes in central Iberia (Sendra et al. 2017). Reported from Romania by Ionescu (1951, 1955) and Italy by Ramellini (1990).

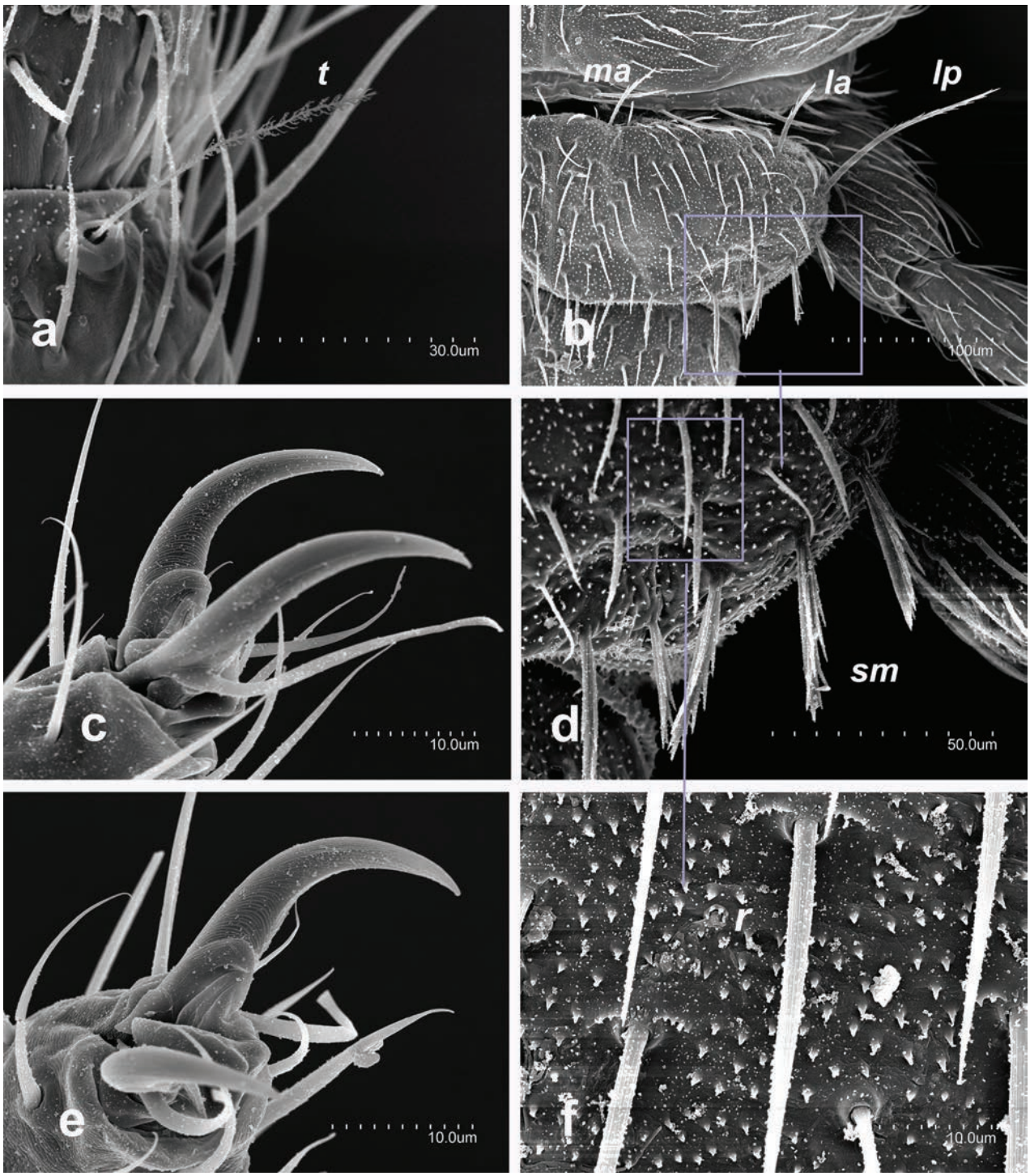

Figure 2. *Campodea* (*Dicampa*) *propinqua* Silvestri, 1932, specimen in Coll. AS **a** latero-anterior view of third antennomere **b** pronotum **c** pretarsus metathoracic leg **d** latero-anterior view of pronotum **e** pretarsus metathoracic leg **f** detail pronotum. Abbreviations: ***t*** trichobothria, ***ma*** medial anterior macrosetae, ***la*** lateral anterior macrosetae, ***lp*** lateral posterior macrosetae, ***sm*** marginal setae, ***r*** rosette gland.

Campodea (*Dicampa*) *sprovieri sprovieri* Silvestri, 1932

Material examined. Romania• 1 ♀, Bârgău Mountains: Leșu, Bistrița-Năsăud County, 47.289248°N, 24.756708°E, 749 m, beach, rarely fir, litter, 02.11.2021, C. Fiera leg.; • 1 ♀, 1 ♂, Brașov County: Pârâul Rece, 45.515038°N, 25.503134°E,

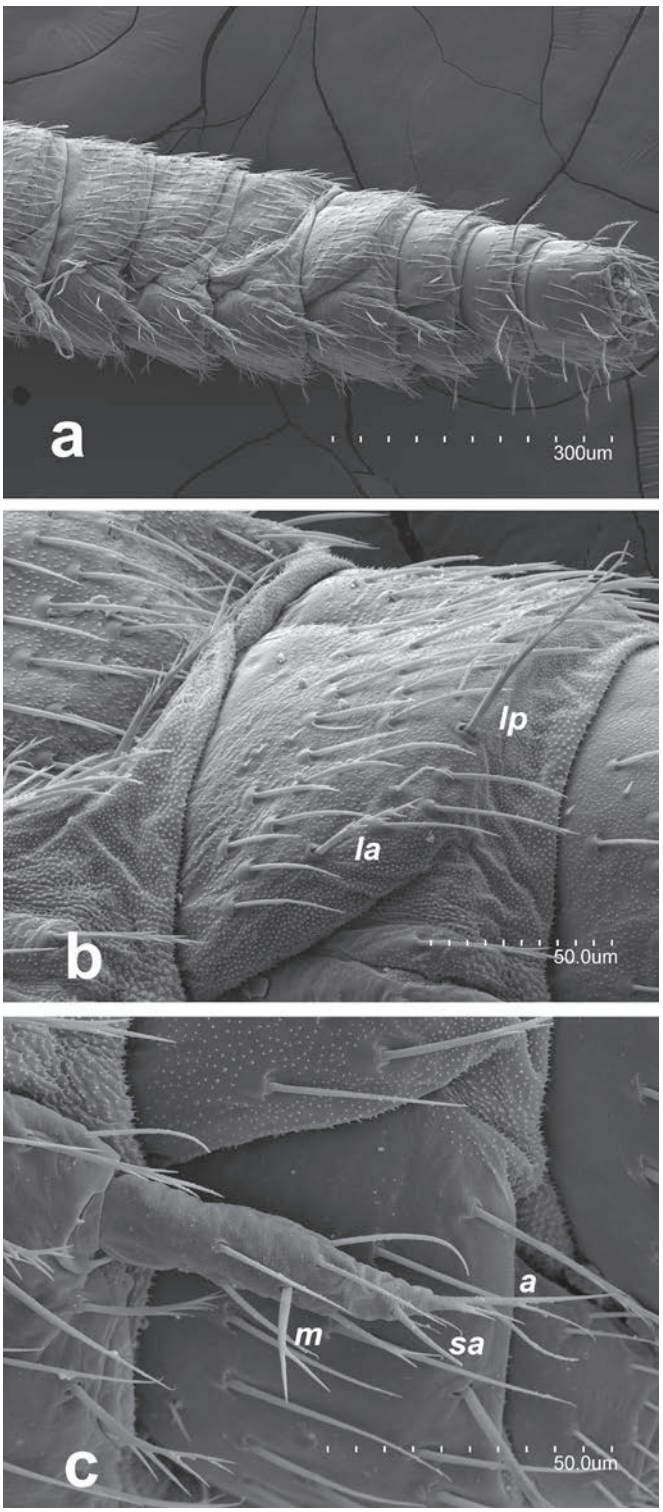

Figure 3. *Campodea* (*Dicampa*) *propinqua* Silvestri, 1932, specimen in Coll. AS **a** abdomen segments 4–10 **b** lateral view abdominal segment 7 **c** stylus abdominal segment 7. Abbreviations: ***la*** lateral anterior macrosetae, ***lp*** lateral posterior macrosetae, ***m*** medial setae, ***sa*** subapical setae, ***a*** apical setae.

994 m a.s.l., spruce forest, soil, 14.07.2018, C. Fiera leg.; • 2 ♂, 3 ♀, 1 juv., Vrancea County: Brădăcești (near Nereju), 45.697641°N, 26.671177°E, 623 m a.s.l., coniferous forest (*Pinus* sp.), soil, 27.05.2021, C. Fiera leg.; • 1 ♂, 2 ♀, Suceava County: Iacobeni, 47.446179°N, 25.311171°E, 895 m a.s.l., mixed forest (fir,

larch, hornbeam), soil and litter, C. Fiera leg.; • 1 ♀, Suceava County: Pătrăuți forest near Răuțeni locality, 47.840511°N, 25.056427°E, 344 m a.s.l., mixed forest (beech, oak, and hornbeam), soil, 13.04.2021, C. Fiera leg.; • 1 juv. Brașov County: Prejmer, site 1, 45.730329°N, 25.737091°E, 510 m a.s.l., mixed forest (maple, lime, hornbeam), soil, 15.11.2018, C. Fiera and Weiner M.W. leg.; • 3 ♀, 2 ♂, 3 juvs, Brașov County: Prejmer, site 3, 45.75037°N, 25.723362°E, 510 m a.s.l., oak forest (*Quercus cerris*), 100 years old, 15.11.2018, C. Fiera and Weiner M.W. leg.; • one juv., Brașov County: Prejmer, site 4, 45.753624°N, 25.707257°E, 501 m a.s.l., oak forest (*Quercus cerris*), less than 70 years old, 15.11.2018, C. Fiera and Weiner M.W. leg.; • 4 ex., Cheile Zugreni, between Bistriţei and Giumalău mountains, 47.407101°N, 25.545952°E, 770 m a.s.l., pine and spruce forest, 18.08.2018, C. Fiera leg.; • 1 ♂, Suceava County: Dornișoara, 47.213982°N, 25.06118°E, 1109 m a.s.l., spruce forest, 18.08.2018, C. Fiera leg.; • 1 ♀, Brașov County, Hărman, site 2, 45.734179°N, 25.671031°E, 508 m a.s.l., peatbog with oak, soil, 16.11.2018, C. Fiera and Weiner M.W. leg.; • 5 ♂, 6 ♀, 7 juvs and 3 specimens kept for DNA, Bucegi Massif: Sinaia, Prahova county, site 1, 45.351264°N, 25.521893°E, 1288 m a.s.l., spruce forest, soil, 14.07.2018, C. Fiera leg.; • 5 ♀, 5 ♂, 7 juvs and 4 specimens kept for DNA, Bucegi Massif: Sinaia, Prahova county, site 2, 45.357541°N, 25.516975°E, 1386 m a.s.l., spruce forest, soil, 14.07.2018, C. Fiera leg.; • 3 juvs, Buzău County: Siriu, 45.559882°N, 26.178259°E, 658 m a.s.l., beech forest, soil, 27.06.2020, C. Fiera leg.; • 2 ♀, 2 juvs, Doftana Valley: Șotriile, 45.227694°N, 25.729119°E, 609 m a.s.l., beech forest, soil, 18.11.2016, C. Fiera leg.; • 2 ♂, 1 ♀, one juv. and one specimen kept for DNA, Bârgău Mountains: Tureac, site 1, Bistrița-Năsăud County, 47.257408°N, 24.856696°E, 862 m a.s.l., beech forest, soil, 18.08.2018, C. Fiera leg. **Bulgaria** • 1 ♀, 4 juvs, Pirin Mountains, Bansko, 41.77552°N, 23.439216°E, 1784 m a.s.l., spruce forest, soil, 13.08.2018, C. Fiera leg.

Habitat and distribution. A soil-dwelling species which is widely spread around the Balkan Peninsula (Ionescu 1955; Rusek 1965b; Condé 1984; Sendra et al. 2012) and Anatolia (Sendra et al. 2006, 2010), including several Aegean islands (Silvestri 1933; Condé 1984).

***Campodea* (*Dicampa*) *transylvanica* Sendra, sp. nov.**

https://zoobank.org/7655C15C-D6CB-4D70-AD16-DA30DA48A7FC

Figs 4a–d, 5a–c, 6a, b

Type material. *Holotype*. Romania • ♂; Turnu Roșu (Sibiu County), Făgăras Mountains (RO Carpathians), soil, 704 m. elevation; mixed forest (spruce, fir, beech) (predominant spruce); 11 November 2021, Fiera C. and I. Vicol leg.; labelled holotype IBB-CTR1. ***Paratypes*. Romania** • 1 ♀, 2 ♂♂, 2 juvs, Turnu Roșu, Făgăraş Mountains (RO Carpathians), Făgăraş, soil, 704 m elevation, mixed forest (spruce, fir, beech) (predominant spruce), 11 November 2021, Fiera C. and I. Vicol leg., labelled IBB-CTR2-5; • 1 ♀, Turnu Roșu, Făgăraş Mountains (RO Carpathians), litter, 704 m. elevation, mixed forest (spruce, fir, beech) (predominant spruce), 11 November 2021, Fiera C. and I. Vicol leg., labelled IBB-CTR6; • 1 ♂, Cârtișoara, Făgăras Mountains (RO Carpathians), litter, beach, 11 November 2021, Fiera C and Vicol I. leg., labelled IBB-CTR7; • 3 ♀♀, Cârtișoara, Făgăras Mountains (RO Carpathians), soil, beach, 11 November 2021, Fiera C. and I.

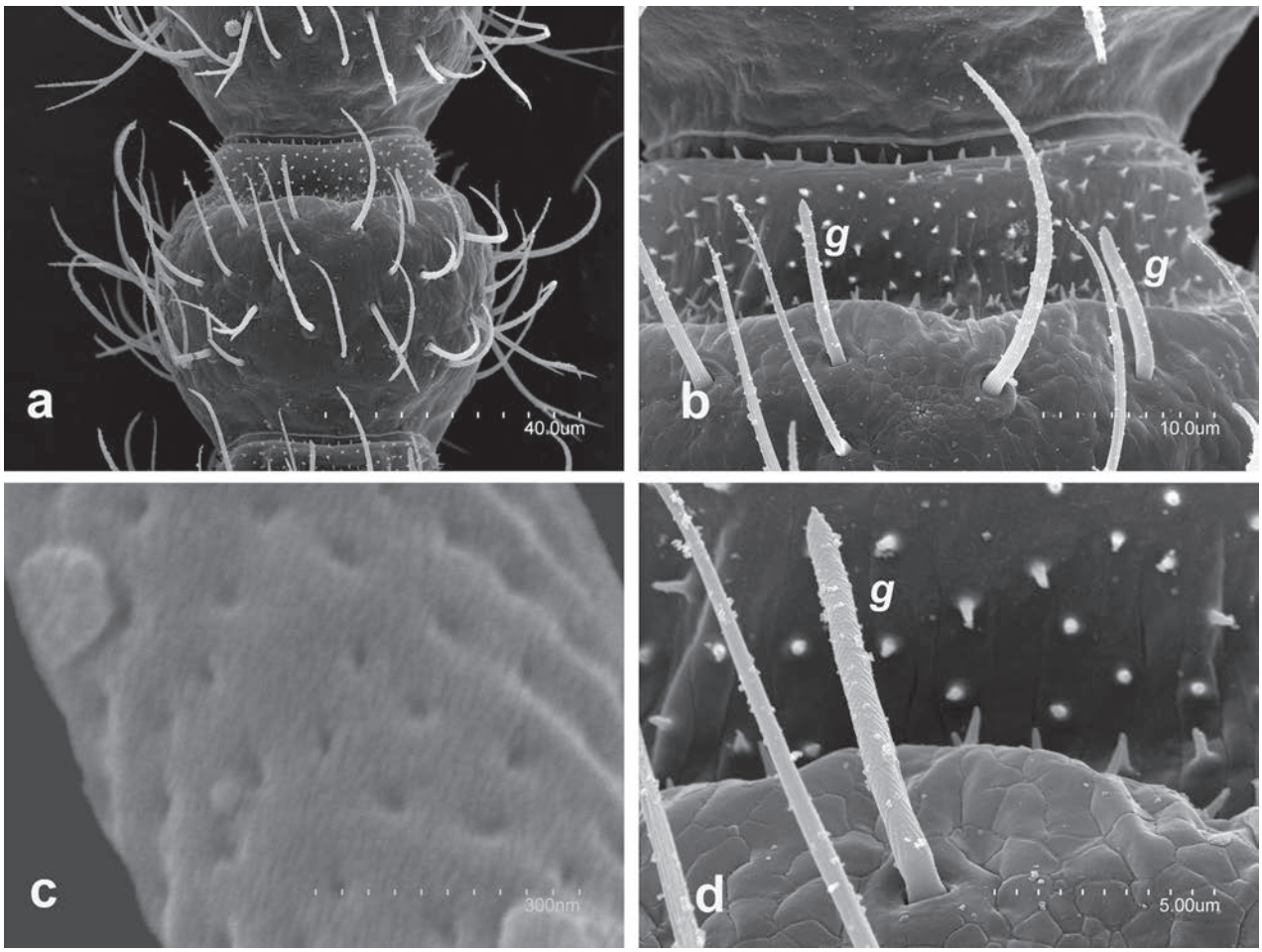

Figure 4. *Campodea* (*Dicampa*) *transylvanica* Sendra, sp. nov., specimen in Coll. AS **a** medial antennomere **b** latero-anterior view of a medial antennomere **c** detail of gouge sensillum **d** gouge sensillum on antennomere. Abbreviation: ***g*** gouge sensillum.

Vicol leg., labelled NMNHS-10832-10834; • 1 juv., Radna (Arad County), Zarand Mountains (RO Carpathians), *Quercus cerris*, *Q. frainetto*, *Betula pendula*, 12 November 2020, Fiera C. and I. Vicol leg., labelled IBB-CTR8; • 1 ♀, 1 ♂, Conop (Arad County), Zarand Mountains (RO Carpathians), *Quercus cerris*, *Q. frainetto*, *Acer campestre*, *Fagus sylvatica*, *Ligustrum vulgare*, *Robinia pseudoacacia*, *Sorbus* sp., *Carpinus betulus*, *Sorbus terminalis*, 11 November 2021, Fiera C. and I. Vicol leg., labelled IBB-CTR9-10.

Other material. Romania • 1 ♀, Turnu Roșu, Făgăraş Mountains (RO Carpathians), Făgăraş, soil, 704 m elevation, mixed forest (spruce, fir, beech) (predominant spruce), 11 November 2021, Fiera C. and I. Vicol leg, Coll AS.

Description. ***Body***. Length 1.9–2.7 mm in male; 2.3–3 mm in females; 1.4–1.7 mm in juveniles. Epicuticle with microdenticles under optical microscope (Fig. 5a) and dense microdenticles under scanning electron microscope (Fig. 5b, c); body with smooth short clothing setae (Fig. 5a–c).

***Head*.** Antennae with 15–19 antennomeres in juveniles and adults, 0.53–0.47 shorter than length of the body in juveniles and 0.45–0.31 in adults; central antennomeres as long as wide with one proximal whorl of bifurcated macrosetae and one distal whorl of smooth macrosetae and uneven short smooth setae; in addition to a single distal whorl of ≤ 4–6 gouge sensilla of 5–6 μm long (Fig. 4a–d). Proximal antennomeres with typical trichobothria disposition and

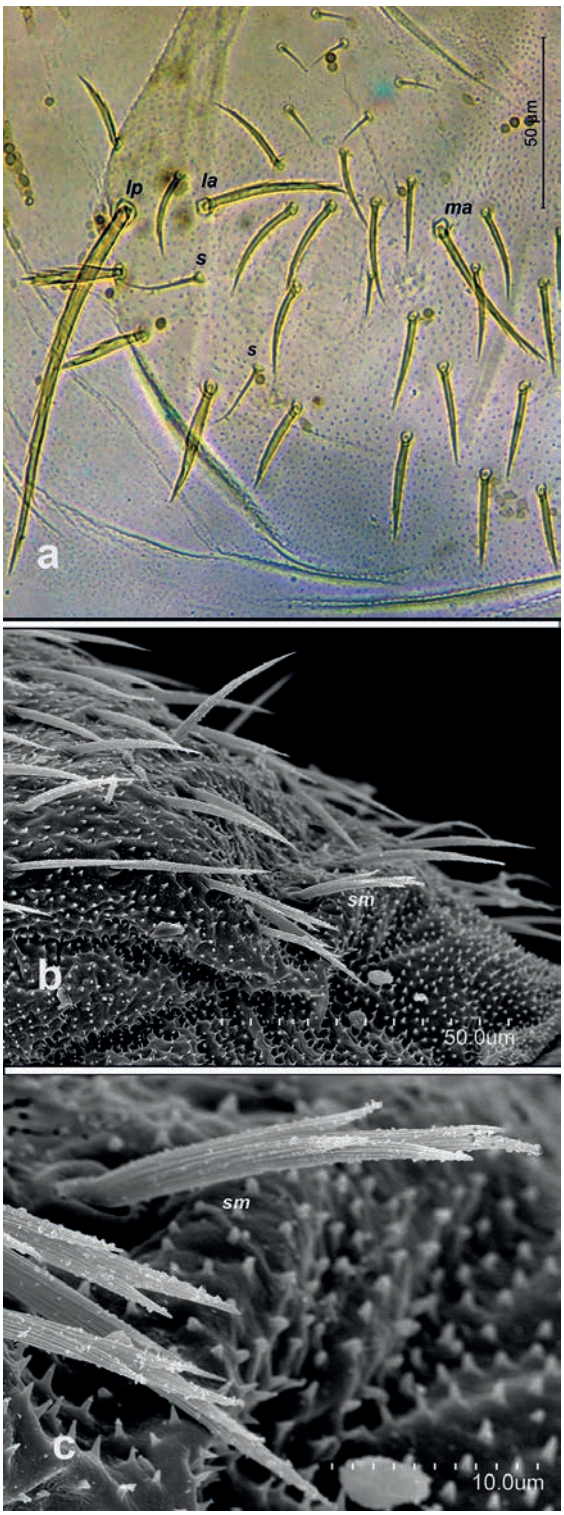

Figure 5. *Campodea* (*Dicampa*) *transylvanica* Sendra, sp. nov., specimens in Coll. AS.) **a** pronotum **b** latero-posterior view of pronotum **c** detail of latero-posterior pronotum. Abbreviations: ***ma*** medial anterior macrosetae, ***la*** latero-anterior macrosetae, ***lp*** latero-posterior macrosetae, ***s*** sensillum, ***sm*** marginal setae.

with small bacilliform sensillum on third antennomere in dorsal position, between *b*–*c* macrosetae. Plain frontal process with one anterior macrosetae, longer than clothing setae. Three macrosetae each with two or three barbs along each side of insertion line of antennomere with length ratios of *a*/*i*/*p*, 11/13/14,

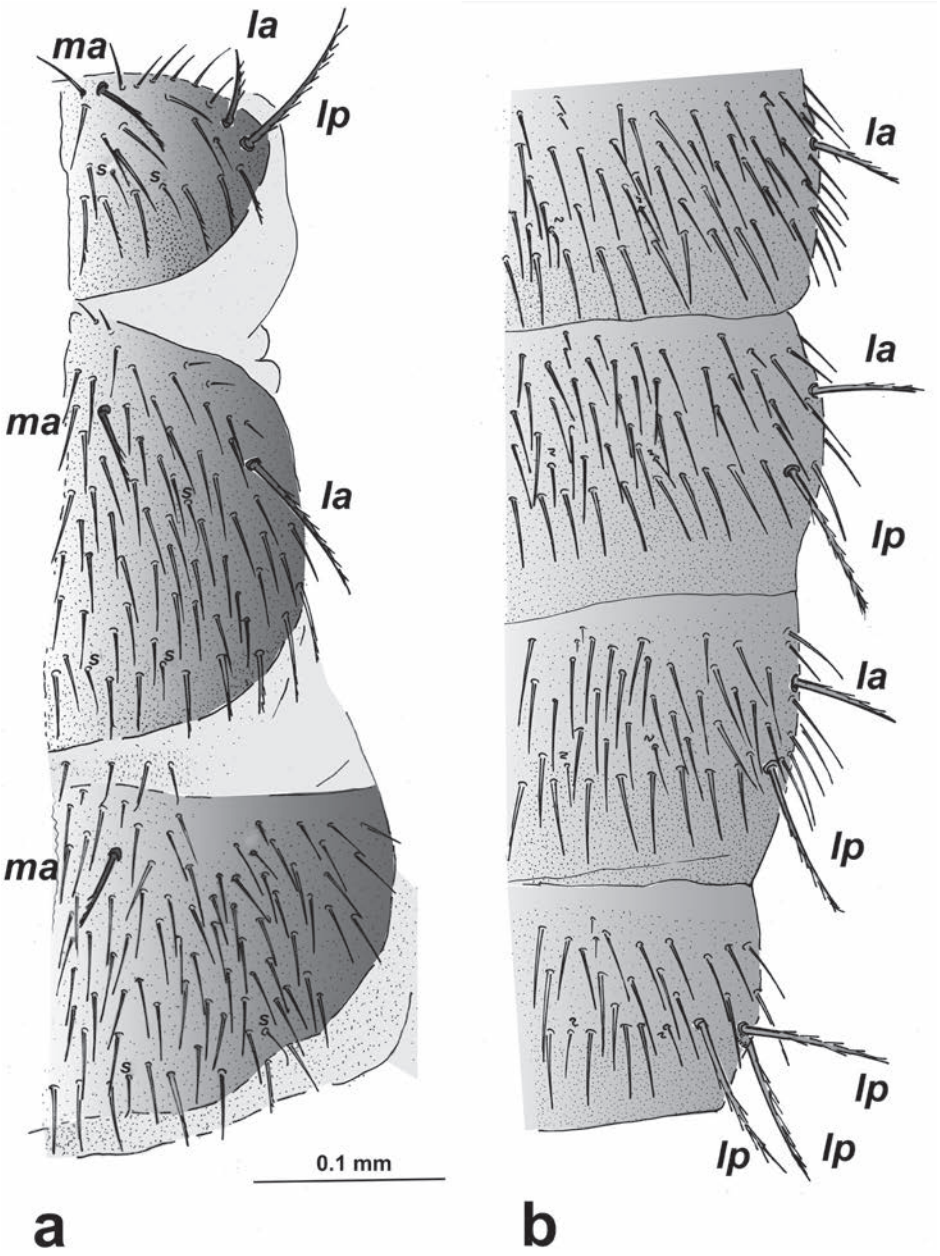

Figure 6. *Campodea* (*Dicampa*) *transylvanica* Sendra, sp. nov. Holotype IBB-CTR1 **a** pronotum, mesonotum, and metanotum **b** urotergites V–VII. Abbreviations: ***ma*** medial anterior macrosetae, ***la*** latero anterior macrosetae, ***lp*** latero posterior macrosetae, ***s*** sensillum.

respectively, in holotype. Large suboval labial palps, each with small latero-external sensillum near two gard setae and five normal setae on anterior portion, ≤ 60 neuroglandular setae in medial and posterior positions.

***Thorax*.** Thoracic macrosetae distribution: pronotum has 1+1 *ma*, 1+1 *la*, 1+1 *lp* macrosetae; mesonotum has 1+1 *ma*, 1+1 *la* macrosetae (Figs 5a, 6a). All macrosetae longer than other setae with barbs in distal ½–3/4 marginal setae barbed and longer than clothing setae. Short legs, metathoracic legs reach border of fourth abdominal segment. Calcars with two or three long barbs in middle. Each tarsus with two separated ventral rows of slightly and thicker smooth setae among clothing setae. Three long smooth dorsal tarsal and one ventral setae. Subequal simple claws and with smooth lateral processes.

***Abdomen*.** Distribution of abdominal macrosetae on tergites (Fig. 6b) shows 1+1 la on V, 1+1 *la*, 1+1 *lp* on VI–VII; 3+3 *lp* on VIII and 5+5 *lp* on IX abdominal; *la* macrosetae with barbs in distal ½–1/3 and *lp* macrosetae bear barbs along distal 4/5. Urosternite I with 7+7 macrosetae; urosternites II to VII with 4+4 macrosetae; urosternite VIII with 1+1 macrosetae; urosternal macrosetae of bifurcated, tri or quadrifurcated. Stylus setae with smooth subapical setae, bifurcated ventromedial seta and with two long basal barbs on apical seta.

Secondary sex features. Female urosternite I with subcylindrical appendages, each bearing ≤ 12 glandular *a*1 setae in apical field. Male urosternite I with subtrapezoidal appendages, each with apical field of ≤ 17 glandular *a*1 setae; a continuous posterior field of ≤ about 100 *g1* glandular setae arranged in 1–3 rows. Two incomplete cerci with basal article plus five primary articles. Internal smooth macrosetae or with one distal barb in proximal articles and other macrosetae with four or five distal barbs; primary articles with up to three whorls of barbed macrosetae, and uneven short smooth setae.

Taxonomic affinities. The distribution of urotergal macrosetae in *Campodea* (*Dicampa*) *transylvanica* Sendra, sp. nov. from the Romanian Carpathians matches that of *Campodea* (*Dicampa*) *plagiaria* Silvestri, 1932 from the Baetic and Riff mountains (Silvestri 1932b). However, *Campodea* (*D.*) *transylvanica* Sendra, sp. nov. differs from *C.* (*D.*) *plagiaria* in several taxonomic features: 15–19 antennomeres in *Campodea* (*D.*) *transylvanica* Sendra, sp. nov. instead of 26–28 antennomeres in soil populations of *Campodea* (*D.*) *plagiaria*; sensillum on the third antennomere in tergal position in *C.* (*D.*) *transylvanica* Sendra, sp. nov. instead of ventral in *C.* (*D.*) *plagiaria*; apical barbs on marginal notal setae in *C.* (*D.*) *transylvanica* Sendra, sp. nov. instead of thin pine marginal setae in *C.* (*D.*) *plagiaria*.

Etymology. Named after Transylvania, a historical and cultural region in Central Europe that encompasses central Romania.

Habitat and distribution. A soil-dwelling species that is found in mixed forests in Zarand and Făgăraș mountains. In two localities it co-occurs with *Campodea* (*Dicampa*) *propinqua* Silvestri, 1932.

Campodea (*Paurocampa*) *ruseki* Condé, 1966

Fig. 7a, b

Material examined. Bulgaria • 2 ♂♂, 1 ♀, Pirin Mountains, Hut Kamenitsa, 1800 m a.s.l., 15.06.1988, P. Beron leg.

Taxonomic notes. Observations under the microscope of the studied material have shown several previously unknown features not mentioned in its original description (Condé 1956, 1966). The antennae have 27 antennomeres in a 3.8 mm female, and 25 in 3.95 mm and 4.2 mm males. The apical antennomere has four simple spheroidal olfactory chemoreceptors on the cupuliform organ. A large bacilliform sensillum is present on the third antennomere in tergal position (between b-c macrosetae). Notal tergites bear microdenticles, and the clothing setae are either smooth or have a distal tiny barb (Fig. 7a). The marginal setae are slightly longer and thicker than clothing setae, with a few bars on distal half to two-thirds. The pronotal macrosetae have a few thin tiny barbs on the distal half, with the longest *lp* macrosetae with one or two thin tiny barbs at the distal position. No trochanteral setae were observed in any of the specimens studied.

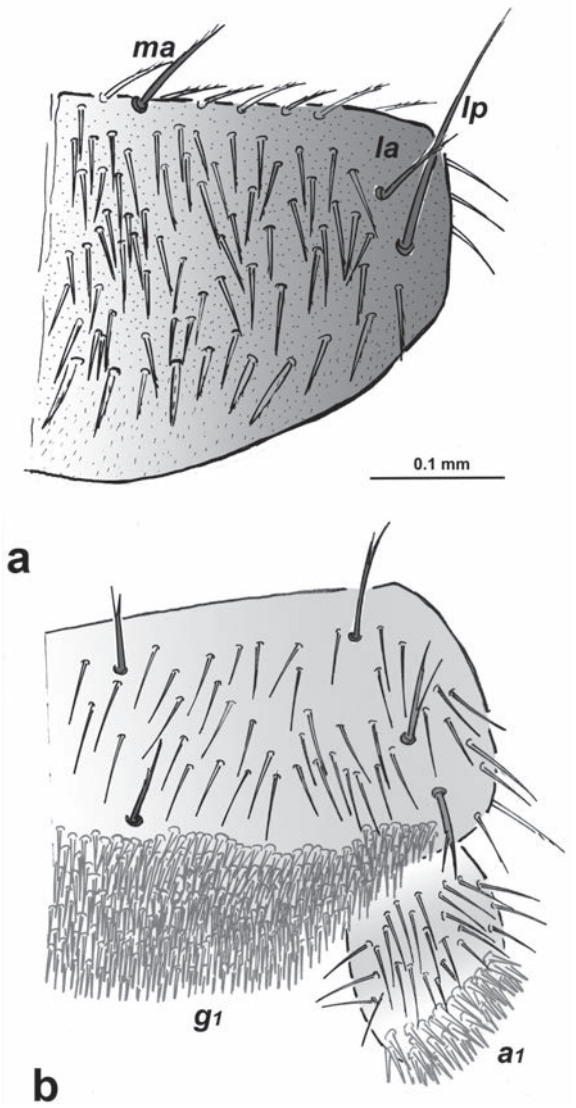

Figure 7. *Campodea* (*Paurocampa*) *ruseki* Condé, 1966 **a** pronotum **b** first urosternite of a male. Abbreviations: ***ma*** medial anterior macrosetae, ***la*** latero-anterior macrosetae, ***lp*** latero-posterior macrosetae, g_1 glandular setae type g1, a_1 glandular setae type a1.

The male urosternite I (Fig. 7b) features slightly spherical appendages, each with an apical field containing ≤ 40 glandular *a*1 setae; a continuous posterior field of ~≤ 240 *g1* glandular setae arranged in 7–9 rows.

Remarks. New record for Bulgaria.

Habitat and distribution. A soil-dwelling species that inhabits high altitudes. It is known from two localities in the Austrian Alps (Condé 1954, 1966) and a single locality in the Pirin Mountains of Bulgaria.

Campodea (*Paurocampa*) *suensoni* Tuxen, 1930

Fig. 8a–f

Material examined. **Romania** • 3 ♂, 1 ♀, 4 juvs, Bârgău Mountains: Leșu, Bistrița-Năsăud County, 47.289248°N, 24.756708°E, 749 m, beach, rarely fir, litter, 02.11.2021, C. Fiera leg.; • 2 juvs, Bârgău Mountains: near Ilva Mică, Bistrița-Năsăud

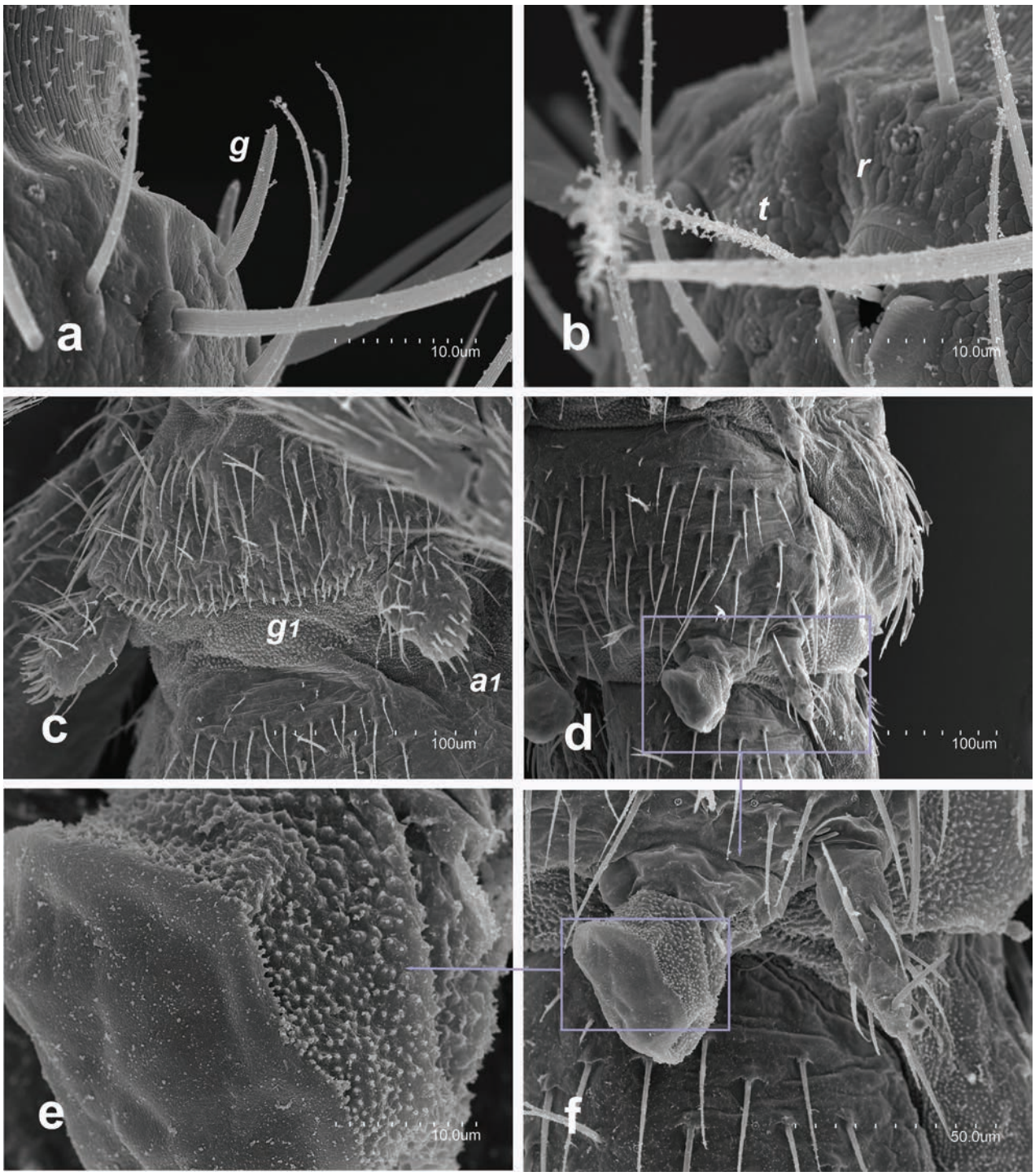

Figure 8. *Campodea* (*Paurocampa*) *suensoni* Tuxen, 1930 **a** antero-lateral view of a medial antennomere **b** distal portion of third antennomere **c** first urosternite of a male **d** sixth urosternite **e** detail exerted vesicle **f** latero-posterior view of sixth urosternite. Abbreviations: ***g*** gouge sensillum, ***t*** trichobothria, ***r*** rosette gland, g_1 glandular setae type g1, a_1 glandular setae type a1.

County, 47.328709°N, 24.702183°E, 494 m a.s.l., beach forest, litter, 02.11.2021, C. Fiera leg.; • 1 ♀, Bârgău Mountains: Tureac, site 8, Bistrița-Năsăud County, 47.257365°N, 24.857551°E, 872 m a.s.l., beach forest, soil, 03.11.2021, C. Fiera leg.; • 2 ♂, 2 ♀, Făgăraș Mountains: Nucșoara, Argeș County, 45.417893°N, 24.733326°E, 1196 m a.s.l., mixed forest (*Fagus sylvatica*, *Betula pendula*, *Alnus viridis*, *Sambucus* sp.), litter, 10.11.2021, C. Fiera and I. Vicol leg.; • 1 ♂, 1 ♀, 2 juvs,

Suceava County: Iacobeni, 47.446179°N, 25.311171°E, 895 m a.s.l., mixed forest (fir, larch, hornbeam), soil and litter, C. Fiera leg.; • 1 ♀, Argeș County: near Râușor Lake, 45.397983°N, 25.056427°E, 431 m a.s.l., rocks, soil, 26.07.2020, C. Fiera leg.; • 3 ♀, 6 ♂, 20 juvs and one specimen kept for DNA, Bârgău Mountains: Tureac, site 1, Bistrița-Năsăud County, 47.257408°N, 24.856696°E, 862 m a.s.l., beech forest, soil, 18.08.2018, C. Fiera leg.; • one juv., Bistriţa-Năsăud County: Valea Străjii near Tiha Bârgăului, 47.211925°N, 24.879244°E, 701 m a.s.l., beech forest, soil, 18.08.2018, C. Fiera leg.; • 2 ♀, Zarand Mountains, site 1, Căsoaia, near Arăneag, Arad county, 46.225324°N, 21.764489°E, 226 m a.s.l., mixed forest (*Abies alba*, *Fagus sylvatica*, *Quercus frainetto*, *Carpinus betulus*, *Acer campestre*), soil, 10.11.2020, C. Fiera and I. Vicol leg. Bulgaria • 2 ♂♂, 2 ♀♀, 3 juvs, Pirin Mountains, above Bansko, 41.77552°N, 23.439216°E, elevation 1784 m, spruce forest, soil, 13.08.2018, leg. C. Fiera; • 2 ex., Pirin Mt., Popina laka Lake, 18 km from Sandanski 1200–1400 m a.s.l., 15.06.1988. P. Beron leg.

Taxonomic notes. Observations under electronic scanning microscope shown several taxonomic morphological characters in details: short gouge sensilla on antennomeres (Fig. 8a); trichobothria with large embase (Fig. 8b); male urosternite I (Fig. 8c) with subspherical appendages, each with an apical field containing glandular a_1 setae in addition to a continuous posterior field of g_1 glandular setae arranged in several rows; and, urosternites I–VII with short stylus and large exerted vesicles with two differentiated cuticle areas (Fig. 8d–f).

Habitat and distribution. A soil-dwelling species that is found also at the entrances of caves and in their deeper zones when abundant organic matter is available (Condé 1974; Sendra et al. 2012). It is common and well-distributed in Central and Eastern Europe (Tuxen 1930; Condé, 1954, 1966; Paclt and Rusek 1961; Condé 1956; Rusek 1965b; Paclt 1961, 1969; Blesić 1984, 1997, 2000b, 2001; Christian 1992; Sendra et al. 2012), extending its distribution southward into central Italy (Condé 1966; Ramellini 2000).

Discussion

Campodeids and other Diplura families have been poorly sampled worldwide, despite their omnipresence in soils and subterranean spaces, including caves accessible or not by humans, as noted by Racovitza (1907) and Sendra (2023). Fortunately, thanks to the Emil Racovita Institute of Speleology in Romania and the National Museum of Natural History in Sofia, the soil and caves campodeid fauna of these two countries has been relatively well documented, primarily in five major contributions (Silvestri 1931; Ionescu 1955; Bareth and Condé 2001; Condé 1996; Sendra et al. 2012). Our study has increased the total number of soil and cave campodeids for Bulgaria and Romania from 19 to 22 species, which include three novelties: *Campodea* (*Paurocampa*) *ruseki* (new record for Bulgaria), *Campodea plusiochaeta* (new record for Romania), and one new species, *Campodea* (*Dicampa*) *transylvanica* Sendra, sp. nov. (Table 1). The soil campodeids in the studied region belong to four genera: *Campodea* Westwood, 1842 with three subgenera *Campodea* s. str. Westwood, 1842 (eight species), *Dicampa* Silvestri, 1932 (nine species) and *Paurocampa* Silvestri, 1932 (two species), *Eutrichocampa* Silvestri, 1902 (one species), *Litocampa* Silvestri, 1933 (one species), and *Plusiocampa* Silvestri, 1912 (one species).

Table 1. Soil campodeid species from Bulgaria and Romania.

Soil species	Country	Reference
Campodea (*Campodea*) *fragilis* Meinert, 1865	Romania	Ionescu 1955
Campodea (*Campodea*) *magna* Ionescu, 1955	Bulgaria, Romania	Ionescu 1955; Sendra et al. 2012; Sendra and Georgiev 2021
Campodea (*Campodea*) *plusiochaeta* Silvestri, 1912	Romania	This study - new species for Romania
Campodea (*Campodea*) *pseudofragilis* Condé, 1984	Romania	Ionescu 1951, 1955; Sendra et al. 2012
Campodea (*Campodea*) *taunica* Marten, 1930	Romania	Ionescu 1951, 1955; Sendra et al. 2012
Campodea (*Campodea*) *tuxeni* Wygodzinsky, 1941	Romania	Sendra et al. 2012
Campodea (*Campodea*) *vihorlatensis* Paclt, 1961	Romania	Sendra et al. 2012
Campodea (*Campodea*) *wallacei* Bagnall, 1918	Romania	Ionescu 1951, 1955; Sendra et al. 2012
Campodea (*Dicampa*) *apula* Silvestri, 1912	Romania	Ionescu 1951, 1955
Campodea (*Dicampa*) *campestris* Ionescu, 1955	Bulgaria, Romania	Ionescu 1955; Sendra et al. 2012; Rusek 1965a
Campodea (*Dicampa*) *caucasica* Rusek, 1965	Bulgaria	Sendra and Georgiev 2021
Campodea (*Dicampa*) *frenata* Silvestri, 1912	Bulgaria, Romania	Ionescu 1951, 1955; Silvestri 1931; Paclt 1969
Campodea (Dicampa) malpighii Silvestri, 1912	Romania	Ionescu 1951, 1955
Campodea (*Dicampa*) *propinqua* Silvestri, 1932	Romania	Ionescu 1951, 1955
Campodea (*Dicampa*) *silvicola* Ionescu, 1955	Romania	Ionescu 1955
Campodea (*Dicampa*) *sprovieri* Silvestri, 1933	Bulgaria, Romania	Ionescu 1951, 1955; Sendra et al. 2012; Rusek 1965a; Sendra and Georgiev 2021
Campodea (*Dicampa*) *transylvanica* sp. nov.	Romania	This study
Campodea (*Paurocampa*) *ruseki* Rusek, 1965	Bulgaria	This study - new species for Bulgaria
Campodea (*Paurocampa*) *suensoni* Tuxen, 1930	Bulgaria & Romania	Ionescu 1951, 1955; Sendra et al. 2012; Rusek 1965b; Paclt 1969
Eutrichocampa collina Ionescu, 1955	Romania	Ionescu 1955; Sendra et al. 2012
Litocampa montana (Ionescu, 1955)	Romania	Ionescu 1955; Sendra et al. 2012
Plusiocampa (*Plusiocampa*) *humicola* Ionescu, 1951	Romania	Ionescu 1951, 1955; Sendra et al. 2012

This biodiversity is higher in terms of both species and genera, including subgenera, than that of other European regions at the same latitude such as Germany, which has a land area similar to that of Bulgaria and Romania combined, and a total of 13 *Campodea* s. str. species. However, France, with nearly twice the land area of Romania and Bulgaria together, has 47 soil and cave species, primarily from the subgenus *Campodea* (32 species) as well as the subgenera *Dicampa* (four species), *Monocampa* Silvestri, 1932 (four species), and *Paurocampa* (two species) plus the genera *Eutrichocampa* (one species), *Litocampa* (two species), *Plusiocampa* (one species), and *Podocampa* Silvestri, 1932 (one species) (Sendra and Reboleira 2020; Sendra et al. 2020). Furthermore, nearby countries such as continental Greece, one third of the combined area of Bulgaria and Romania has eleven species: subgenus *Campodea* (five species), one species in *Dicampa*, one in the subgenus *Paurocampa*, one in *Helladocampa* Condé, 1984, plus three in *Plusiocampa*. In Serbia and Macedonia, with a similar combined area size as continental Greece, there are 19 species distributed within four genera: *Campodea* (8 *Campodea* s. str. species, 5 *Dicampa* species, and 2 *Paurocampa* species), *Eutrichocampa* with two species, *Podocampa* with two species, and finally *Cestocampa* with one species (Sendra and Reboleira 2020; Sendra et al. 2020).

The diversity of soil campodeids in Bulgaria and Romania is consistently higher than in regions at higher latitudes, which is expected due to the decrease in species numbers in northern areas (Sendra et al. 2021a, b). A clear example is the eleven *Campodea* s. str. species inhabiting the United Kingdom and Ireland, a region similar in area to Bulgaria and Romania together. Similarly, only four *Campodea* s. str. species are found in Norway and Sweden (Sendra and Reboleira 2020).

Another notable characteristic of the soil campodeid fauna in Romania and Bulgaria is its diversity in genera and subgenera, comprising four genera and three subgenera with a prevalence of species in the subgenus *Dicampa*. Almost 41% of all species belong to *Dicampa* (nine species). This richness is also high in the southern Mediterranean region, where *Dicampa* likely originated. For example, on the Iberian Peninsula, 30% of species belong to *Dicampa*, and in Morrocco, the figure is 36% (Sendra and Reboleira 2020).

The campodeid diversity in Romania (20 species) compared with Bulgaria (7 species) shows 25% overlap, with five species in common: *C.* (*C.*) *magna*, *C.* (*D.*) *campestris*, *C.* (*D.*) *frenata*, *C.* (*D.*) *sprovieri*, and *C.* (*P.*) *suensoni*. However, there is no overlap among the cave-adapted species, which typically have smaller ranges restricted to karstic areas in each region (Bareth and Condé 2001; Sendra et al. 2012).

Currently, three soil species can be considered as endemic: two are exclusive to Transylvania (Romania), *Plusiocampa humicola* and *C.* (*D.*) *transylvanica* Sendra, sp. nov., and one is found in Lotrului Mountains (Romania), *Litocampa montana*. All nine cave-adapted species are also endemic, with four limited to Romanian caves and five to Bulgarian caves.

Despite the extensive sampling efforts conducted in both countries, new taxonomic discoveries likely await entomologists and bioespeleologists who explore this primitive and fascinating group of Diplura.

Additional information

Conflict of interest

The authors have declared that no competing interests exist.

Ethical statement

No ethical statement was reported.

Funding

For this study, P.S. utilized the facilities of the National Museum of Natural History at the Bulgarian Academy of Sciences, which were acquired or upgraded as part of the DiSSCo-BG project (Upgrade of the Research Infrastructure "Distributed System of Scientific Collections—Bulgaria"). C.F. acknowledges the project number RO1567-IBB01/2024 and 58PHE/2024 - PN-IV-P8-8.1-PRE-HE-ORG-2023-0157.

Author contributions

Conceptualization: AS. Funding acquisition: CF and PS. Supervision: AS. Writing - original draft: AS. Writing - Review and Editing: AS, CF, JS, PS.

Author ORCIDs

Alberto Sendra https://orcid.org/0000-0003-1035-3638
Cristina Fiera https://orcid.org/0000-0002-0125-5879
Jesús Selfa https://orcid.org/0000-0002-0376-7536
Pavel Stoev https://orcid.org/0000-0002-5702-5677

Data availability

All of the data that support the findings of this study are available in the main text.

References

Agrell I (1944) Die schwedischen Thysanuren. Opuscula entomologica 9: 23–36.

Arevad K (1957) Danske Diplura (Insecta, Apterygota). Entomologiske Meddelelser 28: 127–144.

Bagnall RS (1918) On two new species of *Campodea*. The Entomologist's Monthly Magazine 54: 157–159.

Bareth C, Condé B (1985) Campodéidés endogés de Ligurie (Diplura). Annali del Museo Civico di Storia Naturale "Giacomo Doria" 85: 251–258.

Bareth C, Condé B (2001) Campodéidés des grottes de Bulgarie (Insecta: Diplura). Mémoires de Biospéologie 28: 9–27.

Blesić B (1984) Fauna Diplura (Insecta) Sr Srbije. Collection of Scientific Papers of the Faculty of Science Kragujevac 5: 91–96.

Blesić B (1997) Knowledge of Protura and Diplura of Montenegro. The Montenegrin Academy of Sciences and Arts Glasnik of the Section of Natural Sciences 12: 63–70.

Blesić B (1998a) Investigations of Protura and Diplura of South Serbia. Proceedings for Natural Sciences Matica Srpska 94: 87–90.

Blesić B (1998b) Knowledge of Protura and Diplura of Montenegro. The Montenegrin Academy of Sciences and Arts Glasnik of the Section of Natural Sciences 12: 63–70.

Blesić B. (2000a) Investigation of Diplura and Protura in western Serbia. Proceedings for Natural Sciences 99: 69–79. https://www.maticasrpska.org.rs/stariSajt/casopisi/prirodne_nauke_099.pdf

Blesić B (2000b) Of the Subgenus *Paurocampa* Silvestri, 1932 (Insecta: Diplura) on the Balkans and the rest of Europe. BIOS (Macedonia, Greece), Scientific Annals of the School of Biology 5: 23–26.

Blesić B (2001) Protura and Diplura (Insecta: Apterygota) of the Republic of Macedonia. 75 years Macedonian Museum Natural History: 157–162.

Christian E (1992) Verbreitung und Habitatpräferenz von Doppel- und Zangenschwänzen in der Großstadt Wien (Diplura: Campodeidae, Japygidae). Entomologia Generalis 17(3): 195–205. https://doi.org/10.1127/entom.gen/17/1992/195

Christian E (2003) Checklist of the Diplura of Germany. Entomofauna Germanica 6: 26–32.

Condé B (1947a) Campodéidés d'Algérie. Bulletin de la Société entomologique de France 52 (9): 144–146. https://doi.org/10.3406/bsef.1947.15990

Condé B (1947b) Quelques campodéidés du nord-est de la France. Bulletin Société Sciences Nancy nouvelle série 6: 85–92.

Condé B (1947c) Nouvelles stations françaises de campodéidés avec description d'une forme nouvelle. Annales des Sciences naturelles Zoologie 11ème série (9): 139–144.

Condé B (1950) Campodéidés du Var et des Alpes-Maritimes. Bulletin de la Société linnéenne de Lyon 6: 128–132. https://doi.org/10.3406/linly.1950.7321

Condé B (1953) Campodéidés endogés d'Afrique septentrionale. Bulletin de la Société zoologique de France 78 (5–6): 358–377.

Condé B (1954) Ordnung: Entotropha (Diplura). In: Franz H (Eds) Die Nordost-Alpen im Spiegel ihrer Landtierwelt. Universitätsverlag Wagner, Innsbruck, 644–649.

Condé B (1956) Matériaux pour une monographie des Diploures Campodéidés. Mémoires du Muséum national d'histoire naturelle Série A – Zoologie 12: 1–202.

Condé B (1960) Protoures et Diploures Campodéidés des alluvions de la Moselle. Bulletin de la Société des Sciences de Nancy 19: 123–127.

Condé B (1961) Sur la microfaune du sol de Grande-Bretagne. II Diploures Campodédidés. Annales and Magazine of Natural History série 13, 4: 149–154. https://www.tandfonline.com/doi/pdf/10.1080/00222936108655794

Condé B (1962) Géonémie des Diploures troglobies du Jura et du Vercors. Spelunca Mémoires 2: 119–127.

Condé B (1966) Campodéidés de la région de Recoaro (Vénétie). Revue d'Écologie et de Biologie du sol 3(1): 166–169.

Condé B (1974) Les *Paurocampa* du groupe de *suensoni* Tuxen dans les grottes d'Europe centrale (Diploures Campodéidés). Revue suisse de Zoologie 81(2): 561–567. https://doi.org/10.5962/bhl.part.76023

Condé B (1984) Diploures Campodéidés (Insectes) de Grèce (1ère note). Revue suisse de Zoologie 91(1): 173–201. https://doi.org/10.5962/bhl.part.81875

Condé B (1991) Campodéidés des Grottes de Bourgogne (Insectes, Diploures). Mémoires de Biospéologie 18: 243–246.

Condé B (1993) Une lignée danubienne du genre *Plusiocampa* (Diploures Campodéidés). Revue Suisse de Zoologie 100(3): 735–745. https://doi.org/10.5962/bhl.part.79881

Condé B (1996) Diploures Campodéidés de la Pestera de la Movile (Movile Cave), Dobroudja méridionales (Roumanie). Revue suisse de Zoologie 103(1): 101–114. https://doi.org/10.5962/bhl.part.79940

Drĕnovski AK (1937) I prinos za izuĕvane nissăta nasĕkomna fauna – Apterygogenea na Bulgarija i Makadonija. Sofia, 6 pp.

Husson R (1946) Sur quelques récoltes de Diploures Campodéidés. Revue française d'Entomologie 13: 90–92.

Ionescu MA (1951) Contributiuni la studiul Campodeidelor din Republica Populară Română. Buletin Ştiinţific, Secțiunea de Științe, Agronomice, Geologice și Geografice 3(3): 525–532.

Ionescu MA (1955) Diplura. In: Fauna Republicii Populare Române, Insecta VII (3): 1–48.

Olsen KM (1996) Tohalen *Campodea lubbockiii* Silvestri, 1912, "kranstohale". Insekt-Nytt 21(4): 7–8.

Orelli M (1956) Untersuchungen zur postembryonalen Entwicklung von Campodea (Insecta, Apterygota). Verhandlungen der Naturforschenden Gesellschaft in Basel 67(3): 501–574.

Paclt J (1957) Diplura. Genera Insectorum 212E. P. Wytsman, Crainhem.

Paclt J (1961) Campodeidae des Senckenberg-Museums (Ins.-Diplura). Senckenbergiana biologica 42 (5/6): 455–458.

Paclt J (1965) Neue Beiträge zur Kenntnis der Apterygoten-Sammlung des Zoologischen Staatsinstituts und Zoologischen Museums Hamburg. Entomologische Mitteilungen aus dem Zoologischen Staatsinstitut und Zoologischen Museum Hamburg 3(54): 93–104.

Paclt J (1969) Über zwei verkannte *Campodea*-Arten (Insecta, Diplura) aus dem Witoscha bei Sofia. Zoologischer Anzeiger 182 (3/4): 285–287.

Paclt J, Rusek J (1961) *Campodea suensoni* Tuxen (Insecta, Diplura) clenem beskydské. Publications Faculty of Science University of Brno 415: 279–283.

Pagés J (1951) Contribution à la connaissance des Diploures. Supplément du Bulletin scientifique de Bourgogne 9: 1–97.

Racovitza EG (1907) Essai sur les problèmes biospéologiques. Biospeleologica, I. Archives de Zoologie experimentale et génerale premiere serie 6: 371–488.

Ramellini P (1990) Diplura dei Monti Ausoni e Aurunci (Lazio): Fauna ed Ecologia. Bollettino dell'Associazione Romana di Entomologia 44: 13–28.

Ramellini P (1995) Materiali per un catálogo topografico dei Dipluri Italiani. Fragmenta entomológica 27(1): 15–50.

Ramellini P (2000) Note su Campodeidi del Piemonte (Diplura, Campodeidae). Rivista Piemontese di Storia Naturale 21: 103–114.

Rusek J (1964) Über die Diplura (Apterygota) der Tschechoslowakei. Acta Societatis Zoologicae Bohemoslovenicae 28(2): 134–154.

Rusek J (1965a) Zur Kenntnis der Campodeidae (Diplura) Bulgariens. Acta entomologica Bohemoslovaca 62: 92–97.

Rusek J (1965b) Campodeids (Campodeidae, Diplura) of South-Eastern Europe. Zoologichesky Zhurnal 44(6): 1345–1356.

Sendra A (2023) Habitantes de la oscuridad: Fauna Ibero-balear de las cuevas. Sociedad Entomológica Aragonesa, 752 pp.

Sendra A, Georgiev D (2021) Campodeinae (Campodeidae, Diplura) records from Sarnena Gora Mts, Bulgaria. In: Georgiev D, Bechev D, Yancheva V (Eds) Fauna of Sarnena Sredna Gora Mts, Part 2 ZooNotes, Supplement 10: 12–13.

Sendra A, Moreno A (2004) El subgénero *Campodea s.str*. en la Península Ibérica (Hexapoda: Diplura: Campodeidae). Boletin de la Sociedad Entomológica Aragonesa 35: 19–38. https://dialnet.unirioja.es/servlet/articulo?codigo=1047183

Sendra A, Reboleira ASPS (2020) Euro-Mediterranean fauna of Campodeinae (Campodeidae, Diplura). European Journal of Taxonomy 728: 1–130. https://doi.org/10.5852/ejt.2020.728.1181

Sendra A, Satar A, Montagud S (2006) Première contribution à la faune de Diploures Campodéidés de la Péninsule d'Anatolie, Turquie (Diplura: Campodeidae). Revue suisse de Zoologie 113(3): 693–709. https://doi.org/10.5962/bhl.part.80368

Sendra A, Teruel S, Satar A, Tusun S, Özbay C (2010) New species, new records, and distribution of Campodeidae (Diplura) in Anatolia. Zootaxa 2639: 40–52. https://doi.org/10.11646/zootaxa.2639.1.4

Sendra A, Nitzu E, Sanjuan A (2012) Half a century after Ionescu's work on Romanian Diplura – A faunal contribution based on material collected from karst areas. Travaux de l'Institut de Spéologie "Émile Racovitza" 51: 37–66. https://www.travaux-racovitza.com/journals/downloads/12/art02.pdf

Sendra A, García Y, Weber D (2013) Campodeidae (Hexapoda, Diplura) from caves of the Grand Duchy of Luxembourg. In: Weber D (Eds) Die Höhlenfauna Luxemburgs. Ferrantia 69, Musée national d'histoire naturelle, Luxembourg, 216–226. https://ps.mnhn.lu/ferrantia/publications/Ferrantia69/Ferrantia69%20216-226.pdf

Sendra A, Jiménez-Valverde A, Gilgado JD, Ledesma E, Baquero E, Pérez-Suárez G, Cuesta E, Herrero-Borgoñón JJ, Jordana R, Tinaut A, Barranco P, Ortuño VM (2017) Diplurans of subsurface terrestrial habitats in the Iberian Peninsula, with a new

species description (Diplura: Campodeidae). Zootaxa 4291(1): 61–80. https://doi.org/10.11646/zootaxa.4291.1.4

Sendra A, Antić D, Barranco P, Borko Š, Christian E, Delić T, Fadrique F, Faille A, Galli L, Gasparo F, Georgiev D, Giachino PM, Kováč L, Lukić M, Marcia P, Miculinić K, Nicolosi G, Palero F, Paragamian K, Pérez T, Polak S, Prieto CE, Turbanov I, Vailati D, Reboleira ASPS (2020) Flourishing in subterranean ecosystems: Euro-mediterranean Plusiocampinae and tachycampoids (Diplura, Campodeidae). European Journal of Taxonomy 591: 1–138. https://doi.org/10.5852/ejt.2020.728.1181

Sendra A, Jiménez-Valverde A, Selfa J, Reboleira ASPS (2021a) Diversity, ecology, distribution and biogeography of Diplura. Insect Conservation and Diversity, 14: 415–425. https://doi.org/10.1111/icad.12480

Sendra A, Palero F, Jiménez-Valverde A, Reboleira ASPS (2021b) Diplura in caves: diversity, ecology, evolution and biogeography. Zoological Journal of the Linnean Society 192: 675–689. https://doi.org/10.1093/zoolinnean/zlaa116

Silvestri F (1912) Contribuzione alla conoscenza dei Campodeidae (Thysanura) d'Europa. Bolletino del Laboratorio di Zoologia generale e agraria in Portici 6: 110–147.

Silvestri F (1931) Contributo alla conoscenza dei Campodeidae (Thysanura) delle grotte della Bulgaria. Bulletin des Institutions royales d'histoire naturelle à Sofia 4: 97–107.

Silvestri F (1932a) Campodeidae (Thysanura) de España (primera parte). Eos 8: 115–164.

Silvestri F (1932b) Descripción de cinco nuevas Campodea (Thys.) de Marruecos. Boletín de la Sociedad española de Historia Natural 32(1): 75–87.

Silvestri F (1933) Nuovi contributi alla conoscenza della fauna delle isole Italiane dell'Egeo. Bolletino del Laboratorio di Zoologia generale e agraria della R. Scuola superiore d'agricoltura in Portici 27: 61–111. https://publikationen.ub.uni-frankfurt.de/frontdoor/index/index/docId/15218

Stach J (1929) Verzeichnis der Apterygogenea Ungarns. Annales Historico-Naturales Musei Nationalis Hungarici, Budapest 26: 269–312. http://publication.nhmus.hu/annales/cikkreszletes.php?idhoz=468

Stach J (1964) Katalog Fauny Polski. XV. Apterygota. Polska Akademia Nauk, Instytut Zoologiczny, Warszawa.

Szeptycki A (1974) Diplura (Campodeidae) of the Ojców National Park in Poland. Bulletin entomologique de Pologne 46: 745–748.

Tuxen SL (1930) Einige Apterygoten aus Südeuropa nebst Beschreibung zwei neuer Arten von Thysanura. Entomologiske Meddelelser 17: 219–227.

Vellay I (1900) Ordo Apterygogenea. In: Paszlavszky J (Eds): A Magyar Birodalom Állatvilága (Fauna Regni Hungariae) III. Arthropoda. Királyi Magyar Természettudományi Társulat, Budapest, 19–22.

Wygodzinsky PW (1941) Über eine neue *Campodea* und eine neue *Lepismachilis* aus Südeuropa. Entomologiske meddelelser 22: 137–141.

ZooKeys 1224: 283–316 (2025)
DOI: 10.3897/zookeys.1224.131153

Research Article

Biodiversity restated: > 99.9% of global species in Soil Biota

Robert J. Blakemore[1,2,3]

1 *VermEcology, 101 Suidomichi, Nogeyama, Yokohama-shi, Kanagawa-ken 231-0064, Japan*
2 *ENSSER, Marienstr. 19/20, 10117 Berlin, Germany*
3 *IUCN Species Survival Commission, Rue Mauverney 28, 1196 Gland, Switzerland*
Corresponding author: Robert J. Blakemore (rob.blakemore@gmail.com)

Abstract

More than a decade of research led to the conclusion in 2022 that the Soil Biome is home to ~ 2.1 × 10^{24} taxa and thus supports > 99.9% of global species biodiversity, mostly Bacteria or other microbes, based upon topographic field data. A subsequent 2023 report tabulated a central value of just 1.04 × 10^{10} taxa claiming soils had 59 ± 15%, i.e., 44–74% (or truly 10–50%?) of the global total, while incidentally confirming upper values of ~ 90% for soil Bacteria. Incompatibility of these two studies is reviewed, supporting prior biodiversity data with the vast majority of species inhabiting soils, despite excluding viruses (now with ~ 5 × 10^{31} virions and 10^{26} species most, ~ 80%, in soils). The status of Oligochaeta (earthworms) and other taxa marked "?" in the 2023 paper are clarified. Although biota totals are increased considerably, inordinate threats of topsoil erosion and poisoning yet pertain with finality of extinction. Species affected include Keystone taxa, especially earthworms and microbes, essential for a healthy Soil foundation to sustain the Tree-of-Life inhabiting the Earth.

Key words: Bacteria, earthworm, microbes, -Omics, soil organisms, species richness, viruses

Academic editor: Pavel Stoev
Received: 3 July 2024
Accepted: 3 January 2025
Published: 3 February 2025

ZooBank: https://zoobank.org/76623CA5-AAE5-453E-80E2-8B73406FD18F

Citation: Blakemore RJ (2025) Biodiversity restated: > 99.9% of global species in Soil Biota. ZooKeys 1224: 283–316. https://doi.org/10.3897/zookeys.1224.131153

Introduction

Healthy soil is fundamental to sustainable existence of most species evolving on Earth in Darwin's "Tree of Life" (a paradigm defended by Gulik et al. 2024). Soil supports more than 99.9% of species diversity and, now that vascular plants that seed and root in soils are included (Blakemore 2024), it supports 99% biomass hence ~ 98% of Net Primary Productivity (NPP) and also O_2 production. Bar-On and Milo (2019) had 0.7 Gt of photosynthetic/oxygenase Rubisco enzyme powering terrestrial environments (doubled for terrain to 1.4 Gt) with just ≈ 0.03 Gt (2.1%) in the marine environment. Soil filters and stores freshwater stocks (being subject to Earth tides!) and, as well as ~ 99% of human food, it provides most building materials plus many of our essential medicines/antibiotics. Thus, an important metric must be the scope and snapshot status of living or dormant Soil biota. A recent review by Anthony et al. (2023) claimed "two times greater soil biodiversity than previous estimates", seemingly because Decaëns et al. (2006) had 23% "soil animals" in their tally of described species as known at that time (Fig. 1). Both assertions are challenged for several reasons,

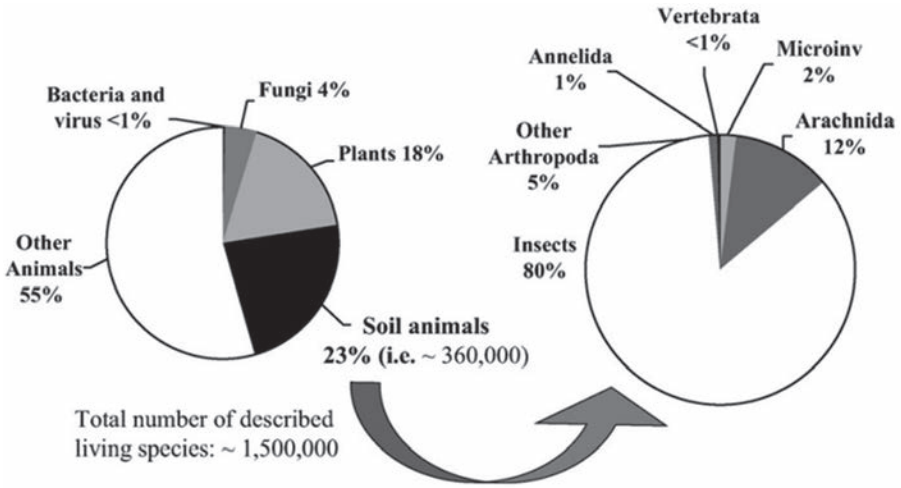

Figure 1. Decaëns et al. (2006: fig. 1) had "soil animals 23%" (i.e., ~ 360,000 in ~ 1.5 million species = 24%?).

not least > 90–99% Soil biota reports by Williamson et al. (2017), Bickel and Or (2020), Zhao et al. (2022), and by Blakemore (2018b, 2022, 2023).

Much higher totals had been determined since 2006, and Williamson et al. (2017) concluded: "Soils represent the greatest reservoir of biodiversity on the planet; prokaryotic diversity in soils is estimated to be three orders of magnitude greater than in all other ecosystems combined." In other words, soils may contain 99.9% of species, mainly microbes. Supporting this were, for example, Bickel and Or (2020) or Zhao et al. (2022) who said: "soil is the most microbiologically abundant (10^{29}) and diverse (10^{11}) environment on the Earth" and, in their figure (Zhao et al. 2022: fig. 3A), these latter authors showed soil taxa at > 10× that of all aquatic species. In other words, > 90% of biodiversity is present in Soil vs Ocean. Independently, around the same time, Blakemore (2022) estimated the "Soil Realm" is home to ~ 2.1×10^{24} taxa, or > 99.9% of global biodiversity, mostly Bacteria/Archaea or other microbes (excluding viruses), based upon published reports and extrapolation of topographic field data. Thus, rather than doubling it to ~ 50%, Anthony et al. (2023) actually halved soil biodiversity from > 99.9%. It is also remarkable that Decaëns et al.'s limited review claiming 23% biota seemed acceptable, unchallenged from 2006 because, instead of appraisal of realistic totals, it merely reported intensity of animal study, notably with terrestrial arthropods or aquatic species greatly overrepresented thus appearing disproportionately high. Such issues require critical re-evaluation and restatement of mainly microbial biota, as is attempted herein.

In 1994 Robert May had assessed ~ 85% of all species as terrestrial (May 1994), and Benton (2001: table 1) extrapolated life on the Land to 12 million species, then being as much as 25× as diverse as in the Sea (just 0.5 million species), i.e., > 96% species on the Land vs < 4% in the Sea. Grosberg et al. (2012: table 1) found most macroscopic organisms were land-based (80%) compared with few in the oceans (15%), and fewer still in freshwater (5%). A recent status paper, like Decaëns et al.'s by Román-Palacios et al. (2022) had only ~ 2 million known species with 80% animals vs 20% plants, plus microbes and fungi needing to be added(!). Claiming combined relative proportions on the Land vs Aquatic of 78% vs 22% (Fig. 2), these authors yet failed to differentiate, making no mention of the Soil nor extrapolating likely totals, again downplaying soil biotic scope.

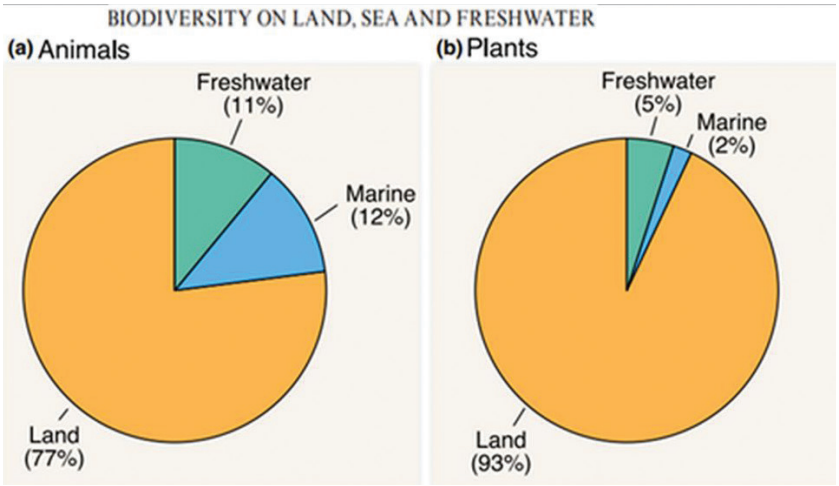

Figure 2. Román-Palacios et al. (2022: fig. 1) summed ~ 1.9 million extant animal and plant species combined, with ~ 80% on Land (~ 1.5 million species) without differentiating those found in Soil. Prokaryotic microbes were not included in their datasets, massively diminishing their terrestrial components (cf. Fierer et al. 2007). Lower still than in Freshwater, speculative claims that the Ocean supports > 80–99% of global biodiversity are readily dismissed by such solidly grounded facts.

Further refinement of these Land vs Aquatic proportions was determined by Blakemore (2022) stating: "Based on topographic field data, an argument is advanced that Soil houses ~ 2.1 × 10^{24} taxa and supports > 99.9% of global species biodiversity, mostly Bacteria or other microbes. Contradictory claims that Soil is home to only a quarter of biota while Ocean harbors 80–99% of Life on Earth are both dismissed." This statement requires clarification against Anthony et al.'s (2023) assertion that Soil hosts around 59% of species whereas their tables show only 10–50% (as tabulated below). Halving true proportions, their data totals are underestimated by orders of magnitude, seemingly due to them using older microbial count sources that have now been far superseded (Fig. 3).

More than a decade ago, prior to Larsen et al. (2017), a call for a "Census of Soil Invertebrates" (CoSI) catalogued 210,000 known soil species (Blakemore 2012: table 1) itself downplaying most microbes. An updated version had > 315,000 soil organisms (Blakemore 2016), but this also tallied just a sixth of total taxa as then known, albeit with massive proportional unknowns (Table 1).

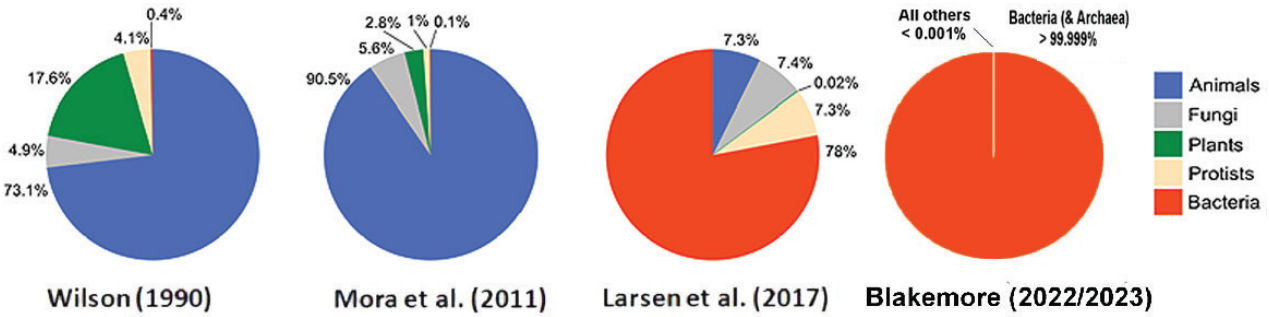

Figure 3. "Micro monde" progressions with microbial proportions greatly increased from Blakemore (2022, 2023: table 1, fig. 9) after Larsen et al. (2017: fig. 1). Of note, Larsen et al. (2017: tabs 1 and 4) in Scenarios already had Bacteria with ≤ 91% of total at up to 5.2 × 10^{9} taxa, compared to Anthony et al.'s (2023) 4.3 or 10 × 10^{8}, these being mainly terrestrial, parasitic, or pathogens related to soil animals.

Table 1. A 2016 "Census of Soil Invertebrates" (CoSI) with counts, mass, and diversity of common soil species.

Soil invertebrate group	Counts (mean) m^{-2}	Biomass (range) g m^{-2}	Total known species	% known
Viruses*	?	?	≈ 2,000–4,577	< 0.5%?
Bacteria and Archaea*	10^{12}	20–500	≈ 7,500	< < 1%?
Fungi*	(500+ several km hyphae)	20–500	≈ 80,000	0.5%
Protozoa*	10^{10}	6–30	1,500	8%
Rotifera (Bdelloid soil rotifers)	10^{5}	?	300	?
Nematoda	10^{6}	1–30	25,000	*"1.3%"*
Lobopodia			**~ 1,200**	**< < 50%**
Lobopodia (Onychophora)	?	?	< 200	50%
Lobopodia (Tardigrada)			~ 1,045	?
Arachnida, Opiliones			6,300	?
Arachnida, Pseudoscorpionida			3,300	?
Acari (mites)	10^{4}	0.2-4	45,200	4%
Hexapoda (totals)	**10^{4}**	**0.2–4**	**~ 9,000**	**17%**
Hexapoda (Collembola)	≤100,000		6,500	
Hexapoda (Diplura)			800	
Hexapoda (Protrura coneheads)			731	
Soil Insecta and their larvae	50–500	4.5	55,000+?	20%?
Myriapoda (centi-, milli-pedes)	**100–1,100**	**1.5–22.5**	**18,000**	**20%**
Myriapoda (Symphyla)			*200*	
Pauropoda (Myriapoda relative)			*700*	
Isopoda (slaters, woodlice, etc.)	≤ 1,800	< 4	5,000	?
Isoptera (termites)	Colonies	?	2,600	60%?
Blattodea (cockroaches)	?	?	4,500	?
Ants (Hymenoptera/ Formicidae)	Colonies	?	13,000	50%
Molluscs (soil gastropods)	?	?	24,000	40%?
Land Turbellaria (planarians)	?	?	830+	?
Terrestrial Polychaeta	?	?	?	?
Oligochaeta (megadriles + mostly aquatic microdriles)**	**50–5,000**	**20–500**	**10,000**	**20%?**
Microdriles (Enchytraeidae)***	1,000–300,000	1-53	~ 700	?
Microdriles (non- enchytraeids) in sodden, waterlogged, or wettish soil	?	?	1,000–2,300?	?
Megadriles ("true" earthworms)	50–4,875	20–500	~ 7,000	< 20%?
Total species (approximate)			**315,500**	**< < 1%?**

Table after Blakemore (2012: table 1, 2016: table 3) "from Brusaard et al. 1997; Wall and Moore 1999; Chapman 2009; Turbe et al. 2010: table 1; Fierer et al. 2007; Blakemore 2012; Wiki (https://en.wikipedia.org/wiki/Global_biodiversity#cite_note-col2016-5) and Pers. Obs.". Fungal hyphae are from https://www.fao.org/agriculture/crops/thematic-sitemap/theme/spi/soil-biodiversity/soil-organisms/by-type/fungi/en/. *These taxa are especially revised upwards in the current study. ** Earthworms from Gobat et al. (2004: table 2.11, p. 42) of ≤ 500 g m^{-2} (to depth?) wet wt. so approximately half for dry weight and a quarter of this for Carbon: ~ 125 g m^{-2} C. Lee (1985: table 7) highest earthworms in NZ pastures (2,020 m^{-2}, 305 fresh g m^{-2} "from McColl and Lautour 1978"); Coupland and McDonald (2008) report *Pontodrilus litoralis* (Grube, 1855) at 750–4,875 m^{-2}. An Earthworm ratio of < 20% known gives expected total (7,000 × 5 =) ~ 35,000 spp (as also in Fig. 4). *** Enchytraeid maxima from Cragg (1963: table 2), Springett (1967: fig. 24) at Moor House, UK; Lavelle and Spain (2001: 281) also reported ≤ 93,600 m^{-2} at Point Barrow, Alaska.

Regarding Table 1 data, it may be noted that higher organisms host many unique symbionts or parasites and, as for microbes, many specific viruses too. For earthworms, Lee (1985: table 7) had highest numbers in NZ pastures (2,020 m^{-2} with 305 g m^{-2}), higher counts are for littoral *Pontodrilus* sp. in WA. Note too that a total number of megadrile earthworms was predicted at ~ 35,000 species. Earthworms are important, as is noted later, due to their activities that greatly enhance other soil biota/microbes. Regarded as superficial soil-dwellers, "Soil Gastropods" were

tabulated. However, viruses were only provisionally included as they fail to meet all criteria of independently living organisms, albeit they are included in several more recent biodiversity surveys. If such a line of argument for viruses were followed, then may not eukaryotic endosymbionts that only actively exist within host cells (Sagan 1967), with their unique genomes, be similarly added in biodiversity totals?

Contemporaneous to CoSI, a Global Soil Biodiversity Atlas (GBIF 2016: table 1) tallied 219,000 soil fauna/microbes while adding 350,700 vascular plants – on a premise plant seeds and roots are grounded in soil – raising totals to 667,000 soil taxa or roughly a third of all ~ 2 million species formally described as that time (Fig. 4).

At around the same time, a 10-year, $1 billion, Census of Marine Life (CoML 2010) funded 2,700 researchers at 670 institutions from > 80 nations to conclude a total of just ~ 230,000 Ocean taxa (or ~ 12% of the 2 million known species!). They claimed this was just one tenth of Ocean's expected total of another two million species, hence a new Ocean Census project "launched" on 27 April 2023 to net the remainder. A similar 2011 Census of Deep Life (CoDL), a central pillar of the Deep Carbon Observatory (DCO - https://deepcarbon.science/), investigated diversity, distribution, and biogeography of obscure subsurface biospheres having little relevance to evolution or extinctions.

As argued in the current report, such expensive sub-marine projects distract funds and efforts from surveys of more crucial soil biota that are much less well-

Organism size	Group	Known species	Estimated species	% described
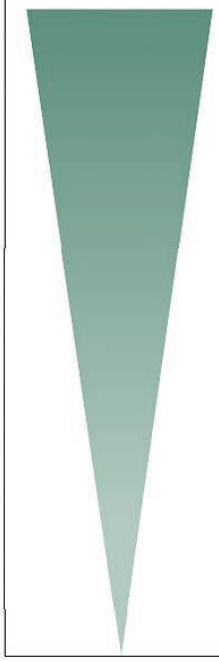	Vascular plants	350700	400000	88 %
	Macrofauna			
	Earthworms	7000*	30000*	23 %
	Ants	14000	25000-30000	60-50 %
	Termites	2700	3100	87 %
	Mesofauna			
	Mites	40000*	100000	55 %
	Collembolans	8500*	50000	17 %
	Microfauna ad microorganisms			
	Nematodes	20000-25000*	1000000-10000000*	0.2-2.5 %
	Protists	21000*	7000000-70000000*	0.03-0.3 %
	Fungi	97000	1500000-5100000	1.9-6.5 %
	Bacteria	15000	>1000000	<1.5 %

Known and estimated number of species of soil organisms and vascular plants organised according to size. Values of estimated diversity comply with the published literature, and are supported by expert judgement. Asterisks indicate numbers of species that live in the soil (updated from Barrios, Ecological Economics, 2007). [1,2]

Figure 4. Global Soil Biodiversity Atlas (GBIF 2016) reporting ~ 667,000 soil biota or just about one third of known 2 million (much above Decaëns et al.'s (2006) 25% total!). Note that earthworms have 7,000 known and > 30,000 estimated species. Bacteria had 15,000 known species but estimated over one million (< 1.5% described). However, when microbes (excluding viruses) are properly considered and counted, as herein, soil unknowns are much higher (likely just < 0.0001% known at best). Vascular plants add ~ 400,000 species (cf. Anthony et al. 2023 with 466,000 angiosperm "Plantae").

known and more endangered, extinctions being time critical. How is it justified to fund long-term abyssal taxonomy at $ millions per species while unknown soil taxa, that may be easily sampled in the field with a spade, are being extincted?

Although primarily concerned with rapid advances in molecular analyses ("Omics") revealing microbial diversity increased by several orders of magnitude (as detailed herein), lesser concerns are upping of counts for topographical terrain and delving into soils to full depth. However, unlike routine biotic surveys via planimetrically flat transect, plot, or quadrat, some surface-area independent inventories (e.g., of farm stocks or people) do not gain from realistic terrain extrapolation, neither do level waterlogged entities (e.g., lakes, mires, or bogs).

In general, prior to 2018 almost all soil inventories were based upon unrealistic, planimetrically flat land areas, thus true soil counts are likely more than doubled, and possibly quadrupled, when properly allowing for terrain and microtopography overlays (Blakemore 2018b), reducing further the marine majority claims. Although such work shows Soil is clearly more crucial and diverse, due to lack of equable support or funding, less than 1% of its meso- and macro-faunal organisms are as yet unearthed (FAO 2020). Furthermore, only a tiny fraction of the enormous soil microbiome is identified, with the proportion of known soil microbiota likely much < 0.0001% (as per Blakemore 2023), thus most of the vast array of Soil Biota remain an unexplored mystery awaiting discovery.

Moreover, rather just scratching the surface to cm or a metre deep, recent studies have mean depth-to-bedrock at 13.1 m plus friable saprock may add 8 m to total > 21 m soil depth (Shangguan et al. 2017: table 1; Hicks-Pries et al. 2023; Blakemore 2024). Consequently, most soil estimates, including those herein, may be an order of magnitude too low and hence the relative soil biomass and diversity values as in Fig. 5 (cf. Fig. 2) are most modest. This dependent upon estimates of full soil depth.

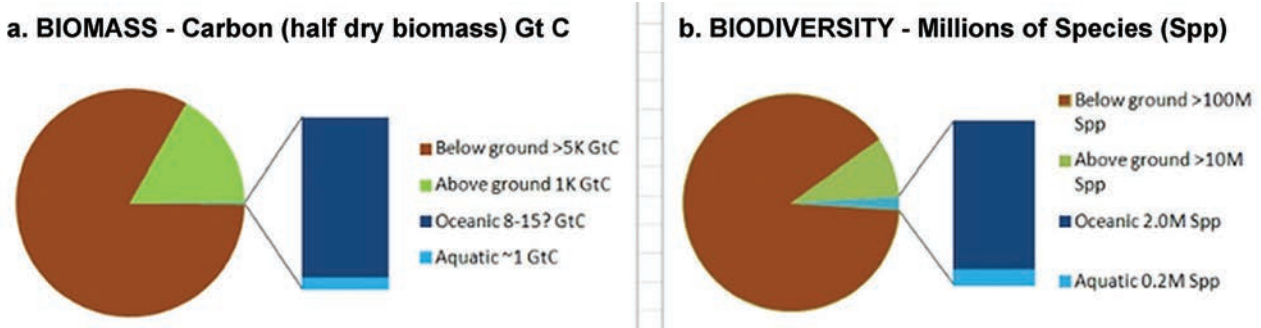

Figure 5. Global biomass (plus dormant/ necromass) and biodiversity in context of biome proportions (from Blakemore 2023 after https://vermecology.wordpress.com/2020/05/27/realms-of-the-soil/: fig. 2 and https://veop.files.wordpress.com/2022/09/new-addendum-file.pdf: fig. 4), being updated in the current report. In the figures above "below ground" or sub-surface refer to soil biotic activity related to surface productivity and not to the deeper subsurface biota.

Extrapolation of soil sampled at just a few superficial centimetres or a metre, to allow for full depth (≤ 21 m as noted above) are not yet applied but in themselves may increase soil stocks by an order of magnitude. Rolando et al. (2021) found soil layers below 90 cm up to 5 m deep accounted for 80% biomass, while the 0–30 cm layer represented only 10% of total soil carbon (i.e., × 10 for > 30 cm).

A further distinction is definition of "deep subsurface" biota that source energy differently to subsoil species. Beaver and Neufeld (2024) state that there is no universal depth that defines the terrestrial subsurface biome, previous publications having described "terrestrial subsurface as deeper than 8 m, and the deep terrestrial subsurface as deeper than 100 m." For the purposes of their review, the deep terrestrial subsurface comprised of rocks and groundwater at least 100 m below the surface of the Continents. Bar-On et al. (2018) "define deep subsurface as the marine subseafloor sediment and the oceanic crust, as well as the terrestrial substratum deeper than 8 m, excluding soil." An important demarcation, although unapplied in the present review, is soil biotic biomass and biodiversity to whole mean depth of soil activity (or frozen in Permafrost), now globally averaged near 21 m.

Soares et al. (2023) suggested 12–20% of Earth's biomass exists in the terrestrial deep subsurface, compared to ~ 1.8% in the deep subseafloor, further confirming "terrestrial deep subsurface holds ca 5-fold more bacterial and archaeal biomass [thus, by proxy, biodiversity?] than the deep marine subsurface." Although the total Ocean biota is again diminished, this deep subsurface data is a much lesser concern in the current global review of Soil biota and is only briefly mentioned in passing.

Abundance of biota relates to both its biomass (living, dead, or dormant forms) and its biodiversity species counts. Initially, a preliminary global microbial abundance estimated by Whitman et al. (1998: tabs 3–5) was 2.6×10^{29} vs 1.2×10^{29} cells in Soils vs Aquatic (marine and freshwater) habitats, and 26.0 vs 2.2 Gt C biomass, respectively. This was an indicator that Soil clearly supports twice the Ocean biota, and ten times its biomass as an early realization that Soil likely supports > 50–90% of Life on Earth. Deep sub-surface microbiota, which are largely irrelevant to most active above-ground Earth processes, were 3.6×10^{30} vs 2.5×10^{30} cells in Oceanic vs Terrestrial sub-surfaces. However, revisions by Kallmeyer et al. (2012), Parkes et al. (2014), Magnabosco et al. (2018), and Hoshino et al. (2020) had just $3–5 \times 10^{29}$ vs $2–6 \times 10^{29}$ cells (biomass of ~ 4 vs 23–31 Gt C), respectively. A global tally of ~ 10^{30} cells was determined independently by Blakemore (2022, 2023), but for somewhat different proportions, for reasons as explained and briefly restated herein.

Soil was shown with ≤ 10^{8} –10^{12} cells/g dry weight or 10^{14} –10^{18} cells/t, there being 10^{6} grams in a tonne. Biodiversity ranges were 10^{2} –10^{6} species/g or 10^{8} –10^{12} species/tonne of soil. Global topsoil was calculated as ~ 2.1×10^{14} t to 1 m depth. Therefore, the total ranges were 2.1×10^{28} –10^{32} cells (median ~ 2.1×10^{30}) and 2.1×10^{22} –10^{26} soil species (median ~ 2.1×10^{24}). Having a new mean soil depth of ~ 21 m would possibly increase these by an order of magnitude, but is not yet applied. Comparatively, Anthony et al.'s (2023) global species total (10^{10}) is mid-range in the biodiversity of a single tonne of topsoil. Moreover, an equivalent to all the Oceans' biodiversity may similarly be held in just a handful of fertile topsoil, or much less than a tonne, albeit, as a general "rule of thumb", a dry tonne of topsoil occupies 0.65 cubic metres, a ground area of < 1 m^2, or a small step for a man.

Prior sources had determined: "species of bacteria per gram of soil vary between 2,000 and 8.3 million" (Gans et al. 2005; Roesch et al. 2007) (= 10^{4}–10^{6} spp/g or 10^{10}–10^{12} spp/t that, if all unique taxa, is equivalent to twenty billion or up to a trillion species per topsoil tonne). Discrepancies in Gans et al. (2005) are samples of 10 g soil so strictly 0.83×10^{6} spp/g, yet their fig. 4 shows total species

number computed as ≤ 10^7 thus a million or so spp per g seems correct. Raynaud and Nunan (2014) had: "a single gram of soil can harbour ≤ 10^{10} bacterial cells and an estimated species diversity of between 4×10^3 to 5×10^4 species" (= 10^{14}–10^{16} cells/t and 4×10^9–5×10^{10} spp/t). Bickel and Or (2020) found: "bacterial phylotypes ranges between 10^2 and 10^6 per gram of soil, with high values similar to the diversity in all of earths environments" (= 10^8–10^{12} spp/t). James et al. (2022) summarized: "Soil microorganisms are the largest biodiversity pool on earth, with more than 10^{30} microbial cells [total surely!?], 10^4 –10^6 species, and nearly 1,000 Gbp of microbial genome per gram of soil". Although fully extrapolated values from the cited reference sources are listed, only the median of the various value ranges are taken as reasonable summaries, these being presented herein.

As already noted, using scaling values, Zhao et al. (2022) found: "Although the estimated total abundance of global airborne bacteria (1.72×10^{24} cells) was 1 to 3 orders of magnitude lower than that of other habitats, such as soil (9.36×10^{28} cells), freshwater (4.70×10^{25} cells), and marine (4.68×10^{28} cells) habitats, estimates of the bacterial richness of the atmosphere (4.71×10^8 to 3.08×10^9) were comparable to those of the hydrosphere". In other words, they confirm Soil at ~ 10^{29} with twice as many microbial cells as the Ocean and, whereas their figure (Zhao et al. 2022: fig. 3A) shows a richness of > 10^{11} soil microbe OTUs, the Ocean or Freshwater and the Air each only have ~ 10^{10} taxa (< 10%). This translates as Soil housing ~ 90% of global biodiversity, as indeed May (1994) had intimated 30 years ago, before the scope of microbial megadiversity was realized as being so vast.

For microbial diversity, recent developments of rapid genomic sequencing and bioinformatics (-omics) allow scaling values such as by Locey and Lennon (2016) to show Earth with ~ 10^{12} microbial OTU taxa (just 10^{10} or ~ 1% in global Ocean). These totals were soon raised to 10^{12}– 10^{14} microbial taxa by Lennon and Locey (2020) and then by Fishman and Lennon (2022) who had "a soft upper constraint of 10^{22}–10^{23} due to neutral drift" for all taxa. Their upper boundary is increased by 20× for median species total in the current study and, regardless of scaling values, confirm Soil's > 99.9% of global biodiversity, being almost entirely microbial. These authors' soft upper constraint of $10^{22–23}$ taxa dispersed in $10^{29–30}$ soil cells is a ratio of one taxon per ~ $10^{6–8}$ cells.

Summarizing the microbial status, Zhao et al. (2022) said**:** "soil is the most microbiologically abundant (10^{29}) and diverse (10^{11}) environment on the Earth". Although their cell count may be within bounds, their diversity – albeit ~ 10× greater than the Ocean's – is disproportionately low due to incomparability of Soil's scaling ratio when compared to any of their other habitats (Fig. 6; Table 2) .

Table 2 contextualizes a current estimate of 2.1×10^{24} soil taxa as 99.99% of a global total. Species values presented herein (e.g., Fig. 6, Table 2) may be contrasted to microbial Spp/OTU counts in Anthony et al. (2023: table 1), arranged in a slightly revised format for better clarity of comparison, as shown in Table 3.

Deep carbon data are of less practical concern to the current study on Land and Soil carbon stocks and cycles, although they again highlight deficiency of Ocean's excessively claimed biota at all scales and at all depths, almost all being downgraded in subsequent reviews.

Anthony et al. (2023: fig. 2) confirm Bacteria richness ≤ 90%, proving their dominance in Soil (Fig. 7) but are mistaken for Oligochaeta, as Earthworms are truly higher with 99% soil occupancy which as is discussed further in the review section below.

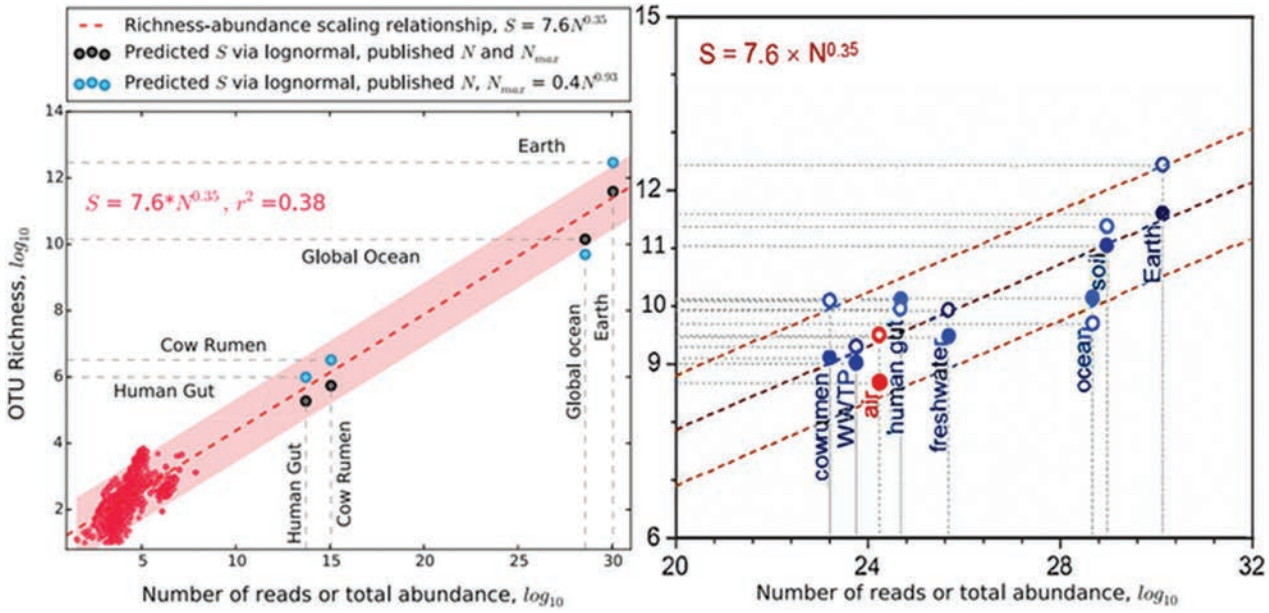

Figure 6. Relative microbial abundance vs diversity after Locey and Lennon (2016: fig. 3), and Zhao et al. (2022: fig. 3A) who added wastewater, air, freshwater, and soil. The Ocean has < 1% of global biodiversity, barely above freshwater or air, and less than the human gut biome! The soil microbiome is revised upwards in Table 2 as its abundance vs richness apogee peak is more extensive than any other major (or minor) habitat.

Table 2. Prokaryote proportional counts and biomass in Earth's six major ecological Realms-of-Life.

Ecological realm	Cells/CFUs × 10^{28} (%) *	Species/OTUs (%) *	Biomass Gt C (%)
1 Soil *	210 (56%)	2.1 × 10^{24} (99.99%)	~ 209.6 (56%)
2 Land superficial **	100 (27%)	10^{12} (< 0.001%)	~ 100? (27%?)
3a Land subsurface ***	~ 20–60 (11%)	< 10^{5}	~ 23–31 (7%)
3b Marine subsurface ***	~ 2.9–35 (4%)	< 10^{6}	< 35 (9.3%)
4 Ocean **	12 (3%)	10^{10} (< 0.0001%)	0.6–2.2 (0.5%)
5 Aquatic on Land **	< 0.02 (< 0.005%)	< 10^{10} (< 0.0001%)	0.3? (< 0.1%?)
6 Atmosphere ****	(10^{24})	(10^{8}–10^{10})	? (< 0.0001%?)
TOTAL	~ 378 × 10^{28} (100%)	~ 2.1 × 10^{24} (100%)	~ 373 (100%)?

* Data from Blakemore (2022, 2023: table 2) greatly modified from Whitman et al. (1998: table 5). Fishman and Lennon (2022) had: "bacterial and archaeal taxa $S_{present}$ is between 10^{6} and 10^{23}"; at ~ 2.1 × 10^{24} soil taxa their upper value is increased by twenty times (Blakemore 2022). CFUs = Colony Forming Units (microbial), OTUs = Operational Taxonomic Units (genetic). Soil microbial biomass is updated to 209.6 in Appendix 1.

** Data extrapolated from Zhao et al. (2022: fig. 3A), Locey and Lennon (2016: fig. 3), Lennon and Locey (2020), and Whitman et al. (1998) who had aquatic habitats, mainly Ocean, with 0.6–2.2. Gt C (just 0.15–0.55%). Grosberg et al. (2012) estimated aquatic habitats occupying ~ 1–2% of land area (now halved to 0.8% due to terrain!) have one-third of the Ocean's biodiversity (and hence likely one-third of its biomass?).

*** Revision of subsurface by Kallmeyer et al. (2012), McMahon and Parnell (2013: table 3), Magnabosco et al. (2018: fig. S23), Bar-On et al. (2018), Hoshino et al. (2020), Blakemore (2022, 2023), Soares et al. (2023).

**** Total 10^{6} cells/m^3 to 1 km altitude (https://en.wikipedia.org/wiki/Aeroplankton) gives 10^{24} cells (> 10^{10} spp?); however, microbes, including Bacteria and Fungi, have been detected in the atmosphere at high altitudes making the atmosphere the Earth's largest biome – much greater than was claimed for the Ocean. Contrary to such Ocean claims, Whitman et al. (1998) said: "By volume, the atmosphere represents the largest compartment of the biosphere, and prokaryotes have been detected at altitudes as high as 57–77 km". Zhao et al. (2022) support these earlier contentions: "While the total abundance of global airborne bacteria in the troposphere (1.72 × 10^{24} cells) is 1 to 3 orders of magnitude lower than that of other habitats, the number of bacterial taxa (i.e., richness) in the atmosphere (4.71 × 10^{8} to 3.08 × 10^{9}) is comparable to that in the hydrosphere". Naturally, many Aeroplankton taxa are shared with the Phytoplankton and Phytomenon. Zhao et al. (2022: fig. 3A) (Fig. 6) also show a human gut biome has greater biodiversity than all the hydrosphere (the realization of which many marine or freshwater researchers may find particularly difficult to stomach). As already noted, aquatic or deep sub-surface biota are of less practical concern to the current study on Land and Soil organisms, although they again highlight deficiency of Ocean's excessively claimed biota at all scales and at all depths, almost all being downgraded in subsequent reviews supporting the need for a "sea change" of appreciation and much increased support for soils.

Table 3. Species (Spp/OTU) biodiversity key values re-formatted from Anthony et al. (2023: table 1).

Biodiversity spp/OTUs *	Lower × 10^8	Central × 10^8	Upper × 10^8
EARTH			
"Phage"	1.000	1,000.0	3,700
Microbe total **	0.067	10.1	10,000–1,000,000
(Microbe just Bacteria)	(0.044)	(10.0)	(37)
Earth total	**1.10**	**1,010.1**	**3,740 *** **
Earth non-Phage total	0.100	10.1	40
Earth non-Phage, non-Bacteria	ND	0.1	ND
SOIL			
"Phage"	0.056	99.0	1,590
Microbe total **	0.060	4.4 ****	"?"
(Microbe just Bacteria)	(0.010)	(4.3)	(33)
Soil total	**0.095**	**104.0**	**1,620**
Soil non-Phage	0.039	5.0	30
Soil non-Phage, non-Bacteria	ND	0.7	ND
% Soil vs Earth totals			
Totals	8.0%	**10.3%**	43.3%
Totals non-Phage	39.0%	**50.0%**	75.0%
Totals non-Phage, non-Bacteria	ND	[-86%!]	ND

*10^8 is 100,000,000 species (Spp) or operational taxonomic units (OTUs). ** Microbe totals are for "bacteria, archaea, and fungi", but the non-Bacteria values are seemingly erroneous as Soil (0.7) has more than all Earth (0.1). *** Upper value "3.74 × 10^{11}" ignores Microbes with "$10^{12\text{-}14}$" taxa. **** Cf. Zhao et al. (2022) have > 10^{11} for soil and > 10^{12} for Earth, and Blakemore (2022, 2023) has total microbes 2.1 × 10^{24} (cf. Table 2) plus total global viral/phage count (as presented herein) of ≤ 10^{26} taxa, found mainly in Soil (see text for details).

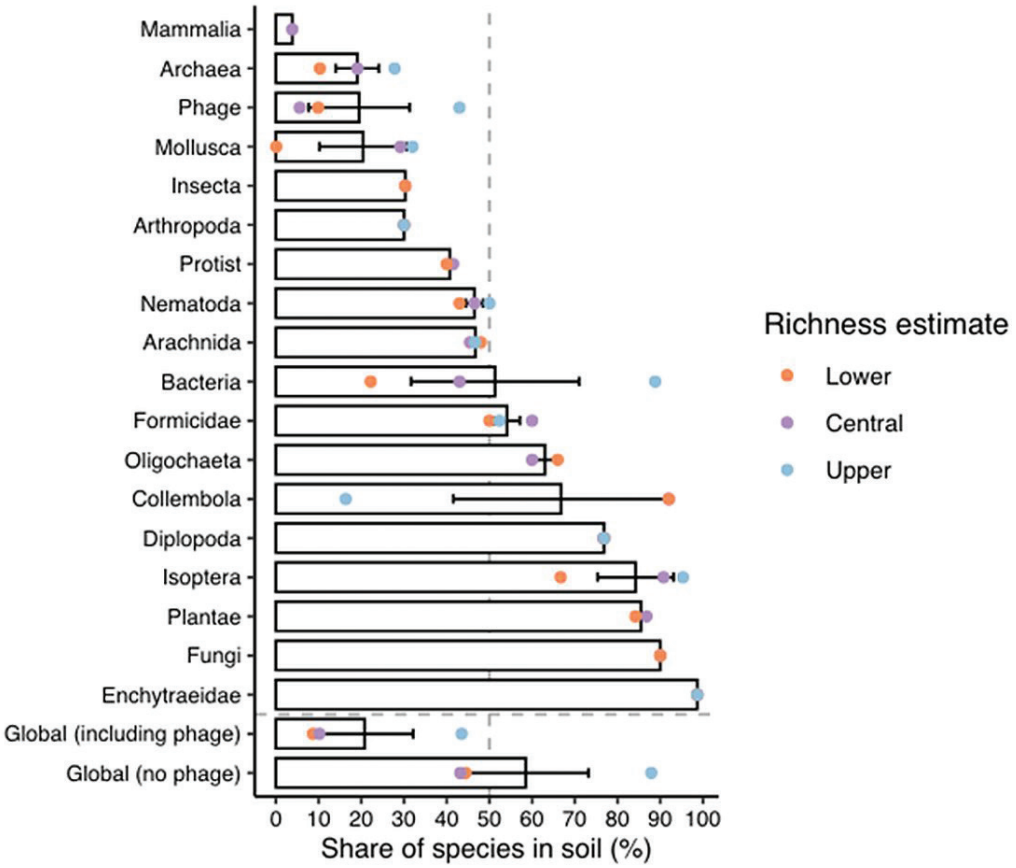

Figure 7. Unsystematically selected taxonomic groups in Anthony et al.'s (2023: fig. 2) (cf. Table 1) appear to show Bacteria's Upper dominance at > 90% in both Soil and "Global (no phage)" totals but, strangely, they omit Megadrile earthworms being > 99% resident in soils, as their name would suggest and as restated below. Comparatively, their Enchytraeidae, according to Martin et al. (2008), are < 47% terrestrial, not 99%!

Materials and methods

The intention of this review is to compile and compare recent Soil Biota studies by Blakemore (2022, 2023) with Anthony et al. (2023). In the last few decades, the advent of high-throughput DNA amplicon sequencing and rapid genetic analyses (-omics) has revealed the complete dominance of microbes in biotic tallies, especially in soils, and a need for realistic biodiversity estimation from projections of their unknown and undescribed components. Realizing our ignorance of soil microbes exposes a stark disparity: Most accounts of global richness reflect historic intensity of study rather than relativistic estimates due to irrational fact of overwhelmingly research effort and funding directed into Aquatic, Oceanic or Space research (e.g., NASA, JAMSTEC, NOAA, Scripps, Woods Hole, https://en.wikipedia.org/wiki/List_of_oceanographic_institutions_and_programs), not Soil. The International Union of Soil Sciences (https://www.iuss.org/) does not list any dedicated institute.

The summary of progress in relative soil biodiversity studies, as introduced above, is further reviewed and where necessary corrected, mostly for microbe counts but also to allow for terrain (after Blakemore 2018b). Factoring soil depth may further double numeric values if not exponentials.

In addition, several omissions and uncertainties ("?") from various published sources are clarified.

Body of review

Regarding Anthony et al. (2023) soil enumeration values questioned with "?"

For Mammalia, Anthony et al. (2023: table 1) had Lower to Median ranges with 75–250 soil species, yet their Upper range was marked "?". Although relatively unimportant, a nominal value in Decaëns et al. (2006: fig. 2) of ≤ 1,000 soil mammals may be a reasonable estimate for this well-known fauna.

However, Anthony et al. (2023) define soil species as "those that live within, on (e.g., insects that feed on the surface of soil), or which complete any part of their life cycle in soil (e.g., organisms with an inactive pupal stage in soil or plant seeds that germinate in soil) or in the tissues of soil-dwelling symbionts (e.g., microbial parasites of soil animals)." Hence, it may be moot to extend inclusion to almost all terrestrial mammals (except, perhaps, some wholly arboreal or semi-aquatic species) that live or feed on soil (or end their life cycle often buried, inhumed, or interred therein!), e.g., *Homo*.

Secondarily, encompassing of many (most?) insects within the definition of soil species adds to an argument for the inclusion of Larsen et al. (2017) insect parasites or pathogens as part of Soil Biota.

Other groups in need of more pertinent "?" clarification are presented in sequential order below.

Regarding Annelida: Oligochaeta (true earthworms and their lesser relatives)

Anthony et al. (2023: table 1) have "?" questioning a possible Upper range of their Oligochaeta which is surprising since they cite the "Global Soil Biodiversity Atlas" (GBIF 2016 - https://esdac.jrc.ec.europa.eu/public_path/shared_folder/Atlases/JRC_global_soilbio_atlas_low_res-2019-06-13.pdf) that states: "Earthworms belong to the phylum Annelida (class Clitellata, subclass Oligochaeta). The Oligochaeta contain 10 400–11 200 species in approximately 800 genera, and 38 families comprised of approximately 7 000 true earthworms." They seem to have missed the subsequent statement: "Although 7 000 'true' earthworms (in 20 families) have been described to date, the total is probably around 30 000 species globally".

This is clearly shown in the GBIF (2016: table data) that is reproduced here in Fig. 4.

Phylum Annelida includes Classes Oligochaeta (earthworms), Polychaeta (marine worms) and, erstwhile, Hirudinea (sanguinivorous or predatory leeches). Due to an inordinate amount of funding for marine research, ~ 13,000 polychaeta are now reported, but only ~ 8,000 are considered valid taxa; similar synonym statistics apply to earthworms but, due to their high endemicity and Soil's heterogeneity, their unknowns are legion. The Oligochaeta comprises mainly soil dwelling Order Megadrilacea from Benham (1890) – the "true" earthworms – and his Microdrilacea for smaller, mainly aquatic worms. Strangely, in Anthony et al. (2023: table 1) their "Oligochaeta" has between 5,000–10,000 total taxa (apparently sourced from Martin et al. 2008 and a GBIF Checklist) and they further claim 3,300–6,000 Oligochaeta in soil (from Martin et al. 2008 and Decaëns et al. 2006). Contrary to Anthony et al. (2023: fig. 2) (see Fig. 7), Martin et al. clearly stated: "Most microdriles are fully aquatic, with the exception of the Enchytraeidae, a family that is primarily terrestrial; of the 650 described species, 200 are aquatic and 150 marine", or primarily > 52% aquatic! These relative figures are treated in further detail below as it is important for facts to be both current and correct.

Martin et al. (2008: table 1) did indeed claim only 5,000 valid species of Oligochaeta *s. stricto* and said 4 of the 14 megadrile families (in actuality six of twenty families) have aquatic or semi-aquatic species (or, for *Pontodrilus* spp., littoral). They further state that "No fewer than 60 species of megadriles are also considered aquatic" and list total aquatics {in squiggly braces} in these stated genera as: Almidae {41 spp.}, Criodrilidae {2}, Lutodrilidae {1}, Sparganophilidae {14}, plus several Lumbricidae claimed to be frequently found in aquatic situations (although this may be questioned as it is often adventitious rather than fixed). Surprisingly they omit other megadrile genera with aquatic species such as Megascolecidae (e.g., a few in NZ lakes) and Pontodrilidae {2 spp.} that is wholly littoral. This biodiversity data requires updating since at least 7,000 truly megadrile taxa are currently described (see Blakemore 2000, 2008, 2016), and whereas names are continually added the more we search and discover, probably less than 20–30% of all species are known, as found by Lee (1959) in New Zealand (cf. Glasby et al. 2009; Blakemore 2011), and by Blakemore (2000) in Tasmania. Numbers of synonyms are un-estimated while likely cryptic species need clarification. If their relative proportions hold true, as Blakemore (2022) suggested, then the average of six cryptics per morphologically described arthropod taxon as in Larsen et al. (2017: table S1) quite counterbalance the ~ 18% eukaryote synonyms that were estimated by Mora et al. (2011).

Anthony et al.'s (2023) preliminary research also overlooked Australian ABRS (2009) global summary with: "7,684 Oligochaeta from Blakemore (2008 and pers. comm.)" and around 30,000 total anticipated global species. As Blakemore (2013) explained, hierarchical classification of true earthworms is: Annelida Lamarck, 1802; Oligochaeta Grube, 1850; Megadrilacea Benham, 1890 with ~ 20 or so families including Moniligastridae, Ocnerodrilidae, Acanthodrilidae, Exxidae, Octochaetidae, Megascolecidae, Lumbricidae and Eudrilidae (all *sensu* Blakemore 2000). Thus, Megadriles have ~ 7,000 known species (with cryptics cancelling synonyms?) compared to mainly aquatic Microdrilacea, composing around 2,300 spp. (Table 1) plus a quite minor microdrile family that these authors – for some unsystematic reason – gave great import: Viz. Enchytraeidae with only around 700 species. Whereas Anthony et al. (2023) claim this family is the most wholly soil-dwelling group with "98.6%" terrestrial members, this is misconstrued as the majority of this Microdrile family is fully- or semi-aquatic; being small, pale and relatively ineffective. Microdrile researchers are classed as aquatic workers, rather than true soil-based, Megadrile eco-taxonomists, consequently they too appear to enjoy greater support and funding for seemingly obscure reasons.

A summary of relative abundance and biodiversity of these Oligochaeta is compiled in Appendix 1.

Another source is García-Roselló et al. (2023: table 1) GBIF database of Annelida: Clitellata with only 8,000 total species but which falsely claims 13.6% are Marine. In comparison, Anthony et al. (2023) strangely state: "Annelids, including the Enchytraeidae and Oligochaeta, with the lowest overall biodiversity but high specializations to soil. We estimate that there are 7.8×10^2 and 1×10^3 Enchytraeidae and Oligochaeta species and that 98.6 ± 0.06% and 63 ± 4.2% of species live in soil, respectively." We may graciously accept this in part as a typing error since the most basic of research reports frequently cite over ~ 7,000 described Megadrile Oligochaeta alone, not just 1,000. Moreover, rather than just 63%, a majority of Megadrile Oligochaeta being wholly soil dwellers is closer to > 99%, as the name, 'Earthworm', suggests (cf. Fig. 7). Although obvious, this is restated.

Thus – contrary to Anthony et al.'s (2023) indication – most of the true earthworm families are terrestrial and nearly 100% resident in soils. Martin et al. (2008) citation of 60 wholly aquatic megadriles may be a reasonable number, that – in a megadrile group of ~ 7,000 taxa – is < 1% making them one of the most specialized of committed soil residents. Other candidates such as the termites or ants are insects living in colonies with winged stages (almost liken to soil "tourists"), thus not as highly endemic nor as specialized as earthworms are. Other taxa such as hexapod Collembola or Acarid mites are typically superficial soil/litter dwellers and depend upon earthworm burrows for their soil ingress. There are several others of less populous soil faunal and floral groups that may also have 100% edaphological species. For instance, components of the ubiquitous superficial cryptogamic Biocrust or extensive Phytomenon that, as well as being most ancient flora, may rival marine Phytoplankton for abundance, diversity, as well as for NPP productivity (Blakemore 2024).

Phytomenon is a recent term for microscopic "plants" that abide, as is appropriate for terrestrial single-celled autotrophs, compared with the marine or aquatic Phytoplankton ("plants" that drift) or the Aeroplankton (aerial floating microbes) as noted already (see Blakemore 2019, 2023, 2024).

Regarding soil Bacteria (plus Archaea)

Anthony et al. (2023: table 1) had Bacteria included within their Microbes often marked with a "?". Global biodiversity is now dominated by Bacteria within the Soil Realm, as Blakemore (2022) showed, with new totals of ~ 2.1×10^{24} taxa in ~ 2.1×10^{30} cells indicating that one species, or operational taxonomic unit (OTUs), exists for around each 10^6 cells. In this review a justified argument is that a unique taxon per million cells is reasonably applicable. As there is no central registry – nor yet a dedicated Soil Ecology Institute – diversity data compiled from diverse sources are updated or corrected as necessary in periodic reviews, such as this present contribution.

In Norway, Torsvik et al. (1990) had found ~ 1.5×10^{10} bacteria cells per gramme of dry forest soil distributed among 4,000 clones with standard genome sizes; a mean number was ~ 4×10^6 bacteria per clone per g of dry soil. This indicated soil bacterial populations comprise many genetically separate clones, with a mean of around ~ 3.75 clones per million cells. This local data suggests more than one species/OTU per million cells is a reasonable approximation.

Worldwide, Roesch et al. (2007) estimated mean microbial populations limited to ~ 1 billion cells per g of soil (10^9 cells/g) comprising 10^3–10^6 Bacteria/Archaea species, or at least one and up to as many as one thousand species per million cells(!). They also found 2,000–10,000 species per gramme of soil were underestimates. Therefore, an extrapolated mean may be closer to 10^5 spp/g (per 10^9 cells/g), suggesting an average nearer to 100 Bacteria/Archaea species per million cells.

As early as 2008, Fulthorpe et al. (2008) had determined that ≤ 87.9% of Bacteria were unique to the soil they were sampled in, and only 1.5% were common to all soils across a large transect of American continents. The same does not hold for the Ocean that is much more homogenous, with intermixing biota widely dispersed. This was clearly shown by Louca (2022: figs 1, 2) with soil habitats four or more orders of magnitude more diverse than marine (etc.) habitats over shorter distances. Dispersal was slowest for terrestrial sub-surfaces, indicating mostly soil environments acting as "isolated islands" of endemic microbial evolution. His "hot-spring" data is interesting as, contrary to claims for Marine origin, most current information point to these being the font of all Life, consistent with Darwin's prescient "Warm little pond" theory of Origin (e.g., Damer 2016).

Whereas Larsen et al. (2017) proposed a new Pie of Life projected for > 1–6 billion ($10^{9–10}$) species on Earth dominated by Bacteria (~ 70–90% of total) which they mainly considered just for insect hosts, Bahram et al. (2018) concluded Soil as Earth's most diverse biome but failed to give figures. For estimates of around 3×10^{29} cells in soils, Flemming and Wuertz (2019), as for Bar-On et al. (2018), also give no species data. Subsequently, Louca et al. (2018, 2019) claimed only "2.2–4.3 million full-length OTUs worldwide" (3×10^6) refuting predictions that billions or trillions of prokaryotic OTUs exist. Yet Wiens (2023) explained how Louca et al. (2019) had made entirely avoidable underestimation errors whilst also revising Larsen et al.'s (2017) projected 1–6 billion estimate downwards to a modest 0.183 to 4.2 billion ($10^{8–9}$) species with 58–88% Bacteria, but again most of these in insect hosts rather than in the much more diverse and extensive Soil habitat.

Conversely, Raynaud and Nunan (2014) said: "The application of novel molecular techniques (such as high throughput sequencing) during the past two decades has uncovered a phenomenal bacterial diversity in soils." They quoted "a single gram of soil can harbour up to 10^{10} bacterial cells and an estimated species diversity of between $4{\cdot}x\ 10^3$ to $5{\cdot}x\ 10^4$ species". But they also noted "when bacterial density is 10^9 cells g^{-1} or less. $\alpha = 1107.53$ corresponds to a species richness of 15000 species for 10^9 cells whereas $\alpha = 264.79$ corresponds to a species richness of 4010 species for the same number of cells." This higher diversity of 4–15 species per million cells is medial to a range estimated earlier of an average one to 100 bacterial species per million cells in Soil as noted above.

At a trans-European transect scale, Plassart et al. (2019) extracted 3×10^6 16S rRNA sequences from 71 × 1 g (dry?) soil samples, detecting a total of 34,190 OTUs ranging from 653 to 1,860 (mean: 1,307) OTUs/g. This ~ 10^3 taxa/g is low to midrange of totals as given elsewhere, possibly due to the methods, soils, or the local climate. Their rarefaction curves of bacterial OTUs followed a logarithmic model without reaching a rarity plateau. Higher richness estimates of between 590 and 100,000 species per gram (10^{2-5} OTUs/g) for similar 16S rRNA PCR sequences were reported by Schloss and Handelsman (2006), their lower range from a remote, presumably wintery, Scottish soil.

In harsh Alpine biomes, Adamczyk et al. (2019) still extracted an average of 1.7×10^4 OTUs per 250 mg sample (thus about 6.8×10^4 OTUs per g?), just a quarter fungal, and they also determined that soil acidity and elevation were the most deleterious variables in these extreme habitats.

Regarding rarity of soil species, Bickel and Or (2020) had most bacterial species classified as rare (99.6%) and these made up ~ 42% of a global relative abundance, they concluded: "The complex structure of soil pores offers numerous refugia for hosting diverse bacterial species. This wide range of microhabitats is particularly important for maintaining the rare components of the soil microbiome". From their global microbial biodiversity of ~ 10,000 OTUs per g dry soil, since Soil harbors ~ 10^{10} cells per g, and these are mostly Bacteria/Archaea, this supports a reasonable average of around one OTU/species per million cells in Soil. Q.E.D.

Recently, Jia et al. (2022) and Sun et al. (2023) confirmed in quite local samples what Fulthorpe et al. (2008) found for trans-continental soils, with rare or unique bacteria being 90–98% while only a minority of species were common. This supports high Soil biodiversity at sample to Continent scale.

Soils naturally include a root-zone Rhizosphere: "the most diverse microbiomes on Earth, containing up to 10^{11} microbial cells and ~ 30,000 bacterial species per gram of root. The rhizosphere microbiome exists through an interwoven tapestry of bacteria, viruses, archaea, protists, fungi, nematodes, and small arthropods interacting directly with plant roots and each other" (White et al. 2021). McNear (2013) found $10^{10} - 10^{12}$ cells per gramme of rhizosphere, endorsing 10^{11} cells/g as a reasonable, but higher, median count in this rich soil microhabitat compared to the Soil environs.

Almost all the studies above are consistent with Blakemore (2022) determining a modest one species per million cells (viz. 2.1×10^{24} species in 2.1×10^{30} cells in Soil globally). However, as noted, underestimations may be one or more orders of magnitude, so all values are approximate. The wide uncertainty range of $10^{22} - 10^{26}$ total species (median ~ 2.1×10^{24}) within $10^{28} - 10^{32}$ cells (median ~ 2.1×10^{30}) shown in this report is commensurate with previous estimations; compared to Fishman and Lennon (2022) the increase is around 20-fold.

This is compliant with Bar-On et al. (2018) who had a 10-fold margin of error in their microbial estimations and a 32-fold error factor for viruses.

Fungal rarity ratios, when simultaneously studied, appear comparable with those for Bacteria, albeit fungal biodiversity, also mainly in soil, is often less by varying factorials (e.g., Labouyrie et al. 2023).

More support for higher Soil Bacteria diversity, both relative and compared to in any other habitat, are indicated by local and global Virus to Bacteria (VtB) ratios which will now be discussed further.

Scaling the Virome – Virus-Like Particles (VLPs) and Virus to Bacteria (VtB) ratios

A virion is an infectious virus particle, while a virus-like particle (VLP) is a non-infectious nanostructure that mimics a virion, but often these terms are used interchangeably. "Phage" is used informally for a bacteriophage that infects and replicates within Bacteria or Archaea, often a synecdochal term for all viruses, not strictly correct thus only quoted and not self-applied in this review. Virus to Microbe (VTM), Virus-Bacteria Ratio (VBR) or Virus to Bacteria Ratio are also interchangeable expressions; hereafter only the latter (VtB) is used.

Tabulated VtB ratios are presented in Appendix 2, revised for microbial counts in Blakemore (2022, 2023), to give a global total of ~ 5.1×10^{31} VLPs with ~ 4.1×10^{31} (~ 80%) virions in soils (to partial depth). This updates the soil virus value, allowing for non-ice and non-desert terrain, that Blakemore (2022) concluded to 1 m depth of ~ 2.1×10^{30} virions, based upon Bar-On et al.'s (2018: 55) summary they accepted had a 32-fold uncertainty. An indication of these uncertainties is from new soil virus data provided in 2023 (https://web.archive.org/web/20220301082457/https://www.soilviral.com/) having: "1 billion viruses g^{-1}, that if calculated over the whole globe amounts to about 4.9×10^{31} soil viruses". Doubled for terrain, this is ~ 1×10^{32} as a new upper value in a range, now of 10^{31}–10^{32} VLPs. A mean value of around 5×10^{31} global total virions on Earth is then a reasonable compromise, which why this value is quoted in the Abstract above.

Virus to Microbe/Bacteria Ratios (VtBs) of Virus-Like Particles (VLPs) interlink (as shown in Appendix 2) indicating likely ranges of both abundance and diversity acting as mutual cross-checks on relative abundance and diversity summaries. Wide ranging VtB estimations, pertinent for soil, mostly vary around 10:1 to 100:1. Emerson (2019) summarized how abundant and important viruses are in the Soil compared to in the Sea. A plausible summary is that viruses are most abundant in Soil and at least ten times, but often ≤ 100 times (or more?), as rich as the Bacteria, their primary hosts, in terms of both abundance and biodiversity.

Conversely, a few studies show a VtB ratio around 1:1 suggesting both be raised to 10^{26} species? From Blakemore (2023), since both global and Soil alone bacterial biodiversity are in the order of 2×10^{24}, then virus diversity may range from at least as many up to 10^{25}–10^{26} total Soil viral species.

Meanwhile, Anthony et al. (2023) in a Supplementary file had an intermediate value of 1,000 "Phage" species per bacterial species. They said: "Using the upper estimate of bacterial diversity (3.7×10^{9}) and a ratio of 1000:1, we predicted the upper and lower ranges of viral diversity." Despite this, they appear not to have applied it to their table 1 having just 3.7×10^{11} global "Phages" rather than 3.7×10^{12} species as they intimated. This again indicates their report needs a through review.

Review of Soil abundance enumerations

An upper diversity "Phage" value in Anthony et al. (2023: table 1) of 3.7×10^{11} species is well below current estimates about 10^{26} viral varieties found mainly in soils. However, viruses are excluded from strict biodiversity assays by failing to conform as free-living and independent entities according to most definitions of the entities of Life with all their attributes and, often mutual, relationships.

Prior to 2022, an oft-repeated claim that soils support 25% of global biota was seemingly attributable to Decaëns et al. (2006: figs 1, 2) that had: "A rapid survey of invertebrate and vertebrate groups reveals that at least 1/4 [i.e., 25%] of described living species are strictly soil or litter dwellers, the main part of which is insects and arachnids (Fig. 1)". [Fig. 1]. Note that key Soil microbes and fungi are entirely ignored. Since those authors' data had total described species numbering ~ 1,500,000, their soils would presumably total just 375,000 species (they show with an unrealistically low < 5% Bacteria, viruses, and Fungi within this total, or ~ 18,750 microbial taxa?). Of ~ 360,000 soil animals in Decaëns et al. (2006: fig. 2), only 1% "Annelida" is shown, presumably 3,600 earthworm species, a wide underestimation, approximately half the true count of described species as known at that time.

Because Anthony et al. (2023) overlooked key studies (not least by Benton 2001; Williamson et al. 2017; Bickel and Or 2020; Blakemore 2018b, 2022, and Zhao et al. 2022) also ignoring GBIF (2016), they implied Decaëns et al. (2006) was the only previous work on soil biodiversity. Thus, Anthony et al. (2023) improperly conceded that, rather than 25% as claimed by soil "experts", soils held 59% (stated as: "an average of 58.5% of life inhabits soil" and "considering most life on Earth together, the average proportion of species in soil across all three estimates (lower, central, and upper) is 58.5 ± 14.7%, excluding phage [sic]"), i.e., with a range of 44–74% of global biodiversity. This conclusion is nonetheless unsupported in their table 1 data with Earth's 1.01×10^{11} and Soil's 1.04×10^{10} of species that is ~ 10% (as in Table 3), mainly composed of "Phages", which their figures show total 1×10^{11} species with 9.9×10^{9} (or implausibly just 9.9% of viruses!) in their soils.

"Phages", if excluded from their totals, give Earth and Soil taxa values of non-Phage biota of 1×10^{9} and 0.5×10^{9}, respectively, or with ~ 50% biota in soil. This value, of 500 million soil species, is orders of magnitude lower than values of 10^{11} soil microbes (mainly Bacteria) reported by Zhao et al. (2022), ≤ 10^{23} in Fishman and Lennon (2022), and 2.1×10^{24} taxa (almost all Bacteria) in Blakemore (2022, 2023). These latter studies reasonably exclude viruses which are difficult to accommodate within most definitions of true living entities, as has already been remarked on and adhered to herein.

In summary, of their 1.04×10^{10} soil species, just 500 million would be non-Phages but, of these, seemingly 4.4×10^{8} are "Microbes" composed mainly of 4.3×10^{8} "Bacteria". Subtracted from 5.0×10^{8} non-Phage soil species, implies there are ~ 0.7×10^{8} or 70 million non-Phage, non-Bacterial species anticipated in their mean soil taxa total. Discrepancy in their table is that this figure appears to be higher than Earth's total 0.1×10^{8} or 10 million non-Phage, non-Bacterial species! Such issues indicate a need for self-correction quality controls, possibly acknowledged correction or retraction.

Restating conclusions as herein, Zhao et al. (2022) reasoned that "soil is the most microbiologically abundant (10^{29}) and diverse (10^{11}) environment on the Earth", however, this data was updated in Blakemore (2022, 2023) to an abundance of 2.1×10^{30} cells and 2.1×10^{24} soil taxa both comparing poorly with Anthony et al.'s (2023) central value of just 1.04×10^{10} total soil taxa. Differing by a factor of two and an order of $\times 10^{14}$, or a hundred trillion times, this disparity needs remedy in properly directed Soil research as an urgent priority if a dedicated Soil Ecology Institute emerges.

Resolution of shortcomings continues, as Wiens (2023) pointed out: "Mora and colleagues estimated approximately 10,000 bacterial species (roughly the number of described species). They acknowledged that these projections were likely underestimates. Yet, prokaryotes may be a major driver of Earth's overall species richness. Recent studies have estimated a staggering range of species numbers for bacteria, from low millions to hundreds of millions, to low trillions. All were based on extrapolations from molecular studies." He continued: "Clearly, controversies about global biodiversity cannot be resolved without better resolving bacterial richness". Accepting that this is still a young and growing area of research, I wholeheartedly concur, adding that Soil is foundational.

Context of Soil species extinctions

As biodiversity estimates climb, actual on-the-ground species decline due to rapidly increasing extinctions, up to 100–1,000 × above expected rates from IPBES (2019: fig. SMP3) of: "background rate of 0.1–2 extinctions per million species per year". However, IPBES lacks both "Context and Triage", thereby losing credibility, appearing to give equal status to Land:Sea:Freshwater when in factual reality these respectively provide 99.9:0.1:0.0% to biodiversity (or to humanity's thriving). Extinction is a large, complex topic, but some key references are E.O. Wilson's (1992) prediction from rain forests of 27,000 extinctions per year (74 per day) and IPBES (2019) reportedly having a rate ≤ 200 species lost per day, mainly on land, and mainly for larger, charismatic taxa rather than the 99% of lesser, understudied invertebrates (so true base rate may be 100 × higher at 20,000 per day?).

Albeit soil faunal lists grow exponentially, our soils are being subjected to severe and accelerating destruction from erosion, desertification, chemical poisoning, capping, and rapidly increasing soil acidity – a critical global issue that is mostly ignored (cf. Raza et al. 2021; Zamanian et al. 2021). Soil loss inevitably results in silent species loss, mostly of microbes that are most dominant in soils (as this report indicates), but also of more obvious soil macrobes (e.g., Veresoglou et al. 2015), and specifically of earthworms (Blakemore 2018a) that in this regard are also remarkably understudied.

In the context of soil losses, no wholly marine mammal, shark/ray, fish nor coral is confirmed extinct in the last 250 years (Vermeij 1993), and nary a polychaete marine worm either (https://recentlyextinctspecies.com/databases/annelids). Freshwater losses have occurred, but the biodiversity of this biome is relatively minor and these almost always relate to the surrounding soils. The next section measures the magnitude of macrobe losses, with terrestrial Gastropoda (e.g., slugs or snails) as a useful model for proportionate extrapolation to the specifics of earthworm extinctions.

Earthworm extinction losses

An extinction website (https://web.archive.org/web/20230718152549/https://en.wikipedia.org/wiki/List_of_recently_extinct_invertebrates) catalogues just three Annelida (earthworms), one each from Tasmania, NZ and Japan (each surveyed, evaluated and reported by myself, as per Blakemore 2018a), against 25 better-studied Arachnids (spiders). For terrestrial Mollusca gastropods (snails and slugs) their link (https://web.archive.org/web/20240406171442/https://en.wikipedia.org/wiki/List_of_recently_extinct_molluscs) has a higher total of about 428 extinct taxa. Compared to earthworms, some confounding factors are approximately an equal number of molluscs are marine or aquatic (although no wholly marine snail, nor worm, is confirmed as extinct in the last 250 years since Linnaeus' Volume 1), while only a few earthworms are littoral or aquatic (~ 60 as remarked on earlier), thus land-based taxa approximations may be reasonably commensurate. Published extinction reports are presumably verifiable, whereas true extinction totals may be much higher since only a proportion of existing species are known, fewer evalutated. For earthworms, ~ 7,000 species are described with 30,000–35,000 total taxa expected; this corresponds well with terrestrial gastropods having a higher proportion of ~ 24,000 known species, but estimated total also around 35,000 species (Barker 2001).

Although gastropods as mostly superficial feeders are provisionally excluded from some soil fauna lists, they are like earthworms in two respects: They are wingless, thus are often highly endemic, plus the predicted total numbers of their taxa are on par. This is important because the better known and researched molluscs have published extinctions of ~ 400 species which may reasonably be applied to earthworms if their researchers had the same level of support as do Malacologists. Seemingly, due to such research disparities, ~ 42% of all studied and reported animal extinctions have occurred within this popular gastropod group (Lydeard et al. 2004). Economic arguments that molluscs attack plants are nullified by primal and proven enhancement of vegetation or crops due to earthworm activities.

How supportable is a > 400 earthworm species extinct estimate? Régnier et al. (2015) said: "Using data on terrestrial invertebrates, this study estimates that we may already have lost 7% of the [described living] species on Earth and that the biodiversity crisis is real." And using this datum, Cardoso et al. (2020) stated: "However, it is likely that insect extinctions since the industrial era are around 5 to 10%, i.e. 250,000 to 500,000 species, based on estimates of 7% extinctions for land snails (Régnier et al. 2015). In total at least one million species are facing extinction in the coming decades, half of them being insects (IPBES, 2019)." Thus, for all ~ 7,000 currently described megadriles, a 7% loss would be ~ 490 species extinct. Q.E.D. Similar loss extrapolated to all > 30,000 of likely total megadrile earthworms (in the unlikely event anyone attempts to describe them all), would be > 2,100 extinct earthworms. Fixing the issue of potential losses of such an essential soil fauna, as was highlighted in a meta-analysis of organic farms by Blakemore (2018a), should be a major priority. A subsequent study from birdwatchers in the UK, while ignoring this global meta-analysis study, yet independently and subsequently came to a similar conclusion (Barnes et al. 2023).

As already noted for terrestrial invertebrates, Régnier et al. (2015) estimated critical 7% species loss while Cowie et al. (2022) had 7.5–13% loss, but the status of most taxa remains unclear. Isbell et al. (2022) regarded ~ 30% terrestrial invertebrates either threatened or extinct, which is similar to ~ 30% threatened or extinct rates in IUCN's "Redlist" of earthworms of Japan and NZ/Australia compiled by the author in 2018. Yet most of the earthworm species in these reports were DD: "data deficient".

Microbial extinction losses

Although the IPBES (2019) report barely considered microbes nor "non-charismatic" invertebrates, they did note: "around 9 per cent of the world's estimated 5.9 million terrestrial species – more than 500,000 species – have insufficient habitat for long-term survival, and are committed to extinction, many within decades, unless their habitats are restored." Yet, their rate estimate of ≤ 200 non-microbe species lost per day, is mainly on land and mainly due to often irreversible Land-Use-Change (LUC for agriculture and/or pasture). If the massive new biodiversity estimates herein have similar and proportional rates, this may increase many-fold for the > 99.9% soil microbes in 10^{24} taxa. Proportionately, a 7% rate of invertebrate loss (noted above) would equate to 2 million microbes per day, or ~ 23 taxa lost per second! This critical issue as alluded to in the Abstract was reported here: http://vermecology.wordpress.com/2021/06/20/tol/ and requires further investigation.

An example for microbes is *Streptomyces avermitilis* (ex Burg et al., 1979) initially found only once in a soil sample collected in 1977 near a golf course at Ito, Shizuoka-ken, Japan. From this single species the Nobel-prized pharmaceutical Avermectins were derived. Just as the loss of the soil biome should be of concern for productivity and natural remedies, increasingly it is being recognized that dysbiosis of the human (or other animal) gut or superficial (skin) biome is also related to good health. This human health issue is outside the current study remit but closely relates to healthy soils.

Regarding microbe extirpations on farms, Blakemore (2018a) also noted microbial declines under artificial compared to organic fertilizers at Rothamstead, UK by -50%, likely from the onset of their chemical farming schemes. A similar loss of -50% Bacteria and fungi in chemical compared to organic husbandry was reported from farms in the Philippines (Blakemore 2017: table 5). A meta-analysis by Lori et al. (2017) obtained similar findings and came to similar conclusions on soil loss.

Bacterial (and lesser fungal) richness relates to soil carbon, and its reduction due to land use (poor farming) and climate change could cause dramatic shifts in the microbial diversity (Bastida et al. 2021). This is tenuously supported by a recent paper (Kačergius et al. 2023) at the Lithuanian Institute of Agriculture on organic, sustainable, and intensive-chemical farming systems that found: "20 years ago, when analyzing soil samples from the same agricultural fields, colonies of culturable bacteria and fungi were grown and up to $1–5 \times 10^6$ CFU of organotrophic bacteria were counted, up to $1–2 \times 10^7$ nitrifying bacteria. In 2022, we counted up to $1–4 \times 10^5$ CFU during culturable bacterial colony counts, which is quite different than 20 years ago." Although there are problems with this study (e.g., having to use "culturable" counts for comparison, and a highly acidic "pine old-growth forest" control), this relative decline, if truly

representative, shows a 10–100 times fall in microbes in just 20 years. Losing a few species per year from just one site if applicable to farmlands globally could be significant. Were this trend more widely manifest it would be a major concern for anyone, not just Soil Ecologists, organic farmers, or policy makers. Confirmatory research is clearly required.

Recently, Thaler (2021) cogently noted: "Darwin's "tangled bank" of interdependent organisms may be composed mostly of other microbes. There is the likelihood that as some classes of microbes become extinct, others evolve and diversify. Lack of insight into the dynamics of evolution of microbial biodiversity is arguably the single most profound and consequential unknown with regard to human knowledge of the biosphere". In light of the current work few could now disagree with this.

Summary, conclusions, and future directions for Soil loss remedy

Shortcomings in Decaëns et al. (2006) soil biodiversity summary as (shown in Fig. 1) are mainly that it only reports intensity of study, not estimated totals, and mostly ignores microbes that have since become paramount. Other flaws in its premise are that since around two million species had already been described at that time (MEA 2005: Chapter 4), then their 23% in 360,000 species would likely have been closer to ~ 18%. Conversely, if their > 23% in Plants, Fungi, Bacteria, and viruses that are all mostly found in soil were added to their 23% total, the soil proportion is doubled, being raised to > 46%, albeit only ~ 1% of soil organisms are known (FAO 2020). Hence, would a likely new total for their study if 100 × and of around~ 38 million species not already have a 99% majority in soils?

Moreover, it appears that estimated soil fungi alone supported as many as their claimed global total of 1.5 million species: "The estimated global fungal diversity has changed dramatically from 100, 000 in the 1940s to 1.5 million in the early 2000s, then 2.8 to 3.8 million in the 2017s, and currently 2.5 million species as the best estimate. However, 155,000 species are currently known; thus, many species are still undescribed and waiting for their discoveries" from https://mycokeys.pensoft.net/topical_collection/254/. These known fungi should also be in soil total.

Anthony et al. (2023) claimed their 1.04×10^{10} soil species estimate as "approximately two times greater soil biodiversity than previous estimates" but it was considerably less than Zhao et al. (2022: fig. 3A) already with 10^{11} soil microbial OTUs that was revised upwards to 2.1×10^{24} species by Blakemore (2022). Both prior studies surpass their subsequent 2023 findings indicating a need either for rebuttal or for a thoroughly refined restatement of both local and global soil biotic enumerations.

This review of vital Soil Biota aimed to clarify its true scope while indicating key areas in need of understanding. The vast array of faunal, floral, fungal, and microbial groups and their roles are mostly unexplored and open for investigation, emphasizing an urgent need to establish a Soil Ecology Institute. Until this is fully realized, in the interim, myriad Aquatic or Atmospheric facilities abound, although the naturally depauperate Ocean and void Space will mostly remain intact regardless as they do not erode, neither do they flood nor burn. Ocean issues are solved in Soil. Due to the most pressing problem of topsoil erosion and irreversible extinction losses, a major shift should be realizing the

overwhelming importance and fragility of our precious Soil. The need for proportionate fund reallocation (hence no extra costs involved) to support urgent and directed soils research – under the principles of true Context with systematic Triage – to benefit all Life on Earth.

A supporting homage to our origins and reliance on Microbes in Soils is a diagrammatic Tree-of-Life, as alluded to in the Abstract and Introduction, showing common microbial ancestry origins and prehistoric extinction events – https://web.archive.org/web/20240705043415/http://evogeneao.s3.amazonaws.com/images/tree_of_life/tree-of-life_2000.png. The author notes that this is a phylogenetic tree not reflecting biodiversity.

This Tree-of_Life is particularly poignant with regards to a mostly mysterious soil virome as expounded by Paez-Espino et al. (2016). Williamson et al. (2017) discuss similar issues, coming to a simple conclusion: "Soils remain the most poorly understood ecosystems on Earth. At the same time, viruses represent the largest pool of untapped genetic diversity and unexplored sequence space on the planet. In this regard, the soil virome comprises an unknown quantity within an unexplored territory: a vast new frontier, ripe with opportunities for discovery." The current report is not alone in realizing such magnitudes, nor in urging for more support for Soil Eco-taxonomic restoration in order to boldly explore this vast new frontier lying in wait directly beneath our feet, while it still exists.

While focusing on fundamental soil microbiome, it is important to note this is enhanced by activities of a literal ground-breaking master of its domain as manifest in Darwin's "humble earthworm".

Promoting earthworm activity, as advocated by Blakemore (2018a, 2022, 2023), increases plant growth and provides microhabitats for soil fauna and flora, viz.: "microbes increase during digestion and after gut passage in their fresh castings by up to × 1,000 (Lee 1985: 27, 206) further enriching soils." Presumably the viral abundance is also increased by a multi-fold magnitude due to such actions. Thus, a simple solution to soil degradation is to attempt, in any way and at all times, to preserve and enhance earthworm populations that are more accessible than microbes. As Bill Mollison, co-founder of Permaculture and author of their Designers Manual (Mollison 1988) said: "There is one, and only one solution, and we almost have no time to try it. We must turn all our resources to repairing the natural World, and train all our young people to help. They want to; we need to give them this last chance to create forests, soils, clean waters, clean energies, secure communities, stable regions, and to know how to do it from hands-on experience." (https://web.archive.org/web/20240719045254/https://www.azquotes.com/quote/873849).

That the Soil hosts > 99.9% of global diversity now requires a major "Sea change" in attitudes and funding to recognize its true scope. This should spur formation of at least one dedicated Soil Ecology Institute (for both natural and managed lands) tasked to catalogue, research and reverse mass degradation of our planet's most crucial, yet most neglected ecosystem – that of the Soil Realm.

Acknowledgements

Dave Loneragan and Rose Andrews of Kangaroo Valley and Rowan and Robbie of Berry, NSW kindly provided accommodations during formulation and compilation of this review. Constructive critiques of editors and referees are

appreciated in helping improve the paper and, although some of the enforced edits detract, I take responsibility for any unintended errors and oversight omissions that remain. The authors of Anthony et al. (2023) soil enumeration paper were emailed for critical comment and respectful collaboration in 2023, but they have yet to respond.

Permission for use of previously published images was sought from original authors as cited, or is compliant with Proceedings of the National Academy of Sciences (PNAS) and GBIF allowed copy.

Additional information

Conflict of interest

The author has declared that no competing interests exist.

Ethical statement

No ethical statement was reported.

Funding

No funding was reported.

Author contributions

The author solely contributed to this work.

Author ORCIDs

Robert J. Blakemore https://orcid.org/0000-0001-9797-8328

Data availability

All of the data that support the findings of this study are available in the main text.

References

ABRS (2009) Australian Biological Resource Service Report. https://www.dcceew.gov.au/sites/default/files/env/pages/2ee3f4a1-f130-465b-9c7a-79373680a067/files/nlsaw-2nd-complete.pdf

Adamczyk M, Hagedorn F, Wipf S, Donhauser J, Vittoz P, Rixen C, Frossard A, Theurillat J P, Frey B (2019) The Soil Microbiome of GLORIA Mountain Summits in the Swiss Alps. Frontiers in Microbiology 10: 1080. https://doi.org/10.3389/fmicb.2019.01080

Anthony MA, Bender SF, van der Heijden MGA (2023) Enumerating soil biodiversity. Proceedings of the National Academy of Sciences of the USA 120(33): e2304663120. https://doi.org/10.1073/pnas.2304663120 [Appendix data – www.pnas.org/doi/suppl/10.1073/pnas.2304663120/suppl_file/pnas.2304663120.sapp.pdf]

Ashelford KE, Day MJ, Fry JC (2003) Elevated abundance of bacteriophage infecting bacteria in soil. Applied and Environmental Microbiology 69: 285–289. https://doi.org/10.1128/AEM.69.1.285-289.2003

Bahram M, Hildebrand F, Forslund SK, Anderson JL, Soudzilovskaia NA, Bodegom PM, Bengtsson-Palme J, Anslan S, Coelho LP, Harend H, Huerta-Cepas J, Medema MH, Maltz MR, Mundra S, Olsson PA, Pent M, Põlme S, Sunagawa S, Ryberg M, Tedersoo L, Bork P (2018) Structure and function of the global topsoil microbiome. Nature 560: 233–237. https://doi.org/10.1038/s41586-018-0386-6

Bar-On YM, Milo R (2019) The global mass and average rate of rubisco. Proceedings of the National Academy of Sciences of the USA 116(10): 4738–4743. https://doi.org/10.1073/pnas.1816654116

Bar-On YM, Phillips R, Milo R (2018) The biomass distribution on Earth. Proceedings of the National Academy of Sciences of the USA 115: 6506–6511. https://doi.org/10.1073/pnas.1711842115

Barker GM (2001) Gastropods on land: Phylogeny, diversity, and adaptive morphology. In: Barker GM (Ed.) The Biology of Terrestrial Molluscs, CABI Publishing, Wallingford, New Zealand, 146 pp. https://doi.org/10.1079/9780851993188.0001

Barnes AE, Robinson RA, Pearce-Higgins JW (2023) Collation of a century of soil invertebrate abundance data suggests long-term declines in earthworms but not tipulids. Public Library of Science ONE 18(4): e0282069. https://doi.org/10.1371/journal.pone.0282069

Bastida F, Eldridge DJ, García C, Kenny Png G, Bardgett RD, Delgado-Baquerizo M. (2021) Soil microbial diversity-biomass relationships are driven by soil carbon content across global biomes. International Society for Microbial Ecology Journal 15: 2081–2091. https://doi.org/10.1038/s41396-021-00906-0

Beaver RC, Neufeld JD (2024) Microbial ecology of the deep terrestrial subsurface. International Society for Microbial Ecology Journal 18(1): wrae091. https://doi.org/10.1093/ismejo/wrae091

Benham WB (1890) An attempt to classify Earthworms. Quarterly Journal of Microscopical Science 31: 201–315. https://doi.org/10.1242/jcs.s2-31.122.201

Benton MJ (2001) Biodiversity on land and in the sea. Geological Journal 36(3–4): 211–230. https://doi.org/10.1002/gj.877

Bergh O, Børsheim KY, Bratbak G, Heldal M (1989) High abundance of viruses found in aquatic environments. Nature 340: 467–468. https://doi.org/10.1038/340467a0

Bickel S, Or D (2020) Soil bacterial diversity mediated by microscale aqueous-phase processes across biomes. Nature Communications 11: 116. https://doi.org/10.1038/s41467-019-13966-w

Blakemore RJ (2000) Tasmanian Earthworms. CD-ROM Monograph with Review of World Families. VermEcology, Kippax, ACT 2615, 800 pp. https://archive.org/details/tasmanianearthw00blak

Blakemore RJ (2008) A Series of Searchable Texts on Earthworm Biodiversity, Ecology and Systematics from Various Regions of the World. Yokohama National University, Tokiwadai, Japan. https://web.archive.org/web/20230501052317 [http://www.annelida.net/earthworm/]

Blakemore RJ (2011) Further records of non-cryptic New Zealand earthworms. ZooKeys 160: 23–46. https://doi.org/10.3897/zookeys.160.2354

Blakemore RJ (2012) Call for a Census of Soil Invertebrates (CoSI). Zoology in the Middle East 58: suppl. 4: 171–176. https://doi.org/10.1080/09397140.2012.10648999

Blakemore RJ (2013) The major megadrile families of the world reviewed again on their taxonomic types (Annelida: Oligochaeta: Megadrilacea). Opuscula Zoologica, Budapest 44(2): 107–127. https://opuscula.elte.hu/PDF/Tomus44_2/Blakemore_Families.pdf

Blakemore RJ (2016) Cosmopolitan Earthworms – an Eco-taxonomic guide to the peregrine species of the world. 5th edn. VermEcology, Yokohama, 800 pp.

Blakemore RJ (2017) Veni, Vidi, Vermi... II. Earthworms in organic fields restore SOM & H_2O and fix CO_2. VermEcology Occasional Papers (Veop) 2(2): 1–26. https://doi.org/10.13140/RG.2.2.11022.97608

Blakemore RJ (2018a) Critical Decline of Earthworms from Organic Origins under Intensive, Humic SOM-Depleting Agriculture. Soil Systems 2(2): 33. https://doi.org/10.3390/soilsystems2020033

Blakemore RJ (2018b) Non-Flat Earth Recalibrated for Terrain and Topsoil. Soil Systems 2(4): 64. https://doi.org/10.3390/soilsystems2040064

Blakemore RJ (2019) Humic Carbon to Fix Extinction, Climate and Health. VermEcology Occasional Papers (Veop) 3: 1–8. https://doi.org/10.20944/preprints201904.0109.v1

Blakemore RJ (2022) New Global Species Biodiversity: Soil soars, Ocean flounders. VermEcology Occasional Papers (Veop) 5: 1–9. https://doi.org/10.32942/OSF.IO/DGPTW

Blakemore RJ (2023) Biotic SOC Stock: What We Had & What We Lost. VermEcology Occasional Papers (Veop) 6: 1–59. https://doi.org/10.5281/zenodo.7825446

Blakemore RJ (2024). Biomass Refined: 99% of Organic Carbon in Soils. Biomass 4(4): 1257–1300. https://doi.org/10.3390/biomass4040070

Cao M-M, Liu S-Y, Bi L, Chen S-J, Wu H-Y, Ge Y, Han B, Zhang L-M, He J-Z, Han L-L (2022) Distribution Characteristics of Soil Viruses Under Different Precipitation Gradients on the Qinghai-Tibet Plateau. Frontiers in Microbiology 13: 848305. https://doi.org/10.3389/fmicb.2022.848305

Cardoso P, Barton PS, Birkhofer L, Chichorro F, Deacon C, Fartmann T, Fukushima CS, Gaigher R, Habel JC, Hallmann CA, Hill MJ, Hochkirch A, Kwak ML, Mammola S, Noriega JA, Orfinger AB, Pedraza F, Pryke JS, Roque FO, Simaika JSP, Stork NE, Suhling F, Vorster C, Samways MJ (2020) Scientists' warning to humanity on insect extinctions. Biological Conservation 242: 108426. https://doi.org/10.1016/j.biocon.2020.108426

Cobián-Güemes AG, Youle M, Cantú VA, Felts B, Nulton J, Rohwer F (2016) Viruses as Winners in the Game of Life. Annual Review of Virology 3(1): 197–214. https://doi.org/10.1146/annurev-virology-100114-054952

CoML (2010) Census of Marine Life. http://www.coml.org/

Coupland GT, McDonald JI (2008) Extraordinarily high earthworm abundance in deposits of marine macrodetritus along two semi-arid beaches. Marine Ecology Progress Series 361: 181–189. https://doi.org/10.3354/meps07351

Cowie RH, Bouchet P, Fontaine B (2022) The Sixth Mass Extinction: fact, fiction or speculation?. Biological Review 97: 640–663. https://doi.org/10.1111/brv.12816

Cragg JB (1963) Some Aspects of the Ecology of Moorland Animals. Journal of Ecology 49(2): 477–506. https://doi.org/10.2307/2257219

Decaëns T, Jiménez CC, Gioia C, Measey G, Lavelle P (2006) The values of soil animals for conservation biology. European Journal of Soil Biology 42: S23–S38. https://doi.org/10.1016/j.ejsobi.2006.07.001

Damer B (2016) A Field Trip to the Archaean in Search of Darwin's Warm Little Pond. Life 6(2): 21. https://doi.org/10.3390/life6020021

Emerson JB (2019) Soil Viruses: A New Hope. mSystems 4. https://doi.org/10.1128/msystems.00120-19

FAO (2020) Food and Agriculture Organization of the UN: State of knowledge of soil biodiversity - Status, challenges and potentialities. Report, FAO, Rome. https://doi.org/10.4060/cb1928en

Fierer N, Breitbart M, Nulton J, Salamon P, Lozupone C, Jones R, Robeson M, Edwards RA, Felts B, Rayhawk S, Knight R, Rohwer F, Jackson RB (2007) Metagenomic and Small-Subunit rRNA Analyses Reveal the Genetic Diversity of Bacteria, Archaea, Fungi, and Viruses in Soil. Applied Environmental Microbiology 73: 21. https://doi.org/10.1128/AEM.00358-07

Fierer N, Strickland MS, Liptzin D, Bradford MA, Cleveland CC (2009) Global patterns in belowground communities. Ecological Letters 12(11): 1238–1249. https://doi.org/10.1111/j.1461-0248.2009.01360.x

Fishman FJ, Lennon JT (2022) Macroevolutionary constraints on global microbial diversity. Ecological Evolution 13(8): e10403. https://doi.org/10.1002/ece3.10403

Flemming HC, Wuertz S (2019) Bacteria and archaea on Earth and their abundance in biofilms. National Review of Microbiology 17: 247–260. https://doi.org/10.1038/s41579-019-0158-9

Fulthorpe RR, Roesch LF, Riva MA, Triplett EW (2008) Distantly sampled soils carry few species in common. Multidisciplinary Journal of Microbial Ecology 2(9): 901–910. https://doi.org/10.1038/ismej.2008.55

Gans J, Woilinsky M, Dunbar J (2005) Computational improvements reveal great bacterial diversity and high metal toxicity in soil. Science 309: 1387–1390. https://doi.org/10.1126/science.1112665

García-Roselló E, González-Dacosta J, Lobo JM (2023) The biased distribution of existing information on biodiversity hinders its use in conservation, and we need an integrative approach to act urgently. Biological Conservation 283: 110118. https://doi.org/10.1016/j.biocon.2023.110118

GBIF (2016) Global Biodiversity Information Facility: Global Soil Biodiversity Atlas. https://esdac.jrc.ec.europa.eu/public_path/shared_folder/Atlases/JRC_global_soilbio_atlas_low_res-2019-06-13.pdf

Gijsman AJ (1991) Deforestation and Land Use: Changes in Physical and Biological Soil Properties in Relation to Sustainability. https://inclusive-finance.tropenbos.org/file.php/1454/tropdoc1.pdf

Glasby CJ, Read GB, Lee KE, Blakemore RJ, Fraser PM, Pinder AM, Erséus C, Moser WE, Burreson EW, Govedich FR, Davies RW, Dawson EW (2009) Chapter 17. Phylum Annelida: Bristle-worms, Earthworms, Leeches. In: The New Zealand Inventory of Biodiversity. Volume 1. Kingdom Animalia: Radiata, Lophotrochozoa, and Deuterostomia. Canterbury University Press, Christchurch, 312–358.

Gobat JM, Aragno M, Matthey W (2004) The living soil: fundamentals of soil science and soil biology. Science Publishers, Enfield, 568 pp.

Graham EB, Camargo AP, Wu R, Neches RY, Nolan M, Paez-Espino D, Kyrpides NC, Jansson JK, McDermott JE, Hofmockel KS (2023) Soil Virosphere Consortium: Global Biogeography of the Soil Virosphere. bioRxiv. 2023.11.02.565391. https://doi.org/10.1101/2023.11.02.565391

Graham EB, Camargo AP, Wu R, Neches RY, Nolan M, Paez-Espino D, Kyrpides NC, Jansson JK, McDermott JE, Hofmockel KS (2024) A global atlas of soil viruses reveals unexplored biodiversity and potential biogeochemical impacts. Nature Microbiology 9: 1873–1883. https://doi.org/10.1038/s41564-024-01686-x

Grosberg RK, Vermeij GJ, Wainwright PC (2012) Biodiversity in water and on land. Current Biology 22: R900-R903. https://doi.org/10.1016/j.cub.2012.09.050

Gulik van der PTS, Hoff WD, Speijer D (2024) The contours of evolution: In defence of Darwin's tree of life paradigm. Bioessays 46(5): e2400012. https://doi.org/10.1002/bies.202400012

Hendrix RW, Smith MC, Burns RN, Ford ME, Hatfull GF (1999) Evolutionary relationships among diverse bacteriophages and prophages: All the World's a phage. Proceedings of the National Academy of Sciences of the USA 96: 2192–2197. https://doi.org/10.1073/pnas.96.5.2192

Hoshino T, Doi H, Uramoto G-I, Wörmer L, Adhikari RR, Xiao N, Morono Y, D'Hondt S, Hinrichs K-U, Inagaki F (2020) Global diversity of microbial communities in marine sediment. Proceedings of the National Academy of Sciences of the USA 117(44): 27587–27597. https://doi.org/10.1073/pnas.1919139117

IPBES (2019) Global assessment report of the Intergovernmental Science-Policy Platform on Biodiversity and Ecosystem Services. IPBES Secretariat: 1753. https://doi.org/10.5281/zenodo.3831673

Isbell F, Balvanera P, Mori AS, He J-S, Bullock JM, Regmi GR, Seabloom EW, Ferrier S, Sala OE, Guerrero-Ramírez NR, Tavella J, Larkin DJ, Schmid B, Outhwaite CL, Pramual P, Borer ET, Loreau M, Omotoriogun TC, Obura DO, Anderson M, Portales-Reyes C, Kirkman K, Vergara PM, Clark AT, Komatsu KJ, Petchey OL, Weiskopf SR, Williams LJ, Collins SL, Eisenhauer N, Trisos CH, Renard D, Wright AJ, Tripathi P, Cowles J, Byrnes JEK, Reich PB, Purvis A, Sharip Z, O'Connor MI, Kazanski CE, Haddad NM, Soto EH, Dee LE, Díaz S, Zirbel CR, Avolio ML, Wang S, Ma Z, Liang J, Farah HC, Johnson JA, Miller BW, Hautier Y, Smith MD, Knops JMH, Myers BJE, Harmáčková ZV, Cortés J, Harfoot MBJ, Gonzalez A, Newbold T, Oehri J, Mazón M, Dobbs C, Palmer MS (2022) Expert perspectives on global biodiversity loss and its drivers and impacts on people. Frontiers of Ecological Environment 21(2): 94–103. https://doi.org/10.1002/fee.2536

James MT, Farrisi ST, Shah S, Shah V (2022) Identification of Major Organisms Involved in Nutritional Ecosystem in the Acidic Soil From Pennsylvania, USA. Frontiers of Environmental Science 10: 766302. https://doi.org/10.3389/fenvs.2022.766302

Jansson JK (2023) Soil viruses: Understudied agents of soil ecology. Environental Microbiology 25(1): 143–146. https://doi.org/10.1111/1462-2920.16258

Jia X, Dini-Andreote F, Salles JF (2022) Unravelling the interplay of ecological processes structuring the bacterial rare biosphere. Multidisciplinary Journal of Microbial Ecology 2: 96. https://doi.org/10.1038/s43705-022-00177-6

Kačergius A, Sivojienė D, Gudiukaitė R, Bakšienė E, Masevičienė A, Žičkienė L (2023) Comparison of the Structure of Soil Microbial Communities of Different Ecosystems Using the Microbiome Sequencing Approach. Soil Systems 7: 70. https://doi.org/10.3390/soilsystems7030070

Kallmeyer J, Pockalny R, Adhikari RR, Smith DC, D'Hondt S (2012) Global distribution of microbial abundance and biomass in subseafloor sediment. Proceedings of the National Academy of Sciences of the USA 109: 16213–16216. https://doi.org/10.1073/pnas.1203849109

Kannoly S, Oken G, Shadan J, Musheyev D, Singh K, Singh A, Dennehy JJ (2022) Single-Cell Approach Reveals Intercellular Heterogeneity in Phage-Producing Capacities. Microbiological Spectroscopy 11(1): e0266321. https://doi.org/10.1128/spectrum.02663-21

Koonin EV, Krupovic M, Dolja VV (2023) The global virome: How much diversity and how many independent origins? Environmental Microbiology 25(1): 40–44. https://doi.org/10.1111/1462-2920.16207

Kuzyakov Y, Mason-Jones K (2018) Viruses in soil: Nano-scale undead drivers of microbial life, biogeochemical turnover and ecosystem functions. Soil Biology and Biochemistry 127: 305–317. https://doi.org/10.1016/j.soilbio.2018.09.032

Labouyrie M, Ballabio C, Romero F, Panagos P, Jones A, Schmid MW, Mikryukov V, Dulya O, Tedersoo L, Bahram M, Lugato E, van der Heijden MGA, Orgiazzi A (2023) Patterns in soil microbial diversity across Europe. Nature Communication 14: 3311. https://doi.org/10.1038/s41467-023-37937-4

Larsen BB, Miller EC, Rhodes MK, Wiens JJ (2017) Inordinate Fondness Multiplied and Redistributed: the Number of Species on Earth and the New Pie of Life. The Quarterly Review of Biology 92: 3. https://doi.org/10.1086/693564

Lavelle P, Spain AV (2001) Soil Ecology. Kluwer Academic Publishers, New York, 654 pp. https://doi.org/10.1007/0-306-48162-6

Lee KE (1959) The Earthworm Fauna of New Zealand. NZ DSIR, Wellington, 600 pp.

Lee KE (1985) Earthworms their Ecology and Relationships with Soils and Land Use. Academic Press, Sydney, 585 pp. https://archive.org/details/earthwormstheire0000leek

Lennon JT, Locey KJ (2020) More support for Earth's massive microbiome. Biology Direct 15: 5. https://doi.org/10.1186/s13062-020-00261-8

Locey KJ, Lennon JT (2016) Scaling laws predict global microbial diversity. Proceedings of the National Academy of Sciences of the USA 113(21): 5970–5975. https://doi.org/10.1073/pnas.1521291113

Lori M, Symnaczik S, Mäder P, De Deyn G, Gattinger A (2017) Organic farming enhances soil microbial abundance and activity—A meta-analysis and meta-regression. Public Library of Science ONE 12(7): e0180442. https://doi.org/10.1371/journal.pone.0180442

Louca S (2022) The rates of global bacterial and archaeal dispersal. Multidisciplinary Journal of Microbial Ecology 16: 159–167. https://doi.org/10.1038/s41396-021-01069-8

Louca S, Shih PM, Pennell MW, Fischer WW, Parfrey LW, Doebeli M (2018) Bacterial diversification through geological time. Nature Ecology & Evolution 2: 1458–1467. https://doi.org/10.1038/s41559-018-0625-0

Louca S, Mazel F, Doebeli M, Parfrey LW (2019) A census-based estimate of Earth's bacterial and archaeal diversity. Public Library of Science Biology 17: e3000106. https://doi.org/10.1371/journal.pbio.3000106

Lydeard C, Cowie RH, Ponder WF, Bogan AE, Bouchet P, Clark SA, Cummings KS, Frest TJ, Gargominy O, Herbert DG, Hershler R, Perez KE, Roth B, Seddon M, Strong EE, Thompson FG (2004) The global decline of nonmarine mollusks. BioScience 54(4): 321–330. https://doi.org/10.1641/0006-3568(2004)054[0321:TGDONM]2.0.CO;2

Magnabosco C, Lin LH, Dong H, Bomberg M, Ghiorse W, Stan-Lotter H, Pedersen K, Kieft TL, van Heerden E, Onstott TC (2018) The biomass and biodiversity of the continental subsurface. Nature Geoscience 11: 707–717. https://doi.org/10.1038/s41561-018-0221-6

Martin P, Martinez-Ansemil E, Pinder A, Timm T, Wetzel MJ (2008) Global diversity of oligochaetous clitellates ("Oligochaeta"; Clitellata) in freshwater. Hydrobiologia 595: 117–127. https://doi.org/10.1007/s10750-007-9009-1

May RM (1994) Biological Diversity: Differences between Land and Sea. Philosophical Transactions of the Royal Society B: Biological Sciences 343(1303): 105–111. https://doi.org/10.1098/rstb.1994.0014

McMahon S, Parnell J (2013) Weighing the deep continental biosphere. FEMS Microbiology Ecology 87(1): 113–120. https://doi.org/10.1111/1574-6941.12196

McNear DH (2013) The Rhizosphere - Roots, Soil and Everything In Between. Nature Education Knowledge 4(3): 1. https://www.nature.com/scitable/knowledge/library/the-rhizosphere-roots-soil-and-67500617/

MEA (2005) Millennium Ecosystem Assessment of Ecosystems and Human Well-being: Biodiversity Synthesis. World Resources Institute, Washington, DC. https://www.millenniumassessment.org/documents/document.273.aspx.pdf

Miller H, Mulhall J, Pfau LA, Palm R, Denkenberger DC (2024) Can Foraging for Earthworms Significantly Reduce Global Famine in a Catastrophe? Biomass 4(3): 765–783. https://doi.org/10.3390/biomass4030043

Mollison, W (1988) Permaculture- A Designer's Manual. Tagari Press, Australia, 576 pp.
Mora C, Tittensor DP, Adl S, Simpson AGB, Worm B (2011) How many species are there on Earth and in the Ocean? Public Library of Science Biology 9: e1001127. https://doi.org/10.1371/journal.pbio.1001127
Muscatt G, Cook R, Millard A, Bending GD, Jameson E (2023) Viral metagenomics reveals diverse virus-host interactions throughout the soil depth profile. mBio 14: e02246-23. https://doi.org/10.1128/mbio.02246-23
Mushegian AR (2020) Are There 10^{31} Virus Particles on Earth, or More, or Fewer? Journal of Microbiology 202(9): 20. https://doi.org/10.1128/JB.00052-20
Paez-Espino D, Eloe-Fadrosh EA, Pavlopoulos GA, Thomas AD, Huntemann M, Mikhailova N, Rubin E, Ivanova NN, Kyrpides NC (2016) Uncovering Earth's virome. Nature 536(7617): 425–430. https://doi.org/10.1038/nature19094
Parkes RJ, Cragg V, Roussel E, Webster G, Weightman A, Sass H (2014) A review of prokaryotic populations and processes in sub-seafloor sediments, including biosphere:-geosphere interactions. Marine Geology 352: 409–425. https://doi.org/10.1016/j.margeo.2014.02.009
Plassart P, Prévost-Bouré NC, Uroz S, Dequiedt S, Stone D, Creamer R, Griffiths RI, Bailey MJ, Ranjard L, Lemanceau P (2019) Soil parameters, land use, and geographical distance drive soil bacterial communities along a European transect. Science Reports 9: 605. https://doi.org/10.1038/s41598-018-36867-2
Pratama AA, Terpstra J, de Oliveria ALM, Salles JF (2020) The role of rhizosphere bacteriophages in plant health. Trends in Microbiology 28(9): 709–718. https://doi.org/10.1016/j.tim.2020.04.005
Raynaud X, Nunan N (2014) Spatial ecology of bacteria at the microscale in soil. Public Library of Science ONE 9: e87217. https://doi.org/10.1371/journal.pone.0087217
Raza S, Irshad A, Margenot A, Zamanian K, Li N, Ullah S, Mehmood K, Khan MA, Siddique N, Zhou J, Mooney SJ, Kurganova I, Zhao X, Kuzyakov Y (2021) Inorganic carbon is overlooked in global soil carbon research: A bibliometric analysis. Geoderma 443: 116831. https://doi.org/10.1016/j.geoderma.2024.116831
Régnier C, Achaz G, Lambert A, Cowie RH, Bouchet P, Fontaine B (2015) Mass extinction in poorly known taxa. Proceedings of the National Academy of Sciences of the USA 112(25): 7761–7766. https://doi.org/10.1073/pnas.1502350112
Roesch LF, Fulthorpe RR, Riva A, Casella G, Hadwin AK, Kent AD, Daroub SH, Camargo FA, Farmerie WG, Triplett EW (2007) Pyrosequencing enumerates and contrasts soil microbial diversity. ISME J. 1: 283–290. https://doi.org/10.1038/ismej.2007.53
Ryals R, Zhu B, Min K, Cooper A, Goldsmith S, Pett-Ridge J, Torn M, Berhe AA (2023) The deep soil organic carbon response to global change. Annual Review of Ecology, Evolution, and Systematics 54: 375–401. https://doi.org/10.1146/annurev-ecolsys-102320-085332
Dubeux JCB, de Souza TC, Mackowiak C, Wright D, George S, Pires T, Santos E (2021) Organic carbon is mostly stored in deep soil and only affected by land use in its superficial layers. Agrosystems, Geosciences and Environment 4(1): e20135. https://doi.org/10.1002/agg2.20135
Román-Palacios C, Moraga-López D, Wiens JJ (2022) The origins of global biodiversity on land, sea and freshwater. Ecology letters 25(6): 1376–1386. https://doi.org/10.1111/ele.13999
Roux S, Emerson JB (2022) Diversity in the soil virosphere: to infinity and beyond? Trends in Microbiology 30(11): 1025–1035. https://doi.org/10.1016/j.tim.2022.05.003
Sagan (Margulis) L (1967) On the Origin of Mitosing Cells. Journal of Theoretical Biology 14: 225–274. https://doi.org/10.1016/0022-5193(67)90079-3

Schloss PD, Handelsman J (2006) Toward a Census of Bacteria in Soil. Public Library of Science Computer Biology 2(7): e92. https://doi.org/10.1371/journal.pcbi.0020092

Shangguan W, Hengl T, Mendes de Jesus J, Yuan H, Dai Y (2017) Mapping the global depth to bedrock for land surface modeling. Journal of Advance Model Earth Systems 9: 65–88. https://doi.org/10.1002/2016MS000686

Soares A, Edwards A, An D, Bagnoud A, Bradley J, Barnhart E, Bomberg M, Budwill K, Caffrey SM, Fields M, Gralnick J, Kadnikov V, Momper L, Osburn M, Mu A, Moreau JW, Moser D, Purkamo L, Rassner SM, Sheik CS, Sherwood Lollar B, Toner BM, Voordouw G, Wouters K, Mitchell AC (2023) A global perspective on bacterial diversity in the terrestrial deep subsurface. Microbiology (Reading) 169(1): 001172. https://doi.org/10.1099/mic.0.001172

Springett JA (1967) An ecological study of moorland Enchytraeidae. Durham PhD theses, Durham University, UK. Available at Durham E-Theses. http://etheses.dur.ac.uk/8869/

Sun Q, Li H-Y, Li K, Zhang X-Q, Shi Y, Wu Y, Li X, Li Z, Zhang J, Wang L-X, Liang C-Z (2023) Climatic factors regulate the assembly processes of abundant and rare microbial communities in desert soil. Journal of Plant Ecology16(6): rtad032. https://doi.org/10.1093/jpe/rtad032

Suttle CA (2005) Viruses in the sea. Nature 437: 356–361. https://doi.org/10.1038/nature04160

Thaler DS (2021) Is Global Microbial Biodiversity Increasing, Decreasing, or Staying the Same? Front. Ecol. Evol. 19 Sec. Phylogenetics, Phylogenomics, and Systematics 9: 2011. https://doi.org/10.3389/fevo.2021.565649

Torsvik V, Goksøyr J, Daae FL (1990) High diversity in DNA of soil bacteria. Applied Environmental Microbiology 56(3): 782–787. https://doi.org/10.1128/aem.56.3.782-787.1990

Veresoglou S, Halley J, Rillig M (2015) Extinction risk of soil biota. Nature Communication 6: 8862. https://doi.org/10.1038/ncomms9862

Vermeij GJ (1993) Biogeography of Recently Extinct Marine Species: Implications for Conservation. Conservation Biology 7(2): 391–397. https://doi.org/10.1046/j.1523-1739.1993.07020391.x

White RA III, Rosnow J, Piehowski PD, Brislawn CJ, Moran JJ (2021) In Situ Non-Destructive Temporal Measurements of the Rhizosphere Microbiome 'Hot-Spots' Using Metaproteomics. Agronomy 11(11): 2248. https://doi.org/10.3390/agronomy11112248

Whitman WB, Coleman DC, Wiebe WJ (1998) Prokaryotes: The Unseen Majority. Proceedings of the National Academy of Sciences of the USA 95: 6578-6583. https://doi.org/10.1073/pnas.95.12.6578

Wiens JJ (2023) How many species are there on Earth? Progress and problems. Public Library of Science Biology 21(11): e3002388. https://doi.org/10.1371/journal.pbio.3002388

Williamson KE, Radosevich M, Wommack KE (2005) Abundance and diversity of viruses in six Delaware soils. Applied Environmental Microbiology 71: 3119–3125. https://doi.org/10.1128/AEM.71.6.3119-3125.2005

Williamson KE, Fuhrmann JJ, Wommack KE, Radosevich M (2017) Viruses in soil ecosystems: an unknown quantity within an unexplored territory. Annual Review of Virology 4: 201–219. https://doi.org/10.1146/annurev-virology-101416-041639

Wilson EO (1992) The diversity of life. Harvard University Press, Cambridge, 424 pp.

Zamanian K, Zhou J, Kuzyakov Y (2021) Soil carbonates: the unaccounted, irrecoverable carbon source. Geoderma 384: 114817. https://doi.org/10.1016/j.geoderma.2020.114817

Zhao J, Jin L, Wu D, Xie JW, Li J, Fu XW, Cong ZY, Fu PQ, Zhang Y, Luo XS, Feng XB, Zhang G, Tiedje JM, Li X (2022) Global airborne bacterial community-interactions with Earth's microbiomes and anthropogenic activities. Proceedings of the National Academy of Sciences of the USA 119(42): e2204465119. https://doi.org/10.1073/pnas.2204465119

Appendix 1

Biomass of earthworms and microbes, as major soil organisms in the various biomes, are compared to minor microdriles (viz. Enchytraeid potworms that were given inordinate importance by Anthony et al. (2023)). These data are presented in Table A1:

Earthworm biomass at 3.8 Gt C and Microbes at 209.6 Gt C are slightly higher than 2.3–3.6 Gt C and 200 Gt C, respectively, as estimated by Blakemore (2023: table 2) confirming importance of both groups to Soil Ecology.

This new earthworm value of 3.8 Gt C may be doubled to ~ 7.6 Gt for dry biomass which is substantially higher than the 0.9 Gt (and thus 0.45 Gt C?) as lately reported in Miller et al. (2024). Their paper overlooked 4.5 Gt dry and 2.25 Gt C data in Blakemore (2017 -https://vermecology.wordpress.com/2017/02/12/nature-article-to-commemorate-charles-darwins-birthday-on-12th-feb/) independently extrapolated from the extensive works compiled by the leading earthworm ecologist and taxonomist, my PhD assessor and mentor, Dr Ken Lee (1985).

Table A1. Biome Carbon biomass of Enchytraeids, Earthworms and Microbes selected from Fierer et al. (2009: table 1– https://onlinelibrary.wiley.com/doi/epdf/10.1111/j.1461-0248.2009.01360.x) in g/m^2 C, with Biome areas from Whitman et al. (1998: table 2 – http://rpdata.caltech.edu/courses/aph161/Handouts/whitman98.pdf) in Gigahectares (Gha).

Biome	Enchytraeid (g/m^2 C)	Earthworm (g/m^2 C)	Microbe (g/m^2 C)	Biome (Gha)	Total Enchy. (Gt C)	Total E/worm (Gt C)	Total Microbe (Gt C)
Boreal forest	0.32	0.3	57	1.2	0.04	0.03	6.84
Desert	0	0	43	1.8	0.00	0.00	7.74
Temp. conif.	0.80	1.2	175	0.5	0.04	0.06	8.75
Temp. decid.	0.64	2.0	116	0.7	0.04	0.14	8.12
Temp. grass	0.31	3.8	131	0.9	0.03	0.34	11.79
Tropical forest*	0.10	4.9	203	2.5	0.03	1.23	50.75
Tundra	0.99	1.4	136	0.8	0.08	0.11	10.88
TOTAL				**8.4**	**0.26**	**1.9**	**104.8**
Terrain × 2**				**16.8**	**0.52**	**3.8**	**209.6**

*Tropical forest Enchytraeid data infilled from (https://edepot.wur.nl/202864 1991: table 2.2 with 0.02–0.20 g dry wt. thus < 0.1 g C similar to FW (fresh weight) data extracted from https://soil-organisms.org/index.php/SO/article/view/155 2021:tabs 4, 5). Note that earthworms are usually the most important elements of Tropical forests biota, contrary to some misguided reports, as clearly explained by practical Soil Ecologist fieldworkers, e.g., Gijsman (1991). Enchytraeids have ~ 700 known species compared to ~ 7,000 described earthworms, or × 10, and biomass of earthworms is × 7 too. **Terrain doubling from Blakemore (2018b) allows for landscape's coarse terrain progressively overlain by finer layers of microtopography and soil rugosity, less so in bogs.

Appendix 2

Virus-Like Particle (VLP) counts (Global and in Soil alone)

All viral estimates in Anthony et al. (2023: table 1) had speculative uncertainty marked "?". Indeed, Williamson et al. (2017) found soil viral diversity severely underestimated and under-sampled, albeit their measures of viral richness were much higher for soils than for aquatic ecosystems. Many soil virus reports show ≤ 10^{10} –10^{11} virions per gram of soil and a global best-estimate tally was of > 10^{31} virus-like-particles (VLP) that are infecting microbial populations at any one time (Mushegian 2020 originally cited from Hendrix et al. 1999).

If 10^{10} –10^{11} virions per g occur, this is 10^{16} –10^{17} per tonne of soil. Further, if there exist 2.1 × 10^{14} t topsoil to 1 m depth (from Blakemore 2022), then a range is 2.1 × 10^{30}–10^{31} virions (with a median value ~ 1.5 × 10^{31}).

This total is approximately the same as that calculated by other authors, e.g., Mushegian (2020) or Cobián-Güemes et al. (2016) of between 10^{31} and 4.8 × 10^{31} viral phages. Comparatively, Suttle (2005) extrapolated counts of Marine viruses from local samples to the entire World, arriving at an estimate of 4 × 10^{30} virus particles in well-mixed oceanic waters (i.e., ~ 10%). Mushegian (2020: table 1) arrived at a similar estimate to this at 2 × 10^{30} virions in the Ocean, i.e., a range of just 2–4% of Ocean virions in a global total of ~ 10^{31} virions.

Previous range of Ocean virus proportions is then just 2–10% of global totals with much of the remainder (90–98%) in Soil. True Soil counts are variable, as shown below, further reducing the proportional Ocean values.

While initial estimates of virus abundance in Soil ranged from 10^{7} to 10^{9} virus like particles (VLP) per gram of dry soil (Williamson et al. 2005, 2017) with a mean ~ 10^{8}, Pratama et al. (2020) found a higher mean of 10^{9} VLP per g from a range of catalogued soils and Graham et al. (2023) had 10^{7} to 10^{10} viruses per g of soil. This agrees with Jansson (2023) for different soil types at 10^{8}–10^{10} VLP per g dry soil (mean also 10^{9}), but she noted the true number may be higher than that obtained by microscopy because many soil viruses are intracellular and not able to be imaged separately. Kannoly et al. (2022) shows ≤ 1,430 plaque-forming-units (PFU) per lysogenic bacterial cell-burst (a so-called "burst size" of viral particles). Thus, an exponential order or two is easily added, possibly to allow reasonable estimates of around 10^{10}–10^{11} VLP per g of dry soil?

Especially relevant, a study by Cobián-Güemes et al. (2016) estimated 4.8 × 10^{31} VLPs on Earth but comprising an unrealistic minimum of 257,698 different viral genotypes (sic). They quoted reports with only 3.9 × 10^{6} ≤ 2 × 10^{9} total varieties (or one variety per 10^{22}–10^{25} VLP), which seems a wide underestimation compared to other studies. Their VtB ratios (in their table 1) were skewed by a low "Human associated" ratio of just 0.1 and a high "Other host-associated" of 25, to give a median ratio for all their biomes of 12. Their Soil VtB was 19.1. Here revised microbial counts in Blakemore (2022, 2023) give a global total of > 5.1 × 10^{31} VLPs with ~ 4.1 × 10^{31} (~ 80%) virions in soils (to full depth?) and a Soil alone VtB near ~ 20:1, as in Table A2:

Whitman et al.'s (1998: table 5) 3.6 and 2.5 × 10^{30} cells in Oceanic or Terrestrial sub-surfaces were downgraded by Kallmeyer et al. (2012), Parkes et al. (2014), Magnabosco et al. (2018) and Hoshino et al. (2020) to just 3–5 and 2–6 × 10^{29}, or ~ 4 × 10^{29} each, and with sub-surface biomass of 4 and 23–31 Gt C, respectively. Bar-On et al. (2018: supp: 62) for Marine, Sub-Ocean, and Sub-Soil,

Table A2. Virus-Like Particles (VLP) from Microbes/Bacteria (VtB) ratios modified after Cobián-Güemes et al. (2016: table 1) and Microbes abundances from (Blakemore 2022, 2023 cf. those given in Table 2 of main text above).

BIOME	Microbes/Biome × 10^{28}	VtB ratio	VLP/Biome × 10^{31}	Microbe %	Virus %
Marine	12	12.76	0.15	4.0	3.0
Freshwater	0.02	14	0.00	0.0	0.0
Sub-Ocean	40	11	0.44	13.2	8.6
Sub-Terrestrial	40	11	0.44	13.2	8.6
Soil *	210	19.5 (~ 20)	4.10	69.5	79.8 (~ 80)
TOTAL	302.0	(Mean 11.4)	5.13	100.0%	100.0%

*Their soil microbe value was 2.50 (truly 2.556) × 10^{29} whereas Blakemore (2022, 2023: table 3) had 210 × 10^{28} (cf. Table 2). Data was based upon Whitman et al. (1998) for Prokaryote cells, as revised by Blakemore (2022) and corrected (as detailed in text), with combined Sub-Ocean and Sub-Terrestrial values averaged out.

had 1.2 × 10^{29}, 4 × 10^{29} and 20 × 10^{29} cells, respectively. For Soil, their Prokaryote total was ≈ 3 × 10^{29} cells, similar to the values presented herein.

The mean VtB ratio 11.4 is approximately the same as Cobián-Güemes et al. (2016: table 1) median VtB of 12, both above Bergh et al. (1989) ~ 10:1 aquatic VtB. If 11.4 is applied to 302 × 10^{28} Microbes a total is ~ 5 × 10^{31} VLPs. However, Soil alone VtB is double at ~ 20:1 that, for 210 × 10^{28} Microbes, is ~ 4 × 10^{31} VLPs (~ 80%). Thus, proportion of viruses in Soil from total viruses is ~ 80% as noted in the Abstract (cf. Ocean 2–10% noted above), with the remainder in the deep-subsurfaces.

Although most samples are superficial, often in just the top 5 or 10 cm of soils, viral activity persists throughout the soil profile, to at least 1 m depth according to Muscatt et al. (2023). Interestingly, these latter authors stated: "Viral contributions to soil ecology are largely unknown due to the extreme diversity of the soil virosphere. Despite variation in estimates of soil viral abundances (10^7 to 10^{10} viruses per gram of soil), it is clear that soils are among the largest viral reservoirs on Earth. Early metagenomics investigations have revealed high genetic diversity in soil viruses, with putative impacts on global biogeochemistry. Still, less than 1% of publicly available viral metagenomic sequences are from soil, reflecting the lack of knowledge about soil viruses and their ecological roles". Accordingly, as soil is so under-represented, Graham et al. (2023, 2024) argue that understanding the rôle of viruses in soil is most pressing of any of our ecological challenges.

Virus to Bacteria (VtB) ratio abundances

As already noted, Mushegian (2020) had an approximate 10-fold excess of phages over bacterial cells (as per Bergh et al. 1989), whereas Cobián-Güemes et al. (2016: table 1, fig. 1) median VtB was around 12:1 and in Soil alone ~ 20:1 (or 100:1 mean soil ratio in their figure which is an order higher that all other ratios). Applied to Table A2 totals, a 12:1 ratio for all ~ 3.78 × 10^{30} global microbe cells would be ~ 4.6 × 10^{31} VLPs with 4.1 × 10^{31}, or 89%, of viruses in Soil. But this too may be out by an order or more, not least to account for those active intracellular virus particles that are mostly overlooked in general surveys, or in the Soil's VtB ratios.

Early on, Ashelford et al. (2003) averaged soil virus numbers at 1.5 × 10^8 per g, which they said was equivalent to 4% of total bacteria population (of 3.6 × 10^9 per g) giving a virus-to-bacterium ratio (VtB) in their soil of 0.04:1. Subsequently, other authors found much higher numbers, e.g. Cobián-Güemes et al. (2016: fig. 1) had mean Soil VtB ratio ~ 100:1 but selected a median value of ~ 20:1 as in their table 1 (cf. Table A2).

Cao et al. (2022) reported highly variable virus-to-bacteria ratios (VtB) in soils as ranging from 0.001 to 8,200 (six orders of magnitude!) although their study found abundance of virus-like particles (VLPs) ranged from 2.0×10^7 to 1.0×10^{10} and microbial abundance ranged from 1.0×10^8 to 8.2×10^8 per gram of dry soil, to give a VtB ratio from ~ 0.1 to 98.3 (near three orders of magnitude range), settling around a median VtB ratio value of 10:1 compliant with Cobián-Güemes et al. (2016: table 1, fig. 1) but including depauperate aquatic biomes. Wide ranging (VTM/VBR = VtB) estimations, pertinent for soil, mostly vary ~ 10:1 to 100:1 which is interesting as this complies with a virus species to host species range as assumed by Koonin et al. (2023).

VtB ratios (= VTM/VBR) for species diversity

Although an answer is complex, a preliminary estimate in Fierer et al. (2007: table 3) had bacterial OTUs of $10^{3–6}$ (median ~ 5×10^4) while viral vOTUs ranged $10^{3–8}$ (median 10^6) thus, extrapolating data, soil viruses may appear 10–100 times more diverse than Bacteria as a rough indication of mutual biodiversity crosscheck. As just noted, Koonin et al. (2023) conservative range estimate was 10:1 to 100:1 for their host species ratio. Muscatt et al. (2023) determined: "overall vOTU per host ratio was 0.42 (median = 0) [sic], reflecting the predominance of unique host associations for individual vOTUs". This suggests viral diversity is commensurate with Bacteria/Archaea diversity (vOTU:bOTU) and vice versa. So, for 2.1×10^{24} soil microbe species, viral diversity would be at least ($2.1 \times 0.42 = 0.88$) or around 0.88×10^{23} vOTUs. Viral richness (~ 10^{23} per $10^{31–32}$ virions) would then be ~ 1 unique 'variety' for each $10^{8–9}$ virions, or roughly two or three orders lower than bacterial richness which, as noted, is around one bacterial taxon per million cells. Q.E.D.

Conversely, Roux and Emerson (2022) quote: "estimates of soil viral richness suggested the presence of 1000 to 1 000 000 genotypes per sample" and samples were traced as ~ 200 g wet soil, say ~ 100 g dry, to give around 10–10,000 soil genotypes per gramme (or around 10^3 in a mean of 10^9 virus particles per g which is also ~ 1 vOTU per million virion cells as with bacterial estimates). Thus, both are at a mutual 1:1 ratio. Recently, Graham et al. (2024) quoted 10^7–10^{10} viruses per gramme of soil showing soils as the largest viral reservoirs on Earth and they reported averages of 40.01 (range 1–2,124), 35.48 (range 1–1,651) and 24.91 (range 1–896) unique viral clusters per soil sample (presumably 1 g?) at the species, genus, and family levels. This suggests four viral species for each one million, up to a billion soil virions, a bit higher than for Bacteria.

A likely summary is that viruses are most abundant in soils and at least ten or 100 times as rich as the Bacteria, their primary hosts. From Blakemore (2023), as both Global and Soil alone bacterial biodiversity are in the order of 2×10^{24}, then virus diversity may range from at least as many, ≤ 10^{25}–10^{26} viral species in total.

Alternatively, as ~ 10^{31} viruses are known, may soil Bacteria reasonably range 10^{29}–10^{30} species?

Support is found in Kuzyakov and Mason-Jones (2018), viz.: "The total number of viruses (including intracellular viruses inside bacteria) is probably 1–2 orders of magnitude higher than the bacterial populations" From this we may again conclude in circular argument that Bacteria are 1–2 orders less in terms of both cells and species.

Finally, we may concur with Williamson et al. (2017): "To understand the soil virome, much work remains."

ZooKeys 1224: 317–348 (2025)
DOI: 10.3897/zookeys.1224.135458

Research Article

On *Cytheridella whitmani* sp. nov. (Crustacea, Ostracoda) from Cape Cod (Massachusetts, USA), with a reappraisal of the taxonomy of the genus

Koen Martens[1,2], Nadiny Martins de Almeida[3], Michael Shribak[4], Janet Higuti[3,5], Isa Schön[1,6]

1 *Royal Belgian Institute of Natural Sciences, Freshwater Biology, Vautierstraat 29, B-1000 Brussels, Belgium*
2 *Department of Biology, Ghent University, K.L. Ledeganckstraat 35, B-9000 Ghent, Belgium*
3 *Graduate Program in Ecology of Inland Water Ecosystems (PEA), Department of Biology (DBI), Centre of Biological Sciences (CCB), State University of Maringá (UEM), Av. Colombo, 5790, CEP 87020-900, Maringá, PR, Brazil*
4 *Marine Biological Laboratory, Woods Hole, MA, USA*
5 *Centre of Research in Limnology, Ichthyology and Aquaculture (Nupélia), Centre of Biological Sciences (CCB), State University of Maringá (UEM), Av. Colombo, 5790, CEP 87020-900. Maringá, PR, Brazil*
6 *Centre of Environmental Sciences (CMK), University of Hasselt, 3590 Diepenbeek, Belgium*
Corresponding author: Koen Martens (darwinula@gmail.com)

Abstract

Cytheridella whitmani Martens, **sp. nov.** is described from lakes on Cape Cod (MA, USA). The species differs from its congeners mainly by the shape of the female carapace and by the morphology of the hemipenis, especially of the distal lobe and the copulatory process. The literature on the genus is reviewed and the synonymy of the fossil *Cytheridella boldii* Purper, 1974 with the type species *C. ilovayi* Daday, 1905, both described from South America, is confirmed. The status of *Cytheridella americana* (Furtos, 1936) is reverted to that of "uncertain species". Beside the type species and the new species, the genus currently includes only three further species from Africa: *C. monodi* Klie, 1936, *C. damasi* Klie, 1944 (with synonym *C. chariessa* Rome, 1977), and *C. tepida* Victor, 1987. The morphology of the new species is discussed in comparison with the congeneric species, especially regarding the valve ornamentation, the structure and function of the third thoracopod, the hemipenis and the caudal ramus. It is suggested that *C. whitmani* is a recent invasive species in the lakes of the Cape Cod peninsula. Its occurrence at northern latitudes is unexpected, as its congeneric species are consistently (sub-) tropical.

Key words: African species, caudal ramus, hemipenis, invasive species, valve ornamentation

Academic editor: Ivana Karanovic
Received: 24 August 2024
Accepted: 4 December 2024
Published: 3 February 2025

ZooBank: https://zoobank.org/77C00701-6AE6-44EA-B634-6A78FD25B356

Citation: Martens K, Almeida NM, Shribak M, Higuti J, Schön I (2025) On *Cytheridella whitmani* sp. nov. (Crustacea, Ostracoda) from Cape Cod (Massachusetts, USA), with a reappraisal of the taxonomy of the genus. ZooKeys 1224: 317–348. https://doi.org/10.3897/zookeys.1224.135458

Introduction

Non-marine ostracods (small, bivalved crustaceans) occur on all continents except Antarctica, and in most aquatic and (semi-) terrestrial environments (Smith et al. 2015). The knowledge on the diversity of non-marine ostracods on different continents and in different zoogeographical regions is highly unequal and this mostly for historical reasons. In Europe, living non-marine ostracods have consistently received much more taxonomic and ecological attention over

the past one and a half century than in North America, whereas for most ostracod groups (genera, subfamilies), the North American fauna is more speciose than the European one (Martens et al. 2008; Meisch et al. 2019).

The non-marine ostracod fauna of Massachusetts has been investigated by Haldeman (1842), Cushmann (1905, 1907), Sharpe (1908, 1910), and Furtos (1935). A total of 22 species has thus far been reported by these authors from Massachusetts, 13 of these from Cape Cod (Table 1). Especially the more extensive survey of Furtos (1935) is of interest here, as most species she described or reported on are from localities on Cape Cod, the peninsula dealt with in the present study.

Cytheridella Daday, 1905 belongs to the family Limnocytheridae Sars, 1925, subfamily Timiriaseviinae Mandelstam, 1960 (at this stage we do not follow Tanaka et al. (2021) in raising this subfamily "to a higher taxonomic level") and tribe Cytheridellini Danielopol & Martens, 1989 (in Danielopol et al. 1989). Its type species, *C. ilosvayi* Daday, 1905, originally described from Paraguay, turned out to be one of the most common inhabitants of Neotropical water bodies (Higuti et al. 2010; Conceição et al. 2020). The morphology of *C. ilosvayi* has been extensively studied over the past decade. For example, Wrozyna et al. (2014, 2016, 2018, 2019) performed quantitative valve outline analyses in search of discrete morphotypes, with implications for ontogeny and zoogeography. Danielopol et al. (2018) and Lord et al. (2020) formalised the different types of sieve-type pore canals and demonstrated their relevance for

Table 1. Ostracod species reported from Massachusetts (M) and from Cape Cod specifically (CC) in the literature. Note: *Cypris scabra* Haldeman, 1842 is here considered an uncertain species, as was already foreshadowed by Furtos (1935), and is not listed here. Martens et al. (2023) reported a sexual population of *Cypridopsis vidua* from Cape Cod.

Genus and species	Authority	Cushman, 1905	Cushman, 1907	Sharpe, 1908	Sharpe, 1910	Furtos, 1935	Present Paper
Heterocypris incongruens	(Ramdohr, 1808)	M		M			
Cyprinotus syn.? *americanus*	Cushman, 1905	M					
Spirocypris passaica	Sharpe, 1903		M	M			
Eucypris virens	(Jurine, 1820)		M	M			
Bradleystrandesia fuscata	(Jurine, 1820)		M				
Bradleystrandesia reticulata	(Zaddach, 1844)		M	M			
Bradleystrandesia splendida	(Furtos, 1933)					M	
Cypridopsis vidua	(O.F. Müller, 1776)		M				
Cypria exculpta	(Fischer, 1855)		CC				
Cypria obesa	(Sharpe, 1897)				CC		
Cypria palustera	(Furtos, 1935)					CC	
Physocypria posterotuberculata	(Furtos, 1935)					CC	
Physocypria globula	(Furtos, 1933)					CC	
Cyclocypris forbesi	(Sharpe, 1897)					CC	
Cyclocypris cruciata	Furtos, 1935					CC	
Candona candida	(O.F. Müller, 1776)		M				
Candona decora	(Furtos, 1933)					CC	
Fabaeformiscandona caudata	(Kaufmann, 1900)					CC	
Pseudocandona annae septentrionalis	(Furtos, 1935)					CC	
Pseudocandona elliptica	(Furtos, 1933)					CC	
Pseudocandona punctata	(Furtos, 1933)					CC	
Darwinula stevensoni	(Brady & Robertson, 1870)					CC	
Cytheridella whitmani	this study						CC

ostracod taxonomy. Danielopol et al. (2023) compiled an extensive diagnosis of *C. ilosvayi*, mostly based on valve morphology, in comparison with several fossil *Cytheridella* species. Here, we describe a new extant species of the genus *Cytheridella* found in several lakes (locally referred to as "ponds") on Cape Cod and re-asses the validity of the known recent species.

Materials and methods

Study area

Samples in the present study were taken in the south-western half of Cape Cod. This peninsula extends into the Atlantic Ocean at the eastern shore of North America, looking like a crooked arm (Fig. 1). It has an east-west oriented basal part and a south-north oriented distal part. It is a sandy peninsula, mostly formed during the last ice age. By ca 18,000 years ago, the ice sheets had retreated past Cape Cod. The resulting landscape, especially of the basal part, is one littered with Holocene (Kettle) lakes of varying shapes, depth and surface sizes (Fisher and Leatherman 1987).

Sampling and sample treatment

Semi-quantitative samples were taken with a rectangular hand net (mesh size 160 µm), using waders, between 10 cm and 1.5 m deep by moving the net amongst vegetation and over the bottom sediment. All available habitats

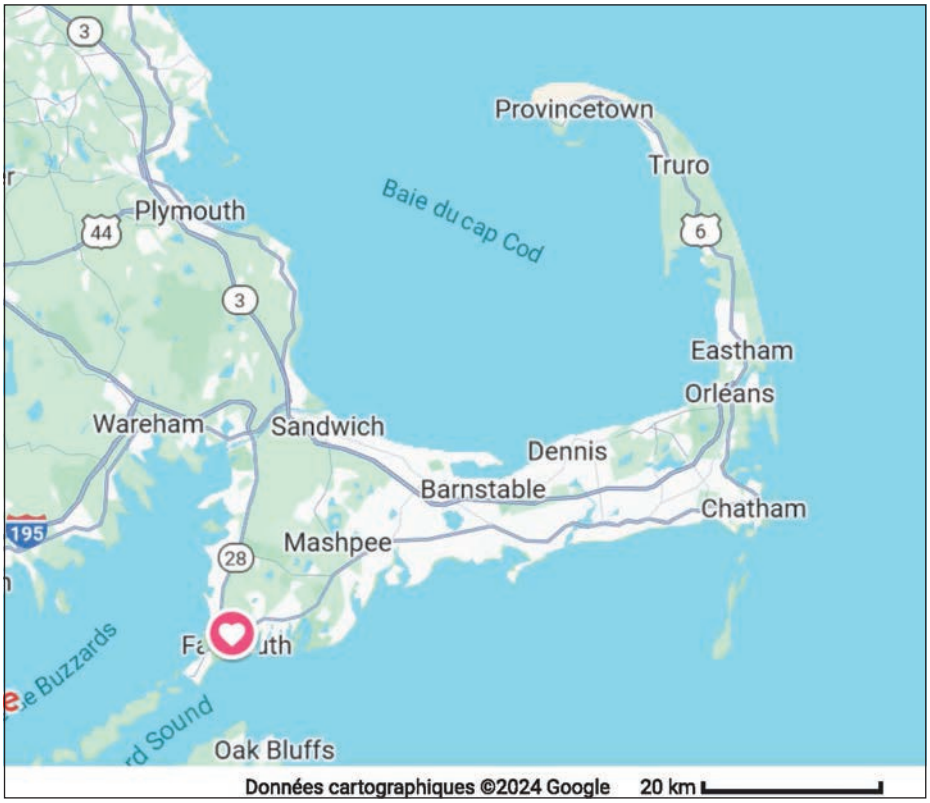

Figure 1. Map of Cape Cod (MA, USA). The symbol indicates the position of Grews Pond (Falmouth), the type locality of *Cytheridella whitmani*.

(exposed sand and gravel beaches, submerged weed beds, emerging macrophyte stands and accumulated debris, fallen leaves etcetera) at the public access areas (boat ramps) of each lake were sampled. In situ measurements were taken with portable meters of water electrical conductivity (Greisinger 480846), pH and temperature (Ebro PHX800). Ostracods were sorted in the laboratory from the total samples under a stereo-binocular microscope (Leica) and were stored in Eppendorf tubes in 100% ethanol, buffered with borax to prevent decalcification of the valves.

Soft parts were separated from the valves using dissection needles and were put in a drop of glycerine for the dissection of the appendages. The dissection was covered with a coverslip and sealed with transparent nail polish. Valves were stored dry in micropaleontological slides. Drawings of soft parts were made using a camera lucida (Olympus U-DA) attached to the microscope (Olympus CX-41). Carapace and valves were illustrated and measured using Scanning Electron Microscopy (SEM, Fei Qanta 200 ESEM, in the Royal Belgian Institute of Natural Sciences, Brussels, Belgium) in different views and details. The hemipenis of the new species was also illustrated using the polychromatic polarisation microscope. The "Polscope" uses polarisation interference colours to show details of tissues that would otherwise be invisible. It was invented by Michael Shribak (Shribak 2014, 2015) at the Marine Biological Laboratory (MBL, Woods Hole, MA, USA). The Polscope setup used here consisted of a microscope Olympus IX81, with objective lens magnification 20 × and total magnification 20 × 16, and a colour CCD camera Olympus DP73. The only previous use of this technology for imaging ostracods was in Martens et al. (2023).

Chaetotaxy of the limbs largely follows the model proposed by Broodbakker and Danielopol (1982). Higher taxonomy of the Ostracoda follows Horne et al. (2002), Meisch et al. (2019, 2024) and for the Timiriaseviinae, Danielopol et al. (2018). Repository: Royal Belgian Institute of Natural Sciences, Brussels, Belgium (**RBINS**; general inventory number IG34899, specimens numbers INV323000-3230021).

Abbreviations used in text and figures

Valves and carapaces

Cp	carapace
CpD	carapace in dorsal view
CpRL	carapace in right lateral view
CpV	carapace in ventral view
H	height
il	inner list
L	length
LV	left valve
LVi	left valve in internal view
ol	outer list
RV	right valve
RVi	right valve in internal view
W	width

Limbs

A1	antennula
A2	antenna
cop	copulatory process on Hp
CR	caudal ramus ("organ fourchu" in female)
d, d_p, e, f, h2, h3	claws and setae on T2 and T3
dej	ductus ejaculatorius in copulatory process
DL	distal lobe of Hp
En1–En4	endopodite segments 1–4 of T1–T3
Hp	hemipenis
Md	mandibula
MdPalp	mandibular palp
Mx1	maxillula
T1	first thoracopod
T2	second thoracopod
T3	third thoracopod
Y, Ya	aesthetascs on A2 and A1 respectively

Results

Class Ostracoda Latreille, 1802
Subclass Podocopa G.O. Sars, 1866
Order Podocopida G.O. Sars, 1866
Suborder Cypridocopina Baird, 1845
Superfamily Cytheroidea Baird, 1850
Family Limnocytheridae Sars, 1928 (fide Danielopol et al. 2018)

Subfamily Timiriaseviinae Mandelstam, 1960

Metacypridinae Danielopol, 1960 (fide Colin and Danielopol 1978). Syn.

Tribe Cytheridellini Danielopol & Martens, 1989

Allocated genera. *Cytheridella* Daday, 1905; *Gomphocythere* Sars, 1924. Note: the genus *Gomphodella* De Deckker, 1981 is now lodged in the tribe Gomphodellini Danielopol et al. 2018.

Genus *Cytheridella* Daday, 1905

Onychocythere Tressler, 1939 (fide Pinto and Sanguinetti 1962). Syn.

Type species. *Cytheridella ilosvayi* Daday, 1905.

Syn.: *Metacypris ometepensis* Swain & Gilby, 1964 (fide Purper 1974; Martens and Behen 1994).

Syn.: *Onychocythere alosa* Tressler, 1939 (fide Purper 1974; Cohuo et al. 2017).

Syn.: *Gomphocythere argentinensis* Ferguson, 1967 (fide Karanovic 2009).

Syn.: *Cytheridella boldii* Purper, 1974 (fide Danielopol et al. 2018).

Diagnosis (partly derived from the extensive analysis of Danielopol et al. 2023). Cp largely sexually dimorphic. Males: CpV and CpD laterally rather flattened, with greatest width slightly behind the middle, both anterior and posterior sides pointed. Females: CpD and CpV with highly developed brood chamber, occupying 2/3 of the posterior part of the Cp, posterior margin almost straight, anterior margin pointed. In both sexes with well-developed lateral sulci and external valve surfaces heavily ornamented, with pits, rimmed pores with setae, and, especially anteriorly and posteriorly, with long and stiff setae and pores on conical elevations with setae (*Porenwarzen*). In inner views, both valves with well-developed anterior and posterior selvages, largely inwardly displaced; anterior calcified inner lamella of both valves set with two connected rows of long and fine cuticular filaments (setulae). Hinge adont. Central Muscle Scars consisting of a vertical row of four scars.

A1 with second segment bearing a long seta on the proximo-ventral side; penultimate segment fully or partly fused (segments 4+5); one of dorso-apical setae on this segment shaped as a trident. A2 with three distal claws. T1 and T2 with segment En4 fused with end claw. T3 a reflexed "cleaning limb", with segment 4 not fused with end claw, seta h3 a spine. In females, with elongated CR ("organ fourchu"), with bifurcated tip. Hp with DL hinging on basal part, copulatory process coiled, short or (very) long. In males, CR simple but robust setae.

Other (African) species. *C. damasi* Klie, 1944 (Congo, syn.: *C. chariessa* Rome, 1977 (Congo, in Rome and De Deckker 1977, fide Karanovic 2009)); *Cytheridella monodi* Klie, 1936 (Cameroon) *Cytheridella tepida* Victor, 1987 (Nigeria).

Remark. *Cytheridella americana* (Furtos, 1936) Danielopol (1981 in Colin and Danielopol 1980) from Yucatan (Mexico) is here considered an uncertain species (see below).

***Cytheridella whitmani* Martens, sp. nov.**

https://zoobank.org/2560DC0D-F302-47F3-BE20-6BCB7C5F3476

Figs 2–12

Type material. ***Holotype*** • 1 ♂ (adult); dissected and stored on a permanent microscopic slide and valves stored dry in a micropalaeontological slide (nr INV323000). ***Allotype*** • 1 ♀ (adult); dissected and stored as the holotype (nr INV323001). ***Paratypes*** • 3 ♂♂ adult Cp used for SEM (nrs INV323002-323004). 1 ♂ dissected and stored as the holotype (nr INV323005). 3 ♀♀ adult Cp used for SEM (nrs INV323006, INV323008, INV323010,). 1 ♀ dissected and stored as the holotype (nr INV3230014). Thirty ♀♀ and ♂♂ in EtOH (INV3230021).

Type locality. USA • Massachusetts, Cape Cod, Grews Pond, Goodwill Park, Falmouth. Coordinates: N: 41.5696816, W: 70.6146054. Altitude: 5 m a.s.l. Collected on 27 July 2023. Leg.: Koen Martens and Isa Schön. Measurements at the time of collecting: Electrical Conductivity: 49 µS/cm, pH: 7.4, Water Temperature: 28 °C (holotype, allotype, and paratypes are all from the type locality).

Other localities on Cape Cod (details on ecology will be provided elsewhere). ***Woods Hole*****:** Miles Pond. ***Falmouth*****:** Mares Pond, Deep Pond, Coonamessett Pond. ***Mashpee*****:** Wakeby Pond, Peters Pond, Pemlico Pond. ***Barnstable*****:** Lorells Pond, Snake Pond, Mystic Pond, Middle Pond, Hamblin Pond, Shubael Pond,

Wequaquet Pond, Dennis Pond. ***Bourne*:** Flax Pond. Sandwich: Laurence Pond, Spectacle Pond. ***Yarmouth*:** Long Pond.

Etymology. The species is named after Dr Charles Otis Whitman (1842–1910), professor at the University of Chicago, and the first director of the Marine Biological Laboratory (MBL) at Woods Hole (Ma, USA), after whom one of the present Research Centres at MBL and a series of fellowships are named (https://en.wikipedia.org/wiki/Charles_Otis_Whitman). The name is a noun in the genitive singular.

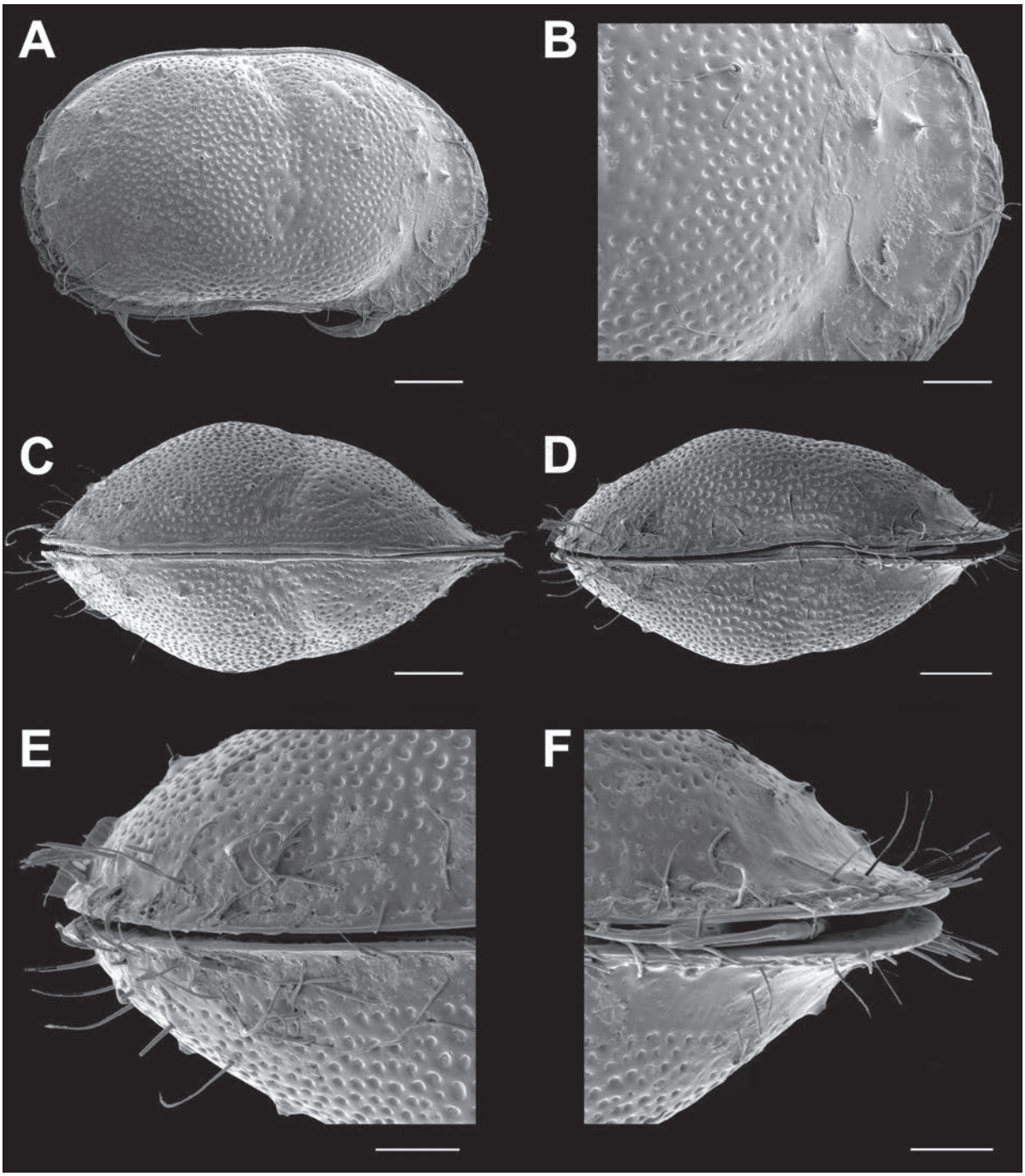

Figure 2. *Cytheridella whitmani*, male **A** CpRL (INV323004) **B** CpRL, detail of anterior part (INV323004) **C** CpD (INV323002) **D** CpV (INV323003) **E** CpV, detail of posterior part (INV323003) **F** CpV, detail of anterior part (INV323003). Scale bars: 100 µm (**A, C, D**); 50 µm (**B, E, F**).

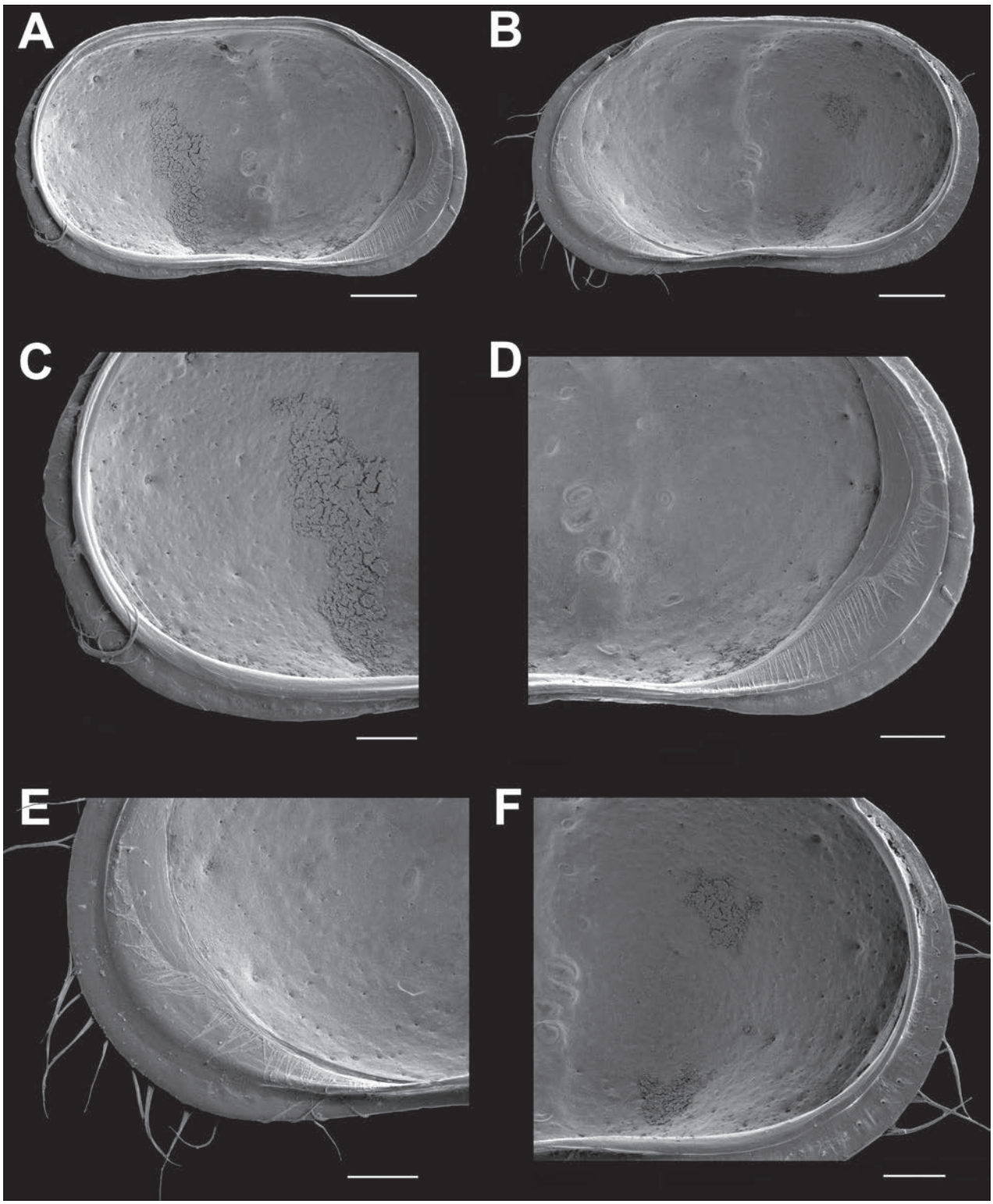

Figure 3. *Cytheridella whitmani*, male **A** LVi (INV323005) **B** RVi (INV323005) **C** LVi, detail of posterior part (INV323005) **D** LVi, detail of anterior part (INV323005) **E** RVi, detail of anterior part (INV323005) **F** RVi, detail of posterior part (INV323005). Scale bars: 100 µm (**A, B**); 50 µm (**C–F**).

Diagnosis. Cp as typical for the genus and in dorsal view most similar to the type species, but significantly smaller. Valves in inner view both with largely inwardly displaced selvage, especially in the poster-ventral corner of the RV. Posterior flanges of both valves on the inner side set with a series of rimmed pores,

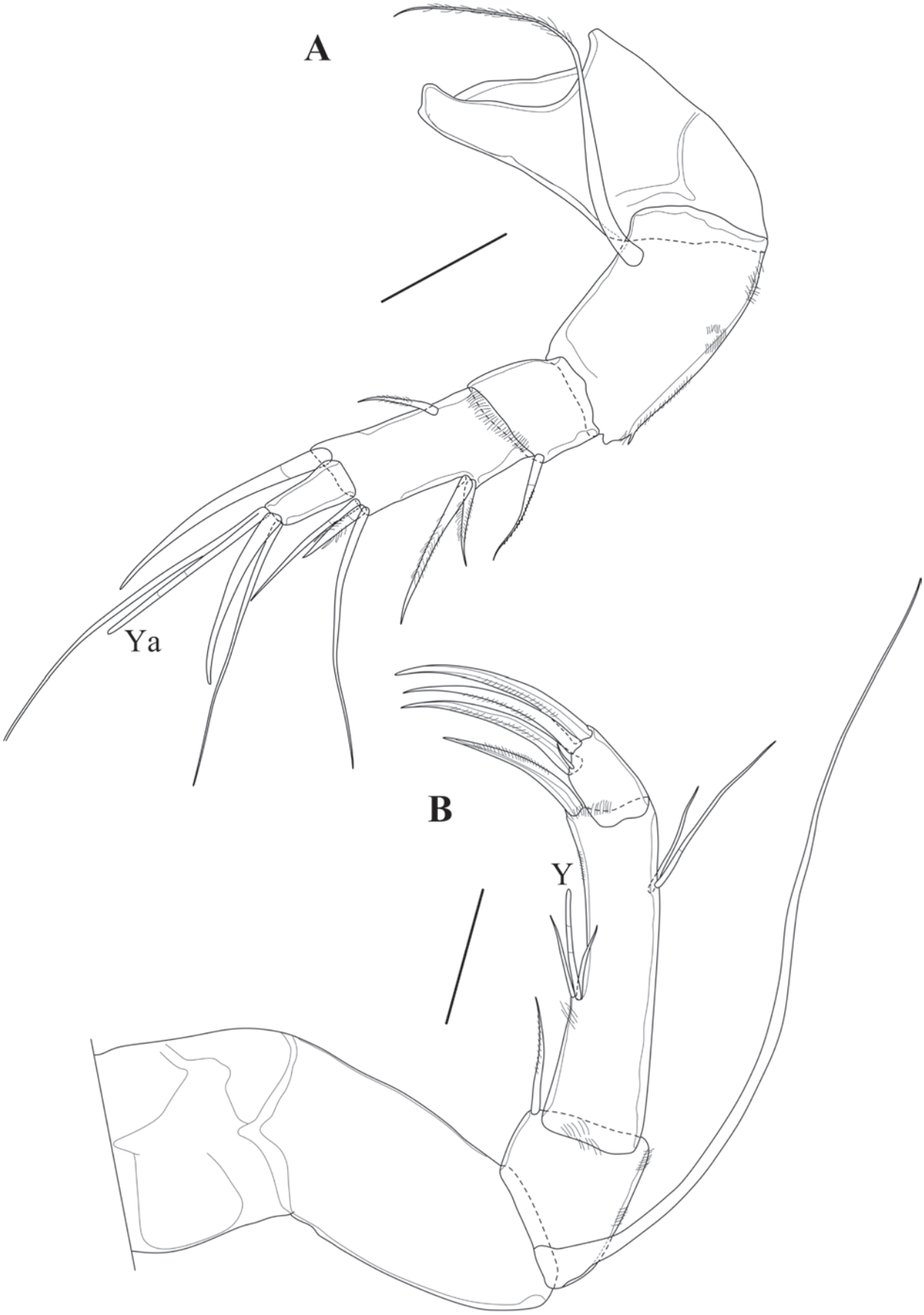

Figure 4. *Cytheridella whitmani*, holotype male **A** A1 (INV323000) **B** A2 (INV323000). Scale bars: 50 µm.

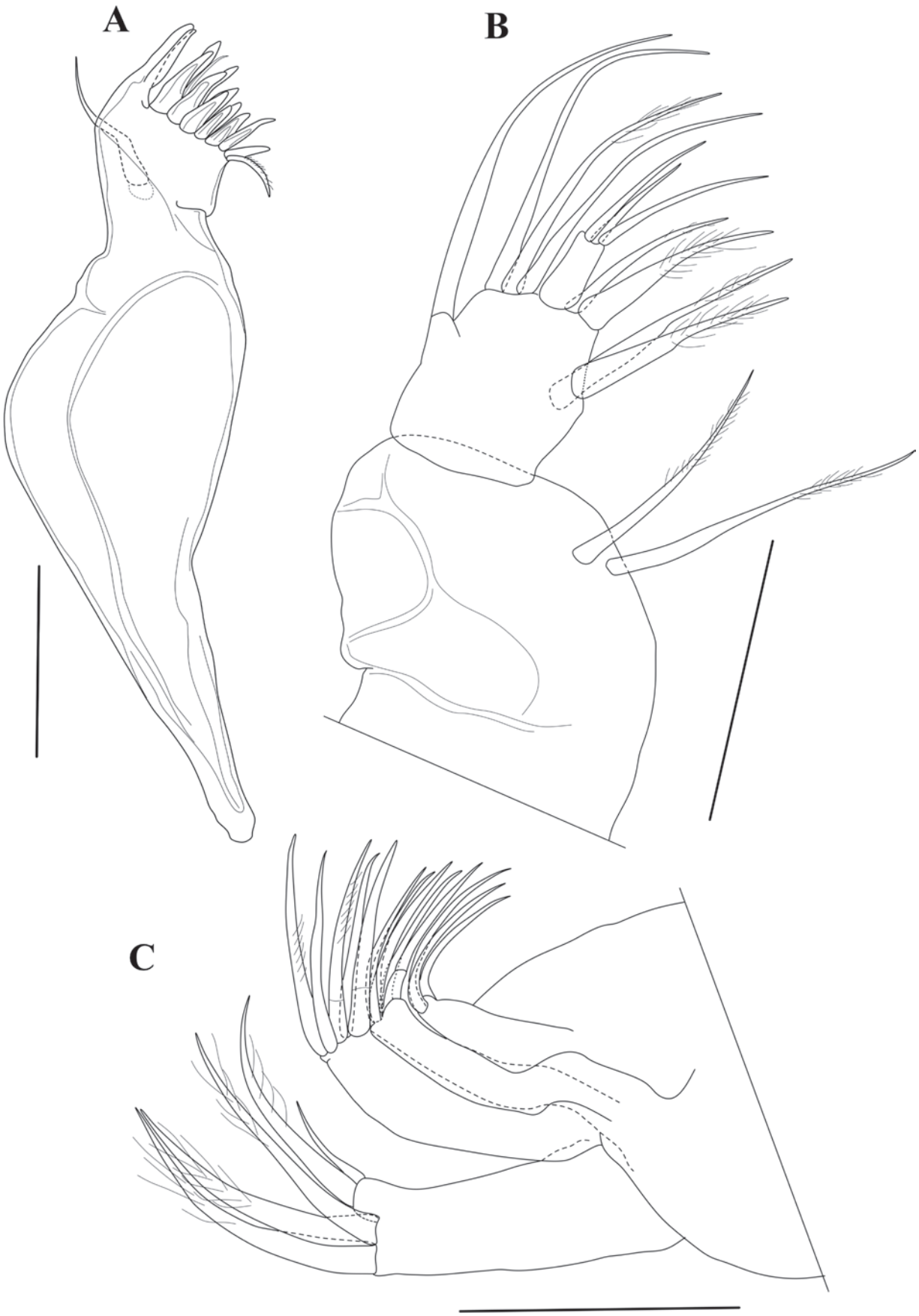

Figure 5. *Cytheridella whitmani*, holotype male **A** Md (INV323000) **B** Md-palp (INV323000) **C** Mx1 (INV323000). Scale bars: 50 µm.

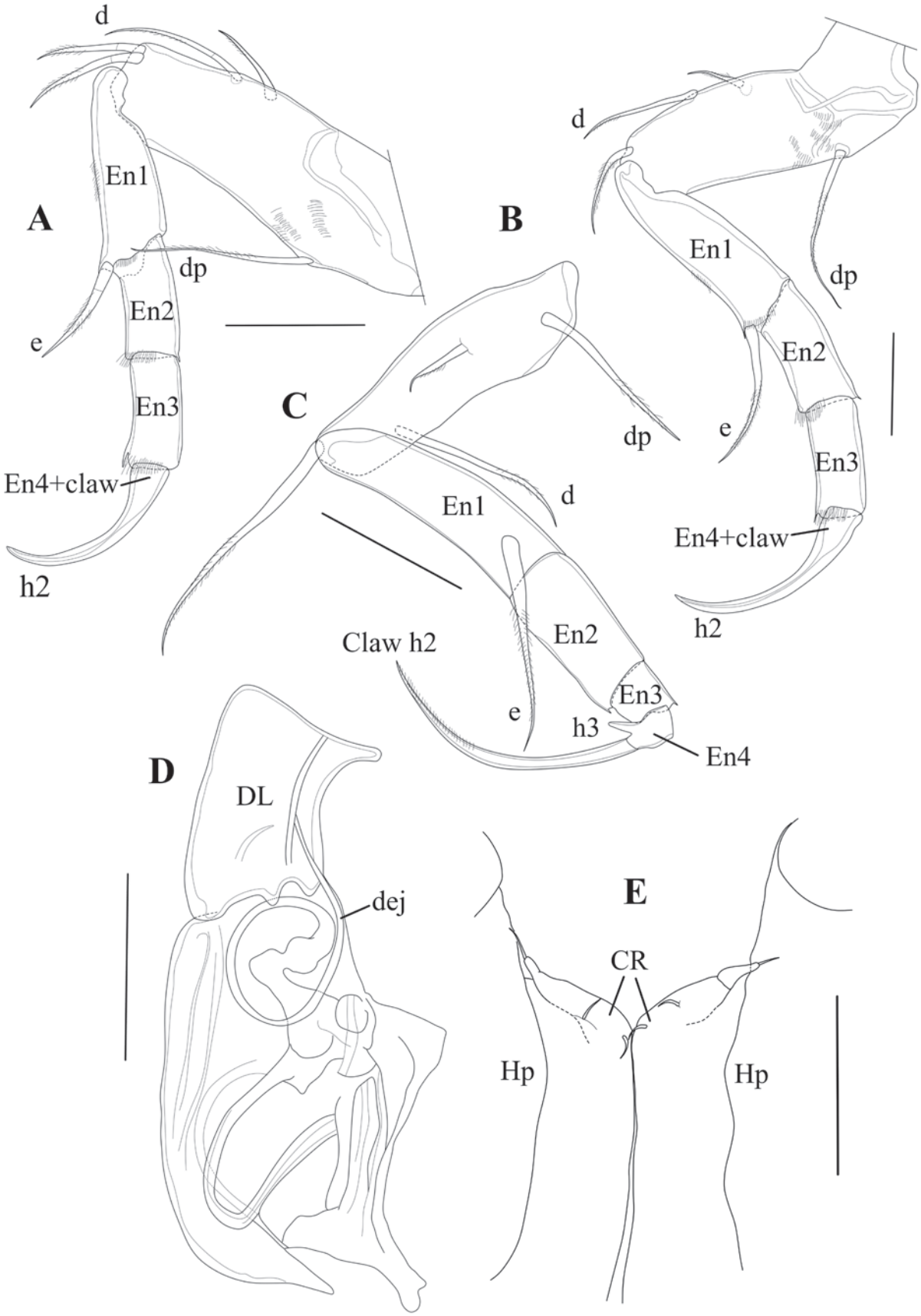

Figure 6. *Cytheridella whitmani*, holotype male **A** T1 (INV323000) **B** T2 (INV323000) **C** T3 (INV323000) **D** Hp (INV323000) **E** CR in between two Hp. (INV323015). Scale bars: 50 µm.

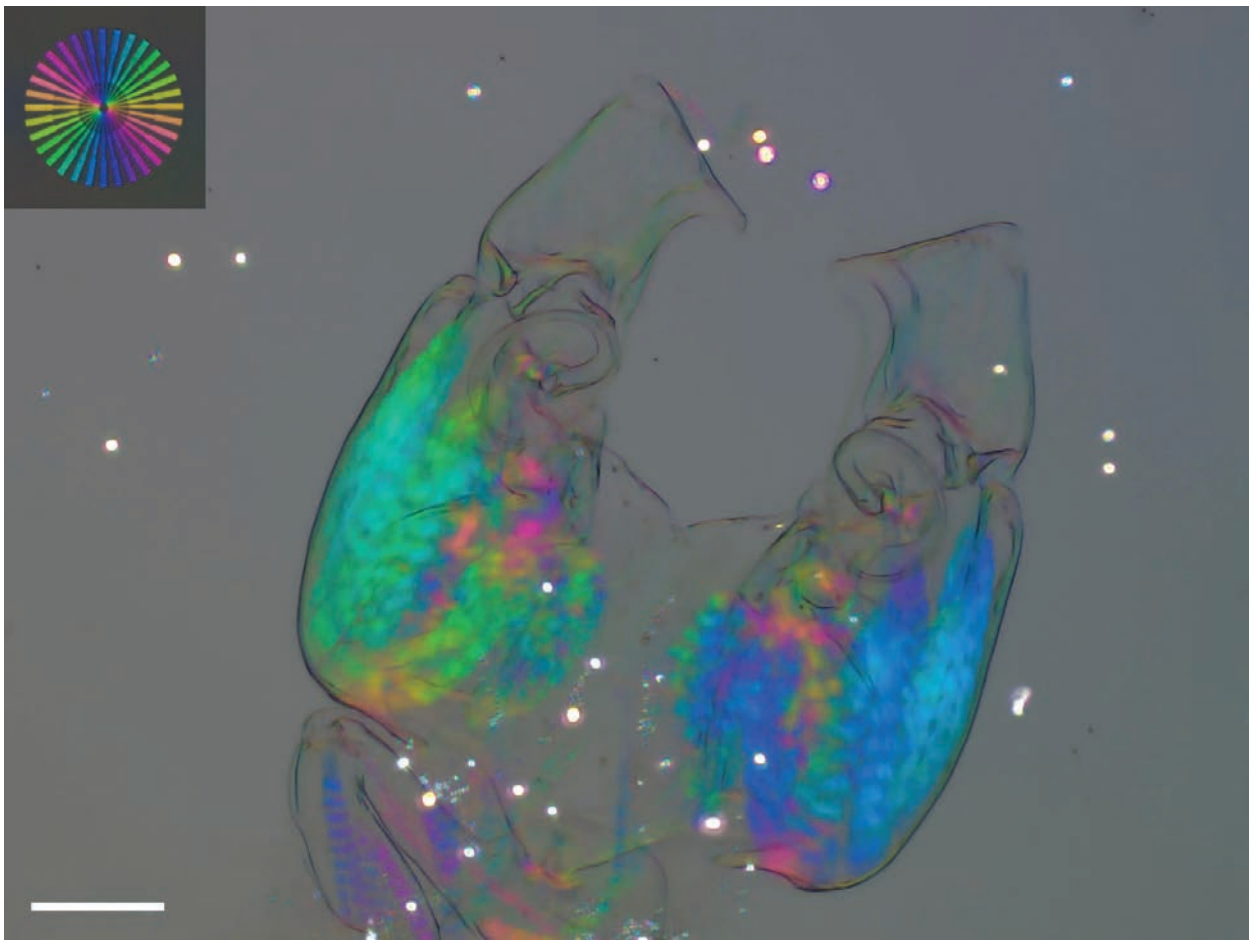

Figure 7. *Cytheridella whitmani*, male, both Hp (INV323015). Image by polychromatic Polscope. Inset: image of the test target. Crucially, the slow axes of the test target are radial, and their hue can be effectively utilized to determine muscle orientation within the Hp. Scale = 50 µm.

each bearing a simple seta. A1 with ventro-apical seta strong and claw-like. Mx1 palp apically with four claws and one seta. T3 a cleaning limb, with endopodal segment 4 fused with terminal claw, seta h3 a spine. Hp with DL elongated, sub-rectangular with bluntly pointed ventro-distal edge, and a long narrow, coiled copulatory process, distally pointed.

Description. Male. CpRL (Fig. 2A, B) view rectangular, with widely rounded posterior and anterior margins, the latter slightly ventrally produced; dorsal margin straight for more than half of its length, ventral margin sinuous slightly anteriorly to the middle; with in both valves a clear lateral dorso-medial sulcus (reaching from dorsal side to more than half the height of the valves) and an antero-ventral sulcus (reaching from ventral side to more than half the height of the valves). CpD (Fig. 2C) and CpV (Fig. 2D–F) with pointed anterior and posterior margins and unevenly rounded lateral sides, the latter interrupted by the lateral sulci, greatest width situated slightly behind the middle. External valve surface heavily ornamented, set with circular and longitudinal pits and rimed pores, the latter especially anteriorly and posteriorly with long and stiff setae (*Porenwarzen*).

RVi (Fig. 3B, E, F) with shape as for the CpRL, with straight dorsal and slightly sinuous ventral sides, both anterior and posterior margins widely rounded; with well-developed selvage widely inwardly displaced along anterior and posterior

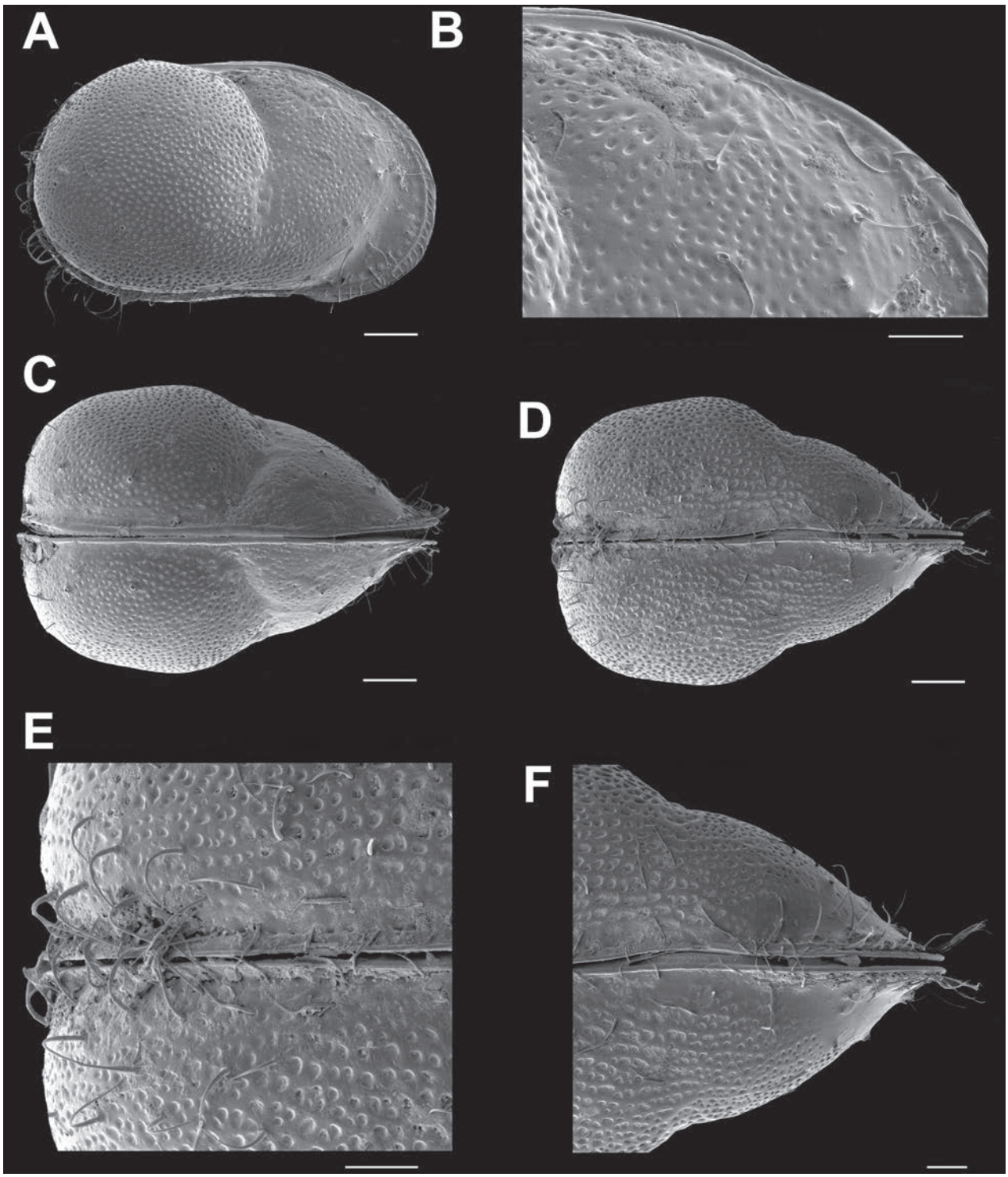

Figure 8. *Cytheridella whitmani*, female **A** CpRL (INV323008) **B** CpRL, detail of anterodorsal part (INV323008) **C** CpD (INV323006) **D** CpV (INV323007) **E** CpV, detail of posterior part (INV323007) **F** CpV, detail of anterior part (INV323007). Scale bars: 100 µm (**A, C, D**); 50 µm (**B, E, F**).

margins, especially in the postero-ventral part; this part of the flange with a circular line of rimmed pores with setae.

LVi (Fig. 3A, C, D) almost symmetrically to RV, but with selvage less inwardly displaced, especially in the postero-ventral part.

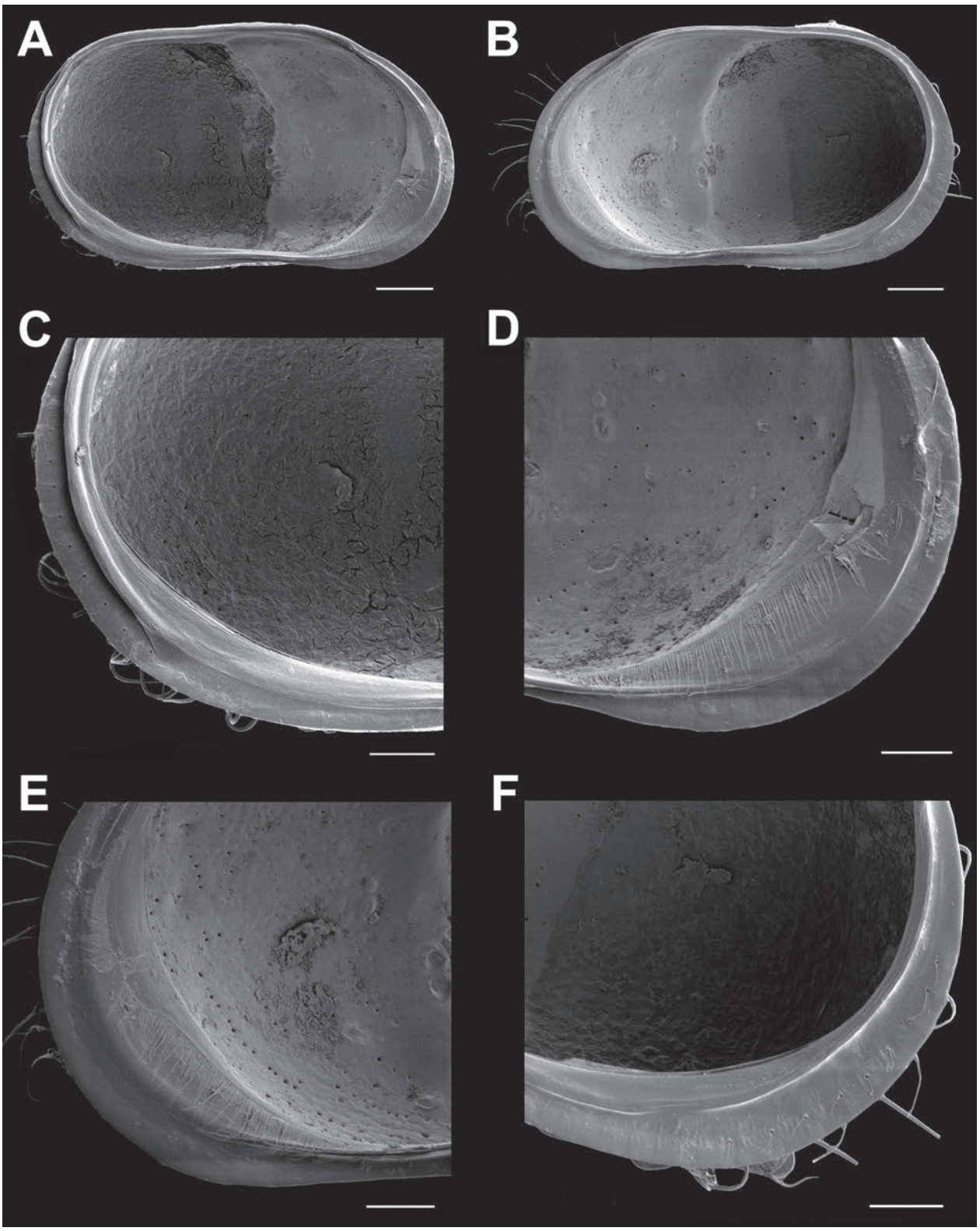

Figure 9. *Cytheridella whitmani*, female **A** LVi (INV3230014) **B** RVi (INV3230014) **C** LVi, detail of posterior part (INV3230014) **D** LVi, detail of anterior part (INV3230014) **E** RVi, detail of anterior part (INV3230014) **F** RVi, detail of posterior part (INV3230014). Scale bars: 100 µm (**A, B**); 50 µm (**C–F**).

A1 (Fig. 4A). Five-segmented. First segment slightly longer than wide. Second segment slightly shorter than the first one, with one long ventral and distally plumose seta, sub-basically inserted and reaching tip of penultimate segment.

Third segment sub-quadrate, with a single dorso-apical seta reaching mid-length of fourth segment. Fourth segment (fusion of ancestral 4th and 5th segments) approximately twice as long as basal width. Setation of ancestral fourth segment: two unequal dorso-medial setae, one ventro-medial seta approximately as long as the shortest dorso-medial seta. Setation of ancestral fifth segment: three dorso-apical setae: one long, one short and one approximately one third the length of the long one; this latter seta broad and distally with two spines, almost looking like a trident, consisting of apical point and two subapical spines) and one seta of intermediate length, slightly longer than half the length of the long seta; further with one long ventro-apical claw-like seta. Fifth (terminal) segment approximately 1.5 times as long as the basal width, apically with aesthetasc Ya and its longer accompanying seta, fused at the base with that of the Ya, one long seta, almost as long as the accompanying seta of Ya and a shorter, but stout claw.

A2 (Fig. 4B). Protopodite two-segmented. First segment short. Second segment approximately twice as long as basal width. Exopodite a long, one-segmented spinneret seta, reaching beyond tips of end claws. Endopodite three-segmented. En1 skewed rectangular, approximately as long as basal width, with a short ventro-apical seta, reaching halfway along the second segment; dorso-apically with some pseudochaeta. En2 approximately five times as long as basal width; mid-ventrally with a short aesthetasc Y, flanked on each side by a subequal seta; dorsally with two sub-apical setae, one approximately half the length of the other and ventro-apically with a large claw, more than two times the length of the third segment. En3 (terminal segment) small, skewed sub-quadrate, apically with three large and subequal pectinate claws.

Md coxa (Fig. 5A) long and curved, apically with eight strong teeth, some doubled, interspaced with thin setae, ventro-apically with a short, reflexed plumose seta; sub-apically with a long and stout seta, not reaching the tips of the claws.

MdPalp (Fig. 5B) three-segmented. First segment ventrally set with two large, plumose sub-apical setae, one approximately 3/4 the length of the other, and a respiratory plate (not illustrated). Second segment (fusion of two segments) mid-ventrally with two large and stout setae, almost equally long and plumose in the distal half; mid-dorsally with one long and smooth seta, reaching beyond all other setae, ventro-apically with one long and stout seta, plumose in the distal half and one short, thin and largely smooth seta; dorso-apically with a bunch of three long, sub-equal setae, mostly smooth. Third (terminal) segment very small, approximately twice as long as the basal width; with three apical setae, one long, one of intermediate length and one shorter than the other two.

Mx1 (Fig. 5C) consisting of a basis, a large respiratory plate (not illustrated), three endites and a one-segmented palp. First endite with three subequal, slender setae. Second endite with five subequal, claw-like setae. Third endite with five claw-like setae, four large and one half the size of the others. Palp with four long claws, distally plumose and one small smooth seta, approximately half the length of the claws. Respiratory plate (exopodite – not illustrated) with approximately 16 plumose rays.

T1 (Fig. 6A) a four-segmented walking leg. Basal segment (Basis) long and broad, with one long ventral seta dp, almost reaching distal tip of segment, two short, subequal dorso-apical setae and a two mid-dorsal seta, the most distally inserted one approximately twice as long as the proximal one and reaching distal tip of segment. Segment En1 with one stout ventro-apical seta (e seta)

Figure 10. *Cytheridella whitmani*, allotype female **A** A1 (INV323001) **B** A2 (INV323001). Scale bars: 50 µm.

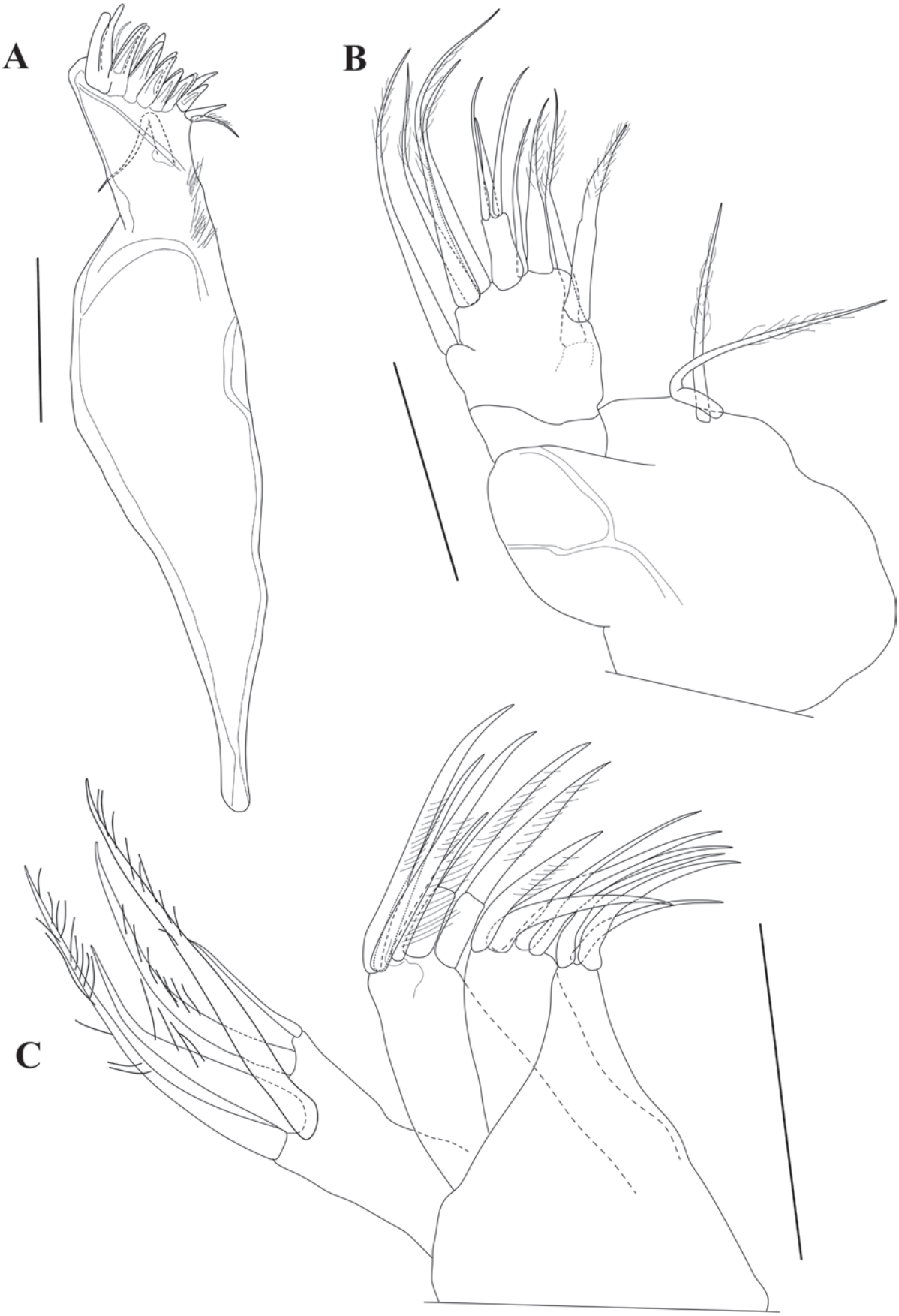

Figure 11. *Cytheridella whitmani*, allotype female **A** Md (INV323001) **B** Md-palp (INV323001) **C** Mx1 (INV323001). Scale bars: 50 µm.

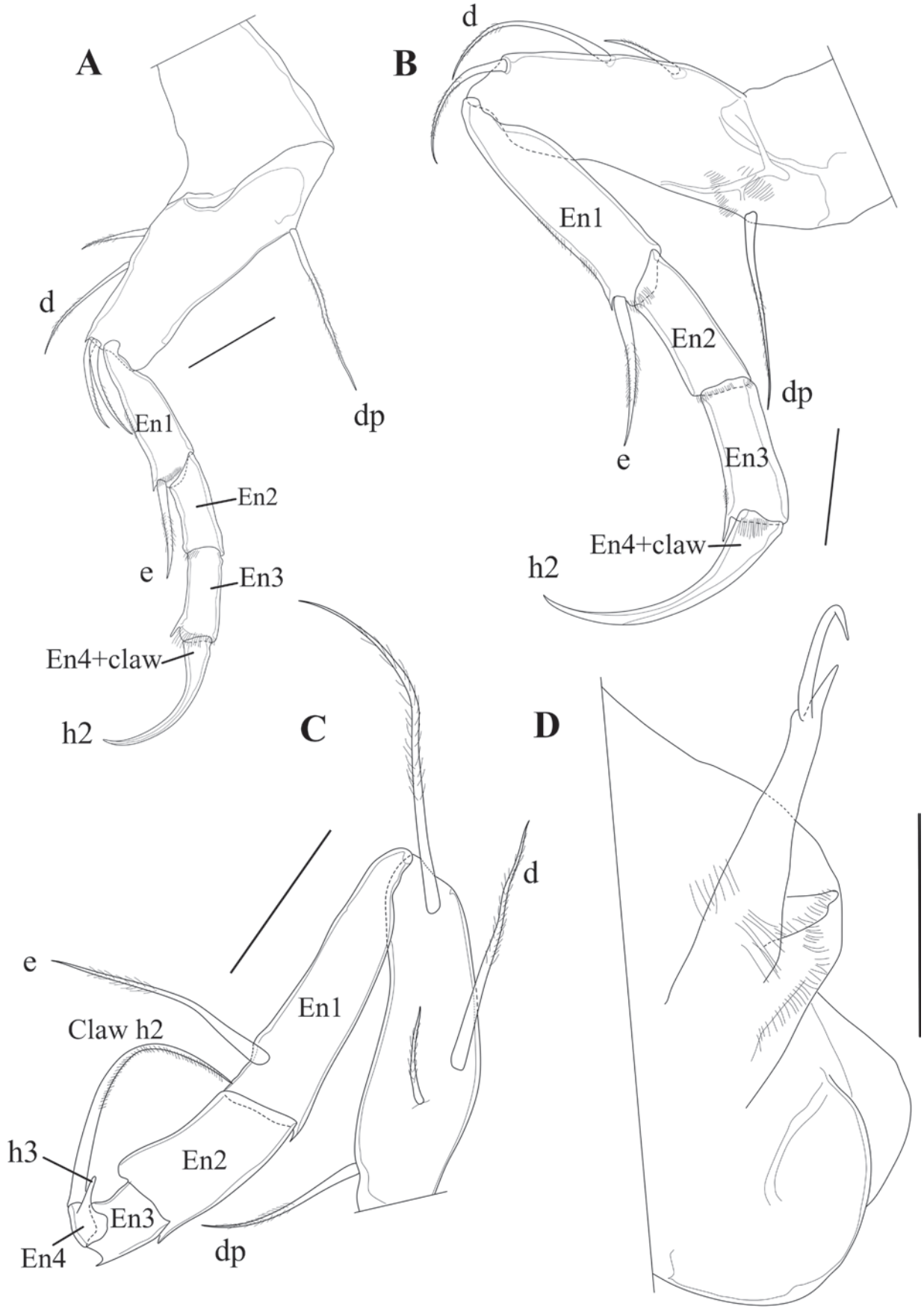

Figure 12. *Cytheridella whitmani*, allotype female **A** T1 (INV323001) **B** T2 (INV323001) **C** T3 (INV323001) **D** CR and post-abdomen (INV323001). Scale bars: 50 µm.

reaching tip of En2. Segment En2 with length approximately 1.5 times basal width and without setae. En3 with length similar to that of second endopodal segment and also without setae; apically with one long and curved distal claw (h2), distally pectinate and basally incorporating segment En4.

T2 (Fig. 6B) also a four-segmented walking leg, slightly larger than the first thoracic limb. Basal segment (Basis) with long and thin mid-ventral seta dp, plumose in the distal 2/3 of its length; one short dorso-apical seta and two mid-dorsal setae, the most distally inserted one approximately three times as long as the proximal one and reaching beyond the distal tip of segment. Segment En1 with ventro-apical seta (e seta) approximately as long as the segment itself. En2 and En3 subequal and without setae, distal claw (h2), basally incorporating segment En4, longer and slightly more arched than equivalent claw on T1.

T3 (Fig. 6C) a cleaning leg. Basal segment (basis) elongated, ventrally with a long basal seta dp; apically with a single, long (as long as the segment itself) and smooth seta, mid-dorsally with two setae, the most distally inserted one approximately three times as long as the proximal one and reaching beyond the distal tip of segment with half of its length. En1 the longest endopodal segment, with subapically a long e seta, plumose in its distal third. En2 shorter than En1 by approximately one third, devoid of setae. En3 short, approximately half the length En2 and devoid of setae. En4 even smaller than En3, slightly obliquely inserted on the latter, carrying a long and curved claw h2 (but not fused with it) and a spine-like h3, fitting in a ventro-apical space of En2, thus forming a cleaning pincer.

Hp (Figs 6D, 7) with broad, elongated and sclerotised muscular body, comprising three or four main bundles of muscles (see Polscope illustration, Fig. 7), an elongated and sub-rectangular distal lobe (DL), with bluntly pointed ventro-distal edge, with a short seta inserted in the middle of the basal part of the lobe DL, and a long narrow, coiled copulatory process, distally pointed. CR (Fig. 6E) consisting of two stout setae at base of each Hp, but not fused with them.

Female (only sexually dimorphic features mentioned).

CpRL (Fig. 8A, B) sub-rectangular, with widely rounded posterior and anterior margins, the latter slightly ventrally produced; dorsal margin not straight, but strongly indented behind the middle at the start of the lateral sulcus, ventral margin slightly sinuous; with a clear dorso-medial sulcus and an anterior ventro-medial sulcus in both valves, as in the male. CpD (Fig. 8C) and CpV (Fig. 8D–F) with pointed anterior margin and posteriorly with highly developed brood chamber, occupying two-thirds of the posterior part of the Cp, posterior margin almost straight. External valve surface heavily ornamented, set with circular and longitudinal pits, rimed pores, especially anteriorly and posteriorly with long and stiff setae in *Porenwarzen*.

RVi (Fig. 9B, E, F) with shape as for the CpRL, but with straight dorsal and slightly sinuous ventral sides, both anterior and posterior margins widely rounded; well-developed selvage widely inwardly displaced along anterior and posterior margins, especially in the postero-ventral part, this part of the flange with a series of rimmed pores with single setae. Posterior brood pouch most prominent.

LVi (Fig. 9A, C, D) almost symmetrically as the RV, but with selvage slightly less inwardly displaced, especially in the postero-ventral part.

A1 (Fig. 10A) with "trident" aspect of short dorso-apical seta on fourth segment pronounced (consisting of apical point and two subapical spines); ventro-apical seta in this segment a long seta, not a claw; accompanying seta to aesthetasc Ya on terminal seta twice as long as aesthetasc itself.

A2 (Fig. 10B) with exopodal seta shorter than in the male, not reaching tips of end claws; these three claws more (sub-) equal than in the male.

Md coxa (Md) (Fig. 11A) less sinuous than in the male. Palp (Fig. 11B) with setae in first segment more subequal in length.

Chaetotaxy of endites and palp of Mx1 (Fig. 11C) highly similar to that in the male, but one distal claw on the palp significantly shorter than the three others.

T1 (Fig. 12A), T2 (Fig. 12B) and T3 (Fig. 12C) largely as in the male, but with En4 in T3 even more obliquely inserted on the tip of En3.

Posterior part of body (Fig. 12D) with CR ("organ fourchu" in Rome and De Deckker 1977) composed of an elongated ramus, ending in bifurcation, with one short, bluntly pointed branch and one longer, hook-like branch; one additional caudal lobe set with pseudochaeta.

Table 2. Measurements of Recent and fossil species of *Cytheridella* (from literature) and from specimens of *C. whitmani* used in the present paper for illustration by SEM (all in µm). F = female. M = Male. FOSS = Fossil. Wrozyna et al. (2014) identified two female morphotypes (large F and small F). Victor (1987) reported on two different populations of *C. tepida*, one from northern and one from southern Nigeria, with large size differences between them. "/" = measurements not given in the reference.

Literature Data				
Species	L	H	W	References
C. ilosvayi F	960–1140	910	770	Purper 1974
C. ilosvayi M	880–950	550	540	Purper 1974
C. ilosvayi large F	1110–1140	/	/	Wrozyna et al. 2014
C. ilosvayi small F	920–990	/	/	Wrozyna et al. 2014
C. monodi F	760	380	480	Klie 1936
C. monodi M	650	350	370	Klie 1936
C. chariessa F	870	430	590	Rome and De Deckker 1977
C. chariessa M	780	390	440	Rome and De Deckker 1977
C. damasi F	900	450	630	Klie 1944
C. damasi M	700	380	380	Klie 1944
C. tepida North Nigeria F	1140–1160	570–590	780–810	Victor 1987
C. tepida North Nigeria M	950–1000	540–550	550–570	Victor 1987
C. tepida South Nigeria F	1180–1640	590–840	780–820	Victor 1987
C. tepida South Nigeria M	1000–1500	540–800	/	Victor 1987
C. danielopoli (FOSS)	880	/	/	Danielopol et al. 2023
C. martingrossi (FOSS)	1020–1120	/	/	Danielopol et al. 2023
Measurements *C. whitmani* in the present paper				
	L	H	W	
Females				
C. whitmani	789		541	INV323006 CpD
C. whitmani	768		541	INV323007 CpV
C. whitmani	766	453		INV323008 CpRL
C. whitmani	768	456		INV3230013 LVi
C. whitmani	770	451		INV3230013 RVi
C. whitmani	773	449		INV3230014 LVi
C. whitmani	775	443		INV3230014 RVi
Males				
C. whitmani	683		366	INV323002 CpD
C. whitmani	678		349	INV323003 CpD
C. whitmani	698	403		INV323004 CpRL
C. whitmani	706	425		INV323009 LVi
C. whitmani	698	416		INV323009 RVi
C. whitmani	689	401		INV323005 LVi
C. whitmani	682	390		INV323005 RVi

Measurements. See Table 2.

Ecology. The species is abundant in the permanent lakes on Cape Cod. It occurs on different types of sediments with detritus and was mostly found at ca 0.5–1 m depth.

Differential diagnosis. This species is especially characterised by the shape of the Cp and of the DL and the cop of the Hp, by which it can be distinguished from all living *Cytheridella* species. The selvage is more inwardly displaced than in other species, especially so in the postero-ventral corner of the RV of both genders, which also allows distinction from fossil species. *Cytheridella whitmani* can be further distinguished from *C. ilosvayi* by the fact that it is significantly smaller (female length approximately 800 µm against 1000 µm or more in *C. ilosvayi*), by the less widely developed posterior brood pouch in the female, and by the fact that the setae on the rimmed pores on the posterior inner flanges (named peripheral marginal infold (pmi) by Danielopol et al. 2023) are simple, whereas these are bi- or multifurcated in *C. ilosvayi*. In addition, the valves and CpRL in males and females of *C. whitmani* have a straight dorsal margin over more than half the length, unlike in *C. ilosvayi* where this margin is curved. The fossil species, *C. martingrossi* Danielopol & Piller, 2023 (in Danielopol et al. 2023), is significantly larger than the new species (female length approximately 1100 µm), and the shape of the CpRL is different in that it is posteriorly upturned. Females of *C. tepida* are between 1100 and 1640 µm long, and as such are the largest species in the genus, much larger than *C. whitmani*. *Cytheridella damasi* (syn. *C. chariessa*), *C. monodi*, and the fossil *C. danielopoli* Purper, 1979 are of similar sizes as *C. whitmani*, but have different valve shapes. Whereas the dorsal margin in males and females in *C. whitmani* is straight and running parallel with the ventral margin, the dorsal margin in *C. monodi* is curved, while in *C. damasi* it is sloping towards the posterior side. In *C. danielopoli*, the shape of the male valves in inner view resembles that of *C. whitmani*, but the female brood chamber in the latter species is much more developed than in *C. danielopoli* in both lateral and dorsal view (see Purper 1974: pl. 7, figs 23, 24).

Discussion

Taxonomy of *Cytheridella* species

Swain and Gilby (1964) described *Metacypris ometepensis* from Lake Nicaragua, but in a rather incomplete way. For example, even though they found males, they did not describe the Hp, and what they called the "third leg of male" does not have the typical "cleaning limb" morphology, so is most likely an illustration of the T2 (1964: fig. 3(2)). However, the carapace shape of both males and females is typical of *Cytheridella ilosvayi*, as is the length of the female carapace of approximately 1 mm. This brought Martens and Behen (1994) to transfer this species to the genus *Cytheridella* and to subsequently sink *M. ometepensis* into the synonymy of *C. ilosvayi*.

Tressler (1939) described *Onychocythere alosa* Tressler, 1939 on a single male and single female, both retrieved from the stomach of a fish, a specimen of the American shad, *Alosa sapidissima* (Wilson, 1811), caught at Welaka (Florida, USA) in the St. Johns River. Four other ostracod specimens were in the same stomach, which Tressler identified as *Cypria ophthalmica* (Jurine, 1820). As the American shad is an amphidromous, migratory species, Tressler

assumed that the cytherid specimens had been eaten in a marine environment, while the specimens of *C. ophthalmica* would have been consumed in freshwater. However, both the incomplete drawing of the female Cp and the accurate drawing of the Hp show that the species is identical to *C. ilosvayi*. Therefore, Pinto and Sanguinetti (1962) synonymised *Onychocythere* with *Cytheridella* and subsequently Cohuo et al. (2017) synonymised *C. alosa* with *C. ilosvayi*.

Ferguson (1967) described *Gomphocythere argentinensis* from Argentina, and illustrated the female Cp and the Hp, which were clearly identical to those of *C. ilosvayi*. Karanovic (2009) sank the former species into the synonymy of the latter.

Danielopol et al. (2018) argued that there were few, if any, differences between *C. ilosvayi* and poorly illustrated *C. boldii* Purper, 1974 and suggested that the latter might be a synonym of the former. We here confirm this opinion.

Finally, *Cytheridella americana* was described by Furtos (1936) from the cenotes of Yucatan (Mexico) as *Metacypris americana* and was transferred to *Cytheridella* by Danielopol (1981, in Colin and Danielopol 1980), based on Furtos (1936: fig. 46) which shows the T3 being transformed into a cleaning limb which is typical of the genus *Cytheridella*. However, the species was described based on a single female and was poorly illustrated, with a single figure of a valve in lateral view and few figures of appendages. We here propose to consider it an "uncertain species" following the procedure described by Müller (1912) and Meisch et al. (2019, 2024). *Cytheridella ilosvayi* is thus left as the only living representative of the genus in the Americas. On the other hand, the fossil species *C. danielopoli* (Cenozoic, from the Upper Amazon Basin) and *C. martingrossi* (in Danielopol et al. 2023) (Sucuriju Solimões Formation; late Middle to early Late Miocene; state of Amazônia) show clear morphological differences with *C. ilosvayi*, especially the latter species. Wrozyna et al. (2014) analysed morphological variability of both limbs and valves of a series of males, females, and juveniles of *Cytheridella ilosvayi* and concluded (especially based on valve parameters) that there were two morphotypes of females, but a single morphotype in males and in the different juvenile stages. Wrozyna et al. (2014: 1043) wrote: "The presence of two morphologically similar females and only one type of males indicates the coexistence of female morphotypes which may represent either two (cryptic) species or a mixed reproduction population in which parthenogenetic and sexual reproduction coexists." In later papers, Wrozyna et al. (2016, 2018, 2019) further confirmed the existence of different morphotypes within *Cytheridella ilosvayi*. These morphotypes could in time be allocated formal taxonomic status, in some cases even with separate geographical distributions. But none of the formal species synonymised above could be allocated to such morphotypes, as either the type material is non-existent, or damaged (e.g., Furtos 1936; Tressler 1939). We thus face the paradox that morphotypes might need to become taxonomically formalised, but that at the same time potential names from the past must be excluded.

Karanovic (2009) formally synonymised *C. chariessa* (in Rome and De Deckker 1977) with *C. damasi* (in Klie 1944), a synonymy which was already foreshadowed by Victor (1987: 900): "*Cytheridella chariessa* and *C. damasi* are morphologically very similar". After that, only three African species remained in *Cytheridella*: the said *C. damasi* from Congo, *C. monodi* from Cameroon, and *C. tepida* from Nigeria. These species differ from the South American type species, from *C. whitmani* and from each other mainly by the shape of the DL of the Hp, which is more rectangular, and not as widely triangular as in *C. ilosvayi* (Figs 6D, 13).

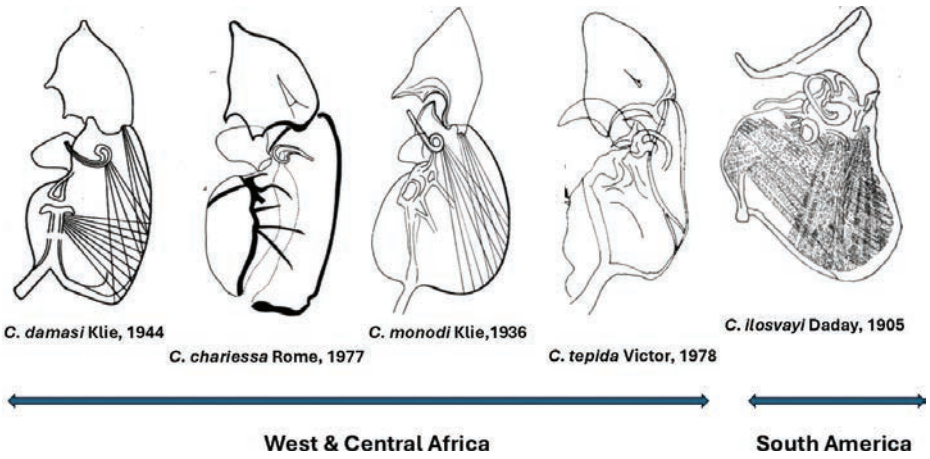

Figure 13. Hemipenes of Recent species of *Cytheridella.* Drawing of *C. ilosvayi* from Purper (1974). All others by original authors. *Cytheridella chariessa* is a synonym of *C. damasi*.

Comparative morphology

Morphology of the T3

The five extant species (two American and three African) share several synapomorphies, of which the female Cp, with the largely inflated brood pouch, and the modified T3 as cleaning limb in both males and females, are especially notable. Yet, the actual chaetotaxy of the T3 differs between some of these species, and Danielopol et al. (2018) stressed the need to compare the chaetotaxy of this limb in the different (extant) species of *Cytheridella*. In both males and females of the African *C. damasi* and *C. tepida*, T1 and T2 have separate endopodal segments En1–En3, while segment En4 is fused with the end claw h2, but where it remains visible as a swollen base of the claw and the occasional presence of a vestigial setula. In the T3 of these species, segment En4 is also fused with the endclaw h2, but much more visible as a swollen base and it carries a spine-like structure, which we here interpret as being homologous to seta h3. Klie (1936) did not illustrate the thoracic legs of his *Cytheridella monodi* from Cameroon, but indicated that the three legs are largely similar, with "some exceptions", from which he cited the presence of an additional hook-like structure at the basis of the end claw in T3. In his key to the genera, he cited for *Cytheridella* "Endklaue mit Sporn" (endclaw with spur – Klie 1936: 307). We can thus assume that the basic chaetotaxy of this leg is similar in all three African species. In *C. ilosvayi* and *C. whitmani*, the situation in both males and females is largely similar to that of the African species, but the fused segment En4 is far less visible at the base of the claw in T1 and T2, while segment En4 of T3 in this species is clearly separated from, and not fused with, the basis of the claw h2 (Purper 1974). Seta h3 is also spine-like, and clearly inserted on the segment En4, which offers support for its homology to seta h3. Based on this small, but significant, morphological difference (the fully separate segment En4 in T3), the South/ Central American species *C. ilosvayi* and *C. whitmani* on the one hand and the three African species on the other, could form two different clusters, with the African one being the more derived one (because of the extra fusion between En4 and claw h2 in T3). This could indicate that the genus, or its ancestral form, already existed before the continental breakup, resulting in South America on the one hand and (west and central) Africa on the other, and that the lineage is thus older than 65 Myr.

Function of the T3

Different morphologies of limbs are nearly always associated with different functions. In most cytheroid ostracod species, the three pairs of thoracic limbs have similar morphologies and are mostly all regarded as walking legs, although in many cases they can also be seen as a means to cling to the (vegetal) surface in habitats with high energy currents. In most Cypridoidea, the three pairs of thoracopods have very different functions: T1 is heavily involved in mating activities in males, T2 is nearly always a walking leg, while in the family Cyprididae, the T3 is modified into a cleaning leg with a pincer-shaped distal part, suitable to clean the natatory setae of the A1 and A2 (Karanovic 2012; Horne et al. 2002).

The morphological differences between T1 and T2 on the one hand and the T3 on the other in species of *Cytheridella* also indicate a different functionality. T3 is more reflexed and, together with the spine-like h3, forms quite a different limb as compared to T1 and T2. The reflexed aspect of the distal part of T3 is more pronounced in the African species, as it starts with the skewed position of segment En2 on En1 and continues with the almost fully reflexed claw h2 with En4 fused to it base. In *C. whitmani*, segments En1 and En2 are in an almost straight (not skewed) position, but En4 and the claws h2 are also fully reflexed (almost 180°). This lead Colin and Danielopol (1980) to interpret the T3 in the species of this genus as a clasping organ, developed to attach the animal to (floating) vegetation, which is very common in Brazilian floodplains, such as Paraná, Pantanal, and Amazon (for example in the genera *Eichhornia*, *Pistia*, *Salvinia* – see Higuti et al. 2007). Here, we interpret the T3 as a functional cleaning limb, where spine h3, the lateral side of En3, and the expanded dorsal tip of En2 form a pincer-like structure, functionally similar, but not homologous, to the pincer-shaped tip of the T3 in most species of Cyprididae.

Caudal ramus

The caudal ramus in cytheroids, unlike in most Cyprididae, is mostly reduced to a relatively simple structure, mostly consisting of some setae. But there are notable exceptions, such as for example in species of the genus *Gomphocythere* Sars, 1924, where the posterior part of the female abdomen comprises two complete caudal rami, each consisting of two setae and three hirsute lobes, while a single furcal organ (FO) is situated dorsally on the abdomen, close to what is assumed to be the caudal seta (CS). In male *Gomphocythere*, the CR consists of one or two simple setae, incorporated in the proximo-ventral part of the Hp (Martens 2003). Regarding the species of *Cytheridella*, the presence/absence and shape of the CR is unclear. Klie (1936) wrote, for both sexes of *C. monodi*, "Eine Furka ist nicht vorhanden" (There is no furca). Klie (1944: fig. 58), on the other hand, illustrated a stout, distally bifurcated rod in the female as "furka" but did not mention it for the male. Rome and De Deckker (1977: pl. 8, fig. q) called this the "organ forchu" in female *C. chariessa*, where it is much smaller than in *C. whitmani* and again, mentioned no CR for the male. For female *C. tepida*, Victor (1987: 898) wrote "Caudal process blunt, devoid of furcal rami", while he did not mention it for the male, also not in the fairly detailed description of the Hp (p. 900). Purper (1974: pl. 5, figs 8, 9) illustrated a bifurcated rod (which

she called caudal ramus) for females *C. ilosvayi*, but did not mention either furca or caudal ramus in the description of the male. In female *C. whitmani* the CR is a single stout rod, distally bifurcate with the larger distal ramus hook-like and pointed; the two distal rods together make for a pincer. In male *C. whitmani*, the CR consists of two stout setae, one of each situated at the base of the Hp, but not fused with it. It is therefore not possible at this stage to interpret the presence/absence and shape of the CR in this genus in a phylogenetic context: were the CR in female *C. monodi* and *C. tepida* missed during the original description or are they really absent in these species? Is *C. whitmani* the only species with CR in the male, or were they missed in all other species of this genus? Re-examination of the type materials of the other species could provide the answers.

Hemipenis

For comparative purposes, the Hp of the other extant species of *Cytheridella* are illustrated in Fig. 13. This figure shows that *C. ilosvayi* from South and Central America has an aberrant DL on the Hp, while the DL of *C. whitmani* is more in line with those of the African species. However, the African species have a well-developed lower ramus, which appears to be absent (*C. whitmani*) or is much smaller (*C. ilosvayi*; see Wrozyna et al. 2018: fig. 4) in the Neotropical species. Fig. 13 also offers support for the synonymy of *C. chariessa* with *C. damasi*, as the Hp of both species is almost identical.

External valve morphology

The external valve ornamentation in both males and females is complex and highly developed. Almost the entire external surface of the valves is covered with pits, mostly organised in circular (anterior and posterior) or random (central parts) patterns. In *C. ilosvayi*, these pits are just shallow and closed indentions. In *C. whitmani*, several of these pits contain what looks like incompletely developed sieve-type pores, although for most of these it is difficult to see as they are cluttered with sticky dirt. A complete sieve-type pore as illustrated by Danielopol et al. (2018) for *C. boldii* was not observed by us in *C. whitmani*, despite the examination of close to 200 SEM images of several male and female carapaces and valves.

The surface of the Cp of the new species carries several rimmed pores, while towards both the anterior and posterior extremities, both setae on conical elevations (so called *Porenwarzen*), as well as long and stiff setae occur. The latter can give the impression that this species is spiny, but these structures are clearly setae and not spines. The term *Porenwarzen* is also used for similar structures in some species of Cyprididae, for example in *Eucypris virens* (Jurine, 1820) (see Meisch 2000), but it is uncertain whether these structures are fully homologous in these distantly related ostracod lineages.

Pseudochaeta on valves and upper lip

Both valves in at least *C. ilosvayi* and *C. whitmani* carry internal rows of long and fine setulae on the anterior calcified inner lamella. Danielopol et al. (2023) have called these “cuticular filaments”. These structures do not follow a con-

tinuous line, but rather form two different half-rows which meet slightly below the middle. The top half row is situated more distally, the bottom one more proximal to the inner margins. These rows do not seem to be associated with inner lists of vestigial selvages, and their origin (and function) remains unclear. In species of *Herpetocypris* Brady & Norman, 1889 (Cyprididae) one or two ancient inward displacements of selvages have left the anterior calcified lamellae with rows of setae (Gonzalez Mozo et al. 1996), but these are clearly associated with (ancient) marginal selvages, which is not the case here. Daday (1905) figured the upper lip of *C. ilosvayi* with distal filaments, probably pseudochaetae. A similar illustration appears in Rome and De Deckker (1977: pl. 8I) for *C. chariessa*. Also, Colin and Danielopol (1980: fig. 11D) illustrated this type of labrum for *Cytheridella* sp. from Los Palacios, Cuba, which has long and dense pseudochaetae distally. One could wonder if the pseudochaeta on the upper lip and those on the valves are interacting with each other, perhaps during (filter) feeding. This will be described and discussed for several non-marine ostracod species elsewhere.

Status of *C. whitmani* in Cape Cod

The African *Cytheridella* species are thus far known from tropical Africa only (Cameroon, Congo, and Niger), while *C. ilosvayi* occurs in the (sub-) tropical regions of South and Central America. However, in Cape Cod, *C. whitmani* survives in a climate with maritime influence, with warm summers and cold winters. Cushman (1907), Sharpe (1910), and especially Furtos (1935) dealt with species collected from localities on Cape Cod, several of which are situated close to Woods Hole, Falmouth, Barnstable, and East Sandwich. Those are the same places from which *C. whitmani* was collected in large numbers during the present survey (in 20 of 24 sampled lakes – see above). However, whereas these older papers together reported 21 species of ostracods (Table 1), none mentioned ostracods that would even remotely resemble a species of *Cytheridella*. It is of course possible that the species was missed during the sampling efforts in the first half of the 20th century on which these papers report. However, as a case in point, one of the localities from which Furtos (1935) described ostracods, is "Marston Mills Pond". There are three likely candidates from this locality (presently called Mystic Lake, Middle Pond, and Hamblin's Pond) and *C. whitmani* presently occurs in all three of these lakes (see above). Therefore, *C. whitmani* could be considered an invasive species in the Cape Cod peninsula and arrived there after 1935. This hypothesis can be tested by analysing cores from lakes which now carry the species in abundance. There could be a link between this presumed recent and successful invasion and the fact that winters are becoming less cold in the peninsula (Valiela and Bowen 2003).

Acknowledgements

The samples of the present study were collected by KM and IS during their 2023 stay at MBL, Woods Hole (Ma, USA). The stays of IS (2019, 2022, 2023) and of KM (2024) as Whitman Fellows at the Marine Biological Laboratory (Woods Hole, USA) were funded by the L. and A. Colwin Fund of the MBL. IS also ac-

knowledges several travel grants to Woods Hole funded by the Flemish Fund for Scientific Research (FWO). IS and KM thank Dr Irina Arkhipova (MBL Bay Paul Centre) for providing lab space during their stays at MBL, Dr Javier Lloret (MBL Ecosystems Centre) for logistic field support and Robert Kaski and Horace Bryant (MBL supporting services) for logistic support with the field vehicles.

It is noteworthy that the work by Norma Furtos (1935), including her sampling in 1933, on the non-marine ostracods from Cape Cod was done "under the auspices of the Marine Biological Laboratory, Woods Hole, Mass., (and that) facilities at Woods Hole were made available through the kindness of Dr. M. H. Jacobs", the Director of MBL at that stage. In 1934, Norma Furtos was a "Fellow in Zoology" at MBL (https://history.archives.mbl.edu/people-and-courses/person/norma-c-furtos).

Laetitia Despontin (RBINS, Brussels, Belgium) provided technical assistance with the SEM illustrations. Dr Claude Meisch (Luxembourg) and Dr Danielopol (Graz, Austria) are thanked for their useful comments, which provoked further research and considerably improved the paper.

Additional information

Conflict of interest

The authors declare that they have no competing or conflicting financial or nonfinancial interests.

Ethical statement

The species used in this study is neither a CITES-listed species nor an endangered species according to IUCN Red Lists.

Funding

The stays of IS (2019, 2022, 2023) and of KM (2024) as Whitman Fellows at the Marine Biological Laboratory (Woods Hole, USA) were funded by the L. and A. Colwin Fund of the MBL. IS also acknowledges several travel grants to Woods Hole funded by the Flemish Fund for Scientific Research (FWO).

Author contributions

KM and IS conceptualised the research and performed the sampling and water chemistry measurements. KM sorted the samples and identified the present species as new to science. MS, NMA and JH assisted with the illustrations. All authors assisted in the writing of the manuscript.

Author ORCIDs

Koen Martens https://orcid.org/0000-0001-8680-973X
Nadiny Martins de Almeida https://orcid.org/0000-0002-4380-125X
Michael Shribak https://orcid.org/0000-0002-5849-6294
Janet Higuti https://orcid.org/0000-0002-3721-9562
Isa Schön https://orcid.org/0000-0001-9269-6487

Data availability

All of the data that support the findings of this study are available in the main text.

References

Baird W (1845) Arrangement of the British Entomostraca, with a list of species, particularly noticing those which have as yet been discovered within the bounds of the Club. Transactions of the Berwicks Naturalists Club 2: 145–158.

Baird W (1850) The natural history of the British Entomostraca. The Ray Society, London, 364 pp [36 plates]. https://doi.org/10.5962/bhl.title.1807

Brady GS, Norman AM (1889) A Monograph of the Marine and Freshwater Ostracoda of the North Atlantic and of North-Western Europe. Section I: Podocopa. Scientific Transactions of the Royal Dublin Society, Series 2(4): 63–270.

Brady GS, Robertson D (1870) The Ostracoda and Foraminifera of tidal rivers. Part 1. Annals and Magazine of Natural History, Series 4(6): 1–33. https://doi.org/10.1080/00222937008696200

Broodbakker NW, Danielopol DL (1982) The chaetotaxy of Cypridoidea (Crustacea, Ostracoda) limbs: proposals for a descriptive model. Bijdragen tot de Dierkunde 52:103–120. https://doi.org/10.1163/26660644-05202003

Cohuo S, Macario-Gonzalez L, Perez L, Schwalb A (2017) Overview of Neotropical-Caribbean freshwater ostracod fauna (Crustacea, Ostracoda): identifying areas of endemism and assessing biogeographical affinities. Hydrobiologia 786: 5–21. https://doi.org/10.1007/s10750-016-2747-1

Colin JP, Danielopol DL (1978) New data on the systematics of the Limnocytheridae (Ostracoda, Cytheracea). Geobios 11: 563–567. [including reference to Danielopol 1960]. https://doi.org/10.1016/S0016-6995(78)80084-9

Colin JP, Danielopol DL (1980) Sur la morphologie, la systématique, la biogéographie et l'évolution des ostracodes Timiriaseviinae (Limnocytheridae). Paléobiologie Continentale 11: 1–51. [published 1981]

Conceição EO, Mantovano T, Campos R, Rangel TF, Martens K, Bailly D, Higuti J (2020) Mapping the observed and modelled intracontinental distribution of non-marine ostracods of South America. Hydrobiologia 847(7): 1663–1687. https://doi.org/10.1007/s10750-019-04136-6

Cushmann JA (1907) Ostracoda from Southeastern Massachusetts. American Society of Naturalists 41(481): 35–39. https://doi.org/10.1086/278701

Cushmann JA (1905) A new ostracod from Nantucket. The American Naturalist 39(47): 791–793. https://doi.org/10.1086/278573

Daday E (1905) Untersuchungen über die Süsswasser-Mikrofauna Paraguays. Zoologica, Stuttgart 44(4): 234–270, Ostracoda.

Danielopol DL, Martens K, Casale LM (1989) Revision of the genus *Leucocythere* Kaufmann, 1892 (Crustacea, Ostracoda, Limnocytheridae), with the description of a new species and two new tribes. Bulletin van het Koninklijk Belgisch Instituut voor Natuurwetenschappen, Biologie 59 (1989): 63–94. [published 1990]

Danielopol DL, Cabral MC, Lord A, Carbonel P, Gross M, Stoica M, Humphreys WF, Namiotko T, Tóth E, Külköylüoglu O, Piller W, Nunes T (2018) Sieve-type pore canals in the Timiriaseviinae. A contribution to the comparative morphology and the systematics of the Limnocytheridae (Ostracoda, Crustacea). Zootaxa 4495(1): 1–64. https://doi.org/10.11646/zootaxa.4495.1.1

Danielopol DL, Gross M, Piller WE (2023) Morphology And Taxonomy Of Three *Cytheridella* Species (Ostracoda, Timiriaseviinae, Cytheridellini) From Western Amazonia. Geo-Eco-Marina 29: 83–109. https://doi.org/10.5281/zenodo.10350901

De Deckker P (1981) Taxonomy and ecological notes of some ostracods from Australian inland waters. Transactions of the Royal Society of South Australia 105 (3): 91–138.

Ferguson Jr E (1967) Three new species of freshwater ostracods (Crustacea) from Argentina. Notulae Naturae (The Academy of Natural Sciences of Philadelphia) 405: 1–7.

Fischer S (1855) Beitrag zur Kenntnis der Ostracoden. Abhandlungen der Mathematisch-Physicalischen Classe der Königlich Bayerischen Akademie der Wissenschaften 7: 635–666.

Fisher JJ, Leatherman SP (1987) Glacial and coastal geology, Cape Cod National Seashore, Massachusetts. Geological Society of America Centennial Field Guide—Northeastern Section, 213–220. https://doi.org/10.1130/0-8137-5405-4.213

Furtos NC (1933) The Ostracoda of Ohio. Bulletin of the Ohio Biological Survey 5 (6): 411–524.

Furtos, NC (1935) Fresh-water Ostracoda from Massachusetts. Journal of the Washington Academy of Sciences 25 (12): 530–544.

Furtos NC (1936) On the Ostracoda from the cenotes of Yucatan and vicinity. Publications of the Carnegie Institution of Washington 457: 89–115.

Gonzalez Mozo M, Martens K, Baltanás A (1996) A taxonomic revision of European *Herpetocypris* Brady and Norman, 1889 (Crustacea, Ostracoda). Bulletin van het Koninklijk Belgisch Instituut voor Natuurwetenschappen, Biologie 66: 93–132.

Haldeman, SS (1842) Description of a new species of *Cypris.* Proceedings of the Philadelphia Academy of Natural Sciences 1: 184.

Higuti J, Machado Velho LF, Lansac Tôha FA, Martens K (2007) Pleuston communities are buffered from regional flood pulses: the example of ostracods in the Paraná River floodplain, Brazil. Freshwater Biology 52: 1930–1943. https://doi.org/10.1111/j.1365-2427.2007.01821.x

Higuti J, Declerck SAJ, Lansac-Tôha FA, Machado Velho LF, Martens K (2010) Variation in ostracod (Crustacea, Ostracoda) communities in the alluvial valley of the upper Paraná River (Brazil) in relation to substrate. Hydrobiologia 644: 261–278. https://doi.org/10.1007/s10750-010-0122-1

Horne DJ, Cohen A, Martens K (2002). Taxonomy, morphology and biology of quaternary and living Ostracoda. In: Holmes JA, Chivas AR (Eds) The Ostracoda applications in Quaternary research. American Geophysical Union, Washington, DC, USA, 131: 5–36. https://doi.org/10.1029/131GM02

Jurine L (1820) Histoire des monocles qui se trouvent aux environs de Genève I–XVI. J. Paschoud, Genève, 260 pp. https://doi.org/10.5962/bhl.title.10137

Karanovic I (2009) Four new species of *Gomphodella* De Deckker, with a phylogenetic analysis and a key to the living representatives of the subfamily Timiriaseviinae. Crustaceana 82: 1133–1176. https://doi.org/10.1163/156854009X452731

Karanovic I (2012) Recent freshwater ostracods of the world. Springer, Heidelberg, 608[+xiii] pp. https://doi.org/10.1007/978-3-642-21810-1

Kaufmann A (1900) Cypriden und Darwinuliden der Schweiz. Revue Suisse de Zoologie 8: 209–423 [pls 15–31]. https://doi.org/10.5962/bhl.part.10584

Klie W (1936) Ostracoden aus Kamerun. Revue de Zoologie et de Botanie Africaine 28(2): 287–302.

Klie W (1944) Ostracoda. Exploration du Parc National Albert, Mission H. Damas (1935–1936) 12: 1–62.

Latreille PA (1802) Histoire naturelle, générale et particulière des Crustacés et des Insectes. Familles Naturelles des Genres. Dufart, Paris, 394 pp. https://doi.org/10.5962/bhl.title.15764

Lord AR, Cabral MC, DL Danielopol (2020) Sieve-type normal pore canals in Jurassic ostracods: a review with description of a new genus. Acta Palaeontologica Polonica 65(2): 313–349. https://doi.org/10.4202/app.00632.2019

Mandelstam MI (1960) The subfamily Timiriaseviinae, Mandelstam, Subfam. nov. In: Orlov Y (Ed.) Fundamentals of Paleontology. In: Chernysheva NE (Ed.) A manual for Paleontology and geologists of the USSR, 8 (Arthropoda-Crustacea): 372–375, National Science-Technical Publishing House, Moscow. [in Russian]

Martens K (2003) On the evolution of *Gomphocythere* (Crustacea, Ostracoda) in Lake Nyassa/ Malawi (East Africa), with the description of 5 new species. Hydrobiologia 497: 121–144. https://doi.org/10.1023/A:1025417822555

Martens K, Behen F (1994) A checklist of the recent non-marine ostracods (Crustacea, Ostracoda) from the inland waters of South America and adjacent islands. Travaux scientifiques du Musée d'Histoire naturelle de Luxembourg 22: 81.

Martens K, Schön I, Meisch C, Horne DJ (2008) Global biodiversity of non-marine Ostracoda (Crustacea). In: Balian EV, Lévêque C, Segers H, Martens K (Eds) Freshwater animal diversity assessment. Hydrobiologia 595: 185–193. https://doi.org/10.1007/s10750-007-9245-4

Martens K, Shribak M, Arkhipova I, Schön I (2023) The common morphospecies *Cypridopsis vidua* (O.F. Müller, 1776) (Crustacea, Ostracoda) is not a obligate parthenogen. Belgian Journal of Zoology 153: 15–34. https://doi.org/10.26496/bjz.2023.107

Meisch C (2000) Freshwater Ostracoda of Western and Central Europe. In: Schwoerbel J, Zwick P (eds) Süßwasserfauna von Mitteleuropa 8/3. Spektrum Akademischer Verlag, Heidelberg, Berlin, 522 pp.

Meisch C, Smith RJ, Martens K (2019) A subjective global checklist of the extant non-marine Ostracoda (Crustacea). European Journal of Taxonomy 492: 1–135. https://doi.org/10.5852/ejt.2019.492

Meisch C, Smith RJ, Martens K (2024) An updated subjective global checklist of the extant non-marine Ostracoda (Crustacea). European Journal of Taxonomy 974: 1–144. https://doi.org/10.5852/ejt.2024.974.2767

Müller OF (1776) Zoologiae Danicae prodromus: seu Animalium Daniae et Norvegiae indigenarum characteres, nomina, et synonyma imprimis popularium. Typis Hallageriis, Havniae, 228 pp. https://doi.org/10.5962/bhl.title.63795

Müller GW (1912) Crustacea: Ostracoda. Das Tierreich 31: 1–434. https://doi.org/10.5962/bhl.title.1079

Pinto RD, Sanguinetti YT (1962) A complete revision of the Genera *Bisulcocypris* and *Theriosynoecum* (Ostracoda) with the world geographical and stratigraphical distribution. Escola de Geologia de Porto Alegre 4: 1–165.

Purper I (1974) *Cytheridella boldii* Purper, sp. nov. (Ostracoda) from Venezuela and a revision of the genus *Cytheridella* Daday, 1905. Anais Academia Brasileira de Ciências 46: 635–662.

Purper I (1979) Cenozoic Ostracodes of the Upper Amazon Basin, Brazil. Pesquisas 12: 209–281. https://doi.org/10.22456/1807-9806.21765

Ramdohr FA (1808) Uber die Gattung *Cypris* Müller und drei zu derselben gehörige neue Arten. Magazin der Gesellschaft Naturforschender Freunde zu Berlin fur die Neuesten Entdeckungen in der Gesammten Naturkunde 2: 85–93.

Rome DR, De Deckker P (1977) Ostracodes du lac Kivu. Mémoires de l'Institut géologiques de l'Université de Louvain 29: 241–287.

Sars GO (1866) Oversigt af Norges marine ostracoder. Forhandlinger I Videnskabs-Selskabet I Christiana 1865: 1–130.

Sars GO (1924) The freshwater Entomostraca of the Cape Province (Union of South Africa). Ostracoda. Annals of the South African Museum 20: 105–193.

Sars GO (1925) Ostracoda. In: Sars GO (Ed.) An account of the Crustacea of Norway with short descriptions and figures of all the species. Vol. 9: 73–208, Taf 33–96.

Sars GO (1928) Ostracoda. In: Sars GO (Ed.) An account of the Crustacea of Norway with short descriptions and figures of all the species. Vol. 9(15–16): 241–271, Annex, Corrections, 6.

Sharpe RW (1897) Contribution to a knowledge of the North American Fresh-water Ostracoda included in the families Cytheridae and Cyprididae. Bulletin of the Illinois State Laboratory of Natural History 4: 414–484. https://doi.org/10.21900/j.inhs.v4.439

Sharpe RW (1908) A further report on the Ostracoda of the United States National Museum. Proceedings of the United States National Museum 35(1651): 399–430, pls 50–65. https://doi.org/10.5479/si.00963801.35-1651.399

Sharpe RW (1910) On some ostracods, mostly new, in the collections of the United States National Museum. Proceedings of the United States National Museum 38(1750): 335–341. https://doi.org/10.5479/si.00963801.38-1750.335

Shribak M (2014) Polychromatic polarization state generator and its application for real-time birefringence imaging, US Patent 9625369.

Shribak M (2015) Polychromatic polarization microscope: bringing colors to a colorless world. Scientific Reports 5: 17340. https://doi.org/10.1038/srep17340

Smith AJ, Horne DJ, Martens K, Schön I (2015) Class Ostracoda. In: Thorpe and Covich's Freshwater Invertebrates, 4th edn., Academic Press and Elsevier, London, 757–780. https://doi.org/10.1016/B978-0-12-385026-3.00030-9

Swain FW, Gilby JM (1964) Ecology and taxonomy of Ostracoda and an alga from Lake Nicaragua. Pubblicazioni della Stazione zoologica di Napoli 33(suppl.): 361–386 [published 1965].

Tanaka H, Hyunsu Y, Pham HTM, Karanovic Y (2021) Two new xylophile cytheroid ostracods (Crustacea) from Kuril-Kamchatka Trench, with remarks on the systematics and phylogeny of the family Keysercytheridae, Limnocytheridae, and Paradoxostomatidae. Arthropod Systematics & Phylogeny 79: 171–188. https://doi.org/10.3897/asp.79.e62282

Tressler WL (1939) *Onychocythere*, a new genus of marine ostracod from Florida. with a description of one species. Journal of the Washington Academy of Science 29(8): 336–339.

Valiela I, Bowen JL (2003) Shifts in Winter Distribution in Birds: Effects of Global Warming and Local Habitat Change. AMBIO 32(7): 476–480. https://doi.org/10.1579/0044-7447-32.7.476

Victor R (1987) A new species of the genus *Cytheridella* (Crustacea, Ostracoda) from Nigeria, West Africa. Journal of Natural History 21: 893–902. https://doi.org/10.1080/00222938700770541

Wrozyna C, Piller WE, Gross M (2014) Morphotypes of *Cytheridella ilosvayi* (Ostracoda) detected by soft and hard part analyses. Crustaceana 87: 1043–1071. https://doi.org/10.1163/15685403-00003342

Wrozyna C, Neubauer TA, Meyer J, Piller WE (2016) Shape variation in Neotropical *Cytheridella* (Ostracoda) using semi landmarks based geometric morphometrics: a methodological approach and possible biogeographical implications. PLoS ONE 11: 1–16. https://doi.org/10.1371/journal.pone.0168438

Wrozyna C, Meyer, J, Gross M, Ramos MIF, Piller WE (2018) Definition of regional ostracod (*Cytheridella*) morphotypes by use of landmark-based morphometrics. Freshwater Science 37: 573–592. https://doi.org/10.1086/699482

Wrozyna C, Meyer J, Gross M, Ramos MIF, Piller WE (2019) Sexual, ontogenetic, and geographic variation of the Neotropical freshwater ostracod *Cytheridella ilosvayi*. BMC Zoology 4: 1–19. https://doi.org/10.1186/s40850-019-0042-0

Zaddach EG (1844) *Synopseos crustaceorum prussicorum prodromus*. Impressit E.J. Dalkowski, Regiomonti, [vi +] 39 pp.